5-14-2023

Design, synthesis, and characterization of monomeric peptide multiagonists for the mitigation of CNS-associated side effects in the treatment of Type II diabetes and Obesity

Kylie Sloane Chichura
Syracuse University

Abstract

Current treatments for type 2 diabetes mellitus (T2DM) and obesity do not reliably achieve long-term weight-loss and up to 50% of patients experience nausea and vomiting. Thus, there is a critical need for obesity medications that provide glycemic control with enhanced weight loss and without side effects. We recently reported on the development of EP45, a first in class monomeric peptide drug, which displayed glucoregulation and profound weight loss in rats, and an absence of visceral malaise in shrews, a mammalian model capable of vomiting (unlike rats). By targeting multiple weight-loss and glucoregulatory pathways simultaneously with a single drug, GEP44, we can address multiple coexisting conditions to more efficaciously reduce body weight and blood glucose levels, all devoid of side-effects to improve patient tolerance and quality of life.

Design, synthesis, and characterization of monomeric peptide multi-agonists for the mitigation of CNS-associated side effects in the treatment of Type II diabetes and Obesity

By

Kylie S. Chichura

B.S., Moravian University, 2019
M.Phil., Syracuse University, 2021

DISSERTATION
Submitted in partial fulfillment for the degree of
Doctor of Philosophy in Chemistry

Syracuse University
May 2023

Table of Contents

List of Figures and Tables

Chapter 1: Introduction

Chapter 2: Hit to lead development of a triple agonist of GLP-1R, Y1-R, and Y2-R

residues present in the Ex-4 and GLP-1, respectively. Green Q3 is known to be important in GlucR agonism. Ser2 of GEP44 is the D-isomer indicated as a lowercase “s”. (B) CD spectroscopy displays the measured α-helical secondary structure of peptides at 35 μM. (C) PEP-FOLD3 simulations of calculations of designed peptides I = EP38; II = EP45; II I= EP40; IV = EP44; V = EP46; VI = EP50; VII = GEP44. Simulations for Ex-4 and $PYY_{3–36}$ were complementary to the published structures for both peptides (data not shown).

Figure 2-2. FRET (tracking cAMP stimulation via FRET at H188 dose-response of GEP44 at the GLP-1R (A), dose-response nonlinear regression of GEP44 at the GLP-1R (B). FRET response of 300 pM GEP44 against GLP-1R antagonist Ex(9-39) pre-treatment at GLP-1R (C), dose-response nonlinear regression of 3000 pM GEP44 against GLP-1R antagonist Ex(9-39) pre-treatment at GLP-1R (D). FRET (E) and dose-response nonlinear regression (F), tracked by mitigation of adenosine (2 μM in all four treatments) stimulated cAMP at the A2b receptor via FRET at H188, of GEP44 at Y2-R. Normalized FRET response of GEP44 against NPY antagonist BIIE0246 [300 nM] at Y2-R (G). FRET response of GEP44 at the Glucagon receptor indicating no agonism (H). EC_{50} values for GEP44 are 10 nM at Y2-R and 330 pM at GLP-1R. The PYY_{3-36} and Ex4 EC50 values in these FRET assays are 16 nM and 16 pM at the Y2-R and GLP-1R, respectively.

Figure 2-3. Dose escalation study averaging food intake for 2 days on each dose relative to vehicle treatment for the 2 d prior shows less of a reduction of food intake in response to EP44 (B) vs Ex-4 (A) in lean rats (male, age 11 weeks, n = 4 per group). However, unlike Ex-4 (A), EP44 (B) did not induce nausea assessed by kaolin intake during 2 day

treatment periods. Modifications were made to improve Y2-R binding with GEP44, resulting in robust reductions in food intake (C) vs Ex-4 (A) without induction of nausea assessed by kaolin intake.

Figure 2-4. Longitudinal study (5 d Tx.; n = 3–5 per group; 10 nmol/kg; cohort 1: age 20 weeks, 16 weeks HFD exposure, 641.9 ± 17.9 g, n = 4; cohort 2: age 28 weeks, 24 weeks HFD exposure, 826.1 ± 35.7 g, n = 9) in DIO rats shows sustained weight loss (A), reduced food intake (B), and reduced fasting blood glucose (C) due to GEP44 treatment. IPGTT was performed prior to the baseline phase and immediately following the last drug treatment. When compared to Ex-4 (E) or vehicle (F), treatment with GEP44 (D) yielded stronger reductions in blood glucose during IPGTTs following 5 d treatments in prediabetic rats. Area under the curve (AUC) analyses of blood glucose from glucose bolus to 60 min indicated a significant effect of GEP44 on glucose clearance (G). For bar graphs, empty bars represent baseline data, and filled bars represent data during drug treatment. Data were analyzed with repeated measurements two-way ANOVA followed by Bonferroni's post-hoc test. When compared to baseline measures or vehicle control: *$p < 0.05$, ***$p < 0.001$.

Figure 2-5. Systemically delivered GEP44 enhances glucose clearance during IPGTT while showing minimal emetogenic effects in shrews n = 9; ~8 months old; 60–65 g. (A) In an IPGTT, GEP44 (10 nmol/kg) suppressed blood glucose levels after IP glucose administration (2 g/kg, IP) compared to saline. (B) AUC analysis from 0 (*i.e.*, postglucose bolus) to 120 min showed that GEP44 reduced AUC compared to vehicle. (C) The number

of single emetic episodes following GEP44 (10 and 60 nmol/kg) or saline systemic administration did not differ across treatment conditions. Indeed, GEP44 caused emesis in only one shrew tested. Data are expressed as mean ± SEM. Data in panel A were analyzed with repeated measurements two-way ANOVA followed by Bonferroni's post-hoc test. Data in panel B were analyzed with the Student's t test for repeated measures. Due to the nonparametric nature of data in panel C, a repeated measurements Friedman test followed by Dunn's post hoc test was used to analyze GEP44 data, while a Wilcoxon test was used to analyze Ex-4 data. *$p < 0.05$, ***$p < 0.001$.

Figure 2-6. Up to 85% FI reduction by GEP44 with the native D-Ser2 residue compared to the no effect observed when using L-Ser2 GEP44.

Figure 2-7. Design of chimeric peptides GEP44 and GEP12. Shown are the amino acid sequences of Ex-4, PYY_{1-36}, and PYY_{3-36} overlaid with those of GEP44 and GEP12 with lowercase single-letter amino acid code denoting a D-isomer.

Figure 2-8. *In vitro* evaluation of chimeric peptides GEP44 and GEP12. (A) Dose-dependent agonism (% change in FRET ratio tracking levels of cAMP) of Ex-4, GEP44, and GEP12 at the GLP-1R. (B) Dose-dependent agonism (% change in FRET ratio tracking levels of cAMP) of PYY_{3-36}, GEP44, and GEP12 at the Y2-R. (C) Dose-dependent agonism of PYY_{1-36}, GEP44, and GEP12 at the Y1-R. (D) Percent binding of Ex-4, GEP44, and GEP12 at the GLP-1R. (E) Percent binding of PYY_{3-36}, GEP44, and GEP12 at the Y2-R. (F) Percent binding of PYY1-36, GEP44, and GEP12 at the Y1-R.

(G) % internalization of GEP44 and GEP12 at the GLP-1R. (H) % recruitment of β-arrestin-2 by Ex-4 and GEP44 at the GLP-1R. (I) % internalization of Ex-4 and GEP44 at the Y2-R.

Figure 2-9. Action of GEP44 and GEP12 are mediated by GLP-1R and Y1-R in isolated pancreatic islets and muscle tissue. Rat (A) and human (B) islets were incubated for 60 min in 20 mM glucose and additional agents as indicated. Supernatants were then assayed for insulin, cAMP, and glucagon concentrations. (C) Insulin secretion rates (ISRs) were measured by perifusion over a one-hour incubation period in rat islets in 20 mM glucose with 5 or 50 nM peptides with or without Y1-R antagonist, as indicated (C). Impact of GEP44 on (D) cAMP, (E) the ISR to cAMP ratio, and (F) glucagon secretion, relative to glucose-mediated stimulation alone in the absence of test compounds. cAMP levels corresponded directly, and glucagon secretion corresponded inversely with the ISR. (G) Uptake of 3H-2-deoxyglucose (2-DG) and (H) lactate production (Å} 5 mM glucose) in response to GEP44 and other agents known to interact with GLP-1R, Y1-R, and Y2-R in the rat quadriceps muscle ex vivo. Horizontal dashed line in 2A, B, D, and F represents response to 20 mM glucose alone in assay as described. a = PD 160170; b = BIIE0246; c = BIBO; d = Bay K, e = Wortmannin.

Figure 2-10. FISH and IHC visualization of *f*Cy5-GEP44 and its colocalization with Y1-R, Y2-R, and GLP-1R in cells in the NTS/AP regions of the rat brain. (A) *f*Cy5-GEP44 (green) administered IP colocalized with Y1-R and GLP-1R (yellow) in the AP. (B) *f*Cy5-GEP44 administered ICVI colocalized with Y1-R (yellow) and GLP-1R (magenta) in the AP. (C)

*f*Cy5-GEP44 administered ICVI colocalized with Y2-R (yellow) and GLP-1R (magenta) in cells of the AP.

Figure 2-11. GEP44-mediated reductions in body weight and food intake were stronger than those elicited by LIRA during a 16-day and 27-day dose escalation protocol. (A, B) DIO Wistar rats were treated with vehicle or with GEP44 or LIRA at 10 nmol/kg/day for 9 days followed by 25 nmol/kg/day for 7 days (n=4–6) rats/group. In a second experiment, (C) changes in body weight and (D) food intake was evaluated during 27 days of treatment with vehicle, GEP44, vehicle-treated rats that were pair-fed to those receiving GEP44, LIRA, and vehicle-treated rats that were pair-fed to those receiving LIRA; n=8 per group. DIO male Wistar rats were matched based on baseline food intake and initial body weight gain trajectory. Changes in body weight were evaluated in response to GEP44 at doses escalating from 5 to 50 nmol/kg/day. Rats underwent pair-feeding to match the amount of food consumed by their GEP44-treated counterparts. Other groups included rats treated with saline vehicle control, LIRA, and rats that were pair-fed to their LIRA-treated counterparts. Symbols representing the results from pair-fed animals are overlayed by those from the GEP44 and LIRA treatment groups. Data shown are means $\pm$ SEM; *p <0.05, ***p <0.001, ****p <0.0001.

Figure 2-12. Sequences of lipidated peptides successfully synthesized and purified to >95% by HPLC. Lowercase letters denote D-amino acids.

(seconds/meal; M-P), and meal size (grams/meal; Q-T) at time intervals 1, 6, 6-12, and 12-24 hours after administration. All data presented as mean ± SEM.

Figure 3-4. Pretreatment with an antibody against DBI attenuates central exendin-4 induced hypophagia in chow fed rats. Rats were pretreated 4th ventricle with a DBI antibody (AB 3 µg/3 µL) or vehicle followed by 4th ventricle treatment with ODN (20 µg/2 µL), Ex-4 (0.3 µg/2 µL), or vehicle. 24 hour food intake in chow (A) and HFD (B) fed rats, kaolin intake in chow (C) and HFD (D) fed rats, and body weight change in chow (E) and HFD (F) fed rats following treatments. # indicates difference from Veh/Veh (P=0.05). All data presented as mean ± SEM.

Figure 3-5. Pretreatment with an ODN antagonist attenuates central exendin-4 induced hypophagia. Rats were pretreated 4th ventricle with an ODN antagonist (AntOP 200 µg/2 µL) or vehicle followed by 4th ventricle treatment with ODN (20 µg/2 µL), Ex-4 (0.3 µg/2 µL), or vehicle. 24 hour food intake in chow (A) and HFD (B) fed rats, kaolin intake in chow (C) and HFD (D) fed rats, and body weight change in chow (E) and HFD (F) fed rats following treatments. # indicates difference from Veh/Veh (P=0.05). All data presented as mean ± SEM.

Figure 3-6. Five-day combined treatment with ODN enhances peripheral Liraglutide induced hypophagia. Rats were treated 4th ventricle with ODN (100 µg/2 µL) or vehicle followed by intraperitoneal treatment with Liraglutide (25 µg/kg) or vehicle for 5 days. Daily (A) and cumulative (B) food intake, daily (C) and cumulative (D) kaolin intake, and daily

body weight (E) in HFD fed rats following treatments. Isolated day 1 food intake (F). All data presented as mean ± SEM.

Figure 3-7. Pretreatment with an ODN antagonist attenuates peripheral Liraglutide induced hypophagia. Rats were pretreated lateral ventricle with an ODN antagonist (AntOP 100 µg/2 µL) or vehicle followed by intraperitoneal treatment with Liraglutide (50 µg/kg), or vehicle. 48 hour food intake in chow (A) and HFD (B) fed rats, kaolin intake in chow (C) and HFD (D) fed rats, and body weight change in chow (E) and HFD (F) fed rats following treatments. All data presented as mean ± SEM.

Chapter 4: Novel peptide antagonists of GPR75

Figure 4-1. Blind SU75-36/GPR75 receptor *in silico* docking using HPEPDOCK. SU75-36 (aqua marine; see arrow) surface binding of GPR75 consistent with SPR binding (Figure 2). Docking score 0.884.

Figure 4-2. SPR assay tracking SU75-36 binding at GPR75. SU75-36 binds to GPR75 with a K_D of 7.76 µM.

Figure 4-3. SPR assay tracking SU75-37 binding at GPR75. SU75-37 binds to GPR75 with a K_D of 23.8 µM.

Figure 4-4. SPR assay comparing SU75-36 binding at hGLP-1R with positive Ex-4 control, negative ODN control, and SU75-37. SU75-37 does not bind at the hGLP-1R, akin with its design.

Figure 4-5. SPR assay tracking SU75-36 binding at hGLP-1R. SU75-36 binds to GPR75 with a K_D of 182 μM.

Figure 4-6. Peptide sequences of novel GPR75 antagonists. Peptides have been synthesized, confirmed, and purified prior to testing. Lowercase letter indicates a D-amino acid. Peptides are C-terminally amidated.

Figure 4-7. Folded state analysis of SU75-36 and SU75-37. Peptides were analyzed by CD spectroscopy. Percent helicities were calculated as 20.9% for SU75-36 and 21.3% for SU75-37.

Figure 4-8. 4th Ventricle GPR75 Ligands Suppress Food Intake and Body Weight in HFD Rats. Effect of 4th ventricle SUODN-36 (20, 100, or 200 μg/2 μL in aCSF) and SUODN-37 (20 μg/2 μL in aCSF) treatment on 24h food intake (A) and body weight change (B) in HFD fed rats. All data presented as mean ± SEM.

Figure 4-9. Lateral Ventricle GPR75 ligands injection suppresses food intake and body weight in chow and HFD-fed rats. Effect of lateral ventricle SUODN-36 (20 or 100 μg/2μL in aCSF) or SUODON-37 (20μg/2μL in aCSF) treatment on 24h food intake in chow (A)

List of abbreviations

2-DG	^{3}H-2-deoxyglucose
5-TG	5-thio-d-glucose
α-MSH	Alpha-melanocyte-stimulating hormone
A2B	Adenosine receptor
AA	Amino acid
AB	Antibody
ACN	Acetonitrile
aCSF	Artificial cerebrospinal fluid
ALT	Alanine aminotransferase
AP	*Area postrema*
ARC	Arcuate nucleus
AST	Aspartate aminotransferase
BBB	Blood-brain barrier
BMI	Body mass index
BSA	Bovine serum albumin
BW	Body weight
Calc	Calculated
cAMP	Cyclic adenosine monophosphate
CDC	Centers for Disease Control and Prevention
CeA	Central nucleus of the amygdala
CHCA	α–cyano–4–hydroxycinnamic acid

CHO	Chinese hamster ovary cells
CI	Confidence interval
CNS	Central nervous system
Cy5	Cyanine5
DAPI	4′,6-diamidino-2-phenylindole
DBCO	Dibenzocyclooctyne
db/*db*	Diabetic mouse
DBI	Diazepam binding inhibitor
DI	Deionized
DIC	*N,N'*-diisopropylcarbodiimide
DIO	Diet-induced obese
DLS	Dynamic light scattering
DMF	*N,N'*-dimethylformamide
DMSO	Dimethylsulfoxide
DPP-IV	Dipeptidyl peptidase 4
DVC	Dorsal vagal complex
EAS	Electron absorption spectrum
EC_{50}	Half-max effective concentration
ECD	Extracellular domain
EE	Energy expenditure
EDTA	Ethylenediaminetetraacetic acid
ELISA	Enzyme-linked immunoassay
ESI-MS	Electrospray ionization mass spectrometry

Ex-4	Exendin-4
Ex9-39	Exendin(9-39)
FDA	US Food and Drug Administration
FI	Food intake
FISH	Fluorescence *in situ* hybridization
Fmoc	Fluorenylmethyloxycarbonyl
FRET	Fluorescence resonance energy transfer
Ga	Gauge
GESR	GPCR Extraction and Stabilization Reagent
GGG	GLP-1/GIP/glucagon
G_i	Inhibitory G-protein
GI	Gastrointestinal
GIP	Glucose-dependent insulinotropic peptide
GIPR	Glucose-dependent insulinotropic peptide receptor
GLP-1	Glucagon-like peptide 1
GLP-1R	Glucagon-like peptide 1 receptor
GlucR	Glucagon receptor
GPCR	G protein-coupled receptor
GPR75	G-protein receptor 75
GSIS	Glucose-stimulated insulin secretion
H_2O	Water
HBSS	Hank’s balanced salt solution
HDL	High-density lipoprotein

HEK293	Human embryonic kidney cells
HPLC	High performance liquid chromatography
IC_{50}	Half-max inhibitory concentration
ICVI	Intracerebroventricular injection
IHC	Immunohistochemistry
IP	Intraperitoneal
ISR	Insulin secretion rate
KAX	Ketamine, xylazine, and acepromazine
Kcal	Kilocalorie
K_D	Dissociation constant
KO	Knockout
KRB	Krebs-Ringer bicarbonate
LCMS	Liquid chromatography mass spectrometer
LDL	Low-density lipoprotein
LIRA	Liraglutide (Victoza®)
MALDI-ToF MS	Matrix-assisted laser desorption ionization time-of-flight mass spectrometry
MC4R	Melanocortin-4 receptor
MED	Minimal effective dose
MeOH	Methanol
MOE	Molecular Operating Environment
mRNA	Messenger ribonucleic acid
MSP	microScout plate
MTD	Maximum tolerated dose

NAFLD	Non-alcoholic fatty liver disease
NIH	National Institutes of Health
NOAEL	‘No observed adverse effect’ level
NPY1R	Neuropeptide Y1 receptor
NPY2R	Neuropeptide Y2 receptor
NTA	Nitrilotriacetic acid
NTS	*Nucleus tractus solitarius*
ob/*ob*	Obese mouse
ODN	Octadecaneuropeptide
OEG	Oligo(ethylene glycol)
OMe	Methoxy
OP	Octapeptide
OtBu	*tert*-butoxy
Pbf	2,2,4,6,7-pentamethyldihydrobenzofuran
PBS	Phosphate-buffered saline
PBST	Phosphate-buffered saline with 0.1% tween
PI3Kg	Phosphatidylinositol 3 kinase g-subunit
PK	Pharmacokinetic
PKA	Protein kinase A
PKC	Protein kinase C
PVN	Paraventricular nucleus
PYY_{1-36}	Peptide tyrosine tyrosine, residues 1-36
PYY_{3-36}	Peptide tyrosine tyrosine, residues 3-36

qPCR	Quantitative polymerase chain reaction
RP-HPLC	Reversed-phase high performance liquid chromatography
RT	Room temperature
RXFP1	Relaxin-1 receptor
RXFP3	Relaxin-3 receptor
RYGB	Roux-en-Y gastric bypass
SD	Standard deviation
SEM	Standard error of the mean
SPPS	Solid-phase peptide synthesis
SPR	Surface plasmon resonance
T2DM	Type 2 diabetes mellitus
TDN	Tridecaneuropeptide
TFA	Trifluoroacetic acid
TIPS	Triisopropylsilane
T_R	Retention time
Trig	Triglycerides
Tx	Treatment
Veh/Veh	Vehicle control
Y2RKO	Y2R-deficient

Chapter 1: Introduction

1.1 Type 2 diabetes (T2DM)

Diabetes is a chronic health condition that affects more than 37 million people in the U.S. alone. The Centers for Disease Control and Prevention (CDC) recognizes three different types of diabetes, namely Type 1, Type 2, and Gestational. Type 2 diabetes mellitus (T2DM) accounts for more than 95% of total diabetes cases and is described as a resistance to insulin resulting in elevated blood sugar levels. Insulin is a hormone released from the pancreas that allows blood sugar to enter cells and be converted to usable energy.

1.1.1 Economical burden of T2DM

Since the incidence and severity of diabetes is growing rapidly, the associated costs of disease management create an enormous, global economic burden. Diabetes has become the costliest chronic condition in the world,[1,2] totaling 12% of healthcare expenditures and approximately $827 billion globally.[3,4]

1.1.2 Comorbidities of T2DM

Of all patients with T2DM, approximately 75% are diagnosed with one or more chronic diseases, or comorbidities, which tend to proliferate the burden of T2DM.[5-8] Some concordant comorbidities of T2DM, which are commonly addressed under diabetes management, include obesity, cardiovascular disease, hypertension, and nephropathy.[5] The risk of comorbidities in those with T2DM increases with disease progression.[8]

1.1.3 Current treatment options for patients with T2DM and/or associated comorbidities

Considering the worldwide prevalence of T2DM and obesity, many treatment options have been made available for patients. Bariatric surgeries, including gastric bypass and gastric sleeve, are an invasive treatment option with many associated risk factors. Some risks and side effects include bowel obstructions, vomiting, and hypoglycemia.[9] The National Institutes of Health (NIH) has strict eligibility criteria for patients to be considered for bariatric surgery, including a T2DM diagnosis and a body mass index (BMI) between 30-34.9 kg/m^2.[10]

1.1.4 Multi-agonists in the clinic

Many prominent academic and industrial research labs have devoted their efforts to lessening the burden of T2DM and obesity. To achieve the weight loss effects of bariatric surgeries with a single therapeutic, the field has embraced the idea of gut hormone co-agonists. Designing monomeric dual or triple agonists based on GLP-1 with glucagon,[11-13] and/or glucose-dependent insulinotropic polypeptide (GIP)[14,15] are promising novel approaches for the development of anti-obesity drugs, although such continue to suffer from significant gastric side effects.[16,17] Groups have also explored the concept of GLP-1/GIP/glucagon (GGG) triple agonism,[18] however, there is a concern that glucagon's hyperglycemic function might reverse, or fully over-ride (*e.g.*, efinopegdutide), some of the improvements in glycemia seen with GLP-1 alone.[18] The first such GGG triple agonist to report human clinical trial data was SAR441255 from Sanofi, who reported the results in a 2022 paper.[19] Sanofi have subsequently announced they will not pursue this drug further, again reiterating the difficulty of achieving the right balance between glucagon

and GLP-1. Recent studies in our group have instead focused on the combination of GLP-1RAs with neuropeptide Y agonists, given the clear clinical data supporting the restoration of impaired islet function, diabetes correction, and weight-loss associated with such post bariatric surgery.[21] Recent literature by this team[21] and other sources[22,23] shows that combination therapy using a Y2-R agonist (PYY_{3-36}) with a GLP-1RA (Ex-4 or GLP-1) offers synergistic effects in terms of weight loss.

1.2 Gut signaling hormones and associated receptors

1.2.1 Areas of the hindbrain involved in appetite regulation

Many studies in human and animal models have revealed the brain's role in controlling appetite. The hypothalamus contains circuits that regulate food intake and body weight by integrating peripheral nutritional signals.[24] Much like the hypothalamus, the circumventricular organ known as the *area postrema* (AP) detects chemical signals and relays them to other parts of the brain. The *nucleus tractus solitarius* (NTS) is a major neuroanatomical site for controlling feeding behavior.[24] These regions of the hindbrain contain many vital receptor targets.

1.2.2 GLP-1/GLP-1R

GLP-1 is a gut hormone and neurotransmitter that mediates insulinotropic effects by binding to GLP-1Rs. This can occur via a direct effect on GLP-1Rs expressed on pancreatic β-cells and via GLP-1R-mediated neuronal activation of an entero-insular or gut-to-brain-pancreas axis.[25-27] Existing GLP-1 mimetics induce insulinotropic effects by binding to GLP-1Rs on pancreatic β-cells, while simultaneously promoting satiety by

binding to GLP-1Rs in brain regions associated with energy homeostasis.[28-32] Control of food intake by GLP-1 is regulated by GLP-1 produced and released from intestinal L-cells and preproglucagon (PPG) neurons of the caudal NTS.[33,34] The therapeutic potential of GLP-1R targeting for the treatment of obesity and T2DM has been extensively validated and several FDA approved treatments are in the clinic,[35-50] including liraglutide (Saxenda®), semaglutide 1.0 mg (Ozempic®) and high-dose 2.4 mg semaglutide (Wegovy®). Liraglutide achieves glucoregulation with moderate long-term of 5.4-6.8% BW reduction over placebo, as adjunct to diet and exercise.[41] Liraglutide binds to the GLP-1R and becomes internalized in key neurons of food intake regulation in the arcuate nucleus (ARC) of the hypothalamus.[51] Semaglutide is a similarly derived GLP-1RA with the advantage of weekly s.c. administration in the treatment of co-morbid T2DM/obesity.[52] In three randomized control trials published in 2021 (STEP 1-3 trials),[53] efficacy and safety data of semaglutide were assessed. Across these trials, mean placebo-subtracted weight loss averaged 12.3%.[54-56] Most recently, high dose semaglutide (Wegovy®) was approved with mean-placebo-subtracted weight-loss of 15.8%.[57] An oral formulation of semaglutide 14 mg (Rybelsus®) is now also FDA approved for T2DM. However, gastrointestinal adverse events were most commonly reported with the oral application.[58] In all cases, however, long term weight-loss (defined as over 1 year) were not sustained and rates of nausea, vomiting and diarrhea were elevated compared with placebo throughout treatment.[59] Indeed, according to a recent report by Merck, over half of T2DM patients initiating GLP-1RA are non-adherent and the majority (>70%) discontinue therapy by 24 months due to side-effects.[60]

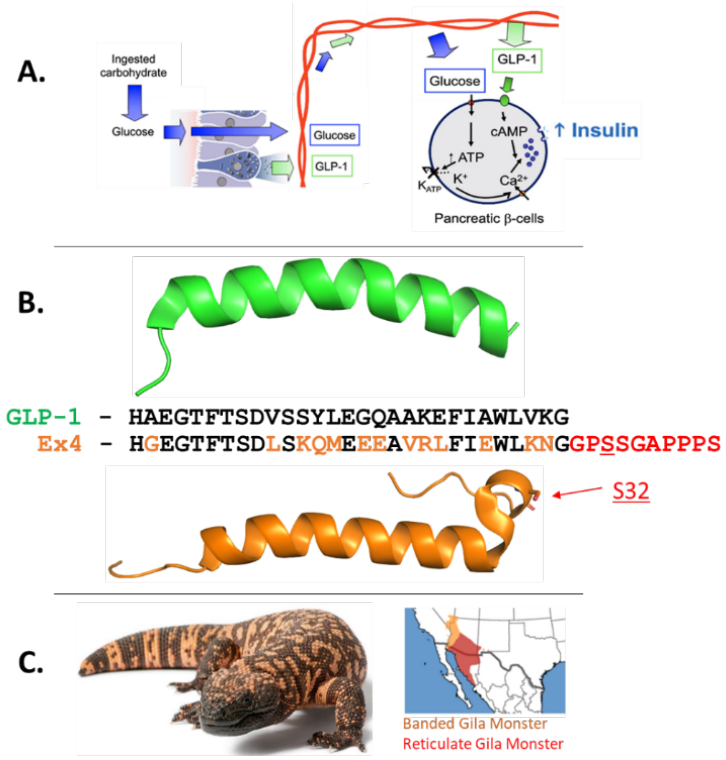

Figure 1-1. Schematic of GLP-1 and GLP-1 analogue, Exendin-4 (Ex-4). (A) Schematic representation of the primary function of GLP-1 to stimulate insulin secretion in a glucose-dependent manner as blood glucose levels rise postprandially. (B) Structure and primary sequence overlay of GLP-1 (green; PDB:3IOL, bound peptide without GLP-1R extracellular domain) and Exendin-4 (orange; PDB:1JRJ). The black letters of the sequence of Ex-4 represent shared residues with GLP-1, orange shows residue variation, and red are the additional residues on the C-terminal domain of Ex-4, highlighting the S32 deemed responsible for the increased binding of Ex-4 to GLP-1R, over the native substrate. (C) Gila monster (*Heloderma suspectum*) and region of natural habitat.

1.2.3 PYY_{1-36}/Y1-R

PYY_{1-36} is a gut hormone that is co-secreted from the L cells together with GLP-1, and which preferentially binds the neuropeptide Y1 receptor (Y1-R), found in pancreatic islets, and areas of appetite regulation in the brain including the AP and NTS, where it has an orectic effect.[61] It has recently been demonstrated that GLP-1R is expressed in NPY neurons in the AP and thus, GLP-1 can directly, and indirectly, inhibit neuronal signaling in the orexigenic NPY system via agonism of GLP-1R.[62] Thus, GLP-1R agonism can work

to over-ride this orectic component of Y1-R agonism. More central to our hypothesis, considerable research indicates that Y1-R agonism by PYY_{1-36} plays a crucial role in β-islet survival, and indeed is increasingly recognized as a key factor in post-bariatric reversal of diabetes via recovery of impaired islet secretory function.[63-65]

1.2.4 PYY_{3-36}/Y2-R

The truncated peptide PYY_{3-36} is derived from PYY_{1-36} via proteolytic processing by DPP-IV and binds preferentially at the Y2-R. PYY_{3-36} crosses the blood-brain barrier (BBB)[66] and inhibits food intake via Y2-R in key brain areas of energy homeostasis, namely the ARC of the hypothalamus, as well as brainstem AP and NTS.[67-71] Consistent with these findings, we found that peripheral administration of an anorexigenic dose of PYY_{3-36} stimulated c-Fos (marker of neuronal activation) in forebrain (ARC) and hindbrain (AP/NTS) regions that contain Y1-R and Y2-Rs and are linked to the control of food intake.[72] Additionally, we, and others, have shown that circulating PYY_{3-36} levels are reduced in obese humans.[73-78] Following BW reduction and/or gastric bypass surgery, circulating concentrations of PYY_{3-36} return to levels representative of average weight individuals.[75,79,80] This indicates that obesity does not result from resistance to PYY_{3-36}, but from a lack of circulating peptide, making it an attractive clinical drug target. Indeed, peripheral administration of PYY_{3-36} reduces caloric intake and increases postprandial insulin levels, enhances insulin sensitivity, thermogenesis, lipolysis and fat oxidation in lean and obese humans and nonhuman primates.[81-85] PYY_{3-36} treatment also improves glucose control, insulin resistance and lipid metabolism in rodents.[84,86,87] There are significant limitations that have hampered the development of PYY_{3-36} as an anti-obesity

drug including short half-life (~12 min),[88] inability to sustain BW reduction beyond a 1-2 week period,[89] possibly due to Y2-R down-regulation and tolerance (tachyphylaxis) or due to stimulation of compensatory mechanisms resulting from reduced food intake.[50,90]

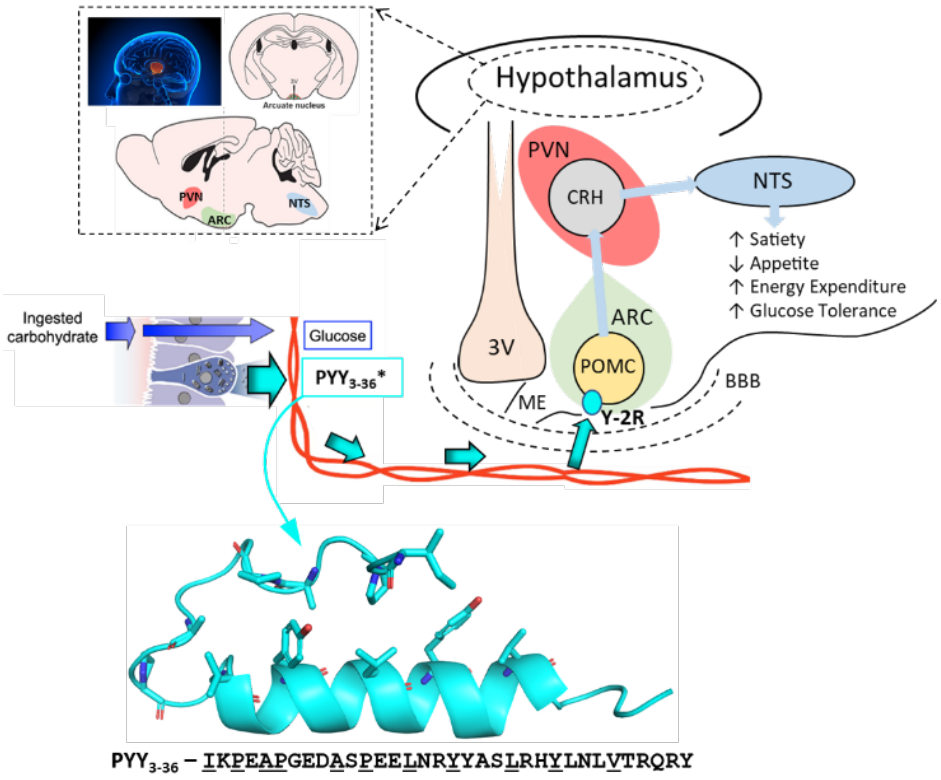

Figure 1-2. Schematic representation of the physiological action of PYY_{3-36}. Structure of PYY_{3-36} with sequence underlining the hydrophobic residues (stick figure of structure) that drive the hydrophobic zipper secondary structure (PDB:2DF0).

1.3 Publications/patents on dual administration of GLP-1R/Y2-R agonists

This review outlines various contributions to the field particularly in combination, conjugation, and dual administration of GLP-1RAs and Y2-RAs. Synergistic administration of Ex-4 and PYY_{3-36} was first reported in 2005 by Talsania, *et al*.[91] They demonstrated that co-administration of Ex-4 and PYY_{3-36} reduces appetite and regulates FI in a C57BL/6 mouse model for up to 8 hrs. This administration strategy decreased FI

in the mice more than the sum of the individual effects of Ex-4 and PYY_{3-36} alone. In addition, through administering each hormone with an antagonist of the other, they found Ex-4 and PYY_{3-36} work by GLP-1R-dependent and Y2-R-dependent pathways, respectively.

In more recent years, Chepurny, *et al*. reported a monomeric agonist of both receptors, GLP-1R and Y2-R.[92] The authors showed how the lead compound, EP45, a 45-amino acid sequence peptide iteratively designed to mimic ligands of the target receptors, was able to show potent, independent agonism at the GLP-1R and Y2-R. They hypothesized targeting both receptors with a single peptide would potentially lower blood glucose and suppress appetite. The idea of dual administration of Ex-4 and PYY_{3-36} was revisited in 2019 by Kjaergaard, *et al*., who examined acute food intake and neuronal activation in C57BL/6J mice.[93] C-fos brain reactivity heat maps revealed potential regulation of multiple unexplored biological responses post-Ex-4/PYY_{3-36} co-administration. In alignment with the focus of this review, PYY_{3-36} was shown to enhance the effect of Ex-4 and subsequent appetite reduction and enhanced neuronal activity.

Considering the increased evidence of the benefits of dual administration of a GLP-1R agonist and PYY_{3-36} in suppressing appetite and food intake in rodent models, our lab published our lead compound, GEP44,[94] which was designed based on our proof-of-concept dual agonist, EP45, mentioned above. The GEP44 sequence contains amino acid substitutions to drive the desired “PP-fold” necessary to optimize multi-receptor activation. Testing of GEP44 in DIO Sprague-Dawley rats and musk shrews showed a significant reduction in FI, BW, and fasting blood glucose in rats and little to no evidence of nausea at doses up to 60 nmol/kg in both animal models. Our group suggested GEP44

caused an unidentified Y1-R-mediated effect, so we dedicated future experiments to understanding the role of activating Y1-R in glucoregulation and weight loss. We also recognized that, due to its peptidyl structure, GEP44 should be further optimized to enhance its half-life.

Simultaneously, Østergaard, *et al*., published their take on a GLP-1 and PYY_{3-36} peptide hybrid.[95] They ran *in vitro* binding against the hGLP-1R and hY2-R of several peptides, some designed to strictly target the Y2-R and others designed to concurrently target both the Y2-R and GLP-1R. Their lead compound 19 had decreased affinity for GLP-1R and Y2-R compared to the native ligands, GLP-1 and PYY_{3-36}, respectively. The *in vivo* FI study was done in lean C57BL/6J male mice with compound 19 and two other peptide mono-agonists of each receptor. Compound 19 showed statistically significant depletion of FI for up to 6 hours post-administration. This article reiterates the synergy between the gut hormones, GLP-1, and PYY_{3-36}, and stresses the benefits of having a single molecule with multiple actions.

Combination therapy of GLP-1 and PYY_{3-36} via Fc-peptide conjugation was investigated by Boland, *et al*.[96] The co-administration of Fc-GLP-1 and Fc-PYY_{3-36} showed profound BW reduction, restoration of glucose homeostasis, and recovery of β-cell function in two mice models: C57BLKS/J *db*/*db* (diabetic) and DIO Y2R-deficient (Y2RKO). They utilized hyperinsulinemic-euglycemic clamps to measure effects of weight-independent insulin action in both mice models and found that activation of Y2-R in regions of the hypothalamus and hindbrain is essential to seeing improved insulin sensitivity and greater hepatic glycogenesis. These findings support the idea of the useful association between the gut-brain axis and metabolic homeostasis.

There's a direct correlation between the growing incidences of T2DM and non-alcoholic fatty liver disease (NAFLD) worldwide.[97] Evidence suggests NAFLD doubles the risk of patients developing T2DM.[98] Bariatric surgery, namely RYGB, elicits positive effects on weight reduction and prevention of NAFLD. The GLP-1RA Ex-4 has been shown to improve insulin sensitivity and ultimately reverse hepatic steatosis in *ob/ob* mice.[99] Metzner, *et al*., used combination therapy by co-administering liraglutide and PYY_{3-36} in DIO male Wistar rats to show the ability of this treatment strategy to partially mimic the effects of RYGB.

Table 1-1. Recent literature evidence of targeting both GLP-1R *and* Y2-R, either by dual administration, combination, or conjugation therapy.

Drug/Concept	Strategy	Originator	Model	Administration
Ex-4 and PYY_{3-36}	Dual administration	Talsania, *et al*.	C57BL/6 mice	IP infusion
Ex-4 and $PYY_{3–36}$	Dual administration	Reidelberger, *et al*.	DIO Sprague-Dawley rats	IP infusion
EP45	Combination	Doyle, *et al*.	Lean Sprague−Dawley rats	s.c. injection
Ex-4 and PYY_{3-36}	Dual administration	Kjaergaard, *et al*.	C57BL/6J mice	s.c. injection
GEP44	Combination	Doyle, *et al*.	DIO and lean Sprague-Dawley rats and musk shrews	s.c. (rats)/ IP (shrews)
GLP-1 and PYY_{3-36} hybrid	Combination	Østergaard, *et al*.	Lean C57BL/6J male mice	s.c. injection
Fc-GLP-1 and Fc-PYY_{3-36}	Conjugation	Boland, *et al*.	C57BLKS/J *db/db* and DIO Y2R-deficient (Y2RKO) mice	IP infusion
Liraglutide and PYY_{3-36}	Dual administration	Metzner, *et al*.	DIO male Wistar rats	s.c. (Liraglutide)/ osmotic minipump (PYY_{3-36} and saline)
Peptide 3b	Conjugation	Yang, *et al*.	Male C57BL/6J and *db/db* mice	s.c. or IP, depending on study
GEP44/GEP12	Combination	Doyle, *et al*.	Male Sprague Dawley rats and DIO Wistar rats	s.c. injection

There is an emerging precedence in literature of gut hormones serving as constructs upon which new T2DM/obesity therapeutics are being built. Known GLP-1RAs in the clinic have serious drawbacks including mild to severe CNS-associated side effects. The field is moving towards mitigation or complete removal of these side effects to increase patient compliance, since, in a 2020 study, 70.1% of patients taking GLP-1RAs for T2DM/obesity were nonadherent after 1 year.[100] Combination therapy of dual agonists of GLP-1R and Y2-R have the potential to serve the dire, unmet clinical need for T2DM and obesity treatments devoid of common side effects.

1.4 References

1. American Diabetes Association. Economic costs of diabetes in the US in 2017. *Diabetes Care.* 2018;41(5):917-928.

2. Dieleman JL, Baral R, Birger M, et al. US spending on personal health care and public health, 1996–2013. *JAMA*. 2016;316(24):2627–2646.

3. Shrestha S.S., Honeycutt A.A., Yang W., Zhang P., Khavjou O.A., Poehler D.C., Neuwahl S.J., Hoerger T.J. Economic costs attributable to diabetes in each US state. *Diabetes Care.* 2018;41:2526–2534.

4. Butt MD, Ong SC, Wahab MU, Rasool MF, Saleem F, Hashmi A, Sajjad A, Chaudhry FA, Babar ZU. Cost of Illness Analysis of Type 2 Diabetes Mellitus: The Findings from a Lower-Middle Income Country. *Int J Environ Res Public Health*. 2022;19(19):12611.

5. Eilat-Tsanani, S., Margalit, A. & Golan, L.N. Occurrence of comorbidities in newly diagnosed type 2 diabetes patients and their impact after 11 years' follow-up. *Sci Rep* 2021;11, 11071.

6. Agborsangaya, C. B., Lau, D., Lahtinen, M., Cooke, T. & Johnson, J. A. Multimorbidity prevalence and patterns across socioeconomic determinants: A cross-sectional survey. *BMC Public Health* 2012;12, 201.

7. Alonso-Morán, E. *et al.* Multimorbidity in persons with type 2 diabetes in the Basque Country (Spain): Prevalence, comorbidity clusters and comparison with other chronic patients. *Eur. J. Intern. Med.* 2015;26, 197–202.

8. Dall, T. M. *et al.* The economic burden of elevated blood glucose levels in 2012: Diagnosed and undiagnosed diabetes, gestational diabetes mellitus, and prediabetes. *Diabetes Care* 2014;37, 3172–3179.

9. https://www.mayoclinic.org/tests-procedures/bariatric-surgery/about/pac-20394258.

10. https://asmbs.org/resources/2022-asmbs-and-ifso-indications-for-metabolic-and-bariatric-surgery.

11. Ambery P, Parker VE, Stumvoll M, *et al.* MEDI0382, a GLP-1 and glucagon receptor dual agonist, in obese or overweight patients with type 2 diabetes: a randomised, controlled, double-blind, ascending dose and phase 2a study. *Lancet* 2018;391:2607-18.

12. Sanchez-Garrido MA, Brandt SJ, Clemmensen C, Muller TD, DiMarchi RD, Tschop MH. GLP-1/glucagon receptor co-agonism for treatment of obesity. *Diabetologia* 2017.

13. Day JW, Gelfanov V, Smiley D, et al. Optimization of co-agonism at GLP-1 and glucagon receptors to safely maximize weight reduction in DIO-rodents. *Biopolymers* 2012;98:443-50.

14. Petersen J, Stromgaard K, Frolund B, Clemmensen C. Designing Poly-agonists for Treatment of Metabolic Diseases: Challenges and Opportunities. *Drugs* 2019;79:1187-97.

15. Finan B, Yang B, Ottaway N, et al. A rationally designed monomeric peptide triagonist corrects obesity and diabetes in rodents. *Nat Med* 2015;21:27-36.

16. Chepurny OG, Bonaccorso RL, Leech CA, et al. Publisher Correction: Chimeric peptide EP45 as a dual agonist at GLP-1 and NPY2R receptors. *Sci Rep* 2018;8:6192.

17. Tanday N, Flatt PR, Irwin N. Amplifying the antidiabetic actions of glucagon-like peptide-1: Potential benefits of new adjunct therapies. *Diabet Med* 2021;38:e14699.

18. Khoo B, Tan TM. Combination gut hormones: prospects and questions for the future of obesity and diabetes therapy. *J Endocrinol* 2020;246:R65-R74.

19. Bossart M, Wagner M, Elvert R, et al. Effects on weight loss and glycemic control with SAR441255, a potent unimolecular peptide GLP-1/GIP/GCG receptor triagonist. *Cell Metab* 2022;34:59-74 e10.

20. Guida C, Ramracheya R. PYY, a Therapeutic Option for Type 2 Diabetes? *Clin Med Insights Endocrinol Diabetes* 2020;13:1179551419892985.

21. Milliken BT, Elfers C, Chepurny OG, et al. Design and Evaluation of Peptide Dual-Agonists of GLP-1 and NPY2 Receptors for Glucoregulation and Weight Loss with Mitigated Nausea and Emesis. *J Med Chem* 2021;64:1127-38.

22. Kjaergaard M, Salinas CBG, Rehfeld JF, Secher A, Raun K, Wulff BS. PYY(3-36) and exendin-4 reduce food intake and activate neuronal circuits in a synergistic manner in mice. *Neuropeptides* 2019;73:89-95.

23. Oldham S, Howard V, Will S., *et al*. 2002-P: A Long-Acting GLP-1 and Y2-Receptor Dual Agonist Improves Body Weight and Glucose Control in Obese and Diabetic Rodent Models. *Diabetes* 2019;Jun; 68(Supplement 1): (Poster Abstract).

24. Dowsett GKC, Lam BYH, Tadross JA, Cimino I, Rimmington D, Coll AP, Polex-Wolf J, Knudsen LB, Pyke C, Yeo GSH. A survey of the mouse hindbrain in the fed and fasted states using single-nucleus RNA sequencing. *Mol Metab.* 2021;53:101240.

25. Nishizawa M, Nakabayashi H, Uehara K, Nakagawa A, Uchida K, Koya D. Intraportal GLP-1 stimulates insulin secretion predominantly through the hepatoportal-pancreatic vagal reflex pathways. *Am J Physiol Endocrinol Metab* 2013;305:E376-87.

26. Wan S, Coleman FH, Travagli RA. Glucagon-like peptide-1 excites pancreas-projecting preganglionic vagal motoneurons. *Am J Physiol Gastrointest Liver Physiol*. 2007;292:G1474-82.

27. Donath MY, Burcelin R. GLP-1 effects on islets: hormonal, neuronal, or paracrine? *Diabetes Care* 2013;36 Suppl 2:S145-8.

28. Lafferty RA, Tanday N, Moffett RC, et al. Positive Effects of NPY1 Receptor Activation on Islet Structure Are Driven by Pancreatic Alpha- and Beta-Cell Transdifferentiation in Diabetic Mice. *Front Endocrinol* (Lausanne) 2021;12:633625.

29. Guida C, Stephen S, Guitton R, Ramracheya RD. The Role of PYY in Pancreatic Islet Physiology and Surgical Control of Diabetes. *Trends Endocrinol Metab* 2017;28:626-36.

30. Zhang Z, Hu Y, Xu N, et al. A New Way for Beta Cell Neogenesis: Transdifferentiation from Alpha Cells Induced by Glucagon-Like Peptide 1. *J Diabetes Res* 2019;2019:2583047.

31. Saleh M, Gittes GK, Prasadan K. Alpha-to-beta cell trans-differentiation for treatment of diabetes. *Biochem Soc Trans* 2021;49:2539-48.

32. Lu J, Jaafer R, Bonnavion R, Bertolino P, Zhang CX. Transdifferentiation of pancreatic alpha-cells into insulin-secreting cells: From experimental models to underlying mechanisms. *World J Diabetes* 2014;5:847-53.

33. Alhadeff AL, Mergler BD, Zimmer DJ, et al. Endogenous Glucagon-like Peptide-1 Receptor Signaling in the Nucleus Tractus Solitarius is Required for Food Intake Control. *Neuropsychopharmacology* 2017;42:1471-9.

34. Reiner DJ, Leon RM, McGrath LE, et al. Glucagon-Like Peptide-1 Receptor Signaling in the Lateral Dorsal Tegmental Nucleus Regulates Energy Balance. *Neuropsychopharmacology* 2018;43:627-37.

35. O'Neil PM, Birkenfeld AL, McGowan B, et al. Efficacy and safety of semaglutide compared with liraglutide and placebo for weight loss in patients with obesity: a randomised, double-blind, placebo and active controlled, dose-ranging, phase 2 trial. *Lancet* 2018;392:637-49.

36. le Roux CW, Astrup A, Fujioka K, et al. 3 years of liraglutide versus placebo for type 2 diabetes risk reduction and weight management in individuals with prediabetes: a randomised, double-blind trial. *Lancet* 2017;389:1399-409.

37. Sorli C. Semaglutide, lipid-lowering drugs, and NAFLD - Author's reply. *Lancet Diabetes Endocrinol* 2017;5:330.

38. Sorli C, Harashima SI, Tsoukas GM, et al. Efficacy and safety of once-weekly semaglutide monotherapy versus placebo in patients with type 2 diabetes (SUSTAIN 1): a double-blind, randomised, placebo-controlled, parallel-group, multinational, multicentre phase 3a trial. *Lancet Diabetes Endocrinol* 2017;5:251-60.

39. Ahren B, Masmiquel L, Kumar H, et al. Efficacy and safety of once-weekly semaglutide versus once-daily sitagliptin as an add-on to metformin, thiazolidinediones, or both, in patients with type 2 diabetes (SUSTAIN 2): a 56-week, double-blind, phase 3a, randomised trial. *Lancet Diabetes Endocrinol* 2017;5:341-54.

40. Pi-Sunyer X, Astrup A, Fujioka K, et al. A Randomized, Controlled Trial of 3.0 mg of Liraglutide in Weight Management. *The New England journal of medicine* 2015;373:11-22.

41. Ard J, Cannon A, Lewis CE, et al. Efficacy and safety of liraglutide 3.0 mg for weight management are similar across races: subgroup analysis across the SCALE and phase II randomized trials. *Diabetes Obes Metab* 2016;18:430-5.

42. O'Neil PM, Aroda VR, Astrup A, et al. Neuropsychiatric safety with liraglutide 3.0 mg for weight management: Results from randomized controlled phase 2 and 3a trials. *Diabetes Obes Metab* 2017;19:1529-36.

43. Yu M, Shankar RR, Zhang R, et al. Efficacy and safety of sitagliptin added to treatment of patients with type 2 diabetes inadequately controlled with premixed insulin. *Diabetes Obes Metab* 2018.

44. Scott R, Morgan J, Zimmer Z, et al. A randomized clinical trial of the efficacy and safety of sitagliptin compared with dapagliflozin in patients with type 2 diabetes mellitus and mild renal insufficiency: The CompoSIT-R study. *Diabetes Obes Metab* 2018.

45. Raji A, Long J, Lam RLH, O'Neill EA, Engel SS. Efficacy and Safety of Sitagliptin in Hispanic/Latino Patients with Type 2 Diabetes: A Pooled Analysis from Ten Randomized, Placebo-Controlled Phase 3 Clinical Trials. *Diabetes Ther* 2018.

46. Home P, Shankar RR, Gantz I, et al. A randomized, double-blind trial evaluating the efficacy and safety of monotherapy with the once-weekly dipeptidyl peptidase-4 inhibitor omarigliptin in people with type 2 diabetes. *Diabetes Res Clin Pract* 2018;138:253-61.

47. Flint A, Raben A, Astrup A, Holst JJ. Glucagon-like peptide 1 promotes satiety and suppresses energy intake in humans. *The Journal of clinical investigation* 1998;101:515-20.

48. Hayes MR, Mietlicki-Baase EG, Kanoski SE, De Jonghe BC. Incretins and amylin: neuroendocrine communication between the gut, pancreas, and brain in control of food intake and blood glucose. *Annual review of nutrition* 2014;34:237-60.

49. Hayes MR, Schmidt HD. GLP-1 influences food and drug reward. *Curr Opin Behav Sci* 2016;9:66-70.

50. Kanoski SE, Hayes MR, Skibicka KP. Glp-1 and Weight Loss: Unraveling the Diverse Neural Circuitry. *Am J Physiol Regul Integr Comp Physiol* 2016:ajpregu 00520 2015.

51. Secher A, Jelsing J, Baquero AF, et al. The arcuate nucleus mediates GLP-1 receptor agonist liraglutide-dependent weight loss. *J Clin Invest* 2014;124:4473-88.

52. Magnone M, Emionite L, Guida L, et al. Insulin-independent stimulation of skeletal muscle glucose uptake by low-dose abscisic acid via AMPK activation. *Sci Rep* 2020;10:1454

53. Kushner RF, Calanna S, Davies M, et al. Semaglutide 2.4 mg for the Treatment of Obesity: Key Elements of the STEP Trials 1 to 5. *Obesity* (Silver Spring) 2020;28:1050-61.

54. Wilding JPH, Batterham RL, Calanna S, et al. Once-Weekly Semaglutide in Adults with Overweight or Obesity. *N Engl J Med* 2021;384:989.

55. Wadden TA, Bailey TS, Billings LK, et al. Effect of Subcutaneous Semaglutide vs Placebo as an Adjunct to Intensive Behavioral Therapy on Body Weight in Adults With Overweight or Obesity: The STEP 3 Randomized Clinical Trial. *JAMA* 2021;325:1403-13.

56. Rubino D, Abrahamsson N, Davies M, et al. Effect of Continued Weekly Subcutaneous Semaglutide vs Placebo on Weight Loss Maintenance in Adults With Overweight or Obesity: The STEP 4 Randomized Clinical Trial. *JAMA* 2021.

57. Rubino DM, Greenway FL, Khalid U, et al. Effect of Weekly Subcutaneous Semaglutide vs Daily Liraglutide on Body Weight in Adults With Overweight or Obesity Without Diabetes: The STEP 8 Randomized Clinical Trial. *JAMA* 2022;327:138-50.

58. Buse JB, Bode BW, Mertens A, et al. Long-term efficacy and safety of oral semaglutide and the effect of switching from sitagliptin to oral semaglutide in patients with type 2 diabetes: a 52-week, randomized, open-label extension of the PIONEER 7 trial. *BMJ Open Diabetes Res Care* 2020;8.

59. Wharton S, Calanna S, Davies M, et al. Gastrointestinal tolerability of once-weekly semaglutide 2.4 mg in adults with overweight or obesity, and the relationship between gastrointestinal adverse events and weight loss. *Diabetes Obes Metab* 2021.

60. Weiss T, Carr RD, Pal S, et al. Real-World Adherence and Discontinuation of Glucagon-Like Peptide-1 Receptor Agonists Therapy in Type 2 Diabetes Mellitus Patients in the United States. *Patient Prefer Adherence* 2020;14:2337-45.

61. Walther C, Morl K, Beck-Sickinger AG. Neuropeptide Y receptors: ligand binding and trafficking suggest novel approaches in drug development. *J Pept Sci* 2011;17:233-46.

62. Ruska Y, Szilvasy-Szabo A, Kovari D, et al. Expression of glucagon-like peptide 1 receptor in neuropeptide Y neurons of the arcuate nucleus in mice. *Brain Struct Funct* 2022;227:77-87.

63. Guida C, Ramracheya R. PYY, a Therapeutic Option for Type 2 Diabetes? *Clin Med Insights Endocrinol Diabetes* 2020;13:1179551419892985.

64. Lafferty RA, Tanday N, Moffett RC, et al. Positive Effects of NPY1 Receptor Activation on Islet Structure Are Driven by Pancreatic Alpha- and Beta-Cell Transdifferentiation in Diabetic Mice. *Front Endocrinol* (Lausanne) 2021;12:633625.

65. Guida C, Stephen S, Guitton R, Ramracheya RD. The Role of PYY in Pancreatic Islet Physiology and Surgical Control of Diabetes. *Trends Endocrinol Metab* 2017;28:626-36.

66. Nonaka N, Shioda S, Niehoff ML, Banks WA. Characterization of blood-brain barrier permeability to PYY3-36 in the mouse. *J Pharmacol Exp Ther* 2003;306:948-53.

67. Fetissov SO, Byrne LC, Hassani H, Ernfors P, Hökfelt T. Characterization of neuropeptide Y Y2 and Y5 receptor expression in the mouse hypothalamus. *Journal of Comparative Neurology* 2004;470:256-65.

68. Parker RMCH, H. Regional distribution of Y-receptor subtype mRNAs in rat brain. *Eur J Neurosci* 1999;11:1431-48.

69. Shaw JL, Gackenheimer SL, Gehlert DR. Functional autoradiography of neuropeptide Y Y1 and Y2 receptor subtypes in rat brain using agonist stimulated [35S]GTPγS binding. *Journal of Chemical Neuroanatomy* 2003;26:179-93.

70. Neary NM, Small CJ, Druce MR, et al. Peptide YY3-36 and glucagon-like peptide-17-36 inhibit food intake additively. *Endocrinology* 2005;146:5120-7.

71. Blevins JE, Chelikani PK, Haver AC, Reidelberger RD. PYY(3-36) induces Fos in the arcuate nucleus and in both catecholaminergic and non-catecholaminergic neurons in the nucleus tractus solitarius of rats. *Peptides* 2008;29:112-9.

72. Henry KE, Elfers CT, Burke RM, *et al*. Vitamin B12 conjugation of peptide-YY(3-36) decreases food intake compared to native peptide-YY(3-36) upon subcutaneous administration in male rats. *Endocrinology* 2015;156:1739-49.

73. Roth CL, Enriori PJ, Harz K, Woelfle J, Cowley MA, Reinehr T. Peptide YY is a regulator of energy homeostasis in obese children before and after weight loss. *J Clin Endocrinol Metab* 2005;90:6386-91.

74. Batterham RL, Cohen MA, Ellis SM, et al. Inhibition of Food Intake in Obese Subjects by Peptide YY(3-36). *N Engl J Med* 2003;349:941-8.

75. le Roux CW, Batterham RL, Aylwin SJ, et al. Attenuated peptide YY release in obese subjects is associated with reduced satiety. *Endocrinology* 2006;147:3-8.

76. Rahardjo GL, Huang X-F, Tan YY, Deng C. Decreased Plasma Peptide YY Accompanied by Elevated Peptide YY and Y2 Receptor Binding Densities in the Medulla Oblongata of Diet-Induced Obese Mice. *Endocrinology* 2007;148:4704-10.

77. Nianhong Y, Chongjian W, Mingjia X, Limei M, Liegang L, Xiufa S. Interaction of Dietary composition and PYY gene expression in diet-induced obesity in rats. *J Huazhong Univ Sci Technol [Med Sci]* 2005;25:243-6.

78. Roth CL, Bongiovanni KD, Gohlke B, Woelfle J. Changes in dynamic insulin and gastrointestinal hormone secretion in obese children. *J Pediatr Endocrinol Metab* 2010;23:1299-309.

79. Roth CL, Enriori PJ, Harz K, Woelfle J, Cowley MA, Reinehr T. Peptide YY is a regulator of energy homeostasis in obese children before and after weight loss. *J Clin Endocrinol Metab* 2005;90:6386-91.

80. Reinehr T, Roth CL, Enriori PJ, Masur K. Changes of dipeptidyl peptidase IV (DPP-IV) in obese children with weight loss: relationships to peptide YY, pancreatic peptide, and insulin sensitivity. *J Pediatr Endocrinol Metab* 2010;23:101-8.

81. Sloth B, Holst JJ, Flint A, Gregersen NT, Astrup A. Effects of PYY1-36 and PYY3-36 on appetite, energy intake, energy expenditure, glucose and fat metabolism in obese and lean subjects. *Am J Physiol Endocrinol Metab* 2007;292:E1062-8.

82. Moran TH, Smedh U, Kinzig KP, Scott KA, Knipp S, Ladenheim EE. Peptide YY(3-36) inhibits gastric emptying and produces acute reductions in food intake in rhesus monkeys. *Am J Physiol Regul Integr Comp Physiol* 2005;288:R384-8.

83. Koegler FH, *et al*. Peptide YY(3–36) Inhibits Morning, but Not Evening, Food Intake and Increases Body Weight in Rhesus Macques. *Diabetes* 2005;54:3198-204.

84. Vrang N, Madsen AN, Tang-Christensen M, Hansen G, Larsen PJ. PYY(3-36) reduces food intake and body weight and improves insulin sensitivity in rodent models of diet-induced obesity. *Am J Physiol Regul Integr Comp Physiol* 2006;291:R367-75.

85. Abdel-Hamid HA, Abdalla MMI, Zenhom NM, Ahmed RF. The effect of peptide tyrosine tyrosine (PYY3-36), a selective Y2 receptor agonist on streptozotocin-induced diabetes in albino rats. *Endocr Regul* 2019;53:26-33.

86. van den Hoek AM, Heijboer AC, Voshol PJ, et al. Chronic PYY3-36 treatment promotes fat oxidation and ameliorates insulin resistance in C57BL6 mice. *Am J Physiol Endocrinol Metab* 2007;292:E238-45.

87. Chandarana K, Gelegen C, Irvine EE, et al. Peripheral activation of the Y2-receptor promotes secretion of GLP-1 and improves glucose tolerance. *Mol Metab* 2013;2:142-52.

88. Addison ML, Minnion JS, Shillito JC, et al. A role for metalloendopeptidases in the breakdown of the gut hormone, PYY 3-36. *Endocrinol* 2011;152:4630-40.

89. Reidelberger R, Haver A, Chelikani PK, et al. Effects of leptin replacement alone and with exendin-4 on food intake and weight regain in weight-reduced diet-induced obese rats. *Am J Physiol Endocrinol Metab.* 2012;302(12):E1576-85.

90. Guida C, Stephen SD, Watson M, et al. PYY plays a key role in the resolution of diabetes following bariatric surgery in humans. *EBioMedicine* 2019;40:67-76.

91. Talsania T, Anini Y, Siu S, Drucker DJ, Brubaker PL. Peripheral exendin-4 and peptide YY(3-36) synergistically reduce food intake through different mechanisms in mice. *Endocrinology*. 2005;146(9):3748-56.

92. Chepurny, O.G., Bonaccorso, R.L., Leech, C.A. *et al.* Chimeric peptide EP45 as a dual agonist at GLP-1 and NPY2R receptors. *Sci Rep* 8, 3749 (2018).

93. Kjaergaard M, Salinas CBG, Rehfeld JF, Secher A, Raun K, Wulff BS. PYY(3-36) and exendin-4 reduce food intake and activate neuronal circuits in a synergistic manner in mice. *Neuropeptides*. 2019;73:89-95.

94. Milliken, B. T., C. Elfers, O. G. Chepurny, K. S. Chichura, I. R. Sweet, T. Borner, M. R. Hayes, B. C. De Jonghe, G. G. Holz, C. L. Roth and R. P. Doyle (2021). "Design and Evaluation of Peptide Dual-Agonists of GLP-1 and NPY2 Receptors for Glucoregulation and Weight Loss with Mitigated Nausea and Emesis." *J Med Chem* 64(2): 1127-1138.

95. Østergaard, S., Paulsson, J.F., Kofoed, J. *et al.* The effect of fatty diacid acylation of human PYY_{3-36} on Y2 receptor potency and half-life in minipigs. *Sci Rep* 11, 21179 (2021).

96. Boland BB, Laker RC. Peptide-YY_{3-36}/glucagon-like peptide-1 combination treatment of obese diabetic mice improves insulin sensitivity associated with recovered pancreatic

β-cell function and synergistic activation of discrete hypothalamic and brainstem neuronal circuitries. *Mol Metab.* 2022;55:101392.

97. Younossi ZM. Non-alcoholic fatty liver disease - A global public health perspective. *J Hepatol.* 2019;70(3):531-544.

98. Targher, G., Corey, K.E., Byrne, C.D. *et al.* The complex link between NAFLD and type 2 diabetes mellitus — mechanisms and treatments. *Nat Rev Gastroenterol Hepatol* 2021;18, 599–612.

99. Ding, X., Saxena, N.K., Lin, S., Gupta, N. and Anania, F.A. (2006), Exendin-4, a glucagon-like protein-1 (GLP-1) receptor agonist, reverses hepatic steatosis in *ob*/*ob* mice. *Hepatology*, 43: 173-181.

100. Weiss T, Carr RD, Pal S, Yang L, Sawhney B, Boggs R, Rajpathak S, Iglay K. Real-World Adherence and Discontinuation of Glucagon-Like Peptide-1 Receptor Agonists Therapy in Type 2 Diabetes Mellitus Patients in the United States. *Patient Prefer Adherence*. 2020;14:2337-2345.

Chapter 2: Hit to lead development of a triple agonist of GLP-1R, Y1-R, and Y2-R

The work on this project has resulted in the following publications and patents:

B. T. Milliken, C. Elfers, O. G. Chepurny, **K. S. Chichura**, I. R. Sweet, T. Borner, M. R. Hayes, B. C. De Jonghe, G. G. Holz, C. L. Roth, and R. P. Doyle (2021). “Design and Evaluation of Peptide Dual-Agonists of GLP-1 and NPY2 Receptors for Glucoregulation and Weight Loss with Mitigated Nausea and Emesis.” *J. Med. Chem*. 64(2): 1127-1138.

Chichura, K. S., Elfers, C., Roth, C. L., Doyle, R. P. (2022) *Melanocortin and GLP-1 Receptor Agonists and Methods of Use*. Provisional Patent. Filed 08/2022.

K. S. Chichura, C. Elfers, T. Salameh, V. Kamat, O. G. Chepurny, A. McGivney, B. T. Milliken, G. G. Holz, S. V. Applebey, M. R. Hayes, I. R. Sweet, C. L. Roth, and R. P. Doyle (2023). “A Peptide Triple Agonist of GLP-1, Neuropeptide Y1, and Neuropeptide Y2 Receptors Promotes Glycemic Control and Weight Loss.” Accepted to *Sci. Rep*.

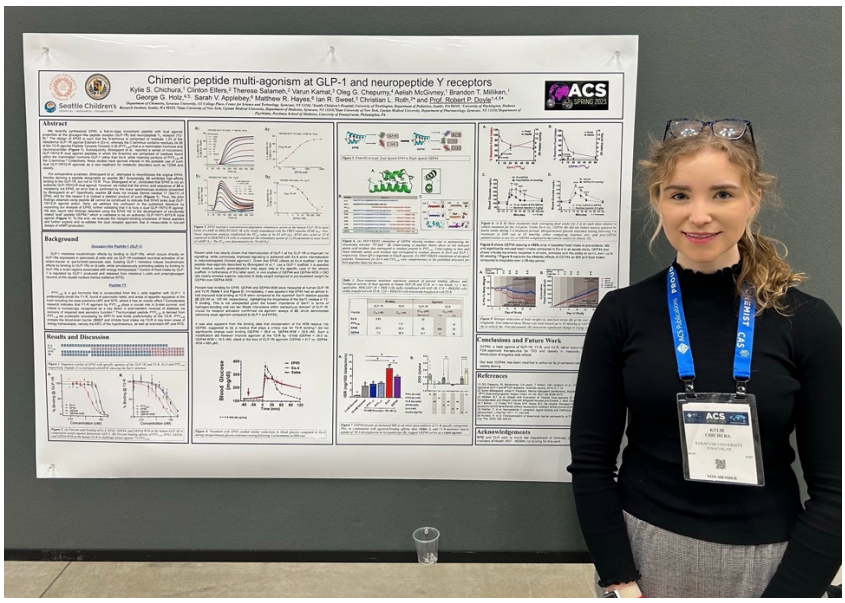

American Chemical Society National Meeting and Exposition, General Orals session and poster presentation, Indianapolis, IN, March 2023.

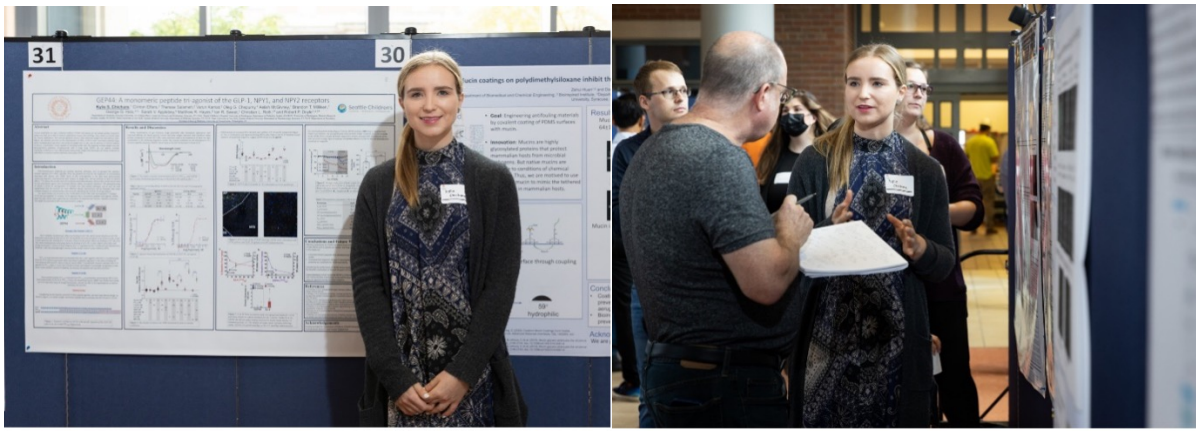

Bioinspired Institute poster presentation, Syracuse University, October 2022.

60th Annual Meeting of the European Society for Pediatric Endocrinology (ESPE), Henning Anderson award recipients, pictured with collaborator Prof. Christian Roth, M.D. (Seattle Children's Research Institute; SCRI), in Rome, Italy, September 2022.

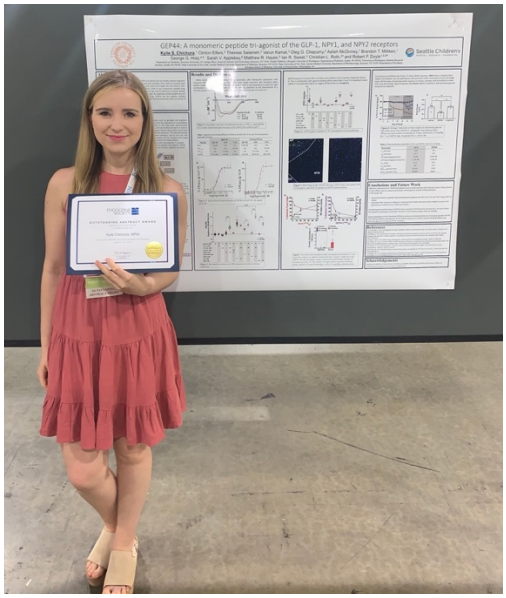

The Endocrine Society's Annual General Meeting ('Endo') 2022 poster presentation, Outstanding Abstract Award recipient, in Atlanta, GA, June 2022.

The author working in the SCRI, pictured with Clinton Elfers (Senior researcher). March 2022.

Seattle Children's Research Institute, pictured with Aelish McGivney (Doyle group undergraduate '23), August 2021.

The author pictured with the CEM microwave-assisted Liberty Blue peptide synthesizer in the Doyle lab at Syracuse University.

2.1 Proof-of-concept chimeric, peptide-based dual agonists

Obesity and its comorbidities cause significant, yet preventable, morbidity and mortality in the U.S. Current treatments have limited long-term efficacy with little or no impact on disease reversal.[1] While therapies based on endogenous gut peptides such as GLP-1 receptor agonists (GLP-1RAs) have been compelling therapeutic agents for obesity and T2DM, only a few have achieved partial long-term weight loss (≥5-15% in adults at 1 year),[2-7] and all have shown significant side effects, including nausea/malaise and gastrointestinal (GI) ailments.[6,8-10] In attempts to overcome these issues, the field has created novel *dual or triple agonists* based on gut hormones to complement GLP-1, such as glucagon or glucose-dependent insulinotropic polypeptide (GIP); none however, have demonstrated convincing long-term improvements with respect to weight loss, and all continue to exert GI adverse effects.[11-15] The pathophysiology of obesity is driven by dysregulation of multiple, but inter-related pathways, and as such we hypothesize the solution for more effective obesity interventions will be therapies that target multiple receptors of complementary neurocircuits regulating the controls of energy balance.

2.1.1 Design and secondary structure of GEP44

The design of GEP44 was inspired by our proof-of-concept dual agonist, EP45,[16] which is the first chimeric peptide to have simultaneous dual action at GLP-1R and Y2-R. The transition from our hit compound, EP45, to GEP44 involved various design and screening strategies including *in silico* prediction, *in vitro* agonism, binding, internalization and β-arrestin recruitment measurements [at GLP-1R, Y1-R, Y2-R, and Glucagon receptor (GlucR)]. The secondary structure of these compounds was screened by CD

spectroscopy, and the helicity was determined and compared to Ex-4 and PYY_{3-36} controls. The chimeric peptides had comparable α-helical structures (10.6-19.1% helicity) to those of Ex-4 (18.7%) and PYY_{3-36} (21.6%), and calculations were done using PEP-FOLD3[17] to predict their folded states. In the structure of EP45, the two α-helices formed a hydrophobic pocket which generated a perpendicular interaction occurring on the face of the peptide believed to interact with the extracellular domain (ECD) of GLP-1R. Several iterative substitutions were made to increase the hydrophobic interaction between both helices. The docking software HPEPDOCK[18] or MOE 2.0[19] were used to predict the lowest-energy interactions of the peptides and GLP-1R and Y2-R. *In silico* modeling methods allowed for the determination of additional residues to replace.

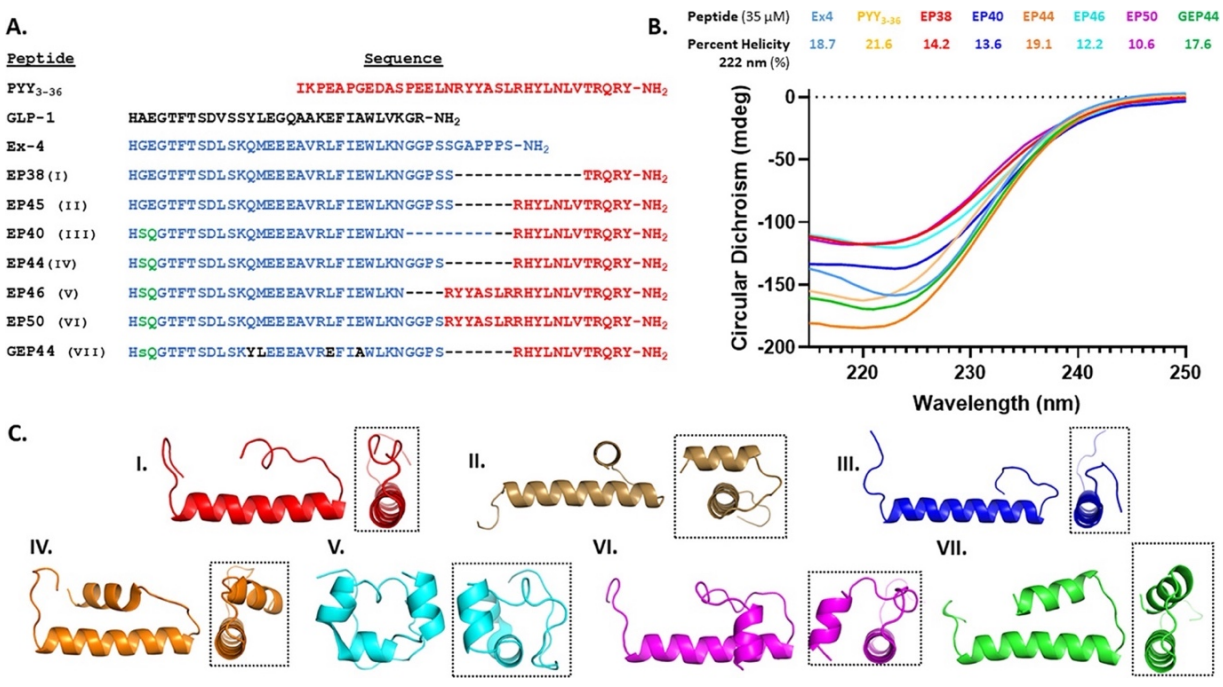

Figure 2-1. (A) Color-coding of peptides shown above in red indicates amino acid residues within EP44 and GEP44 that correspond to residues present in $PYY_{3–36}$. Color-coding in blue and black indicates amino acid residues within GEP44 that correspond to residues present in the Ex-4 and GLP-1, respectively. Green Q3 is known to be important in GlucR agonism. Ser2 of GEP44 is the D-isomer indicated as a lowercase “s”. (B) CD

spectroscopy displays the measured α-helical secondary structure of peptides at 35 μM. (C) PEP-FOLD3 simulations of calculations of designed peptides I = EP38; II = EP45; II I= EP40; IV = EP44; V = EP46; VI = EP50; VII = GEP44. Simulations for Ex-4 and $PYY_{3–36}$ were complementary to the published structures for both peptides (data not shown).

2.1.2 *In vitro* binding and function of GEP44

After being synthesized by solid-phase chemistry, the various chimeric peptides had to be assayed for *in vitro* activity and binding. GEP44 proved to be a potent agonist of Y2-R (IC_{50} 10 nM vs 16 nM for native $PYY_{3–36}$), implying at least equipotency between both ligands at the Y2-R) and GLP-1R (EC_{50} 330 pM at GLP-1R vs EC_{50} 16 pM for Ex-4). To confirm receptor potency and selectivity, the GLP-1R antagonist, exendin(9-39) (Ex9-39), and Y2-R antagonist, BIIE0246, blocked GEP44 agonism in FRET assays in cells expressing each receptor individually. Competitive binding of the peptides was measured at GLP-1R against GLP-1 (as a red fluorescent analogue), specifically to gauge what effects increased PYY peptide components had on GLP-1R binding. Despite GEP44 having comparable agonism to PYY_{3-36} at Y2-R, it still displays moderate binding (IC_{50} 113 nM) at GLP-1R, in line with the moderate agonism (EC_{50} 330 pM) observed at GLP-1R. Glucose stimulated insulin secretion (GSIS) by pancreatic islets was also measured in response to GEP44. Compared to Ex-4, GEP44 had a 25% lower static insulin secretion rate (ISR), which is potentially due to its decreased GLP-1R potency.

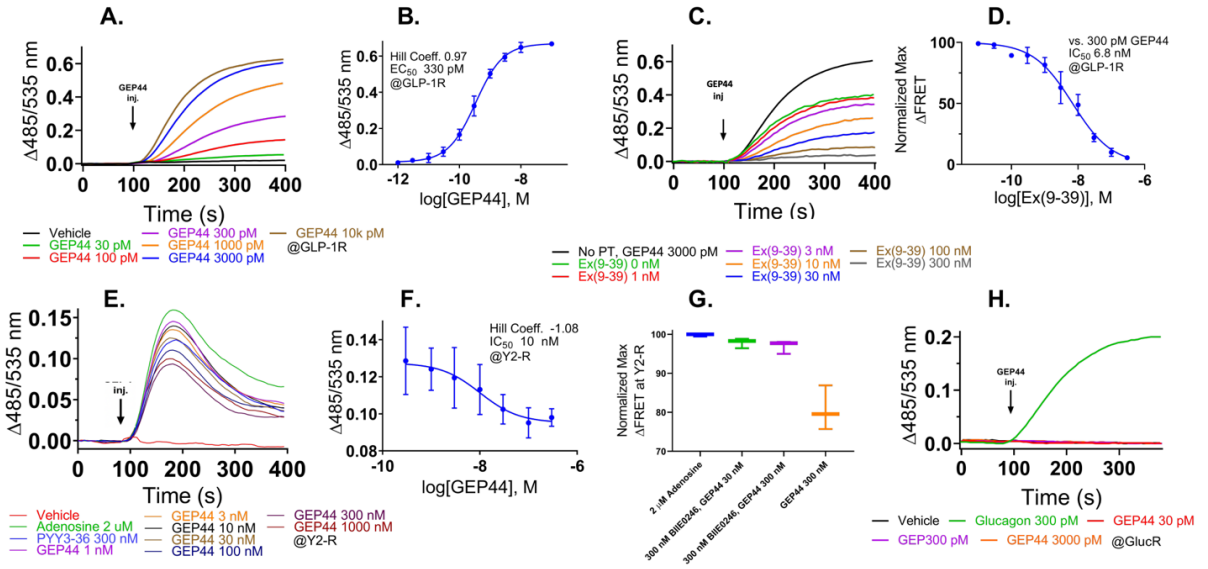

Figure 2-2. FRET (tracking cAMP stimulation via FRET at H188 dose-response of GEP44 at the GLP-1R (A), dose-response nonlinear regression of GEP44 at the GLP-1R (B). FRET response of 300 pM GEP44 against GLP-1R antagonist Ex(9-39) pre-treatment at GLP-1R (C), dose-response nonlinear regression of 3000 pM GEP44 against GLP-1R antagonist Ex(9-39) pre-treatment at GLP-1R (D). FRET (E) and dose-response nonlinear regression (F), tracked by mitigation of adenosine (2 μM in all four treatments) stimulated cAMP at the A2b receptor via FRET at H188, of GEP44 at Y2-R. Normalized FRET response of GEP44 against NPY antagonist BIIE0246 [300 nM] at Y2-R (G). FRET response of GEP44 at the Glucagon receptor indicating no agonism (H). EC_{50} values for GEP44 are 10 nM at Y2-R and 330 pM at GLP-1R. The PYY_{3-36} and Ex-4 EC_{50} values in these FRET assays are 16 nM and 16 pM at the Y2-R and GLP-1R, respectively.

2.1.3 *In vivo* analyses GEP44 and applicable controls

These peptides, Ex-4 and GEP44, were screened in a dose escalation study which revealed the effects of combining Y2-R agonism, or lack thereof, into a GLP-1R agonist to reduce food intake and nausea/emesis while maintaining glucoregulation. Screening of GEP44 in lean Sprague-Dawley rats resulted in robust reductions in food intake vs Ex-4 without induction of nausea assessed by kaolin intake. Further studies in DIO Sprague-Dawley rats yielded similar reductions in food intake to the GEP44 dose escalation study in lean rats with significant weight reduction and a significant reduction in fasting blood

glucose at a 10 nmol/kg dose. Since rodents are a nonvomiting species, additional experiments were performed in the musk shrew (*Suncus murinus*), an emetic mammalian model, to test GEP44 on glycemic profile and vomiting. GEP44 caused emesis in only one shrew receiving a 60 nmol/kg dose, compared to the numerous emetic episodes seen in Ex-4 shrews at just 5 nmol/kg.

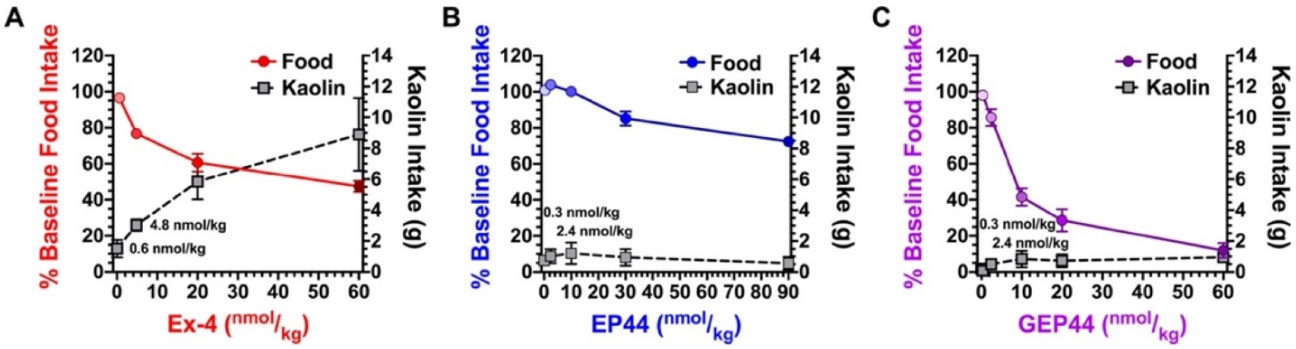

Figure 2-3. Dose escalation study averaging food intake for 2 days on each dose relative to vehicle treatment for the 2 days prior shows less of a reduction of food intake in response to EP44 (B) vs Ex-4 (A) in lean rats (male, age 11 weeks, n = 4 per group). However, unlike Ex-4 (A), EP44 (B) did not induce nausea assessed by kaolin intake during 2-day treatment periods. Modifications were made to improve Y2-R binding with GEP44, resulting in robust reductions in food intake (C) vs Ex-4 (A) without induction of nausea assessed by kaolin intake.

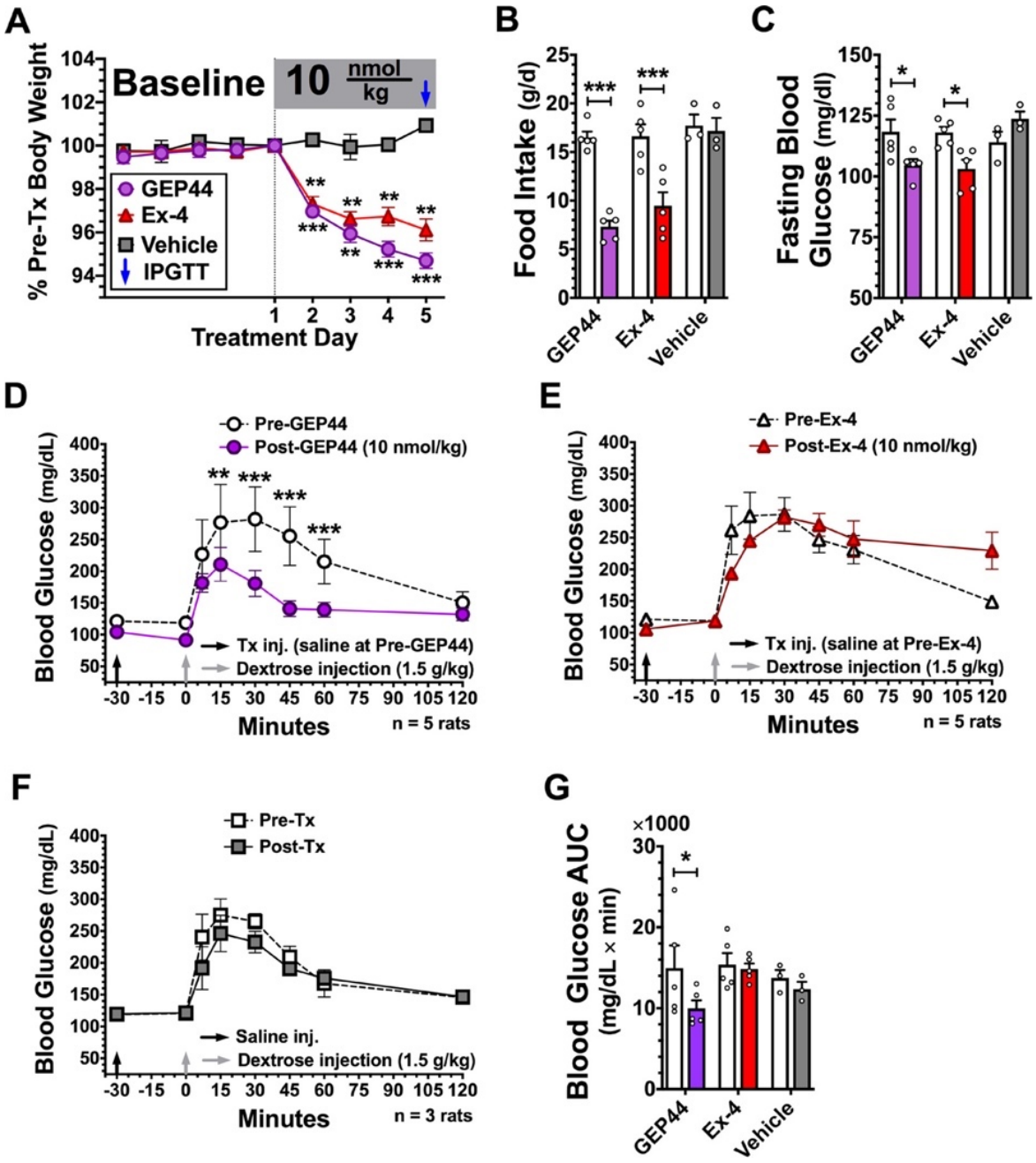

Figure 2-4. Longitudinal study (5 d Tx.; n = 3–5 per group; 10 nmol/kg; cohort 1: age 20 weeks, 16 weeks HFD exposure, 641.9 ± 17.9 g, n = 4; cohort 2: age 28 weeks, 24 weeks HFD exposure, 826.1 ± 35.7 g, n = 9) in DIO rats shows sustained weight loss (A), reduced food intake (B), and reduced fasting blood glucose (C) due to GEP44 treatment. IPGTT was performed prior to the baseline phase and immediately following the last drug treatment. When compared to Ex-4 (E) or vehicle (F), treatment with GEP44 (D) yielded stronger reductions in blood glucose during IPGTTs following 5-d treatments in prediabetic rats. Area under the curve (AUC) analyses of blood glucose from glucose bolus to 60 min indicated a significant effect of GEP44 on glucose clearance (G). For bar graphs, empty bars represent baseline data, and filled bars represent data during drug

treatment. Data were analyzed with repeated measurements two-way ANOVA followed by Bonferroni's *post-hoc* test. When compared to baseline measures or vehicle control: *p < 0.05, ***p < 0.001.

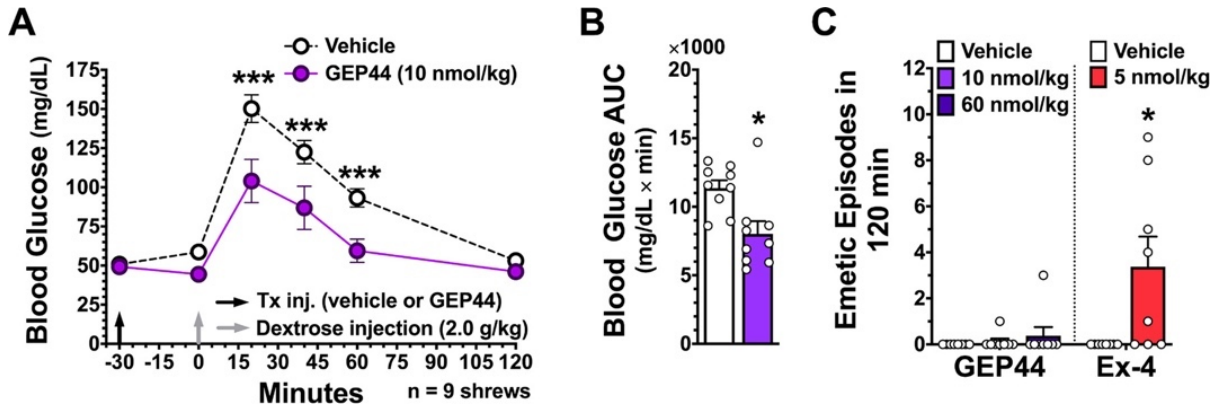

Figure 2-5. Systemically delivered GEP44 enhances glucose clearance during IPGTT while showing minimal emetogenic effects in shrews n = 9; ~8 months old; 60–65 g. (A) In an IPGTT, GEP44 (10 nmol/kg) suppressed blood glucose levels after IP glucose administration (2 g/kg, IP) compared to saline. (B) AUC analysis from 0 (*i.e*., post-glucose bolus) to 120 min showed that GEP44 reduced AUC compared to vehicle. (C) The number of single emetic episodes following GEP44 (10 and 60 nmol/kg) or saline systemic administration did not differ across treatment conditions. Indeed, GEP44 caused emesis in only one shrew tested. Data are expressed as mean ± SEM. Data in panel A were analyzed with repeated measurements two-way ANOVA followed by Bonferroni's post-hoc test. Data in panel B were analyzed with the Student's t-test for repeated measures. Due to the nonparametric nature of data in panel C, a repeated measurements Friedman test followed by Dunn's post hoc test was used to analyze GEP44 data, while a Wilcoxon test was used to analyze Ex-4 data. *p < 0.05, ***p < 0.001.

2.2 GEP44 as a triple agonist

We demonstrate that two peptide biased agonists (GEP44 and GEP12) of the GLP-1R, Y1-R, and Y2-R elicit Y1-R antagonist-controlled, GLP-1R-dependent stimulation of insulin secretion in both rat and human pancreatic islets, thus revealing the counteracting effects of Y1-R and GLP-1R agonism. These agonists also promote insulin-independent Y1-R-mediated glucose uptake in muscle tissue *ex vivo* and more profound reductions in food intake and body weight than liraglutide when administered to DIO rats. Our findings

support a role for Y1-R signaling in glucoregulation and highlight the therapeutic potential of simultaneous receptor targeting to achieve long-term benefits for millions of patients.

2.2.1 Design and synthesis of GEP44 and selected analogues

Predictive software was used to develop many additional peptide sequences that would simultaneously agonize the GLP-1R and Y2-R and potentially have activity at the Y1-R (GEP01-GEP11). One peptide, GEP12, was designed to have an enhanced ISR in pancreatic islets. The H1F amino acid substitution from GEP44 to GEP12 shut down GLP-1R-based internalization and ended up increasing ISR compared to controls.[20] The D-Ser in position 2 of GEP44 was maintained for future iterations due to the stability and *in vivo* validation differences.

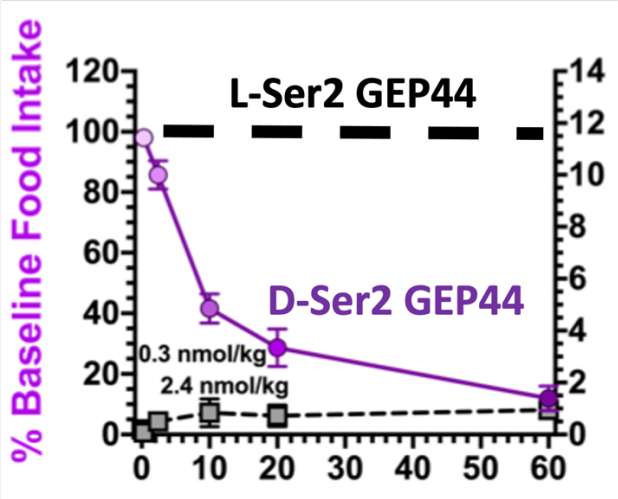

Figure 2-6. Up to 85% FI reduction by GEP44 with the native D-Ser^2 residue compared to the no effect observed when using L-Ser^2 GEP44.

The peptides were synthesized in-house via SPPS and purified by HPLC. Once purified, the peptides were screened for binding and function.

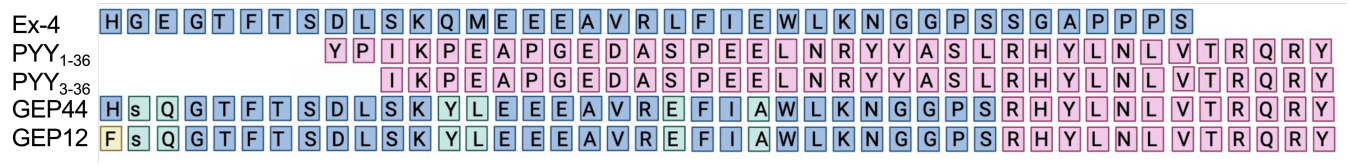

Figure 2-7. Design of chimeric peptides GEP44 and GEP12. Shown are the amino acid sequences of Ex-4, PYY_{1-36}, and PYY_{3-36} overlaid with those of GEP44 and GEP12 with lowercase single-letter amino acid code denoting a D-isomer.

2.2.2 Measurements of binding, agonism, receptor internalization, and β-arrestin-2 recruitment of GEP44 and selected analogues

The addition of these peptides to H188-GLP-1R transduced HEK293 cells resulted in elevated levels of cAMP with varying levels of potency. After analysis of the ease of synthesis and purification, solubility, and potency, GEP44 still appeared to be a lead candidate compared to other peptides. GEP44 resulted in an EC_{50} value of 417 pM, and the overall magnitude of response at GLP-1R was nearly equivalent to that of Ex-4 (EC_{50} 28.7 pM). To gauge the triple agonist behavior of GEP44, activity at Y1-R and Y2-R was validated in assays that monitored their ability to counteract adenosine stimulated cAMP production in HEK293 C24 cells that were transiently transfected with Y1-R or Y2-R. As we reported previously, pre-treatment of these cells with GEP44 for 20 min resulted in a concentration-dependent inhibitory effect with IC_{50} values of 34 nM and 27 nM for Y2-R and Y1-R, respectively. Binding affinity at the GLP-1R, Y2-R, and Y1-R was measured in-house using an SPR instrument. The half-maximal GEP44 binding at GLP-1R was observed at 113 nM (versus 5.85 nM for Ex-4), 65.8 nM at Y2-R (versus 1.51 nM for PYY_{3-36}), and 86.6 nM at Y1-R (versus 7.9 nM for PYY_{1-36}).

A publication by Jones *et al.*, reported the impact of GLP-1R trafficking on insulin release and noted specifically that Ex-4 analogs with reduced capacity to elicit

internalization and β-arrestin recruitment were more efficacious at inducing insulin release than the parent Ex-4 peptide. The authors reported that conversion of the N-terminal His (H) to Phe (F) amino acid substitution resulted in an Ex-4 analog (Ex-4-Phe1) with improved efficacy at inducing insulin release while eliciting reduced levels of GLP-1R internalization and β-arrestin-2 recruitment.[21] We incorporated this idea into our GEP44 scaffold and came up with, GEP12, a GEP44 analog with an analogous N-terminal H1F modification. We found that GEP12 functioned as a GLP-1R agonist with an EC_{50} of 17.3 nM and bound to this receptor with an K_D of 19.2 nM. As predicted, we observed no measurable GEP12-mediated internalization of GLP-1R in response to concentrations as high as 400 nM. We then explored the responses to both peptides in *ex vivo* studies of insulin secretion in pancreatic islets.

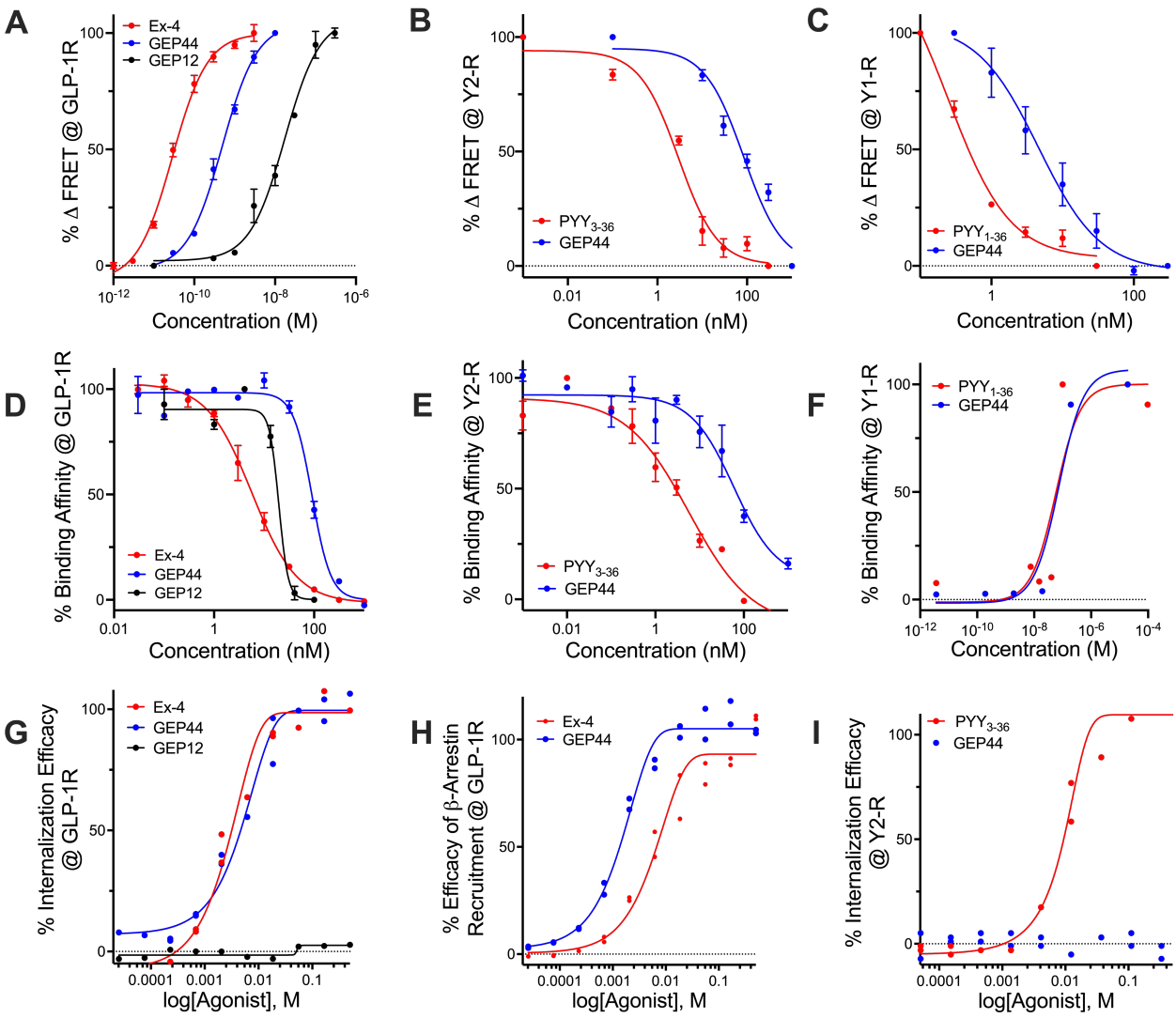

Figure 2-8. *In vitro* evaluation of chimeric peptides GEP44 and GEP12. (A) Dose-dependent agonism (% change in FRET ratio tracking levels of cAMP) of Ex-4, GEP44, and GEP12 at the GLP-1R. (B) Dose-dependent agonism (% change in FRET ratio tracking levels of cAMP) of PYY_{3-36}, GEP44, and GEP12 at the Y2-R. (C) Dose-dependent agonism of PYY_{1-36}, GEP44, and GEP12 at the Y1-R. (D) Percent binding of Ex-4, GEP44, and GEP12 at the GLP-1R. (E) Percent binding of PYY_{3-36}, GEP44, and GEP12 at the Y2-R. (F) Percent binding of PYY1-36, GEP44, and GEP12 at the Y1-R. (G) % internalization of GEP44 and GEP12 at the GLP-1R. (H) % recruitment of β-arrestin-2 by Ex-4 and GEP44 at the GLP-1R. (I) % internalization of Ex-4 and GEP44 at the Y2-R.

2.2.3 Islet and muscle effects of GEP44 and selected analogues

Insulin secretion from rat and human islets was measured in the presence of 20 mM glucose using both static and perifusion analyses. By either including or excluding various test compounds, we were able to see that the effects of GEP44 and GEP12 on islets are mediated by both GLP-1R and Y1-R. A static analysis in rat and human islets showed that both Ex-4 and GEP44 were able to potentiate ISR by 62% and 37%, respectively, in reference to the 20 mM glucose control. As hypothesized, GEP12 showed even stronger increases in ISR. GEP44 had a stimulatory effect on ISR *only* in the presence of a Y1-R antagonist. Both GEP44 and GEP12 increased cAMP levels in rat and human islet in the presence of glucose and Y1-R antagonists.

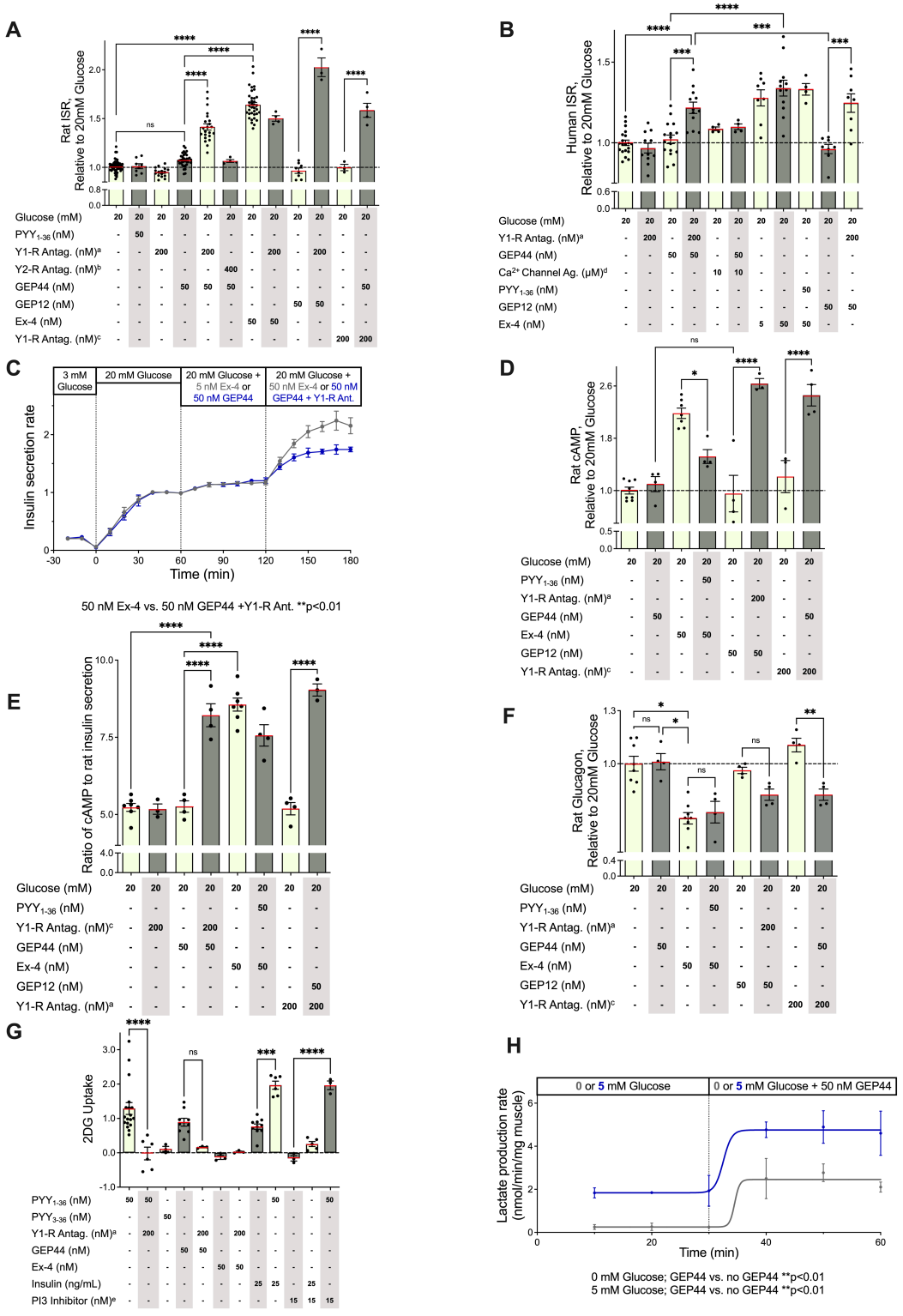

Figure 2-9. Action of GEP44 and GEP12 are mediated by GLP-1R and Y1-R in isolated pancreatic islets and muscle tissue. Rat (A) and human (B) islets were incubated for 60 min in 20 mM glucose and additional agents as indicated. Supernatants were then assayed for insulin, cAMP, and glucagon concentrations. (C) Insulin secretion rates

(ISRs) were measured by perifusion over a one-hour incubation period in rat islets in 20 mM glucose with 5 or 50 nM peptides with or without Y1-R antagonist, as indicated (C). Impact of GEP44 on (D) cAMP, (E) the ISR to cAMP ratio, and (F) glucagon secretion, relative to glucose-mediated stimulation alone in the absence of test compounds. cAMP levels corresponded directly, and glucagon secretion corresponded inversely with the ISR. (G) Uptake of ^{3}H-2-deoxyglucose (2-DG) and (H) lactate production (5 mM glucose) in response to GEP44 and other agents known to interact with GLP-1R, Y1-R, and Y2-R in the rat quadriceps muscle *ex vivo*. Horizontal dashed line in 2A, B, D, and F represents response to 20 mM glucose alone in assay as described. a = PD 160170; b = BIIE0246; c = BIBO; d = Bay K, e = Wortmannin.

2.2.4 Fluorescent in situ hybridization (FISH) and immunohistochemistry (IHC) with fluorescent GEP44

Areas in the hindbrain associated with appetite control (AP/NTS) are imperative to this research because of their involvement in food intake and control of nausea/malaise. To visualize GEP44 localization, an IP (15.5 µg/kg) or ICVI (1 µg/µL) injection of *f*Cy5-GEP44 was administered to rats, and coronal sections of the rat brainstem were isolated. RNAscope fluorescent *in situ* hybridization (FISH) with immunohistochemistry (IHC) was performed to visualize GEP44 colocalized with the GLP-1R, Y1-R, and Y2-R on neurons in the hindbrain.

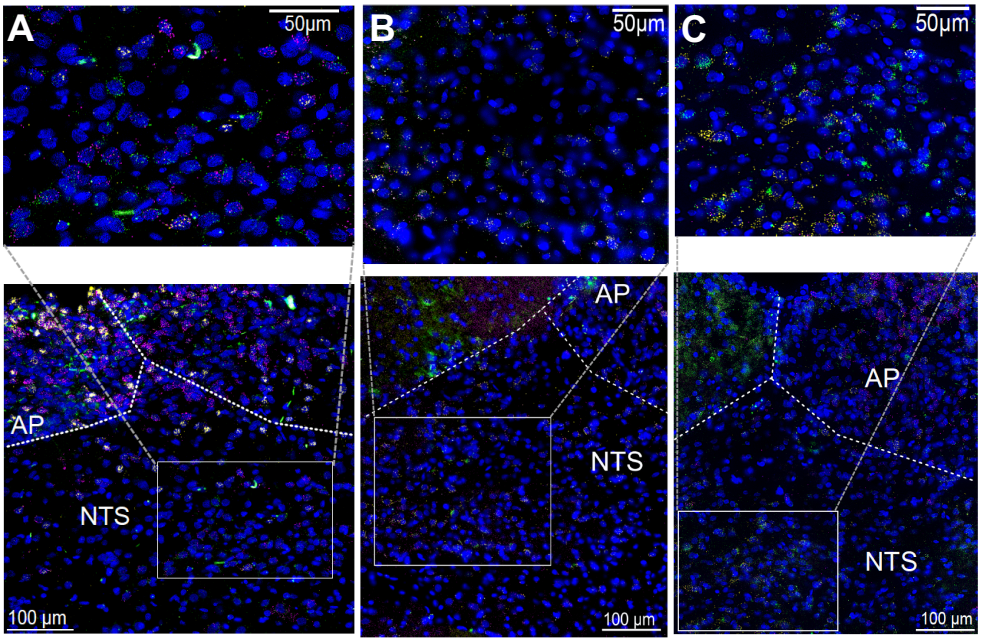

Figure 2-10. FISH and IHC visualization of *f*Cy5-GEP44 and its colocalization with Y1-R, Y2-R, and GLP-1R in cells in the NTS/AP regions of the rat brain. (A) *f*Cy5-GEP44 (green) administered IP colocalized with Y1-R and GLP-1R (yellow) in the AP. (B) *f*Cy5-GEP44 administered ICVI colocalized with Y1-R (yellow) and GLP-1R (magenta) in the AP. (C) *f*Cy5-GEP44 administered ICVI colocalized with Y2-R (yellow) and GLP-1R (magenta) in cells of the AP.

2.2.4.1 Synthesis of *f*Cy5-GEP44 and *f*Cy5-PYY_{3-36}

The fluorescent analogs of GEP44 and PYY_{3-36} were synthesized using Copper-free CLICK chemistry. First, GEP44 and PYY_{3-36} analogs with an Fmoc-Lys(N_3)-OH (ChemPep Inc.) substitution in the 27th and 2nd positions, respectively, were synthesized on the peptide synthesizer. The peptides were purified using an Agilent 1200 series HPLC tracking at 280 nm. The pure peptides were mixed at a 1:1 mole ratio with sulfo-Cy5 DBCO (Lumiprobe) for 16 hours at RT in 4:1 DMF:H_2O. The excitation/emission profiles were analyzed using a fluorimeter, and the fluorescent peptides were confirmed by MALDI-MS and HPLC tracked at 600 nm. Any excess sulfo-Cy5 DBCO was removed during purification.

2.2.5 Long-term *in vivo* study vs. liraglutide (LIRA)

Male Wistar rats (n=4) were fed a 60% HFD for 20 weeks before the start of the study. Baseline measures of body weight and food intake were collected for one week to balance the groups and create feeding pairs. Two independent experiments were performed. In the first experiment, three cohorts of eight animals each received daily injections of vehicle or increasing doses of either GEP44 or LIRA, which is a well-established GLP-1RA currently approved for the treatment of obesity, starting at 10 nmol/kg for 9 days and followed by 25 nmol/kg for 7 days. In the second experiment, five cohorts of eight animals each received daily injections of GEP44 alone, vehicle pair-fed with GEP44, LIRA alone, vehicle pair-fed to LIRA, and vehicle alone. GEP44 was administered as follows: 5 nmol/kg/day for 4 days, 10 nmol/kg/day for 4 days, 25 nmol/kg/day for 12 days, and 50 nmol/kg/day for 8 days. LIRA was administered as follows: 5 nmol/kg/day for 4 days, 10 nmol/kg/day for 4 days, 25 nmol/kg/day for 4 days, and 50 nmol/kg/day for 16 days. GEP44 treatment resulted in more profound reductions of food intake and body compared to treatment with equimolar doses (10 and 25 nmol/kg/day) of LIRA. Similar results were observed in a follow-up 27-day treatment study, in which GEP44 continued to elicit more profound reductions in food intake than equimolar doses of LIRA (5, 10, and 25 nmol/kg/day).

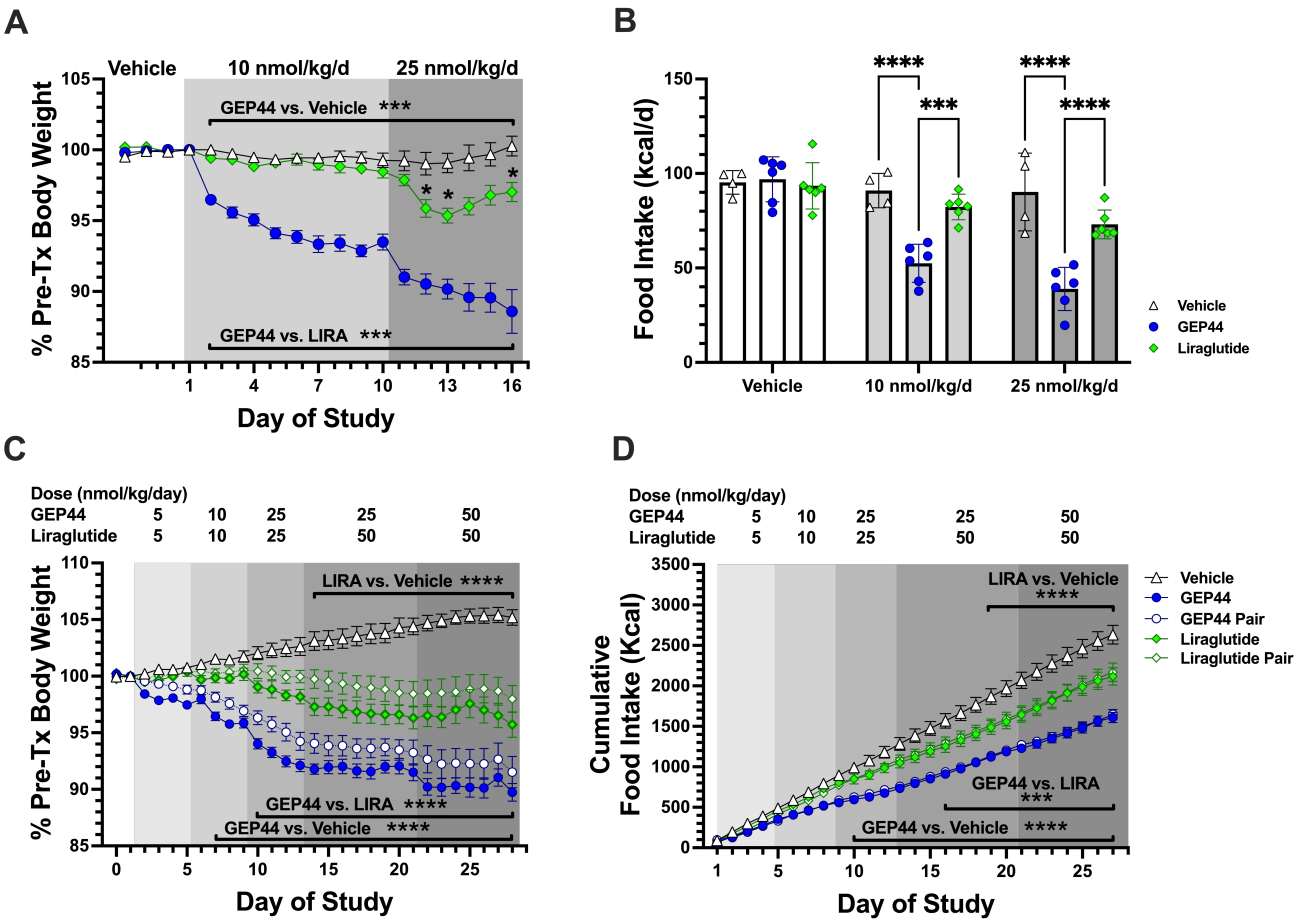

Figure 2-11. GEP44-mediated reductions in body weight and food intake were stronger than those elicited by LIRA during a 16-day and 27-day dose escalation protocol. (A, B) DIO Wistar rats were treated with vehicle or with GEP44 or LIRA at 10 nmol/kg/day for 9 days followed by 25 nmol/kg/day for 7 days (n=4–6) rats/group. In a second experiment, (C) changes in body weight and (D) food intake was evaluated during 27 days of treatment with vehicle, GEP44, vehicle-treated rats that were pair-fed to those receiving GEP44, LIRA, and vehicle-treated rats that were pair-fed to those receiving LIRA; n=8 per group. DIO male Wistar rats were matched based on baseline food intake and initial body weight gain trajectory. Changes in body weight were evaluated in response to GEP44 at doses escalating from 5 to 50 nmol/kg/day. Rats underwent pair-feeding to match the amount of food consumed by their GEP44-treated counterparts. Other groups included rats treated with saline vehicle control, LIRA, and rats that were pair-fed to their LIRA-treated counterparts. Symbols representing the results from pair-fed animals are overlayed by those from the GEP44 and LIRA treatment groups. Data shown are means ± SEM; *p <0.05, ***p <0.001, ****p <0.0001.

2.3 Pharmacokinetic enhancement of GEP44

Many FDA-approved pharmacotherapies used to treat T2DM and obesity are administered in the form of an injection.[22-24] Since approximately 70% of users discontinue treatment for a variety of reasons including CNS-associated side effects and frequent dosing,[25] the field is moving towards increasing patient compliance by lowering the frequency of dosing. The drug Ex-4 (Byetta®) is an unmodified GLP-1RA that requires once-daily dosing because of its short *in vivo* half-life ($T_{1/2}$) of under 2½ hours.[26] A snapshot pharmacokinetic (PK) experiment in lean rats administered 1 nmol/kg GEP44 showed the need for an improved PK profile. More recent T2DM/obesity therapeutics, *i.e*., liraglutide (Ozempic®) and semaglutide (Wegovy®), are modified with lipid-based molecules containing varying linkers. Semaglutide contains a C18 fatty diacid attached to a hydrophilic γGlu-2xOEG linker which is incorporated in its 26th position. This combination of diacid and linker successfully enhances albumin binding and reduces renal clearance resulting in an increased *in vivo* $T_{1/2}$.[27]

2.3.1 Design and synthesis of lipidated peptides

The methodology used for PK enhancement was adopted and applied to GEP44, and we developed sequences of potential long-acting peptides (KSCGG1-4). A modified amino acid residue, Fmoc-Lys(Ggu-L-Glu(AA-AA))-OH (Iris Biotech, FAA7640), was purchased and incorporated into the peptide synthesizer using double coupling onto the resin at 90°C with extended coupling time (from 4 to 8 minutes) to ensure it was effectively added. In two of the peptides, a D-Arg was used to replace the L-Arg in the 43rd position based on work by Lafferty *et al*. This research demonstrated a D-Arg^{35} PYY_{1-36} molecule with

improved resistance to plasma enzymatic degradation compared to the L-Arg version.[20] We hypothesized that the replacement of L-Arg with D-Arg would further improve the $T_{1/2}$ of the lipidated peptides, since they would better resist enzymatic degradation.

KSCGG1: GEP44-K27GG
HsQGTFTSDLSKYLEEEAVREFIAWL**X**NGGPSSGAPPPSRHYLNLVTRQRY-NH_2

KSCGG2: GEP44-K27GG D-Arg[43]
HsQGTFTSDLSKYLEEEAVREFIAWL**X**NGGPSSGAPPPSRHYLNLVTRQrY-NH_2

KSCGG3: GEP44-K12GG D-Arg[43]
HsQGTFTSDLS**X**YLEEEAVREFIAWLKNGGPSSGAPPPSRHYLNLVTRQrY-NH_2

KSCGG4: GEP44-K12GG
HsQGTFTSDLS**X**YLEEEAVREFIAWLKNGGPSSGAPPPSRHYLNLVTRQRY-NH_2

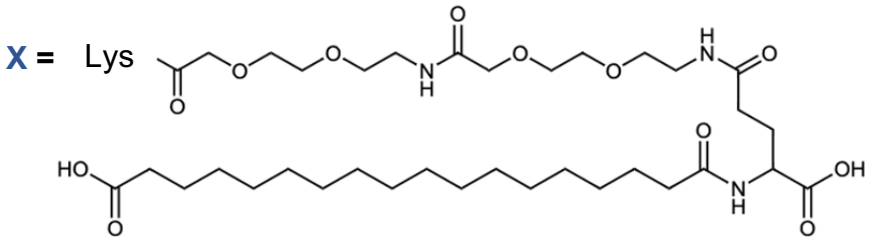

Figure 2-12. Sequences of lipidated peptides successfully synthesized and purified to >95% by HPLC. Lowercase letters denote D-amino acids.

2.3.2 Formulation differences of lipidated peptides

Since the lipidated peptides have increased hydrophobicity due to the fatty diacid component, there were many formulation differences compared to unmodified peptides. Once the lipidated peptides were cleaved from the resin and precipitated, they needed to be dissolved in 10% acetic acid to solubilize at a low volume for ease of purification. When lipidated peptides were dissolved directly in water or 0.9% saline, they appeared very

cloudy and had lower stability at 4°C. After the peptides were purified and freeze-dried, various solubility and stability tests had to be completed to ensure they could be administered *in vivo* at the desired concentrations. Solubility tests consisted of weighing out a known amount of solid, pure peptide and gradually adding water or 0.9% saline 10 µL at a time until the peptide was fully dissolved. The concentration would then be verified on a NanoDrop. For the stability tests, a known amount of solid, pure (>95% by HPLC) peptide would be weighted and dissolved in water or 0.9% saline at varying concentrations. An HPLC trace would be taken prior to the beginning of the test. The peptide in solution was left in the 4°C refrigerator for multiple days or weeks, and HPLC traces were gathered every day or once per week. The assays would be terminated once the HPLC traces began to show evidence of peptide degradation in the form of the appearance of new peaks and the disappearance of the main peptide peak. Any new peaks growing in would be collected and checked via MS. This could give valuable insight about how exactly a specific peptide fragments in solution and how to potentially mitigate degradation in future designs.

2.3.3 *Ex vivo* ISR in pancreatic islets

Lipidated peptides are currently being screened for their ability to increase glucose-dependent ISR in pancreatic islets.

2.3.4 *In vitro* evaluation of lipidated peptides

The addition of these lipidated peptides to H188-GLP-1R transduced HEK293 cells resulted in elevated levels of cAMP with varying levels of potency. The FRET ratios were

normalized and graphed with GEP44 for comparison. The EC_{50} values for the lipidated peptides were all in the low nanomolar range at 29.7, 18.3, 10.1, and 29.0 nM for KSCGG1, KSCGG2, KSCGG3, and KSCGG4, respectively.

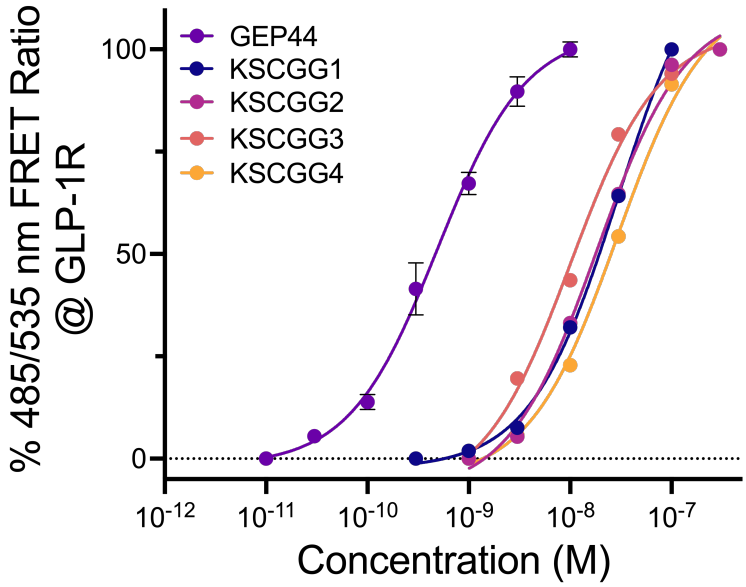

Figure 2-13. Dose-dependent agonism (% change in FRET ratio tracking levels of cAMP) of GEP44 and lipidated peptides (KSCGG1, KSCGG2, KSCGG3, and KSCGG4) at the GLP-1R.

2.3.5 Preliminary *in vivo* analysis of long-acting peptides

KSCGG1 was tested in male DIO Wistar rats. The rats were immediately placed on a HFD (Research Diets D12492, 60% kcal from fat) at 4 weeks old. At the time of the 200 nmol/kg dose, the rats had 42 weeks of HFD exposure. All treatments were administered just before the start of the dark cycle via subcutaneous injection. Administration of 200 nmol/kg KSCGG1 resulted in a 6% decrease both BW and FI, relative to baseline. The BW of these rats did not return to the baseline measurements even after 7 days.

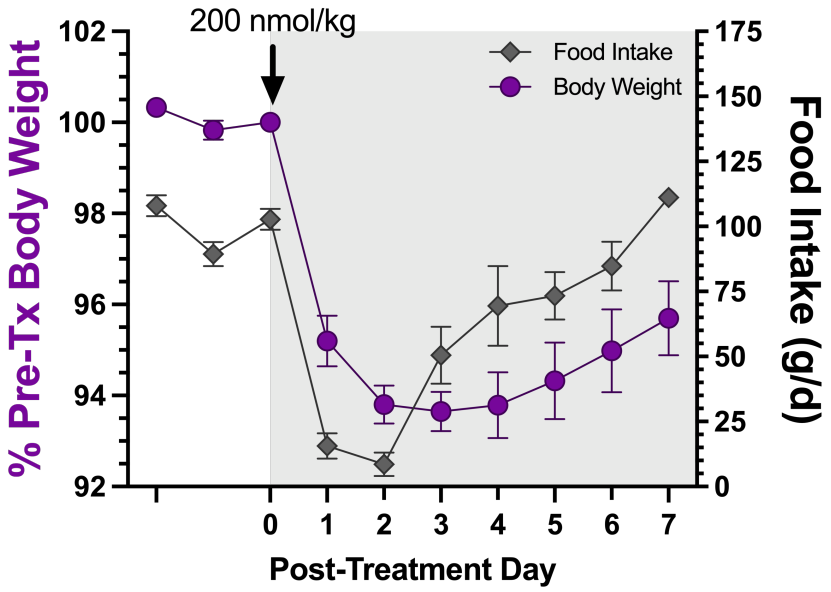

Figure 2-14. Body weight and food intake reduction in Wistar rats following a 200 nmol/kg s.c. injection of KSCGG1.

The remaining lipidated analogues are currently being tested *in vivo* at SCRI in tandem with semaglutide. All peptides will be compared by their ability to reduce BW and FI for several days without causing CNS-associated side effects. The peptide with the ability to meet these criteria will be considered our *lead* compound.

2.4 Triple agonists of GLP-1R, Y1-R, and Y2-R as potential opioid use disorder (OUD) therapeutics

2.4.1 OUD prevalence and impact

Opioid use disorder (OUD) is a substantial public health crisis in the United States. Despite recent attempts to reduce prescription of opioid analgesics and increase treatment access, more than 100,000 U.S. adults died from a drug-involved overdose in 2021.[28] Current FDA-approved medications for OUD all directly target the brain's opioid system. Despite the effectiveness of these medications to treat OUD,[29] there is still a high

rate of relapse following detoxification.[30-31] Thus, there is a dire unmet clinical need for conceptually innovative approaches to treating OUD.[32]

2.4.2 Design and synthesis of potential OUD therapeutics

Recent studies from our lab and others show that systemic administration of a GLP-1R agonist is sufficient to reduce opioid-taking and -seeking behaviors in rats.[33-36] From a translational perspective, these findings are suggest that GLP-1R agonists could be repurposed from treating T2DM and/or obesity to treat OUD.[37] While the doses of GLP-1R agonists that reduce opioid taking and seeking do not produce malaise-like effects in rats, the propensity of GLP-1R agonists to elicit nausea/emesis in humans is a valid concern.[37] Emerging literature indicates that co-administration of a GLP-1R agonist and a Y2-R agonist produces greater behavioral responses and fewer adverse effects than either monotherapy alone.[38-44] While the exact mechanism(s) underlying these effects is not clear, there is some evidence that activation of Y2-Rs enhances GLP-1R signaling in the brain.[45] Recently, we and others developed chimeric peptides that function as dual agonists of GLP-1Rs and Y2-Rs.[16, 46-47] We showed that our novel triple agonist, GEP44, reduced voluntary fentanyl taking and seeking in male rats at doses that did not produce adverse emetic or malaise-like effects commonly associated with GLP-1R agonists.[34] Moreover, these behaviorally relevant doses of GEP44 did not affect *ad libitum* feeding or alter body weight gain in fentanyl-experienced rats.[34] Together, these findings support the development of chimeric peptide triple agonists of GLP-1R, Y2-R, and Y1-R as a novel class of pharmacotherapies for treating OUD. GEP12 was designed to decrease GLP-1R-based internalization and enhance the potency at GLP-1R. These peptides

would be verified for parameters such as Y2-R-, Y1-R-, *and* GLP-1R-based assays, as described in earlier in this chapter.

Table 2-1. Chimeric peptide sequences designed by the author to be synthesized and screened at GLP-1R, Y2-R, and Y1-R.

Code	Peptide Sequence	Agonism	
		GLP-1R	Y2-R
GEP44	HsQGTFTSDLSKYLEEEAVREFIAWLKNGGPSRHYLNLVTRQRY-NH_2	330 pM	10 nM
GEP01	HsQGTFTSDLSKYLEEEAVREFIAWLKNGGPSSRHYLNLVTRQRY-NH_2	86 pM	
GEP02	HsQGTFTSDLSKQMEEEAVREFIAWLKNGGPSRHYLNLVTRQRY-NH_2	294 pM	
GEP03	HsQGTFTSDLSKQLEEEAVRLFIAWLKNGGPSRHYLNLVTRQRY-NH_2		209 nM
GEP04	HsQGTFTSDLSKQMEEEAVRLFIAWLKNGGPSSGAPRHYLNLVTRQRY-NH_2	115 pM	
GEP05	YsQGTFTSDLSKQMEEEAVRLFIAWLKNGGPSSGAPRHYLNLVTRQRY-NH_2	6.2 nM	
GEP06	YPQGTFTSDVSKQMEEEAVREFIAWLKNGGPSRHYLNLVTRQRY-NH_2	>3000 nM	
GEP07	YPQGTFTSDLSKYMEEEAVREFIAWLKNGGPSRHYLNLVTRQRY-NH_2	66 nM	
GEP08	YLDGTFTSDLSKYLEEEAVREFIAWLKNGGPSSRHYLNLVTRQRY-NH_2	334 pM	
GEP09	DLSKYLEEEAVREFIAWLKNGGPSRHYLNLVTRQRY-NH_2		
GEP10	HsQGTFTSDLSKYLEEEAVREFIAWLKNGGPSRHYLNWVTRQRY-NH_2	685 pM	307 nM
GEP11	HsQGTFTSDLSKYLEEEAVREFIAWLKNGGPSRHYLNWLTRQRY-NH_2	396 pM	427 nM
	↓ GLP-1R internalization; ↑ GLP-1R agonism; ↑ $T_{1/2}$; ↑ V_D		
GEP12	FsQGTFTSDLSKYLEEEAVREFIAWLKNGGPSRHYLNLVTRQrY-NH_2	13.7 nM	

2.5. Melanocortin-4 and GLP-1 Receptor Dual Agonists

2.5.1 Melanocortin-4 receptor (MC4R)

As mentioned previously, therapies based on endogenous gut peptides such as GLP-1RAs have been compelling therapeutic agents for obesity and T2DM. However, only a few of these have achieved partial long-term weight loss (≥5-15% in adults at 1 year), and all have shown significant side effects, including nausea/malaise and gastrointestinal ailments. There is a dire unmet clinical need for new anti-obesity agents with increased efficacy, safety, and patient tolerance.

In recent years, melanocortin-4 receptor (MC4R) agonists have been developed and tested in forms of obesity caused by deficient hypothalamic melanocortin signaling. The MC4R plays a significant role in energy balance and appetite,[48-49] and activation of MC4R by its endogenous ligand, α-melanocyte-stimulating hormone (α-MSH), leads to appetite reduction.[48] To lessen the burden of the aforementioned metabolic diseases, chimeric dual agonists of GLP-1R and MC4R have been designed, synthesized, and preliminarily tested in animal models of T2DM/obesity.

2.5.2 Design and synthesis of dual GLP-1R/MC4R agonists

The design of dual GLP-1R/MC4R agonists involves the combination of the N-terminal end of GEP44, a peptide with activity at GLP-1R and significant metabolic benefits in various animal models, with an MC4R-agonizing peptide. The native ligand of MC4R, α-MSH, a 13-amino acid neuropeptide, was incorporated onto the C-terminal end. The resulting chimeric sequence was termed KSCEM01 and synthesized by the author. The additional peptides comprising Table 2-2 were designed based on literature reports of short, peptide-based agonists of MC4R.[50-51] Briefly, KSCEM02 was inspired by a publication by Sawyer, *et al*., who published data on a ligand with enhanced potency, increased resistance to proteolysis, and increased duration of action compared to α-MSH.[50] KSCEM03 and KSCEM04 were designed based on truncation studies done by Haskell-Luevano, *et al*., who utilized a frog skin bioassay to find the minimally active fragment of α-MSH.[51] All peptides were synthesized by the author and purified to >95% by HPLC.

Table 2-2. Sequences of GLP-1R/MCR chimeric dual agonists designed by the author. KSCEM01, KSCEM02, KSCEM03, and KSCEM04 have been synthesized and purified to >95% by HPLC. Lowercase letters denote D-amino acids; Nle = norleucine.

Peptide	Sequence
KSCEM01	HsQGTFTSDLSKYLEEEAVREFIAWLKNGGPSYSMEHFRWGKPV-NH_2
KSCEM02	HsQGTFTSDLSKYLEEEAVREFIAWLKNGGPSYS(Nle)EHfRWGKPV-NH_2
KSCEM03	HsQGTFTSDLSKYLEEEAVREFIAWLKNGGPSYS(Nle)EHfRW-NH_2
KSCEM04	HsQGTFTSDLSKYLEEEAVREFIAWLKNGGPSHfRW-NH_2

2.5.3 Measurements of activity and binding affinity of KSCEM01 at GLP-1R

KSCEM01 was assayed for activity in HEK293 cells expressing GLP-1R to ensure it retained functional agonism despite having a different C-terminus compared to GEP44. KSCEM01 successfully elevated cAMP levels, and FRET ratio was plotted with Ex-4 and GEP44 for comparison. The EC_{50} values at GLP-1R of KSCEM01 and Ex-4 were 4.08 nM and 0.29 pM, respectively. KSCEM01 was designed to have complementary activity at GLP-1R and MC4R. Although KSCEM01 was less potent than both Ex-4 and GEP44 in activity assays, it had approximately equipotent binding affinity compared to Ex-4 at GLP-1R (K_D KSCEM01 9.9 nM vs. Ex-4 5.9 nM). Considering the potent GLP-1R binding affinity, we decided to perform preliminary *in vivo* studies.

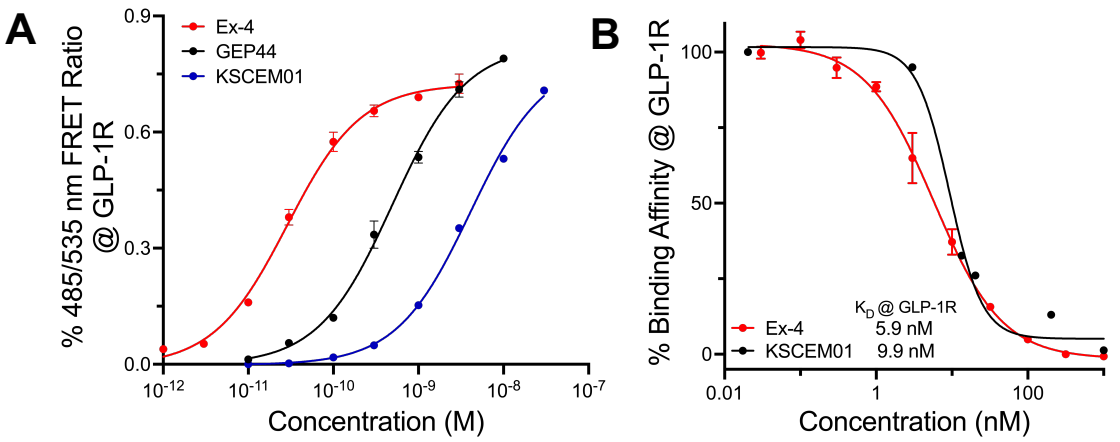

Figure 2-15. *In vitro* evaluation of the chimeric peptide, KSCEM01. (A) Dose-dependent agonism (% change in FRET ratio tracking levels of cAMP) of Ex-4, GEP44, and KSCEM01 at the GLP-1R. (B) Percent binding of Ex-4 and KSCEM01 at the GLP-1R with their respective K_D values.

2.5.4 Effects of KSCEM01 on food intake and body weight *in vivo*

To gauge effects on FI in rodents, KSCEM01 was administered to male Sprague-Dawley rats at multiple doses and the percent baseline FI was reported. At the 2, 5, and 10 nmol/kg doses, we see an approximately 60% decline in FI compared to the vehicle control. Since the 10 nmol/kg dose was well-tolerated, it was used in an 11-day study measuring FI and BW decline in Sprague-Dawley rats. KSCEM01 caused about a 5% decrease in pre-treatment BW which lasted several days. Since this peptide showed sustained weight loss over an extended period, it was compared to the long-acting, FDA-approved therapeutic, LIRA, in a dose-escalation study. In this 17-day study in Sprague-Dawley rats, KSCEM01 showed a dose-dependent decline in BW stronger than that of LIRA.

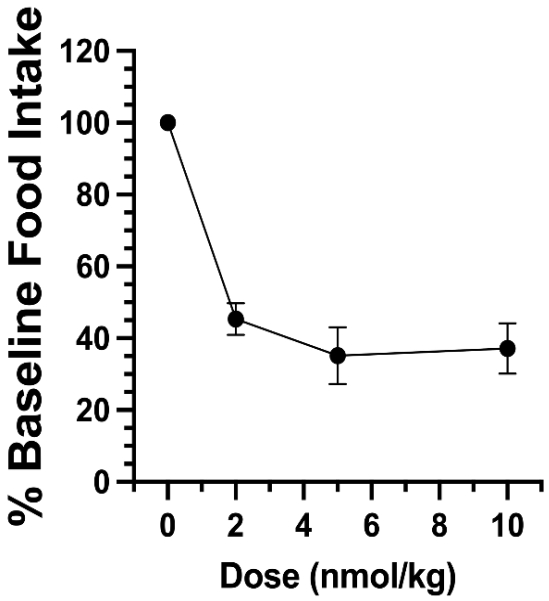

Figure 2-16. Dose escalation study in male Sprague-Dawley rats showing food intake reduction vs. baseline after administration of KSCEM01.

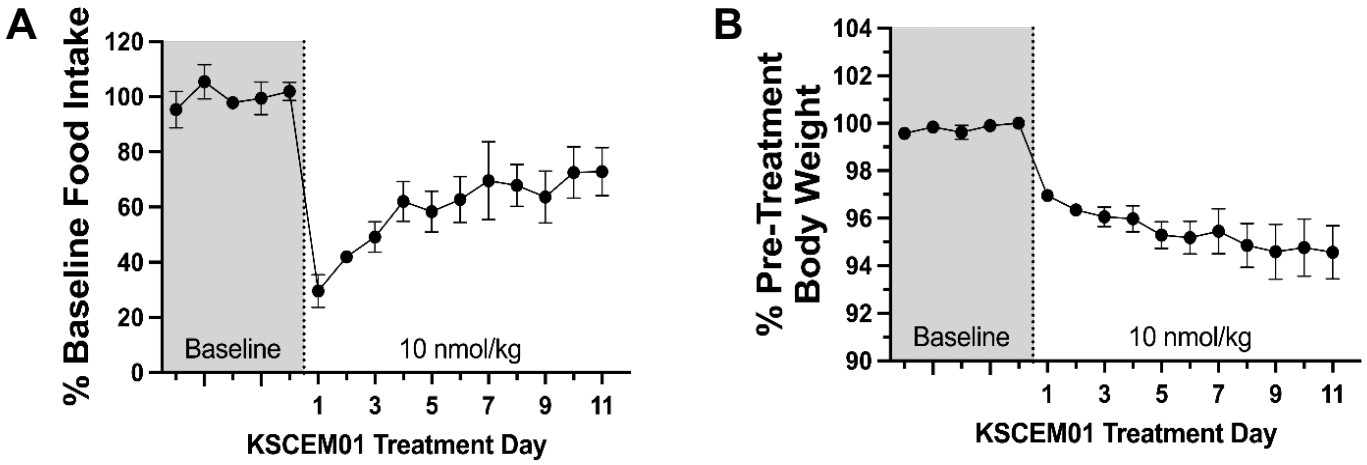

Figure 2-17. Effects of a single administration of 10 nmol/kg KSCEM01 on food intake (A) and body weight (B) in male Sprague-Dawley rats.

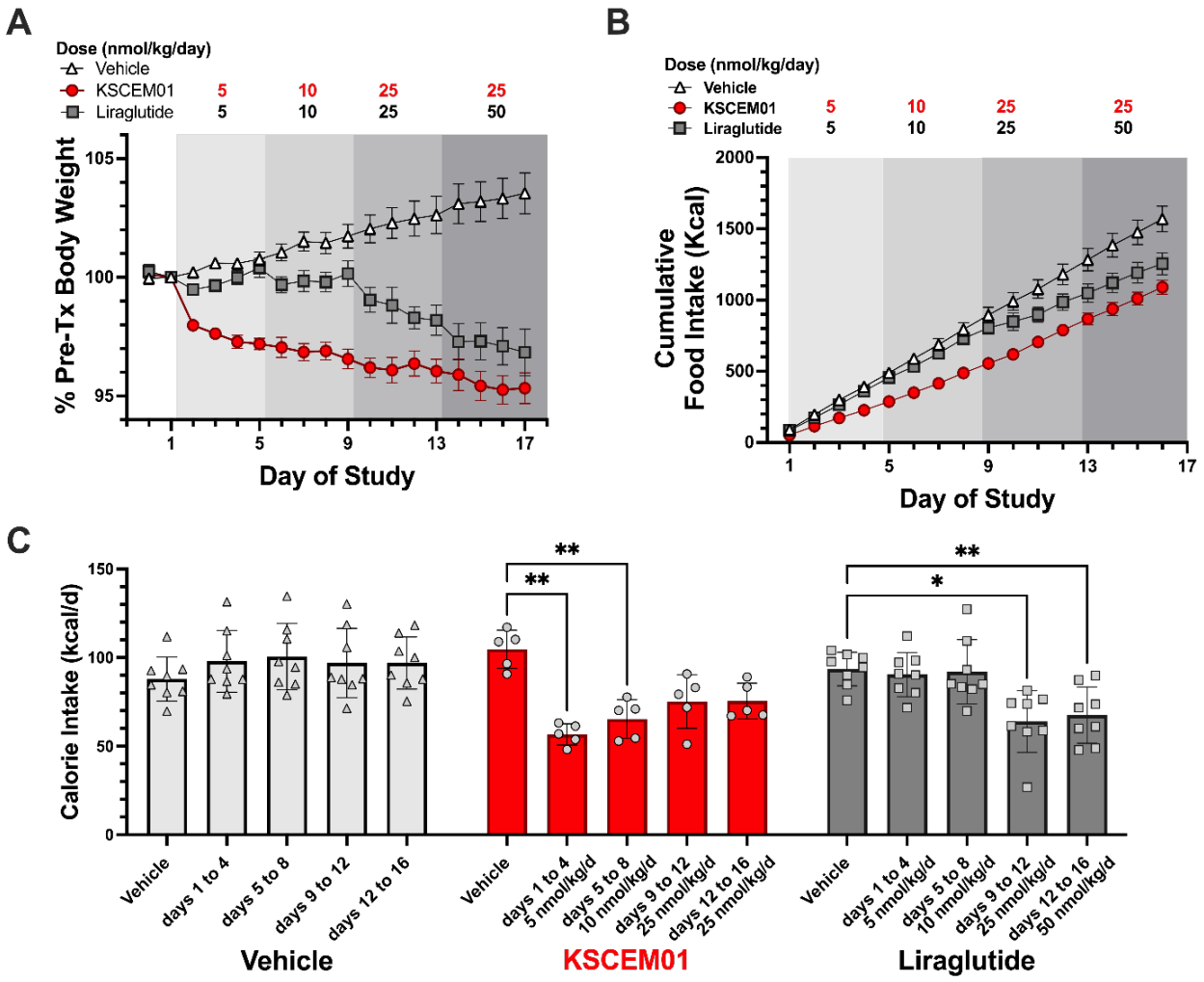

Figure 2-18. Dose escalation experiments in male Sprague-Dawley Rats of KSCEM01, liraglutide, and vehicle control administration showing changes in body weight (A), cumulative food intake (B), and calorie intake (C).

The dose-dependent decrease in BW and robust decline in FI compared to LIRA and vehicle cohorts seen after administration of KSCEM01 has prompted us to design additional potential GLP-1R and MC4R dual agonists. The outcome of metabolic testing of these peptides will allow us to determine a lead candidate that can be further optimized. These preliminary metabolic results of the proof-of-concept peptide, KSCEM01, reveal a potential future for therapeutics targeting both the GLP-1R and MC4R simultaneously.

2.6 References

1. Petersen J, Stromgaard K, Frolund B, Clemmensen C. Designing Poly-agonists for Treatment of Metabolic Diseases: Challenges and Opportunities. *Drugs* 2019;79:1187-97.

2. Wilding JPH, Batterham RL, Calanna S, et al. Once-Weekly Semaglutide in Adults with Overweight or Obesity. *N Engl J Med* 2021;384:989.

3. Wadden TA, Bailey TS, Billings LK, et al. Effect of Subcutaneous Semaglutide vs Placebo as an Adjunct to Intensive Behavioral Therapy on Body Weight in Adults With Overweight or Obesity: The STEP 3 Randomized Clinical Trial. *JAMA* 2021;325:1403-13.

4. Rubino D, Abrahamsson N, Davies M, et al. Effect of Continued Weekly Subcutaneous Semaglutide vs Placebo on Weight Loss Maintenance in Adults With Overweight or Obesity: The STEP 4 Randomized Clinical Trial. *JAMA* 2021.

5. Nauck MA, Meier JJ. MANAGEMENT OF ENDOCRINE DISEASE: Are all GLP-1 agonists equal in the treatment of type 2 diabetes? *Eur J Endocrinol* 2019;181:R211-R34.

6. Andreadis P, Karagiannis T, Malandris K, et al. Semaglutide for type 2 diabetes mellitus: A systematic review and meta-analysis. *Diabetes Obes Metab* 2018;20:2255-63.

7. Zaccardi F, Htike ZZ, Webb DR, Khunti K, Davies MJ. Benefits and Harms of Once-Weekly Glucagon-like Peptide-1 Receptor Agonist Treatments: A Systematic Review and Network Meta-analysis. *Ann Intern Med* 2016;164:102-13.

8. Li J, He K, Ge J, Li C, Jing Z. Efficacy and safety of the glucagon-like peptide-1 receptor agonist oral semaglutide in patients with type 2 diabetes mellitus: A systematic review and meta-analysis. *Diabetes Res Clin Pract* 2021;172:108656.

9. Bettge K, *et al*. Occurrence of nausea, vomiting and diarrhoea reported as adverse events in clinical trials studying glucagon-like peptide-1 receptor agonists: A systematic analysis of published clinical trials. *Diabetes Obes Metab* 2017;19:336-47.

10. Weiss T, Carr RD, Pal S, *et al*. Real-World Adherence and Discontinuation of Glucagon-Like Peptide-1 Receptor Agonists Therapy in Type 2 Diabetes Mellitus Patients in the United States. *Patient Prefer Adherence* 2020;14:2337-45.

11. Sanchez-Garrido MA, Brandt SJ, Clemmensen C, Muller TD, DiMarchi RD, Tschop MH. GLP-1/glucagon receptor co-agonism for treatment of obesity. *Diabetologia* 2017;60:1851-61.

12. Frias JP, Bastyr EJ, 3rd, Vignati L, et al. The Sustained Effects of a Dual GIP/GLP-1 Receptor Agonist, NNC0090-2746, in Patients with Type 2 Diabetes. *Cell Metab* 2017;26:343-52 e2.

13. Ambery P, Parker VE, Stumvoll M, et al. MEDI0382, a GLP-1 and glucagon receptor dual agonist, in obese or overweight patients with type 2 diabetes: a randomised, controlled, double-blind, ascending dose and phase 2a study. *Lancet* 2018;391:2607-18.

14. Bastin M, Andreelli F. Dual GIP-GLP1-Receptor Agonists In The Treatment Of Type 2 Diabetes: A Short Review On Emerging Data And Therapeutic Potential. *Diabetes Metab Syndr Obes* 2019;12:1973-85.

15. Khoo B, Tan TM. Combination gut hormones: prospects and questions for the future of obesity and diabetes therapy. *J Endocrinol* 2020;246:R65-R74.

16. Chepurny OG, Bonaccorso RL, Leech CA, Wöllert T, Langford GM, Schwede F, Roth CL, Doyle RP, Holz GG. Chimeric peptide EP45 as a dual agonist at GLP-1 and NPY2R receptors. *Sci Rep*. 2018;8(1):3749.

17. Lamiable A, Thévenet P, Rey J, Vavrusa M, Derreumaux P, Tufféry P. PEP-FOLD3: faster de novo structure prediction for linear peptides in solution and in complex. *Nucleic Acids Res*. 2016;44(W1):W449-W454.

18. Zhou P, Jin B, Li H, Huang SY. HPEPDOCK: a web server for blind peptide-protein docking based on a hierarchical algorithm. *Nucleic Acids Res*. 2018;46(W1):W443-W450.

19. https://www.chemcomp.com/index.htm.

20. Lafferty RA, Tanday N, Flatt PR, Irwin N. Development and characterisation of a peptidergic N-and C-terminally stabilised mammalian NPY1R agonist which protects against diabetes induction. *Biochim Biophys Acta Gen Subj*. 2020;1864(5):129543.

21. Jones B, Buenaventura T, Kanda N, Chabosseau P, Owen BM, Scott R, Goldin R, Angkathunyakul N, Corrêa IR Jr, Bosco D, Johnson PR, Piemonti L, Marchetti P, Shapiro AMJ, Cochran BJ, Hanyaloglu AC, Inoue A, Tan T, Rutter GA, Tomas A, Bloom SR. Targeting GLP-1 receptor trafficking to improve agonist efficacy. *Nat Commun*. 2018;9(1):1602.

22. Morieri ML, Avogaro A, Fadini GP. Long-Acting Injectable GLP-1 Receptor Agonists for the Treatment of Adults with Type 2 Diabetes: Perspectives from Clinical Practice. *Diabetes Metab Syndr Obes*. 2020;13:4221-4234

23. Villela R, Correa R. Semaglutide 2.4 mg: the latest GLP-1RA approved for obesity *Journal of Investigative Medicine* 2022;70:3-4.

24. Chavda VP, Ajabiya J, Teli D, Bojarska J, Apostolopoulos V. Tirzepatide, a New Era of Dual-Targeted Treatment for Diabetes and Obesity: A Mini-Review. *Molecules* 2022;27(13):4315.

25. Weiss T, Carr RD, Pal S, Yang L, Sawhney B, Boggs R, Rajpathak S, Iglay K. Real-World Adherence and Discontinuation of Glucagon-Like Peptide-1 Receptor Agonists Therapy in Type 2 Diabetes Mellitus Patients in the United States. *Patient Prefer Adherence*. 2020;14:2337-2345.

26. Huang YS, Chen Z, Chen YQ, Ma GC, Shan JF, Liu W, Zhou LF. Preparation and characterization of a novel exendin-4 human serum albumin fusion protein expressed in Pichia pastoris. *J Pept Sci.* 2008;14(5):588-95.

27. Mahapatra, M.K., Karuppasamy, M. & Sahoo, B.M. Semaglutide, a glucagon like peptide-1 receptor agonist with cardiovascular benefits for management of type 2 diabetes. *Rev Endocr Metab Disord* 2022;23, 521–539.

28. https://nida.nih.gov/research-topics/trends-statistics/overdose-death-rates

29. Dennis, B.B.*, et al.* The effectiveness of opioid substitution treatments for patients with opioid dependence: a systematic review and multiple treatment comparison protocol. *Syst Rev* 3, 105 (2014).

30. Nunes, E.V.*, et al.* Relapse to opioid use disorder after inpatient treatment: Protective effect of injection naltrexone. *J Subst Abuse Treat* 2018;85, 49-55.

31. Chalana, H., Kundal, T., Gupta, V. & Malhari, A.S. Predictors of Relapse after Inpatient Opioid Detoxification during 1-Year Follow-Up. *J Addict* 2016, 7620860.

32. Humphreys, K.*, et al.* Responding to the opioid crisis in North America and beyond: recommendations of the Stanford-Lancet Commission. *Lancet* 2022;399, 555-604.

33. Zhang, Y.*, et al.* Activation of GLP-1 receptors attenuates oxycodone taking and seeking without compromising the antinociceptive effects of oxycodone in rats.

Neuropsychopharmacology:official publication of the American College of Neuropsychopharmacology 2020;45, 451-461.

34. Zhang, Y.*, et al.* A novel dual agonist of glucagon-like peptide-1 receptors and neuropeptide Y2 receptors attenuates fentanyl taking and seeking in male rats. *Neuropharmacology* 2021;192, 108599.

35. Douton, J.E.*, et al.* Glucagon-like peptide-1 receptor agonist, exendin-4, reduces reinstatement of heroin-seeking behavior in rats. *Behav Pharmacol* 2021;32, 265-277.

36. Douton, J.E.*, et al.* Glucagon-like peptide-1 receptor agonist, liraglutide, reduces heroin self-administration and drug-induced reinstatement of heroin-seeking behaviour in rats. *Addiction biology* 2021;e13117.

37. Merkel, R.*, et al.* A novel approach to treating opioid use disorders: Dual agonists of glucagon-like peptide-1 receptors and neuropeptide Y2 receptors. *Neurosci Biobehav Rev* 2021;131, 1169-1179.

38. De Silva, A.*, et al.* The gut hormones PYY 3-36 and GLP-1 7-36 amide reduce food intake and modulate brain activity in appetite centers in humans. *Cell Metab* 2011*;*14, 700-706.

39. Neary, N.M.*, et al.* Peptide YY3-36 and glucagon-like peptide-17-36 inhibit food intake additively. *Endocrinology* 2005;146, 5120-5127.

40. Fenske, W.K.*, et al.* Exogenous peptide YY3-36 and Exendin-4 further decrease food intake, whereas octreotide increases food intake in rats after Roux-en-Y gastric bypass. *Int J Obes* (Lond) 2012;36, 379-384.

41. Reidelberger, R.D., Haver, A.C., Apenteng, B.A., Anders, K.L., Steenson, S.M. Effects of exendin-4 alone and with peptide YY(3-36) on food intake and body weight in diet-induced obese rats. *Obesity* 2011;19, 121-127.

42. Talsania, T., Anini, Y., Siu, S., Drucker, D.J., Brubaker, P.L. Peripheral exendin-4 and peptide YY(3-36) synergistically reduce food intake through different mechanisms in mice. *Endocrinology* 2005*;*146, 3748-3756.

43. Schmidt, J.B.*, et al.* Effects of PYY3-36 and GLP-1 on energy intake, energy expenditure, and appetite in overweight men. *American journal of physiology. Endocrinology and metabolism* 2014;306, E1248-1256.

44. Dischinger, U.*, et al.* Toward a Medical Gastric Bypass: Chronic Feeding Studies With Liraglutide + PYY3-36 Combination Therapy in Diet-Induced Obese Rats. *Front Endocrinol (Lausanne)* 2020;11, 598843.

45. Kjaergaard, M.*, et al.* PYY(3-36) and exendin-4 reduce food intake and activate neuronal circuits in a synergistic manner in mice. *Neuropeptides* 2019;73, 89-95.

46. Ostergaard, S., Paulsson, J.F., Kjaergaard Gerstenberg, M., Wulff, B.S. The Design of a GLP-1/PYY Dual Acting Agonist. *Angew Chem Int Ed Engl* 2021;60, 8268-8275.

47. Milliken, B.T.*, et al.* Design and Evaluation of Peptide Dual-Agonists of GLP-1 and NPY2 Receptors for Glucoregulation and Weight Loss with Mitigated Nausea and Emesis. *J Med Chem* 2021;64, 1127-1138.

48. Heyder, N.A., Kleinau, G., Speck, D. *et al.* Structures of active melanocortin-4 receptor–G_s-protein complexes with NDP-α-MSH and setmelanotide. *Cell Res* 2021;31, 1176–1189.

49. Krashes, M. J., Lowell, B. B., Garfield, A. S. Melanocortin-4 receptor-regulated energy homeostasis. *Nat. Neurosci.* 2016;19, 206–219.

50. Sawyer, T.K. *et al*. 4-Norleucine, 7-D-phenylalanine-α-melanocyte-stimulating hormone: A highly potent α-melanotropin with ultralong biological activity. *Proceedings of the National Academy of Sciences.* 1980;77, 5754–5758.

51. Haskell-Luevano, C. *et al*. Truncation Studies of α-Melanotropin Peptides Identify Tripeptide Analogues Exhibiting Prolonged Agonist Bioactivity. *Peptides*. 1996;17, 6, 995-1002.

Chapter 3: Neuropeptides and related analogues to treat metabolic diseases

The work on this project has resulted in the following patent:

Chichura, K. S., Geisler, C. E., Reiner, B. C., Crist, R. C., Hayes, M. R., Doyle, R. P. *Octadecaneuropeptide (ODN) and novel derived neuropeptides activity in the brain for food intake, obesity, body weight and prevention of nausea/emesis*. Provisional Patent. Filed 08/2022.

The author at the University of Pennsylvania to meet with collaborators, Prof. Matt Hayes, Caroline Geisler, Ph.D., and Tito Borner, Ph.D.

3.1 Octapeptide (OP), octadecaneuropeptide (ODN), and novel iterations.

Endozepines are a family of astroglia-secreted proteins that were originally isolated and characterized as endogenous ligands of benzodiazepine receptors.[1] It is now clearly established that the octadecaneuropeptide (ODN), acting through the central-type benzodiazepine receptor or an orphan metabotropic receptor, is an endozepine that exerts pro-conflict behavior, induction of anxiety,[2] decrease of water consumption, and reduction of food intake.[3] ODN also stimulates astrocyte proliferation and protects both neurons and astrocytes from oxidative stress.[4] ODN is an *in situ*-produced cleavage product of the endozepine diazepam binding inhibitor (DBI). In cultured astrocytes, DBI expression is upregulated during moderate oxidative stress, and authentic ODN production is subsequently increased, suggesting that ODN may also have actions as a paracrine factor protecting neighboring neurons.[4]

Obesity alters multiple aspects of hindbrain ODN signaling, including a longer time course of ODN hypophagia, including possible difference in DBI cleavage to ODN (recombinant DBI protein is hypophagic in chow but not HFD-fed rats),[1] the ODN antagonist AntOP is hypophagic in HFD-fed but not chow-fed rats providing a possible new site of action and/or modified target interactions.

ODN signaling may be downstream of, and partially mediate, the effects of GLP-1R signaling, and thus partially mediates all existing GLP-1-based pharmacotherapies currently used to treat diabetes and obesity. Nonetheless, ODN and novel peptide derivatives (*e.g.*, TDN) thereof signaling appears to not be maxed out by GLP-1R agonism as ODN and GLP-1R agonist co-treatment have additive hypophagia effects.

Antagonizing ODN signaling with either an antibody targeted against DBI or a peptide antagonist of the ODN receptor (AntOP), attenuates the hypophagic and body weight effects of central and peripheral GLP-1R agonists.[1] Because nutritional state regulates hindbrain DBI protein expression,[5] GLP-1R signaling may contribute to this effect. ODN may facilitate transport of GLP-1R agonists across the blood brain barrier, specifically at the tanycyte borders, both across the 4th ventricle and the sub-postrema border, to regulate brain penetrance of GLP-1R agonists. Multiple cleavage products of ODN are physiologically active and suppress food intake, allowing for the creation of new forms of non-naturally occurring optimized peptides.

In the present studies the ODN receptor has been deorphanized. We have discovered that ODN is an endogenous antagonist of the relaxin-3 receptor (RXFP3) and novel peptide derivatives of ODN (*e.g.*, TDN; tridecaneuropeptide) also antagonize the RXFP3. Relaxin-3 is an orexigenic neuropeptide that promotes weight gain and becomes upregulated in obesity to defend against weight loss. Thus, antagonizing this signal to preserve a lower body weight may help overcome the typically observed weight loss plateau seen with current anti-obesity pharmacotherapies.

3.1.1 Synthesis of OP/ODN peptides

The synthesis of OP, ODN, and various analogues was conducted using a CEM microwave-assisted Liberty Blue synthesizer with Fmoc-protected amino acids.

Table 3-1. List of linear and cyclic analogues of ODN and OP.

Peptide	Sequence
Linear analogues	
ODN	QATVGDVNTDRPGLLDLK
AntOP	RPGL(D-L)DLK
TDN (SUODN-01)	DVNTDRPGLLDLK
OP (SUODN-02)	RPGLLDLK
SUODN-03	RPGLL
SUODN-04	DVNTDRPG
SUODN-05	DVNTDRPGLL
SUODN-06	QATVGDVNTDRPG
SUODN-07	QATVGDVNTDRPGLL
Cyclic analogues	
SUODN-08	XATVGDVNTDRPGLLDLZ
SUODN-09	XATVGDVNTDRPGZLDLK
SUODN-10	XATVGDVNTDRPGLZDLK
SUODN-11	XATVGDVNTDRPGLLDZK
SUODN-12	QXTVGDVNTDRPGLLDLZ
SUODN-13	QXTVGDVNTDRPGZLDLK
SUODN-14	QXTVGDVNTDRPGLZDLK
SUODN-15	QXTVGDVNTDRPGLLDZK
SUODN-16	QATVXDVNTDRPGLLDLZ
SUODN-17	QATVXDVNTDRPGZLDLK
SUODN-18	QATVXDVNTDRPGLZDLK
SUODN-19	QATVXDVNTDRPGLLDZK

X = alkyne-Q,A,G
Z = Lys(N_3)

3.1.1.1 ODN-biotin

A biotinylated Lys residue (Fmoc-Lys(Biotin)-OH, Aapptec) was incorporated directly onto the peptide synthesizer and double-coupled onto the resin at 90°C for an extended

coupling time. The peptide was reconstituted in 10% acetic acid after synthesis to mitigate solubility issues and purified using an Agilent 1200 series HPLC tracking at 220 nm.

3.1.1.2 AntOP

The OP antagonist, AntOP, was synthesized as described for OP above except for the substitution of a D-Leu residue for the L-Leu in OP.[1] Since the 4th and 5th residues of AntOP are an L-Leu and D-Leu, respectively, there seems to be extra steric strain that prevents the >70% purity of AntOP right off the synthesizer. Mass spectrometry data showed almost 50% of a Leu deletion product. To bypass this issue and yield a higher percentage of the desired product, both residues in the 4th and 5th positions were double coupled for an extended coupling time. The peptide was reconstituted and purified using an Agilent 1200 series HPLC tracking at 220 nm.

3.1.1.3 *f*Cy5-OP and *f*Cy5-TDN

The fluorescent analogs of OP and TDN were synthesized using Copper-free CLICK chemistry. First, OP and TDN analogs with Fmoc-Lys(N_3)-OH substitutions in the 8th and 13th positions, respectively, were synthesized on the peptide synthesizer. The peptides were purified using an Agilent 1200 series HPLC tracking at 220 nm. The pure peptides were mixed at a 1:1 mole ratio with sulfo-Cy5 DBCO for 16 hours at RT in 4:1 DMF:H_2O. The excitation/emission profile was analyzed using a fluorimeter, and the fluorescent peptides were confirmed by MALDI-MS and HPLC tracked at 600 nm. Any excess sulfo-Cy5 DBCO was removed during purification.

3.1.2 GPCR extraction from rat brain tissue

Membrane proteins were extracted from rat brain tissue sent from the Hayes lab at the University of Pennsylvania based on the protocol for tissues on the GPCR Extraction and Stabilization Reagent (GESR) (ThermoFisher Scientific, Rockford, Il). Briefly, the tissue samples were suspended in 1 mL of cold (4°C) PBS and washed repeatedly. The PBS was decanted, and 1 mL of cold (4°C) GESR was added to the tissue samples. The tissue samples were homogenized until an even suspension was obtained by pipetting up and down 15-20 times. The homogenate was transferred to a new tube and was incubated at 4°C for 30 minutes with end-over-end mixing. The sample was centrifuged at 16,000 x g for 20 minutes at 4°C. The supernatant containing stabilized protein receptors was saved and stored at 4°C until being analyzed.

3.1.3 Surface plasmon resonance using ODN-biotin

Binding analysis was done on a Nicoya Open Surface plasmon resonance instrument using a Nicoya streptavidin sensor chip. The coupling procedure was according to the streptavidin sensor chip protocol, including the steps of surface conditioning and surface activation. For ligand immobilization, ODN-biotin (20 µg/mL in the PBST pH 7 running buffer) was injected over channel 2 for a 5-minute interaction time. This process was repeated several times to ensure optimal immobilization. The supernatant from the GPCR extraction procedure was injected over channels 1 and 2 of the chip, and a background-corrected binding curve was obtained. The chip was then soaked for 16 hours in 5 mL of MeOH at 4°C. An electron absorption spectrum of the MeOH used to soak the chip was

obtained using a Nanodrop One. The remaining MeOH was mixed with water, freeze-dried, and sent out for MS/MS sequencing.

3.1.4 Metabolic effects *in vivo*

The results of this work demonstrate that central ODN and novel ODN based peptides decrease food intake in chow and HFD-maintained rats, that hindbrain DBI protein expression is regulated by nutritional state and GLP-1 agonism in chow-fed rats and that this is blunted in HFD-fed rats, that central GLP-1 agonism upregulates DBI mRNA expression in chow-fed rats, that blocking ODN signaling with either an antibody targeting DBI or an ODN antagonist attenuates the anorectic effect of central and peripheral GLP-1 analogues, that ODN and GLP-1 signaling are cooperative to suppress food intake, and that ODN is involved in the hindbrain glucose sensing response.

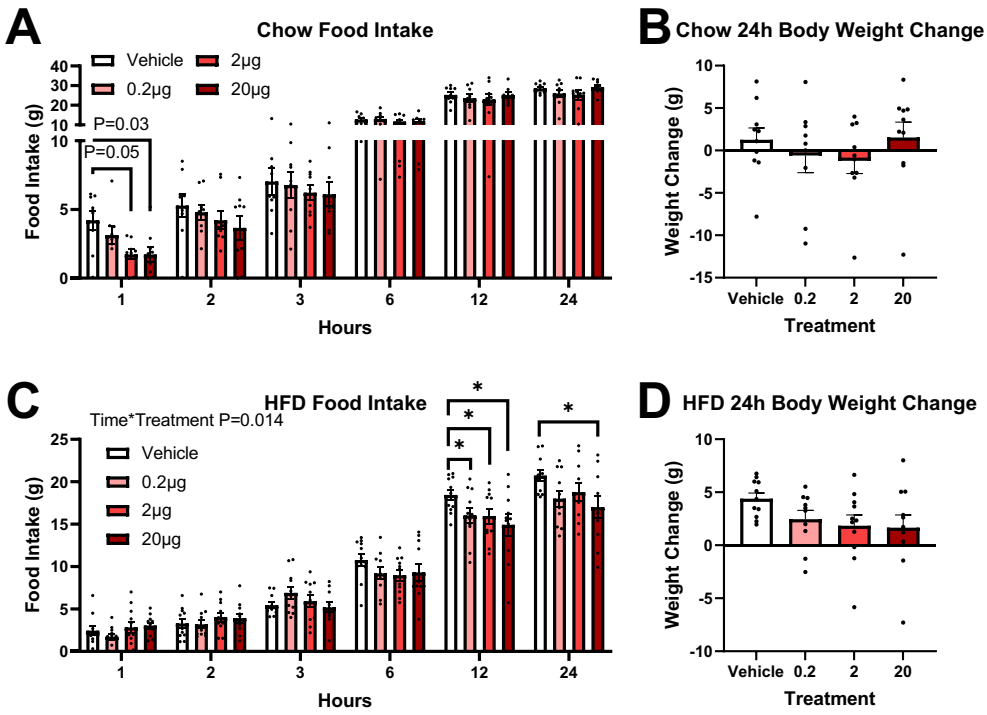

Figure 3-1. Central ODN dose dependently suppresses food intake in chow and HFD-fed rats. Effect of 4th ventricle ODN (0.2, 2, or 20 µg/2 µL in aCSF) treatment on 24h food intake (grams; A, C) and body weight change (B, D) in chow and HFD fed rats. All data presented as mean ± SEM.

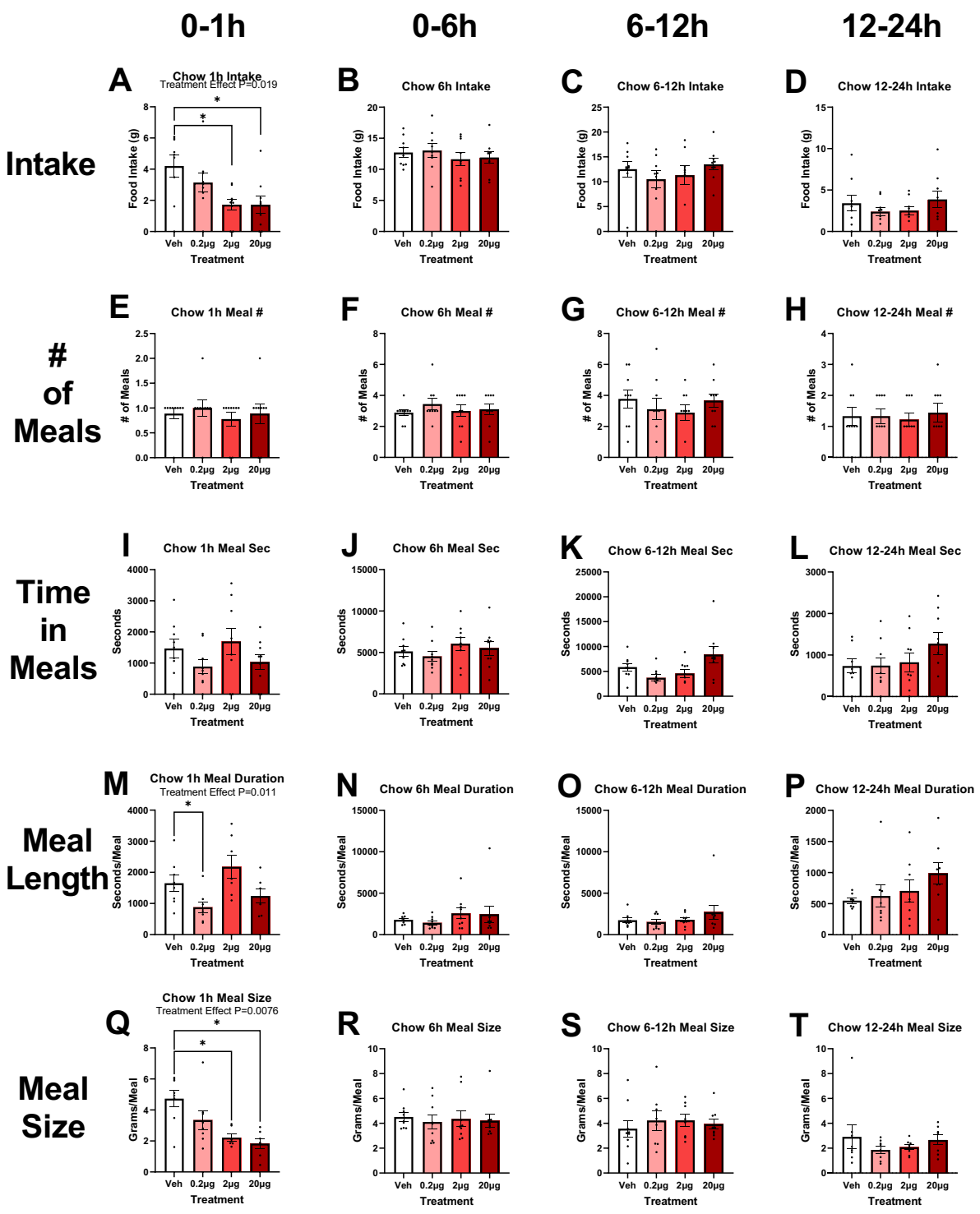

Figure 3-2. Meal pattern data following central ODN administration in chow-fed rats. Effect of 4th ventricle ODN (0.2, 2, or 20 µg/2 µL in aCSF) treatment on food intake (grams; A-D), number of meals (E-H), time spent eating meals (seconds; I-L), meal length (seconds/meal; M-P), and meal size (grams/meal; Q-T) at time intervals 1, 6, 6-12, and 12-24 hours after administration. All data presented as mean ± SEM.

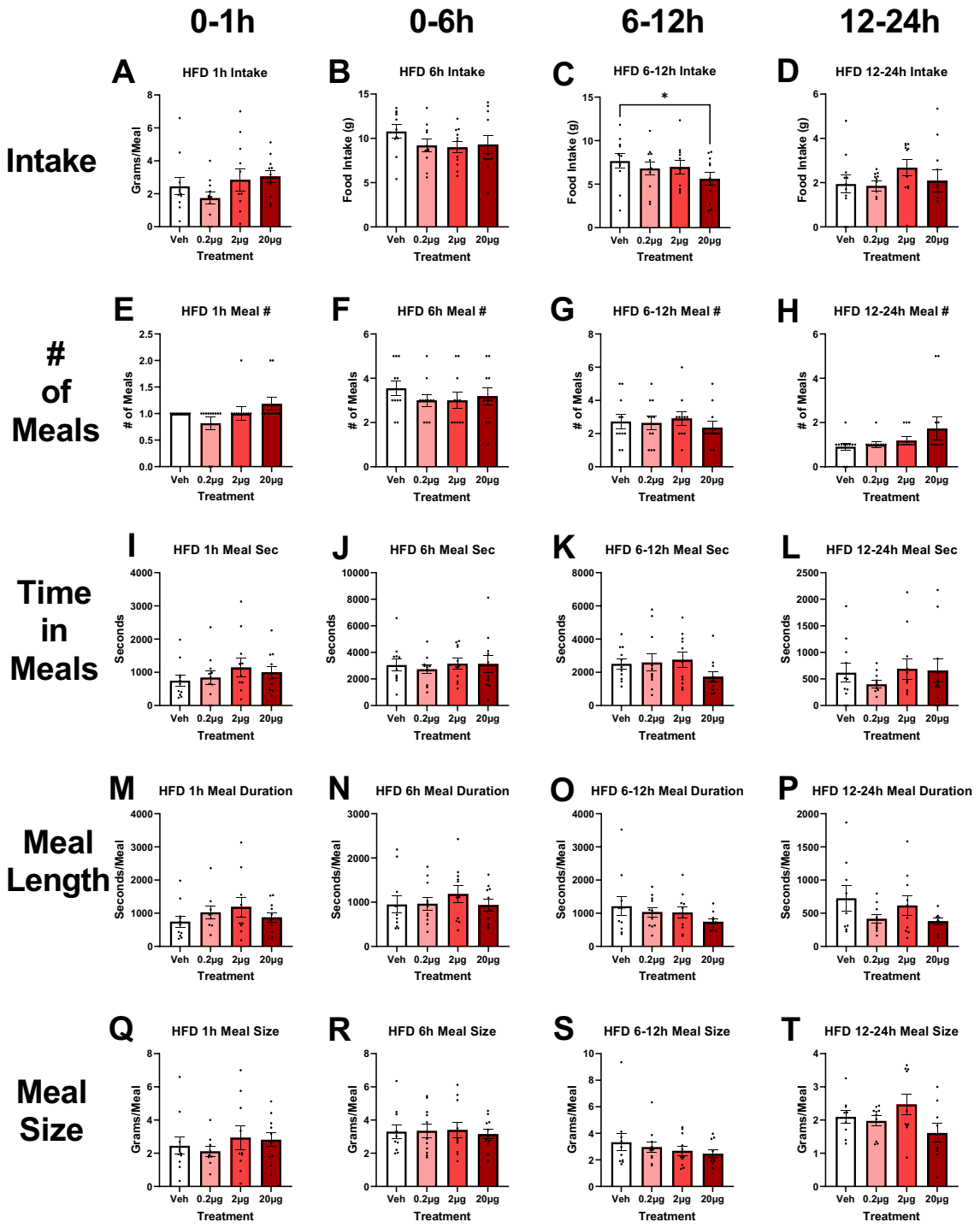

Figure 3-3. Meal pattern data following central ODN administration in HFD-fed rats. Effect of 4th ventricle ODN (0.2, 2, or 20 µg/2 µL in aCSF) treatment on food intake (grams; A-D), number of meals (E-H), time spent eating meals (seconds; I-L), meal length (seconds/meal; M-P), and meal size (grams/meal; Q-T) at time intervals 1, 6, 6-12, and 12-24 hours after administration. All data presented as mean ± SEM.

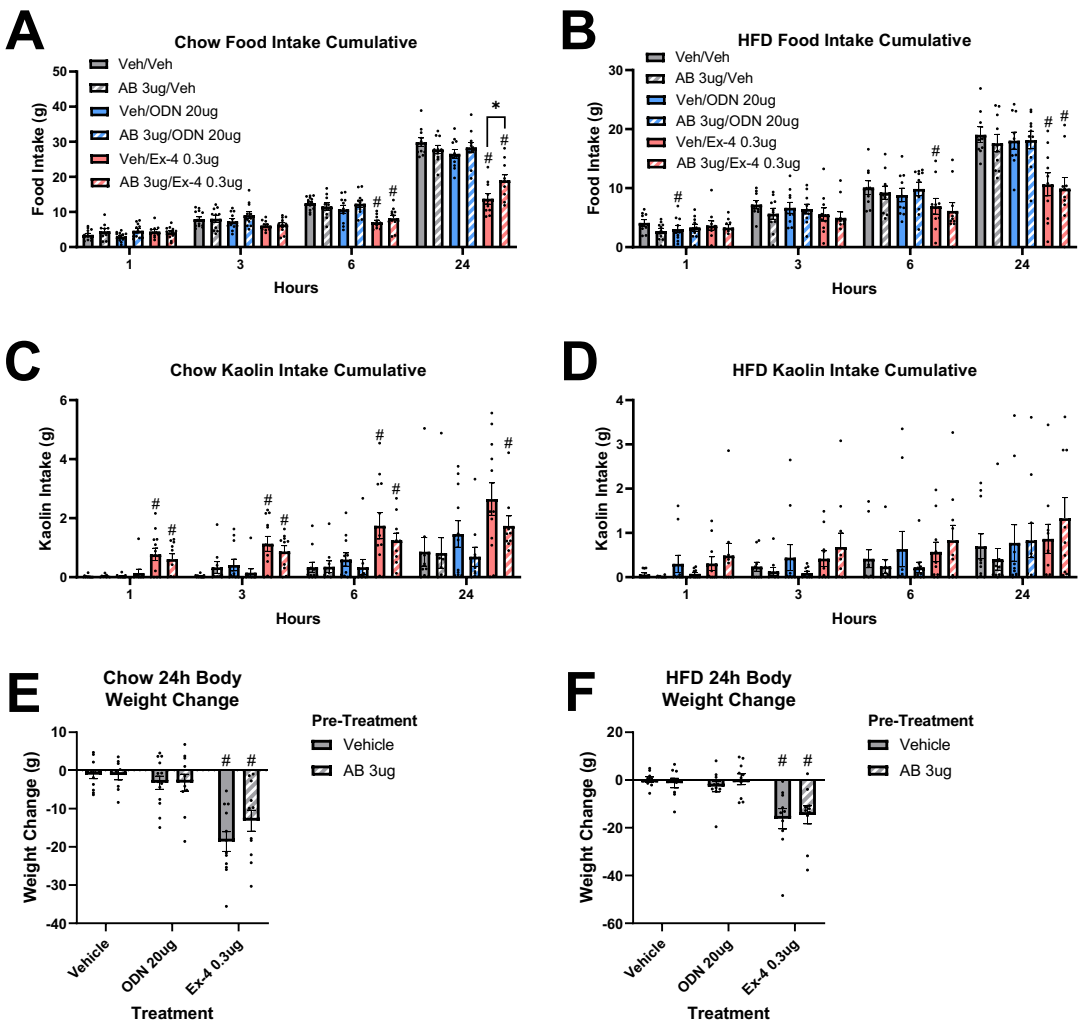

Figure 3-4. Pretreatment with an antibody against DBI attenuates central Ex-4-induced hypophagia in chow fed rats. Rats were pretreated 4th ventricle with a DBI antibody (AB 3 µg/3 µL) or vehicle followed by 4th ventricle treatment with ODN (20 µg/2 µL), Ex-4 (0.3 µg/2 µL), or vehicle. 24 hour food intake in chow (A) and HFD (B) fed rats, kaolin intake in chow (C) and HFD (D) fed rats, and body weight change in chow (E) and HFD (F) fed rats following treatments. # indicates difference from Veh/Veh (P=0.05). All data presented as mean ± SEM.

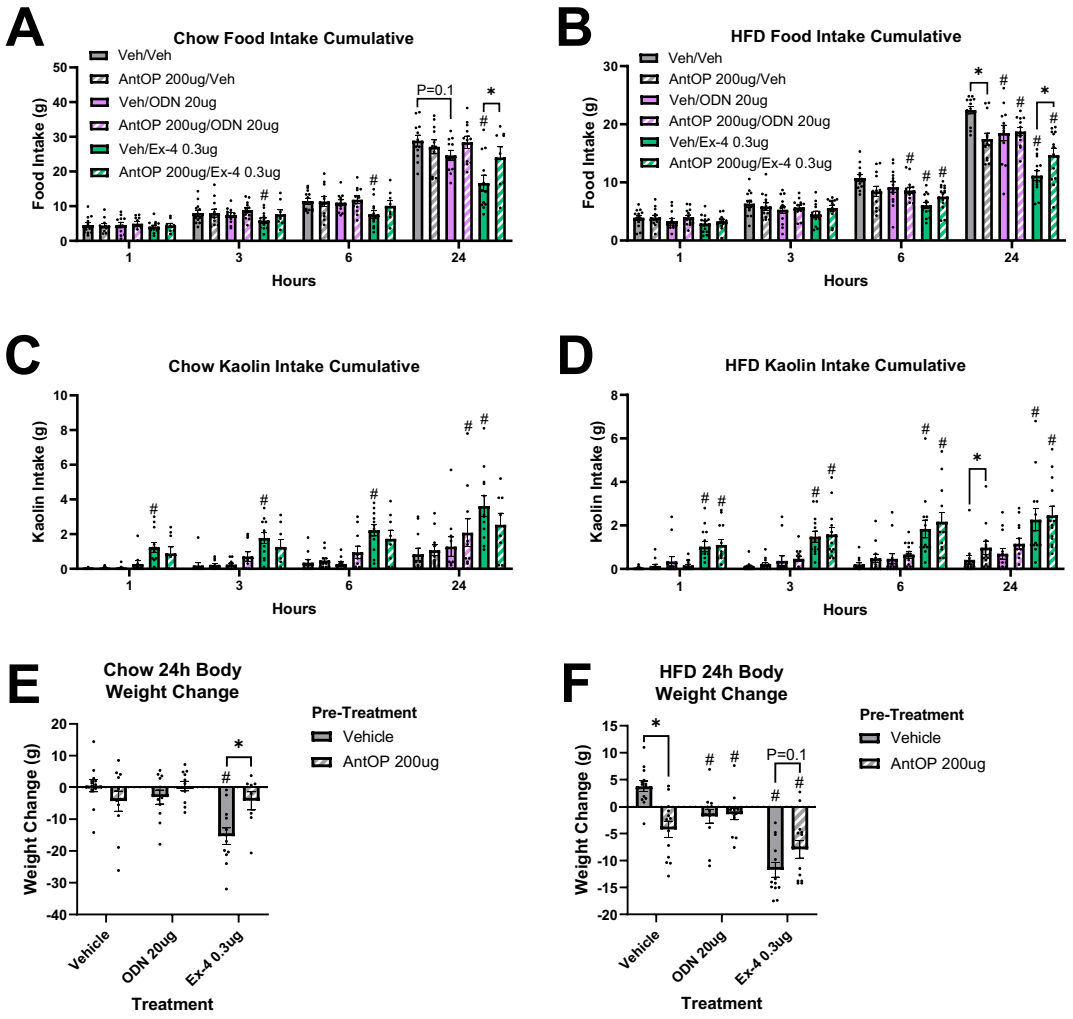

Figure 3-5. Pretreatment with an ODN antagonist attenuates central Ex-4-induced hypophagia. Rats were pretreated 4th ventricle with an ODN antagonist (AntOP 200 µg/2 µL) or vehicle followed by 4th ventricle treatment with ODN (20 µg/2 µL), Ex-4 (0.3 µg/2 µL), or vehicle. 24 hour food intake in chow (A) and HFD (B) fed rats, kaolin intake in chow (C) and HFD (D) fed rats, and body weight change in chow (E) and HFD (F) fed rats following treatments. # indicates difference from Veh/Veh (P=0.05). All data presented as mean ± SEM.

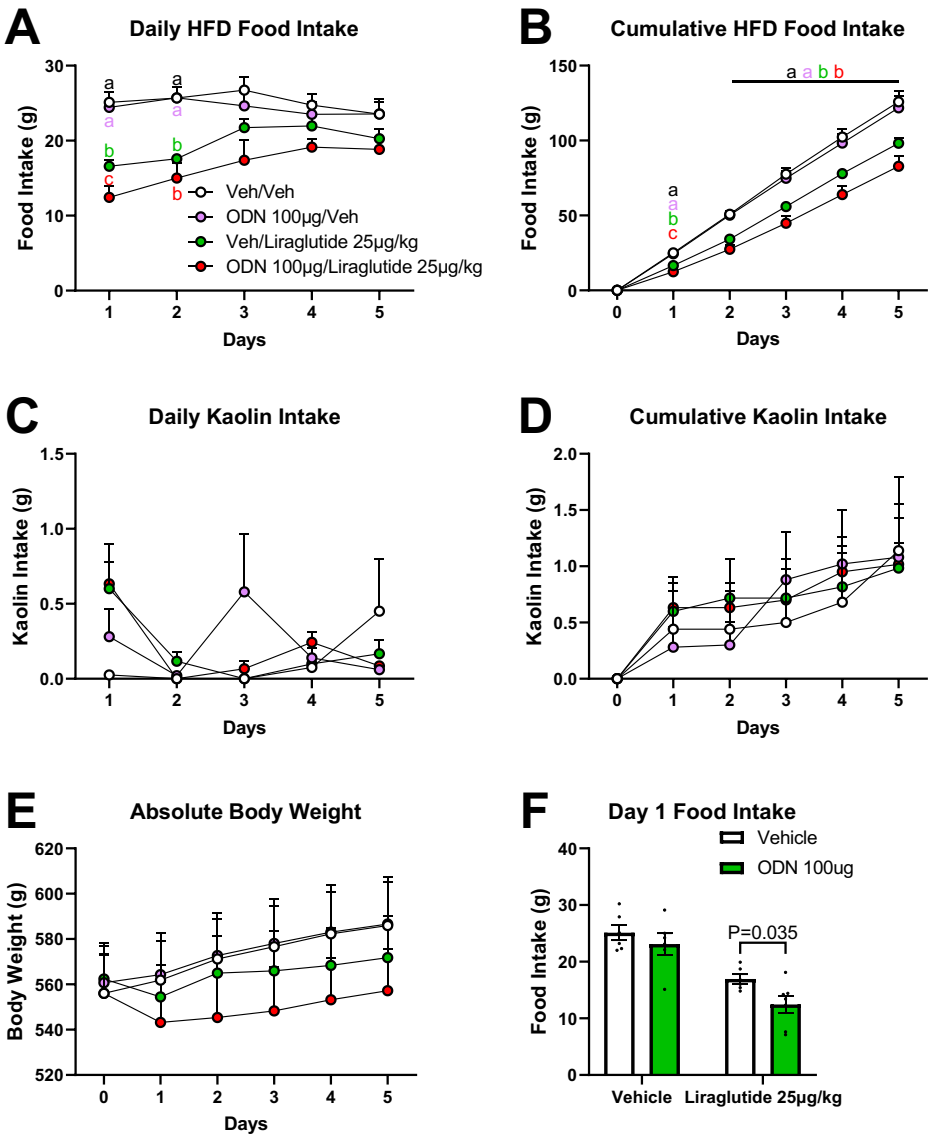

Figure 3-6. Five-day combined treatment with ODN enhances peripheral LIRA-induced hypophagia. Rats were treated 4th ventricle with ODN (100 µg/2 µL) or vehicle followed by intraperitoneal treatment with LIRA (25 µg/kg) or vehicle for 5 days. Daily (A) and cumulative (B) food intake, daily (C) and cumulative (D) kaolin intake, and daily body weight (E) in HFD-fed rats following treatments. Isolated day 1 food intake (F). All data presented as mean ± SEM.

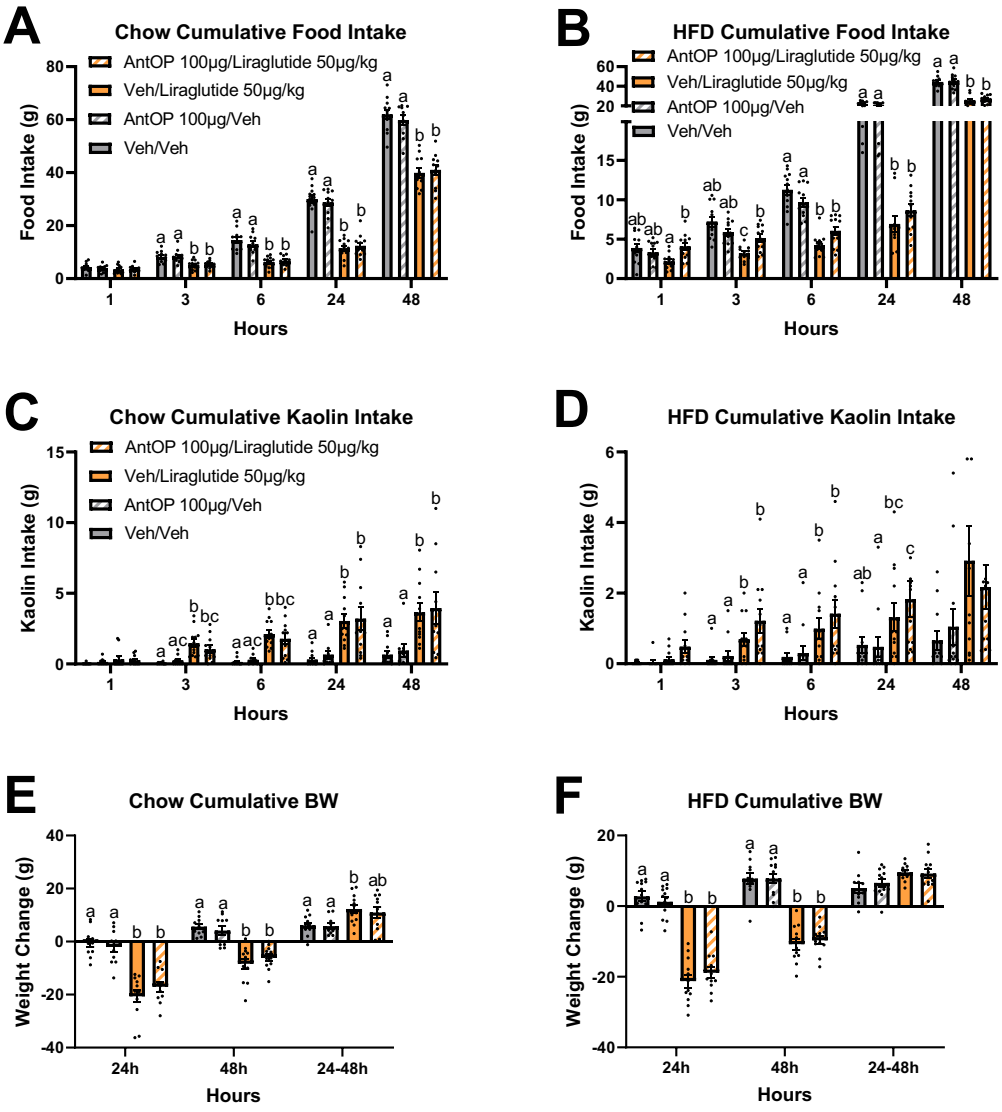

Figure 3-7. Pretreatment with an ODN antagonist attenuates peripheral LIRA-induced hypophagia. Rats were pretreated lateral ventricle with an ODN antagonist (AntOP 100 µg/2 µL) or vehicle followed by intraperitoneal treatment with LIRA (50 µg/kg), or vehicle. 48 hour food intake in chow (A) and HFD (B) fed rats, kaolin intake in chow (C) and HFD (D) fed rats, and body weight change in chow (E) and HFD (F) fed rats following treatments. All data presented as mean ± SEM.

3.1.5 FISH and IHC analysis of *f*Cy5-OP and *f*Cy5-TDN

Areas in the hindbrain associated with appetite control (AP/NTS) are imperative to this research because of their involvement in food intake and control of nausea/malaise. To visualize OP and TDN localization, an IP (15.5 µg/kg) or ICVI (1 µg/µL) injection of *f*Cy5-OP and *f*Cy5-TDN will be administered to rats, and coronal sections of the rat brainstem will be isolated to perform FISH with IHC.

3.2 References

1. Jérôme Leprince, Pierrick Gandolfo, Jean-Louis Thoumas, Christine Patte, Jean-Luc Fauchère, Hubert Vaudry, and Marie-Christine Tonon Structure−Activity Relationships of a Series of Analogues of the Octadecaneuropeptide ODN on Calcium Mobilization in Rat Astrocytes. *Journal of Medicinal Chemistry* 1998;41 (23), 4433-4438.

2. Garcia de Mateos-Verchère, J.; Leprince, J.; Tonon, M.-C.; Vaudry, H.; Costentin, J. The octadecaneuropeptide ODN induces anxiety in rodents: Possible involvement of a shorter biologically active fragment. *Peptides.* 1998;19, 841−848.

3. do Rego, JC., Orta, MH., Leprince, J. *et al.* Pharmacological Characterization of the Receptor Mediating the Anorexigenic Action of the Octadecaneuropeptide: Evidence for an Endozepinergic Tone Regulating Food Intake. *Neuropsychopharmacol* 2007;32, 1641–1648.

4. Masmoudi-Kouki O, Namsi A, Hamdi Y, Bahdoudi S, Ghouili I, Chuquet J, Leprince J, Lefranc B, Ghrairi T, Tonon M-C, Lizard G and Vaudry D. Cytoprotective and Neurotrophic Effects of Octadecaneuropeptide (ODN) in *in vitro* and *in vivo* Models of Neurodegenerative Diseases. *Front. Endocrinol.* 2020;11:566026.

5. Guillebaud F, Girardet C, Abysique A, Gaigé S, Barbouche R, Verneuil J, Jean A, Leprince J, Tonon M-C, Dallaporta M, Lebrun B and Troadec J-D. Glial Endozepines Inhibit Feeding-Related Autonomic Functions by Acting at the Brainstem Level. *Front. Neurosci*. 2017;11:308.

Chapter 4: Novel peptide antagonists of GPR75

The work on this project has resulted in the following patent:

Chichura, K. S., Geisler, C. E., Hayes, M. R., Doyle, R. P. *Novel GPR75 ligands for controlling food intake, energy expenditure, body weight and treatment of obesity and metabolic diseases*. Provisional Patent. Filed 08/2022.

4.1 Orphan GPCRs, specifically GPR75

G-protein coupled receptors (GPCRs) are common biological targets in drug discovery.[1] There are over 140 GPCRs with unknown endogenous ligands,[2] which are termed orphan GPCRs. G-protein receptor 75 (GPR75) is a member of the G protein-coupled cell surface receptor family.[3] Many reports have linked GPR75 with obesity and metabolic diseases.[4-7] A study in *GPR75* knockout (KO) mice suggests that inhibiting GPR75 may decrease food intake and body fat while improving glucose tolerance and insulin sensitivity.[8]

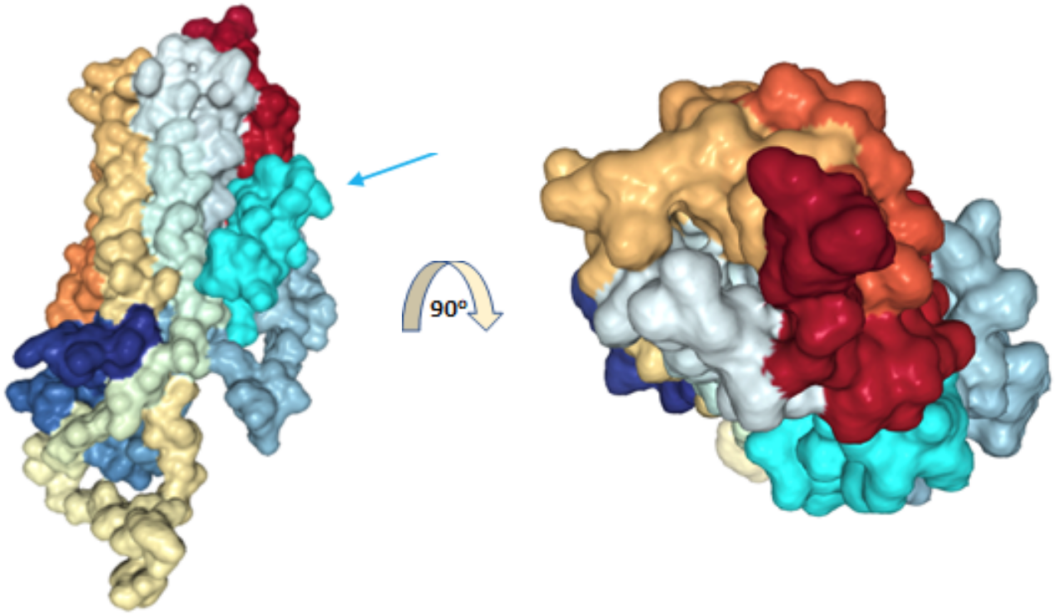

Figure 4-1. Blind SU75-36/GPR75 receptor *in silico* docking using HPEPDOCK. SU75-36 (aqua marine; see arrow) surface binding of GPR75 consistent with SPR binding (Figure 4-2). Docking score 0.884.

4.1.1 SPR experiments with GPR75 and hGLP-1R

The binding of SU75-36 was analyzed using a Surface Plasmon Resonance (SPR) assay, which tracked binding of SU75-36 at GPR75 over time. The assay indicated that SU75-36 binds to GPR75 with a K_D of 7.76 μM. This assay was further analyzed using Nicoya

OpenSPR software which showed the best fit parameters using a one-to-one model. K_D was observed to be 7.76 x 10^{-6} M (7.76 µM). The SPR assay was duplicated to determine the binding of SU75-37 at GPR75 over time. The assay indicated that SU75-37 binds to GPR75 with a K_D of 23.8 µM. As with SU75-36, this assay was further analyzed using Nicoya OpenSPR software. K_D was observed to be 2.38 x 10^{-5} M (23.8 µM). To confirm the specificity of the peptide ligand binding, the SPR assay was duplicated for both SU75-36 and SU75-37 to determine binding at hGLP-1R with Ex-4 and ODN used as a positive and negative controls, respectively. SU75-37 did not bind to the hGLP-1R receptor. Although SU75-36 showed the ability to bind the hGLP-1R receptor, the measured binding constant K_D of 182 µM is indicative of weak binding.

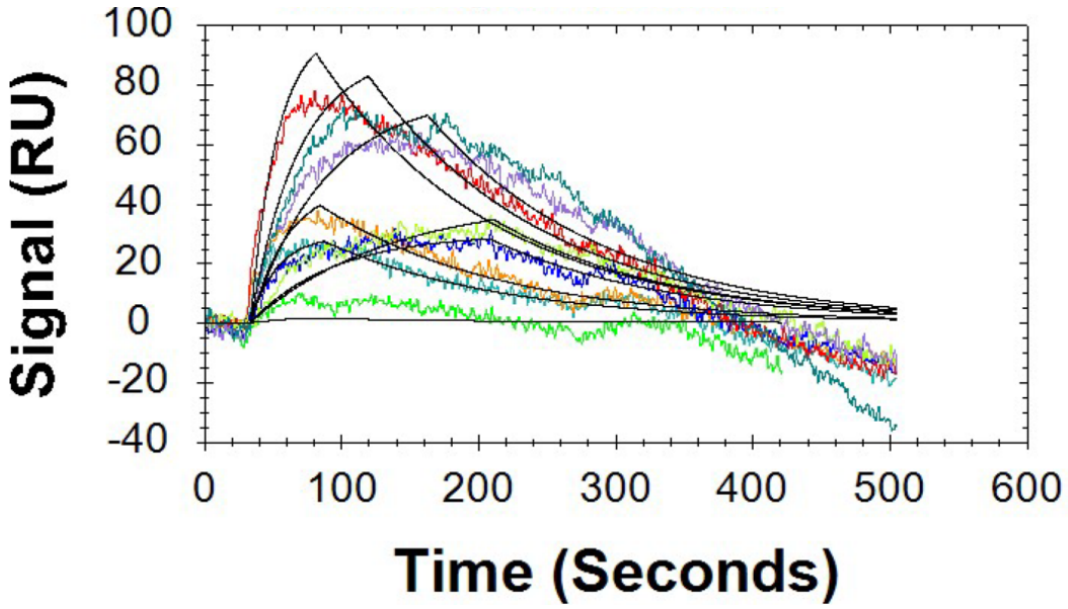

Figure 4-2. SPR assay tracking SU75-36 binding at GPR75. SU75-36 binds to GPR75 with a K_D of 7.76 µM.

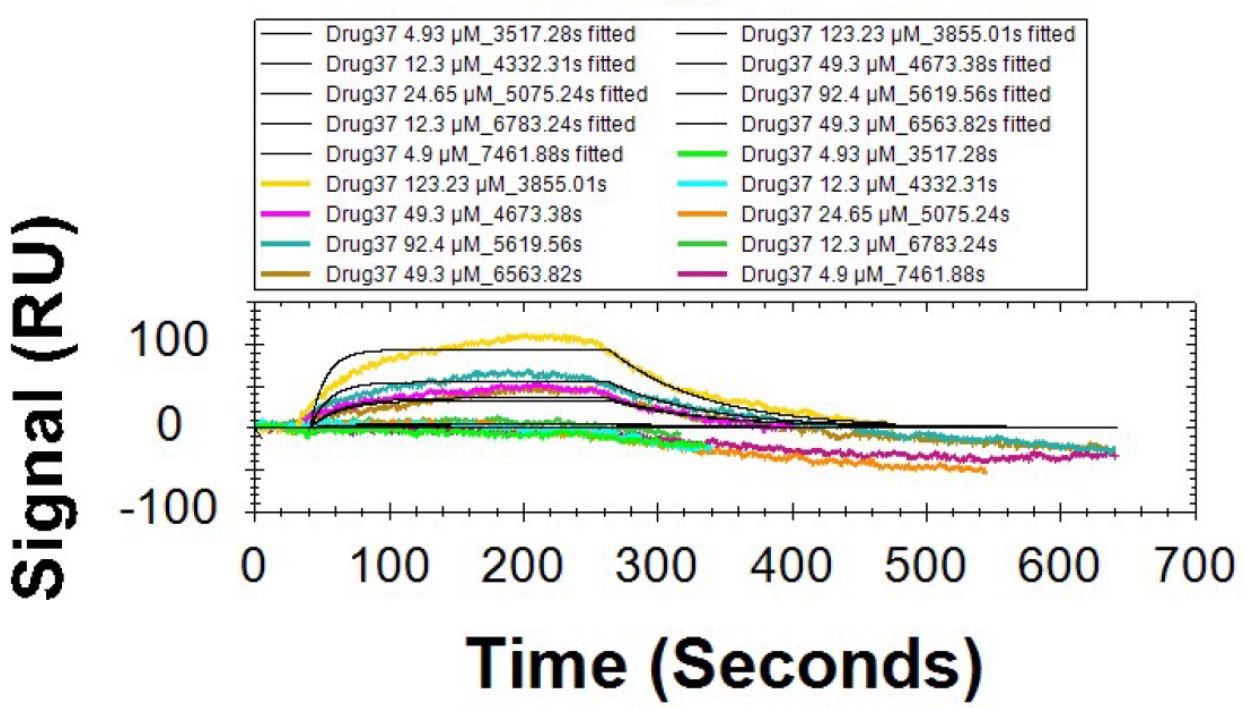

Figure 4-3. SPR assay tracking SU75-37 binding at GPR75. SU75-37 binds to GPR75 with a K_D of 23.8 µM.

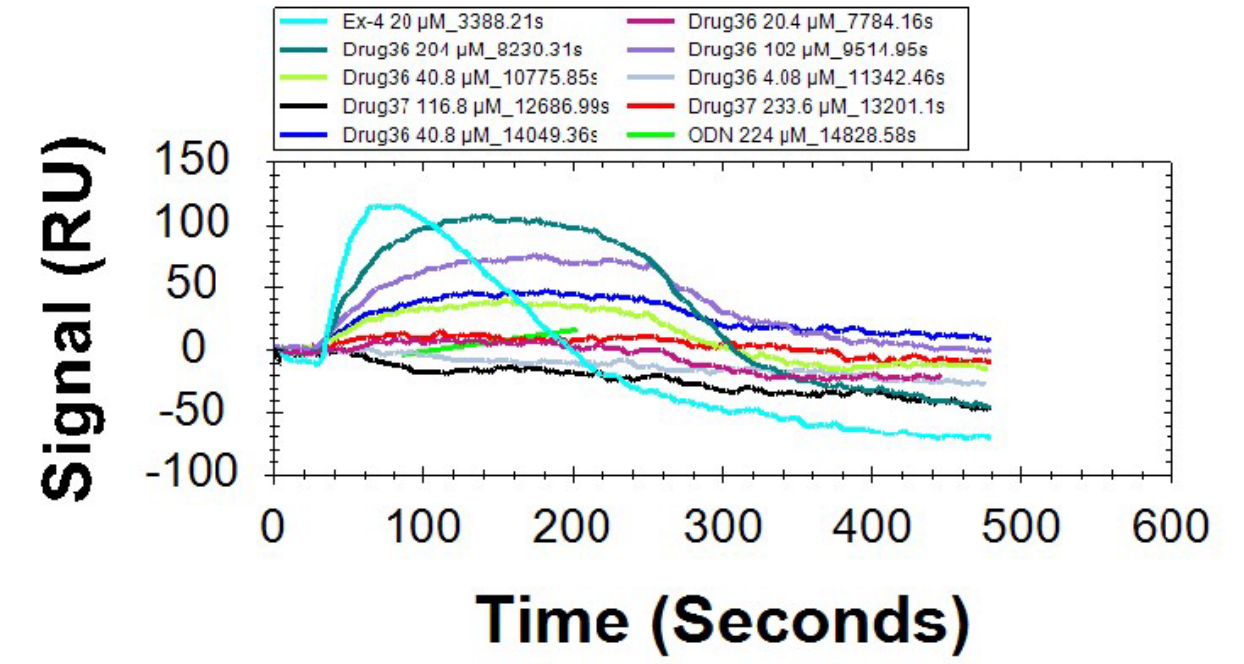

Figure 4-4. SPR assay comparing SU75-36 binding at hGLP-1R with positive Ex-4 control, negative ODN control, and SU75-37. SU75-37 does not bind at the hGLP-1R, akin with its design.

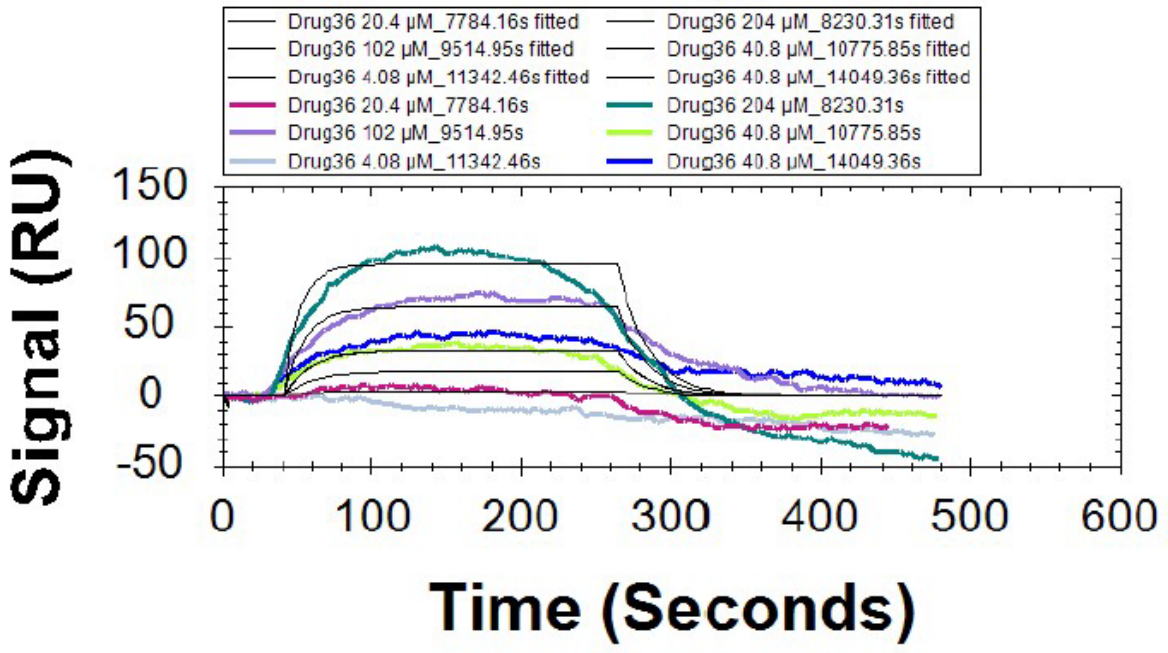

Figure 4-5. SPR assay tracking SU75-36 binding at hGLP-1R. SU75-36 binds to GPR75 with a K_D of 182 µM.

4.1.2 Design and synthesis of peptide-based antagonists of GPR75

4.1.2.1 SU75-36 and SU75-37

SU75-36 is a chimeric peptide that contains a GLP-1R agonizing portion and a C-terminal region mimicking octadecaneuropeptide (ODN). This peptide was designed to allow us to analyze GLP-1R-based metabolic effects *in vivo* as well as effects downstream of GLP-1R signaling. SU75-37 has the same C-terminal sequence as SU75-36, but its N-terminal end has the first four residues removed to terminate activity GLP-1R. Both peptides were synthesized on the peptide synthesizer and purified on an Agilent 1200 series HPLC tracking at 280 nm to >95% purity, as confirmed by HPLC.

Figure 4-6. Peptide sequences of novel GPR75 antagonists. Peptides have been synthesized, confirmed, and purified prior to testing. Lowercase letter indicates a D-amino acid. Peptides are C-terminally amidated.

4.1.2.2 *f*Cy5-SU75-36 and *f*Cy5-SU75-37

The fluorescent analogs of *f*Cy5-SU75-36 and *f*Cy5-SU75-37 were synthesized using Copper-free CLICK chemistry. First, SU75-36 and SU75-37 analogs with Fmoc-Lys(N_3)-OH (ChemPep Inc.) substitutions in the 25th and 21st positions, respectively, were synthesized on the peptide synthesizer. The peptides were purified using an Agilent 1200 series HPLC tracking at 280 nm. The peptides were confirmed by HPLC and MALDI-MS and mixed at a 1:1 mole ratio with sulfo-Cy5 DBCO (Lumiprobe) for 16 hours at RT in 4:1 DMF:H_2O. The excitation/emission profile was analyzed using a fluorimeter, and the fluorescent peptides were confirmed by MALDI-MS and HPLC tracked at 600 nm. Any excess sulfo-Cy5 DBCO was removed during purification by HPLC.

4.1.2.3 Secondary structure analysis of SU75-36 and SU75-37

SU75-36 and SU75-37 were dissolved at 40 μM in 0.9% saline and analyzed using a Chirascan VX (Applied Photophysics) spectrophotometer at a 250-200 nm measurement range, 100 nm/min scanning speed, 1 nm bandwidth, 4 second response time, and 1.0 nm data pitch. The percent helicities of SU75-36 and SU75-37 are 20.9% and 21.3%, respectively.

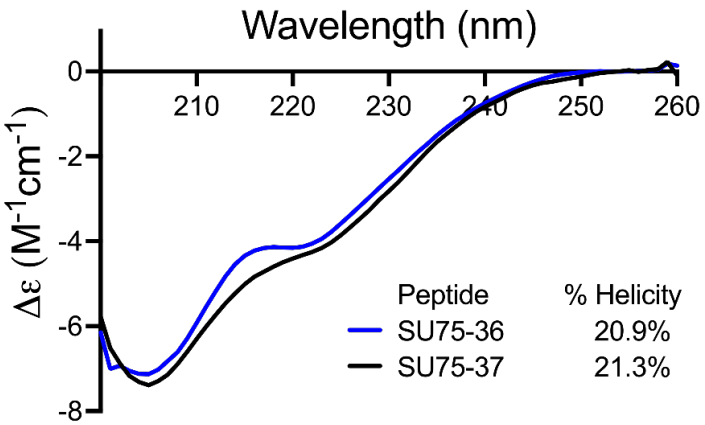

Figure 4-7. Folded state analysis of SU75-36 and SU75-37. Peptides were analyzed by CD spectroscopy. Percent helicities were calculated as 20.9% for SU75-36 and 21.3% for SU75-37.

4.1.3 Metabolic effects of SU75-36 and SU75-37 *in vivo*

Experiments to track the metabolic effects resulting from administration of SU75-36 and SU75-37 included intramuscular injections into the 4th ventricle of DIO rats. One group of rats was administered a vehicle without a GPR75 inhibitor as a negative control. The FI of each rat was observed 1, 3, 6, and 24 hours after administration of the GPR75 inhibitor. Rats were weighed at the beginning of the experiment and 24 hours after administration of the GPR75 inhibitor to ultimately calculate a change in BW. Rats that were administered SU75-36 and SU75-37 showed a further decrease in FI and a significant decrease in BW when compared to the other groups.

An additional experiment in DIO rats monitored the same FI and BW changes mentioned previously, and it simultaneously tracked kaolin intake which is an established model of nausea/malaise. There was an absence of kaolin intake in rats administered these novel antagonists of GPR75. This indicates that SU75-36 and SU75-37 successfully suppress energy balance without producing nausea/malaise.

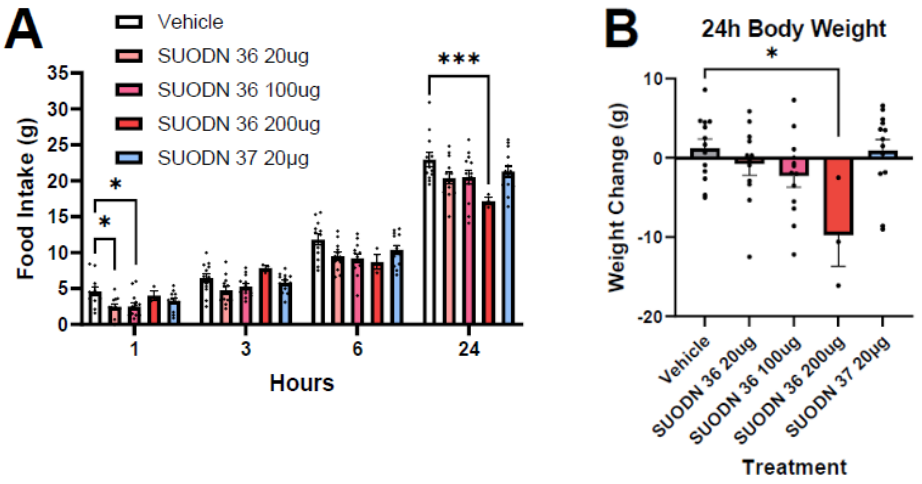

Figure 4-8. 4th Ventricle GPR75 Ligands Suppress Food Intake and Body Weight in HFD-fed rats. Effect of 4th ventricle SUODN-36 (20, 100, or 200 µg/2 µL in aCSF) and SUODN-37 (20 µg/2 µL in aCSF) treatment on 24h food intake (A) and body weight change (B) in HFD fed rats. All data presented as mean ± SEM.

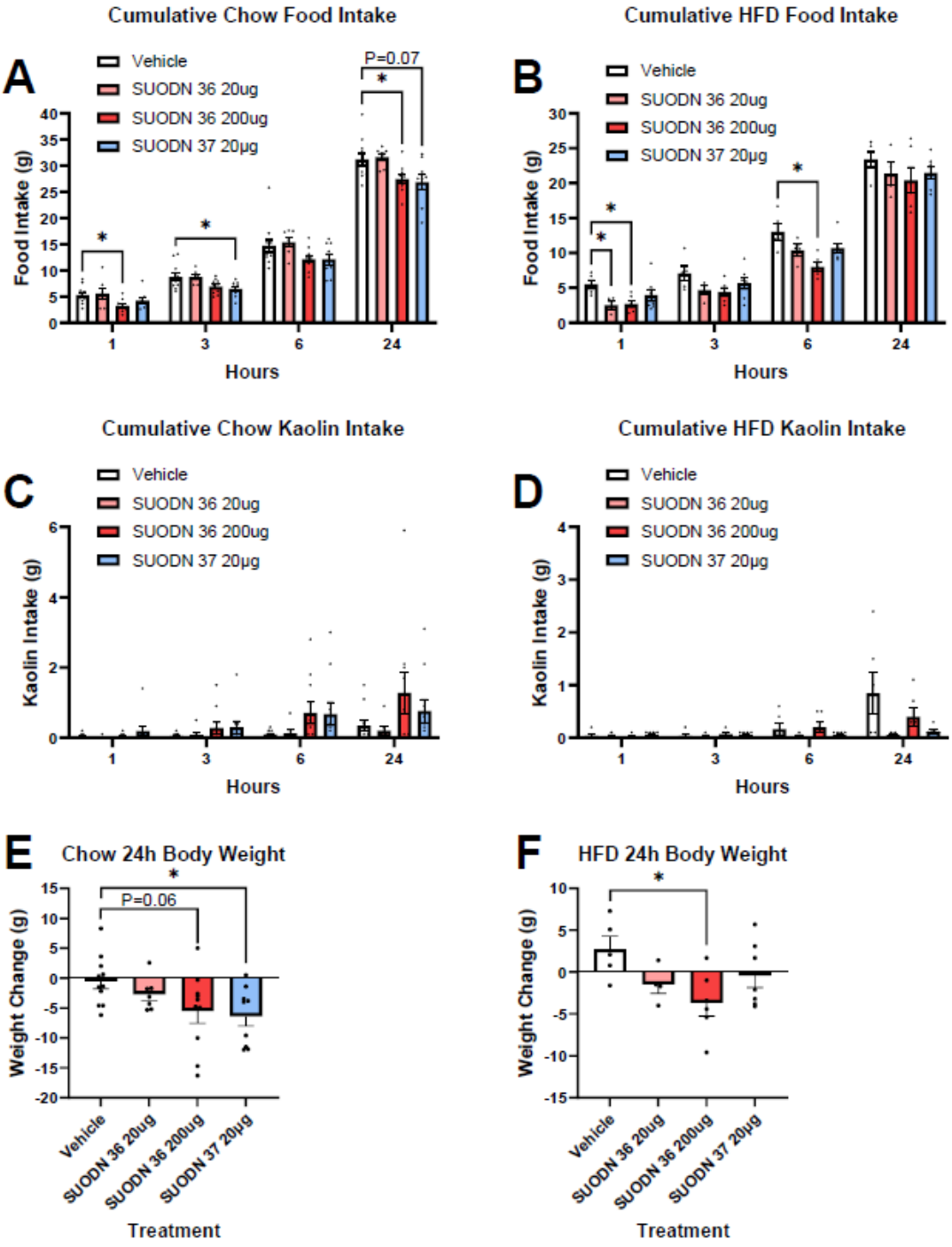

Figure 4-9. Lateral ventricle GPR75 ligands injection suppresses food intake and body weight in chow and HFD-fed rats. Effect of lateral ventricle SUODN-36 (20 or 100 µg/2µL in aCSF) or SUODON-37 (20µg/2µL in aCSF) treatment on 24h food intake in chow- (A) and HFD-fed rats (B), kaolin intake in chow (C) and HFD-fed rats (D) and body weight change in chow (E) and HFD-fed rats (F). All data presented as mean ± SEM.

4.1.4 FISH and IHC analysis of *f*Cy5-SU75-36 and *f*Cy5-SU75-37

Areas in the hindbrain associated with appetite control (AP/NTS) are imperative to this research because of their involvement in food intake and control of nausea/malaise. To visualize SU75-36 and SU75-37 localization, an IP (15.5 µg/kg) or ICVI (1 µg/µL) injection of *f*Cy5-SU75-36 and *f*Cy5-SU75-37 will be administered to rats, and coronal sections of the rat brainstem will be isolated to perform FISH with IHC.

4.2 References

1. Stockert, J. A. & Devi, L. A. Advancements in therapeutically targeting orphan GPCRs. *Front. Pharmacol.* 2015;6.

2. Tang, Xl., Wang, Y., Li, Dl. *et al.* Orphan G protein-coupled receptors (GPCRs): biological functions and potential drug targets. *Acta Pharmacol Sin* 2012;33, 363–371.

3. https://www.ncbi.nlm.nih.gov/gene?Db=gene&Cmd=ShowDetailView&TermToSearch=10936.

4. Akbari P, Gilani A, Sequencing of 640,000 exomes identifies *GPR75* variants associated with protection from obesity. *Science*. 2021;373(6550):eabf8683.

5. Hossain, S., DIRICE, E.; 244-LB: GPR75 Ablation Protects against Diet-Induced Obesity, Inflammation, and Insulin Resistance. *Diabetes*. 2022; 71 (Supplement_1): 244–LB.

6. Hossain S, Gilani A, Pascale J, Villegas E, Diegisser D, Agostinucci K, Kulaprathazhe MM, Dirice E, Garcia V, Schwartzman ML. *Gpr75*-deficient mice are protected from high-fat diet-induced obesity. Obesity (Silver Spring). 2023

7. Murtaza, B., Asghar, F., Patoli D. GPR75: An exciting new target in metabolic syndrome and related disorders. *Biochimie*. 2022, 195, 19-26.

8. Powell, DR, *et al*. Mice Lacking *Gpr75* are Hypophagic and Thin. *Diabetes, Metabolic Syndrome and Obesity*, 2022;15, 45-58.

Chapter 5: Experimental methods and materials

5.1 General methods

The design, syntheses, and all purification of peptides was completed at Syracuse University by the author, unless otherwise noted. *In silico* modeling software (HPEPDOCK and MOE 2.0) was used to evaluate docking simulations between ligands and receptors. Peptides designed using the 20 natural amino acids and few unnatural amino acids can be programmed into the Liberty Blue peptide synthesizer. The automated synthesizer can synthesize peptides between 5 and 60 amino acid residues. Crude peptides were typically 70% pure and require further purification in-house using an Agilent 1200 series HPLC or a larger-scale Biotage instrument. Determination of the molecular weight of the peptides and side products is done in-house using an ESI-MS or MALDI-TOF MS. Some of the necessary screening is completed at Syracuse University using a Nicoya SPR instrument to determine binding affinity. *In vitro* assays measuring activity at relevant receptors were completed by Dr. Oleg Chepurny at SUNY Upstate Medical University in the lab of Prof. George Holz. Any data measuring ISR in pancreatic islets or glucose uptake in muscle is done at the University of Washington. *In vivo* experiments are done outside of Syracuse University by our collaborators at Seattle Children's Research Institute or the University of Pennsylvania.

5.2 Syntheses of peptides via SPPS

5.2.1 Synthesis of chimeric dual/triple agonists of GLP-1R and NPYR(s)

All peptides were synthesized in-house by the author using solid-phase peptide synthesis performed on ProTide Rink amide resin using a microwave-assisted CEM Liberty Blue

peptide synthesizer (Matthews, NC, USA). Fmoc-protected amino acids were coupled to the resin using Oxyma Pure (0.25 M) and *N, N'*-diisopropyl carbodiimide (0.125 M) as the activator and activator base, respectively. Fmoc was removed between couplings with 20% piperidine. Global deprotection and cleavage of the peptides from the solid-support resin was achieved using a CEM Razor instrument via a 40-minute incubation at 40°C in a mixture of 95% trifluoroacetic acid, 2.5% triisopropylsilane, and 2.5% water. The peptides were precipitated with cold (4°C) diethyl ether.

5.2.1.1 EP45

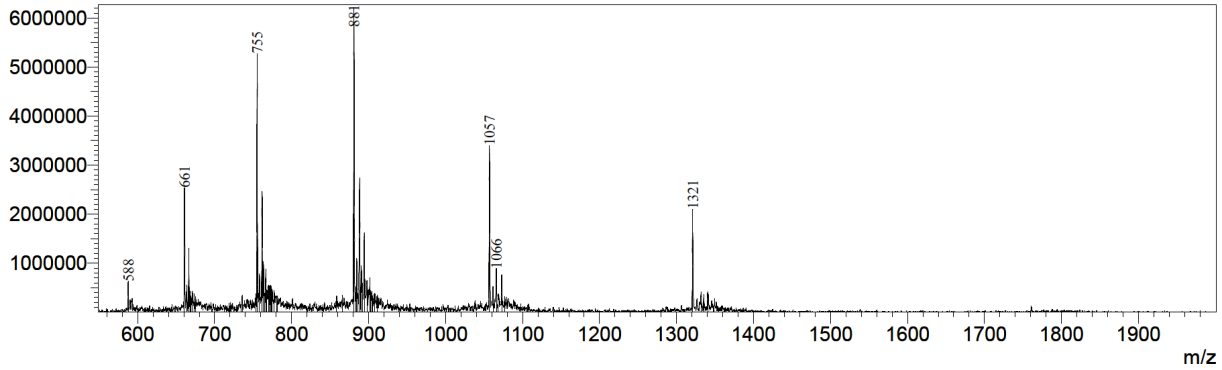

Figure 5-1. ESI-MS trace of EP45, expected *m/z* = 5280, observed *m/z* = 1321 $[M+4H]^{+4}$, 1057 $[M+5H]^{+5}$, 881 $[M+6H]^{+6}$, 755 $[M+7H]^{+7}$, 661 $[M+8H]^{+8}$.

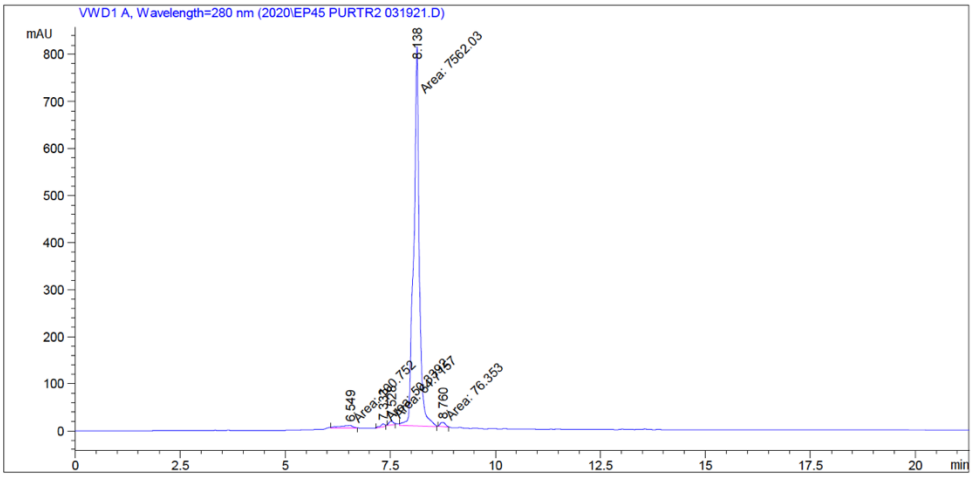

Figure 5-2. RP-HPLC purity trace showing product at 8.138 min.

5.2.1.2 GEP44

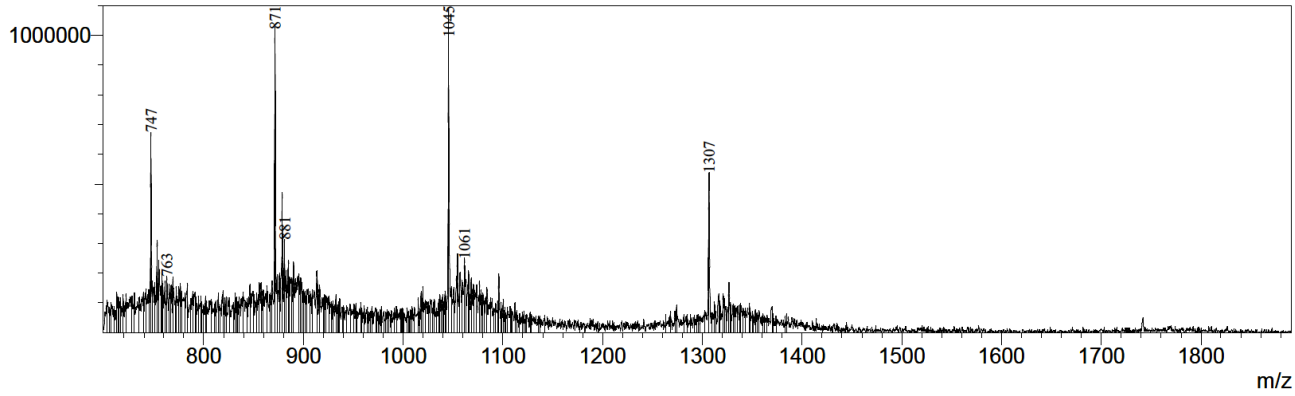

Figure 5-3. ESI-MS trace of GEP44, expected *m/z* = 5198, observed *m/z* = 1307 $[M+4H]^{+4}$, 1045 $[M+5H]^{+5}$, 872 $[M+6H]^{+6}$, 747 $[M+7H]^{+7}$.

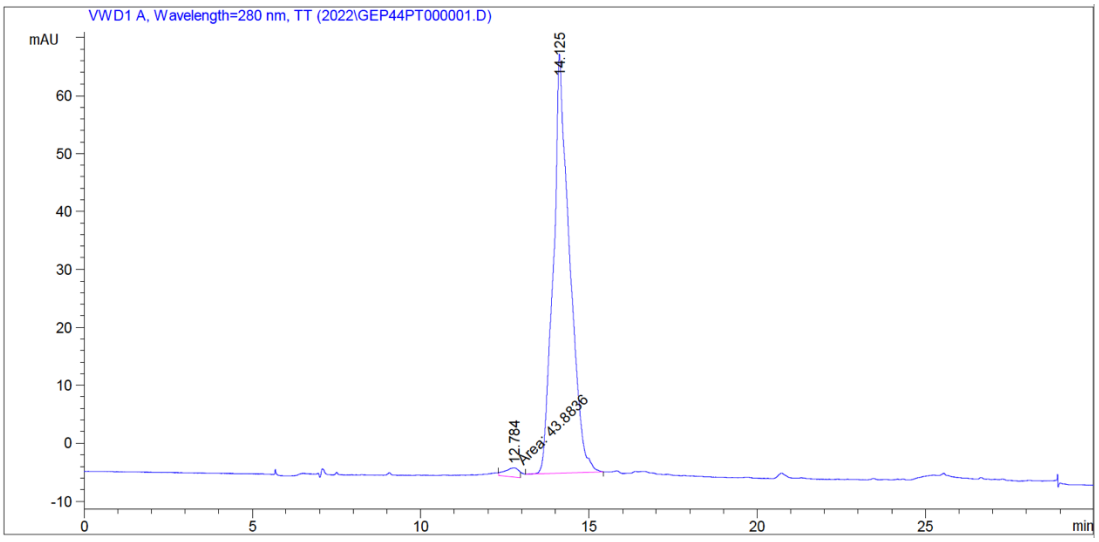

Figure 5-4. RP-HPLC purity trace showing product at 14.125 min.

5.2.1.3 GEP03

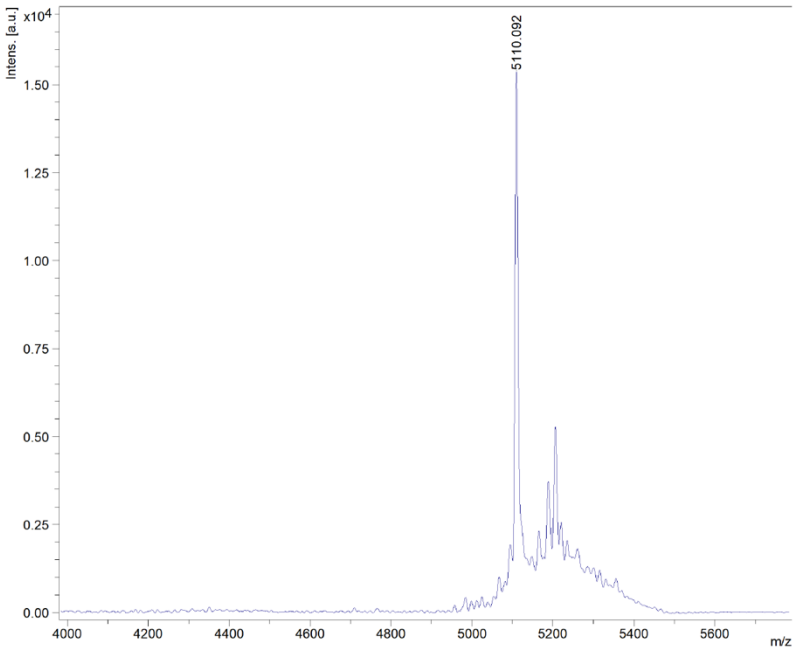

Figure 5-5. MALDI-TOF MS trace of GEP03, expected *m/z* = 5109, observed *m/z* = 5110.

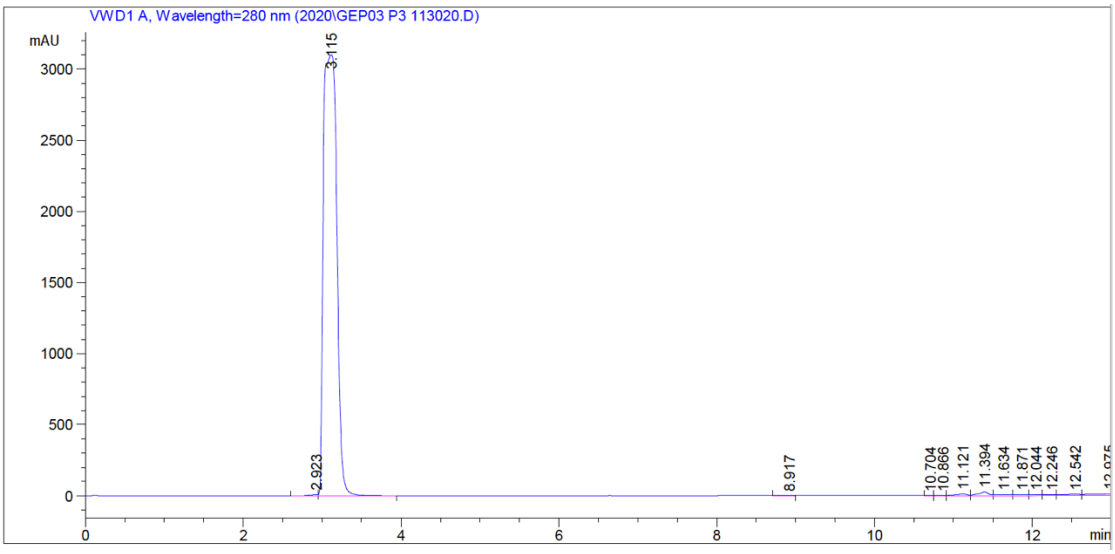

Figure 5-6. RP-HPLC purity trace showing product at 3.115 min.

5.2.1.4 GEP04

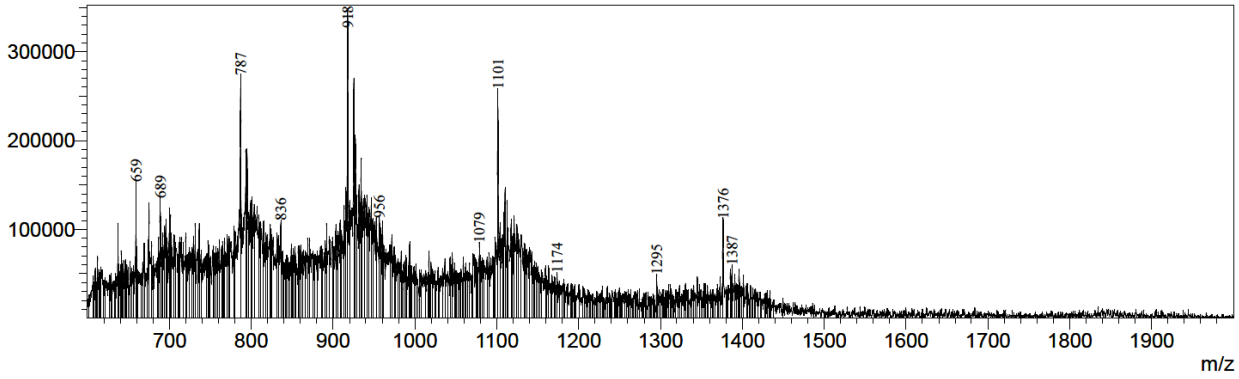

Figure 5-7. ESI-MS trace of GEP04, expected *m/z* = 5500, observed *m/z* = 1376 $[M+4H]^{+4}$, 1101 $[M+5H]^{+5}$, 918 $[M+6H]^{+6}$, 787 $[M+7H]^{+7}$.

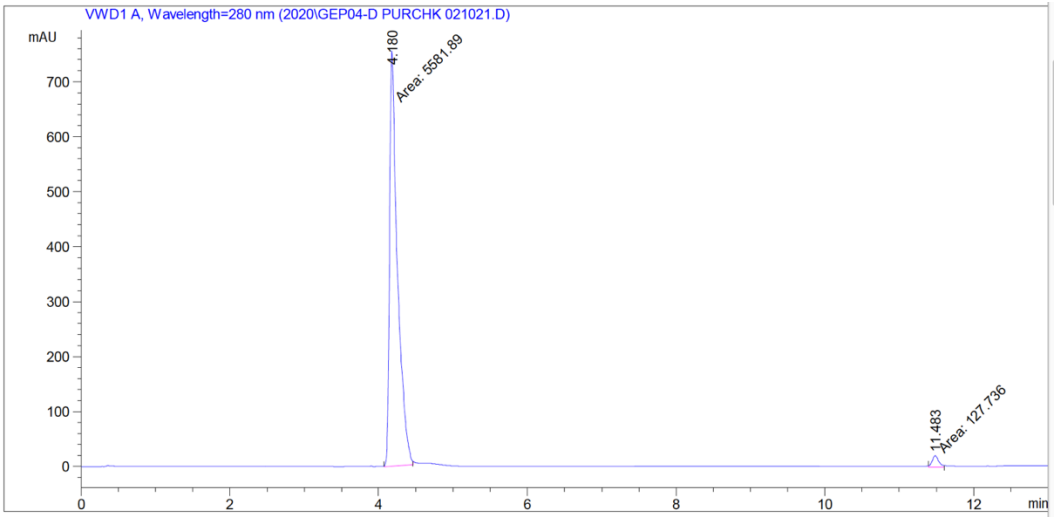

Figure 5-8. RP-HPLC purity trace showing product at 4.180 min.

5.2.1.5 GEP06

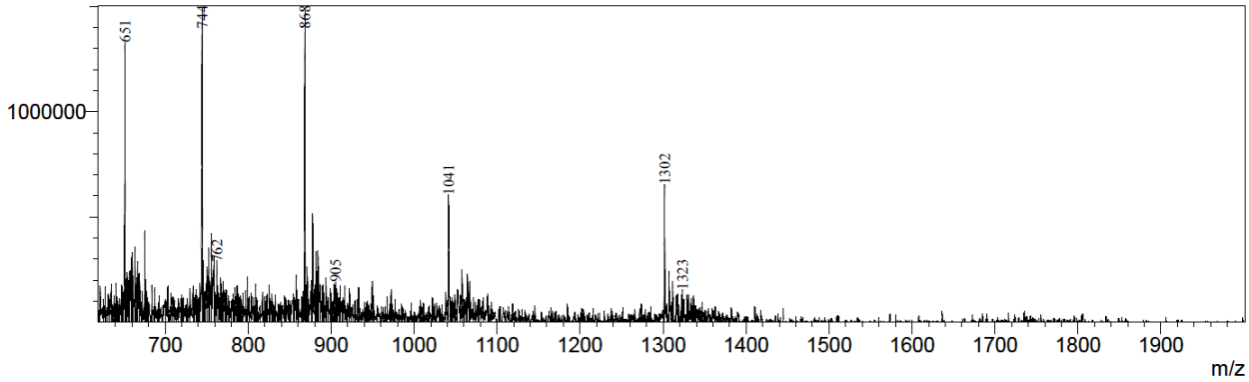

Figure 5-9. ESI-MS trace of GEP06, expected *m/z* = 5202, observed *m/z* = 1302 $[M+4H]^{+4}$, 1041 $[M+5H]^{+5}$, 868 $[M+6H]^{+6}$, 744 $[M+7H]^{+7}$, 651 $[M+8H]^{+8}$.

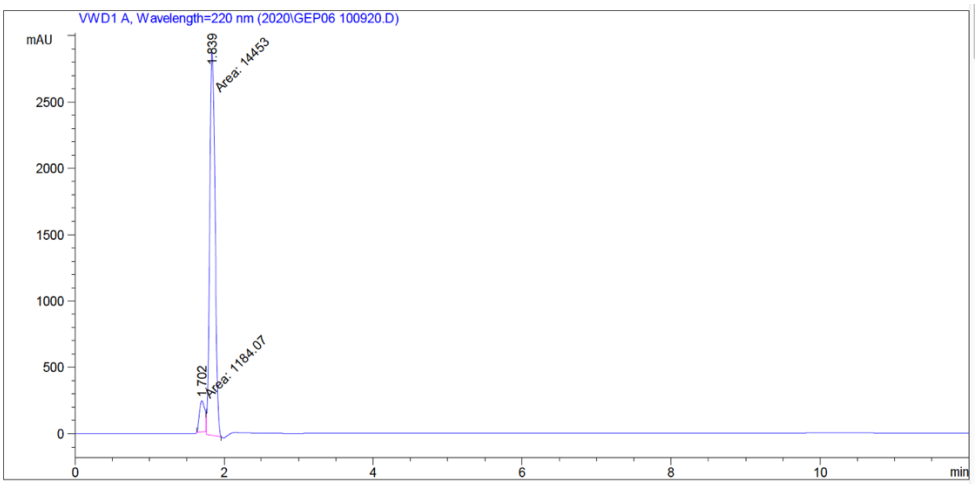

Figure 5-10. RP-HPLC purity trace showing product at 1.839 min.

5.2.1.6 GEP08

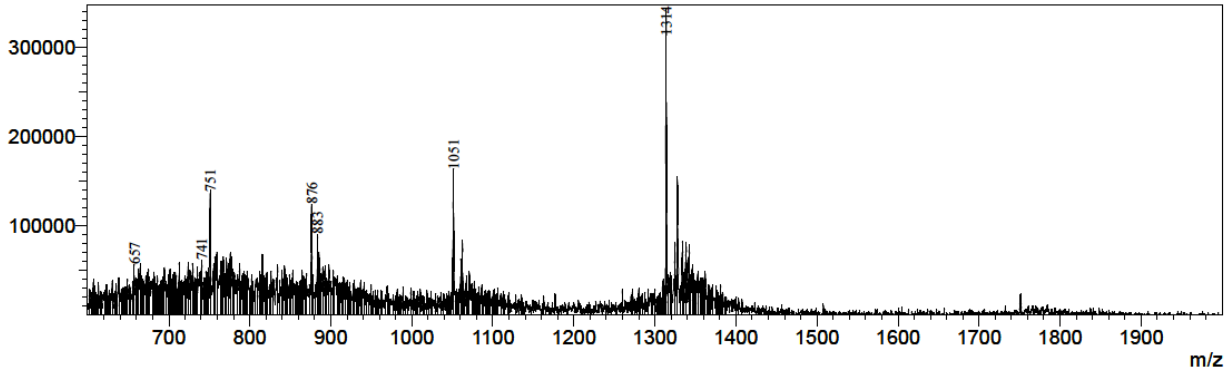

Figure 5-11. ESI-MS trace of GEP08, expected *m/z* = 5250, observed *m/z* = 1314 $[M+4H]^{+4}$, 1051 $[M+5H]^{+5}$, 876 $[M+6H]^{+6}$, 751 $[M+7H]^{+7}$, 657 $[M+8H]^{+8}$.

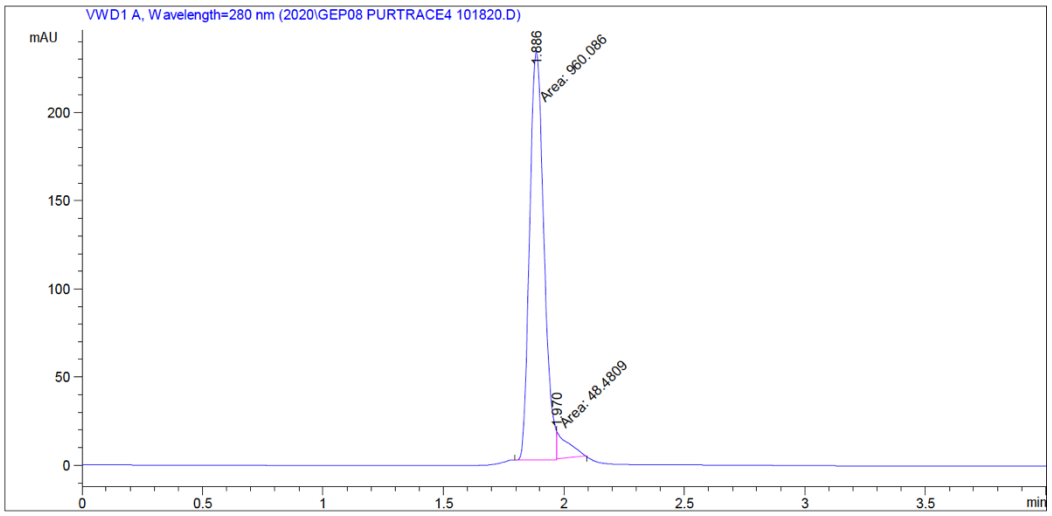

Figure 5-12. RP-HPLC purity trace showing product at 1.886 min.

5.2.1.11 GEP09

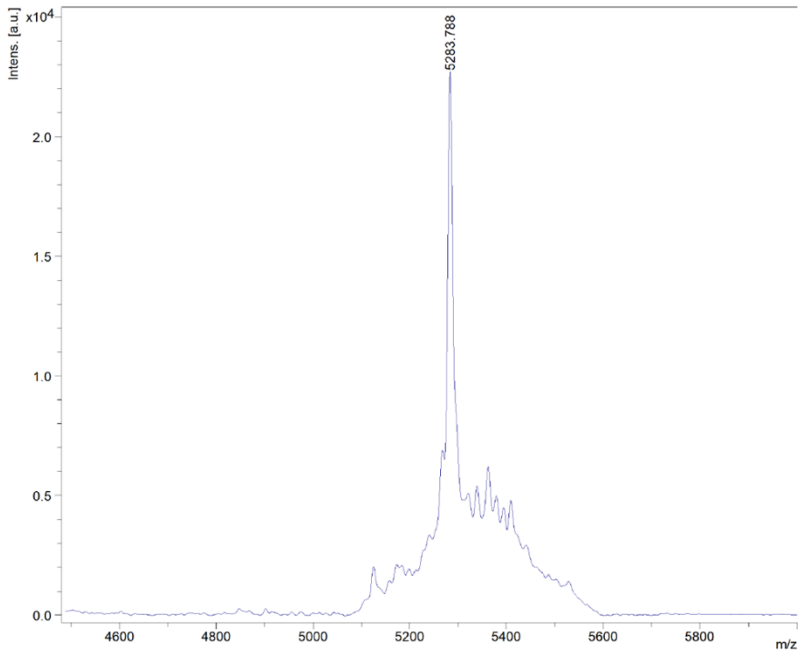

Figure 5-13. MALDI-TOF MS trace of GEP09, expected *m/z* = 5283, observed *m/z* = 5283.

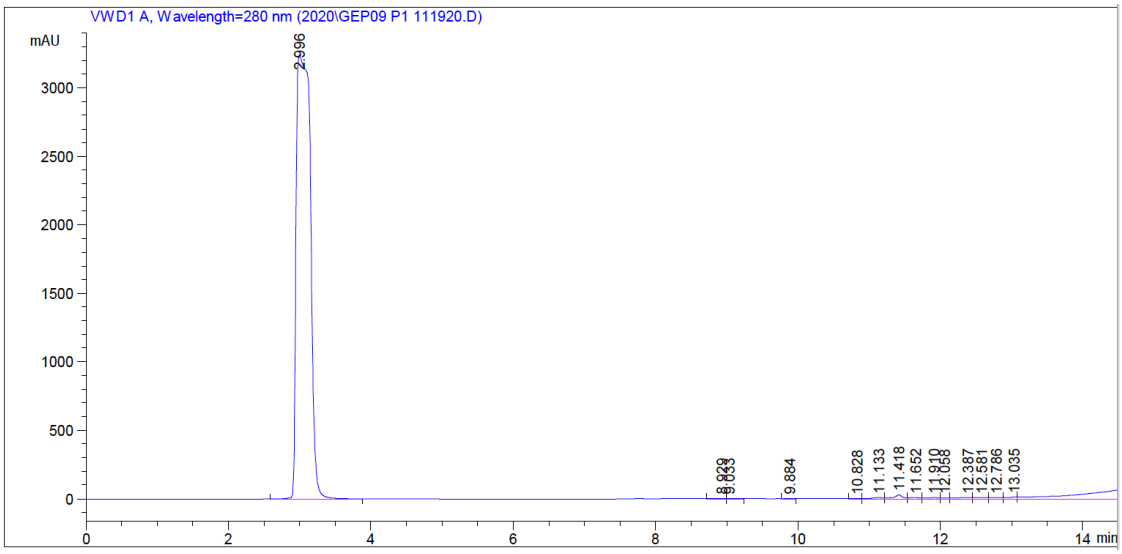

Figure 5-14. RP-HPLC purity trace showing product at 2.996 min.

5.2.1.7 GEP10

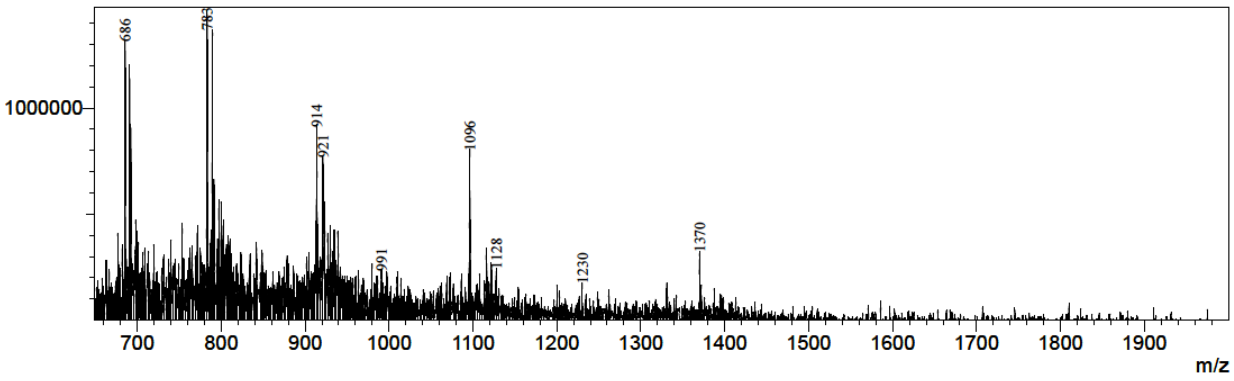

Figure 5-15. ESI-MS trace of GEP10, expected *m/z* = 5475, observed *m/z* = 1314 $[M+4H]^{+4}$, 1096 $[M+5H]^{+5}$, 914 $[M+6H]^{+6}$, 783 $[M+7H]^{+7}$, 686 $[M+8H]^{+8}$.

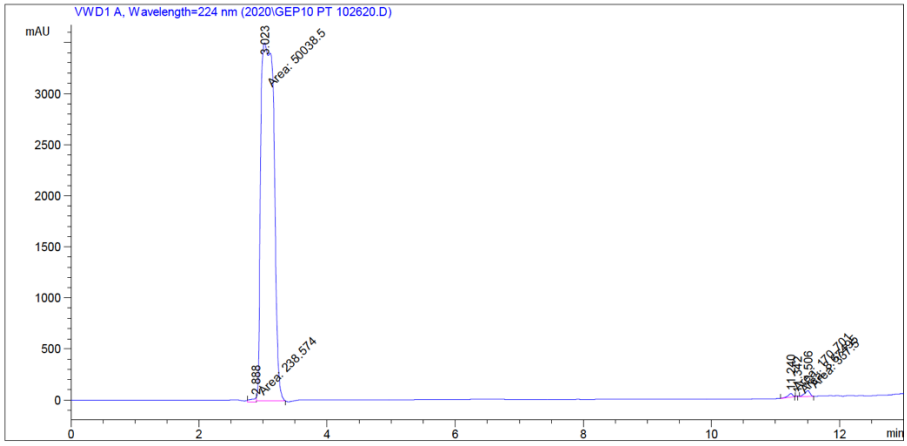

Figure 5-16. RP-HPLC purity trace showing product at 3.023 min.

5.2.1.8 GEP12

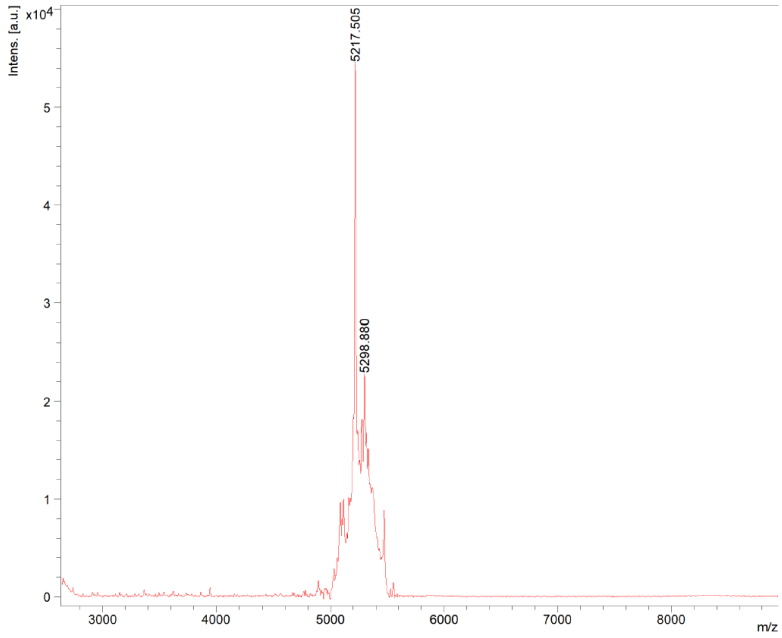

Figure 5-17. MALDI-TOF MS trace of GEP12, expected *m/z* = 5216.76, observed *m/z* = 5217.

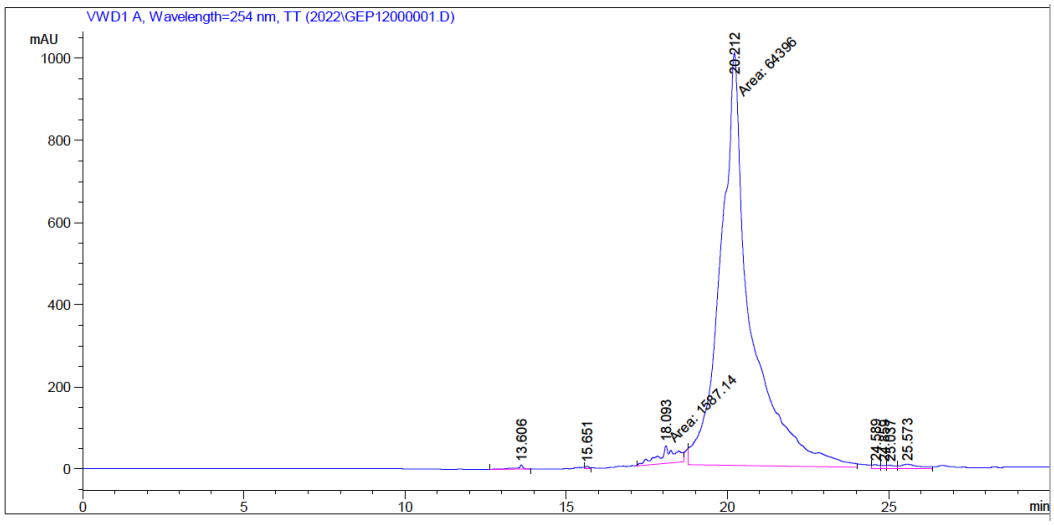

Figure 5-18. RP-HPLC purity trace showing product at 20.212 min.

5.2.1.9 GEP44 W38

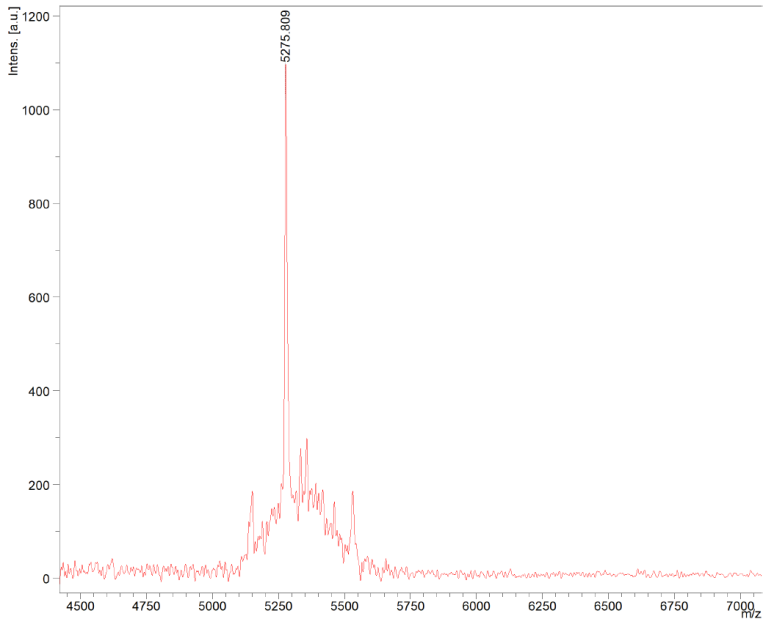

Figure 5-19. MALDI-TOF MS trace of GEP44 W38, expected *m/z* = 5270.79, observed *m/z* = 5275.

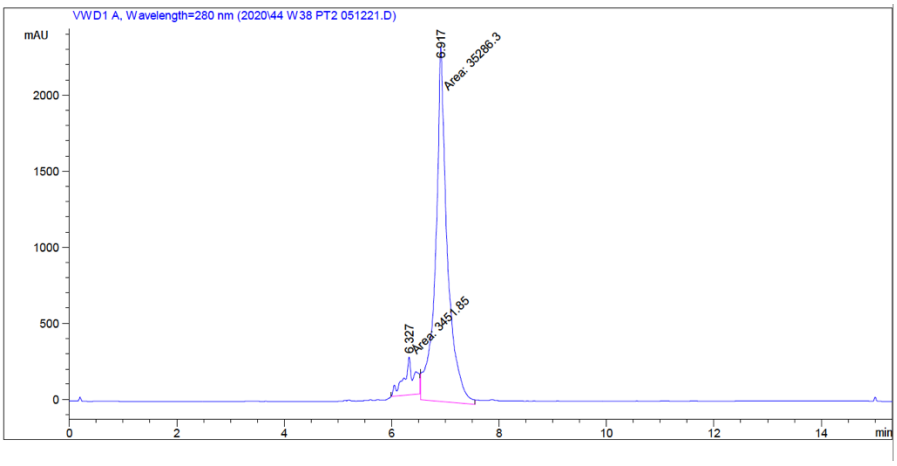

Figure 5-20. RP-HPLC purity trace showing product at 6.917 min.

5.2.1.10 GEP44 W38 L39

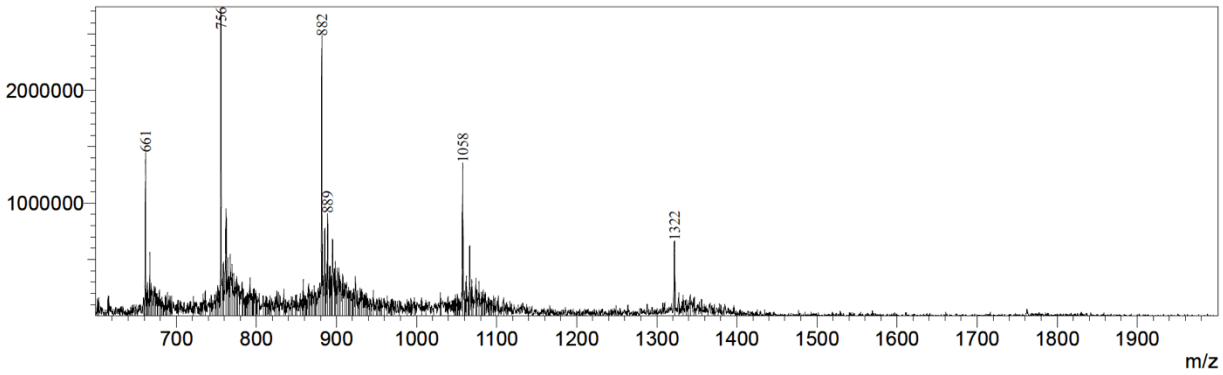

Figure 5-21. ESI-MS trace of GEP44 W38 L39, expected *m/z* = 5285, observed *m/z* = 1322 $[M+4H]^{+4}$, 1058 $[M+5H]^{+5}$, 882 $[M+6H]^{+6}$, 756 $[M+7H]^{+7}$, 661 $[M+8H]^{+8}$.

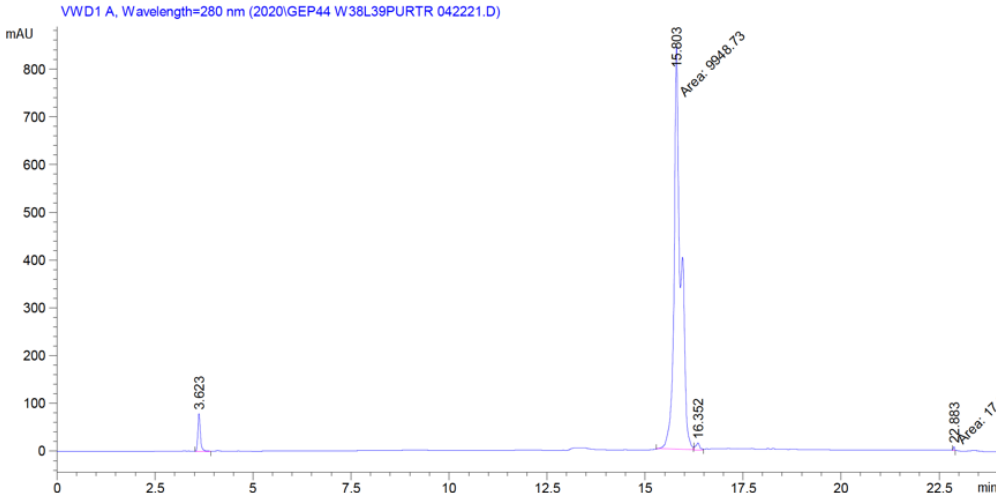

Figure 5-22. RP-HPLC purity trace showing product at 15.803 min.

5.2.1.11 EP45 W39

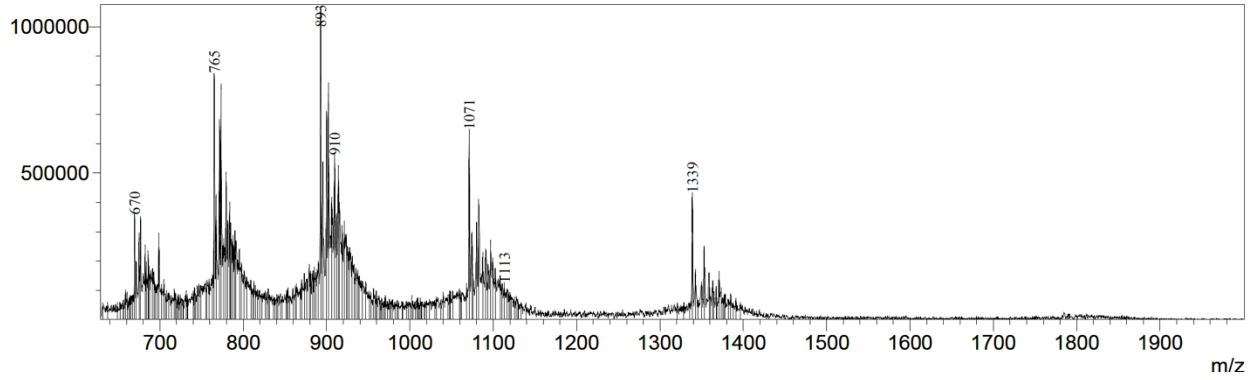

Figure 5-23. ESI-MS trace of EP45 W39, expected *m/z* = 5352, observed *m/z* = 1339 $[M+4H]^{+4}$, 1071 $[M+5H]^{+5}$, 893 $[M+6H]^{+6}$, 765 $[M+7H]^{+7}$, 670 $[M+8H]^{+8}$.

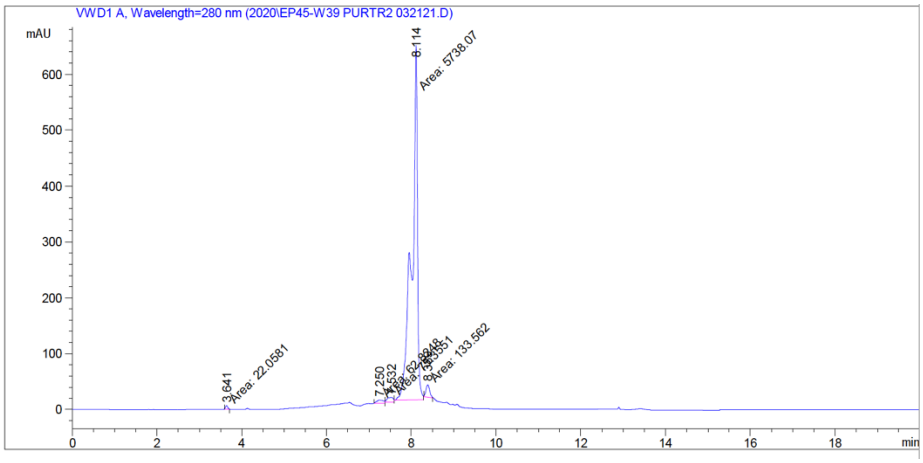

Figure 5-24. RP-HPLC purity trace showing product at 8.114 min.

5.2.1.12 Exendin-4 (Ex-4)

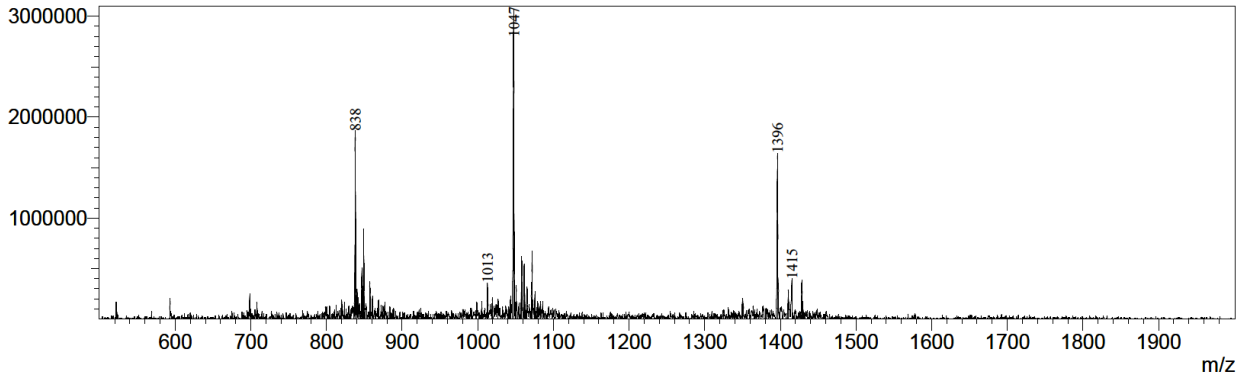

Figure 5-25. ESI-MS trace of Ex-4, expected *m/z* = 4185, observed *m/z* = 1396 $[M+3H]^{+3}$, 1047 $[M+4H]^{+4}$, 838 $[M+5H]^{+5}$.

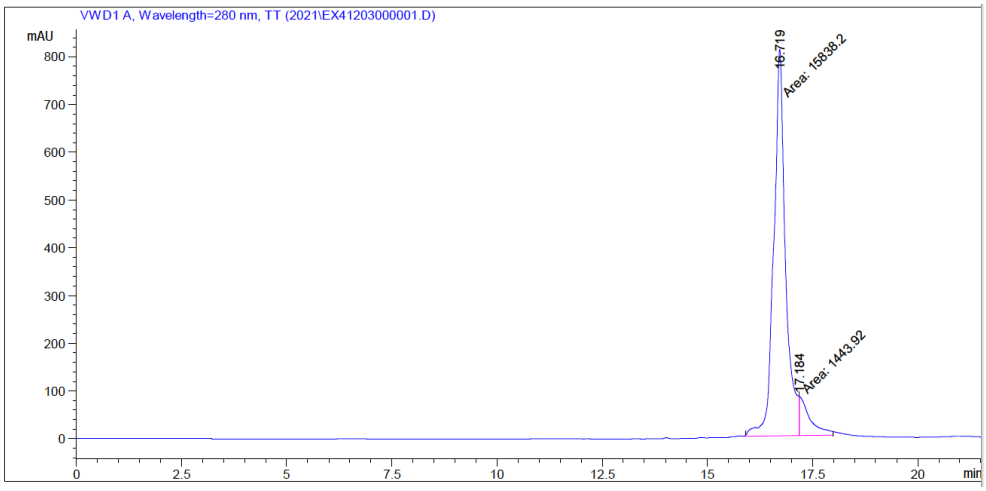

Figure 5-26. RP-HPLC purity trace showing product at 16.719 min.

5.2.1.13 Lipidated GEP44 analogs

5.2.1.13.1 KSCGG1

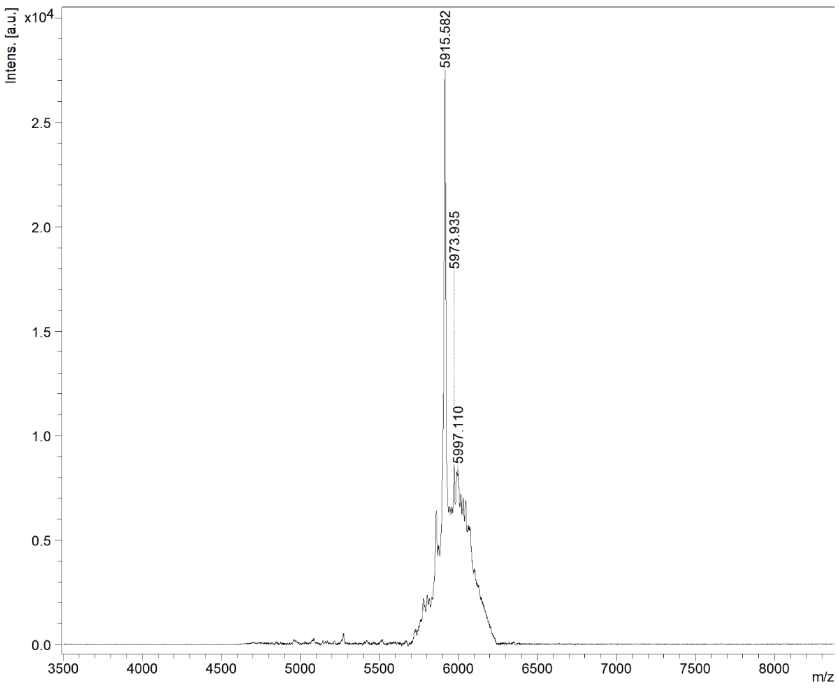

Figure 5-27. MALDI-TOF MS trace of KSCGG1, expected *m/z* = 5914, observed *m/z* = 5915.

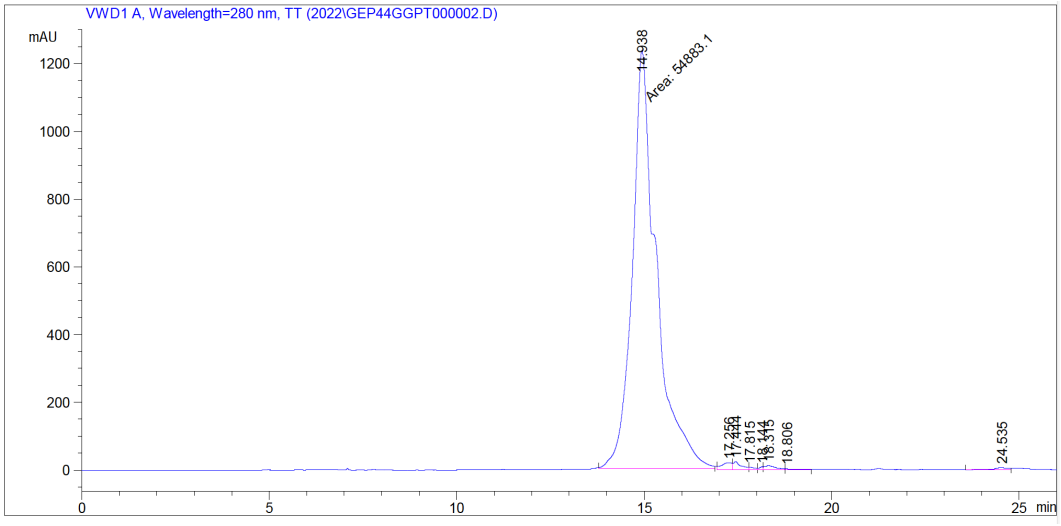

Figure 5-28. RP-HPLC purity trace showing product at 14.938 min.

5.2.1.13.2 KSCGG2

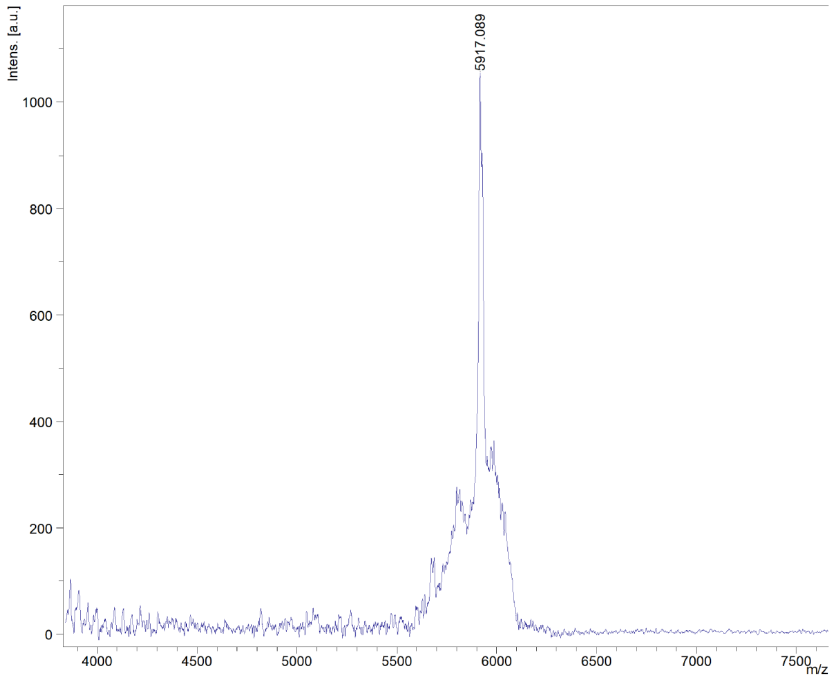

Figure 5-29. MALDI-TOF MS trace of KSCGG2, expected *m/z* = 5914, observed *m/z* = 5917.

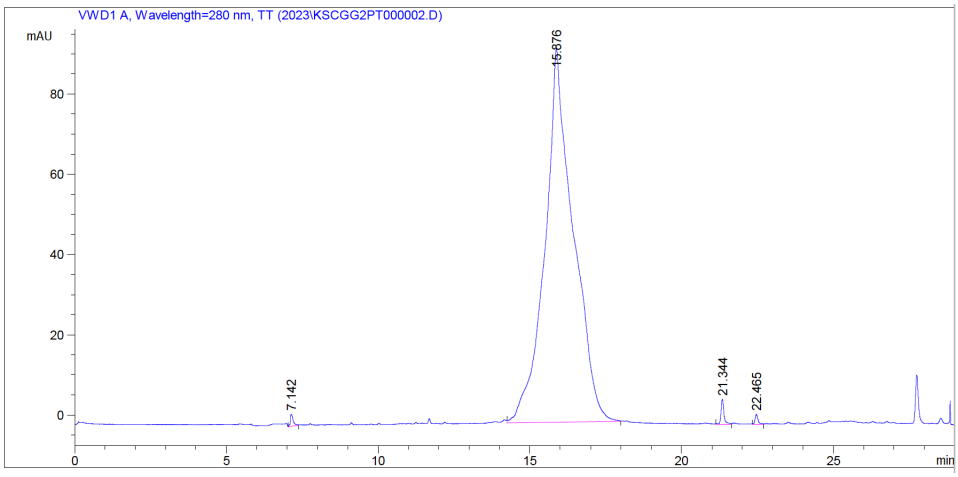

Figure 5-30. RP-HPLC purity trace showing product at 15.876 min.

5.2.1.13.3 KSCGG3

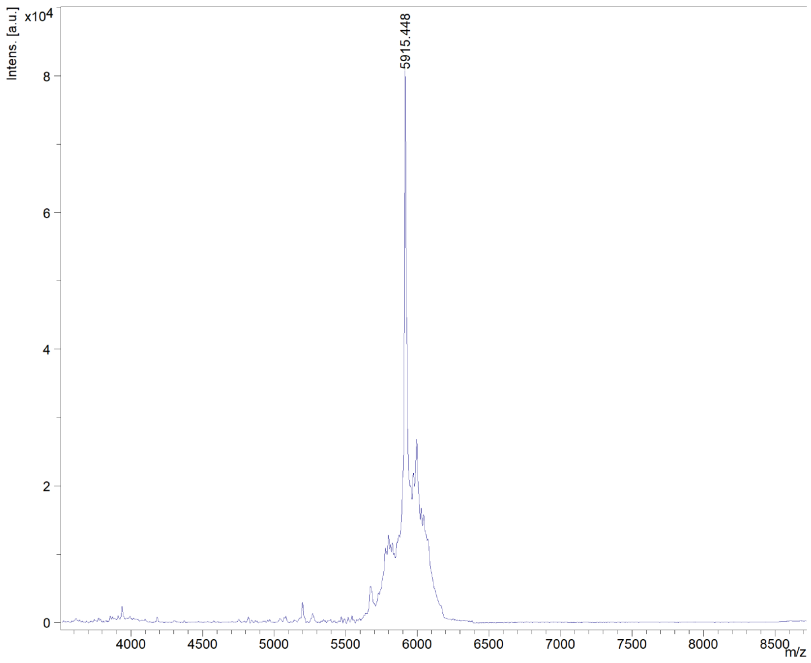

Figure 5-31. MALDI-TOF MS trace of KSCGG3, expected *m/z* = 5914, observed *m/z* = 5915.

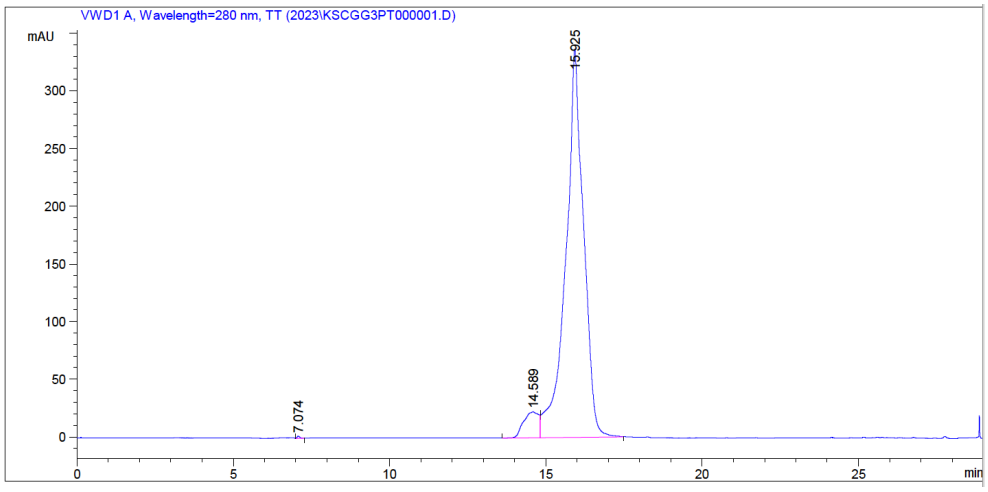

Figure 5-32. RP-HPLC purity trace showing product at 15.925 min.

5.2.1.13.4 KSCGG4

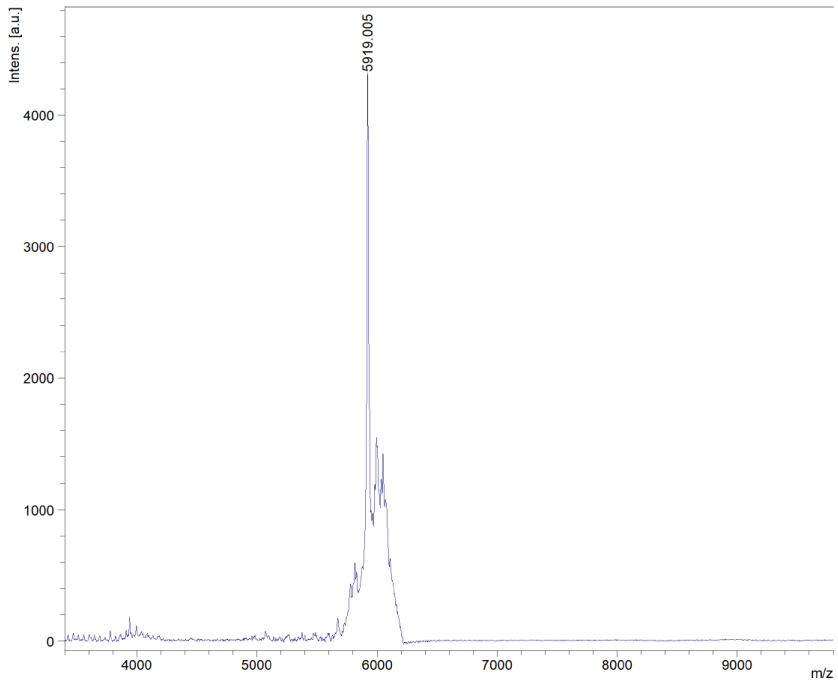

Figure 5-33. MALDI-TOF MS trace of KSCGG4, expected *m/z* = 5914, observed *m/z* = 5915.

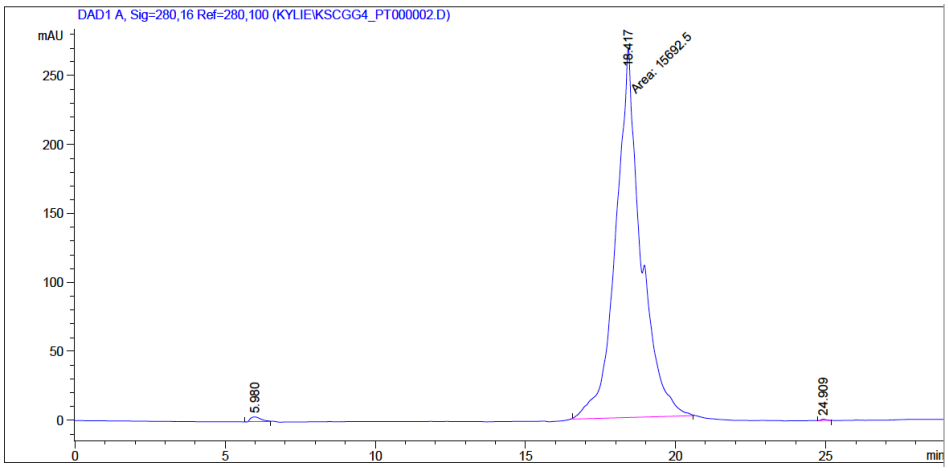

Figure 5-34. RP-HPLC purity trace showing product at 18.417 min.

5.2.1.22 Azido-modified peptides and fluorescent analogs

All fluorescently-tagged peptides were synthesized in-house by the author. Solid-phase peptide synthesis of the peptides with an Fmoc-Lys(N_3)-OH modification were performed on ProTide Rink amide resin using a microwave-assisted CEM Liberty Blue peptide synthesizer. The azido-modified peptides were reacted with sulfo-Cyanine5 DBCO (Lumiprobe) at a 1:4 molar ratio. The reagents were dissolved in 4:1 DMF:H_2O and were left spinning for 16 hours at room temperature.

5.2.1.22.1 GEP44 K(N_3)

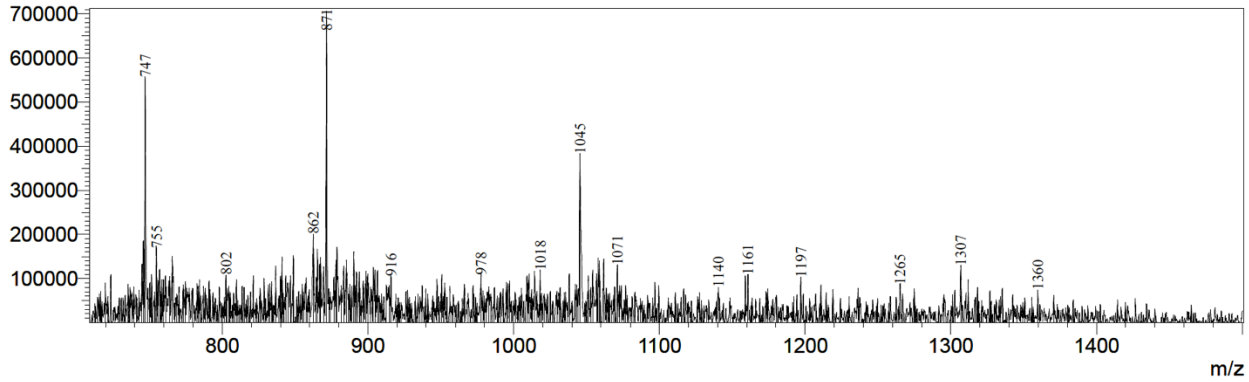

Figure 5-35. ESI-MS trace of GEP44 K(N_3), expected *m/z* = 5220, observed *m/z* = $[M+4H]^{+4}$, 1045 $[M+5H]^{+5}$, 871 $[M+6H]^{+6}$, 747 $[M+7H]^{+7}$.

5.2.1.22.2 *f*Cy5-GEP44

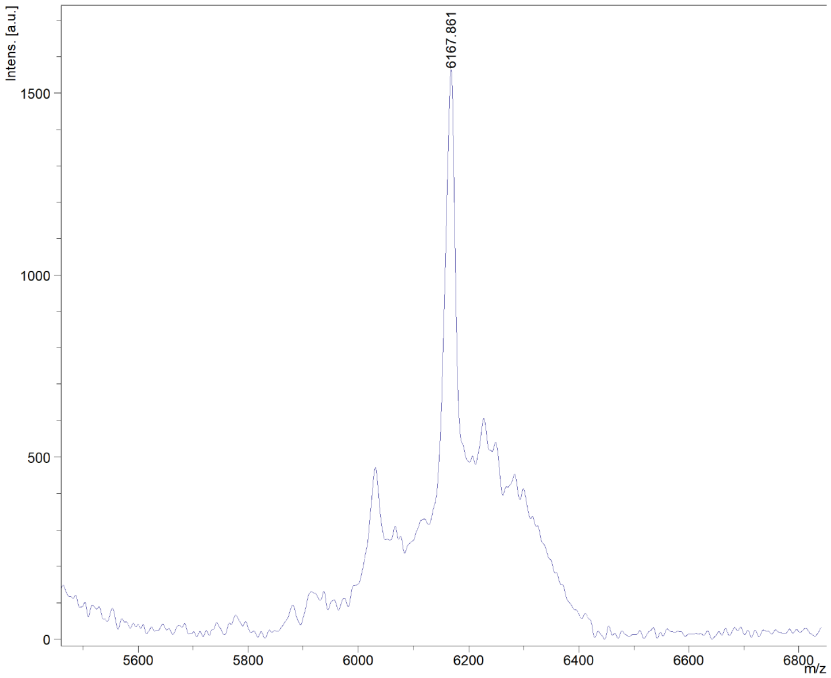

Figure 5-36. MALDI-TOF MS trace of *f*Cy5-GEP44, expected *m/z* = 6167, observed *m/z* = 6167.

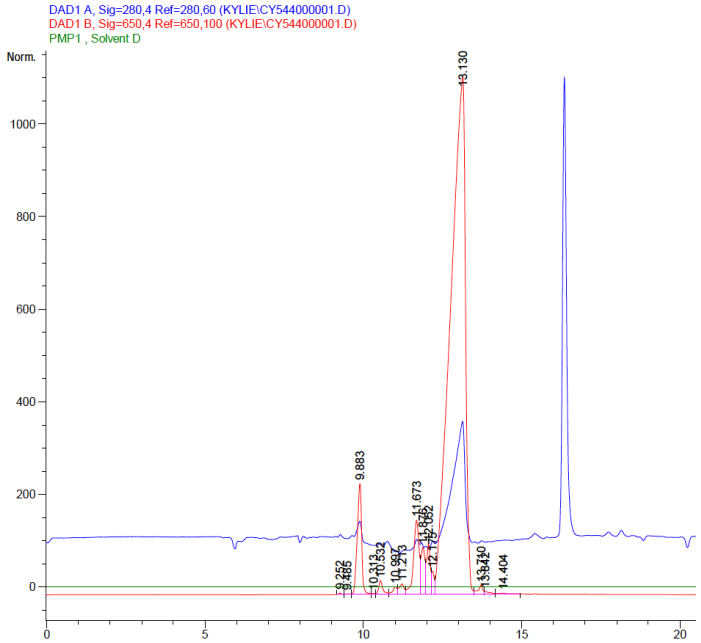

Figure 5-37. RP-HPLC trace showing product at 13.13 min.

5.2.1.22.3 GEP12 K(N_3)

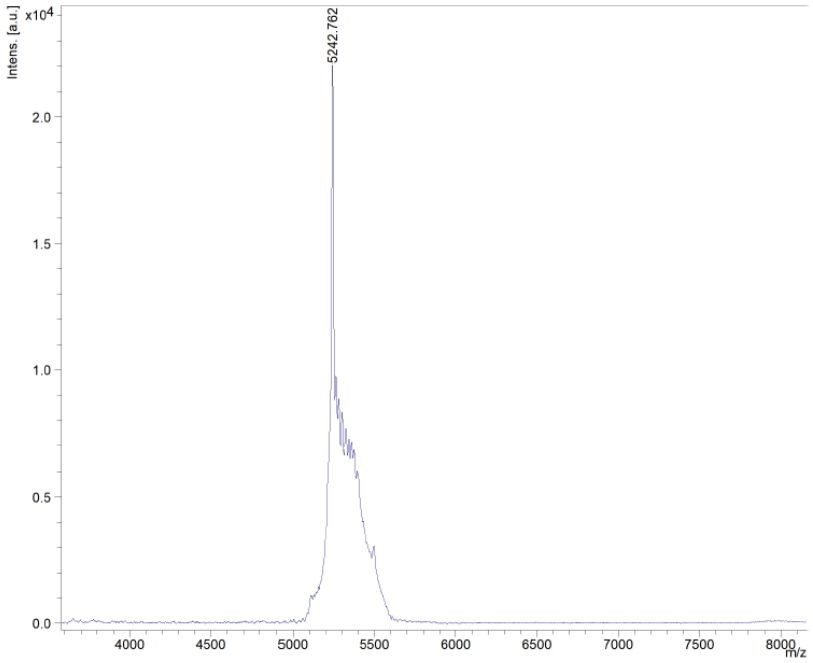

Figure 5-38. MALDI-TOF MS trace of GEP12 K(N_3), expected *m/z* = 5242, observed *m/z* = 5242.

5.2.1.22.4 *f*Cy5-GEP12

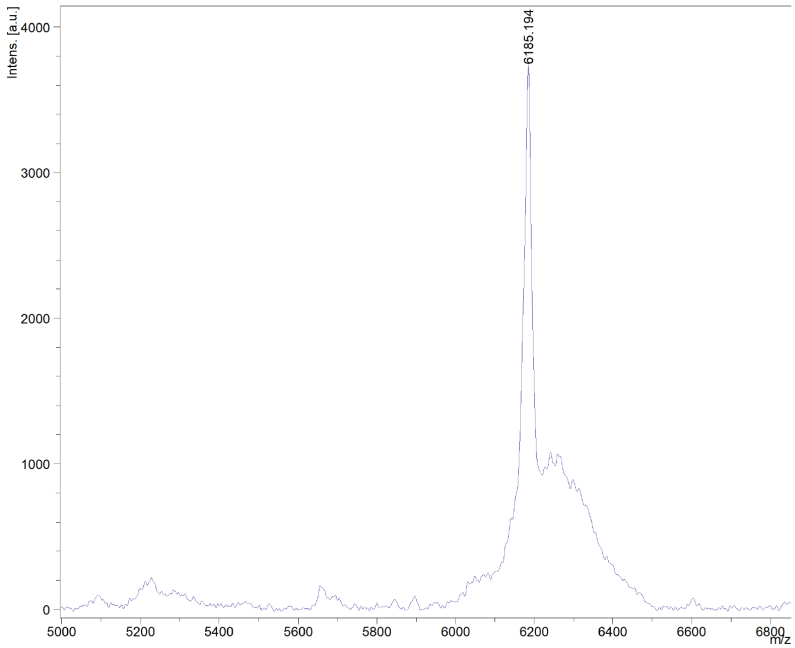

Figure 5-39. MALDI-TOF MS trace of *f*Cy5-GEP12, expected *m/z* = 6184, observed *m/z* = 6185.

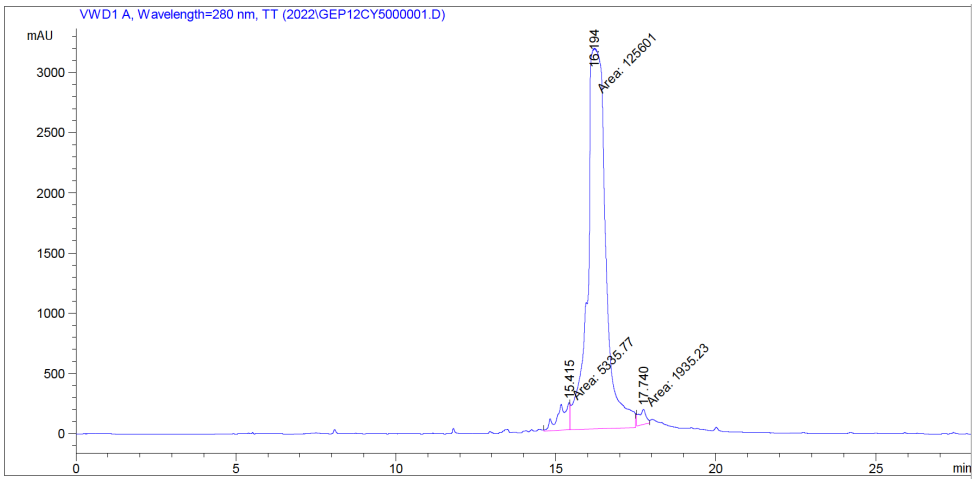

Figure 5-40. RP-HPLC purity trace showing product at 16.194 min.

5.2.1.22.5 PYY_{3-36} $K(N_3)$

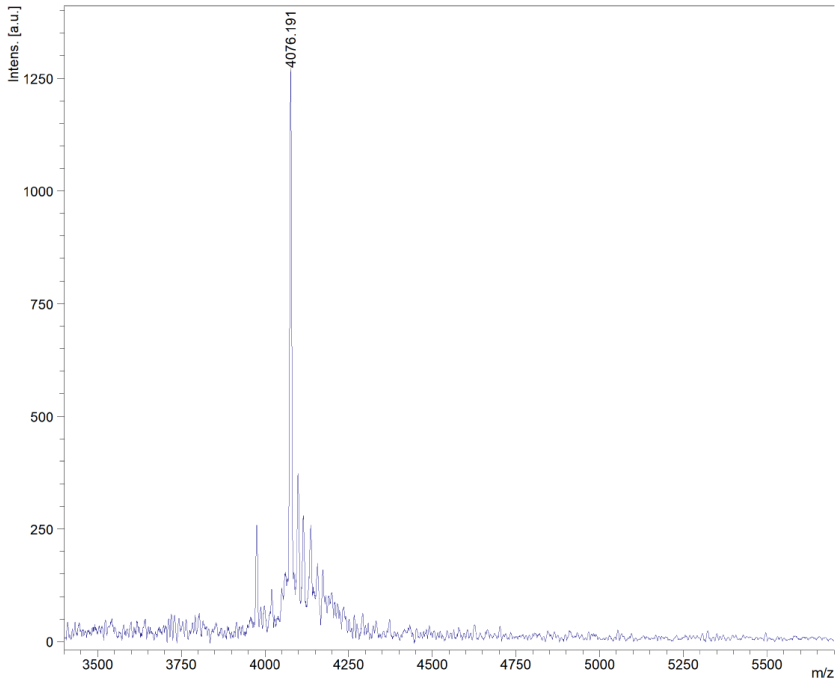

Figure 5-41. MALDI-TOF MS trace of PYY_{3-36} $K(N_3)$, expected *m/z* = 4075, observed *m/z* = 4076.

5.2.1.22.6 *f*Cy5-PYY$_{3-36}$

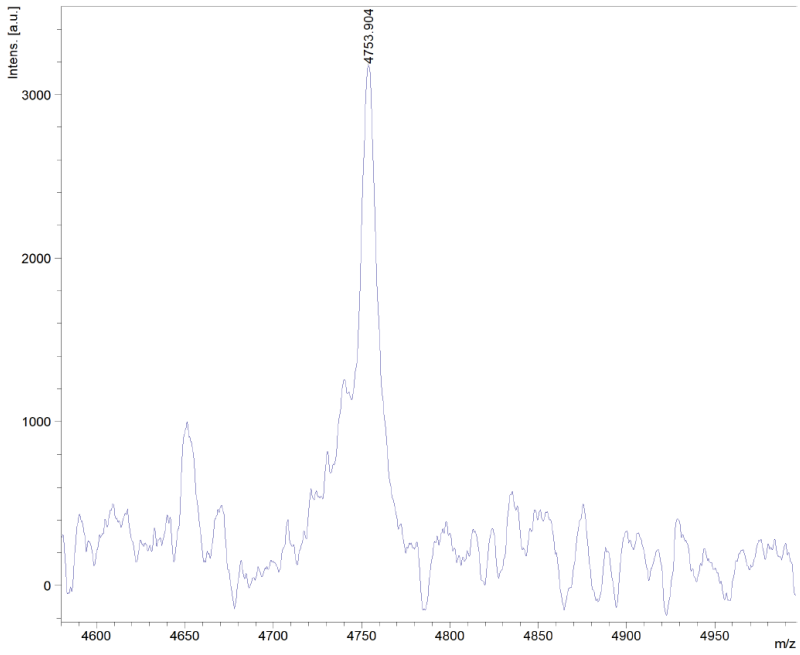

Figure 5-42. MALDI-TOF MS trace of *f*Cy5-PYY$_{3-36}$, expected *m/z* = 4753, observed *m/z* = 4754.

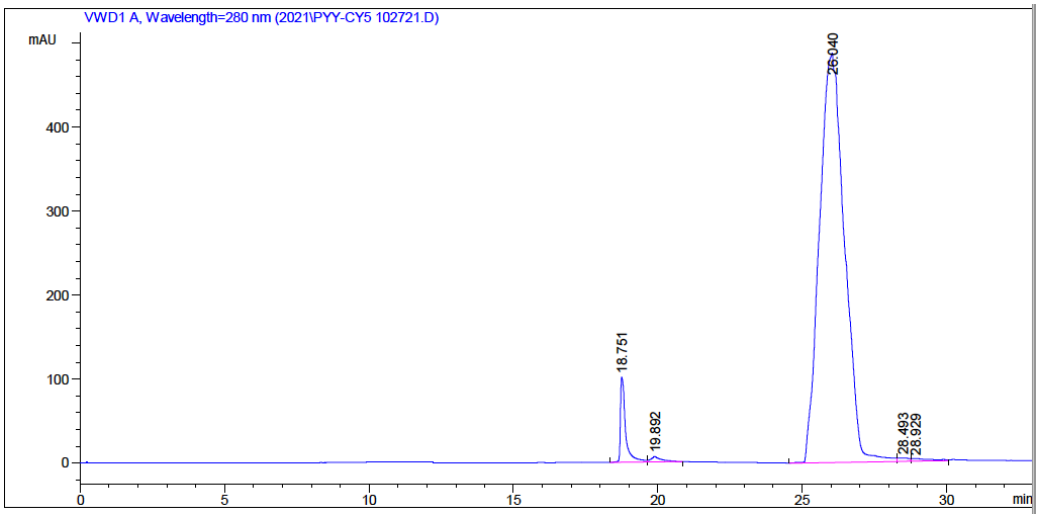

Figure 5-43. RP-HPLC purity trace showing product at 26.04 min.

5.2.2 Neuropeptides based on Octadecaneuropeptide (ODN)

5.2.2.1 ODN

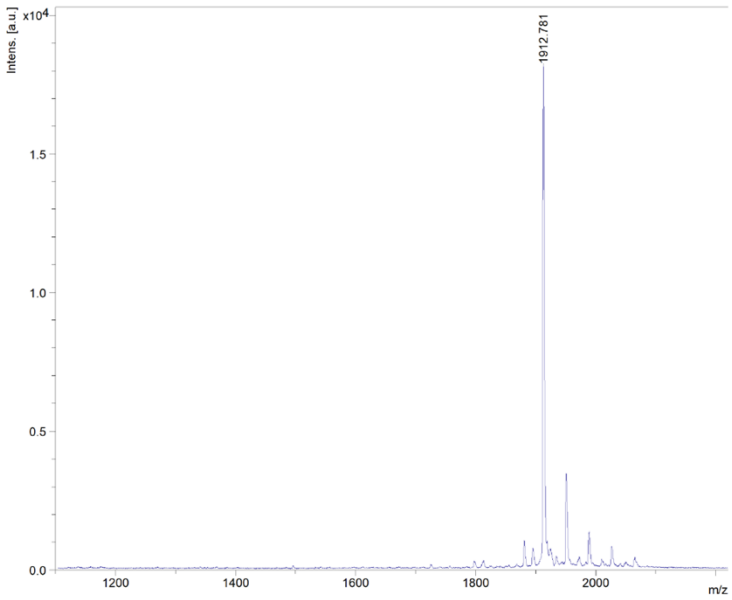

Figure 5-44. MALDI-TOF MS trace of ODN, expected *m/z* = 1911, observed *m/z* = 1912.

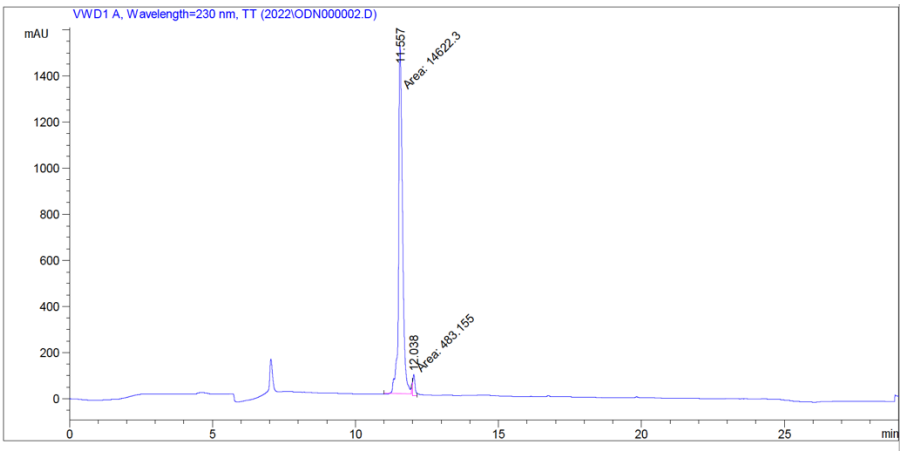

Figure 5-45. RP-HPLC purity trace showing product at 11.557 min.

5.2.2.2 Octapeptide (OP)

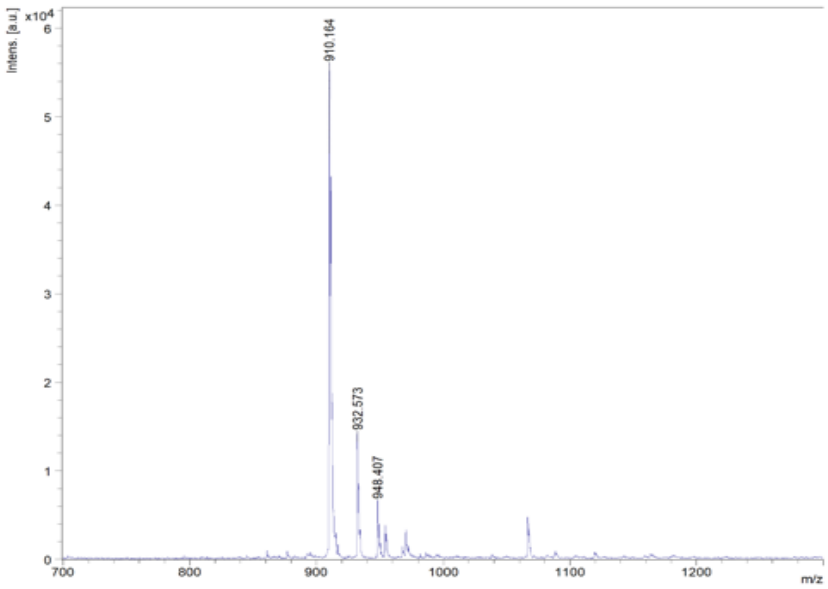

Figure 5-46. MALDI-TOF MS trace of OP, expected *m/z* = 910, observed *m/z* = 910.

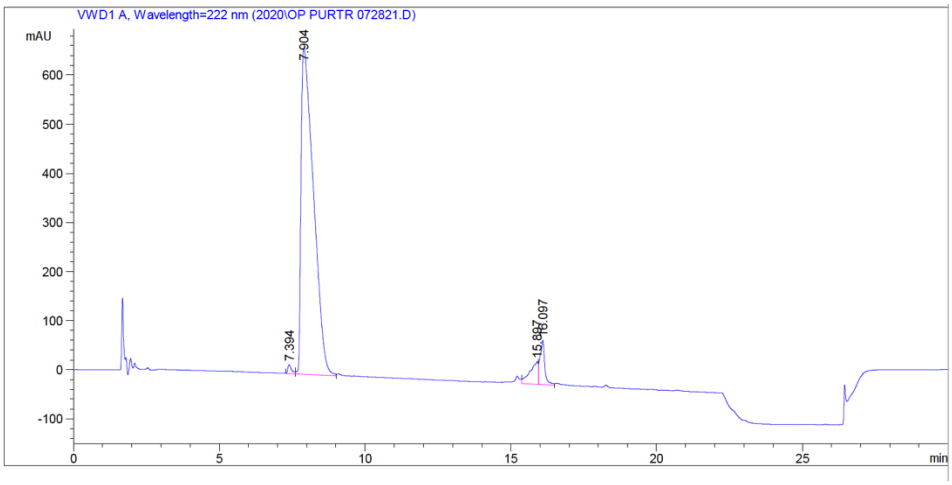

Figure 5-47. RP-HPLC purity trace showing product at 7.904 min.

5.2.2.3 OP antagonist (AntOP)

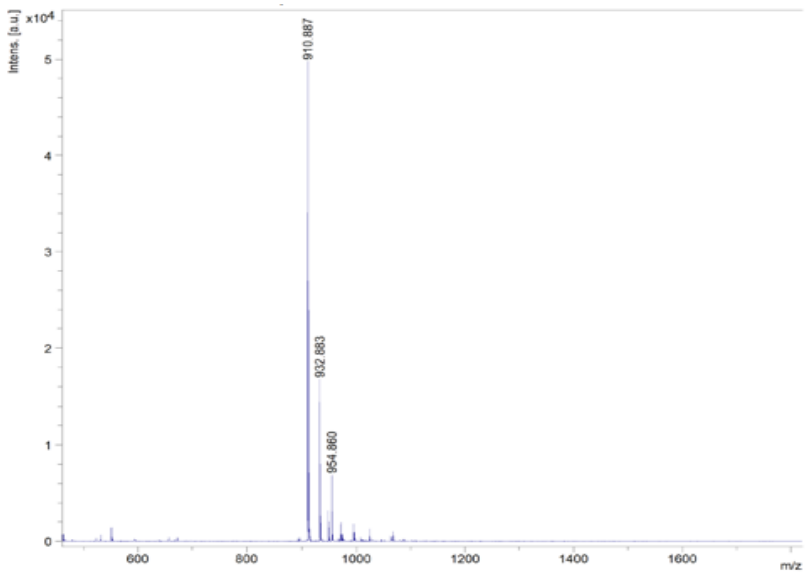

Figure 5-48. MALDI-TOF MS trace of AntOP, expected *m/z* = 910, observed *m/z* = 910.

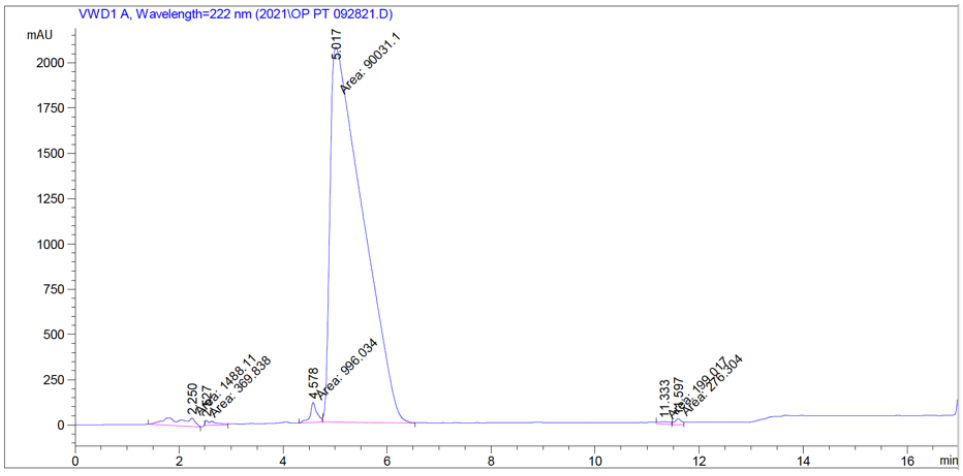

Figure 5-49. RP-HPLC purity trace showing product at 5.017 min.

5.2.2.4 TDN

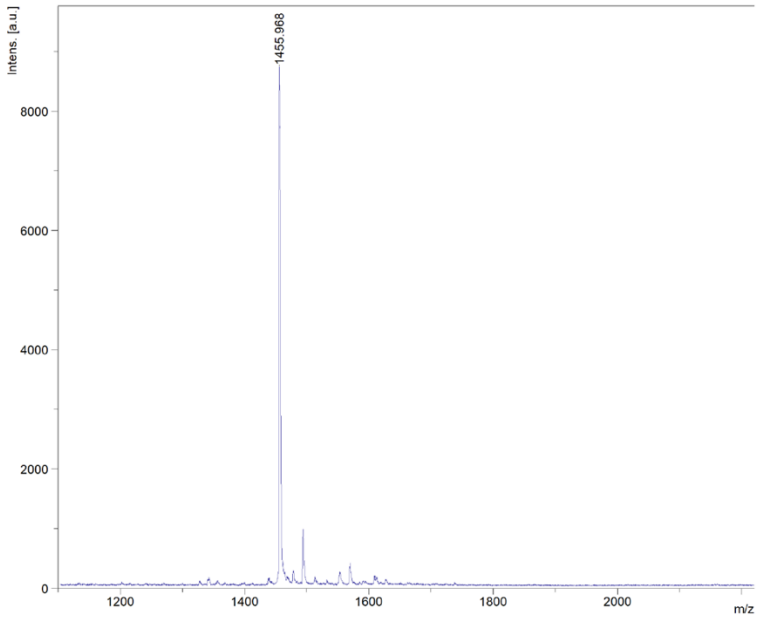

Figure 5-50. MALDI-TOF MS trace of TDN, expected *m/z* = 1455, observed *m/z* = 1455.

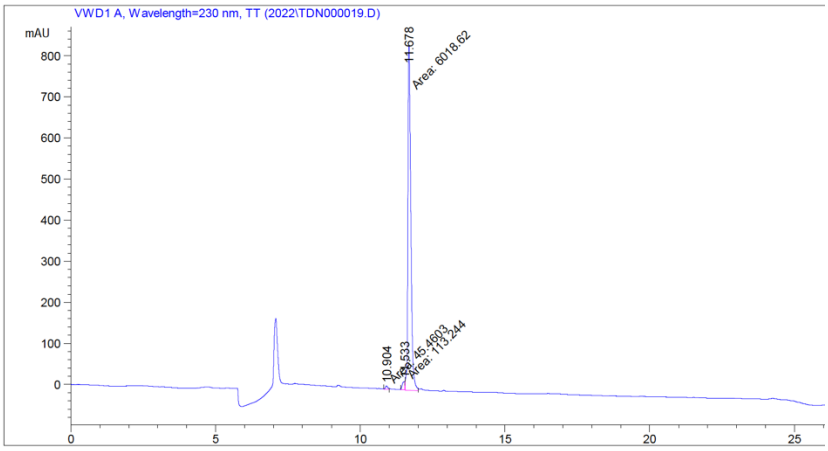

Figure 5-51. RP-HPLC purity trace showing product at 11.678 min.

5.2.2.5 ODN-Biotin

Solid-phase peptide synthesis of ODN-Biotin was performed using an Fmoc-Lys(Biotin)-OH (ChemPep Inc.) incorporated into the peptide synthesizer.

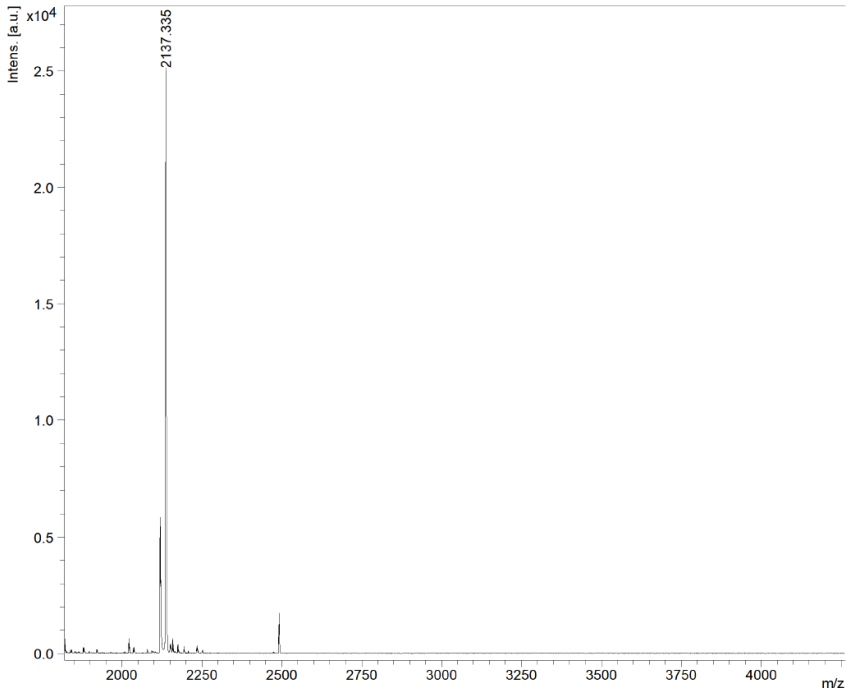

Figure 5-52. MALDI-TOF MS trace of ODN-Biotin, expected *m/z* = 2136, observed *m/z* = 2137.

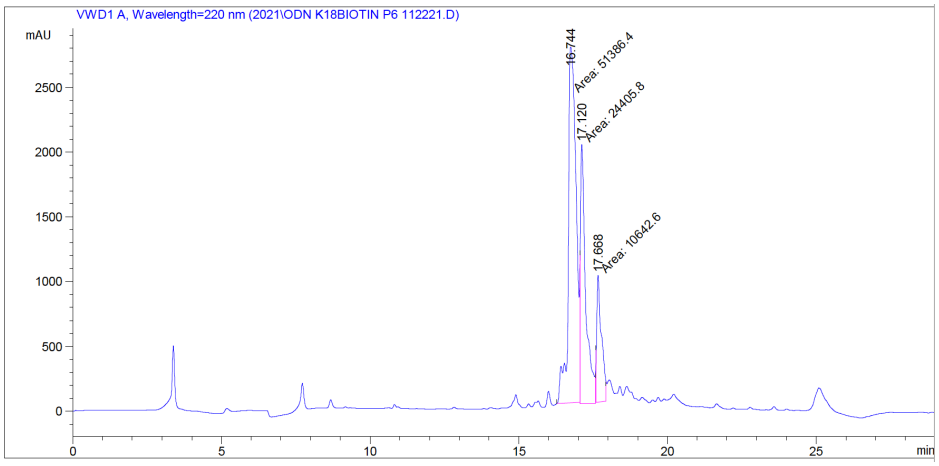

Figure 5-53. RP-HPLC trace showing product at 16.744 min.

5.2.2.6 SUODN-03

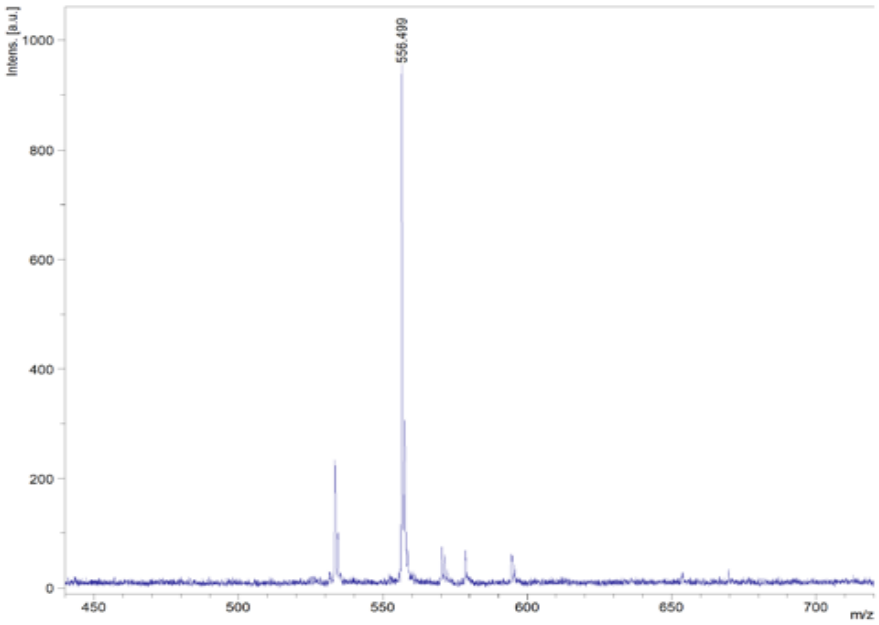

Figure 5-54. MALDI-TOF MS trace of SUODN-03, expected *m/z* = 556, observed *m/z* = 556.

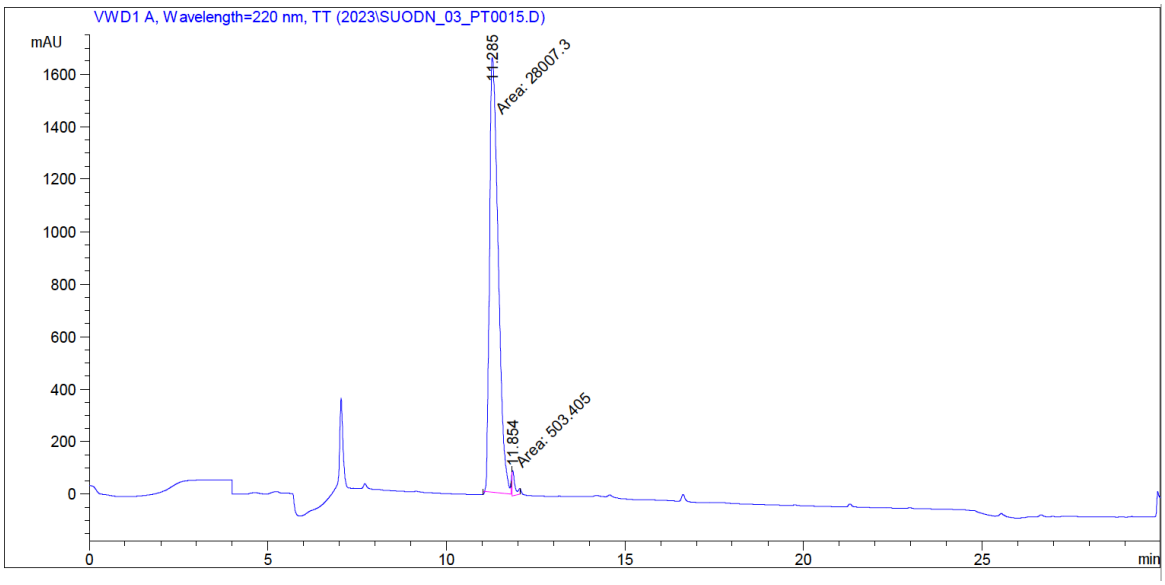

Figure 5-55. RP-HPLC purity trace showing product at 11.285 min.

5.2.2.7 SUODN-04

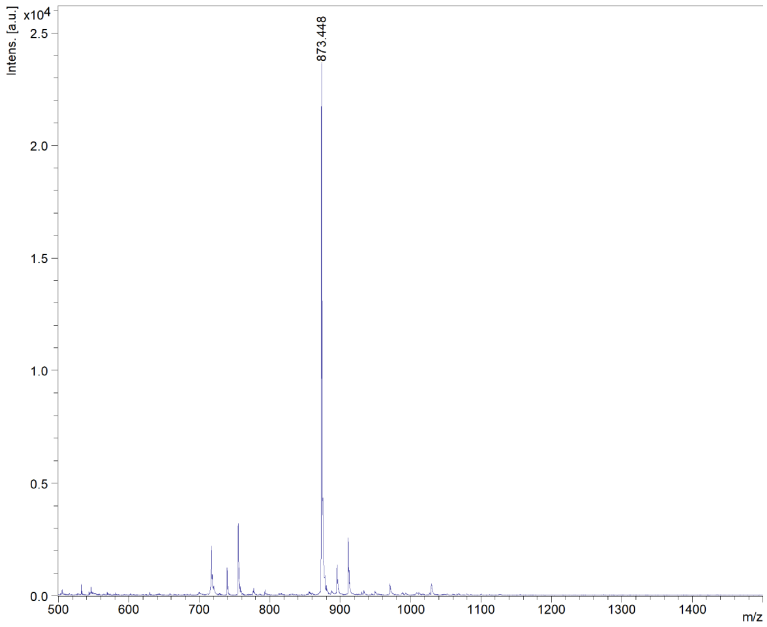

Figure 5-56. MALDI-TOF MS trace of SUODN-04, expected *m/z* = 873, observed *m/z* = 873.

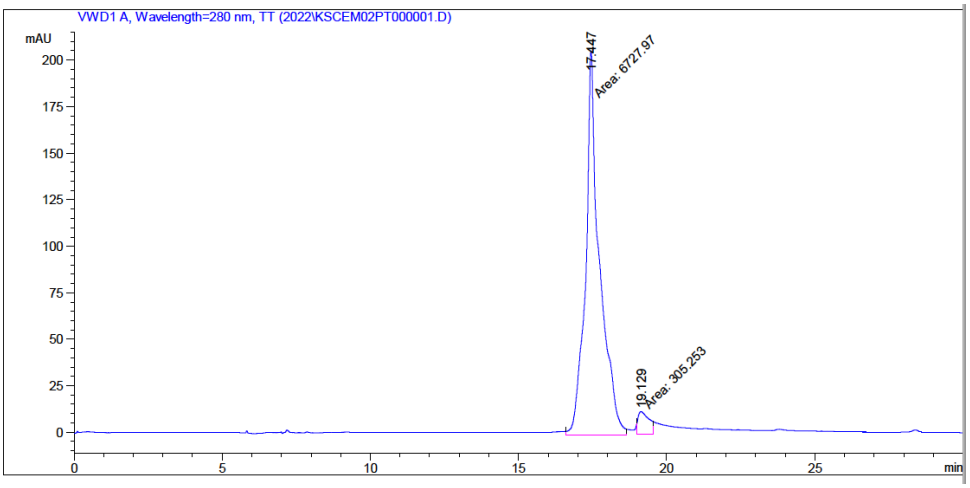

Figure 5-57. RP-HPLC purity trace showing product at 17.447 min.

5.2.2.8 SUODN-05

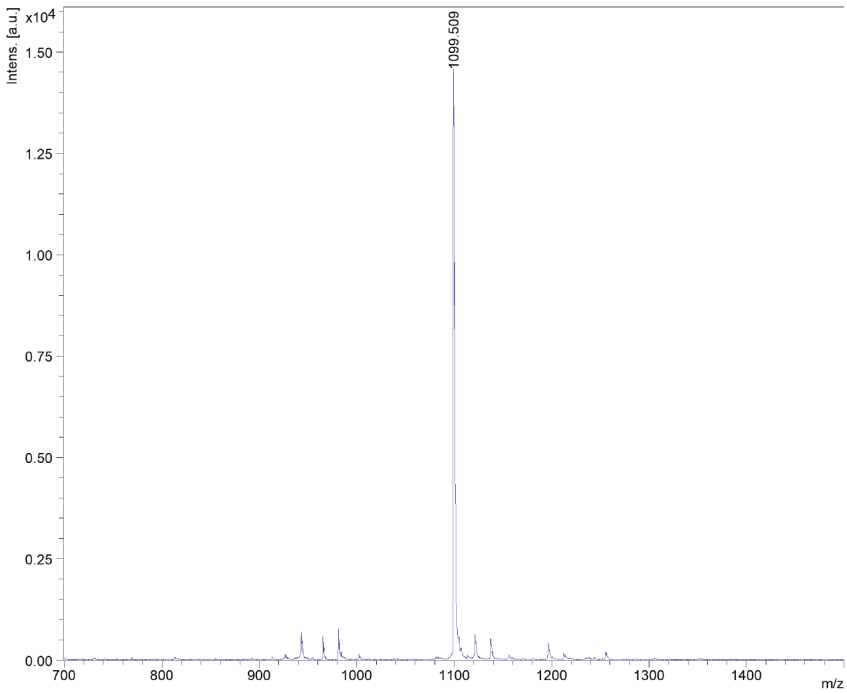

Figure 5-58. MALDI-TOF MS trace of SUODN-05, expected *m/z* = 1099, observed *m/z* = 1099.

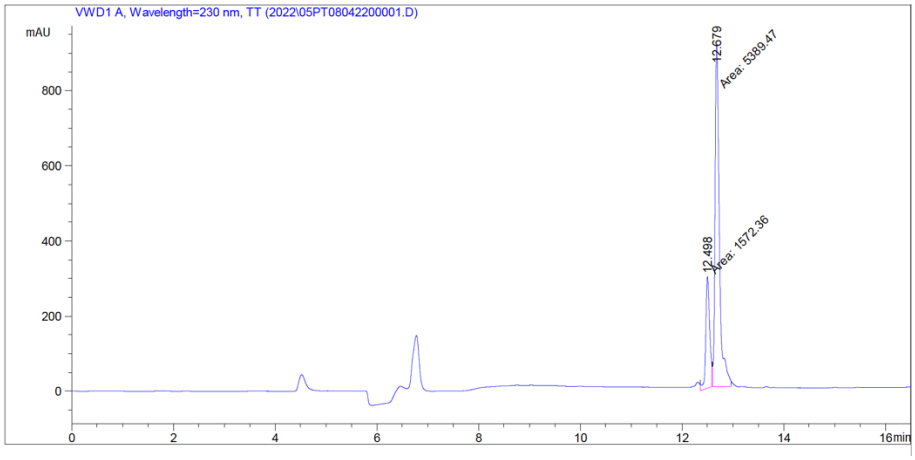

Figure 5-59. RP-HPLC trace showing product at 12.679 min.

5.2.2.9 SUODN-06

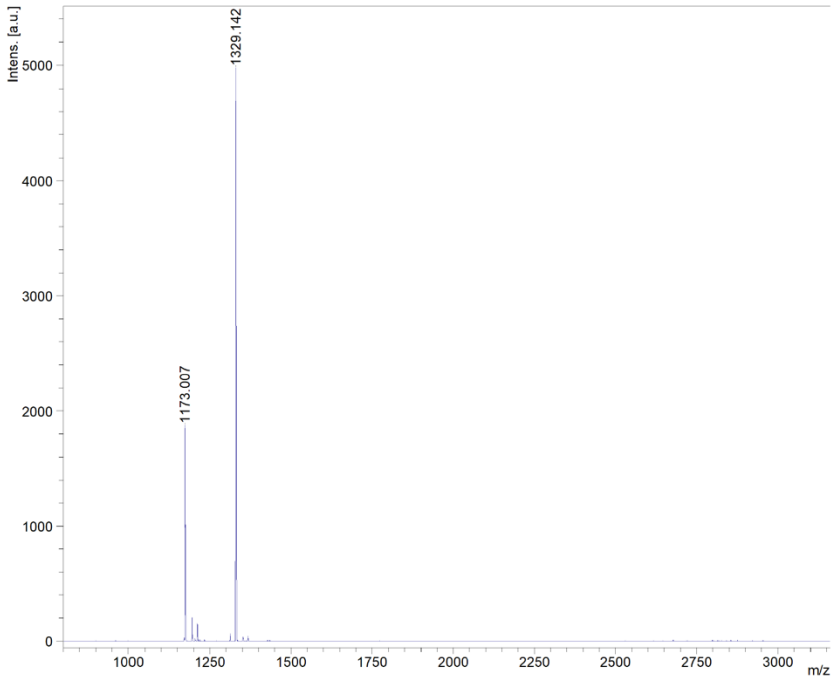

Figure 5-60. MALDI-TOF MS trace of SUODN-06, expected *m/z* = 1329, observed *m/z* = 1329.

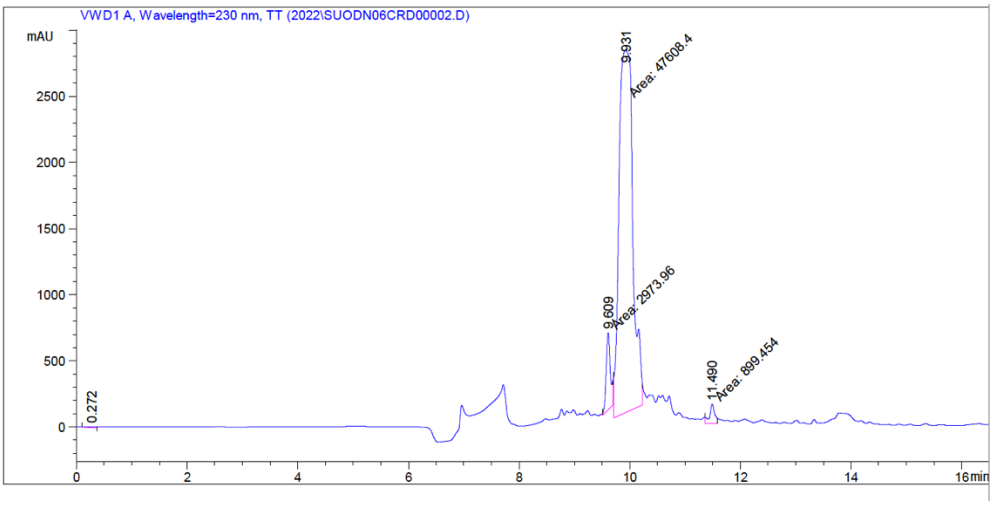

Figure 5-61. RP-HPLC trace showing product at 9.931 min.

5.2.2.10 Azido-modified peptides and fluorescent analogs

5.2.2.10.1 OP K(N_3)

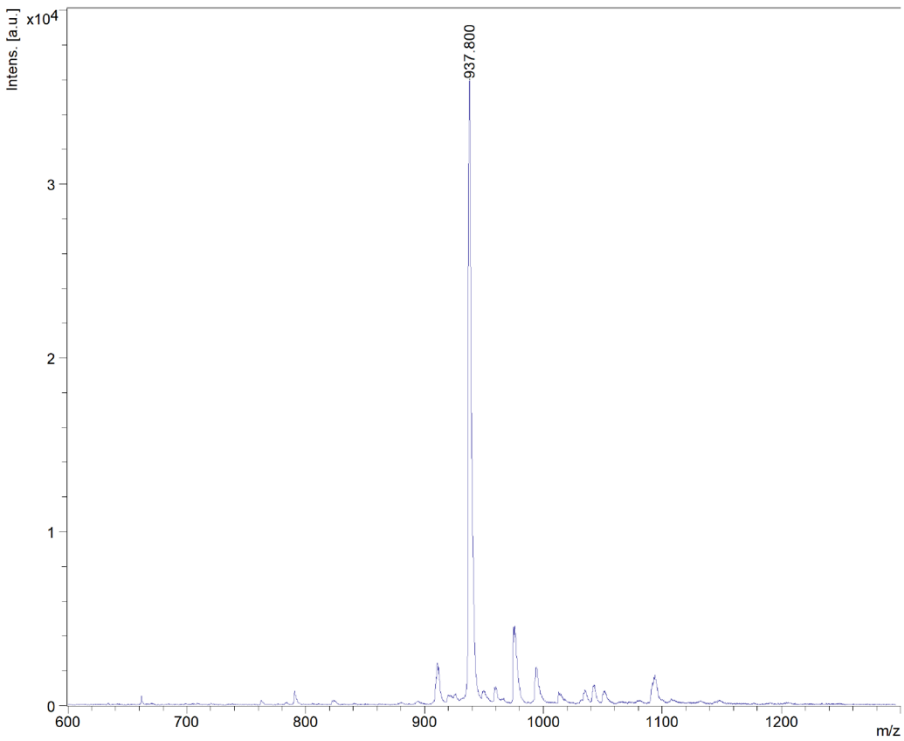

Figure 5-62. MALDI-TOF MS trace of OP K(N_3), expected *m/z* = 937, observed *m/z* = 938.

5.2.2.10.2 *f*Cy5-OP

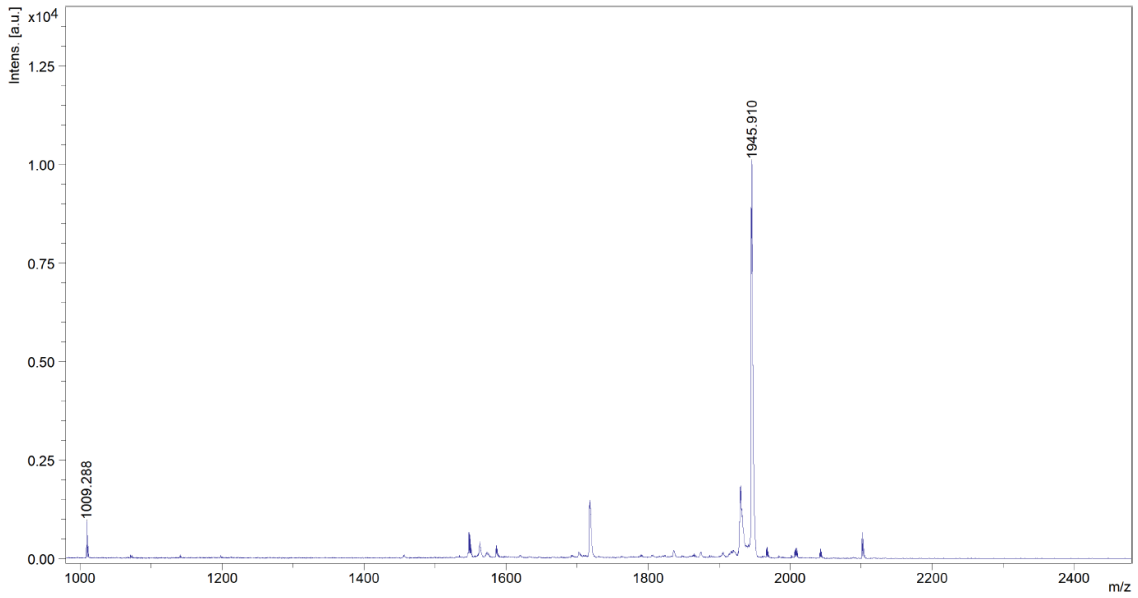

Figure 5-63. MALDI-TOF MS trace of *f*Cy5-OP, expected *m/z* = 1946, observed *m/z* = 1945.

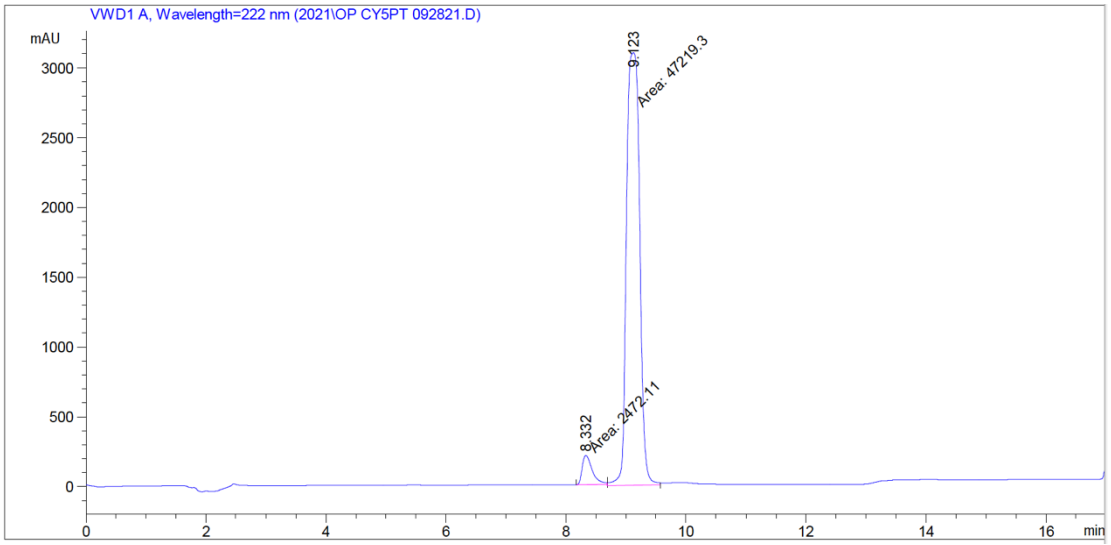

Figure 5-64. RP-HPLC purity trace showing product at 9.123 min.

5.2.2.10.2 TDN K(N_3)

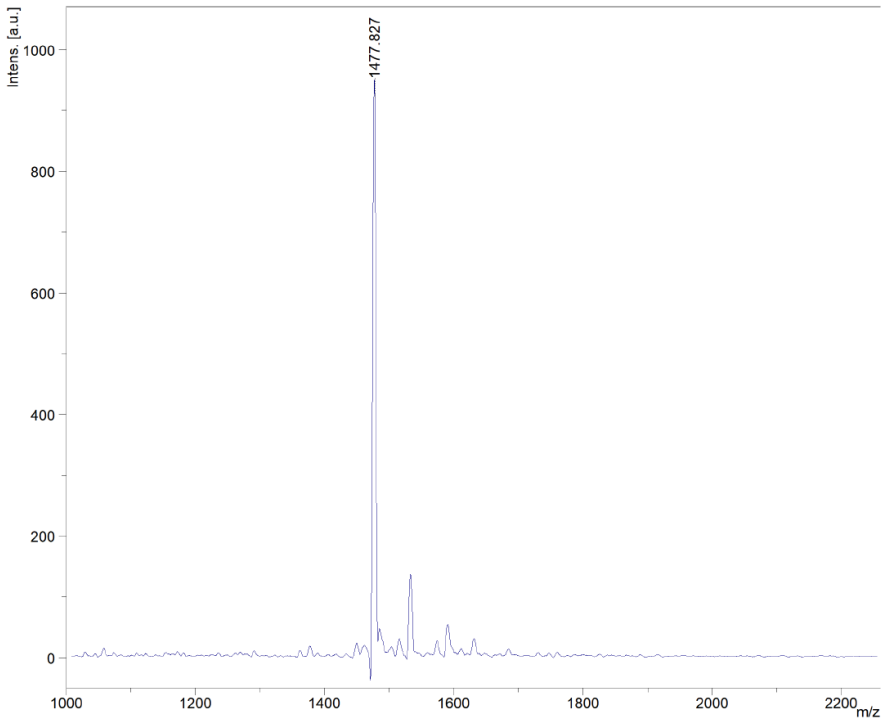

Figure 5-65. MALDI-TOF MS trace of TDN K(N_3), expected *m/z* = 1477, observed *m/z* = 1477.

5.2.2.10.3 *f*Cy5-TDN

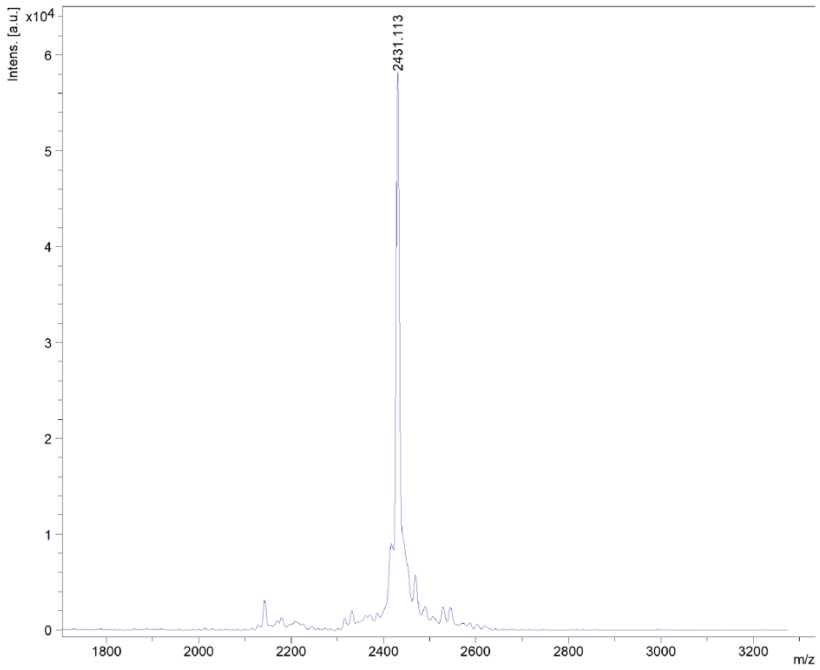

Figure 5-66. MALDI-TOF MS trace of *f*Cy5-TDN, expected *m/z* = 2430, observed *m/z* = 2431.

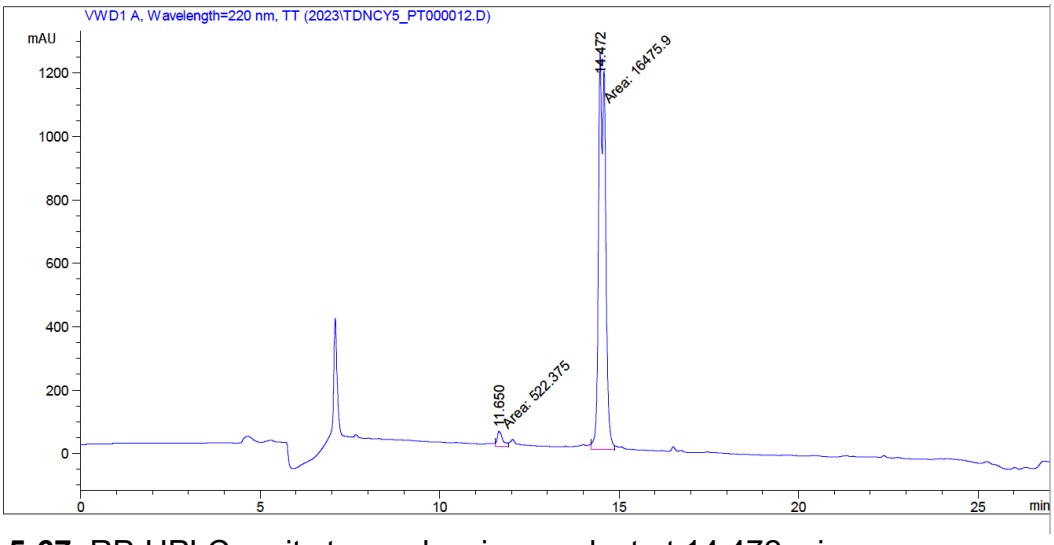

Figure 5-67. RP-HPLC purity trace showing product at 14.472 min.

5.2.3 GPR75 antagonists

5.2.3.1 SU75-36

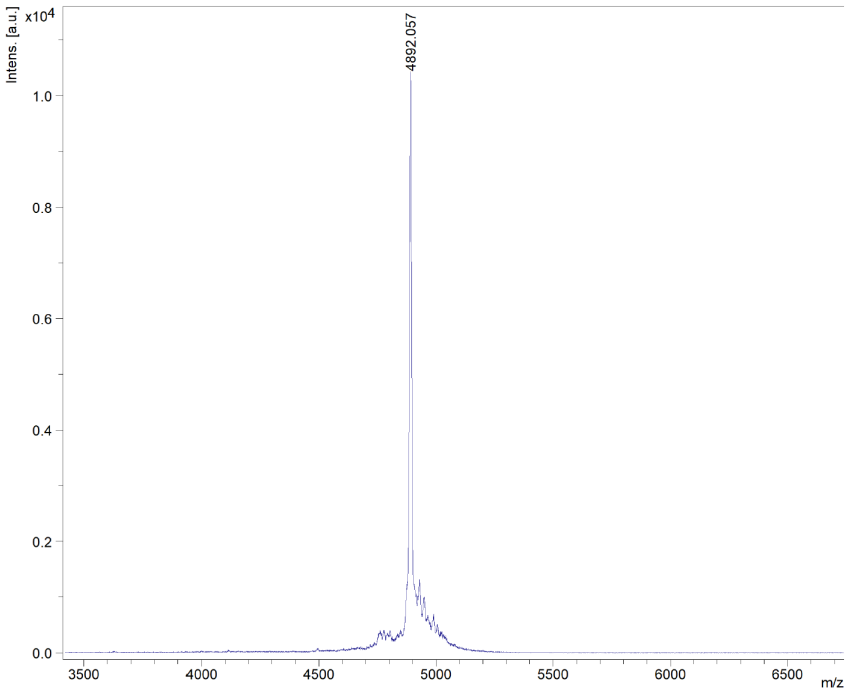

Figure 5-68. MALDI-TOF MS trace of SU75-36, expected *m/z* = 4892, observed *m/z* = 4892.

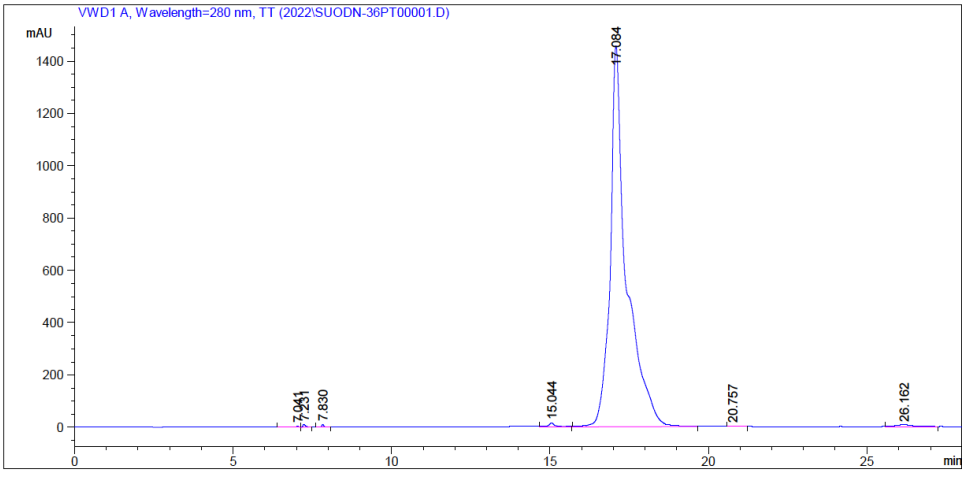

Figure 5-69. RP-HPLC purity trace showing product at 17.084 min.

5.2.3.2 SU75-37

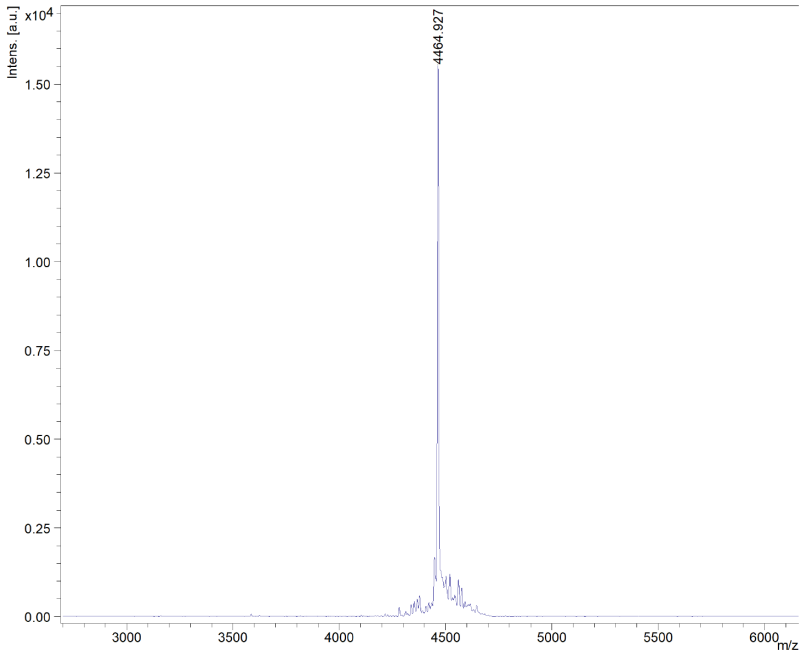

Figure 5-70. MALDI-TOF MS trace of SU75-36, expected *m/z* = 4462, observed *m/z* = 4464.

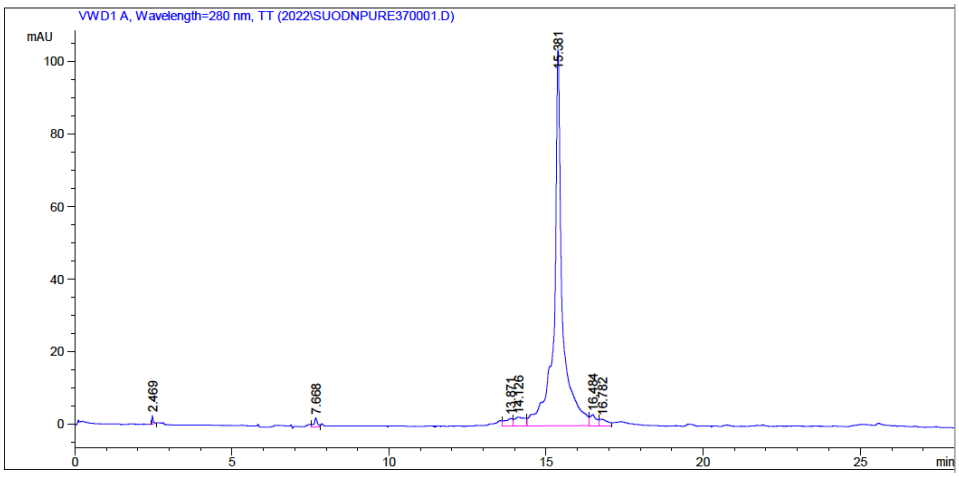

Figure 5-71. RP-HPLC purity trace showing product at 15.381 min.

5.2.3.3 Azido-modified peptides and fluorescent analogs

5.2.3.3.1 SU75-36 K(N_3)

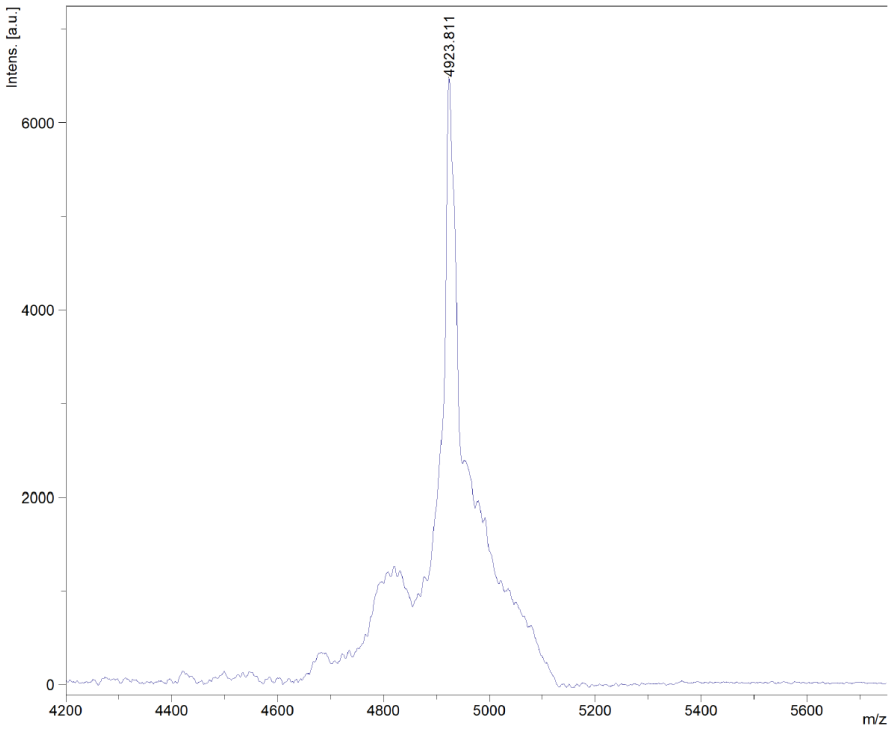

Figure 5-72. MALDI-TOF MS trace of SU75-36 K(N_3), expected *m/z* = 4923, observed *m/z* = 4923.

5.2.3.3.2 *f*Cy5-SU75-36

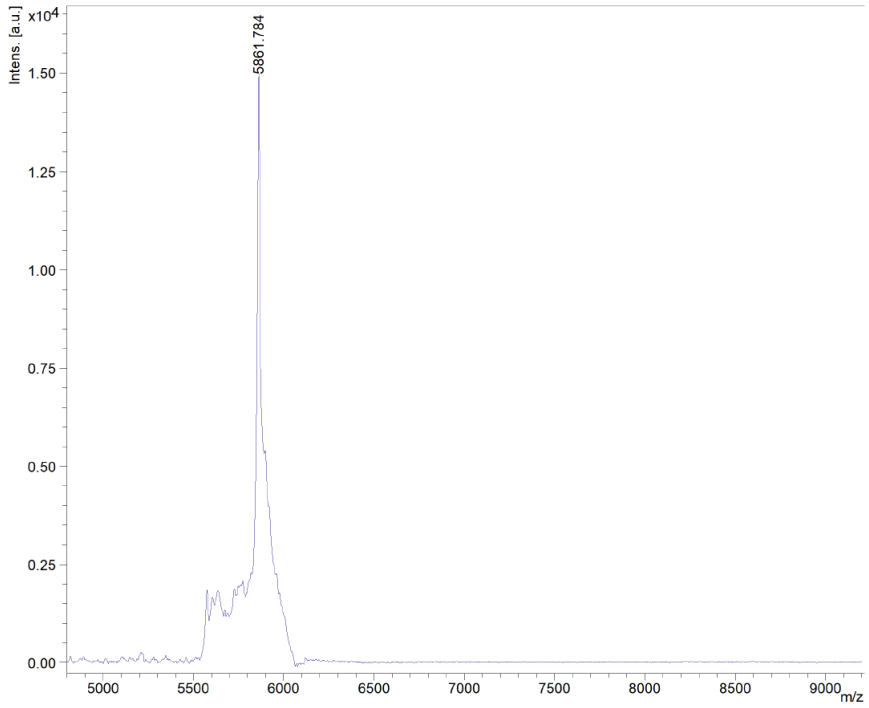

Figure 5-73. MALDI-TOF MS trace of *f*Cy5-SU75-36, expected *m/z* = 5861, observed *m/z* = 5861.

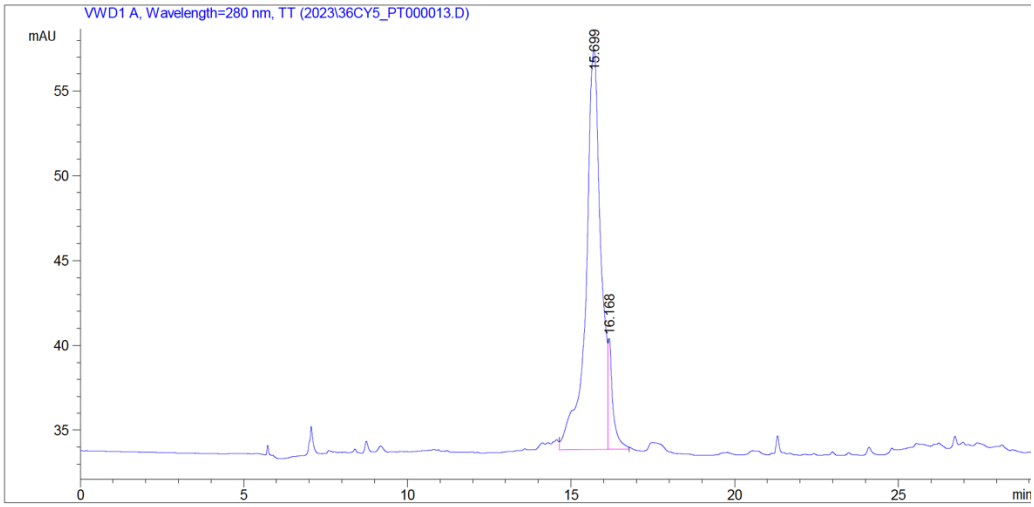

Figure 5-74. RP-HPLC purity trace showing product at 15.699 min.

5.2.3.3.3 SU75-37 K(N_3)

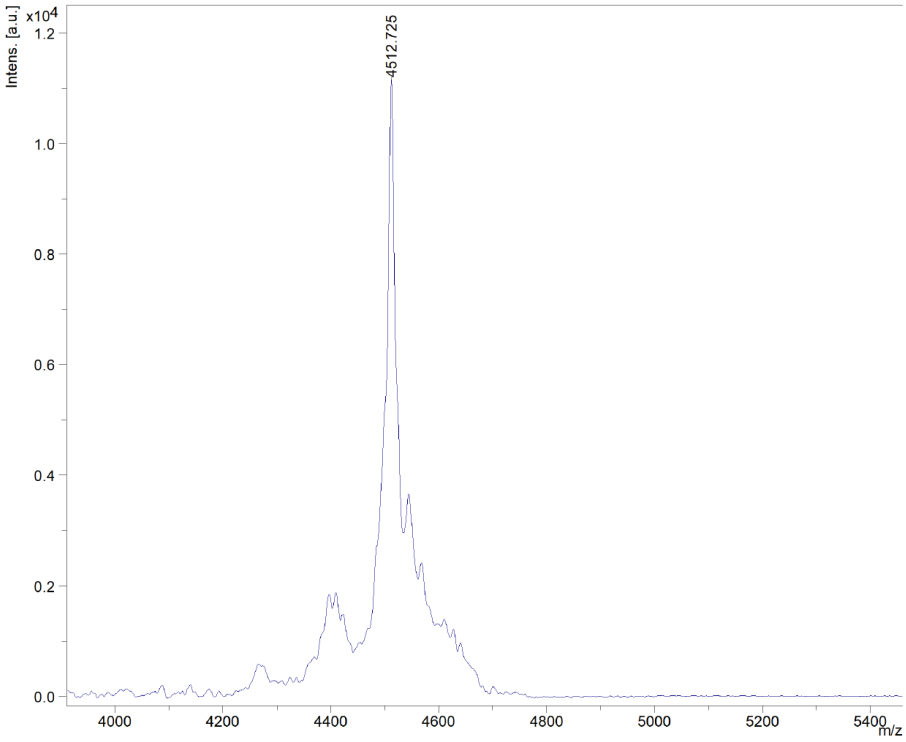

Figure 5-75. MALDI-TOF MS trace of SU75-37 K(N_3), expected *m/z* = 4512, observed *m/z* = 4512.

5.2.3.3.4 *f*Cy5-SU75-37

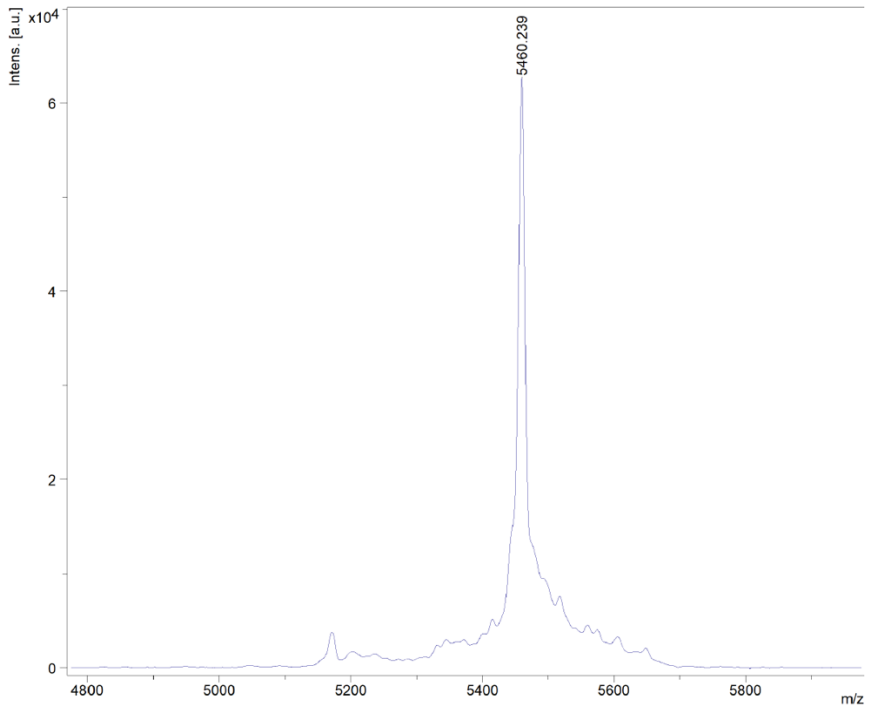

Figure 5-76. MALDI-TOF MS trace of *f*Cy5-SU75-37, expected *m/z* = 5460, observed *m/z* = 5460.

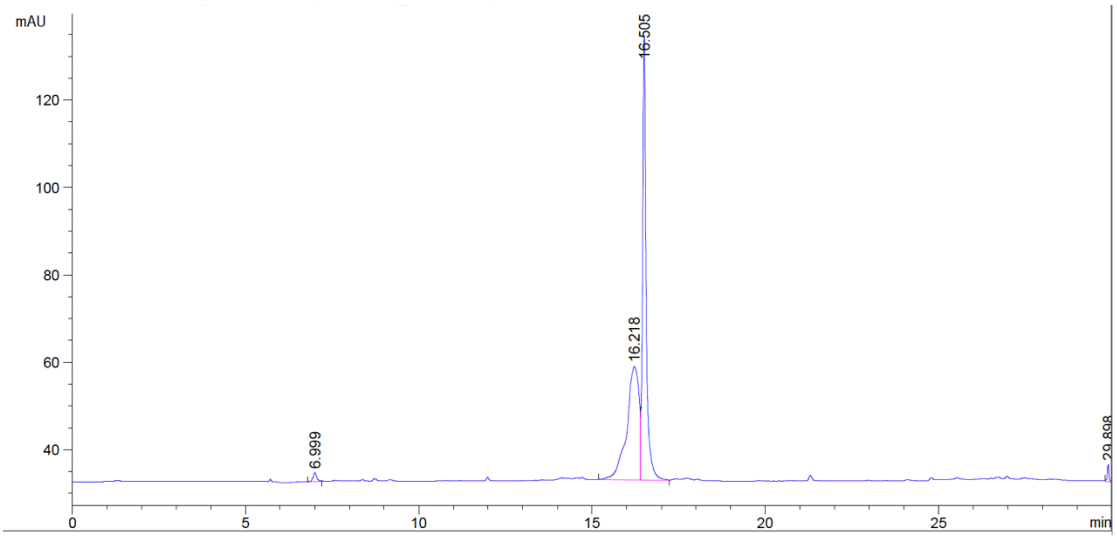

Figure 5-77. RP-HPLC purity trace showing product at 16.505 min.

5.2.4 Dual GLP-1R and MC4R agonists

5.2.4.1 KSCEM01

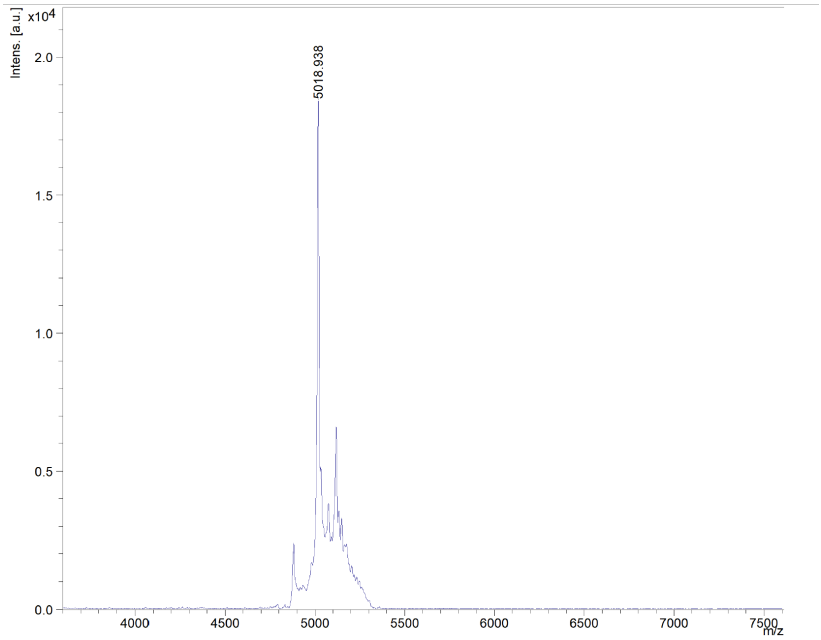

Figure 5-78. MALDI-TOF MS trace of KSCEM01, expected *m/z* = 5018, observed *m/z* = 5018.

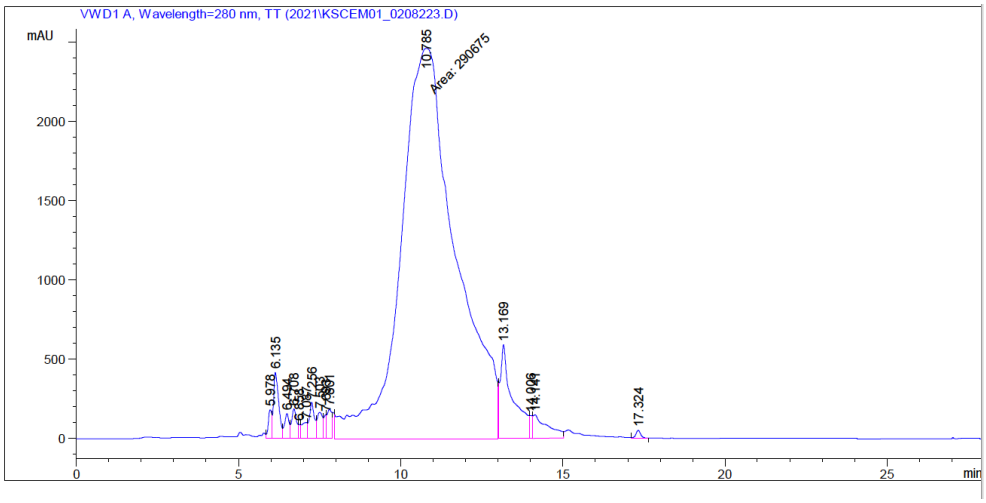

Figure 5-79. RP-HPLC purity trace showing product at 10.785 min.

5.2.4.2 KSCEM02

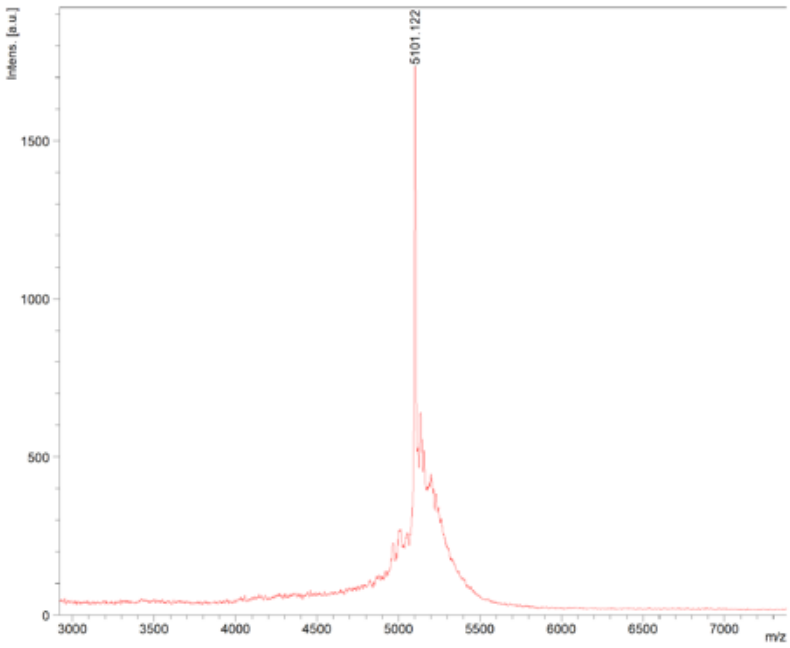

Figure 5-80. MALDI-TOF MS trace of KSCEM02, expected *m/z* = 5100, observed *m/z* = 5101.

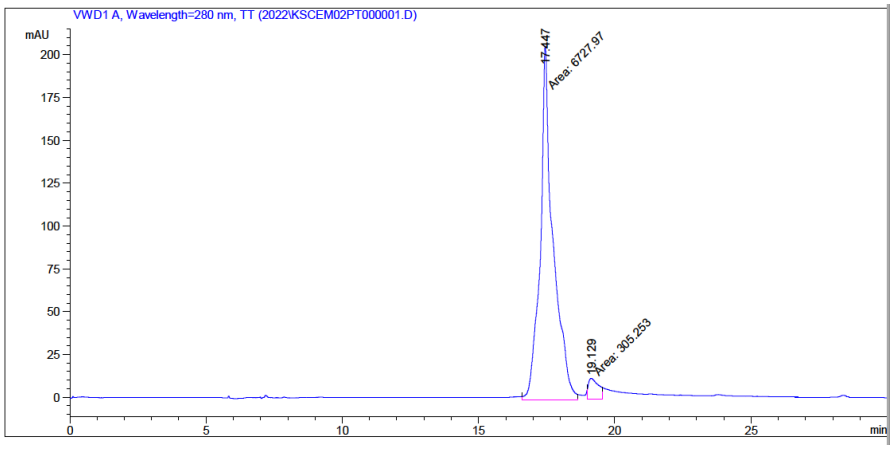

Figure 5-81. RP-HPLC purity trace showing product at 17.447 min.

5.2.4.3 KSCEM03

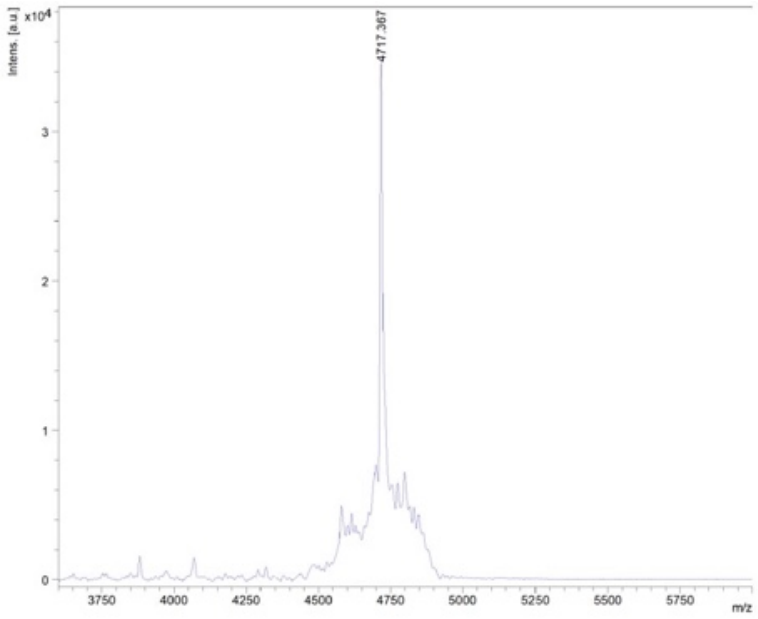

Figure 5-82. MALDI-TOF MS trace of KSCEM03, expected *m/z* = 4716, observed *m/z* = 4717.

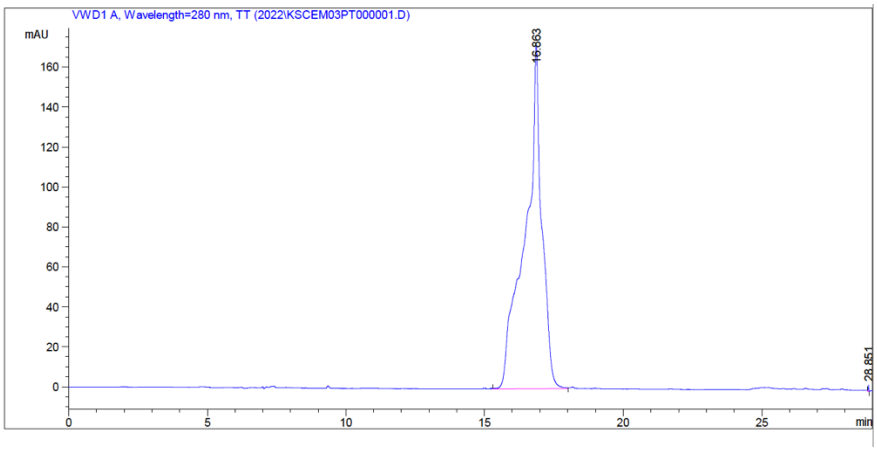

Figure 5-83. RP-HPLC purity trace showing product at 16.663 min.

5.2.4.4 KSCEM04

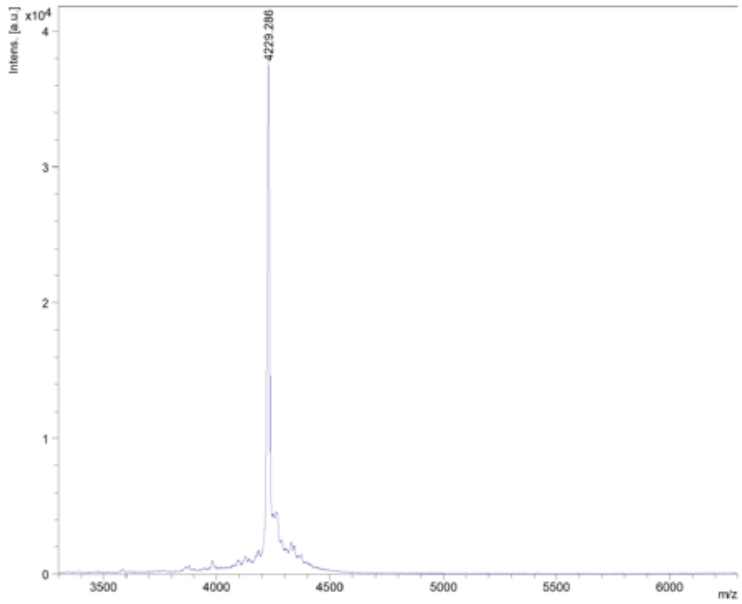

Figure 5-84. MALDI-TOF MS trace of KSCEM04, expected *m/z* = 4229, observed *m/z* = 4229.

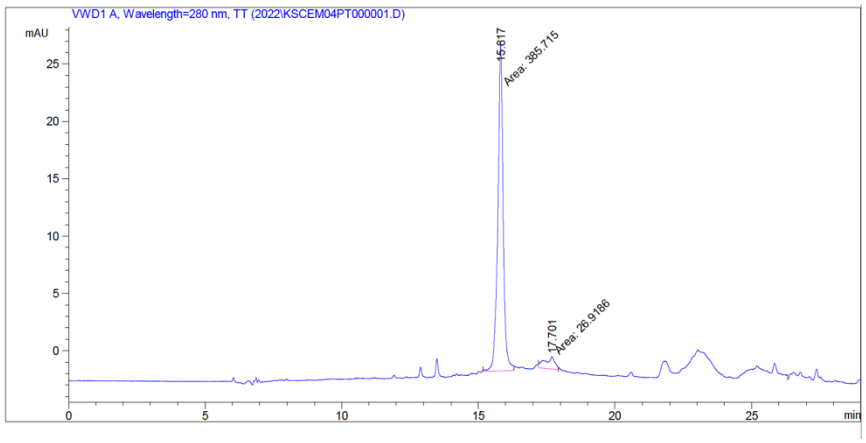

Figure 5-85. RP-HPLC purity trace showing product at 15.617 min.

5.3 Peptide purification and characterization

5.3.1 Agilent High-Performance Liquid Chromatography (HPLC)

Peptides were dissolved at 5-10 mg/mL in DI H_2O and purified on an Agilent 1200 series HPLC instrument (10–75% HPLC-grade acetonitrile for 20 minutes) at a 2 mL/min flow rate over an Agilent Zorbax C18 column (5 μm, 9.4 x 250 mm) tracked at 220, 254, and 280 nm. Peptides were purified to >95% as confirmed by HPLC.

5.3.2 Preparative scale purification via Flash Chromatography (≥ 30 mg)

Peptides were dissolved at 10-15 mg/mL in DI H_2O and purified on a Biotage Isolera LS instrument (10-95% HPLC-grade acetonitrile for 23 column volumes) at a 12 mL/min flow rate over a Biotage Sfär C4 or C18 reverse phase column (300 Å, 20 μm pore size) tracked at 220 and 280 nm. Peptides were purified to >95% as confirmed by HPLC.

5.3.3 Circular Dichroism (CD) Spectroscopy

Peptides were dissolved at 400 μM and diluted to 40 μM in 0.9% saline or H_2O. A Chirascan VX (Applied Photophysics) was used to analyze peptide folded states at a 250-200 nm measurement range, 100 nm/min scanning speed, 1 nm bandwidth, 4 second response time, and 1.0 nm data pitch.

5.3.4 Mass Spectrometry (MS)

5.3.4.1 Electrospray Ionization (ESI) MS

A Shimadzu liquid chromatography mass spectrometer (LCMS) 8040 instrument was used to confirm molecular weights of some peptides and reaction products, especially

those that didn't readily ionize. Solvent A was a 50/50 mixture of MeOH and H_2O, and solvent B was MeOH spiked with 0.1% formic acid.

5.3.4.2 MALDI-TOF MS

Confirmation of the molecular weights of most peptides and reaction products was obtained on a Bruker matrix-assisted laser desorption ionization time-of-flight mass spectrometer (MALDI-TOF MS). Samples were plated on a microScout 96-target polished steel plate (Bruker) in a 50/50 mixture of ACN and H_2O, and the spots were covered in a supersaturated solution of α–cyano–4–hydroxycinnamic acid (CHCA) matrix.

5.3.4.3 High Resolution MS/MS

High resolution MS/MS was completed at SUNY Upstate Medical University using an Orbitrap mass spectrometer.

5.4 Surface plasmon resonance (SPR) experiments

5.4.1 Measurement of GLP-1R competitive binding of GEP44 and GEP12

GEP44 and Ex-4 binding to the human GLP-1R was measured using a TagLite fluorescent competitive binding assay in CHO-K1 cells. GLP-1red was used as the agonist tracer and Ex-4 as the reference competitor. IC_{50} values were measured in duplicate in independent runs at eight concentrations per run. GEP12 binding to the human GLP-1R was measured in-house by SPR using His-tagged GLP-1R bound to a nitrilotriacetic acid (NTA) sensor. The GEP12 dose-response (0.1 nM–100 nM) binding assay was performed in a duplicate.

5.4.2 Measurement of Y1-R competitive binding of GEP44 and GEP12

Peptide binding to human Y1-R was performed in-house by SPR. The dose response to GEP44 (4 pM -19 μM) was evaluated using PYY_{1-36} as positive and PYY_{3-36} as negative controls.

5.4.3 Measurement of Y2-R competitive binding of GEP44 and GEP12

Peptide binding to the human Y2-R was measured in a dose-responsive manner (1 pM–1 μM) using a radioligand competitive binding assay in CHO-K1 cells. Peptide binding was assayed in duplicate independent runs with eight concentrations per run. The peptide PYY_{3-36} was used as a positive control.

5.4.4 Binding of SU75-36 and SU75-37 to GPR75 and hGLP-1R

5.4.4.1 Binding of SU75-36 and SU75-37 at hGLP-1R

SU75-36, SU75-37, Ex-4, and ODN binding at the human GLP-1R (21-139aa region; www.rndsystems.com cat # 10956-GL) was measured via a Nicoya Open SPR instrument using His-tagged hGLP-1R bound to an NTA-coated gold sensor (Nicoya cat # SEN-AU-100-10-NTA) using HBSS (in-house) at 20 μL/min flow rate. Data was fit via a global, one-to-one model using Nicoya OpenSPR software. In-house Ex-4 and ODN were used as the positive and negative controls, respectively.

5.4.4.1 Binding of SU75-36 and SU75-37 at GPR75

SU75-36 binding at the human GPR75 (372-540 aa region; www.antibodies-online.com cat # ABIN5709609) was measured via a Nicoya OpenSPR instrument using His-tagged GPR75 bound to an NTA-coated gold sensor (Nicoya cat # SEN-AU-100-10-NTA, range = 4.08-204 μM) using HBSS (in-house) at 20 μL/min flow rate. Data was fit via a global, one-to-one model using Nicoya OpenSPR software.

5.4.5 ODN-Biotin GPCR screening

Binding analysis was done on a Nicoya Open Surface plasmon resonance instrument using a Nicoya streptavidin sensor chip. The coupling procedure was according to the streptavidin sensor chip protocol, including the steps of surface conditioning and surface activation. For ligand immobilization, ODN-biotin (20 μg/mL in the PBST pH 7 running buffer) was injected over channel 2 for a 5-minute interaction time. This process was repeated several times to ensure optimal immobilization. The supernatant from the GPCR extraction procedure was injected over channels 1 and 2 of the chip, and a background-corrected binding curve was obtained. The chip was then soaked for 16 hours in 5 mL of MeOH at 4°C. An electron absorption spectrum of the MeOH used to soak the chip was obtained using a Nanodrop One. The remaining MeOH was mixed with water, freeze-dried, and sent out for MS/MS sequencing.

5.5 *In vitro* methods

5.5.1 Functional activity screening at human GLP-1R, Y2-R, and Y1-R

H188 virally transduced HEK293 cells stably expressing human GLP-1R were obtained from Novo Nordisk A/S for use in FRET assays. HEK293 C24 cells stably expressing the H188 FRET reporter were obtained by G418 selection and grown in monolayers to ~70% confluency in 100 cm^2 tissue culture dishes and were then transfected with plasmids (11 µg/dish) encoding human GLP-1R, human Y2-R, or human Y1-R. Transfected cells were then incubated for 48 hours in fresh culture media. For real-time FRET kinetic assays, cells were harvested, resuspended in 21 mL of SES buffer, and plated at 196 µL per well. Plated cells were pretreated with 4 µL of agonist, or antagonist (Ex9-39 (GLP-1R antagonist) or BIIE0246 (Y2-R antagonist)), at a given target concentration and incubated for 20 min before performing the assay. Y1-R and Y2-R agonism to stimulate Gi proteins and to inhibit adenylyl cyclase was monitored by detecting the ability of PYY peptides, GEP44, or GEP12 to counteract the ability of Adenosine (acting through endogenous A2B receptor and G_s proteins) to increase levels of cAMP. For these assays, increased levels of cAMP were measured as an increase of the 485/535 nm FRET ratio serving as a readout for binding of cAMP to the H188 biosensor that is based on the exchange protein activated by cAMP.

5.6 *In vivo* methods

5.6.1 Animal studies of GEP44 and related peptides

5.6.1.1 Dose escalation studies of GEP44 and GEP12 in male rats

Male Wistar rats (Ex-4 group, n=4; GEP44 group, n=8) were provided with a HFD (60% kcal from fat, 5.21 kcal/g) for 20 weeks before the start of the study. Rats were singly

housed in BioDAQ cages and allowed to acclimate for at least 10 days before the start of this study. The average baseline weight of the rats in this study was 685 g. Baseline measurements of body weight and food intake were taken for three days to balance the groups. The study design included sequential rounds of a three-day vehicle-treated baseline phase, a three-day treatment phase, and a two-to-three-day washout phase. Dosing began at 0.5 nmol/kg/day and was increased in approximately one-third-log increments ($10^{n/3}$) until the MTD was established. The doses tested included 0.5, 1, 2, 5, 10, 20, 50, and 100 nmol/kg/day administered subcutaneously just before the start of the dark cycle. The 100 nmol/kg dose of GEP44 was tested for one day only. Body weight was assessed daily just before the start of the dark cycle. Food and water were available *ad libitum* and consumption was monitored continuously. A preliminary GEP12 dosing test was performed in male DIO Wistar rats (n=8). These rats were fed the HFD for 40 weeks before the start of the study and weighed an average of 862 g at baseline. The study design included two rounds of a three-day vehicle-treated baseline phase, a three-day treatment phase, and a two-to-three-day washout phase. Doses of 5 to 10 nmol/kg/day were administered via subcutaneous injection just before the start of the dark cycle. Body weight was assessed daily just before the start of the dark cycle. Food and water were available *ad libitum* and consumption was continuously monitored using a BioDAQ system. In this experiment, cages were modified to facilitate the use of the DietMax food monitor system for continuous recording of powdered kaolin consumption. Animals were allowed to acclimate for at least 10 days before the start of the study.

5.6.1.2 Long-term *in vivo* study of GEP44 and LIRA

Male Wistar rats (n=4) were fed a 60% HFD for 20 weeks before the start of the study. Rats were then housed singly in BioDAQ cages and allowed to acclimate to their new environment for 10 days. Baseline measurements of body weight and food intake were collected for one week to balance the groups and create feeding pairs. Two independent experiments were performed. In the first experiment, three cohorts of eight animals each received daily injections of vehicle or increasing doses of either GEP44 or LIRA starting at 10 nmol/kg for 9 days and followed by 25 nmol/kg for 7 days. In the second experiment, five cohorts of eight animals each received daily injections of GEP44 alone, vehicle pair-fed with GEP44, LIRA alone, vehicle pair-fed to LIRA, and vehicle alone. Rats averaged 661 g at baseline with equivalent variances between the groups. GEP44 was administered as follows: 5 nmol/kg/day for 4 days, 10 nmol/kg/day for 4 days, 25 nmol/kg/day for 12 days, and 50 nmol/kg/day for 8 days. LIRA was administered as follows: 5 nmol/kg/day for 4 days, 10 nmol/kg/day for 4 days, 25 nmol/kg/day for 4 days, and 50 nmol/kg/day for 16 days. Food intake was monitored continuously throughout the experiment. Body weights were measured daily immediately before the start of the dark cycle. Pre- and post-treatment fasting plasma samples were obtained from blood collected via tail nick using a microvette to assess insulin levels. Blood glucose concentrations were obtained at the same time using a handheld glucometer. Blood was collected by cardiac puncture at the time of euthanasia which was two hours after the final injection. Commercially available ELISAs were used to perform quantitative assessments of both insulin and adiponectin. Serum levels of glucose, cholesterol (total, high-density lipoprotein [HDL], and calculated low-density lipoprotein [LDL]), triglycerides,

alanine transaminase (ALT), and aspartate transaminase (AST) were determined using a Modular P chemistry analyzer (Roche Diagnostics, Germany) by the University of Washington NORC Core, Seattle, WA.

5.6.2 *In vivo* work with SU75-36 and SU75-37, antagonists of GPR75

5.6.2.1 SU75-36 and SU75-37 in HFD-fed DIO rats

DIO rats were administered 20 µg SU75-36, 100 µg SU75-36, 200 µg SU75-36, or 20 µg SU75-37 by intramuscular injection to the 4th ventricle and observed over 24 hours. One group of rats was administered a vehicle without a GPR75 inhibitor as a negative control. All rats were given *ad libitum* access to access to water 60% HFD chow. The food intake of each rat was observed 1, 3, 6, and 24 hours after administration of the GPR75 inhibitor. Rats were weighed at the beginning of the experiment and 24 hours after administration of the GPR75 inhibitor. The weight change of each rat after 24 hours was then calculated.

5.6.2.2 SU75-36 and SU75-37 in HFD-fed DIO rats with kaolin intake analysis

DIO rats were administered 20 µg SU75-36, 200 µg SU75-36, or 20 µg SU75-37 by intramuscular injection to the 4th ventricle and observed over 24 hours. One group of rats was administered a vehicle without a GPR75 inhibitor as a negative control. All rats were given *ad libitum* access to access to water and chow, 60% HFD chow, chow with Kaolin, or 60% HFD chow with Kaolin. The food intake of each rat was observed 1, 3, 6, and 24 hours after administration of the GPR75 inhibitor. Rats were weighed at the beginning of the experiment and 24 hours after administration of the GPR75 inhibitor. The weight change of each rat after 24 hours was then calculated.

5.6.3 *In vivo* work with ODN and related neuropeptides

5.6.3.1 Cannula implantation surgery

For cannula implantation, rats were anesthetized by an IP injection of a mixture containing ketamine (90 mg/kg, Butler Animal Health Supply), xylazine (2.7 mg/kg, Anased), and acepromazine (0.64 mg/kg, Butler Animal Health Supply) (KAX) and then placed into a stereotaxic apparatus. Each rat was stereotaxically implanted with a guide cannula (26-ga, Plastics One) aimed at the fourth ventricle (guide cannula coordinates: on midline, 2.5 mm anterior to occipital suture, 5.2 mm ventral to skull; internal cannula aimed 7.2 mm ventral to skull) or the lateral ventricle (guide cannula coordinates: 1.5 mm lateral to midline, 0.9 mm posterior to bregma, 1.8 mm ventral to skull; internal cannula aimed 3.8 mm ventral to skull). For all cannulas, dummies (no projection beyond guide) were inserted in the guide cannula and left until infusions were performed. For all surgeries, rats received post-operative temperature support and analgesia was provided immediately following surgery and for two post-operative days (2 mg/kg meloxicam).

5.6.3.2 Food and kaolin intake studies of ODN and related neuropeptides

For all studies measuring food intake following drug treatment, central injections were given at volume of 2 µL were administered using a Hamilton syringe terminating in an injector tip extending 2.0 mm beyond the guide cannula, and intraperitoneal injections were given based on body weight (0.1 mL/100 g body weight). For acute treatment days, rats were food deprived 2 hours before the dark cycle and injections were done immediately prior to the dark cycle onset. Food and kaolin intake was measured 1, 3, 6,

and 24 hours after injections were completed and food crumbs were weighed and accounted for between each timepoint. Body weight was measured during injections and 24 hours after. Injection treatments were organized in a counterbalanced, within-subjects design and separated by ≥72 hours. For chronic intake studies, once daily drug injections and recording of body weight, food, and kaolin intake were performed every 24h immediately prior to the dark cycle onset. For meal pattern analysis, rats living in a BioDAQ system (Research Diets, Inc) were injected similarly. The BioDAQ system records on a second-by-second basis for undisturbed measurements of episodic food intake. Individual bouts are initiated by the animal at onset and termination of feeding; bouts are separated by 5 second inter-bout interval. A meal is defined as at least one bout with a minimum meal size of 0.02 g and separated by a 5-minute undisturbed inter-meal interval. Cumulative food intake, the number of meals, time spent consuming meals, average meal size (g/meal), and average meal length (sec/meal) was calculated for hours 0-1, 0-6, 6-12, and 12-24 relative to drug injection. Additionally, cumulative food intake (g), number of bouts, time in bouts, number of meals, and time in meals were calculated for 20 min intervals for the first 3 hours post injection in chow fed rats and for 1 hour intervals for 24 hours post injections in HFD-fed rats.

5.6.3.3 Hindbrain DBI immunohistochemistry and quantification

Rats maintained on chow or HFD were either *ad libitum* fed or fasted for 24h. All rats received a 4^{th} ventricle injection of aCSF or Ex-4 (0.3 µg/2 µL) 90 minutes prior to sacrifice. Rats were deeply anesthetized with KAX and transcardially perfused with 0.1 M phosphate-buffered saline (PBS; pH 7.4) followed by 4% paraformaldehyde in 0.1 M PBS

on ice. Brains were removed from the crania and post-fixed in 4% paraformaldehyde for 24h, then stored in 20% sucrose in 0.1 M PBS at 4 °C until sunk. Coronal dorsal vagal complex (DVC) sections (30 µm) were sliced and collected directly onto slides (12-550-15; Superfrost Plus, Fisher Scientific) using a cryostat and stored at −80 °C until the start of IHC. Briefly, tissue was washed with 0.1 M PBS 3 times for 8 minutes and then incubated in blocking solution [5% normal donkey serum (Jackson Immunoresearch) in PBST; PBS with 0.3% triton X] followed by overnight incubation in rabbit anti-DBI primary antibody (1:500; ab231910, Abcam) and chicken anti-vimentin primary antibody (1:2000; ab24525, Abcam) at 4 °C. The next morning slides were washed 3 times for 8 minutes in PBST and then incubated in donkey anti-rabbit fluorescent secondary antibody (1:500; AlexaFluor 647, Jackson Immunoresearch) and donkey anti-chicken fluorescent secondary antibody (1:500; AlexaFluor 488, Jackson Immunoresearch) for 3 hours at RT. Finally, slides were washed 3 times for 5 minutes in PBST and one time in PBS before cover-slipped with antifade mounting media with DAPI (H-1200, Vector Laboratories, Inc.). Slides were visualized using fluorescence microscopy (BZ-X810, Keyence). Image analyses to quantify the fluorescent intensity of DBI protein staining in the NTS and AP as well as the % colocalization of DBI and vimentin staining in the AP, subpostrema, and 4th ventricle boarder was done using the HALO® FISH-IF and Area Quantification FL modules.

5.6.3.4 Quantitative real-time (qPCR) studies

Chow-maintained rats received a 4th ventricle injection of aCSF or Ex-4 (0.3 µg/2 µL) 90 minutes prior to sacrifice. Brains were rapidly removed, flash-frozen in −70°C isopentane,

and stored at −80°C until processing. Micro-punched tissue from the DVC was collected from each brain. Total RNA was extracted from tissue from each site using TRIzol (Invitrogen) and the RNeasy kit (Qiagen). The Advantage RT-for-PCR Kit (Clontech) was used to synthesize cDNA from 200 ng of total RNA. Relative mRNA levels of DBI were quantified using quantitative real-time PCR. Rat GapDH (VIC-MGB) was used as an internal control. PCR reactions were completed using TaqMan gene expression kits (DBI: Rn00821402_g1 and GapDH: Rn01775763_g1) and PCR reagents from Applied Biosystems. Samples were analyzed with the QuantStudio 6 Pro system (Applied Biosciences). Relative mRNA expression calculations were completed using the comparative threshold cycle method.

5.6.3.5 Hindbrain glucose sensing studies

Chow-maintained rats were food deprived 2 hours before the dark cycle and 4th ventricle injections were done immediately prior to the dark cycle onset. Baseline glucose values were taken from tail vein blood by glucometer (Concur) prior to injections and 30 and 60 minutes after injections. In one study rats received a pretreatment injection of vehicle (aCSF) or OP (20 µg/2 µL) followed by treatment with vehicle or 5-thio-d-glucose (5-TG; 210 µg/2 µL). In the other study rats received a pretreatment injection of vehicle or AntOP (20 µg/2 µL) followed by treatment with vehicle or D-glucose (5.5 M in 3 µL). Food was returned 1h after injections following measurement of the last blood glucose concentrations and food intake was recorded 2, 4, 6, and 24 hours post injections. Body weight was measured during injections and 24 hours after.

5.6.3.6 Relaxin-3 antagonism model

Rats were stereotaxically implanted with a bilateral guide cannula (26-ga, Plastics One) aimed at the *nucleus incertus* (guide cannula coordinates: ± 0.5 lateral to midline, 9.5 mm anterior to bregma, 5.8 mm ventral to skull; internal cannula aimed 7.8 mm ventral to skull). Recombinant human relaxin-3 was purchased (130-10, PreproTech Inc.) and ODN was synthesized by the author. Injection treatments [pretreatment with ODN (10 µg) or vehicle and treatment with relaxin-3 (32.4 nmol) or vehicle] were organized in a counterbalanced, within-subjects design and separated by ≥72 hours. Rats were food deprived 2 hours before the dark cycle and injections were done immediately prior to the dark cycle onset. All injection were given at a volume of 100nL in aCSF at a rate of 20nL/second using a micropump-depressed (PHD 2000, Harvard Apparatus) loaded with a Hamilton syringe terminating in an injector tip extending 2.0 mm beyond the bilateral guide cannula implanted at the *nucleus incertus* coordinates above. 24h food intake was recorded in a BioDAQ system (Research Diets, Inc). Body weight was measured during injections and 24 hours after.

5.6.3.7 DVC tissue extraction from male rats

Male Sprague Dawley rats were anesthetized by isoflurane and rapidly decapitated, the brains removed, and flash frozen in -70°C isopentane and stored at -80°C. Using a cryostat, the DVC (comprised of the *area postrema*, *nucleus tractus solitarius*, and dorsal motor nucleus of the vagus) of the rat brainstem was micro-punched 1 mm^3 per subnuclei at the level of the AP and pooled together in a cryovial and restored at -80°C for protein/GPCR tissue extraction procedures (5.3.5).

5.7 *Ex vivo* experimental methods and materials

5.7.1 Islet and muscle work relating to GEP project

5.7.1.1 Static measurements to determine rates of insulin secretion, glucagon secretion, and cAMP release

Rates of insulin, glucagon, and cAMP release were determined statically under multiple conditions as previously described.[1] Briefly, islets were handpicked, transferred to a petri dish containing 11 mL of Krebs-Ringer bicarbonate (KRB) buffer supplemented with 0.1% bovine serum albumin (BSA) and 3 mM glucose, and incubated at 37°C and 5% CO_2 for 60 min. Islets were then selected and transferred into wells of 96-well plates containing 0.2 mL of KRB with 20 mM glucose and various test compounds as indicated and incubated for an additional 60 min. Subsequently, the supernatants were assayed for insulin, glucagon, and cAMP. These values were used to calculate the secretion rate as the concentration in the assay (ng/mL for insulin and glucagon, and pmol/mL for cAMP) times the volume of KRB in each well during the assay (0.2 mL) divided by the assay time (60 minutes). Data was then normalized by dividing by the secretion rate in the presence of test compounds over that obtained at 20 mM glucose alone.

5.7.1.2 Perifusion measurements to determine rates of insulin secretion

Insulin production was evaluated using a commercially available perifusion system (BaroFuse; EnTox Sciences, Mercer Island, WA). Ten isolated rat islets were placed into each of eight channels that were operating at a flow rate of 50 µL/min of KRB (continuously equilibrated with 21% O_2, 5% CO_2, and balance of N_2) containing 0.1% BSA

and 3 mM glucose for 90 minutes. Subsequently, varying amounts of glucose and test compounds were injected into the inflow of the flow system as indicated and outflow fractions were collected every 10 minutes and assayed for insulin as described in the section to follow. The insulin secretion rate was calculated as insulin times the flow rate of KRB divided by the number of islet x 100 yielding the ng/min/100 islets. Data was graphed after normalizing each insulin time course by dividing by the secretion rate at each time point by the rate obtained in the presence of 20 mM glucose prior to the addition of test compounds.

5.7.1.3 Glucose uptake in muscle

^{3}H-2-deoxyglucose uptake into muscle tissue was evaluated as previously described, with the exception that the bound radiolabeled compound was separated from free radiolabel by washing the tissue multiple times in radiolabel-free medium. Sprague-Dawley rats (~250 g) were anesthetized by intraperitoneal injection of Beuthanasia-D (38 mg pentobarbital sodium and 6 mg phenytoin sodium/230 g rat) (Schering-Plough Animal Health Corp., Union, NJ). While the rats remained under anesthesia, strips of quadriceps muscle were collected and transferred to a Petri dish containing HBSS with 0.1% BSA. While still under anesthesia, animals were then euthanized by cutting the diaphragm. The muscle strip was cut into smaller pieces (~2 mg each) using a scalpel. Three pieces were then transferred into polystyrene 12 x 75 test tubes containing 190 mL of KRB (with 5 mM bicarbonate) solution and compounds as described in each experiment. Each condition was evaluated in triplicate. The tubes were placed in racks that were partially submerged in a shaking water bath maintained at 37°C. At precisely the times indicated, 10 µL of the

radioactive dose (typically 0.25 µCi) was spiked into each tube to bring the final volume to 200 mL. The tubes were capped and shaken in the water bath at 120 rpm for 45 minutes. Free radiolabel was removed by washing the muscle fragments three times with 5 mL cold (4°C) KRB solution. After the third wash, 100 µL of KRB was added to each tube and the muscle and solution were then transferred to a microcentrifuge tube. The muscle pieces were then fragmented further by sonication (Branson) at maximum power and 50% duty cycle for 20 seconds. The contents of the microfuge tube were then transferred to a 7-mL scintillation vial. A liquid scintillation cocktail (5 mL, Ecolume) was added, the samples were shaken, and radioactivity was evaluated using a liquid scintillation counter.

5.7.1.4 Lactate production by perifused muscle tissue

Muscle fragments (6 x 2 mg each) were placed into each of six channels of a commercially available perifusion system (BaroFuse) operating at a flow rate of 30 µL/min of KRB with 0.1% BSA and varying amounts of glucose. Outflow fractions were collected every 10 minutes and measured using a glucose/glucose oxidase kit in which lactate oxidase was used to replace glucose oxidase. Manufacturer-supplied solutions of horseradish peroxidase, Amplex Red, and lactate oxidase were added to samples in wells of a 96-well microplate which was then incubated at room temperature for 30 minutes. Fluorescence was measured with a spectrophotometer.

5.7.2 GPCR extraction from DVC tissue

Membrane proteins were extracted from rat brain tissue sent from the Hayes lab at the University of Pennsylvania based on the protocol for tissues on the GPCR Extraction and Stabilization Reagent (GESR) (ThermoFisher Scientific, Rockford, Il). Briefly, the tissue samples were suspended in 1 mL of cold (4°C) PBS and washed repeatedly. The PBS was decanted, and 1 mL of cold (4°C) GESR was added to the tissue samples. The tissue samples were homogenized until an even suspension was obtained by pipetting up and down 15-20 times. The homogenate was transferred to a new tube and was incubated at 4°C for 30 minutes with end-over-end mixing. The sample was centrifuged at 16,000 x g for 20 minutes at 4°C. The supernatant containing stabilized protein receptors was saved and stored at 4°C until being analyzed.

5.8 Reference

1. Jung, Reed *et al.* A highly energetic process couples calcium influx through L-type calcium channels to insulin secretion in pancreatic beta-cells. *Am J Physiol Endocrinol Metab* 2009;297: E717–E727.

Chapter 6: On-going and future work

6.1 GEP Project

6.1.1 Expansion of lead triple agonist to help treat other comorbidities of T2DM (NAFLD, NASH, cardiovascular issues, etc.)

There's a direct correlation between the growing incidences of T2DM and non-alcoholic fatty liver disease (NAFLD) worldwide.[1] Bariatric surgery has positive effects on weight reduction and prevention of NAFLD. Evidence suggests NAFLD doubles the risk of patients developing T2DM.[2] The GLP-1RA Ex-4 has been shown to improve insulin sensitivity and ultimately reverse hepatic steatosis in *ob/ob* mice.[3] By expanding the potential therapeutic uses for a triple agonist of GLP-1R, Y2-R, and Y1-R, we can try to guarantee our lead will have sustained clinical relevance.

6.1.2 Multiple dose (50, 100, 200 nmol/kg) pharmacokinetic (PK) experiment in DIO rats

The snapshot PK experiment at 1 nmol/kg dose of unmodified GEP44 gave an indication of its $T_{1/2}$ and clearance compared to Ex-4. Ex-4 (Byetta®) is not modified with a lipid-based residue and, in turn, does not have an enhanced PK profile. The field has progressed to lipidation of GLP-1RAs and marketing them as once-weekly therapeutics (*i.e.*, semaglutide/Wegovy®). To attain a more accurate comparison of our current lead, KSCGG3, and semaglutide, it would be beneficial to repeat the PK experiment with these long-acting compounds. DIO male and female rats would be administered 50, 100, or 200 nmol/kg of KSCGG3, 50, 100, or 200 nmol/kg of semaglutide, or a vehicle control. Blood samples of at least 50 µL should be obtained from the tail vein at frequent time points and deposited into EDTA-coated tubes. The plasma would be flash-frozen and used for an

enzyme-linked immunoassay (ELISA) to ultimately measure the concentration of drug at the various timepoints. PK parameters could be extrapolated from this data to successfully compare our lead to the current, best-in-class T2DM therapeutics.

6.1.3 Determine how long lipidated peptides and semaglutide remain bound to albumin

Peptides KSCGG1-4 contain a fatty diacid which is predicted to bind to serum albumin, resulting in a longer *in vivo* $T_{1/2}$. Wegovy® (Semaglutide), an FDA-approved therapeutic with the same lipid construct, was designed to bind to albumin while maintaining GLP-1R potency.[4] To effectively compare KSCGG1-4 to Wegovy®, it's important to measure several parameters and ensure our peptides are competing with the pharmaceutical standards. Binding of KSCGG1-4 should be measured vs. Wegovy® using a method similar to the one described by Dargó, *et al*.[5]

6.1.4 Synthesize additional potential triple agonists of GLP-1R, Y2-R, and Y1-R

To expand upon the triple agonist scaffold, additional peptide sequences were designed with the intention of decreasing GLP-1R-based internalization and enhancing the potency at GLP-1R (GEP12-19, GEP49). GEP12 was synthesized, assayed for internalization, and served as our proof-of-concept design, since it successfully shut down GLP-1R-based internalization compared to GEP44. Despite GEP12 showing decreased GLP-1R internalization and a greater ISR in rat and human islets relative to GEP44 and the glucose control, it was less potent at GLP-1R in functional assays compared to GEP44, which contributed to its lack of effect in *in vivo* models of T2DM. The additional compounds in this section should be synthesized by methods explained previously and

assayed for GLP-1R function and internalization. In addition, it is vital for these compounds to maintain or improve potency at Y2-R and Y1-R. Peptides GEP28-37 were designed to have improved function and binding at Y2-R and Y1-R. These parameters would be verified by Y2-R-, Y1-R-, *and* GLP-1R-based assays described in chapter 2. Lastly, the peptides comprising the final section of Table 6-1, GEP38-48 and GEP50-51 were designed to have balanced agonism at GLP-1R, Y2-R, and Y1-R.

Table 6-1. Potential triple agonists of GLP-1R, Y2-R, and Y1-R.

Code	Peptide Sequence	Agonism	
		GLP-1R	Y2-R
GEP44	HsQGTFTSDLSKYLEEEAVREFIAWLKNGGPSRHYLNLVTRQRY-NH_2	330 pM	10 nM
GEP01	HsQGTFTSDLSKYLEEEAVREFIAWLKNGGPSSRHYLNLVTRQRY-NH_2	86 pM	
GEP02	HsQGTFTSDLSKQMEEEAVREFIAWLKNGGPSRHYLNLVTRQRY-NH_2	294 pM	
GEP03	HsQGTFTSDLSKQLEEEAVRLFIAWLKNGGPSRHYLNLVTRQRY-NH_2		209 nM
GEP04	HsQGTFTSDLSKQMEEEAVRLFIAWLKNGGPSSGAPRHYLNLVTRQRY-NH_2	115 pM	
GEP05	YsQGTFTSDLSKQMEEEAVRLFIAWLKNGGPSSGAPRHYLNLVTRQRY-NH_2	6.2 nM	
GEP06	YPQGTFTSDVSKQMEEEAVREFIAWLKNGGPSRHYLNLVTRQRY-NH_2	>3000 nM	
GEP07	YPQGTFTSDLSKYMEEEAVREFIAWLKNGGPSRHYLNLVTRQRY-NH_2	66 nM	
GEP08	YLDGTFTSDLSKYLEEEAVREFIAWLKNGGPSSRHYLNLVTRQRY-NH_2	334 pM	
GEP09	DLSKYLEEEAVREFIAWLKNGGPSRHYLNLVTRQRY-NH_2		
GEP10	HsQGTFTSDLSKYLEEEAVREFIAWLKNGGPSRHYLNWVTRQRY-NH_2	685 pM	307 nM
GEP11	HsQGTFTSDLSKYLEEEAVREFIAWLKNGGPSRHYLNWLTRQRY-NH_2	396 pM	427 nM
	↓ GLP-1R internalization; ↑ GLP-1R agonism; ↑ $T_{1/2}$; ↑ V_D		
GEP12	FsQGTFTSDLSKYLEEEAVREFIAWLKNGGPSRHYLNLVTRQrY-NH_2	13.7 nM	
GEP13	FsHGTFTSDLSKLKEEQRQ(Aib)EFIEWLKAGGPPSRHYLNLVTRQrY-NH_2		
GEP14	FsHGTFTSDLSKYLEEQRQ(Aib)EFIEWLKAGGPPSRHYLNLVTRQrY-NH_2		
GEP15	FsHGTFTSDLSKYLEEQRQ(Aib)EFIAWLKAGGPPSRHYLNLVTRQrY-NH_2		
GEP16	FsEGTFTSDYSIYLDKQAA(Aib)EFVNWLLAGGPSRHYLNLVTRQrY-NH_2		
GEP17	FsEGTFTSDYSKYLDKQAA(Aib)EFVNWLLAGGPSRHYLNLVTRQrY-NH_2		
GEP18	FsEGTFTSDYSKYLDKQAA(Aib)EFVAWLLAGGPSRHYLNLVTRQrY-NH_2		
GEP19	FsEGTFISDYSIAMDVSSYLEGQAAKEFIAWLVKGGPSRHYLNLVTRQrY-NH_2		
GEP49	FsEGS(αF)TSDV(αS)SKLEGEAA(αK)E(αF)IAKVVEGGPSRHYLNLVTRQrY-NH_2		
	↑ Y2-R agonism and binding; ↑ $T_{1/2}$; ↑ V_D		
GEP28	FsQGTFTSDLSKYLEEEAVREFIAWLKYGGPLRHYLNLVTRQrY-NH_2		
GEP29	FsQGTFTSDLSKYLEEEAVREFIAWLKNGGPSLRHYLNLVTRQrY-NH_2		
GEP30	FsQGTFTSDLSKYLEEEAVREFIAWLKNGGPSSLRHYLNLVTRQrY-NH_2		
GEP31	FsQGTFTSDLSKYLEEEAVREFIAWLKNGGPSSLRHYINLVTRQrY-NH_2		
GEP32	FsQGTFTSDLSKYLEEEAVREFIAWLKNGGPSLRHYINLVTRQrY-NH_2		
GEP33	FsQGTFTSDLSKYLEEEAVREFIAWLKNGGPSLRHFINWLTRQrY-NH_2		
GEP34	FsQGTFTSDLSKYLEEEAVREFIAWLKNGGPSRHFINWLTRQrY-NH_2		
GEP35	FsQGTFTSDLSKYLEEEAVREFIAWLKNGGPSRHYLNLVTRQ(N_{me}Arg)Y-NH_2		
GEP36	FsQGTFTSDLSKYLEEEAVREFIAWQKNGGPSRHYLNLVTRQ(N_{me}Arg)Y-NH_2		
GEP37	FsQGTFTSDLSKYLEEEAVREFIAWLKNGGPSRHYLNLVTRQrY-NH_2		
GEP38	FsHGTFTSDLSKLKEEQRQ(Aib)EFIEWLKAGGPPLRHYLNLVTRQrY-NH_2		
GEP39	HsHGTFTSDLSKYLEEQRQ(Aib)EFIEWLKAGGPPLRHYLNLVTRQrY-NH_2		
GEP40	FsHGTFTSDLSKYLEEQRQ(Aib)EFIEWLKAGGPPSLRHYLNLVTRQrY-NH_2		
GEP41	FsEGTFTSDYSIYLDKQAA(Aib)EFVNWLLAGGPSRHYINLVTRQrY-NH_2		
GEP42	HsEGTFISDYSIAMDVSSYLEGQAAKEFIAWLVKGGPSLRHYINLVTRQrY-NH_2		
GEP43	FsEGTFTSDYSKYLDKQAA(Aib)EFVNWLLAGGPSLRHFINWLTRQrY-NH_2		
GEP45	FsQGTFTSDLSKYLEEEAVREFIAWLKNGGPSRHFINWLTRQrY-NH_2		
GEP46	FsEGTFTSDYSKYLDKQAA(Aib)EFVNWLLAGGPSRHYLNLVTRQ(N_{me}Arg)Y-NH_2		
GEP47	HsEGTFTSDYSKYLDKQAA(Aib)EFVNWLLAGGPSRHYLNLVTRQ(N_{me}Arg)Y-NH_2		
GEP48	HsHGTFTSDLSKYLEEQRQ(Aib)EFIEWQKAGGPPLRHYLNLVTRQ(N_{me}Arg)Y-NH_2		
GEP50	FsEGS(αF)TSDV(αS)SKLEGEAA(αK)E(αF)IAKVVEGGPSRHYLNLVTRQ(N_{me}Arg)Y-NH_2		
GEP51	FsEGS(αF)TSDV(αS)SKLEGEAA(αK)E(αF)IAKVVEGGPSLRHYINLVTRQrY-NH_2		

6.1.4.1 Encapsulation of the lead peptide for oral delivery

Oral semaglutide (Rybelsus®) is the first GLP-1RA with the ability to be administered orally. Rybelsus® is co-formulated with an absorption enhancer, sodium *N*-(8-[2-hydroxylbenzoyl] amino) caprylate (SNAC), which increases solubility of the drug and helps it to resist proteolytic cleavage.[6] The route of administration of semaglutide (oral vs. subcutaneous injection) does not have a significant effect on the efficacy or tolerability of the therapeutic.[7] Our lead, long-acting peptide should be formulated by the same or similar methods so oral administration is an option.

6.1.4.2 The use of diselenium bonds to stabilize chimeric peptides

It is hypothesized that the ability of GEP44 to effectively act as a multi-agonist and create such potent *in vivo* metabolic effects is in part due to its folded state. As mentioned previously, GEP44 contains two α-helices separated by amino acids put in place to facilitate a β-turn and allow the α-helices to align parallel to each other. Since the helices are in close proximity, the residues are able to interact, and a hydrophobic pocket is formed. This leaves critical residues exposed which engage in binding to the key receptors. If the folded structure of GEP44 is indicative of its function, it is vital the secondary structure is consistently optimal to obtain reliable metabolic effects. Work by Weil-Ktorza, *et al.*, to stabilize insulin reveals their use of a diselenium bond within the peptide to enhance its foldability.[8] Findings included the added thermal stability and increased resistance to enzymatic cleavage of this modified form of insulin compared to the WT. They determined by 2D-NMR and X-ray crystallography that the diselenium

intercalates into a hydrophobic pocket without introducing a steric clash. Given their success with this peptidyl modification, it's hypothesized that incorporating a diselenium bridge into the construct of GEP44 can "staple" the two α-helices and keep the peptide in the desired conformation to optimize receptor activity.

6.1.5 Gather and publish data on lipidated GEP-peptides

Several long-acting iterations of GEP44 have been synthesized, screened for function in cell-based assays, and briefly monitored for BW and FI reduction in animal models of T2DM. If any peptides from section 6.1.4 show potent function at GLP-1R, Y2-R, and Y1-R and improved metabolic effects *in vivo*, they can be synthesized with a lipidated amino acid residue as described previously. Dynamic light scattering (DLS) assays can be used to gauge the level of aggregation or the propensity of the peptides to form aggregates in solution. The lead, long-acting peptide should be assayed for PK and toxicity and published in a peer-reviewed journal.

6.1.6 MC4R/GLP-1R dual agonists

Setmelanotide is a synthetic cyclic peptide that binds to human MC4R with high affinity and activates MC4R at nanomolar concentrations (EC_{50} = 0.27 nM). Setmelanotide reduces food intake and body weight and restores insulin sensitivity in DIO rodents and higher animal models.[9] A novel dual agonist of MC4R and GLP-1R with a sequence shown below should be synthesized via SPPS, purified, and cyclized. To cyclize the peptide, it should be dissolved in 10% aqueous DMSO and left spinning at RT for 48 hours. The reaction would be tracked by HPLC to observe the formation of a new peak

and disappearance of the linear peptide. Once the reaction has gone to completion, the cyclized peptide should be analyzed by HRMS to clearly see the loss of two protons.

Figure 6-1. Primary sequence of a potential MC4R/GLP-1R dual agonist, KSCEM05. Lowercase letters denote D-amino acids.

Once KSCEM05 is successfully cyclized, it's pertinent to ensure the cyclized C-terminal end of the peptide doesn't prevent it from binding to and activating the GLP-1R. *In vitro* confirmatory assays can be completed to confirm functional agonism. In addition, the binding and activity of KSCEM01-05 at MC4R should be measured either in-house via SPR binding or by an external screening source (*i.e.,* Eurofins DiscoverX).

6.2 OP/ODN Project

6.2.1 Publish data on OP/ODN and related neuropeptides

All data on the design, synthesis, and *in vivo* evaluation of OP, ODN, AntOP, and related peptides should be compiled and published in a peer-reviewed journal to complement the submitted patent.

6.2.2 Lipidate the lead peptide to enhance PK profile

The same strategy used to covert GEP44 to a long-acting therapeutic should be applied to ODN, TDN, and/or future analogues, depending on which one of these show the most

potent *in vivo* metabolic effects. Solubility and stability assays should be performed post-synthesis to ensure there's minimal aggregation and a high synthetic reproducibility rate.

6.2.3 Synthesize the shortest possible effective analog of OP/ODN and test its BBB penetrance

To date, the shortest OP analogue is SUODN-03, a pentamer currently being tested for *in vivo* metabolic effects. This peptide will be synthesized with an Fmoc-Lys(N_3)-OH residue at position 5 and reacted with sulfo-Cyanine5 DBCO to yield the fluorescent analogue. The *f*Cy5-SUODN03 can be used as a probe to test penetrance, or lack thereof, into the brain. Fragments of SUODN-03 can be synthesized and tested *in vivo* for metabolic effects. The most effective analogue can be resynthesized with an azido modification, fluorescently-tagged, and assayed for brain penetrance.

6.3 GPR75 Project

6.3.1 Publish data on SU75-36 and SU75-37

All design, synthesis, purification, SPR, and *in vivo* work on SU75-36 and SU75-37 should be gathered and published in a peer-reviewed journal to complement the submitted patent.

6.3.2 Use *in silico* modeling to predict amino acid substitutions that optimize interactions between the peptides and GLP-1R and GPR75

The secondary structures of SU75-36 and SU75-37 are currently not well-understood. A folded-state analysis of these peptides at 40 μM in 0.9% saline was performed using a

CD spectrophotometer. Both peptides adopted an α-helical secondary structure with percent helicities calculated for SU75-36 and SU75-37 as 20.9% and 21.3%, respectively. We are currently utilizing MOE 2.0 to dock the lowest energy conformations of the peptides into the binding or allosteric sites of GLP-1R and GPR75.

6.3.2.1 Use molecular modeling (*i.e.*, MOE 2.0) to predict the optimal position to incorporate a lipid-based residue

Our industrial-standard modeling software, MOE 2.0, should be used to create docking simulations to determine the best position to incorporate a lipidated amino acid. It is pertinent to ensure the lipid isn't interfering with the binding interactions between analytes and their receptors. However, this is strictly a *predictive* software. Solubility and stability assays should be performed post-synthesis to ensure the most stable analogue is pursued. Dynamic light scattering (DLS) assays can also be used to gauge the level of aggregation or the propensity of the peptides to form aggregates in solution.

6.3.3 Lipidate the lead peptide to enhance PK profile and test PK parameters

The same strategy used to covert GEP44 to a long-acting therapeutic should be applied to SU75-36 and/or SU75-37, depending on which one of these or future analogs show the most potent *in vivo* metabolic effects. Solubility and stability assays should be performed post-synthesis to ensure there's minimal aggregation and a high synthetic reproducibility rate.

6.3.4 Measure functional activity of peptides at GLP-1R, GPR75, or both receptors

There are few ways to screen SU75-36, SU75-37, and future analogues prior to *in vivo* testing. It would be beneficial to screen SU75-36 for function at GLP-1R and SU75-37 for lack of function at GLP-1R. SU75-36 and SU75-37 should both be screened at GPR75 by an external company (*e.g.,* Eurofins DiscoverX) or in-house using HEK293 cells transfected with plasmids encoding GPR75.

6.4 References

1. Younossi, Z.M. Non-alcoholic fatty liver disease - A global public health perspective. *J Hepatol.* 2019;70(3):531-544.

2. Targher, G., Corey, K.E., Byrne, C.D. *et al.* The complex link between NAFLD and type 2 diabetes mellitus-mechanisms and treatments. *Nat Rev Gastroenterol Hepatol.* 2021;18, 599–612.

3. Ding, X., Saxena, N.K., Lin, S., Gupta, N. and Anania, F.A. Exendin-4, a glucagon-like protein-1 (GLP-1) receptor agonist, reverses hepatic steatosis in *ob*/*ob* mice. *Hepatology*. 2006;43: 173-181.

4. Knudsen, L.B., Lau, J. The Discovery and Development of Liraglutide and Semaglutide. *Front Endocrinol* (Lausanne). 2019;10:155.

5. Dargó, G.; Bajusz, D.; Simon, K.; Müller, J.; Balogh, G.T. Human Serum Albumin Binding in a Vial: A Novel UV-pH Titration Method To Assist Drug Design. *J. Med. Chem.* 2020;63, 1763–1774.

6. Hughes S, Neumiller JJ. Oral Semaglutide. *Clin Diabetes*. 2020;38(1):109-111.

7. Meier, J. J. Efficacy of Semaglutide in a Subcutaneous and an Oral Formulation. *Front. Endocrinol.* 2021;12: 645617.

8. Weil-Ktorza O, Rege N, Lansky S, Shalev DE, Shoham G, Weiss MA, Metanis N. Substitution of an Internal Disulfide Bridge with a Diselenide Enhances both Foldability and Stability of Human Insulin. *Chemistry*. 2019;25(36):8513-8521.

9. Collet TH, Dubern B, Mokrosinski J, Connors H, Keogh JM, Mendes de Oliveira E, Henning E, Poitou-Bernert C, Oppert JM, Tounian P, Marchelli F, Alili R, Le Beyec J, Pépin D, Lacorte JM, Gottesdiener A, Bounds R, Sharma S, Folster C, Henderson B,

O'Rahilly S, Stoner E, Gottesdiener K, Panaro BL, Cone RD, Clément K, Farooqi IS, Van der Ploeg LHT. Evaluation of a melanocortin-4 receptor (MC4R) agonist (Setmelanotide) in MC4R deficiency. *Mol Metab*. 2017;(10):1321-1329.

Chapter 7: Appendix

7.1 Publications and patents

B. T. Milliken, C. Elfers, O. G. Chepurny, **K. S. Chichura**, I. R. Sweet, T. Borner, M. R. Hayes, B. C. De Jonghe, G. G. Holz, C. L. Roth, and R. P. Doyle (2021). “Design and Evaluation of Peptide Dual-Agonists of GLP-1 and NPY2 Receptors for Glucoregulation and Weight Loss with Mitigated Nausea and Emesis.” *J. Med. Chem*. 64(2): 1127-1138.

Chichura, K. S., Elfers, C., Roth, C. L., Doyle, R. P. (2022) *Melanocortin and GLP-1 Receptor Agonists and Methods of Use*. Provisional Patent. Filed 08/2022.

Chichura, K. S., Geisler, C. E., Hayes, M. R., Doyle, R. P. *Novel GPR75 ligands for controlling food intake, energy expenditure, body weight and treatment of obesity and metabolic diseases*. Provisional Patent. Filed 08/2022.

Chichura, K. S., Geisler, C. E., Reiner, B. C., Crist, R. C., Hayes, M. R., Doyle, R. P. *Octadecaneuropeptide (ODN) and novel derived neuropeptides activity in the brain for food intake, obesity, body weight and prevention of nausea/emesis*. Provisional Patent. Filed 08/2022.

K. S. Chichura, C. Elfers, T. Salameh, V. Kamat, O. G. Chepurny, A. McGivney, B. T. Milliken, G. G. Holz, S. V. Applebey, M. R. Hayes, I. R. Sweet, C. L. Roth, and R. P. Doyle (2023). “A Peptide Triple Agonist of GLP-1, Neuropeptide Y1, and Neuropeptide Y2 Receptors Promotes Glycemic Control and Weight Loss.” Accepted to *Sci. Rep*.

Journal of Medicinal Chemistry

pubs.acs.org/jmc

Article

Design and Evaluation of Peptide Dual-Agonists of GLP-1 and NPY2 Receptors for Glucoregulation and Weight Loss with Mitigated Nausea and Emesis

Brandon T. Milliken,[□] Clinton Elfers,[□] Oleg G. Chepurny, Kylie S. Chichura, Ian R. Sweet, Tito Borner, Matthew R. Hayes, Bart C. De Jonghe, George G. Holz, Christian L. Roth,* and Robert P. Doyle*

Cite This: *J. Med. Chem.* 2021, 64, 1127−1138

Read Online

ACCESS | Metrics & More | Article Recommendations | Supporting Information

ABSTRACT: There is a critical unmet need for therapeutics to treat the epidemic of comorbidities associated with obesity and type 2 diabetes, ideally devoid of nausea/emesis. This study developed monomeric peptide agonists of glucagon-like peptide 1 receptor (GLP-1R) and neuropeptide Y2 receptor (Y2-R) based on exendin-4 (Ex-4) and PYY_{3-36}. A novel peptide, GEP44, was obtained via *in vitro* receptor screens, insulin secretion in islets, stability assays, and *in vivo* rat and shrew studies of glucoregulation, weight loss, nausea, and emesis. GEP44 in lean and diet-induced obese rats produced greater reduction in body weight compared to Ex-4 without triggering nausea associated behavior. Studies in the shrew demonstrated a near absence of emesis for GEP44 in contrast to Ex-4. Collectively, these data demonstrate that targeting GLP-1R and Y2-R with chimeric single peptides offers a route to new glucoregulatory treatments that are well-tolerated and have improved weight loss when compared directly to Ex-4.

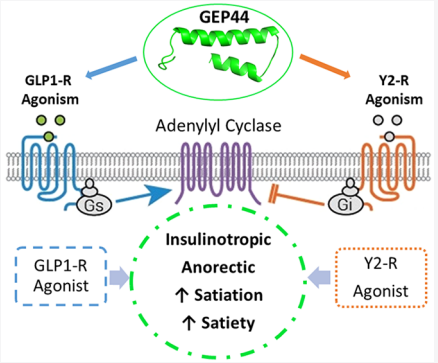

INTRODUCTION

Comorbidities associated with obesity and type 2 diabetes (T2D) continue to be great health challenges with the global population seeing rising child and adult obesity and diabetes rates.[1,2] Pharmacotherapies targeting gut peptide signaling pathways, such as glucagon-like peptide-1 receptor agonists (GLP-1RAs), arguably show the greatest promise for the treatment of comorbidities associated with obesity and T2D. GLP-1RAs are potent stimulators of glucose-dependent insulin secretion and modulate satiety and energy intake via peripheral and central GLP-1Rs.[3−7] Existing GLP-1 mimetics induce insulinotropic effects by binding to GLP-1Rs on pancreatic β-cells while simultaneously promoting satiety by binding to GLP-1Rs in brain regions associated with energy homeostasis.[3,8,9] Initial GLP-1RAs prescribed for the management of T2D also produced modest weight loss that was associated with nausea in 20−50% of patients.[10−15] More recently, GLP-1RAs such as liraglutide and semaglutide have shown significant improvements in weight loss relative to earlier analogues, although semaglutide is currently only prescribed for T2D treatment.

Drug combinations (e.g., phentermine + topiramate, naltrexone + bupropion) achieve stronger reductions of body weight compared to monotherapy with either component individually.[16] An alternative approach involves targeting two or more signaling pathways with the same molecule such as monomeric multiagonists based on GLP-1 and glucagon,[17−20] or GLP-1 and glucose-dependent insulinotropic polypeptide (GIP), with[21] and without[22] glucagon receptor (GlucR) agonism. Such novel therapies show considerable promise, although nausea/emesis and GI side effects in general continue to be unwanted factors.[23]

PYY_{3-36} is a gut derived hormone that crosses the blood−brain barrier (BBB)[24] and reduces food intake via neuropeptide NPY2 receptors (Y2-R) in key forebrain and brainstem areas of energy homeostasis, such as the arcuate (ARC), paraventricular (PVN), ventromedial (VMN), and dorsomedial (DMN) nuclei of the hypothalamus, as well as the lateral hypothalamus, amygdala, ventral tegmental area, area postrema (AP), and nucleus tractus solitarius (NTS).[24−27] Consistent with these findings, peripheral administration of an anorexigenic dose of PYY_{3-36} stimulates Fos (a marker of neuronal activation) in forebrain (e.g., ARC) and hindbrain regions (e.g., AP, NTS) that contain Y2-R and control food intake.[28,29] Furthermore, low central doses of PYY_{3-36} into the ARC inhibit food intake,[30] whereas peripheral injection of PYY_{3-36} decreases expression of the orexigenic hormone neuropeptide Y (NPY) in the ARC.[30,31] Inhibition of food intake by circulating PYY_{3-36} is also transmitted via PYY_{3-36} binding to

Received: October 12, 2020
Published: January 15, 2021

https://dx.doi.org/10.1021/acs.jmedchem.0c01783
J. Med. Chem. 2021, 64, 1127−1138

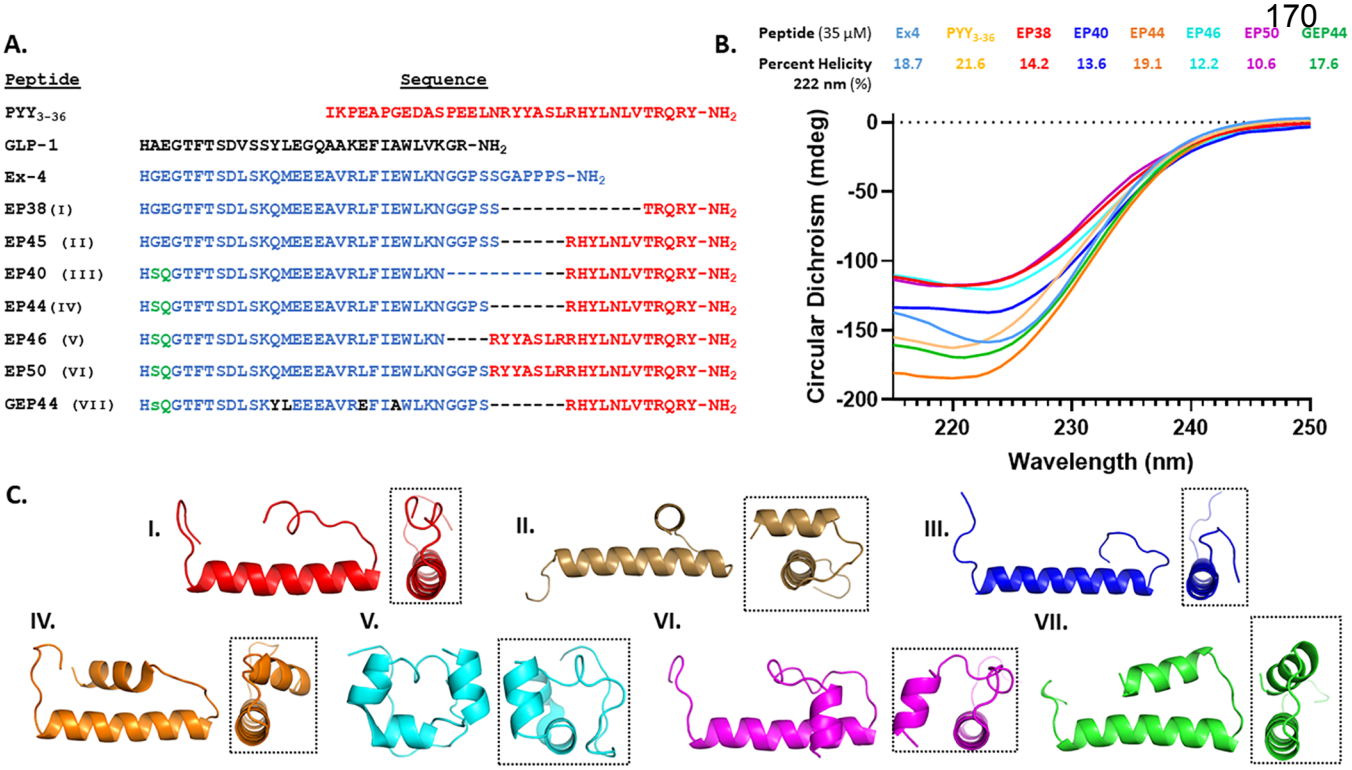

Figure 1. (A) Color-coding of peptides shown above in red indicates amino acid residues within EP44 and GEP44 that correspond to residues present in PYY_{3-36}. Color-coding in blue and black indicates amino acid residues within GEP44 that correspond to residues present in the Ex-4 and GLP-1, respectively. Green Q3 is known to be important in GlucR agonism. Ser2 of GEP44 is the D-isomer indicated as a lowercase "s". (B) CD spectroscopy displays the measured α-helical secondary structure of peptides at 35 μM. (C) PEP-FOLD3 simulations of calculations of designed peptides I = EP38; II = EP45; II I= EP40; IV = EP44; V = EP46; VI = EP50; VII = GEP44. Simulations for Ex-4 and PYY_{3-36} were complementary to the published structures for both peptides (data not shown).

peripheral Y2-Rs that are abundantly expressed on sensory afferent vagus nerve terminals innervating the intestine as well as vagus nerve cell bodies of the nodose ganglion (vagal-brain afferent signaling).[32−34] Beyond its effects on food intake, PYY_{3-36} treatment improves glucose control, insulin resistance, and lipid metabolism in rodents[35−37] while also having a positive impact on β-cell adaptation and survival in models of diabetes.[38] Peripheral administration of PYY_{3-36} reduces food intake and increases postprandial insulin levels, thermogenesis, lipolysis, and fat oxidation in lean and obese humans and nonhuman primates.[35,39−41] Circulating PYY_{3-36} levels are also reduced in obese humans.[42−47] Following body weight (BW) reduction and/or gastric bypass surgery in humans, circulating concentrations of PYY_{3-36} return to levels representative of average weight individuals,[42,44,48] suggesting that obesity does not result from resistance to PYY_{3-36} but may in part be due to a lack of circulating peptide, making it an attractive clinical drug target. PYY_{3-36} is highly sensitive to hydrolysis and proteolysis and has a short half-life of ∼8 min.[49] It is difficult to achieve sustained BW reduction beyond a 1−2 week period,[50] possibly due to Y2-R downregulation and tolerance (tachyphylaxis) to frequent doses of PYY_{3-36} or due to stimulation of compensatory mechanisms resulting from reduced food intake.[24,51] Although body weight reduction via Y2-R stimulation alone in humans is nonsustainable,[24,51,52] a 2019 study in mice demonstrated that peripheral coadministration of exendin-4 (Ex-4) together with PYY_{3-36} resulted in a synergistic effect on food intake reduction and body weight reduction.[52] To this end, the current experiments tested the hypothesis that a single monomeric peptide that activates both the Y2-R and GLP-1R concomitantly would produce a potent, sustained weight loss and also maintain glucose regulation superior to individual agonists of either the Y2-R or GLP-1R alone. Our initial approach led us to the development of EP45 (Figure 1A), a monomeric peptide with confirmed agonism at both the GLP-1R and Y2-R *in vitro*.[53] Herein, we describe the further optimization, *in vitro* screening, and *in vivo* validation in both rodents (rats) and mammals capable of emesis (musk shrews) of GEP44 (Figure 1A). The development of GEP44 was based on results gained by testing preliminary chimeric peptides such as EP45[53] and subsequently EP38, EP44, EP46, and EP50 (described herein). GEP44 is a monomeric, chimeric peptide with polypharmacy at both the GLP-1R and Y2-R. Consistent with the known actions of their targets, administration of GEP44 reduced food intake and body weight, increased glucose stimulated insulin secretion in islets, and tightened glucoregulation relative to Ex-4 controls. Notably, GEP44 induced little to no nausea behavior (in rats) or emesis (in: musk shrews).

RESULTS AND DISCUSSION

Design and *in Vitro* Cell Screening. The design approach from EP45[53] to GEP44 focused on developing a chimeric peptide based on the GLP-1, Ex-4, PYY_{3-36}, and glucagon peptide sequences, initially screened by circular dichroism (CD) (Figure 1B) and *in vitro* receptor agonism assays at GLP-1R, Y2-R, and GlucR (Table 1 and Figure S1). CD was performed at pH 7.4 to assay secondary structure and determine helicity (eqs 1 and 2) compared to Ex-4 and PYY_{3-36} in standard extracellular saline (SES) buffer, used

https://dx.doi.org/10.1021/acs.jmedchem.0c01783
J. Med. Chem. 2021, 64, 1127−1138

Table 1. Dose−Response Nonlinear Regression Analysis of Peptide Agonist Action at the Human GLP-1R, GlucR, Y1-, and Y2-R Using the cAMP Biosensor H188 Expressed in HEK Cells that Coexpressed Each of These GPCRs Individually[a]

peptide	GLP-1R	Y2-R	Yl-R	GlucR
PYY_{3-36}	n/t	16 nM (13.2−17.9)	n/t	n/t
PYY_{1-36}	n/t	n/t	12 nM (3.1−16.8)	n/t
Ex-4	16 pM (11.8−22.3)	n/t	n/t	n/t
EP38	80 pM (59.2−209)	>300 nM	n/t	n/t
EP45	473 pM (297−624)	47 nM (22.1−61.3)	n/t	n/t
EP40	533 pM (407−688)	61 nM (38.3−90.9)	n/t	>3 μM
EP44	240 pM (78.6−500)	32 nM (13.4−86.3)	41 nM (14.8−87.3)	30 nM
EP46	28 nM (11.7−54.9)	18 nM (11.9−28.7)	82 nM (53.8−112)	>3 μM
EP50	2.3 nM (0.12−6.03)	25 nM (3.47−56.8)	n/t	>3 μM
GEP44	330 pM (267−428)	10 nM (4.97−16.8)	27 nM (14.7−39.4)	>3 μM

[a]GLP-1R and GlucR agonist action (EC_{50} values) was measured as the increase of cytosolic [cAMP] in living cells in real time. Y1-R/Y2-R agonist action (IC_{50} values) was monitored in HEK cells that coexpress endogenous adenosine A2b receptors and recombinant Y1-R and Y2-R. Adenosine was administered to initially raise levels of cAMP so that Y1R/Y2-R agonist action to counteract the effect of adenosine could be measured by a decrease of [cAMP]. All values are (±SEM; 95% CI) and are the result of at least triplicate independent data sets, aside from GlucR, which was assayed in duplicate. n/t = not tested. Data represents values obtained using nonlinear regression analysis of data from highest FRET values obtained for each data point.

subsequently in the *in vitro* screening assays (Table 1 and Figure S1).[54] Compared to Ex-4 and PYY_{3-36}, all peptides assayed maintained a comparable α-helical secondary structure (Figure 1B). Calculations were then performed using PEP-FOLD3[55] to predict the peptides' folded states (Figure 1C and Figure S2).

EP38 modeling suggested a similar "PP-fold" to PYY_{3-36} (Figure 1C), although the terminal Tyr38 of EP38 displayed interactions driving the fold, which may contribute to the observed lack of potency at the Y2-R (see IC_{50} values in Table 1). In simulations designing GEP44, it was essential the terminal Tyr was not impeded. EP46 does not possess P31, a residue that drives the formation of the PP-fold[56] observed in the rest of the series and deemed essential for development of GEP44 (Figure 1C). Interestingly, EP46 agonism at GLP-1R was essentially lost (EC_{50} 28 nM), although strong potency was observed at Y2-R (IC_{50} 18 nM) (see also Table 1). EP44 forms a slight hydrophobic zipper that possesses a partial kink due to Q13 hydrogen bonding with E17 and R43 (Figure 1C). Investigation into modifications for Q13, and subsequently neighboring M14, to improve formation of the PP-fold led to Q13Y and M14L incorporated from GLP-1, ultimately used in GEP44.

EP45 and EP50 displayed very similar interactions that formed a hydrophobic pocket (Figure S2) generating a perpendicular interaction occurring on the face of the peptide believed to interact with the extracellular domain (ECD) of GLP-1R. In each model of EP45 and EP50, GLP-1R amino acid W25 forms hydrogen bonds with the backbone of the peptides at residues S32 and P31 for EP45 and EP50 (Figure S2), respectively. Studies into modifications within the PP-fold that might eliminate these undesired interactions led to modifying the peptides via a L21E modification. This modification, when modeled *in silico*, rotated GLP-1R residue W25, opening up hydrogen bonding with the incorporated peptide E21 *and* pi-pi stacking with peptide residue Y35, aiding in the creation of the targeted PP-fold (Figure 1C and Figure S2). With computational models generated, we subsequently conducted *in silico* blind protein−peptide docking using HPEPDOCK[57] (Figure 2 and Figure S3). The HPEPDOCK

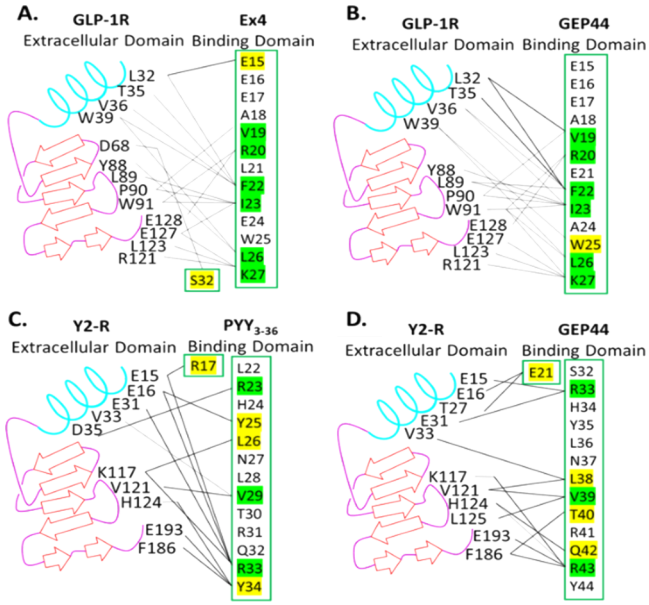

Figure 2. Diagrams summarizing observed integrations from HPEPDOCK molecular docking peptide−receptor simulations. (A, B) GLP-1R (PDB: 3IOL[58]) with Ex-4 and GEP44, respectively. (C, D) Y2-R (PDB: 2IK3) with PYY_{3-36} and GEP44, respectively. Green are common interactions, yellow are unique interactions.

docking results (Figure 2 and Figure S3) offered insights into modifications that could improve agonism focusing on GLP-1R. It was suggested *in silico* that L21 of EP38, EP44, and EP46 displaced hydrophobic interactions in the ECD of the GLP-1R, causing the peptides to protrude to a greater degree from the binding pocket when compared to Ex-4. This observation suggested that a peptide E24A modification, as was then placed into GEP44, would overcome this protrusion.

All peptides of interest from *in silico* studies marked for synthesis were then produced via solid-phase chemistry. We initially completed *in vitro* screening for all such peptides along with Ex-4 controls in HEK cells expressing rat or human GLP-1R (GLP-1R), human Y1-R, human Y2-R, or rat GlucR (Table 1), as described in the Experimental Section. GEP44 proved to be a potent agonist of Y2-R (IC_{50} 10 nM vs 16 nM for native PYY_{3-36}), implying at least equipotency between both ligands at the Y2-R) and GLP-1R (EC_{50} 330 pM at GLP-1R vs EC_{50} 16 pM for Ex-4) (Table 1). Despite the addition of Q3 into GEP44, no agonism (tested up to 3 μM) was observed at the GlucR (Figure S1(H)). Indeed, no agonism was noted at the rat GlucR for any of the peptides, aside from EP44, which returned an EC_{50} of 30 nM (Table 1 and Figure S16). To

https://dx.doi.org/10.1021/acs.jmedchem.0c01783
J. Med. Chem. 2021, 64, 1127−1138

further confirm this receptor selective agonism, we also demonstrated that the potent GLP-1R antagonist exendin9-39 (Ex9-39) and Y2-R antagonist BIIE0246[58] blocked GEP44 agonism in our FRET assays in cells expressing each receptor individually (Figure S1(C) and S1(G), respectively). We also screened EP44 and GEP44 at rat GLP-1R and observed EC_{50} values of 120 pM and 480 pM, respectively (Figure S10).

***In Vitro* Competitive Binding (IC_{50}) at GLP-1R.** We then measured competitive binding of the peptides at GLP-1R against GLP-1 (as a red fluorescent analogue, GLP-1red) specifically to gauge what effects increased PYY peptide components had on GLP-1R binding (Table 2). The *in vitro* binding assay utilized Ex-4 as a reference competitor (see methods). Of immediate note was that EP38 had a comparable IC_{50} value (7.13 nM) to that of Ex-4 (5.98 nM). EP44 also demonstrated significant binding (IC_{50} 27.5 nM) with weaker binding relative to Ex-4 and EP38, aligning with weaker agonism (EC_{50} 240 pM) at GLP-1R. On the other hand, EP40, EP46, and EP50 had weak binding such that the IC_{50} values were 321 nM, >1000 nM, and >1000 nM, respectively. This trend of weaker agonism with weaker binding observed for Ex-4, EP38, and EP44 continues with EP40, EP46, and EP50 with EC_{50} values of 533 pM for EP40 and then into the nanomolar range for both EP46 and EP50. The structure of EP46 as predicted by HPEPDOCK (Figure 1C) does not have the same hydrophobic zipper that is present in EP44. As mentioned previously, EP46 does not possess the P31 residue vital to the formation of the PP-fold observed in the rest of the peptides. A similar analysis of the structure of EP50 can be made and suggests unfavorable interactions between W25 and P31 allowing for suboptimal binding of EP50 at the GLP-1R. Despite GEP44 having comparable agonism at the Y2-R, it still displays moderate binding (IC_{50} 113 nM) at GLP-1R, in line with the moderate agonism (EC_{50} 330 pM) observed at GLP-1R, supporting the design taken from the EP series of peptides into GEP44 while also suggestive of a route to further optimize the dual-agonist series moving forward.

Table 2. IC_{50} Values for GPCR Agonist Peptides Measured at the GLP-1R in Competition Binding Assays Using Red Fluorescent GLP-1

peptide	IC_{50} (nM)	hill
Ex-4	5.98 (2.32−8.18)	−1.30
EP38	7.13 (4.54−8.66)	−1.44
EP40	321 (252−325)	−0.96
EP44	27.5 (20.8−28.3)	−1.56
EP46	>1000	n/d
EP50	>1000	n/d
GEP44	113 (99.1−116)	−1.08

Glucose Stimulated Insulin Secretion (GSIS) in Rat Pancreatic Islets. We next evaluated GSIS by rat pancreatic islets in response to GEP44 *in vitro* (Figure 3). GSIS was increased by GEP44 and Ex-4 at 10 mM glucose (but not at 3 mM glucose), although about 25% lower for GEP44 compared to Ex-4, no doubt a consequence of the lower EC_{50} observed for GEP44 relative to Ex-4 (Table 1). No effect occurred in the presence of PYY_{3-36}, confirming that GEP44 can and does stimulate insulin secretion via islet GLP-1Rs.

Microsomal Stability Assays in Pooled Rat Liver Microsomes. *In vitro* stability assays in pooled rat liver microsomes were conducted for the two peptides tested *in vivo*, namely EP44 and GEP44, and compared to the Ex-4 control. As shown in Table 3, both EP44 and GEP44 have comparable half-lives (125 and 136 min, respectively) and compare reasonably with the Ex-4 control half-life recorded (221 min). Both EP44 and GEP44 also had comparable intrinsic clearance (CL_{int}) values at 35.1 and 32.5 μL/min/mg peptide, respectively. These values of CL_{int} again compare favorably with those of the Ex-4 control (24.7 μL/min/mg peptide). These data support that both EP44 and GEP44 have similar metabolic stability to liver metabolism (primarily cytochrome P450 system) as to Ex-4, which has a suitable PK profile for use twice daily (b.i.d) in humans.

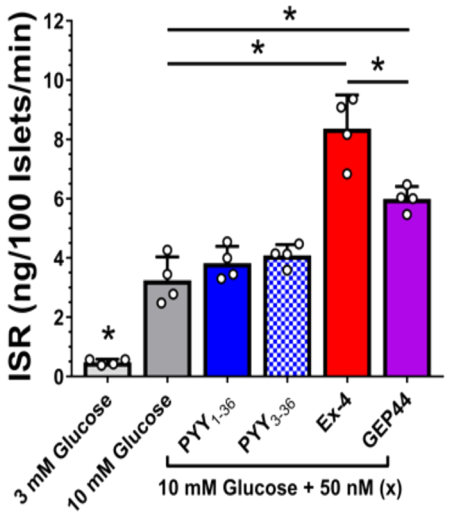

Figure 3. GSIS recorded as static insulin secretion rate (ISR) in rat islets in response to 10 mM glucose and 50 nM peptides, as indicated. Ex-4 and GEP44 both stimulated GSIS, while PYY_{3-36} did not. *p < 0.05.

Table 3. Half-Life and Intrinsic Clearance Measured in Triplicate Rat Liver Pooled Microsomes for Ex-4, EP44, and GEP44 as Measured over 120 min via HPLC[a]

peptide	slope	R^2	$t_{1/2}$ (min)	CL_{int} (μL/min/mg peptide)[b]
Ex-4	−0.003125	0.95	221	24.7 (2.51)
EP44	−0.005526	>0.99	125	35.1 (0.56)
GEP44	−0.005087	>0.99	136	32.5 (1.18)

[a]See also Figure S12. [b]Standard error values.

***In Vivo* Screening in Lean and Diet-Induced Obese Rats.** Comparing *in vitro* data for EP45,[53] the initial proof-of-concept dual agonist, with EP44 and GEP44 against Ex-4 as a control revealed that EP44, EP45, and GEP44 have near comparable GLP-1R agonism (~30% increased potency for GEP44 over EP45 and a further ~30% for EP44 over GEP44), but all are ~12- to 20-fold lower in potency compared to Ex-4 to the hGLP-1R. Screening these peptides *in vivo* offered scope to investigate the effects of combining Y2-R agonism, or lack thereof, into a GLP-1R agonist. As such, we screened Ex-4 (control), EP45 (moderate agonism; 47 nM), EP44 [2-fold lower agonism (32 nM) relative to PYY_{3-36} (16 nM)], and GEP44 (10 nM, equipotent with the *bona fide* ligand PYY_{3-36}). The goal was to focus on the effects of increased Y2-R agonism, coupled with GLP-1R agonism, on reducing food intake and nausea/emesis, while at least maintaining

https://dx.doi.org/10.1021/acs.jmedchem.0c01783
J. Med. Chem. 2021, 64, 1127−1138

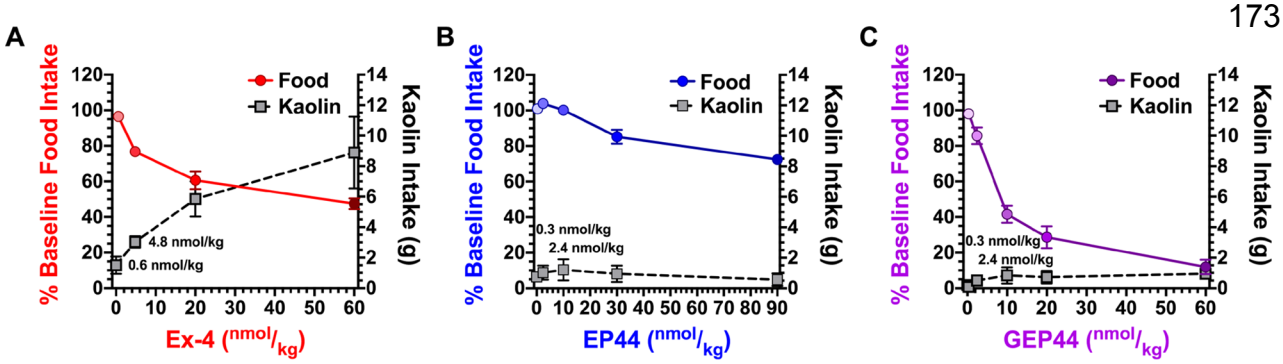

Figure 4. Dose escalation study averaging food intake for 2 d on each dose relative to vehicle treatment for the 2 d prior shows less of a reduction of food intake in response to EP44 (B) vs Ex-4 (A) in lean rats (male, age 11 weeks, $n = 4$ per group). However, unlike Ex-4 (A), EP44 (B) did not induce nausea assessed by kaolin intake during 2 d treatment periods. Modifications were made to improve Y-2R binding with GEP44, resulting in robust reductions in food intake (C) vs Ex-4 (A) without induction of nausea assessed by kaolin intake.

glucoregulation. We performed an initial experiment in lean Sprague−Dawley rats which, not surprisingly, revealed weak food intake reduction for EP45 relative to Ex-4 (Figure S11). Subsequent screening of EP44 and GEP44 revealed remarkable differences in the observed reduction in food intake (−71.4% reduction over 2 days; Figure 4C) following GEP44 administration (20 nmol/kg daily) relative to EP44 (Figure 4B) and Ex-4 (Figure 4A). With respect to changes in food intake, throughout the dosing range, GEP44 dose efficacy was consistent between treatment days, and the dose effect was consistent throughout the day (see Figure S14).

In terms of nausea, rodents lack an emetic reflex, but rather engage in pica behavior (i.e., the consumption of non-nutritive substances following emetic stimuli). In laboratory rats, pica is measured by kaolin consumption (i.e., clay) and is a well-established proxy for nausea.[59,60] While EP44 showed less food intake reduction compared to Ex-4, it showed no incidence of pica, suggesting a lack of nausea. This finding was in stark contrast with the pica observed in Ex-4 control treated rats (all across a dose range of 0.6 nmol/kg to 60 nmol/kg per day for 2 days) (Figures 4A and 4B). It is interesting to note that while GEP44 had an EC_{50} of 480 pM at the rat GLP-1R, EP44 had an EC_{50} of 120 pM, and yet the latter showed little to no evidence of nausea at doses up to 60 nmol/kg, suggesting that any lack of nausea observed is not simply due to weak agonism of the GLP-1R. When nausea was tracked for GEP44, again no incidence of pica was indicated (Figure 4C), even at supraphysiological levels of the peptide (as high as 60 nmol/kg/d for 2 days). The incorporation of a potent Y2-R agonistic component to a weak-moderate GLP-1R agonist has therefore seemed to drive down nausea and, in the case of GEP44, also improved food intake reduction (71.2% drop over 2 days).

Further studies in diet-induced obese (DIO) Sprague−Dawley rats yielded similar reductions in food intake (Figure 5B) to the GEP44 dose escalation study, above, with significant weight reduction (Figure 5A) and a significant reduction in fasting blood glucose (Figure 5C) due to five daily treatments (10 nmol/kg). AUC analyses of blood glucose from glucose bolus to 60 min also indicated a significant effect of GEP44 on glucose clearance (Figure 5G). Additionally, we assessed changes in glucose tolerance due to the five daily treatments (10 nmol/kg) of GEP44 (Figure 5D) vs Ex-4 (Figure 5E) with pre- and post-treatment intraperitoneal glucose tolerance tests (IPGTTs) in prediabetic rats; a vehicle treated group (Figure 5F) was used as a control. We observed significant reductions in postdextrose bolus blood glucose for GEP44, while no changes were observed due to Ex-4 treatment. While changes in fasting blood glucose (Figure 5C) may be due to reduced food intake in both GEP44 and Ex-4, acute changes in body weight (∼5% in GEP44 treated rats) are insufficient to fully account for changes in glucose clearance during the IPGTT. This observation is further supported by the changes in IPGTT glucose clearance following EP44 treatment and independent of weight loss in a similar experiment (see Figure S13).

***In Vivo* Glucoregulation and Emesis Studies in the Mammalian Musk Shrew.** Because rodents are a non-vomiting species, additional *in vivo* experiments were performed in the musk shrew (*Suncus murinus*), an emetic mammalian model, to test GEP44 on glycemic profile and vomiting.[61] The presence of PYY and its receptors has been confirmed in the shrew,[62] and it also represents a powerful tool for the study of the GLP-1R system, as it shares several features with humans, including glucoregulation and emetic sensitivity to current FDA-approved GLP-1R agonists.[63,64]

Therefore, as a proof of concept, we first tested whether GEP44 maintains its glucose-lowering ability during an IPGTT. We observed that shrews treated with 10 nmol/kg of GEP44 displayed improved glucose clearance following glucose administration compared to vehicle injections (at 20, 40, and 60 min post glucose; all p-values <0.001; Figure 6A). This was also reflected by a higher plasma glucose clearing rate compared to vehicle treated animals, indicative of an improved glucoregulatory activity in this species as well (Figure 6B).

We then investigated the potential emetogenicity of GEP44 at 10 and 60 nmol/kg in our shrew model and compared such to an Ex-4 control. Results showed that only one shrew experienced (mild) emesis after GEP44 administrations at doses up to 60 nmol/kg, while Ex-4 demonstrated emesis in 5/8 shews at only 5 nmol/kg (Figure 6C). Collectively, these data also further validate the large therapeutic index of GEP44 observed in rodents (Figure 4C).

CONCLUSION

In summary, effective medications to treat T2D and obesity need to provide long-term control of blood glucose while also potently attenuating caloric intake without nausea/emesis to offer optimal health outcomes with improved tolerance. We demonstrate herein a novel single chimeric peptide approach targeting GLP-1R and Y2-R receptors, which has potentially high impact on the field as evidenced by the combination of significant weight loss, glucoregulation and reduced incidence

https://dx.doi.org/10.1021/acs.jmedchem.0c01783
J. Med. Chem. 2021, 64, 1127−1138

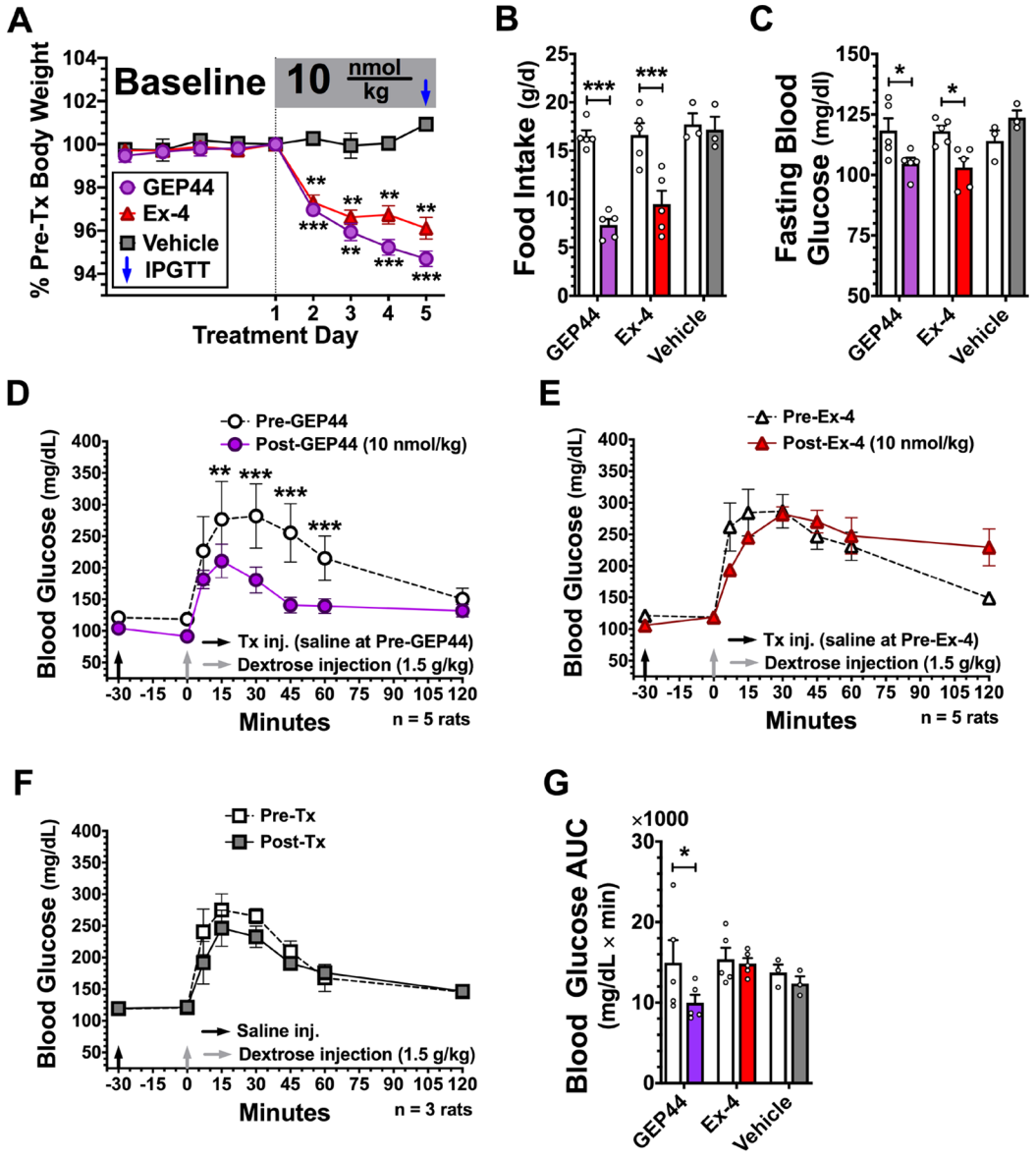

Figure 5. Longitudinal study (5 d Tx.; n = 3−5 per group; 10 nmol/kg; cohort 1: age 20 weeks, 16 weeks HFD exposure, 641.9 ± 17.9 g, n = 4; cohort 2: age 28 weeks, 24 weeks HFD exposure, 826.1 ± 35.7 g, n = 9; group stratification factors in Figure S15) in diet-induced obese rats shows sustained weight loss (A), reduced food intake (B), and reduced fasting blood glucose (C) due to GEP44 treatment. IPGTT was performed prior to the baseline phase and immediately following the last drug treatment. When compared to Ex-4 (E) or vehicle (F), treatment with GEP44 (D) yielded stronger reductions in blood glucose during IPGTTs following 5 d treatments in prediabetic rats. Area under the curve (AUC) analyses of blood glucose from glucose bolus to 60 min indicated a significant effect of GEP44 on glucose clearance (G). For bar graphs, empty bars represent baseline data, and filled bars represent data during drug treatment. Data were analyzed with repeated measurements two-way ANOVA followed by Bonferroni's posthoc test. When compared to baseline measures or vehicle control: *p < 0.05, ***p < 0.001.

of nausea/emesis. Limited pica and emetic response following GEP44 administration is in stark contrast to that observed in a dose-dependent manner for Ex-4 and at doses given in considerable excess to Ex-4 (60 nmol/kg versus 5 nmol/kg), supporting the idea that coactivating NPY receptors along with GLP-1R results in modified signaling compared to each receptor alone, as recently suggested for coadministered PYY_{3-36} and Ex-4.[52] Future work is needed then to elucidate the mechanisms underpinning the observed effects herein with a focus on modifications of gene regulation in the hindbrain. The effects of the agonism noted at the Y1-R for GEP44 (EC_{50} 27 nM) will also be investigated. While empirically we observe an anorectic response, the Y1-R has been associated, beyond an orectic response, with protection of beta islets against the inflammatory damage of diabetes.[65,66] GEP44 may then be a triagonist with additional beneficial effects to be gleaned. Finally, optimization of peptides for PK to allow future translation will also be investigated.

EXPERIMENTAL SECTION

Materials. Novel chimeric peptides (GEP44 and EP series) were produced by Genscript (Piscataway, NJ) or in-house using a microwave assisted CEM liberty Blue peptide synthesizer. Peptides were synthesized with C-terminal amidation and K12-azido modification (in place for future bioconjugations) and confirmed for sequence via MS/MS and purity by RP-HPLC (all at least >95%) (Figure S4−S9). GLP-1, glucagon, Ex-4, Ex(9−39), PYY_{3-36}, and adenosine were obtained from Sigma-Aldrich. BIIE024643 was obtained from Tocris Biosciences (Minneapolis, MN).

https://dx.doi.org/10.1021/acs.jmedchem.0c01783
J. Med. Chem. 2021, 64, 1127−1138

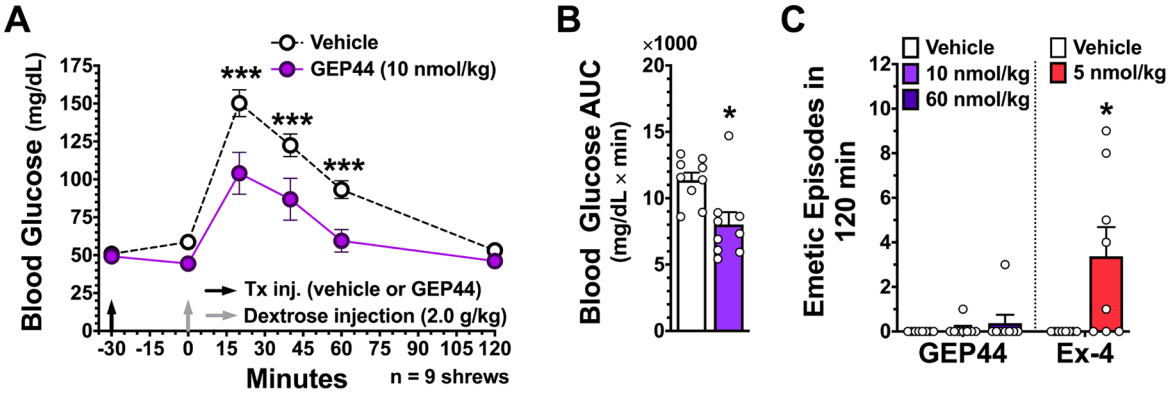

Figure 6. Systemically delivered GEP44 enhances glucose clearance during IPGTT while showing minimal emetogenic effects in shrews $n = 9$; ∼8 months old; 60−65 g. (A) In an IPGTT, GEP44 (10 nmol/kg) suppressed blood glucose levels after IP glucose administration (2 g/kg, IP) compared to saline. (B) AUC analysis from 0 (i.e., postglucose bolus) to 120 min showed that GEP44 reduced AUC compared to vehicle. (C) The number of single emetic episodes following GEP44 (10 and 60 nmol/kg) or saline systemic administration did not differ across treatment conditions. Indeed, GEP44 caused emesis in only one shrew tested. Data are expressed as mean ± SEM. Data in panel A were analyzed with repeated measurements two-way ANOVA followed by Bonferroni's posthoc test. Data in panel B were analyzed with the Student's t test for repeated measures. Due to the nonparametric nature of data in panel C, a repeated measurements Friedman test followed by Dunn's post hoc test was used to analyze GEP44 data, while a Wilcoxon test was used to analyze Ex-4 data. *$p < 0.05$, ***$p < 0.001$.

Cell Culture and Transfection. HEK293 cells were obtained from the American Type Culture Collection (Manassas, VA). HEK293 cells stably expressing the human GLP-1R and virally transduced with H188 for FRET assays were obtained from Novo Nordisk A/S (Bagsvaerd, Denmark).[67] HEK293 C24 cells stably expressing the H188 FRET reporter obtained by G418 antibiotic resistance selection,[68] and grown in monolayers were transfected with either rat GLP-1R,[69] human Y2-R, or human Y1-R at ∼70% confluency in 100 cm^2 tissue culture dishes with 11 μg of plasmid per dish. Post-transfection, cells were incubated for 48 h in fresh culture media. For real-time kinetic assays of FRET, cells were harvested and resuspended in 21 mL of SES buffer and plated at 196 μL per well. Plated cells were pretreated with 4 μL of agonist or antagonist (Ex9-39 or BIIE0246)[70,71] at target concentration and incubated for 20 min prior to performing assay. FRET assays and data analysis were performed using a FlexStation 3 microplate reader as described. Peptide agonism for G_i is screened against the inhibition of a 50 μL injection of 2 μM adenosine (final concentration) in SES as previously described.[70,71]

Plasmid encoding human Y2-R (I.D. NPYR20TN00) in pcDNA3.1 and human Y1-R (NPYR10TN00) were obtained from the cDNA Resource Center (Bloomsburg, PA). HEK293 cells stably expressing the rat GlucR were obtained from C. G. Unson and A. M. Cypess (The Rockefeller University).[72,73] Adenovirus for transduction of HEK293 cells was generated by a commercial vendor (Vira-Quest, North Liberty, IA) using the shuttle vector pVQAd CMV K-NpA and the H188 plasmid provided by Prof. Kees Jalink.[74]

FRET Reporter Assay for Rat and Human GLP-1R and Rat GlucR Agonism Measurement. These assays were conducted as fully described by us previously.[70,71] Briefly, HEK293 cells transiently or stably expressing recombinant GPCRs were plated at 80% confluency on 96-well clear-bottom assay plates (Costar 3904, Corning, NY). Cells were then transduced for 16 h with H188 virus at a density of 60 000 cells/well under conditions in which the multiplicity of infection was equivalent to 25 viral particles per cell. The culture media was removed and replaced by 200 μL/well of a standard extracellular saline (SES) solution supplemented with 11 mM glucose and 0.1% BSA. The composition of the SES was (in mM): 138 NaCl, 5.6 KCl, 2.6 $CaCl_2$, 1.2 $MgCl_2$, 11.1 glucose, and 10 HEPES (295 mosmol, pH 7.4). Real-time kinetic assays of FRET were performed using a FlexStation 3 microplate reader equipped with excitation and emission light monochromators (Molecular Devices, Sunnyvale, CA). Excitation light was delivered at 435/9 nm (455 nm cutoff), and emitted light was detected at 485 ± 15 nm (cyan fluorescent protein) or 535 ± 15 nm (yellow fluorescent protein).[68,75] The emission intensities were the averages of 15 excitation flashes for each time point per well. Test solutions dissolved in SES were placed in V-bottom 96-well plates (Greiner Bio-One, Monroe, NC), and an automated pipetting procedure was used to transfer 50 μL of each test solution to each well of the assay plate containing monolayers of these cells. Assays for each peptide screened at all receptors were performed in triplicate, aside from those at the GlucR, which were conducted as duplicate independent experiments. The 485/535 emission ratio was calculated for each well, and the mean ± SD values for 12 wells were averaged. These FRET ratio values were normalized using baseline subtraction so that a y-axis value of 0 corresponded to the initial baseline FRET ratio, whereas a value of 100 corresponded to a 100% increase (i.e., doubling) of the FRET ratio. The time course of the FRET ratio was plotted after exporting data to GraphPad Prism 8.1 (GraphPad Software, San Diego, CA). Prism 8.1 was also used for nonlinear regression analysis to quantify dose−response relationships.

Competitive Binding Assay at GLP-1R. IC_{50} values were measured in CHO-K1 cells at the human GLP-1R by Euroscreen Fast (Gosselies, Belgium) using their proprietary Taglite fluorescent competitive binding assay (Cat No. FAST0154B). Agonist tracer was GLP-1red at 4 nM with reference competitor Ex-4. Peptides were assayed in duplicate independent runs at nine concentrations per run ranging from 1 pM to 1 μM.

Circular Dichroism. Peptides for CD were constituted at 35 μM in nonsupplemented SES solution at pH 7.4 (Figure 1B). CD measurements were conducted as duplicate independent data sets, each as triplet replicates, with a JASCO J-715 Spectropolarimeter at 25 °C using a 1 cm quartz cell, 250−215 nm measurement range, 100 nm/min scanning speed, 1 nm bandwidth, 4 s response time, and 1.0 nm data pitch. The measured triplets were averaged, baseline subtracted, and smoothened by ProData Viewer software. The CD measurements were converted to molar ellipticity (Equation 1), then to percent helicity (Equation 2).

PEP-FOLD3, Simulated Secondary Structure Prediction. The PEP-FOLD3[55] de novo peptide structure simulating software was used to predict secondary structure for the chimeric peptides screened herein (Figure 1C).

HPEPDOCK, Protein-Peptide Docking Prediction. The PDB files obtained from the PEP-FOLD3 simulations were input into HPEPDOCK[57] blind protein-peptide online docking server to simulate docking for each chimeric peptide with the ECD of the targeted receptors GLP-1R (PDB: 3IOL) and Y2-R (PDB: 2IK3). The HPEPDOCK server utilizes a hierarchical docking protocol that accepts sequence and structure as input for both protein and peptide.

https://dx.doi.org/10.1021/acs.jmedchem.0c01783
J. Med. Chem. 2021, 64, 1127−1138

Outputs from HPEPDOCK received a Z-score for binding energy and were analyzed in PyMOL to evaluate protein-peptide interactions, or lack thereof, within the binding domain. Primary aim for HPEPDOCK targeted establishing a Z-score comparable to the native substrates and known interactions between Ex-4 and the ECD of GLP-1R (Figure S3).

Pooled Rat Liver Microsomal Assay (n = 3 Independent Assays). Pooled liver microsomes from a male Sprague−Dawley rat were purchased from Sigma-Aldrich. Microsomal incubations were performed in triplicate as independent data sets in 3 mM $MgCl_2$, 25 mM KH_2PO_4 buffer at pH 7.4. Assays were performed at 500 μL total volume with 30 μM peptide, 1 mM NADPH, and 1 mg/mL pooled liver microsomes. Kanamycin at 200 μM was used as an internal standard. Pooled rat liver microsome assay showing data collected by HPLC. Conditions: 3 mM $MgCl_2$ and 25 mM KH_2PO_4 pH 7.4 buffer at 0.5 mL with 30 μM peptide, 1 mM NADPH, and 1 mg/mL pooled liver microsomes. Assays were conducted at 37 °C with gentle rocking. Assays were monitored by extracting 30 μL of reaction solution every 20 min and injecting onto a 20 μL loop on an Agilent 1200 Series HPLC with an Eclipse XDB-C18 5 μm 4.6 × 150 mm column. A HPLC method was developed using aqueous acetonitrile and 0.1% trifluoroacetic acid in water with a flow rate of 1 mL/min and gradient optimized to elute out soluble proteins allowing clean separation of the parent peptide and metabolites tracked at 206 nm. Data were fit utilizing eqs 3−6.

Statement on Animal Experiments. All procedures were approved and conducted in compliance with US federal law and institutional guidelines and are congruent with the NIH guide for the Care and Use of Laboratory Animals. Specially, Seattle Children's Research Institute or the University of Washington Institutional Animal Care and Use Committee (SCRI Protocol IACUC00064; UW Protocol 409101) approved these experiments. All procedures conducted in shrews were approved by the Institutional Care and Use Committee of the University of Pennsylvania. All rats were supplied by Charles River, strain code 001, Male CD IGS (Sprague−Dawley) rats. Adult male shrews (*Suncus murinus*) bred at the University of Pennsylvania by coauthor Prof. Bart C. De Jonghe and weighing ∼50−80 g (n = 17 total) were used. The animals generated in the De Jonghe lab were originally derived from a colony maintained at the University of Pittsburgh Cancer Institute (a Taiwanese strain derived from stock supplied by the Chinese University of Hong Kong).

Dose Escalation Study in Lean Rats. Lean Sprague−Dawley rats (male, age 11 weeks, n = 4 per group) were individually housed in cages capable of recording food intake (Accuscan Diet cages) in an animal room maintained on a 12 h light/12 h dark cycle. The study design consisted of sequential rounds of a 2 day baseline phase, a 2 day treatment phase, and a 2 day washout phase. Body weight was assessed daily just prior to the start of the dark cycle; food and kaolin intake were available *ad libitum*, and consumption was continuously recorded. Treatment doses were administered just prior to the start of the dark cycle via subcutaneous injection. EP44 and Ex-4 were tested initially, and treatment groups were balanced for BW.

Five Day Treatment Induced Changes in Glucose Tolerance in DIO Rats. Male Sprague−Dawley rats were group housed in an animal room was maintained on a 12 h light/12 h dark cycle and placed on a high fat diet (HFD; Research Diets, D12492, 60% kcal from fat) beginning at age 4 weeks. Two cohorts of animals were used for this experiment (cohort 1: age 20 weeks; 16 weeks HFD exposure, 641.9 ± 17.9 g, n = 4; cohort 2: age 28 weeks; 24 weeks HFD exposure, 826.1 ± 35.7 g, n = 9); both cohorts were run concurrently. Testing consisted of a pretreatment intraperitoneal glucose tolerance test (IPGTT), a 4 day post-IPGTT recovery period, a 5 day vehicle-treated (0.9% sterile saline solution, injectable) baseline phase, a 5 day drug treatment phase, and a post-treatment IPGTT (immediately following the last treatment dose). Two groups of n = 5 rats were assigned to either GEP44 or Ex-4 by flip of a coin, and one group of n = 3 rats was used as a vehicle control. Assigned treatments (vehicle vs 10 nmol/kg GEP44 vs 10 nmol/kg Ex-4) were administered once daily just prior to the start of the dark cycle. Throughout the experiment, body weight and food intake (via hopper weighs) were assessed daily just prior to the start of the dark cycle. Stratification variables at baseline for group determination of DIO animals for the 5 day treatment experiment is shown in Figure S15.

IPGTTs were performed following a 6 h fast such that the glucose bolus occurred at the start of the dark cycle; all animal handling is performed under red light. Baseline blood glucose measurements were taken immediately before administration of the assigned treatment (vehicle at pretreatment IPGTT; GEP44 [10 nmol/kg], Ex-4 [10 nmol/kg], or vehicle at post-treatment). A second baseline sample was obtained 30 min later, immediately prior to the dextrose bolus (1.5 g/kg dextrose, 20% solution). Additional blood glucose measurements were taken per tail snip 7, 15, 30, 45, 60, and 120 min postbolus. All blood glucose measurements were made via hand-held glucometers (One Touch Ultra) in duplicate; if the variation between the two measures was >5%, a third measurement was taken.

Experiments in Musk Shrews. Animals were single housed in plastic cages (37.3 × 23.4 × 14 cm, Innovive) under a 12 h:12 h light/dark cycle in a temperature- and humidity- controlled environment. Shrews were fed *ad libitum* with a mixture of feline (75%, Laboratory Feline Diet 5003, Lab Diet) and mink food (25%, High Density Ferret Diet 5LI4, Lab Diet) and had *ad libitum* access to tap water except where noted.

Effects of GEP44 on Glycemic Control in Shrews. The protocol for performing the IPGTT in shrews was as follows: Two hours before dark onset, shrews were food- and water-deprived. Three hours later, baseline blood glucose levels were determined from a small drop of tail blood and measured using a standard glucometer (AccuCheck). Immediately following, each shrew (n = 9; ∼8 months old +60−65g) received IP injection of GEP44 (10 nmol/kg) or vehicle (1 mL/100g BW sterile saline). BG was measured 30 min later (t = 0 min), then each shrew received an IP bolus of glucose (2g/kg). Subsequent BG readings were taken at 20, 40, 60, and 120 min after glucose injection. After the final BG reading, food and water were returned. IPGTT studies were carried out in a within-subject, counterbalanced design.

Emetogenic Properties of GEP44 in Shrews. Shrews (male; ∼6 months old; 60−70 g; n = 8 per group) were habituated to IP injections and to clear plastic observation chambers (23.5 × 15.25 × 17.8 cm) for two consecutive days prior to experimentation. The animals were injected IP with GEP44 (10 or 60 nmol/kg), Ex-4 (5 nmol/kg) or vehicle, then video-recorded (Vixia HF-R62, Canon) for 120 min. After 120 min, the animals were returned to their cages. Treatments were separated by 72 h, and treatment order was determined using a randomized complete block design. Analysis of emetic episodes were measured by an observer blinded to treatment groups. Emetic episodes were characterized by strong rhythmic abdominal contractions associated with either oral expulsion from the gastrointestinal tract (i.e., vomiting) or without the passage of materials (i.e., retching).

Rat Islet Isolation and Culture. Islets were harvested from Sprague−Dawley rats (approximately 250 g; Envigo/Harlan) anesthetized by intraperitoneal injection of pentobarbital sodium (150 mg/kg rat). Islets were prepared and purified as described.[76] Islets were then cultured for 18 h in a 37 °C, 5% CO_2 incubator prior to experiments in RPMI medium supplemented with 10% heat inactivated FBS (Invitrogen).

Static Measurement of Insulin Secretion Rate. ISR was determined statically with multiple conditions, as described previously.[77] Briefly, islets were handpicked into a Petri dish containing Krebs-Ringer bicarbonate buffer supplemented with 0.1% bovine serum albumin and 3 mM glucose and incubated at 37 °C, 5% CO_2 for 60 min. Subsequently, islets were picked into wells of 96-well plates containing desired amounts of glucose and agents as indicated and incubated for an additional 60 min. At the end of this period, supernatant was assayed for insulin.

Data Analysis and Statistics. All data were expressed as mean ± SD for descriptive measures of groups at baseline (e.g., body weight and food intake) and mean ± SEM for outcome measures. For all statistical tests, a p-value less than 0.05 was considered significant.

https://dx.doi.org/10.1021/acs.jmedchem.0c01783
J. Med. Chem. 2021, 64, 1127−1138

Longitudinal data were analyzed using repeated measurements two-way ANOVA followed by Bonferroni's posthoc test or a Student's *t* test as appropriate. AUCs were calculated from 0 to 60 min (for rat data) or 0 to 120 min (for shrew data) using the trapezoidal method. ISR data were analyzed using a one-way ANOVA with Dunnett's post-test. Total number of emetic episodes was analyzed using a repeated measurements Friedman test for nonparametric data followed by Dunn's post hoc test or a Wilcoxon test as appropriate.

Equations. Eqs 1 and 2 are used for calculating the molar ellipticity and percent helicity, respectively, from CD measurements (see Figure 1B).

$$\text{molar ellipticity } (\Theta) = \frac{(AM \times 3298)}{(LC)} \quad (1)$$

In eq 1, A = absorbance (abs), C = concentration (g/L), M = average molecular weight (g/mol), and L = path length of cell (cm).

$$\text{percent helicity } (\%) = \frac{\begin{pmatrix}\Theta 100\\ (39\,500(1-2.57))\end{pmatrix}}{n} \quad (2)$$

In eq 2, n = number of residues.

Eqs 3−6 are used to calculate the elimination rate constant, half-life, volume of distribution, and intrinsic clearance, respectively, of Ex-4, EP44, and GEP44 (see Table 3).

$$\text{elimination rate constant } (k) = (-\text{gradient}) \quad (3)$$

$$\text{half-life } (t_{1/2}) \text{ (min)} = \frac{0.693}{k} \quad (4)$$

$$V\left(\frac{\mu\text{L}}{\text{mg}}\right) = \frac{\text{volume of incubation } (\mu\text{L})}{\text{protein in the incubation (mg)}} \quad (5)$$

$$\text{intrinsic clearance } (\text{CL}_{\text{INT}}) \ (\mu\text{L/min /mg protein}) = \frac{V \times 0.693}{t_{1/2}} \quad (6)$$

■ ASSOCIATED CONTENT

Supporting Information

The Supporting Information is available free of charge at https://pubs.acs.org/doi/10.1021/acs.jmedchem.0c01783.

Structure of GLP-1R 310L (PDB)

In vitro dose−response curves, summary of PEP-FOLD3 structural modeling, HPEPDOCK molecular docking peptide−receptor simulations, ESMS and RP-HPLC purity traces, dose−response nonlinear regression, *in vivo* studies, pooled rat liver microsome assays, body weight data from a longitudinal study assessing glucose tolerance, dose escalation experiments, and stratification factors (PDF)

Structure of Y2-R 21K3 (PDB)

Raw PYMOL docking data(ZIP)

■ AUTHOR INFORMATION

Corresponding Authors

Robert P. Doyle − *Department of Chemistry, Syracuse University, Syracuse, New York 13244, United States; Department of Medicine, State University of New York, Upstate Medical University, Syracuse, New York 13210, United States;* orcid.org/0000-0001-6786-5656; Email: rpdoyle@syr.edu

Christian L. Roth − *Department of Pediatrics, Seattle Children's Hospital, University of Washington, Seattle, Washington 98105, United States;* Email: christian.roth@seattlechildrens.org

Authors

Brandon T. Milliken − *Department of Chemistry, Syracuse University, Syracuse, New York 13244, United States*

Clinton Elfers − *Department of Pediatrics, Seattle Children's Hospital, University of Washington, Seattle, Washington 98105, United States*

Oleg G. Chepurny − *Department of Medicine, State University of New York, Upstate Medical University, Syracuse, New York 13210, United States*

Kylie S. Chichura − *Department of Chemistry, Syracuse University, Syracuse, New York 13244, United States*

Ian R. Sweet − *Diabetes Research Institute, University of Washington, Seattle, Washington 98105, United States*

Tito Borner − *Department of Biobehavioral Health Sciences, School of Nursing, University of Pennsylvania, Philadelphia, Pennsylvania 19104, United States*

Matthew R. Hayes − *Department of Psychiatry, Perelman School of Medicine, University of Pennsylvania, Philadelphia, Pennsylvania 19104, United States*

Bart C. De Jonghe − *Department of Biobehavioral Health Sciences, School of Nursing, University of Pennsylvania, Philadelphia, Pennsylvania 19104, United States*

George G. Holz − *Department of Medicine, State University of New York, Upstate Medical University, Syracuse, New York 13210, United States*

Complete contact information is available at: https://pubs.acs.org/10.1021/acs.jmedchem.0c01783

Author Contributions

R.P.D. and C.L.R. conceived and oversaw the project. B.T.M. and R.P.D. designed peptides. B.T.M. and O.G.C. conducted all *in vitro* assays aside from IC_{50} binding measurement, with analyses of such conducted by B.T.M., O.G.C., R.P.D., and G.G.H. Binding experiments were conducted by Euroscreen Fast (Gosselies, Belgium) using peptides synthesized by B.T.M. and K.S.C. B.T.M. conducted all computational calculations and CD experiments. C.E. conducted all rat *in vivo* experiments with help in part by B.T.M. T.B. conducted *in vivo* shrew experiments. I.R.S. conducted ISR. B.T.M., C.E., C.L.R., and R.P.D. wrote the main manuscript with the assistance of all authors (C.E., K.S.C., O.G.C., T.B., M.R.H., B.D.J., I.S.R., and G.G.H.). All authors approved the final submitted manuscript.

Author Contributions

□B.T.M. and C.E. contributed equally to this work.

Notes

The authors declare no competing financial interest.

■ ACKNOWLEDGMENTS

This work was supported in part by Department of Defense Grant 6W81XWH201029901 to C.L.R. and R.P.D., by Diabetes Research Center Grant P30 DK017047 (Cell Function Analysis Core), by National Institutes of Health Grant R01 DK069525 to G.G.H., by pilot study awards to R.P.D. (CUSE award) and C.L.R. (Seattle Children's Hospital, Center for Integrative Brain Research), and by the Swiss National Science Foundation (Grant P400PB_186728) to T.B.

■ ABBREVIATIONS

GPCR, G-coupled protein receptor; GLP-1, glucagon-like peptide-1; GLP-1R, glucagon-like peptide-1 receptor; Ex-4, exendin-4; T2D, type 2 diabetes; GIP, glucose-dependent insulinotropic polypeptide; GlucR, glucagon receptor; PYY_{3-36}, peptide YY_{3-36}; Y1-R, neuropeptide Y-1 receptor; Y2-R, neuropeptide Y-2 receptor; CD, circular dichroism; ECD, extracellular domain; IC_{50}, half maximal inhibitory concentration; EC_{50}, half maximal effective concentration; GSIS, glucose stimulated insulin secretion; SES, standard extracellular saline solution.

■ REFERENCES

(1) Afshin, A.; Reitsma, M. B.; Murray, C. J. L. Health effects of overweight and obesity in 195 Countries over 25 Years. *N. Engl. J. Med.* **2017**, *377*, 1496−1497.
(2) Skinner, A. C.; Perrin, E. M.; Moss, L. A.; Skelton, J. A. Cardiometabolic risks and severity of obesity in children and young adults. *N. Engl. J. Med.* **2015**, *373*, 1307−1317.
(3) O'Neil, P. M.; Birkenfeld, A. L.; McGowan, B.; Mosenzon, O.; Pedersen, S. D.; Wharton, S.; Carson, C. G.; Jepsen, C. H.; Kabisch, M.; Wilding, J. Efficacy and safety of semaglutide compared with liraglutide and placebo for weight loss in patients with obesity: a randomized, double-blind, placebo and active controlled, dose-ranging, phase 2 trial. *Lancet* **2018**, *392*, 637−649.
(4) Flint, A.; Raben, A.; Astrup, A.; Holst, J. J. Glucagon-like peptide 1 promotes satiety and suppresses energy intake in humans. *J. Clin. Invest.* **1998**, *101*, 515−520.
(5) Kanoski, S. E.; Hayes, M. R.; Skibicka, K. P. Glp-1 and weight loss: unraveling the diverse neural circuitry. *Am. J. Physiol. Regul. Integr. Comp. Physiol.* **2016**, *310*, R885−895.
(6) van Bloemendaal, L.; Ijzerman, R. G.; Ten Kulve, J. S.; Barkhof, F.; Konrad, R. J.; Drent, M. L.; Veltman, D. J.; Diamant, M. GLP-1 receptor activation modulates appetite- and reward-related brain areas in humans. *Diabetes* **2014**, *63*, 4186−4196.
(7) Ten Kulve, J. S.; Veltman, D. J.; van Bloemendaal, L.; Barkhof, F.; Drent, M. L.; Diamant, M.; Ijzerman, R. G. Liraglutide reduces CNS activation in response to visual food cues only after short-term treatment in patients with type 2 diabetes. *Diabetes Care* **2015**, *39*, 214−221.
(8) van Bloemendaal, L.; Veltman, D. J.; ten Kulve, J. S.; Groot, P. F. C.; Ruhe, H. G.; Barkhof, F.; Sloan, J. H.; Diamant, M.; Ijzerman, R. G. Brain reward-system activation in response to anticipation and consumption of palatable food is altered by glucagon-like peptide-1 receptor activation in humans. *Diabetes, Obes. Metab.* **2015**, *17*, 878−886.
(9) Fortin, S. M.; Lipsky, R. K.; Lhamo, R.; Chen, J.; Kim, E.; Borner, T.; Schmidt, H. D.; Hayes, M. R. GABA neurons in the nucleus tractus solitarius express GLP-1 receptors and mediate anorectic effects of liraglutide in rats. *Sci. Transl. Med.* **2020**, *533*, No. eaay8071.
(10) Ten Kulve, J. S.; Veltman, D. J.; van Bloemendaal, L.; Barkhof, F.; Deacon, C. F.; Holst, J. J.; Konrad, R. J.; Sloan, J. H.; Drent, M. L.; Diamant, M.; Ijzerman, R. G. Endogenous GLP-1 mediates postprandial reductions in activation in central reward and satiety areas in patients with type 2 diabetes. *Diabetologia* **2015**, *58*, 2688−2698.
(11) le Roux, C. W.; Astrup, A.; Fujioka, K.; Greenway, F.; Lau, D.; Van Gaal, L.; Ortiz, R. V.; Wilding, J.; Skjøth, T. V.; Manning, L. S.; Pi-Sunyer, X. SCALE obesity prediabetes NN8022−1839 study group. 3 years of liraglutide versus placebo for type 2 diabetes risk reduction and weight management in individuals with prediabetes: a randomised, double-blind trial. *Lancet* **2017**, *389*, 1399−1409.
(12) Tomlinson, B.; Hu, M.; Zhang, Y.; Chan, P.; Liu, Z. M. Investigational glucagon-like peptide-1 agonists for the treatment of obesity. *Expert Opin. Invest. Drugs* **2016**, *25*, 1167−1179.
(13) Bettge, K.; Kahle, M.; Abd El Aziz, M. S.; Meier, J. J.; Nauck, M. A. Occurrence of nausea, vomiting and diarrhoea reported as adverse events in clinical trials studying glucagon-like peptide-1 receptor agonists: A systematic analysis of published clinical trials. *Diabetes, Obes. Metab.* **2017**, *19*, 336−347.
(14) Shiomi, M.; Takada, T.; Tanaka, Y.; Yajima, K.; Isomoto, A.; Sakamoto, M.; Otori, K. Clinical factors associated with the occurrence of nausea and vomiting in type 2 diabetes patients treated with glucagon-like peptide-1 receptor agonists. *J. Diabetes Investig.* **2019**, *10*, 408−417.
(15) Horowitz, M.; Aroda, V. R.; Han, J.; Hardy, E.; Rayner, C. K. Upper and/or lower gastrointestinal adverse events with glucagon-like peptide-1 receptor agonists: Incidence and consequences. *Diabetes, Obes. Metab.* **2017**, *19*, 672−681.
(16) Yanovski, S. Z.; Yanovski, J. A. Long-term drug treatment for obesity: a systematic and clinical review. *JAMA* **2014**, *311*, 74−86.
(17) Pocai, A.; Carrington, P. E.; Adams, J. R.; Wright, M.; Eiermann, G.; Zhu, L.; Du, X.; Petrov, A.; Lassman, M. E.; Jiang, G.; Liu, F.; Miller, C.; Tota, L. M.; Zhou, G.; Zhang, X.; Sountis, M. M.; Santoprete, A.; Capito, E.; Chicchi, G. G.; Thornberry, N.; Bianchi, E.; Pessi, A.; Marsh, D. J.; SinhaRoy, R. Glucagon-like peptide 1/Glucagon receptor dual agonism reverses obesity in mice. *Diabetes* **2009**, *58*, 2258−2266.
(18) Sanchez-Garrido, M. A.; Brandt, S. J.; Clemmensen, C.; Muller, T. D.; DiMarchi, R. D.; Tschop, M. H. GLP1/glucagon receptor co-agonism for treatment of obesity. *Diabetologia* **2017**, *60*, 1851−1861.
(19) Ambery, P.; Parker, V. E.; Stumvoll, M.; Posch, M. G.; Heise, T.; Plum-Moerschel, L.; Tsai, L. F.; Robertson, D.; Jain, M.; Petrone, M.; Rondinone, C.; Hirshberg, B.; Jermutus, L. MEDI0382, a GLP-1 and glucagon receptor dual agonist, in obese or overweight patients with type 2 diabetes: a randomised, controlled, double-blind, ascending dose and phase 2a study. *Lancet* **2018**, *391*, 2607−2618.
(20) Day, J. W.; Gelfanov, V.; Smiley, D.; Carrington, P. E.; Eiermann, G.; Chicchi, G.; Erion, M. D.; Gidda, J.; Thornberry, N. A.; Tschöp, M. H.; Marsh, D. J.; SinhaRoy, R.; DiMarchi, R.; Pocai, A. Optimization of co-agonism at GLP-1 and glucagon receptors to safely maximize weight reduction in DIO-rodents. *Biopolymers* **2012**, *98*, 443−450.
(21) Finan, B.; Yang, B.; Ottaway, N.; Smiley, D. L; Ma, T.; Clemmensen, C.; Chabenne, J.; Zhang, L.; Habegger, K. M; Fischer, K.; Campbell, J. E; Sandoval, D.; Seeley, R. J; Bleicher, K.; Uhles, S.; Riboulet, W.; Funk, J.; Hertel, C.; Belli, S.; Sebokova, E.; Conde-Knape, K.; Konkar, A.; Drucker, D. J; Gelfanov, V.; Pfluger, P. T; Muller, T. D; Perez-Tilve, D.; DiMarchi, R. D; Tschop, M. H A rationally designed monomeric peptide triagonist corrects obesity and diabetes in rodents. *Nat. Med.* **2015**, *21*, 27−36.
(22) Frias, J. P.; Bastyr, E. J., 3rd; Vignati, L.; Tschop, M. H.; Schmitt, C.; Owen, K.; Christensen, R. H.; DiMarchi, R. D. The sustained effects of a dual GIP/GLP-1 receptor agonist, NNC0090−2746, in patients with type 2 diabetes. *Cell Metab.* **2017**, *26*, 343−352.
(23) Bastin, M.; Andreelli, F. Dual GIP-GLP1-receptor agonist in the treatment of type 2 diabetes- A short review on emerging data and therapeutic potential. *Diabetes, Metab. Syndr. Obes.: Targets Ther.* **2019**, *12*, 1973−1985.
(24) Nonaka, N.; Shioda, S.; Niehoff, M. L.; Banks, W. A. Characterization of blood-brain barrier permeability to PYY3−36 in the mouse. *J. Pharmacol. Exp. Ther.* **2003**, *306*, 948−953.
(25) Parker, R. M. C.; Herzog, H. Regional distribution of Y-receptor subtype mRNAs in rat brain. *Eur. J. Neurosci.* **1999**, *11*, 1431−1448.
(26) Shaw, J. L.; Gackenheimer, S. L.; Gehlert, D. R. Functional autoradiography of neuropeptide Y Y1 and Y2 receptor subtypes in rat brain using agonist stimulated [35S]GTPγS binding. *J. Chem. Neuroanat.* **2003**, *26*, 179−193.
(27) Neary, N. M.; Small, C. J.; Druce, M. R.; Park, A. J.; Ellis, S. M.; Semjonous, N. M.; Dakin, C. L.; Filipsson, K.; Wang, F.; Kent, A. S.; Frost, G. S.; Ghatei, M. A.; Bloom, S. R. Peptide YY3−36 and glucagon-like peptide-17−36 inhibit food intake additively. *Endocrinology* **2005**, *146*, 5120−5127.

https://dx.doi.org/10.1021/acs.jmedchem.0c01783
J. Med. Chem. 2021, 64, 1127−1138

(28) Blevins, J. E.; Chelikani, P. K.; Haver, A. C.; Reidelberger, R. D. PYY(3−36) induces Fos in the arcuate nucleus and in both catecholaminergic and non-catecholaminergic neurons in the nucleus tractus solitarius of rats. *Peptides* **2008**, *29*, 112−119.
(29) Henry, K. E.; Elfers, C. T.; Burke, R. M.; Chepurny, O. G.; Holz, G. G.; Blevins, J. E.; Roth, C. L.; Doyle, R. P. Vitamin B12 conjugation of peptide-YY(3−36) decreases food intake compared to native peptide-YY(3−36) upon subcutaneous administration in male rats. *Endocrinology* **2015**, *156*, 1739−1749.
(30) Batterham, R. L.; Cowley, M. A.; Small, C. J.; Herzog, H.; Cohen, M. A.; Dakin, C. L.; Wren, A. M.; Brynes, A. E.; Low, M. J.; Ghatei, M. A.; Cone, R. D.; Bloom, S. R. Gut hormone PYY(3−36) physiologically inhibits food intake. *Nature* **2002**, *418*, 650−654.
(31) Challis, B. G.; Pinnock, S. B.; Coll, A. P.; Carter, R. N.; Dickson, S. L.; O'Rahilly, S. Acute effects of PYY3−36 on food intake and hypothalamic neuropeptide expression in the mouse. *Biochem. Biophys. Res. Commun.* **2003**, *311*, 915−919.
(32) Abbott, C. R.; Monteiro, M.; Small, C. J.; Sajedi, A.; Smith, K. L.; Parkinson, J. R.; Ghatei, M. A.; Bloom, S. R. The inhibitory effects of peripheral administration of peptide YY(3−36) and Glucagon-like peptide-1 on food intake are attenuated by ablation of the vagal-brainstem-hypothalamic pathway. *Brain Res.* **2005**, *1044*, 127−131.
(33) Koda, S.; Date, Y.; Murakami, N.; Shimbara, T.; Hanada, T.; Toshinai, K.; Niijima, A.; Furuya, M.; Inomata, N.; Osuye, K.; Nakazato, M. The role of the vagal nerve in peripheral PYY3−36-induced feeding reduction in rats. *Endocrinology* **2005**, *146*, 2369−2375.
(34) Coelho, E. F.; Ferrari, M. F. R.; Maximino, J. R.; Fior-Chadi, D. R. Change in the expression of NPY receptor subtypes Y1 and Y2 in central and peripheral neurons related to the control of blood pressure in rats following experimental hypertension. *Neuropeptides* **2004**, *38*, 77−82.
(35) Vrang, N.; Madsen, A. N.; Tang-Christensen, M.; Hansen, G.; Larsen, P. J. PYY(3−36) reduces food intake and body weight and improves insulin sensitivity in rodent models of diet-induced obesity. *Am. J. Physiol. Regul. Integr. Comp. Physiol.* **2006**, *291*, R367−375.
(36) van den Hoek, A. M.; Heijboer, A. C.; Voshol, P. J.; Havekes, L. M.; Romijn, J. A.; Corssmit, E. P.; Pijl, H. Chronic PYY3−36 treatment promotes fat oxidation and ameliorates insulin resistance in C57BL6 mice. *Am. J. Physiol Endocrinol Metab.* **2007**, *292*, E238−245.
(37) Chandarana, K.; Gelegen, C.; Irvine, E. E.; Choudhury, A. I.; Amouyal, C.; Andreelli, F.; Withers, D. J.; Batterham, R. L. Peripheral activation of the Y2-receptor promotes secretion of GLP-1 and improves glucose tolerance. *Mol. Metab.* **2013**, *2*, 142−152.
(38) Guida, C.; Stephen, S.; Guitton, R.; Ramracheya, R. D. The role of PYY in pancreatic islet physiology and surgical control of diabetes. *Trends Endocrinol. Metab.* **2017**, *28*, 626−636.
(39) Sloth, B.; Holst, J. J.; Flint, A.; Gregersen, N. T.; Astrup, A. Effects of PYY1−36 and PYY3−36 on appetite, energy intake, energy expenditure, glucose and fat metabolism in obese and lean subjects. *Am. J. Physiol. Endocrinol. Metab.* **2007**, *292*, E1062−1068.
(40) Moran, T. H.; Smedh, U.; Kinzig, K. P.; Scott, K. A.; Knipp, S.; Ladenheim, E. E. Peptide YY(3−36) inhibits gastric emptying and produces acute reductions in food intake in rhesus monkeys. *Am. J. Physiol. Regul. Integr. Comp. Physiol.* **2005**, *288*, R384−388.
(41) Koegler, F. H.; Enriori, P. J.; Billes, S. K.; Takahashi, D. L.; Martin, M. S.; Clark, R. L.; Evans, A. E.; Grove, K. L.; Cameron, J. L.; Cowley, M. A. Peptide YY(3−36) inhibits morning, but not evening, food intake and increases body weight in Rhesus macques. *Diabetes* **2005**, *54*, 3198−3204.
(42) Roth, C. L.; Enriori, P. J.; Harz, K.; Woelfle, J.; Cowley, M. A.; Reinehr, T. Peptide YY is a regulator of energy homeostasis in obese children before and after weight loss. *J. Clin. Endocrinol. Metab.* **2005**, *90*, 6386−6391.
(43) Batterham, R. L.; Cohen, M. A.; Ellis, S. M.; Le Roux, C. W.; Withers, D. J.; Frost, G. S.; Ghatei, M. A.; Bloom, S. R. Inhibition of food intake in obese subjects by peptide YY(3−36). *N. Engl. J. Med.* **2003**, *349*, 941−948.
(44) le Roux, C. W.; Batterham, R. L.; Aylwin, S. J.; Patterson, M.; Borg, C. M.; Wynne, K. J.; Kent, A.; Vincent, R. P.; Gardiner, J.; Ghatei, M. A.; Bloom, S. R. Attenuated peptide YY release in obese subjects is associated with reduced satiety. *Endocrinology* **2006**, *147*, 3−8.
(45) Rahardjo, G. L.; Huang, X.-F.; Tan, Y. Y.; Deng, C. Decreased plasma peptide YY accompanied by elevated Peptide YY and Y2 receptor binding densities in the medulla oblongata of diet-induced obese mice. *Endocrinology* **2007**, *148*, 4704−4710.
(46) Nianhong, Y.; Chongjian, W.; Mingjia, X.; Limei, M.; Liegang, L.; Xiufa, S. Interaction of dietary composition and PYY gene expression in diet-induced obesity in rats. *J. Huazhong Univ. Sci. Technol., Med. Sci.* **2005**, *25*, 243−246.
(47) Roth, C. L.; Bongiovanni, K. D.; Gohlke, B.; Woelfle, J. Changes in dynamic insulin and gastrointestinal hormone secretion in obese children. *J. Pediatr. Endocrinol. Metab.* **2010**, *23*, 1299−1309.
(48) Reinehr, T.; Roth, C. L.; Enriori, P. J.; Masur, K. Changes of dipeptidyl peptidase IV (DPP-IV) in obese children with weight loss: relationships to peptide YY, pancreatic peptide, and insulin sensitivity. *J. Pediatr. Endocrinol. Metab.* **2010**, *23*, 101−108.
(49) Addison, M. L.; Minnion, J. S.; Shillito, J. C.; Suzuki, K.; Tan, T. M.; Field, B. C. T.; Germain-Zito, N.; Becker-Pauly, C.; Ghatei, M. A.; Bloom, S. R.; Murphy, K. G. A role for metalloendopeptidases in the breakdown of the gut hormone, PYY 3−36. *Endocrinology* **2011**, *152*, 4630−4640.
(50) Reidelberger, R.; Haver, A.; Chelikani, P. K.; Apenteng, B.; Perriotte-Olson, C.; Anders, K.; Steenson, S.; Blevins, J. E. Effects of leptin replacement alone and with exendin-4 on food intake and weight regain in weight-reduced diet-induced obese rats. *Am. J. Physiol. Endocrinol. Metab.* **2012**, *302*, 1576−1585.
(51) De Silva, A.; Bloom, S. R. Gut hormones and appetite control: A focus on PYY and GLP-1 as therapeutic targets in obesity. *Gut Liver* **2012**, *6*, 10−20.
(52) Kjaergaard, M.; Salinas, C. B. G.; Rehfeld, J. F.; Secher, A.; Raun, K.; Wulff, B. S. PYY(3−36) and exendin-4 reduce food intake and activate neuronal circuits in a synergistic manner in mice. *Neuropeptides* **2019**, *73*, 89−95.
(53) Chepurny, O. G.; Bonaccorso, R. L.; Leech, C. A.; Wöllert, T.; Langford, G. M.; Schwede, F.; Roth, C. L.; Doyle, R. P.; Holz, G. G. Chimeric peptide EP45 as a dual agonist at GLP-1 and NPY2R receptors. *Sci. Rep.* **2018**, *8*, 3749.
(54) Swedberg, J. E.; Schroeder, C. I.; Mitchell, J. M.; Fairlie, D. P.; Edmonds, D. J.; Griffith, D. A.; Ruggeri, R. B.; Derksen, D. R.; Loria, P. M.; Price, D. A.; Liras, S.; Craik, D. J. Truncated Glucagon-like peptide-1 and exendin-4-conotoxin pl14a peptide chimeras maintain potency and -helicity and reveal interactions vital for cAMP signaling in vitro. *J. Biol. Chem.* **2016**, *291*, 15778−15787.
(55) Lamiable, A.; Thévenet, P.; Rey, J.; Vavrusa, M.; Derreumaux, P.; Tufféry, P. PEP-FOLD3: faster de novo structure prediction for linear peptides in solution and in complex. *Nucleic Acids Res.* **2016**, *44* (W1), W449−454.
(56) Nygaard, R.; Nielbo, S.; Schwartz, T. W.; Poulsen, F. M. The PP-Fold solution structure of human polypeptide YY and human PYY3−36 as determined by NMR. *Biochemistry* **2006**, *45*, 8350−8357.
(57) Zhou, P.; Jin, B.; Li, H.; Huang, S. Y. HPEPDOCK: a web server for blind peptide-protein docking based on a hierarchical algorithm. *Nucleic Acids Res.* **2018**, *46*, W443−W450.
(58) Dumont, Y. BIIE0246, a potent and highly selective non-peptide neuropeptide Y Y2 receptor antagonist. *Pharmacol.* **2000**, *129*, 1075−1088.
(59) Liu, Y. L.; Malik, N.; Sanger, G. J.; Friedman, M. I.; Andrews, P. L. Pica-a model of nausea? Species differences in response to cisplatin. *Physiol. Behav.* **2005**, *85*, 271−277.
(60) De Jonghe, B. C.; Lawler, M. P.; Horn, C. C.; Tordoff, M. G. Pica as an adaptive response: kaolin consumption helps rats recover from chemotherapy-induced illness. *Physiol. Behav.* **2009**, *97*, 87−90.
(61) Ueno, S.; Matsuki, N.; Saito, H. *Suncus murinus*: a new experimental model in emesis research. *Life Sci.* **1987**, *41*, 513−518.

https://dx.doi.org/10.1021/acs.jmedchem.0c01783
J. Med. Chem. 2021, 64, 1127−1138

(62) Yi, S. Q.; Li, J.; Yamaguchi, T.; Hori, K.; Hayashi, K.; Itoh, M. Immunolocalization of the PP family and its receptors in the gastrointestinal tract of house musk shrew, *Suncus murinus*. *Neuro Endocrinology Letters* **2011**, *32*, 212−219.
(63) Chan, S. W.; Lin, G.; Yew, D. T.; Rudd, J. A. A physiological role of glucagon-like peptide-1 receptors in the central nervous system of *Suncus murinus* (house musk shrew). *Eur. J. Pharmacol.* **2011**, *668*, 340−346.
(64) Chan, S. W.; Lin, G.; Yew, D. T.; Yeung, C. K.; Rudd, J. A. Separation of emetic and anorexic responses of exendin-4, a GLP-1 receptor agonist in Suncus murinus (house musk shrew). *Neuropharmacology* **2013**, *70*, 141−147.
(65) Persaud, S. J.; Bewick, G. A. Peptide YY: more than just an appetite regulator. *Diabetologia* **2014**, *57*, 1762−1769.
(66) Sam, A. H.; Gunner, D. J.; King, A.; Persoud, S. J.; Brooks, L.; Hostomska, H.; Ford, H. E.; Liu, B.; Ghatei, M. A.; Bloom, S. R.; Bewick, G. A. Selective ablation of peptide YY cells in adult mice reveals their role in beta cell survival. *Gastroenterology* **2012**, *143*, 459−468.
(67) Gromada, J.; Rorsman, P.; Dissing, S.; Wulff, B. S. Stimulation of cloned human glucagon-like peptide 1 receptor expressed in HEK 293 cells induces cAMP-dependent activation of calcium-induced calcium release. *FEBS Lett.* **1995**, *373*, 182−186.
(68) Chepurny, O. G.; Leech, C. A.; Kelley, G. G.; Dzhura, I.; Dzhura, E.; Li, X.; Rindler, M. J.; Schwede, F.; Genieser, H. G.; Holz, G. G. Enhanced Rap1 activation and insulin secretagogue properties of an acetoxymethyl ester of an Epac-selective cyclic AMP analog in rat INS-1 cells studies with 8-pCPT-2'-O-Me-cAMP-AM. *J. Biol. Chem.* **2009**, *284*, 10728−10736.
(69) Thorens, B. Expression cloning of the pancreatic J8 cell receptor for the gluco-incretin hormone glucagon-like peptide 1. *Proc. Natl. Acad. Sci. U. S. A.* **1992**, *89*, 8641−8645.
(70) Milliken, B. T.; Doyle, R. P.; Holz, G. G.; Chepurny, O. G. FRET reporter assays for cAMP and calcium in a 96-well format using genetically encoded biosensors expressed in living cells. *Bio-protocol* **2020**, *10*, No. e3641.
(71) Chepurny, O. G.; Matsoukas, G. L.; Liapakis, G.; Leech, C. A.; Milliken, B. T.; Doyle, R. P.; Holz, G. G. Nonconventional glucagon and GLP-1 receptor agonist and antagonist interplay at the GLP-1 receptor revealed in high-throughput FRET assays for cAMP. *J. Biol. Chem.* **2019**, *294*, 3514−3531.
(72) Jiang, Y.; Cypess, A. M.; Muse, E. D.; Wu, C. R.; Unson, C. G.; Merrifield, R. B.; Sakmar, T. P. Glucagon receptor activates extracellular signal-regulated protein kinase 1/2 via cAMP-dependent protein kinase. *Proc. Natl. Acad. Sci. U. S. A.* **2001**, *98*, 10102−10107.
(73) Cypess, A. M. Signal Transduction by the Glucagon Receptor: Characterization of Ligand Binding, G Protein-Coupling, Second Messenger Generation, and Downstream Effector Activation. Ph.D. Thesis, The Rockefeller University, 1999.
(74) Klarenbeek, J.; Goedhart, J.; van Batenburg, A.; Groenewald, D.; Jalink, K. Fourth-generation Epac-based FRET sensors for cAMP feature exceptional brightness, photostability and dynamic range: Characterization of dedicated sensors for FLIM, for ratiometry and with high affinity. *PLoS One* **2015**, *10*, No. e0122513.
(75) Schwede, F.; Chepurny, O. G.; Kaufholz, M.; Bertinetti, D.; Leech, C. A.; Cabrera, O.; Zhu, Y.; Mei, F.; Cheng, X.; Manning Fox, J. E.; MacDonald, P. E.; Genieser, H. G.; Herberg, F. W.; Holz, G. G. Rp-cAMPS prodrugs reveal the cAMP dependence of first-phase glucose-stimulated insulin secretion. *Mol. Endocrinol.* **2015**, *29*, 988−1005.
(76) Sweet, I. R.; Cook, D. L.; DeJulio, E.; Wallen, A. R.; Khalil, G.; Callis, J.; Reems, J. Regulation of ATP/ADP in pancreatic islets. *Diabetes* **2004**, *53*, 401−409.
(77) Jung, S.-R.; Reed, B. J.; Sweet, I. R. A highly energetic process couples calcium influx through L-type calcium channels to insulin secretion in pancreatic beta-cells. *Am. J. Physiol.* **2009**, *297*, E717−727.

TITLE OF THE INVENTION

Melanocortin and GLP-1 Receptor Agonists and Methods of Use

BACKGROUND

Despite public health education and other initiatives, obesity and type 2 diabetes (T2D) are among the greatest health challenges facing not only the U.S, but the entire world. Weight loss significantly improves morbidity and mortality associated with obesity and associated metabolic disease, such as T2D. However, rigid dietary intervention increases the risk for disinhibited eating and weight regain. In recent years it became clear that hypothalamic dysfunction plays a major role in many forms of severe obesity, such as common obesity, monogenic obesity, and hypothalamic obesity. While therapies based on endogenous gut peptides such as glucagon-like peptide-1 (GLP-1) receptor agonists (GLP-1RAs) have been compelling therapeutic agents for obesity and T2D, only a few have achieved partial long-term weight loss (≥5-15% in adults at 1 year), and all have shown significant side-effects, including nausea/malaise and gastrointestinal ailments.

In recent years, melanocortin receptor agonists have been developed and tested in forms of obesity caused by deficient hypothalamic melanocortin signaling as in patients with pro-opiomelanocortin or leptin receptor deficiency. To reduce the burden and risk of obesity-associated diseases, there is dire unmet clinical need for new anti-obesity agents with increased efficacy, safety and patient tolerance. The present disclosure addresses this unmet need.

BRIEF DESCRIPTION OF THE FIGURES

The drawings illustrate generally, by way of example, but not by way of limitation, various embodiments of the present application.

FIGs. 1A-1D show confirmation of synthesis and purity of non-limiting chimeric peptides, according to various embodiments. (FIG. 1A) KSCEM01 (5016.52 g/mol; 15.244 min T_R; 96.4% pure), (FIG. 1B) KSCEM02 (5097.61 g/mol; 17.447 min T_R; 95.6% pure), (FIG. 1C) KSCEM03 (4716.14 g/mol; 16.863 min T_R; 99.9% pure), (FIG. 1D) KSCEM04 (4223.62 g/mol; 15.817 min T_R; 98.8% pure).

FIG. 2 shows a non-limiting competitive binding assay at hGLP-1R. KSCEM01 (K_D = 9.9 nM) binding at the human GLP-1R, as measured via SPR vs. an Ex-4 (K_D = 5.9 nM) control.

Ex-4 is Exendin-4, His-Gly-Glu-Gly-Thr-Phe-Thr-Ser-Asp-Leu-Ser-Lys-Gln-Met-Glu-Glu-Glu-Ala-Val-Arg-Leu-Phe-Ile-Glu-Trp-Leu-Lys-Asn-Gly-Gly-Pro-Ser-Ser-Gly-Ala-Pro-Pro-Pro-Ser-NH_2.

FIG. 3 shows non-limiting *in vitro* evaluation of KSCEM01 at the hGLP-1R. Dose-dependent agonism (% change in FRET ratio tracking levels of cAMP) of KSCEM01 (EC_{50} = 4.08 nM) at the human GLP-1R vs. an Ex-4 (EC_{50} = 0.29 pM) control.

FIG. 4 illustrates the MALDI mass spectrum of KSCEM01.

FIG. 5 illustrates the reduction in food intake as a result of KSCEM01 administration to male Sprague-Dawley Rats.

FIG. 6 illustrates the reduction in food intake as a result of single dose KSCEM01 administration to male Sprague-Dawley Rats.

FIGs. 7A-7C illustrates the comparative metabolic as a result of KSCEM01, liraglutide, and control administration to male Sprague-Dawley Rats in dose escalation experiments. Shown are changes in body weight (FIG. 7A), cumulative food intake (FIG. 7B), and calorie intake (FIG. 7C).

DETAILED DESCRIPTION OF THE INVENTION

Reference will now be made in detail to certain embodiments of the disclosed subject. While the disclosed subject matter will be described in conjunction with the enumerated claims, it will be understood that the exemplified subject matter is not intended to limit the claims to the disclosed subject matter.

Throughout this document, values expressed in a range format should be interpreted in a flexible manner to include not only the numerical values explicitly recited as the limits of the range, but also to include all the individual numerical values or sub-ranges encompassed within that range as if each numerical value and sub-range is explicitly recited. For example, a range of "about 0.1% to about 5%" or "about 0.1% to 5%" should be interpreted to include not just about 0.1% to about 5%, but also the individual values (*e.g.*, 1%, 2%, 3%, and 4%) and the sub-ranges (*e.g.*, 0.1% to 0.5%, 1.1% to 2.2%, 3.3% to 4.4%) within the indicated range. The statement "about X to Y" has the same meaning as "about X to about Y," unless indicated otherwise. Likewise, the statement "about X, Y, or about Z" has the same meaning as "about X, about Y, or about Z," unless indicated otherwise.

In this document, the terms "a," "an," or "the" are used to include one or more than one unless the context clearly dictates otherwise. The term "or" is used to refer to a nonexclusive "or" unless otherwise indicated. The statement "at least one of A and B" or "at least one of A or B" has the same meaning as "A, B, or A and B." In addition, it is to be understood that the phraseology or terminology employed herein, and not otherwise defined, is for the purpose of description only and not of limitation. Any use of section headings is intended to aid reading of the document and is not to be interpreted as limiting; information that is relevant to a section heading may occur within or outside of that particular section. All publications, patents, and patent documents referred to in this document are incorporated by reference herein in their entirety, as though individually incorporated by reference.

In the methods described herein, the acts can be carried out in any order, except when a temporal or operational sequence is explicitly recited. Furthermore, specified acts can be carried out concurrently unless explicit claim language recites that they be carried out separately. For example, a claimed act of doing X and a claimed act of doing Y can be conducted simultaneously within a single operation, and the resulting process will fall within the literal scope of the claimed process.

Definitions

The term "about" as used herein can allow for a degree of variability in a value or range, for example, within 10%, within 5%, or within 1% of a stated value or of a stated limit of a range, and includes the exact stated value or range.

A disease or disorder is "alleviated" if the severity of a symptom of the disease or disorder, the frequency with which such a symptom is experienced by a patient, or both, is reduced.

As used herein, the terms "alteration," "defect," "variation," or "mutation" refer to a mutation in a gene in a cell that affects the function, activity, expression (transcription or translation) or conformation of the polypeptide it encodes, including missense and nonsense mutations, insertions, deletions, frameshifts, and premature terminations.

As used herein, the term "composition" or "pharmaceutical composition" refers to a mixture of at least one compound described herein with a pharmaceutically acceptable carrier. The pharmaceutical composition facilitates administration of the compound to a patient or

subject. Multiple techniques of administering a compound exist in the art including, but not limited to, intravenous, oral, aerosol, parenteral, ophthalmic, pulmonary, and topical administration.

As used herein, the terms “conservative variation” or “conservative substitution” as used herein refers to the replacement of an amino acid residue by another, biologically similar residue. Conservative variations or substitutions are not likely to change the shape of the peptide chain. Examples of conservative variations, or substitutions, include the replacement of one hydrophobic residue such as isoleucine, valine, leucine, or methionine for another, or the substitution of one polar residue for another, such as the substitution of arginine for lysine, glutamic for aspartic acid, or glutamine for asparagine. Additional examples include swaps within groups such as Gly / Ala; Val / Ile / Leu; Asp / Glu; Asn / Gln; Ser / Thr; Lys / Arg; and Phe / Tyr.

The degree of identity between two polypeptides is determined using computer algorithms and methods that are widely known for the persons skilled in the art. The identity between two amino acid sequences is preferably determined by using the BLASTP algorithm (BLAST Manual, Altschul et al., NCBI NLM NIH Bethesda, Md. 20894, Altschul et al., J. Mol. Biol. 215: 403-410 (1990)), though other similar algorithms can also be used. BLAST and BLAST 2.0 are used, with the parameters described herein, to determine percent sequence identity. Software for performing BLAST analyses is publicly available through the National Center for Biotechnology Information.

A "disease" is a state of health of an animal wherein the animal cannot maintain homeostasis, and wherein if the disease is not ameliorated then the animal's health continues to deteriorate.

In contrast, a "disorder" in an animal is a state of health in which the animal is able to maintain homeostasis, but in which the animal's state of health is less favorable than it would be in the absence of the disorder. Left untreated, a disorder does not necessarily cause a further decrease in the animal's state of health.

As used herein, the terms "effective amount," "pharmaceutically effective amount," and "therapeutically effective amount" refer to a nontoxic but sufficient amount of an agent to provide the desired biological result. That result may be reduction and/or alleviation of the signs, symptoms, or causes of a disease, or any other desired alteration of a biological system. An

appropriate therapeutic amount in any individual case may be determined by one of ordinary skill in the art using routine experimentation.

As used herein, the term "efficacy" refers to the maximal effect (E_{max}) achieved within an assay.

The term "independently selected from" as used herein refers to referenced groups being the same, different, or a mixture thereof, unless the context clearly indicates otherwise. Thus, under this definition, the phrase "X^1, X^2, and X^3 are independently selected from noble gases" would include the scenario where, for example, X^1, X^2, and X^3 are all the same, where X^1, X^2, and X^3 are all different, where X^1 and X^2 are the same but X^3 is different, and other analogous permutations.

"Isolated" means altered or removed from the natural state. For example, a nucleic acid or a polypeptide naturally present in a living animal is not "isolated," but the same nucleic acid or polypeptide partially or completely separated from the coexisting materials of its natural state is "isolated." An isolated nucleic acid or protein can exist in substantially purified form, or can exist in a non-native environment such as, for example, a host cell.

The terms "patient," "subject," or "individual" are used interchangeably herein, and refer to any animal, or cells thereof whether in vitro or in situ, amenable to the methods described herein. In a non-limiting embodiment, the patient, subject, or individual is a human.

As used herein, the term "peptide(s)" and "compound(s)" are used interchangeably.

As used herein, the term "pharmaceutically acceptable" refers to a material, such as a carrier or diluent, which does not abrogate the biological activity or properties of the compound, and is relatively nontoxic, *i.e.*, the material may be administered to an individual without causing undesirable biological effects or interacting in a deleterious manner with any of the components of the composition in which it is contained.

As used herein, the language "pharmaceutically acceptable salt" refers to a salt of the administered compounds prepared from pharmaceutically acceptable nontoxic acids or bases, including inorganic acids or bases, organic acids or bases, solvates, hydrates, or clathrates thereof.

Suitable pharmaceutically acceptable acid addition salts may be prepared from an inorganic acid or from an organic acid. Examples of inorganic acids include hydrochloric, hydrobromic, hydriodic, nitric, carbonic, sulfuric (including sulfate and hydrogen sulfate), and

phosphoric acids (including hydrogen phosphate and dihydrogen phosphate). Appropriate organic acids may be selected from aliphatic, cycloaliphatic, aromatic, araliphatic, heterocyclic, carboxylic and sulfonic classes of organic acids, examples of which include formic, acetic, propionic, succinic, glycolic, gluconic, lactic, malic, tartaric, citric, ascorbic, glucuronic, maleic, malonic, saccharin, fumaric, pyruvic, aspartic, glutamic, benzoic, anthranilic, 4-hydroxybenzoic, phenylacetic, mandelic, embonic (pamoic), methanesulfonic, ethanesulfonic, benzenesulfonic, pantothenic, trifluoromethanesulfonic, 2-hydroxyethanesulfonic, p-toluenesulfonic, sulfanilic, cyclohexylaminosulfonic, stearic, alginic, β-hydroxybutyric, salicylic, galactaric and galacturonic acid.

Suitable pharmaceutically acceptable base addition salts of compounds described herein include, for example, ammonium salts, metallic salts including alkali metal, alkaline earth metal, and transition metal salts such as, for example, calcium, magnesium, potassium, sodium, and zinc salts. Pharmaceutically acceptable base addition salts also include organic salts made from basic amines such as, for example, N,N'-dibenzylethylene-diamine, chloroprocaine, choline, diethanolamine, ethylenediamine, meglumine (N-methylglucamine), and procaine. All of these salts may be prepared from the corresponding compound by reacting, for example, the appropriate acid or base with the compound.

As used herein, the term "pharmaceutically acceptable carrier" or "pharmaceutically acceptable excipient" means a pharmaceutically acceptable material, composition, or carrier, such as a liquid or solid filler, stabilizer, dispersing agent, suspending agent, diluent, excipient, thickening agent, solvent or encapsulating material, involved in carrying or transporting a compound described herein within or to the patient such that it may perform its intended function. Typically, such constructs are carried or transported from one organ, or portion of the body, to another organ, or portion of the body. Each carrier must be "acceptable" in the sense of being compatible with the other ingredients of the formulation, including the compound(s) described herein, and not injurious to the patient. Some examples of materials that may serve as pharmaceutically acceptable carriers include: sugars, such as lactose, glucose, and sucrose; starches, such as corn starch and potato starch; cellulose, and its derivatives, such as sodium carboxymethyl cellulose, ethyl cellulose, and cellulose acetate; powdered tragacanth; malt; gelatin; talc; excipients, such as cocoa butter and suppository waxes; oils, such as peanut oil, cottonseed oil, safflower oil, sesame oil, olive oil, corn oil, and soybean oil; glycols, such as

propylene glycol; polyols, such as glycerin, sorbitol, mannitol, and polyethylene glycol; esters, such as ethyl oleate and ethyl laurate; agar; buffering agents, such as magnesium hydroxide and aluminum hydroxide; surface active agents; alginic acid; pyrogen-free water; isotonic saline; Ringer's solution; ethyl alcohol; phosphate buffer solutions; and other non-toxic compatible substances employed in pharmaceutical formulations. As used herein, "pharmaceutically acceptable carrier" also includes any and all coatings, antibacterial and antifungal agents, and absorption delaying agents, and the like that are compatible with the activity of the compound(s) described herein, and are physiologically acceptable to the patient. Supplementary active compounds may also be incorporated into the compositions. The "pharmaceutically acceptable carrier" may further include a pharmaceutically acceptable salt of the compound(s) described herein. Other additional ingredients that may be included in the pharmaceutical compositions used with the methods or compounds described herein are known in the art and described, for example in Remington's Pharmaceutical Sciences (Genaro, Ed., Mack Publishing Co., 1985, Easton, PA), which is incorporated herein by reference.

As used herein, the term "potency" refers to the dose needed to produce half the maximal response (ED_{50}).

The terms "prevent," "preventing," and "prevention", as used herein, refer to inhibiting the inception or decreasing the occurrence of a disease in a subject. Prevention may be complete (e.g., the total absence of pathological cells in a subject) or partial. Prevention also refers to a reduced susceptibility to a clinical condition. In certain embodiments, "preventing" comprises preventing onset of a disease or disorder.

The term "room temperature" as used herein refers to a temperature of about 15 °C to 28°C.

The term "solvent" as used herein refers to a liquid that can dissolve a solid, liquid, or gas. Non-limiting examples of solvents are silicones, organic compounds, water, alcohols, ionic liquids, and supercritical fluids.

The term "standard temperature and pressure" as used herein refers to 20°C and 101 kPa.

As used herein, "substantially purified" refers to being essentially free of other components. For example, a substantially purified polypeptide is a polypeptide that has been separated from other components with which it is normally associated in its naturally occurring

state. Non-limiting embodiments include 95% purity, 99% purity, 99.5% purity, 99.9% purity and 100% purity.

The term "substantially" as used herein refers to a majority of, or mostly, as in at least about 50%, 60%, 70%, 80%, 90%, 95%, 96%, 97%, 98%, 99%, 99.5%, 99.9%, 99.99%, or at least about 99.999% or more, or 100%. The term "substantially free of" as used herein can mean having none or having a trivial amount of, such that the amount of material present does not affect the material properties of the composition including the material, such that the composition is about 0 wt% to about 5 wt% of the material, or about 0 wt% to about 1 wt%, or about 5 wt% or less, or less than, equal to, or greater than about 4.5 wt%, 4, 3.5, 3, 2.5, 2, 1.5, 1, 0.9, 0.8, 0.7, 0.6, 0.5, 0.4, 0.3, 0.2, 0.1, 0.01, or about 0.001 wt% or less. The term "substantially free of" can mean having a trivial amount of, such that a composition is about 0 wt% to about 5 wt% of the material, or about 0 wt% to about 1 wt%, or about 5 wt% or less, or less than, equal to, or greater than about 4.5 wt%, 4, 3.5, 3, 2.5, 2, 1.5, 1, 0.9, 0.8, 0.7, 0.6, 0.5, 0.4, 0.3, 0.2, 0.1, 0.01, or about 0.001 wt% or less, or about 0 wt%.

The term "substituted" as used herein in conjunction with a molecule or an organic group as defined herein refers to the state in which one or more hydrogen atoms contained therein are replaced by one or more non-hydrogen atoms. The substitution can be direct substitution, whereby the hydrogen atom is replaced by a functional group or substituent, or an indirect substitution, whereby an intervening linker group replaces the hydrogen atom, and the substituent or functional group is bonded to the intervening linker group. A non-limiting example of direct substitution is: RR-H → RR-Cl, wherein RR is an organic moiety/fragment/molecule. A non-limiting example of indirect substitution is: RR-H → RR-$(LL)_{zz}$-Cl, wherein RR is an organic moiety/fragment/molecule, LL is an intervening linker group, and zz is an integer from 0 to 100 inclusive. When zz is 0, LL is absent, and direct substitution results. The intervening linker group LL is at each occurrence independently selected from the group consisting of -H, -O-, -OR, -S-, -S(=O)-, -$S(=O)_2$-, -SR, -N(R)-, -NR_2, -CR=, -C≡, -CH_2-, -CHR-, -CR_2-, -CH_3, -C(=O)-, -C(=NR)-, and combinations thereof. $(LL)_{zz}$ can be linear, branched, cyclic, acyclic, and combinations thereof.

The term "substituent" or "functional group" as used herein refers to a group that can be or is substituted onto a molecule or onto an organic group. Examples of substituents or functional groups include, but are not limited to, a halogen (*e.g.*, F, Cl, Br, and I); an oxygen atom in groups

such as hydroxy groups, alkoxy groups, aryloxy groups, aralkyloxy groups, oxo(carbonyl) groups, carboxyl groups including carboxylic acids, carboxylates, and carboxylate esters; a sulfur atom in groups such as thiol groups, alkyl and aryl sulfide groups, sulfoxide groups, sulfone groups, sulfonyl groups, and sulfonamide groups; a nitrogen atom in groups such as amines, hydroxyamines, nitriles, nitro groups, N-oxides, hydrazides, azides, and enamines; and other heteroatoms in various other groups. Non-limiting examples of substituents that can be bonded to a substituted carbon (or other) atom include F, Cl, Br, I, OR, $OC(O)N(R)_2$, CN, NO, NO_2, ONO_2, azido, CF_3, OCF_3, R, O (oxo), S (thiono), C(O), S(O), methylenedioxy, ethylenedioxy, $N(R)_2$, SR, SOR, SO_2R, $SO_2N(R)_2$, SO_3R, C(O)R, C(O)C(O)R, $C(O)CH_2C(O)R$, C(S)R, C(O)OR, OC(O)R, $C(O)N(R)_2$, $OC(O)N(R)_2$, $C(S)N(R)_2$, $(CH_2)_{0-2}N(R)C(O)R$, $(CH_2)_{0-2}N(R)N(R)_2$, N(R)N(R)C(O)R, N(R)N(R)C(O)OR, $N(R)N(R)CON(R)_2$, $N(R)SO_2R$, $N(R)SO_2N(R)_2$, N(R)C(O)OR, N(R)C(O)R, N(R)C(S)R, $N(R)C(O)N(R)_2$, $N(R)C(S)N(R)_2$, N(COR)COR, N(OR)R, $C(=NH)N(R)_2$, C(O)N(OR)R, and C(=NOR)R, wherein R can be hydrogen or a carbon-based moiety; for example, R can be hydrogen, $(C_1\text{-}C_{100})$hydrocarbyl, alkyl, acyl, cycloalkyl, aryl, aralkyl, heterocyclyl, heteroaryl, or heteroarylalkyl; or wherein two R groups bonded to a nitrogen atom or to adjacent nitrogen atoms can together with the nitrogen atom or atoms form a heterocyclyl.

A "therapeutic" treatment is a treatment administered to a subject who exhibits signs of pathology, for the purpose of diminishing or eliminating those signs.

As used herein, the term "treatment" or "treating" is defined as the application or administration of a therapeutic agent, *i.e.*, a compound or compounds as described herein (alone or in combination with another pharmaceutical agent), to a patient, or application or administration of a therapeutic agent to an isolated tissue or cell line from a patient (*e.g.*, for diagnosis or *ex vivo* applications), who has a condition contemplated herein or a symptom of a condition contemplated herein, with the purpose to alleviate, relieve, alter, remedy, ameliorate, improve, or affect a condition contemplated herein, or the symptoms of a condition contemplated herein. Such treatments may be specifically tailored or modified, based on knowledge obtained from the field of pharmacogenomics.

GLP-1 and MCR Dual Agonist Peptides

Compounds (peptides) described herein can be prepared by the general schemes described herein, using the synthetic method known by those skilled in the art. The following examples illustrate non-limiting embodiments of the compound(s) described herein and their preparation.

In various embodiments, provided herein are chimeric dual-agonist peptides having agonistic function at both GLP-1 (glucagon like peptide) and MCR (melanocortin) receptors. In various embodiments, the dual agonist peptide is less than or equal to 20, 21, 22, 23, 24, 25, 26, 27, 28, 29, 30, 31, 32, 33, 34, 35, 36, 37, 38, 39, 40, 41, 42, 43, 44, 45, 46, 47, 48, 49, 50, 51, 52, 53, 54, 55, 56, 57, 58, 59, or 60 amino acids in length.

In various embodiments, the dual agonist peptide has the sequence:
X1-X2-X3-X4-X5-X6-X7-X8-X9-X10-X11-X12-X13-X14-X15-X16-X17-X18-X19-X20-X21-X22-X23-X24-X25-X26-X27-X28-X29-X30-X31-X32-X33-X34-X35-X36-X37-X38-X39-X40-X41-X42-X43-X44-X45-X46-X46-X47-X48-X49-X50-X51-X52-X53-X54-X55-X56-X57-X58-X59-X60-NH_2 (SEQ ID NO: 1),
wherein the amino acid residues X1-X60 have the definitions listed in Table 1.

Table 1: Definitions for residues in SEQ ID NO. 1.

Position	Definition in SEQ ID NO: 1
X1	H, h, or any other analog or derivative described herein
X2	S, s, α-methyl-Ser, or any other analog or derivative described herein
X3	Q, q, or any other analog or derivative described herein
X4	G
X5	T, t, or any other analog or derivative described herein
X6	F, f, α-methyl-Phe, or any other analog or derivative described herein
X7	T, t, or any other analog or derivative described herein
X8	S, s, α-methyl-Ser, or any other analog or derivative described herein
X9	D, d, or any other analog or derivative described herein
X10	L, l, Nle, or any other analog or derivative described herein

X11	S, s, α-methyl-Ser, or any other analog or derivative described herein
X12	K, k, α-methyl-Lys, K*, K[a], or any other analog or derivative described herein
X13	Y, y, or any other analog or derivative described herein
X14	L, l, Nle, or any other analog or derivative described herein
X15	E, e, or any other analog or derivative described herein
X16	E, e, or any other analog or derivative described herein
X17	E, e, or any other analog or derivative described herein
X18	A, a, α-methyl-Ala, or any other analog or derivative described herein
X19	V, v, Nva or any other analog or derivative described herein
X20	R, r, or any other analog or derivative described herein
X21	E, e, or any other analog or derivative described herein
X22	F, f, α-methyl-Phe, or any other analog or derivative described herein
X23	I, I, or any other analog or derivative described herein
X24	A, a, α-methyl-Ala, or any other analog or derivative described herein
X25	W, w, or any other analog or derivative described herein
X26	L, l, Nle, or any other analog or derivative described herein
X27	K, k, α-methyl-Lys, K*, K[a], or any other analog or derivative described herein
X28	N, n, or any other analog or derivative described herein
X29	G
X30	G
X31	P, p, or any other analog or derivative described herein
X32	S, s, α-methyl-Ser, or any other analog or derivative described herein
X33	H, h, Y, y, or any other analog or derivative described herein
X34	S, s, F, f, α-methyl-Phe, α-methyl-Ser, or any other analog or derivative described herein
X35	M, m, R, r, L, l, Nle, or any other analog or derivative described herein
X36	E, e, W, w, or any other analog or derivative described herein

X37	Absent, H, h, or any other analog or derivative described herein
X38	Absent, F, f, α-methyl-Phe, or any other analog or derivative described herein
X39	Absent, R, r, or any other analog or derivative described herein
X40	Absent, W, w, or any other analog or derivative described herein
X41	Absent or G
X42	Absent, K, k, α-methyl-Lys, K*, K^a, or any other analog or derivative described herein
X43	Absent, P, p, or any other analog or derivative described herein
X44	Absent, V, v, Nva, or any other analog or derivative described herein
X45	Absent, A, R, N, D, C, E, Q, G, H, I, L, K, M, F, P, S, T, W, Y, V, a, r, n, d, c, e, q, g, h, i, l, k, m, f, p, s, t, w, y, v, Nle, Nva, α-methyl-Phe, α-methyl-Ala, α-methyl-Ser, α-methyl-Lys, K*, K^a, or any other analog or derivative described herein
X46	Absent, A, R, N, D, C, E, Q, G, H, I, L, K, M, F, P, S, T, W, Y, V, a, r, n, d, c, e, q, g, h, i, l, k, m, f, p, s, t, w, y, v, Nle, Nva, α-methyl-Phe, α-methyl-Ala, α-methyl-Ser, α-methyl-Lys, K*, K^a, or any other analog or derivative described herein
X47	Absent, A, R, N, D, C, E, Q, G, H, I, L, K, M, F, P, S, T, W, Y, V, a, r, n, d, c, e, q, g, h, i, l, k, m, f, p, s, t, w, y, v, Nle, Nva, α-methyl-Phe, α-methyl-Ala, α-methyl-Ser, α-methyl-Lys, K*, K^a, or any other analog or derivative described herein
X48	Absent, A, R, N, D, C, E, Q, G, H, I, L, K, M, F, P, S, T, W, Y, V, a, r, n, d, c, e, q, g, h, i, l, k, m, f, p, s, t, w, y, v, Nle, Nva, α-methyl-Phe, α-methyl-Ala, α-methyl-Ser, α-methyl-Lys, K*, K^a, or any other analog or derivative described herein
X49	Absent, A, R, N, D, C, E, Q, G, H, I, L, K, M, F, P, S, T, W, Y, V, a, r, n, d, c, e, q, g, h, i, l, k, m, f, p, s, t, w, y, v, Nle, Nva, α-methyl-Phe, α-methyl-Ala, α-methyl-Ser, α-methyl-Lys, K*, K^a, or any other analog or derivative described herein
X50	Absent, A, R, N, D, C, E, Q, G, H, I, L, K, M, F, P, S, T, W, Y, V, a, r, n, d, c, e, q, g, h, i, l, k, m, f, p, s, t, w, y, v, Nle, Nva, α-methyl-Phe, α-methyl-Ala, α-methyl-Ser, α-methyl-Lys, K*, K^a, or any other analog or derivative described herein
X51	Absent, A, R, N, D, C, E, Q, G, H, I, L, K, M, F, P, S, T, W, Y, V, a, r, n, d, c, e, q, g, h, i, l, k, m, f, p, s, t, w, y, v, Nle, Nva, α-methyl-Phe, α-methyl-Ala, α-

	methyl-Ser, α-methyl-Lys, K*, K[a], or any other analog or derivative described herein
X52	Absent, A, R, N, D, C, E, Q, G, H, I, L, K, M, F, P, S, T, W, Y, V, a, r, n, d, c, e, q, g, h, i, l, k, m, f, p, s, t, w, y, v, Nle, Nva, α-methyl-Phe, α-methyl-Ala, α-methyl-Ser, α-methyl-Lys, K*, K[a], or any other analog or derivative described herein
X53	Absent, A, R, N, D, C, E, Q, G, H, I, L, K, M, F, P, S, T, W, Y, V, a, r, n, d, c, e, q, g, h, i, l, k, m, f, p, s, t, w, y, v, Nle, Nva, α-methyl-Phe, α-methyl-Ala, α-methyl-Ser, α-methyl-Lys, K*, K[a], or any other analog or derivative described herein
X54	Absent, A, R, N, D, C, E, Q, G, H, I, L, K, M, F, P, S, T, W, Y, V, a, r, n, d, c, e, q, g, h, i, l, k, m, f, p, s, t, w, y, v, Nle, Nva, α-methyl-Phe, α-methyl-Ala, α-methyl-Ser, α-methyl-Lys, K*, K[a], or any other analog or derivative described herein
X55	Absent, A, R, N, D, C, E, Q, G, H, I, L, K, M, F, P, S, T, W, Y, V, a, r, n, d, c, e, q, g, h, i, l, k, m, f, p, s, t, w, y, v, Nle, Nva, α-methyl-Phe, α-methyl-Ala, α-methyl-Ser, α-methyl-Lys, K*, K[a], or any other analog or derivative described herein
X56	Absent, A, R, N, D, C, E, Q, G, H, I, L, K, M, F, P, S, T, W, Y, V, a, r, n, d, c, e, q, g, h, i, l, k, m, f, p, s, t, w, y, v, Nle, Nva, α-methyl-Phe, α-methyl-Ala, α-methyl-Ser, α-methyl-Lys, K*, K[a], or any other analog or derivative described herein
X57	Absent, A, R, N, D, C, E, Q, G, H, I, L, K, M, F, P, S, T, W, Y, V, a, r, n, d, c, e, q, g, h, i, l, k, m, f, p, s, t, w, y, v, Nle, Nva, α-methyl-Phe, α-methyl-Ala, α-methyl-Ser, α-methyl-Lys, K*, K[a], or any other analog or derivative described herein
X58	Absent, A, R, N, D, C, E, Q, G, H, I, L, K, M, F, P, S, T, W, Y, V, a, r, n, d, c, e, q, g, h, i, l, k, m, f, p, s, t, w, y, v, Nle, Nva, α-methyl-Phe, α-methyl-Ala, α-methyl-Ser, α-methyl-Lys, K*, K[a], or any other analog or derivative described herein
X59	Absent, A, R, N, D, C, E, Q, G, H, I, L, K, M, F, P, S, T, W, Y, V, a, r, n, d, c, e, q, g, h, i, l, k, m, f, p, s, t, w, y, v, Nle, Nva, α-methyl-Phe, α-methyl-Ala, α-methyl-Ser, α-methyl-Lys, K*, K[a], or any other analog or derivative described herein
X60	Absent, A, R, N, D, C, E, Q, G, H, I, L, K, M, F, P, S, T, W, Y, V, a, r, n, d, c, e, q, g, h, i, l, k, m, f, p, s, t, w, y, v, Nle, Nva, α-methyl-Phe, α-methyl-Ala, α-methyl-Ser, α-methyl-Lys, K*, K[a], or any other analog or derivative described herein

In Table 1, the term "any other analog or derivative described herein" refers to any other analog described herein of the naturally occurring amino acid as defined for a given position, and any derivatives as described herein of the naturally occurring amino acid as defined for a given position.

In various embodiments, the dual agonist peptide has the sequence: HsQGTFTSDLSKYLEEEAVREFIAWLKNGGPSYSMEHFRWGKPV-NH_2 (SEQ ID NO. 2).

In various embodiments, the dual agonist peptide has the sequence: HSQGTFTSDLSKYLEEEAVREFIAWLKNGGPSYSMEHFRWGKPV-NH_2 (SEQ ID NO. 3).

In various embodiments, the dual agonist peptide has the sequence: HsQGTFTSDLSKYLEEEAVREFIAWLKNGGPSYS(Nle)EHfRWGKPV-NH_2 (SEQ NO. 4).

In various embodiments, the dual agonist peptide has the sequence: HsQGTFTSDLSKYLEEEAVREFIAWLKNGGPSYS(Nle)EHfRW-NH_2 (SEQ ID NO: 5).

In various embodiments, the dual agonist peptide has the sequence: HsQGTFTSDLSKYLEEEAVREFIAWLKNGGPSHfRW-NH_2 (SEQ ID NO: 6).

In various embodiments, the dual agonist peptide has a sequence that is at least 80, 85, 90, 95, 96, 97, 98, or 99% homologous to the dual agonist peptide of SEQ ID NO. 2.

In various embodiments, the dual agonist peptide has a sequence that is at least 80, 85, 90, 95, 96, 97, 98, or 99% homologous to the dual agonist peptide of SEQ ID NO. 3.

In various embodiments, the dual agonist peptide has a sequence that is at least 80, 85, 90, 95, 96, 97, 98, or 99% homologous to the dual agonist peptide of SEQ ID NO. 4.

In various embodiments, the dual agonist peptide has a sequence that is at least 80, 85, 90, 95, 96, 97, 98, or 99% homologous to the dual agonist peptide of SEQ ID NO. 5.

In various embodiments, the dual agonist peptide has a sequence that is at least 80, 85, 90, 95, 96, 97, 98, or 99% homologous to the dual agonist peptide of SEQ ID NO. 6.

In various embodiments, peptides of SEQ ID NO. 1-6 are dual agonists of GLP-1 and MCR3. In various embodiments, peptides of SEQ ID NO. 1-6 are dual agonists of GLP-1 and MCR4. In various embodiments, peptides of SEQ ID NO. 1-6 are dual agonists of GLP-1 and MCR3/4.

Analogs and Derivatives of Naturally Occurring Amino Acids in SEQ ID NOs. 1-6

In the peptides described herein, an amino acid single-letter code in lower-case represents the corresponding D-amino acid. For example, in SEQ ID NO. 1, the lower-case "s" represents D-serine. The peptides described herein can include L-amino acids, D-amino acids, or a combination of both. In various embodiments, the peptides are D retro-inverso peptides. The term "retro-inverso isomer" refers to an isomer of a linear peptide in which the direction of the sequence is reversed and the chirality of each amino acid residue is inverted. *See, e.g.*, Jameson *et al.*, *Nature,* 368, 744-746 (1994); Brady *et al.*, Nature, 368, 692-693 (1994), which is incorporated herein in its entirety by reference. The net result of combining D-enantiomers and reverse synthesis is that the positions of carbonyl and amino groups in each amide bond are exchanged, while the position of the side-chain groups at each alpha carbon is preserved. Unless specifically stated otherwise, it is presumed that any given L-amino acid sequence of the invention may be made into a D retro-inverso peptide by synthesizing a reverse of the sequence for the corresponding native L-amino acid sequence.

In various embodiments, one or more amino acids in the peptides described herein can be replaced by a non-naturally occurring amino acid or a naturally or non-naturally occurring amino acid analog. For example, an aromatic amino acid can be replaced by 3,4-dihydroxy-L-phenylalanine, 3-iodo-L-tyrosine, triiodothyronine, L-thyroxine, phenylglycine (Phg), or nor-tyrosine (norTyr). Phg, norTyr, and other amino acids including Phe and Tyr can be substituted by, *e.g.*, a halogen, $-CH_3$, -OH, $-CH_2NH_3$, -C(O)H, $-CH_2CH_3$, - CN, $-CH_2CH_2CH_3$, -SH, or another group.

With regard to non-naturally occurring amino acids or naturally and non-naturally occurring amino acid analogs, a number of substitutions in dual agonist peptides described herein are possible alone or in combination. For example, glutamine residues can be substituted with gamma-hydroxy-Glu or gamma-carboxy-Glu. Tyrosine residues can be substituted with an alpha substituted amino acid such as L-alpha-methylphenylalanine or by analogues such as: 3-amino-Tyr; Tyr(CH_3); Tyr($PO_3(CH_3)_2$); Tyr(SO_3H); β-cyclohexyl-Ala; β-(l-cyclopentenyl)-Ala; β-cyclopentyl-Ala; β-cyclopropyl-Ala; β-quinolyl-Ala; β-(2-thiazolyl)-Ala; β-(triazole-l-yl)-Ala; β-(2-pyridyl)-Ala; β-(3-pyridyl)-Ala; amino-Phe; fluoro-Phe; cyclohexyl-Gly; t-Bu-Gly; β-(3-benzothienyl)-Ala; β-(2-thienyl)-Ala; 5-methyl-Trp; and α-methyl-Trp.

Proline residues can be substituted with homo-Pro (L-pipecolic acid); hydroxy-Pro; 3,4-dehydro-Pro; 4-fluoro-Pro; or α-methyl-Pro. Alanine residues can be substituted with alpha-

substituted or N-methylated amino acid such as alpha-amino isobutyric acid (aib), L/D-alpha-ethylalanine (L/D-isovaline), L/D-methylvaline, or L/D-alpha-methylleucine or a non-natural amino acid such as β-fluoro-Ala. Alanine can also be substituted with: n = 0, 1, 2, 3; Glycine residues can be substituted with alpha-amino iso-butyric acid (aib) or L/D-alpha- ethylalanine (L/D-isovaline). Other non-standard amino acid residues that can, in various embodiments, replace one or more standard amino acid residues in the dual agonist peptides described herein include, norleucine (Nle), norvaline (Nva), citrulline (Cit), ornithine (Orn), Naphthylalanine (Nal), α-aminobutryic acid (Abu), 2,4-diaminobutyric acid (Dab), methionine sulfoxide, methionine sulfone, and the like.

The peptides described herein can be modified using standard modifications. Modifications may occur at the amino (N-) terminus, carboxy (C-) terminus, internally, or a combination of any of the preceding. In various embodiments, there may be more than one type of modification in the dual agonist peptide. Modifications include, but are not limited to: acetylation, amidation, biotinylation, cinnamoylation, farnesylation, formylation, myristoylation, palmitoylation, phosphorylation (Ser, Tyr or Thr), stearoylation, succinylation, sulfurylation, and cyclisation (via disulfide bridges or amide cyclisation). The dual agonist peptides described herein may also be modified by 2, 4-dinitrophenyl (DNP), DNP-lysine, modification by 7-amino-4-methyl-coumarin (AMC), flourescein, NBD (7-nitrobenz-2-oxa-l,3-diazole), p-nitro-anilide, rhodamine B, EDANS (5-((2-aminoethyl)amino)naphthalene-1-sulfonic acid), dabcyl, dabsyl, dansyl, Texas red, FMOC, and Tamra (tetramethylrhodamine).

The dual agonist peptides described herein may also be conjugated to, for example, polyethylene glycol (PEG); alkyl groups (*e.g.*, C_1-C_{30} straight or branched alkyl groups); fatty acid radicals (*e.g.*, C_1-C_{30} straight or branched fatty acid radicals); as well as combinations of PEG, alkyl groups, and fatty acid radicals. In various embodiments, PEG groups, $(-CH_2CH_2-O)_m$, can have m equal to 1 to 50. The conjugation can be at any suitable amino acid side chain, such as at a side chain containing a carboxyl group (Asp or Glu), an amine (His, Lys, Arg), or an alcohol (Ser, Thr).

Contemplated herein is a dual-agonist peptide sequence having a D-amino acid, α-amino acid, β-amino acid, methylated amino acid, acetylated amino acid, amidated amino acid, biotinylated amino acid, cinnamoylated amino acid, farnesylated amino acid, formylated amino acid, myristoylated amino acid, palmitoylated amino acid, phosphorylated amino acid (Ser, Tyr

or Thr), stearoylated amino acid, succinylated amino acid, a sulfurylated amino acid, or any other non-standard/non-natural amino acid analog described herein at any one residue position in the peptides of SEQ ID NO. 1-6.

Contemplated herein is a dual-agonist peptide sequence having a D-amino acid, α-amino acid, β-amino acid, methylated amino acid, acetylated amino acid, amidated amino acid, biotinylated amino acid, cinnamoylated amino acid, farnesylated amino acid, formylated amino acid, myristoylated amino acid, palmitoylated amino acid, phosphorylated amino acid (Ser, Tyr or Thr), stearoylated amino acid, succinylated amino acid, a sulfurylated amino acid, or any other non-standard/non-natural amino acid analog described herein at any two residue positions in the peptides of SEQ ID NO. 1-6, wherein any of the preceding unnatural amino acids can be independently present.

Contemplated herein is a dual-agonist peptide sequence having a D-amino acid, α-amino acid, β-amino acid, methylated amino acid, acetylated amino acid, amidated amino acid, biotinylated amino acid, cinnamoylated amino acid, farnesylated amino acid, formylated amino acid, myristoylated amino acid, palmitoylated amino acid, phosphorylated amino acid (Ser, Tyr or Thr), stearoylated amino acid, succinylated amino acid, a sulfurylated amino acid, or any other non-standard/non-natural amino acid analog described herein at any three residue positions in the peptides of SEQ ID NO. 1-6, wherein any of the preceding unnatural amino acids can be independently present.

Contemplated herein is a dual-agonist peptide sequence having a D-amino acid, α-amino acid, β-amino acid, methylated amino acid, acetylated amino acid, amidated amino acid, biotinylated amino acid, cinnamoylated amino acid, farnesylated amino acid, formylated amino acid, myristoylated amino acid, palmitoylated amino acid, phosphorylated amino acid (Ser, Tyr or Thr), stearoylated amino acid, succinylated amino acid, a sulfurylated amino acid, or any other non-standard/non-natural amino acid analog described herein at any four, five, six, seven, eight, nine, or ten residue positions in the peptides of SEQ ID NO. 1-6, wherein any of the preceding unnatural amino acids can be independently present.

In various embodiments, K* is a lysine residue in which the amino side chain is substituted according to the structure:

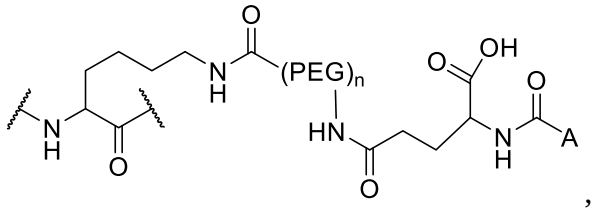

,

wherein n is an integer from 1 to 12;

PEG is a moiety that contains one or more ethylene glycol units; and

A is a linear or branched C_{4-18} alkyl, linear or branched C_{4-18} alkenyl, or linear or branched C_{4-18} alkynyl.

In various embodiments, K* is a lysine residue in which the amino side chain is substituted according to the structure:

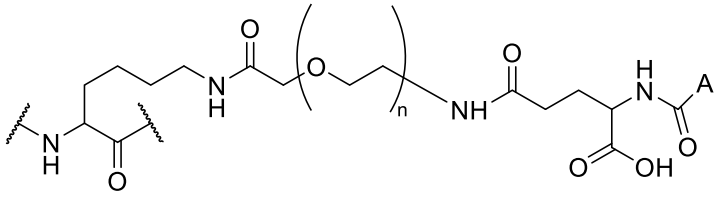

.

In various embodiments, A is a linear or branched C4, C5, C6, C7, C8, C9, C10, C11, C12, C13, C14, C15, C16, C17, or C18 alkyl.

In various embodiments, A is a linear or branched C4, C5, C6, C7, C8, C9, C10, C11, C12, C13, C14, C15, C16, C17, or C18 alkenyl.

In various embodiments, A is a linear or branched C4, C5, C6, C7, C8, C9, C10, C11, C12, C13, C14, C15, C16, C17, or C18 alkynyl.

In various embodiments, A is C12 alkyl.

In various embodiments, K^a is a lysine residue in which the amino side chain is substituted according to the structure:

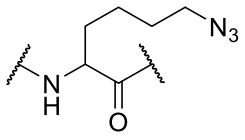

.

Lysine residue derivatives with the structure of K^a can be further reacted or bio-conjugated to other chemical or biological moieties (*in vitro* or *in vivo*), in various embodiments, using copper-free or copper-mediated click-chemistry.

In various embodiments, the dual agonist peptide of SEQ ID NO: 1 does not contain any of the following amino acid sequences:

HAEGTFTSDVSSYLEGQAAKEFIAWLVRGR (SEQ ID NO: 7),

HAEGTFTSDVSSYLEGQAAKEFIAWLVKGR (SEQ ID NO: 8), or

any continuous sequence of 4, 5, 6, 7, 8, 9, 10, 11, 12, 13, 14, 15, 16, 17, 18, 19, 20, 21, 22, 23, 24, 25, 26, 27, 28, 29, or 30 amino acids starting with the first amino acid in either SEQ ID NO. 7 or 8 (His1), or

any sequence that has at least 80, 85, 90, 95, 96, 97, 98, or 99% sequence homology to SEQ ID NO. 7 or SEQ ID NO. 8.

Table 2. **Sequences of GLP-1R/MC4R chimeric dual agonists**.

Peptide	Sequence ID
KSCEM01	2
KSCEM02	4
KSCEM03	5
KSCEM04	6

KSCEM01, KSCEM02, KSCEM03, and KSCEM04 were synthesized and purified to >95% purity. Lowercase letters denote D-amino acids; Nle = norleucine.

The compounds described herein can possess one or more stereocenters, and each stereocenter can exist independently in either the (*R*) or (*S*) configuration. In certain embodiments, compounds described herein are present in optically active or racemic forms. It is to be understood that the compounds described herein encompass racemic, optically-active, regioisomeric and stereoisomeric forms, or combinations thereof that possess the therapeutically useful properties described herein. Preparation of optically active forms is achieved in any suitable manner, including by way of non-limiting example, by resolution of the racemic form with recrystallization techniques, synthesis from optically-active starting materials, chiral synthesis, or chromatographic separation using a chiral stationary phase. In certain embodiments, a mixture of one or more isomer is utilized as the therapeutic compound described herein. In other embodiments, compounds described herein contain one or more chiral centers. These compounds are prepared by any means, including stereoselective synthesis, enantioselective synthesis and/or separation of a mixture of enantiomers and/ or diastereomers. Resolution of

compounds and isomers thereof is achieved by any means including, by way of non-limiting example, chemical processes, enzymatic processes, fractional crystallization, distillation, and chromatography.

The methods and formulations described herein include the use of N-oxides (if appropriate), crystalline forms (also known as polymorphs), solvates, amorphous phases, and/or pharmaceutically acceptable salts of compounds having the structure of any compound(s) described herein, as well as metabolites and active metabolites of these compounds having the same type of activity. Solvates include water, ether (*e.g.*, tetrahydrofuran, methyl tert-butyl ether) or alcohol (*e.g.*, ethanol) solvates, acetates and the like. In certain embodiments, the compounds described herein exist in solvated forms with pharmaceutically acceptable solvents such as water, and ethanol. In other embodiments, the compounds described herein exist in unsolvated form.

In certain embodiments, the compound(s) described herein can exist as tautomers. All tautomers are included within the scope of the compounds presented herein.

In certain embodiments, compounds described herein are prepared as prodrugs. A "prodrug" refers to an agent that is converted into the parent drug *in vivo.* In certain embodiments, upon *in vivo* administration, a prodrug is chemically converted to the biologically, pharmaceutically or therapeutically active form of the compound. In other embodiments, a prodrug is enzymatically metabolized by one or more steps or processes to the biologically, pharmaceutically or therapeutically active form of the compound.

In certain embodiments, sites on, for example, the aromatic ring portion of compound(s) described herein are susceptible to various metabolic reactions. Incorporation of appropriate substituents on the aromatic ring structures may reduce, minimize or eliminate this metabolic pathway. In certain embodiments, the appropriate substituent to decrease or eliminate the susceptibility of the aromatic ring to metabolic reactions is, by way of example only, a deuterium, a halogen, or an alkyl group.

Compounds described herein also include isotopically-labeled compounds wherein one or more atoms is replaced by an atom having the same atomic number, but an atomic mass or mass number different from the atomic mass or mass number usually found in nature. Examples of isotopes suitable for inclusion in the compounds described herein include and are not limited to ^{2}H, ^{3}H, ^{11}C, ^{13}C, ^{14}C, ^{36}Cl, ^{18}F, ^{123}I, ^{125}I, ^{13}N, ^{15}N, ^{15}O, ^{17}O, ^{18}O, ^{32}P, and ^{35}S. In certain embodiments, isotopically-labeled compounds are useful in drug and/or substrate tissue

distribution studies. In other embodiments, substitution with heavier isotopes such as deuterium affords greater metabolic stability (for example, increased *in vivo* half-life or reduced dosage requirements). In yet other embodiments, substitution with positron emitting isotopes, such as ^{11}C, ^{18}F, ^{15}O and ^{13}N, is useful in Positron Emission Topography (PET) studies for examining substrate receptor occupancy. Isotopically-labeled compounds are prepared by any suitable method or by processes using an appropriate isotopically-labeled reagent in place of the non-labeled reagent otherwise employed.

In certain embodiments, the compounds described herein are labeled by other means, including, but not limited to, the use of chromophores or fluorescent moieties, bioluminescent labels, or chemiluminescent labels.

The compounds described herein, and other related compounds having different substituents are synthesized using techniques and materials described herein and as described, for example, in Fieser & Fieser's Reagents for Organic Synthesis, Volumes 1-17 (John Wiley and Sons, 1991); Rodd's Chemistry of Carbon Compounds, Volumes 1-5 and Supplementals (Elsevier Science Publishers, 1989); Organic Reactions, Volumes 1-40 (John Wiley and Sons, 1991), Larock's Comprehensive Organic Transformations (VCH Publishers Inc., 1989), March, Advanced Organic Chemistry 4th Ed., (Wiley 1992); Carey & Sundberg, Advanced Organic Chemistry 4th Ed., Vols. A and B (Plenum 2000,2001), and Green & Wuts, Protective Groups in Organic Synthesis 3rd Ed., (Wiley 1999) (all of which are incorporated by reference for such disclosure). General methods for the preparation of compounds as described herein are modified by the use of appropriate reagents and conditions, for the introduction of the various moieties found in the formula as provided herein.

Compounds described herein are synthesized using any suitable procedures starting from compounds that are available from commercial sources, or are prepared using procedures described herein.

In certain embodiments, reactive functional groups, such as hydroxyl, amino, imino, thio, or carboxy groups, are protected in order to avoid their unwanted participation in reactions. Protecting groups are used to block some or all of the reactive moieties and prevent such groups from participating in chemical reactions until the protective group is removed. In other embodiments, each protective group is removable by different means. Protective groups that are cleaved under totally disparate reaction conditions fulfill the requirement of differential removal.

In certain embodiments, protective groups are removed by acid, base, reducing conditions (such as, for example, hydrogenolysis), and/or oxidative conditions. Groups such as trityl, dimethoxytrityl, acetal and t-butyldimethylsilyl are acid labile and are used to protect carboxy and hydroxy reactive moieties in the presence of amino groups protected with Cbz groups, which are removable by hydrogenolysis, and Fmoc groups, which are base labile. Carboxylic acid and hydroxy reactive moieties are blocked with base labile groups such as, but not limited to, methyl, ethyl, and acetyl, in the presence of amines that are blocked with acid labile groups, such as t-butyl carbamate, or with carbamates that are both acid and base stable but hydrolytically removable.

In certain embodiments, carboxylic acid and hydroxy reactive moieties are blocked with hydrolytically removable protective groups such as the benzyl group, while amino groups capable of hydrogen bonding with acids are blocked with base labile groups such as Fmoc. Carboxylic acid reactive moieties are protected by conversion to simple ester compounds as exemplified herein, which include conversion to alkyl esters, or are blocked with oxidatively-removable protective groups such as 2,4-dimethoxybenzyl, while co-existing amino groups are blocked with fluoride labile silyl carbamates.

Allyl blocking groups are useful in the presence of acid- and base- protecting groups since the former are stable and are subsequently removed by metal or pi-acid catalysts. For example, an allyl-blocked carboxylic acid is deprotected with a palladium-catalyzed reaction in the presence of acid labile t-butyl carbamate or base-labile acetate amine protecting groups. Yet another form of protecting group is a resin to which a compound or intermediate is attached. As long as the residue is attached to the resin, that functional group is blocked and does not react. Once released from the resin, the functional group is available to react.

Typically blocking/protecting groups may be selected from:

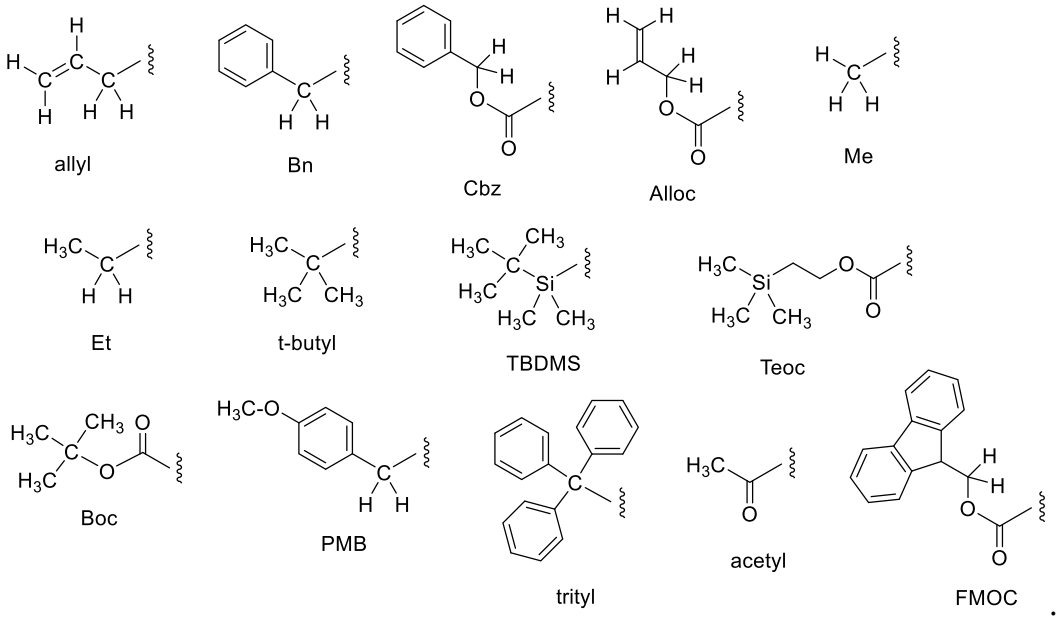

Other protecting groups, plus a detailed description of techniques applicable to the creation of protecting groups and their removal are described in Greene & Wuts, Protective Groups in Organic Synthesis, 3rd Ed., John Wiley & Sons, New York, NY, 1999, and Kocienski, Protective Groups, Thieme Verlag, New York, NY, 1994, which are incorporated herein by reference for such disclosure.

Pharmacology

In various embodiments, the compound(s) described herein can be administered to a subject in an amount ranging from about 0.01 mg/kg to about 200 mg/kg, or about 0.5 mg/kg to about 190 mg/kg, or about 0.75 mg/kg to about 180 mg/kg, or about 1 mg/kg to about 170 mg/kg, or about 1.5 mg/kg to about 160 mg/kg, or about 2 mg/kg to about 150 mg/kg, or about 2.5 mg/kg to about 140 mg/kg, or about 3 mg/kg to about 130 mg/kg, or about 3.5 mg/kg to about 120 mg/kg, or about 4 mg/kg to about 110 mg/kg, or about 4.5 mg/kg to about 100 mg/kg, or about 5 mg/kg to about 95 mg/kg, or about 5.5 mg/kg to about 90 mg/kg, or about 6 mg/kg to about 85 mg/kg, or about 6.5 mg/kg to about 80 mg/kg, or about 7 mg/kg to about 75 mg/kg, or about 7.5 mg/kg to about 70 mg/kg, or about 8 mg/kg to about 65 mg/kg, or about 8.5 mg/kg to about 60 mg/kg, or about 9 mg/kg to about 55 mg/kg or about 9.5 mg/kg to about 50 mg/kg, or about 10 mg/kg to about 45 mg/kg.

In various embodiments, the compound(s) described herein can be administered to a subject in an amount that is less than, equal to, or greater than about 0.01 mg/kg, 0.05 mg/kg, 0.1

mg/kg, 0.25 mg/kg, 0.5 mg/kg, 0.75 mg/kg, 1 mg/kg, 1.5 mg/kg, 2 mg/kg, 2.5 mg/kg, 3 mg/kg, 3.5 mg/kg, 4 mg/kg, 4.5 mg/kg, 5 mg/kg, 5.5 mg/kg, 6 mg/kg, 6.5 mg/kg, 7 mg/kg, 7.5 mg/kg, 8 mg/kg, 8.5 mg/kg, 9 mg/kg, 9.5 mg/kg, 10 mg/kg, 12 mg/kg, 14 mg/kg, 16 mg/kg, 18 mg/kg, 20 mg/kg, 25 mg/kg, 30 mg/kg, 35 mg/kg, 40 mg/kg, 45 mg/kg, 50 mg/kg, 55 mg/kg, 60 mg/kg, 65 mg/kg, 70 mg/kg, 75 mg/kg, 80 mg/kg, 85 mg/kg, 90 mg/kg, 100 mg/kg, 105 mg/kg, 110 mg/kg, 115 mg/kg, 120 mg/kg, 125 mg/kg, 130 mg/kg, 140 mg/kg, 145 mg/kg, 150 mg/kg, 155 mg/kg, 160 mg/kg, 170 mg/kg, 175 mg/kg, 180 mg/kg, 185 mg/kg, 190 mg/kg, 195 mg/kg, or 200 mg/kg.

Compositions

The compositions containing the compound(s) described herein include a pharmaceutical composition comprising at least one compound as described herein and at least one pharmaceutically acceptable carrier. In certain embodiments, the composition is formulated for an administration route such as oral or parenteral, for example, transdermal, transmucosal (*e.g.*, sublingual), lingual, (trans)buccal, (trans)urethral, vaginal (*e.g.*, trans- and perivaginally), (intra)nasal and (trans)rectal, intravesical, intrapulmonary, intraduodenal, intragastrical, intrathecal, subcutaneous, intramuscular, intradermal, intra-arterial, intravenous, intrabronchial, inhalation, and topical administration.

Methods of Treatment, Amelioration, and/or Prevention

The disclosure includes a method of treating, ameliorating, and/or preventing a metabolic disease or disorder using the peptides of SEQ ID NO. 1-6. Non-limiting examples of metabolic diseases or disorders include type 2 diabetes, obesity, nonalcoholic fatty liver disease, hypothalamic obesity, prediabetes, and nonalcoholic steatohepatitis.

In various embodiments, a method of treating, preventing, and/or ameliorating a metabolic condition in the subject includes administering to the subject a therapeutically effective amount of any peptide of the disclosure, thereby treating, preventing, and/or ameliorating the metabolic condition. Administering peptides of SEQ ID NO. 1-6 results in fewer or no significant side-effects, including nausea/malaise and gastrointestinal ailments and/or discomfort as compared to administration of endogenous gut peptides such as glucagon-like peptide-1 (GLP-1) receptor agonists (GLP-1RAs). In various embodiments, administration

of peptides of the disclosure (such as but not limited to any one of SEQ ID NOs. 1-6) results in synergistic effects such that the therapeutic benefits and/or reduction in side effects as a result of their administrations is superior to the administration of a combination of a GLP-1 agonist and a MCR agonist as individual therapeutic agents. In various embodiments, the methods of treating, preventing, and/or ameliorating a metabolic condition in the subject includes reduction of energy intake in the subject (reduced food intake and/or reduced appetite), stimulation of energy expenditure (*e.g.* increased metabolic rate), reduction or elimination of hypothalamic dysfunction, and improvement of glucoregulation.

In various embodiments, the metabolic condition is selected from the group consisting of type 2 diabetes, obesity, nonalcoholic fatty liver disease, and nonalcoholic steatohepatitis.

In various embodiments, the administration is by a route selected from the group consisting of oral, transdermal, transmucosal, intrapulmonary, intraduodenal, intragastrical, intrathecal, subcutaneous, intramuscular, intradermal, intra-arterial, intravenous, intrabronchial, inhalation, and topical administration.

In various embodiments, the subject is a mammal. In various embodiments, the mammal is a human.

The methods described herein include administering to the subject a therapeutically effective amount of at least one compound described herein, which is optionally formulated in a pharmaceutical composition. In various embodiments, a therapeutically effective amount of at least one compound described herein present in a pharmaceutical composition is the only therapeutically active compound in a pharmaceutical composition. In certain embodiments, the method further comprises administering to the subject an additional therapeutic agent that treats metabolic diseases or disorders.

In certain embodiments, administering the compound(s) described herein to the subject allows for administering a lower dose of the additional therapeutic agent as compared to the dose of the additional therapeutic agent alone that is required to achieve similar results in treating a metabolic disease or disorder in the subject. For example, in certain embodiments, the compound(s) described herein enhance(s) the activity of the additional therapeutic compound, thereby allowing for a lower dose of the additional therapeutic compound to provide the same effect.

In certain embodiments, the compound(s) described herein and the therapeutic agent are co-administered to the subject. In other embodiments, the compound(s) described herein and the therapeutic agent are coformulated and co-administered to the subject.

In certain embodiments, the subject is a mammal. In other embodiments, the mammal is a human.

Combination Therapies

The compounds useful within the methods described herein can be used in combination with one or more additional therapeutic agents useful for treating metabolic diseases or disorders. These additional therapeutic agents may comprise compounds that are commercially available or synthetically accessible to those skilled in the art. These additional therapeutic agents are known to treat or reduce the symptoms, of a metabolic disease or disorder.

In various embodiments, a synergistic effect is observed when a compound as described herein is administered with one or more additional therapeutic agents or compounds. A synergistic effect may be calculated, for example, using suitable methods such as, for example, the Sigmoid-E_{max} equation (Holford & Scheiner, 1981, Clin. Pharmacokinet. 6:429-453), the equation of Loewe additivity (Loewe & Muischnek, 1926, Arch. Exp. Pathol Pharmacol. 114:313-326) and the median-effect equation (Chou & Talalay, 1984, Adv. Enzyme Regul. 22:27-55). Each equation referred to above may be applied to experimental data to generate a corresponding graph to aid in assessing the effects of the drug combination. The corresponding graphs associated with the equations referred to above are the concentration-effect curve, isobologram curve and combination index curve, respectively.

Administration/Dosage/Formulations

The regimen of administration may affect what constitutes an effective amount. The therapeutic formulations may be administered to the subject either prior to or after the onset of a metabolic disease or disorder. Further, several divided dosages, as well as staggered dosages may be administered daily or sequentially, or the dose may be continuously infused, or may be a bolus injection. Further, the dosages of the therapeutic formulations may be proportionally increased or decreased as indicated by the exigencies of the therapeutic or prophylactic situation.

Administration of the compositions described herein to a patient, preferably a mammal, more preferably a human, may be carried out using known procedures, at dosages and for periods of time effective to treat a metabolic disease or disorder in the patient. An effective amount of the therapeutic compound necessary to achieve a therapeutic effect may vary according to factors such as the state of the disease or disorder in the patient; the age, sex, and weight of the patient; and the ability of the therapeutic compound to treat a metabolic disease or disorder in the patient. Dosage regimens may be adjusted to provide the optimum therapeutic response. For example, several divided doses may be administered daily or the dose may be proportionally reduced as indicated by the exigencies of the therapeutic situation. A non-limiting example of an effective dose range for a therapeutic compound described herein is from about 1 and 5,000 mg/kg of body weight/per day. One of ordinary skill in the art would be able to study the relevant factors and make the determination regarding the effective amount of the therapeutic compound without undue experimentation.

Actual dosage levels of the active ingredients in the pharmaceutical compositions described herein may be varied so as to obtain an amount of the active ingredient that is effective to achieve the desired therapeutic response for a particular patient, composition, and mode of administration, without being toxic to the patient.

In particular, the selected dosage level depends upon a variety of factors including the activity of the particular compound employed, the time of administration, the rate of excretion of the compound, the duration of the treatment, other drugs, compounds or materials used in combination with the compound, the age, sex, weight, condition, general health and prior medical history of the patient being treated, and like factors well known in the medical arts.

A medical doctor, *e.g.*, physician or veterinarian, having ordinary skill in the art may readily determine and prescribe the effective amount of the pharmaceutical composition required. For example, the physician or veterinarian could start doses of the compounds described herein employed in the pharmaceutical composition at levels lower than that required in order to achieve the desired therapeutic effect and gradually increase the dosage until the desired effect is achieved.

In certain embodiments, it is especially advantageous to formulate the compound in dosage unit form for ease of administration and uniformity of dosage. Dosage unit form as used herein refers to physically discrete units suited as unitary dosages for the patients to be treated;

each unit containing a predetermined quantity of therapeutic compound calculated to produce the desired therapeutic effect in association with the required pharmaceutical vehicle. The dosage unit forms of the compound(s) described herein are dictated by and directly dependent on (a) the unique characteristics of the therapeutic compound and the particular therapeutic effect to be achieved, and (b) the limitations inherent in the art of compounding/formulating such a therapeutic compound.

In certain embodiments, the compositions described herein are formulated using one or more pharmaceutically acceptable excipients or carriers. In certain embodiments, the pharmaceutical compositions described herein comprise a therapeutically effective amount of a compound described herein and a pharmaceutically acceptable carrier.

The carrier may be a solvent or dispersion medium containing, for example, water, ethanol, polyol (*e.g.*, glycerol, propylene glycol, and liquid polyethylene glycol, and the like), suitable mixtures thereof, and vegetable oils. The proper fluidity may be maintained, for example, by the use of a coating such as lecithin, by the maintenance of the required particle size in the case of dispersion, and by the use of surfactants. Prevention of the action of microorganisms may be achieved by various antibacterial and antifungal agents, for example, parabens, chlorobutanol, phenol, ascorbic acid, thimerosal, and the like. In many cases, it is preferable to include isotonic agents, for example, sugars, sodium chloride, or polyalcohols such as mannitol and sorbitol, in the composition. Prolonged absorption of the injectable compositions may be brought about by including in the composition an agent which delays absorption, for example, aluminum monostearate or gelatin.

In certain embodiments, the compositions described herein are administered to the patient in dosages that range from one to five times per day or more. In other embodiments, the compositions described herein are administered to the patient in range of dosages that include, but are not limited to, once every day, every two days, every three days to once a week, and once every two weeks. It is readily apparent to one skilled in the art that the frequency of administration of the various combination compositions described herein varies from individual to individual depending on many factors including, but not limited to, age, disease or disorder to be treated, gender, overall health, and other factors. Thus, administration of the compounds and compositions described herein should not be construed to be limited to any particular dosage

regime and the precise dosage and composition to be administered to any patient is determined by the attending physician taking all other factors about the patient into account.

The compound(s) described herein for administration may be in the range of from about 1 µg to about 10,000 mg, about 20 µg to about 9,500 mg, about 40 µg to about 9,000 mg, about 75 µg to about 8,500 mg, about 150 µg to about 7,500 mg, about 200 µg to about 7,000 mg, about 350 µg to about 6,000 mg, about 500 µg to about 5,000 mg, about 750 µg to about 4,000 mg, about 1 mg to about 3,000 mg, about 10 mg to about 2,500 mg, about 20 mg to about 2,000 mg, about 25 mg to about 1,500 mg, about 30 mg to about 1,000 mg, about 40 mg to about 900 mg, about 50 mg to about 800 mg, about 60 mg to about 750 mg, about 70 mg to about 600 mg, about 80 mg to about 500 mg, and any and all whole or partial increments therebetween.

In some embodiments, the dose of a compound described herein is from about 1 mg to about 2,500 mg. In some embodiments, a dose of a compound described herein used in compositions described herein is less than about 10,000 mg, or less than about 8,000 mg, or less than about 6,000 mg, or less than about 5,000 mg, or less than about 3,000 mg, or less than about 2,000 mg, or less than about 1,000 mg, or less than about 500 mg, or less than about 200 mg, or less than about 50 mg. Similarly, in some embodiments, a dose of a second compound as described herein is less than about 1,000 mg, or less than about 800 mg, or less than about 600 mg, or less than about 500 mg, or less than about 400 mg, or less than about 300 mg, or less than about 200 mg, or less than about 100 mg, or less than about 50 mg, or less than about 40 mg, or less than about 30 mg, or less than about 25 mg, or less than about 20 mg, or less than about 15 mg, or less than about 10 mg, or less than about 5 mg, or less than about 2 mg, or less than about 1 mg, or less than about 0.5 mg, and any and all whole or partial increments thereof.

In certain embodiments, a composition as described herein is a packaged pharmaceutical composition comprising a container holding a therapeutically effective amount of a compound described herein, alone or in combination with a second pharmaceutical agent; and instructions for using the compound to treat, prevent, or reduce one or more symptoms of a metabolic disease or disorder in a patient.

Formulations may be employed in admixtures with conventional excipients, *i.e.*, pharmaceutically acceptable organic or inorganic carrier substances suitable for oral, parenteral, nasal, intravenous, subcutaneous, enteral, or any other suitable mode of administration, known to the art. The pharmaceutical preparations may be sterilized and if desired mixed with auxiliary

agents, *e.g.*, lubricants, preservatives, stabilizers, wetting agents, emulsifiers, salts for influencing osmotic pressure buffers, coloring, flavoring, and/or aromatic substances and the like. They may also be combined where desired with other active agents, *e.g.*, other analgesic agents.

Routes of administration of any of the compositions described herein include oral, nasal, rectal, intravaginal, parenteral, buccal, sublingual or topical. The compounds for use in the compositions described herein can be formulated for administration by any suitable route, such as for oral or parenteral, for example, transdermal, transmucosal (*e.g.*, sublingual), lingual, (trans)buccal, (trans)urethral, vaginal (*e.g.*, trans- and perivaginally), (intra)nasal and (trans)rectal), intravesical, intrapulmonary, intraduodenal, intragastrical, intrathecal, subcutaneous, intramuscular, intradermal, intra-arterial, intravenous, intrabronchial, inhalation, and topical administration.

Suitable compositions and dosage forms include, for example, tablets, capsules, caplets, pills, gel caps, troches, dispersions, suspensions, solutions, syrups, granules, beads, transdermal patches, gels, powders, pellets, magmas, lozenges, creams, pastes, plasters, lotions, discs, suppositories, liquid sprays for nasal or oral administration, dry powder or aerosolized formulations for inhalation, compositions and formulations for intravesical administration and the like. It should be understood that the formulations and compositions described herein are not limited to the particular formulations and compositions that are described herein.

Oral Administration

For oral application, particularly suitable are tablets, dragees, liquids, drops, suppositories, or capsules, caplets and gelcaps. The compositions intended for oral use may be prepared according to any method known in the art and such compositions may contain one or more agents selected from the group consisting of inert, non-toxic pharmaceutically excipients that are suitable for the manufacture of tablets. Such excipients include, for example an inert diluent such as lactose; granulating and disintegrating agents such as cornstarch; binding agents such as starch; and lubricating agents such as magnesium stearate. The tablets may be uncoated or they may be coated by known techniques for elegance or to delay the release of the active ingredients. Formulations for oral use may also be presented as hard gelatin capsules wherein the active ingredient is mixed with an inert diluent.

For oral administration, the compound(s) described herein can be in the form of tablets or capsules prepared by conventional means with pharmaceutically acceptable excipients such as binding agents (*e.g.*, polyvinylpyrrolidone, hydroxypropylcellulose or hydroxypropyl methylcellulose); fillers (*e.g.*, cornstarch, lactose, microcrystalline cellulose or calcium phosphate); lubricants (*e.g.*, magnesium stearate, talc, or silica); disintegrates (*e.g.*, sodium starch glycollate); or wetting agents (*e.g.*, sodium lauryl sulphate). If desired, the tablets may be coated using suitable methods and coating materials such as OPADRY™ film coating systems available from Colorcon, West Point, Pa. (*e.g.*, OPADRY™ OY Type, OYC Type, Organic Enteric OY-P Type, Aqueous Enteric OY-A Type, OY-PM Type, and OPADRY™ White, 32K18400). Liquid preparation for oral administration may be in the form of solutions, syrups, or suspensions. The liquid preparations may be prepared by conventional means with pharmaceutically acceptable additives such as suspending agents (*e.g.*, sorbitol syrup, methyl cellulose or hydrogenated edible fats); emulsifying agent (*e.g.*, lecithin or acacia); non-aqueous vehicles (*e.g.*, almond oil, oily esters, or ethyl alcohol); and preservatives (*e.g.*, methyl or propyl p-hydroxy benzoates or sorbic acid).

Compositions as described herein can be prepared, packaged, or sold in a formulation suitable for oral or buccal administration. A tablet that includes a compound as described herein can, for example, be made by compressing or molding the active ingredient, optionally with one or more additional ingredients. Compressed tablets may be prepared by compressing, in a suitable device, the active ingredient in a free-flowing form such as a powder or granular preparation, optionally mixed with one or more of a binder, a lubricant, an excipient, a surface active agent, and a dispersing agent. Molded tablets may be made by molding, in a suitable device, a mixture of the active ingredient, a pharmaceutically acceptable carrier, and at least sufficient liquid to moisten the mixture. Pharmaceutically acceptable excipients used in the manufacture of tablets include, but are not limited to, inert diluents, granulating and disintegrating agents, dispersing agents, surface-active agents, disintegrating agents, binding agents, and lubricating agents.

Suitable dispersing agents include, but are not limited to, potato starch, sodium starch glycollate, poloxamer 407, or poloxamer 188. One or more dispersing agents can each be individually present in the composition in an amount of about 0.01% w/w to about 90% w/w relative to weight of the dosage form. One or more dispersing agents can each be individually

present in the composition in an amount of at least, greater than, or less than about 0.01%, 0.05%, 0.1%, 0.5%, 1%, 2%, 3%, 4%, 5%, 10%, 15%, 20%, 25%, 30%, 35%, 40%, 45%, 50%, 55%, 60%, 65%, 70%, 75%, 80%, 85%, or 90% w/w relative to weight of the dosage form.

Surface-active agents (surfactants) include cationic, anionic, or non-ionic surfactants, or combinations thereof. Suitable surfactants include, but are not limited to, behentrimonium chloride, benzalkonium chloride, benzethonium chloride, benzododecinium bromide, carbethopendecinium bromide, cetalkonium chloride, cetrimonium bromide, cetrimonium chloride, cetylpyridine chloride, didecyldimethylammonium chloride, dimethyldioctadecylammonium bromide, dimethyldioctadecylammonium chloride, domiphen bromide, lauryl methyl gluceth-10 hydroxypropyl dimonium chloride, tetramethylammonium hydroxide, thonzonium bromide, stearalkonium chloride, octenidine dihydrochloride, olaflur, N-oleyl-1,3-propanediamine, 2-acrylamido-2-methylpropane sulfonic acid, alkylbenzene sulfonates, ammonium lauryl sulfate, ammonium perfluorononanoate, docusate, disodium cocoamphodiacetate, magnesium laureth sulfate, perfluorobutanesulfonic acid, perfluorononanoic acid, perfluorooctanesulfonic acid, perfluorooctanoic acid, potassium lauryl sulfate, sodium alkyl sulfate, sodium dodecyl sulfate, sodium laurate, sodium laureth sulfate, sodium lauroyl sarcosinate, sodium myreth sulfate, sodium nonanoyloxybenzenesulfonate, sodium pareth sulfate, sodium stearate, sodium sulfosuccinate esters, cetomacrogol 1000, cetostearyl alcohol, cetyl alcohol, cocamide diethanolamine, cocamide monoethanolamine, decyl glucoside, decyl polyglucose, glycerol monostearate, octylphenoxypolyethoxyethanol CA-630, isoceteth-20, lauryl glucoside, octylphenoxypolyethoxyethanol P-40, Nonoxynol-9, Nonoxynols, nonyl phenoxypolyethoxylethanol (NP-40), octaethylene glycol monododecyl ether, N-octyl beta-D-thioglucopyranoside, octyl glucoside, oleyl alcohol, PEG-10 sunflower glycerides, pentaethylene glycol monododecyl ether, polidocanol, poloxamer, poloxamer 407, polyethoxylated tallow amine, polyglycerol polyricinoleate, polysorbate, polysorbate 20, polysorbate 80, sorbitan, sorbitan monolaurate, sorbitan monostearate, sorbitan tristearate, stearyl alcohol, surfactin, Triton X-100, and Tween 80. One or more surfactants can each be individually present in the composition in an amount of about 0.01% w/w to about 90% w/w relative to weight of the dosage form. One or more surfactants can each be individually present in the composition in an amount of at least, greater than, or less than about 0.01%, 0.05%, 0.1%,

0.5%, 1%, 2%, 3%, 4%, 5%, 10%, 15%, 20%, 25%, 30%, 35%, 40%, 45%, 50%, 55%, 60%, 65%, 70%, 75%, 80%, 85%, or 90% w/w relative to weight of the dosage form.

Suitable diluents include, but are not limited to, calcium carbonate, magnesium carbonate, magnesium oxide, sodium carbonate, lactose, microcrystalline cellulose, calcium phosphate, calcium hydrogen phosphate, and sodium phosphate, Cellactose® 80 (75% α-lactose monohydrate and 25% cellulose powder), mannitol, pre-gelatinized starch, starch, sucrose, sodium chloride, talc, anhydrous lactose, and granulated lactose. One or more diluents can each be individually present in the composition in an amount of about 0.01% w/w to about 90% w/w relative to weight of the dosage form. One or more diluents can each be individually present in the composition in an amount of at least, greater than, or less than about 0.01%, 0.05%, 0.1%, 0.5%, 1%, 2%, 3%, 4%, 5%, 10%, 15%, 20%, 25%, 30%, 35%, 40%, 45%, 50%, 55%, 60%, 65%, 70%, 75%, 80%, 85%, or 90% w/w relative to weight of the dosage form.

Suitable granulating and disintegrating agents include, but are not limited to, sucrose, copovidone, corn starch, microcrystalline cellulose, methyl cellulose, sodium starch glycollate, pregelatinized starch, povidone, sodium carboxy methyl cellulose, sodium alginate, citric acid, croscarmellose sodium, cellulose, carboxymethylcellulose calcium, colloidal silicone dioxide, crosspovidone and alginic acid. One or more granulating or disintegrating agents can each be individually present in the composition in an amount of about 0.01% w/w to about 90% w/w relative to weight of the dosage form. One or more granulating or disintegrating agents can each be individually present in the composition in an amount of at least, greater than, or less than about 0.01%, 0.05%, 0.1%, 0.5%, 1%, 2%, 3%, 4%, 5%, 10%, 15%, 20%, 25%, 30%, 35%, 40%, 45%, 50%, 55%, 60%, 65%, 70%, 75%, 80%, 85%, or 90% w/w relative to weight of the dosage form.

Suitable binding agents include, but are not limited to, gelatin, acacia, pre-gelatinized maize starch, polyvinylpyrrolidone, anhydrous lactose, lactose monohydrate, hydroxypropyl methylcellulose, methylcellulose, povidone, polyacrylamides, sucrose, dextrose, maltose, gelatin, and polyethylene glycol. One or more binding agents can each be individually present in the composition in an amount of about 0.01% w/w to about 90% w/w relative to weight of the dosage form. One or more binding agents can each be individually present in the composition in an amount of at least, greater than, or less than about 0.01%, 0.05%, 0.1%, 0.5%, 1%, 2%, 3%,

4%, 5%, 10%, 15%, 20%, 25%, 30%, 35%, 40%, 45%, 50%, 55%, 60%, 65%, 70%, 75%, 80%, 85%, or 90% w/w relative to weight of the dosage form.

Suitable lubricating agents include, but are not limited to, magnesium stearate, calcium stearate, hydrogenated castor oil, glyceryl monostearate, glyceryl behenate, mineral oil, polyethylene glycol, poloxamer 407, poloxamer 188, sodium laureth sulfate, sodium benzoate, stearic acid, sodium stearyl fumarate, silica, and talc. One or more lubricating agents can each be individually present in the composition in an amount of about 0.01% w/w to about 90% w/w relative to weight of the dosage form. One or more lubricating agents can each be individually present in the composition in an amount of at least, greater than, or less than about 0.01%, 0.05%, 0.1%, 0.5%, 1%, 2%, 3%, 4%, 5%, 10%, 15%, 20%, 25%, 30%, 35%, 40%, 45%, 50%, 55%, 60%, 65%, 70%, 75%, 80%, 85%, or 90% w/w relative to weight of the dosage form.

Tablets can be non-coated or they may be coated using known methods to achieve delayed disintegration in the gastrointestinal tract of a subject, thereby providing sustained release and absorption of the active ingredient. By way of example, a material such as glyceryl monostearate or glyceryl distearate may be used to coat tablets. Further by way of example, tablets may be coated using methods described in U.S. Patent Nos. 4,256,108; 4,160,452; and 4,265,874 to form osmotically controlled release tablets. Tablets may further comprise a sweetening agent, a flavoring agent, a coloring agent, a preservative, or some combination of these in order to provide for pharmaceutically elegant and palatable preparation.

Tablets can also be enterically coated such that the coating begins to dissolve at a certain pH, such as at about pH 5.0 to about pH 7.5, thereby releasing a compound as described herein. The coating can contain, for example, EUDRAGIT® L, S, FS, and/or E polymers with acidic or alkaline groups to allow release of a compound as described herein in a particular location, including in any desired section(s) of the intestine. The coating can also contain, for example, EUDRAGIT® RL and/or RS polymers with cationic or neutral groups to allow for time-controlled release of a compound as described herein by pH-independent swelling.

Parenteral Administration

For parenteral administration, the compounds as described herein may be formulated for injection or infusion, for example, intravenous, intramuscular or subcutaneous injection or infusion, or for administration in a bolus dose and/or continuous infusion. Suspensions,

solutions, or emulsions in an oily or aqueous vehicle, optionally containing other formulatory agents such as suspending, stabilizing, and/or dispersing agents, may be used.

Sterile injectable forms of the compositions described herein may be aqueous or oleaginous suspensions. These suspensions may be formulated according to techniques known in the art using suitable dispersing or wetting agents and suspending agents. The sterile injectable preparation may also be a sterile injectable solution or suspension in a nontoxic, parenterally-acceptable diluent or solvent, for example as a solution in 1, 3-butanediol. Among the acceptable vehicles and solvents that may be employed are water, Ringer's solution, and isotonic sodium chloride solution. Sterile, fixed oils are conventionally employed as a solvent or suspending medium. For this purpose, any bland fixed oil may be employed including synthetic mono- or di-glycerides. Fatty acids, such as oleic acid and its glyceride derivatives are useful in the preparation of injectables, as are natural pharmaceutically acceptable oils, such as olive oil or castor oil, especially in their polyoxyethylated versions. These oil solutions or suspensions may also contain a long-chain alcohol diluent or dispersant, such as such as lauryl, stearyl, or oleyl alcohols, or similar alcohol.

Additional Administration Forms

Additional dosage forms suitable for use with the compound(s) and compositions described herein include dosage forms as described in U.S. Patents Nos. 6,340,475; 6,488,962; 6,451,808; 5,972,389; 5,582,837; and 5,007,790. Additional dosage forms suitable for use with the compound(s) and compositions described herein also include dosage forms as described in U.S. Patent Applications Nos. 20030147952; 20030104062; 20030104053; 20030044466; 20030039688; and 20020051820. Additional dosage forms suitable for use with the compound(s) and compositions described herein also include dosage forms as described in PCT Applications Nos. WO 03/35041; WO 03/35040; WO 03/35029; WO 03/35177; WO 03/35039; WO 02/96404; WO 02/32416; WO 01/97783; WO 01/56544; WO 01/32217; WO 98/55107; WO 98/11879; WO 97/47285; WO 93/18755; and WO 90/11757.

Controlled Release Formulations and Drug Delivery Systems

In certain embodiments, the formulations described herein can be, but are not limited to, short-term, rapid-offset, as well as controlled, for example, sustained release, delayed release, and pulsatile release formulations.

The term “sustained release” is used in its conventional sense to refer to a drug formulation that provides for gradual release of a drug over an extended period of time, and that may, although not necessarily, result in substantially constant blood levels of a drug over an extended time period. The period of time may be as long as a month or more and should be a release which is longer that the same amount of agent administered in bolus form.

For sustained release, the compounds may be formulated with a suitable polymer or hydrophobic material which provides sustained release properties to the compounds. As such, the compounds for use with the method(s) described herein may be administered in the form of microparticles, for example, by injection or in the form of wafers or discs by implantation.

In some cases, the dosage forms to be used can be provided as slow or controlled-release of one or more active ingredients therein using, for example, hydropropylmethyl cellulose, other polymer matrices, gels, permeable membranes, osmotic systems, multilayer coatings, microparticles, liposomes, or microspheres or a combination thereof to provide the desired release profile in varying proportions. Suitable controlled-release formulations known to those of ordinary skill in the art, including those described herein, can be readily selected for use with the pharmaceutical compositions described herein. Thus, single unit dosage forms suitable for oral administration, such as tablets, capsules, gelcaps, and caplets, that are adapted for controlled-release are encompassed by the compositions and dosage forms described herein.

Most controlled-release pharmaceutical products have a common goal of improving drug therapy over that achieved by their non-controlled counterparts. Ideally, the use of an optimally designed controlled-release preparation in medical treatment is characterized by a minimum of drug substance being employed to cure or control the condition in a minimum amount of time. Advantages of controlled-release formulations include extended activity of the drug, reduced dosage frequency, and increased patient compliance. In addition, controlled-release formulations can be used to affect the time of onset of action or other characteristics, such as blood level of the drug, and thus can affect the occurrence of side effects.

Most controlled-release formulations are designed to initially release an amount of drug that promptly produces the desired therapeutic effect, and gradually and continually release of other amounts of drug to maintain this level of therapeutic effect over an extended period of time. In order to maintain this constant level of drug in the body, the drug must be released from

the dosage form at a rate that will replace the amount of drug being metabolized and excreted from the body.

Controlled-release of an active ingredient can be stimulated by various inducers, for example pH, temperature, enzymes, water, or other physiological conditions or compounds. The term "controlled-release component" is defined herein as a compound or compounds, including, but not limited to, polymers, polymer matrices, gels, permeable membranes, liposomes, or microspheres or a combination thereof that facilitates the controlled-release of the active ingredient. In certain embodiments, the compound(s) described herein are administered to a patient, alone or in combination with another pharmaceutical agent, using a sustained release formulation.

The term “delayed release” is used herein in its conventional sense to refer to a drug formulation that provides for an initial release of the drug after some delay following drug administration and that mat, although not necessarily, includes a delay of from about 10 minutes up to about 12 hours.

The term “pulsatile release” is used herein in its conventional sense to refer to a drug formulation that provides release of the drug in such a way as to produce pulsed plasma profiles of the drug after drug administration.

The term “immediate release” is used in its conventional sense to refer to a drug formulation that provides for release of the drug immediately after drug administration.

As used herein, short-term refers to any period of time up to and including about 8 hours, about 7 hours, about 6 hours, about 5 hours, about 4 hours, about 3 hours, about 2 hours, about 1 hour, about 40 minutes, about 20 minutes, or about 10 minutes and any or all whole or partial increments thereof after drug administration.

As used herein, rapid-offset refers to any period of time up to and including about 8 hours, about 7 hours, about 6 hours, about 5 hours, about 4 hours, about 3 hours, about 2 hours, about 1 hour, about 40 minutes, about 20 minutes, or about 10 minutes, and any and all whole or partial increments thereof after drug administration.

Dosing

The therapeutically effective amount or dose of a compound described herein depends on the age, sex, and weight of the patient, the current medical condition of the patient, and the

progression of a metabolic disease or disorder in the patient being treated. The skilled artisan is able to determine appropriate dosages depending on these and other factors.

A suitable dose of a compound described herein can be in the range of from about 0.01 mg to about 5,000 mg per day, such as from about 0.1 mg to about 1,000 mg, for example, from about 1 mg to about 500 mg, such as about 5 mg to about 250 mg per day. The dose may be administered in a single dosage or in multiple dosages, for example from 1 to 4 or more times per day. When multiple dosages are used, the amount of each dosage may be the same or different. For example, a dose of 1 mg per day may be administered as two 0.5 mg doses, with about a 12-hour interval between doses.

It is understood that the amount of compound dosed per day may be administered, in non-limiting examples, every day, every other day, every 2 days, every 3 days, every 4 days, or every 5 days. For example, with every other day administration, a 5 mg per day dose may be initiated on Monday with a first subsequent 5 mg per day dose administered on Wednesday, a second subsequent 5 mg per day dose administered on Friday, and so on.

In the case wherein the patient's status does improve, upon the doctor's discretion the administration of the compound(s) described herein is optionally given continuously; alternatively, the dose of drug being administered is temporarily reduced or temporarily suspended for a certain length of time (*i.e.*, a “drug holiday”). The length of the drug holiday optionally varies between 2 days and 1 year, including by way of example only, 2 days, 3 days, 4 days, 5 days, 6 days, 7 days, 10 days, 12 days, 15 days, 20 days, 28 days, 35 days, 50 days, 70 days, 100 days, 120 days, 150 days, 180 days, 200 days, 250 days, 280 days, 300 days, 320 days, 350 days, or 365 days. The dose reduction during a drug holiday includes from 10%-100%, including, by way of example only, 10%, 15%, 20%, 25%, 30%, 35%, 40%, 45%, 50%, 55%, 60%, 65%, 70%, 75%, 80%, 85%, 90%, 95%, or 100%.

Once improvement of the patient's conditions has occurred, a maintenance dosage is administered if necessary. Subsequently, the dosage or the frequency of administration, or both, is reduced to a level at which the improved disease is retained. In certain embodiments, patients require intermittent treatment on a long-term basis upon any recurrence of symptoms and/or infection.

The compounds described herein can be formulated in unit dosage form. The term “unit dosage form” refers to physically discrete units suitable as unitary dosage for patients

undergoing treatment, with each unit containing a predetermined quantity of active material calculated to produce the desired therapeutic effect, optionally in association with a suitable pharmaceutical carrier. The unit dosage form may be for a single daily dose or one of multiple daily doses (*e.g.*, about 1 to 4 or more times per day). When multiple daily doses are used, the unit dosage form may be the same or different for each dose.

Toxicity and therapeutic efficacy of such therapeutic regimens are optionally determined in cell cultures or experimental animals, including, but not limited to, the determination of the LD_{50} (the dose lethal to 50% of the population) and the ED_{50} (the dose therapeutically effective in 50% of the population). The dose ratio between the toxic and therapeutic effects is the therapeutic index, which is expressed as the ratio between LD_{50} and ED_{50}. The data obtained from cell culture assays and animal studies are optionally used in formulating a range of dosage for use in humans. The dosage of such compounds lies preferably within a range of circulating concentrations that include the ED_{50} with minimal toxicity. The dosage optionally varies within this range depending upon the dosage form employed and the route of administration utilized.

Examples

Various embodiments of the present application can be better understood by reference to the following Examples which are offered by way of illustration. The scope of the present application is not limited to the Examples given herein.

Methods

Peptide Syntheses and Purification

Solid-Phase Peptide Synthesis was performed on ProTide Rink amide resin using a microwave-assisted CEM Liberty Blue peptide synthesizer (Matthews, NC). Fmoc-protected amino acids were coupled to the resin using Oxyma Pure (0.25 M) and N, N'-diisopropylcarbodiimide (0.125 M) as the activator and activator base, respectively. Fmoc was removed between couplings with 20% Piperidine. Global deprotection and cleavage of the peptides from the solid-support resin was achieved using a CEM Razor instrument over a 40-minute incubation period at 40°C in a mixture of 95% TFA, 2.5% TIPS, and 2.5% water. Peptides were purified on an Agilent 1200 series High-Performance Liquid Chromatography

(HPLC) instrument (10-75% HPLC-grade acetonitrile for 20 minutes at 2 mL/min flow rate using an Agilent Zorbax C18 column (5µm, 9.4 x 250 mm) tracked at 280 nm. Peptides were purified to >95%.

Competitive Binding Assay at GLP-1R

KSCEM01 binding at the human GLP-1R was measured via a Nicoya Open SPR instrument in-house using His-tagged hGLP-1R bound to an NTA sensor. The Ex-4 was run in a duplicate, dose response manner (0.1 nM-150 nM) and the KSCEM01 was ran once in a dose-response manner (0.1 nM-150 nM).

***In vitro* Receptor Agonism at hGLP-1R**

H188 virally transduced HEK293 cells stably expressing human GLP-1R were obtained from Novo Nordisk A/S for use in FRET assays. HEK293 C24 cells stably expressing the H188 FRET reporter were obtained by G418 selection and grown in monolayers to ~70% confluency in 100 cm^2 tissue culture dishes and were then transfected with plasmids (11 µg/dish) encoding human GLP-1R. Transfected cells were then incubated for 48 h in fresh culture media. For real-time FRET kinetic assays, cells were harvested, resuspended in 21 mL of SES buffer, and plated at 196 µL per well. Plated cells were pretreated with 4 µL of agonist at a given target concentration and incubated for 20 min before performing the assay. For these assays, increased levels of cAMP were measured as an increase of the 485/535 nm FRET ratio serving as a readout for binding of cAMP to the H188 biosensor that is based on the exchange protein activated by cAMP.

Dose Escalation Experiment

Referring to FIG. 5, male Sprague Dawley rats (n=4) were fed a 60% HF diet for 48 weeks before the start of the study. Rats were then housed singly and allowed to acclimate to their new environment for 10 days. A dose escalation study was performed consisting of three days of baseline measures, followed by KSCEM01 administered via subcutaneous injection at 2 nmol/kg/day for 3 days, 5 nmol/kg/day for 3 days, and 10 nmol/kg/day for 3 days; treatments were administered 30 minutes prior to the start of the dark cycle. Rats averaged 947 ± 145 g at the start of treatment. Food intake was recorded daily by hopper weighs, and body weight was

measured daily immediately before the start of the dark cycle. KSCEM01 treatment resulted in a 54.7% reduction in food intake at 2 nmol/kg/day, a 64.8% reduction in food intake at 5 nmol/kg/day, and a 62.9% reduction in food intake at 10 nmol/kg/day.

11-Day Treatment Experiment at Single Dose

Referring to FIG. 6, male Sprague Dawley rats (n=4) were fed a 60% HF diet for 48 weeks before the start of the study. Rats were then housed singly and allowed to acclimate to their new environment for 10 days. Baseline measures of body weight and food intake were collected for five days, and rats averaged 969 ± 227 g at start of treatment. KSCEM01 was administered via subcutaneous injection just prior to the start of the dark cycle at 10 nmol/kg/day for eleven days. Food intake was recorded daily by hopper weighs, and body weight was measured daily immediately before the start of the dark cycle. Eleven-day KSCEM01 treatment at 10 nmol/kg/day resulted in a 5.4% reduction in body weight and an average 40.9% reduction in food intake.

16-Day Treatment Experiment with Increasing Doses

Referring to FIGs. 7A-7C, male Wistar rats (n=5) were fed a 60% HF diet for 40 weeks before the start of the study. Rats were then housed singly in BioDAQ cages and allowed to acclimate to their new environment for 10 days. Baseline measures of body weight and food intake were collected for four days, and rats averaged 850 ± 41 g at start of treatment. KSCEM01 was administered via subcutaneous injection just prior to the start of the dark cycle on the following dosing schedule: 5 nmol/kg/day for 4 days, 10 nmol/kg/day for 4 days, and 25 nmol/kg/day for 8 days. Food intake was monitored continuously throughout the experiment. Body weights were measured daily immediately before the start of the dark cycle. Outcomes for Liraglutide and vehicle treated groups from a prior experiment using the same study design were included for reference. At the start of treatment, rats treated with Liraglutide weighed 658 ± 68 g and rats treated with vehicle weighed 661 ± 96 g; animals from both groups were on 60% HF diet for 20 weeks before the start of the study. Sixteen-day KSCEM01 treatment resulted in a 4.7% reduction in body weight relative to pre-treatment.

The terms and expressions employed herein are used as terms of description and not of limitation, and there is no intention in the use of such terms and expressions of excluding any equivalents of the features shown and described or portions thereof, but it is recognized that various modifications are possible within the scope of the embodiments of the present application. Thus, it should be understood that although the present application describes specific embodiments and optional features, modification and variation of the compositions, methods, and concepts herein disclosed may be resorted to by those of ordinary skill in the art, and that such modifications and variations are considered to be within the scope of embodiments of the present application.

CLAIMS

What is claimed is:

1. A dual melanocortin receptor (MCR) and glucagon like peptide (GLP-1) agonist peptide, or a pharmaceutically acceptable salt thereof, comprising the amino acid sequence: X1-X2-X3-X4-X5-X6-X7-X8-X9-X10-X11-X12-X13-X14-X15-X16-X17-X18-X19-X20-X21-X22-X23-X24-X25-X26-X27-X28-X29-X30-X31-X32-X33-X34-X35-X36-X37-X38-X39-X40-X41-X42-X43-X44-X45-X46-X46-X47-X48-X49-X50-X51-X52-X53-X54-X55-X56-X57-X58-X59-X60-NH_2 (SEQ ID NO. 1),

wherein the residues X1-X60 are as defined in Table 1.

2. The peptide of claim 1, wherein the sequence is at least 80, 85, 90, 95, 96, 97, 98, or 99% homologous to a peptide of SEQ ID NO. 2.

3. The peptide of claim 1, wherein residues X51-X60 are absent.

4. The peptide of claim 1, having a sequence selected from the group consisting of SEQ ID NO. 2, SEQ ID NO. 3, SEQ ID NO. 4, SEQ ID NO. 5, and SEQ ID NO. 6.

5. The peptide of claim 4, wherein the peptide has the sequence of SEQ ID NO. 2.

6. The peptide of claim 1, wherein X12 and X27 are each independently selected from the group consisting of K, k, α-methyl-Lys, K*, and K^a,

wherein K* has the structure:

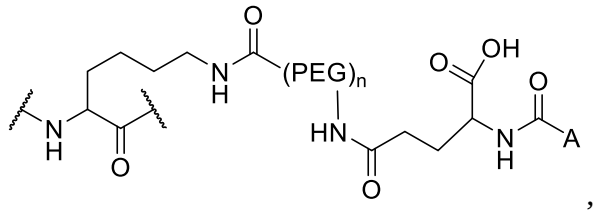

,

wherein:

n is an integer from 1 to 12;

PEG is a moiety comprising one or more ethylene glycol units; and

A is a linear or branched C_{4-18} alkyl, linear or branched C_{4-18} alkenyl, or linear or branched C_{4-18} alkynyl; and

wherein K^a has the structure:

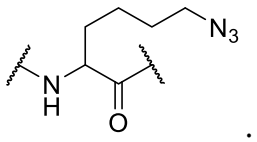

.

7. A pharmaceutical composition comprising the peptide of any one of claims 1-6 and at least one pharmaceutically acceptable carrier or excipient.

8. A method of treating, preventing, and/or ameliorating a metabolic condition in the subject, the method comprising:

administering to the subject a therapeutically effective amount of the peptide of any one of claims 1-7.

9. The method of claim 8, wherein the metabolic condition is selected from the group consisting of type 2 diabetes, obesity, nonalcoholic fatty liver disease, hypothalamic obesity, prediabetes, and nonalcoholic steatohepatitis.

10. The method of claim 10, wherein the peptide is selected from the group consisting of SEQ ID NO. 2, SEQ ID NO. 3, SEQ ID NO. 4, SEQ ID NO. 5, and SEQ ID NO. 6.

11. The method of claim 10, wherein the peptide has the sequence of SEQ ID NO: 2.

12. The method of claim 8, wherein the administration is by a route selected from the group consisting of oral, transdermal, transmucosal, intrapulmonary, intraduodenal, intragastrical, intrathecal, subcutaneous, intramuscular, intradermal, intra-arterial, intravenous, intrabronchial, inhalation, and topical administration.

13. The method of claim 8, wherein the subject is a mammal.

14. The method of claim 13, wherein the mammal is a human.

ABSTRACT OF THE DISCLOSURE

Provided herein are chimeric dual-agonist peptides having agonistic function at both GLP-1 (glucagon-like peptide) and MCR (melanocortin) receptors.

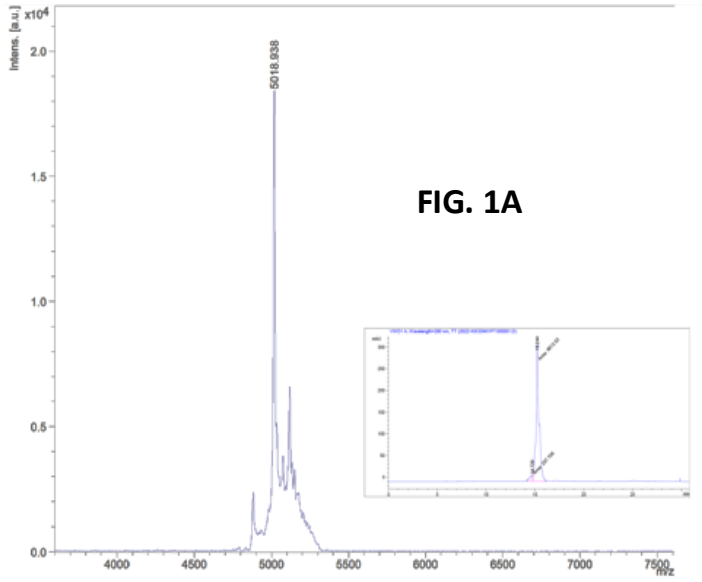

FIG. 1A

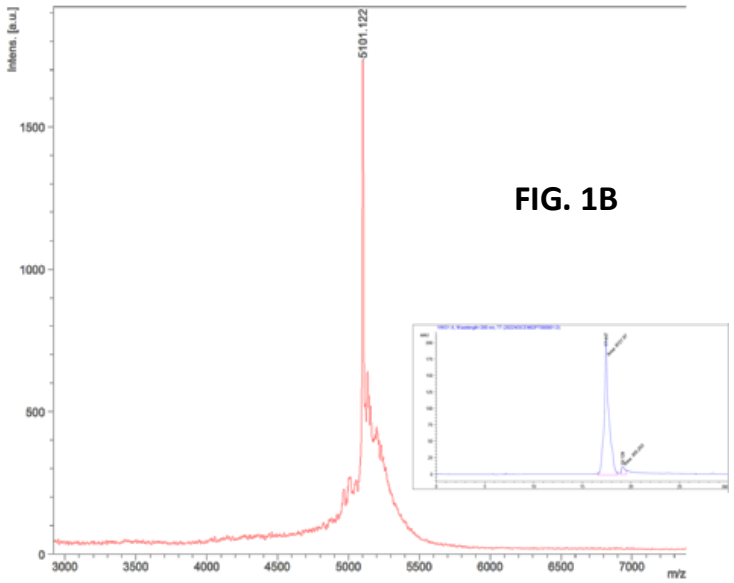

FIG. 1B

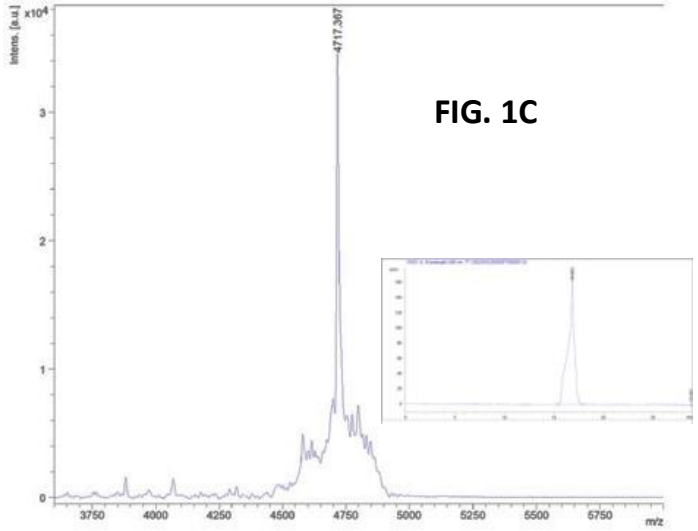

FIG. 1C

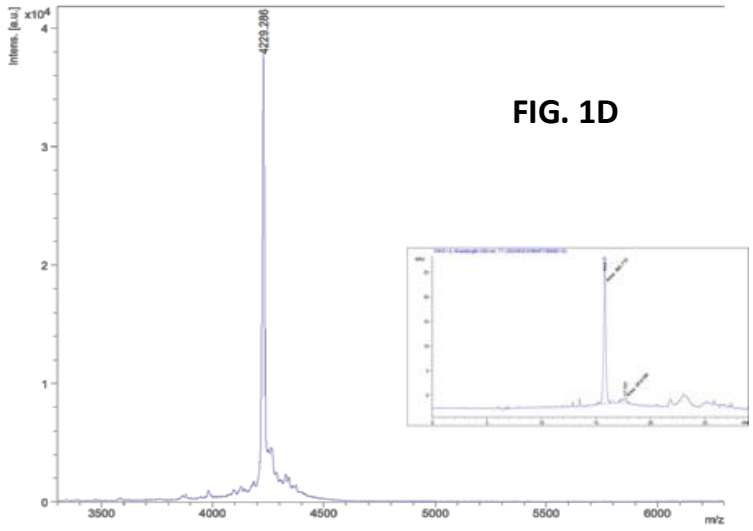

FIG. 1D

FIG. 2

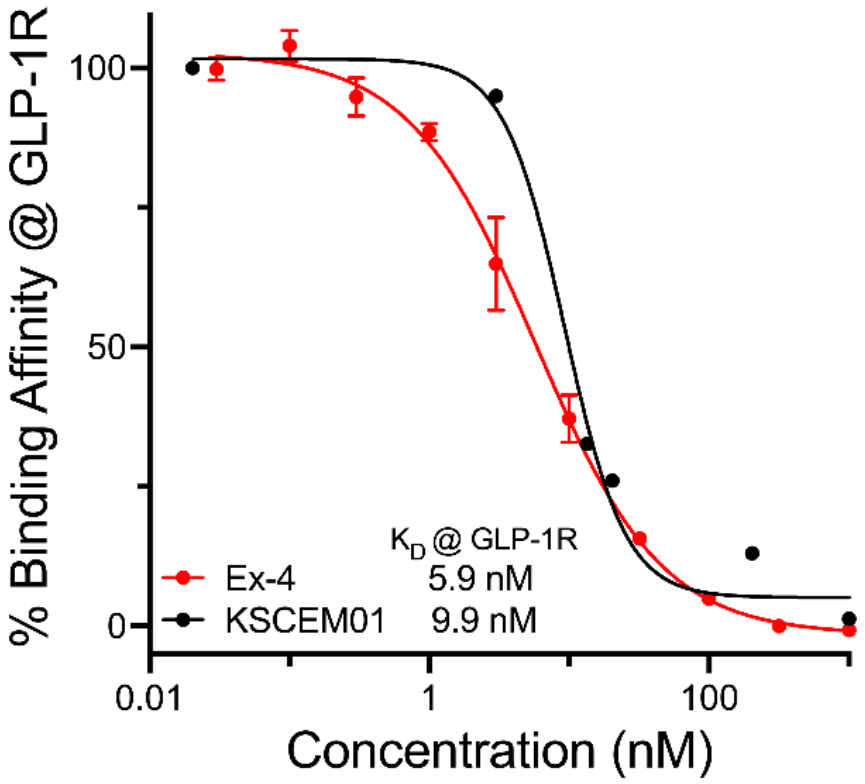
% Binding Affinity @ GLP-1R
100
50
0
0.01
1
100
Concentration (nM)
K_D @ GLP-1R
Ex-4 5.9 nM
KSCEM01 9.9 nM

FIG. 3

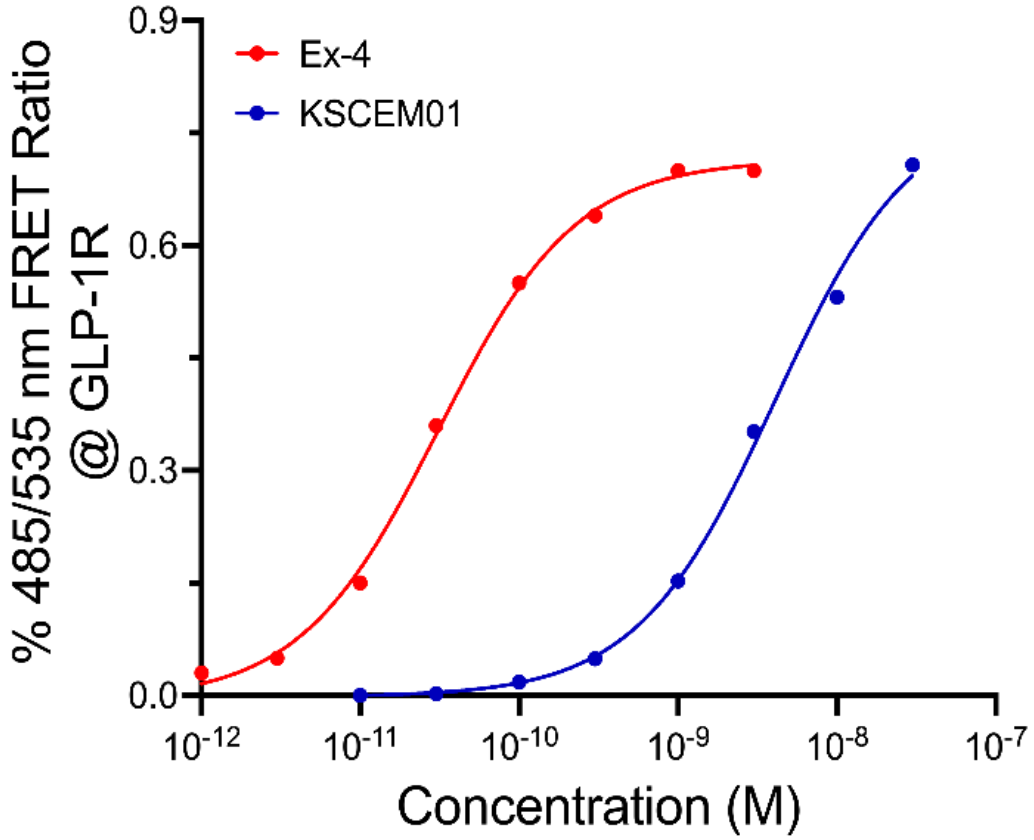
0.9
0.6
0.3
0.0
% 485/535 nm FRET Ratio @ GLP-1R
Ex-4
KSCEM01
10-12
10-11
10-10
10-9
10-8
10-7
Concentration (M)

FIG. 4

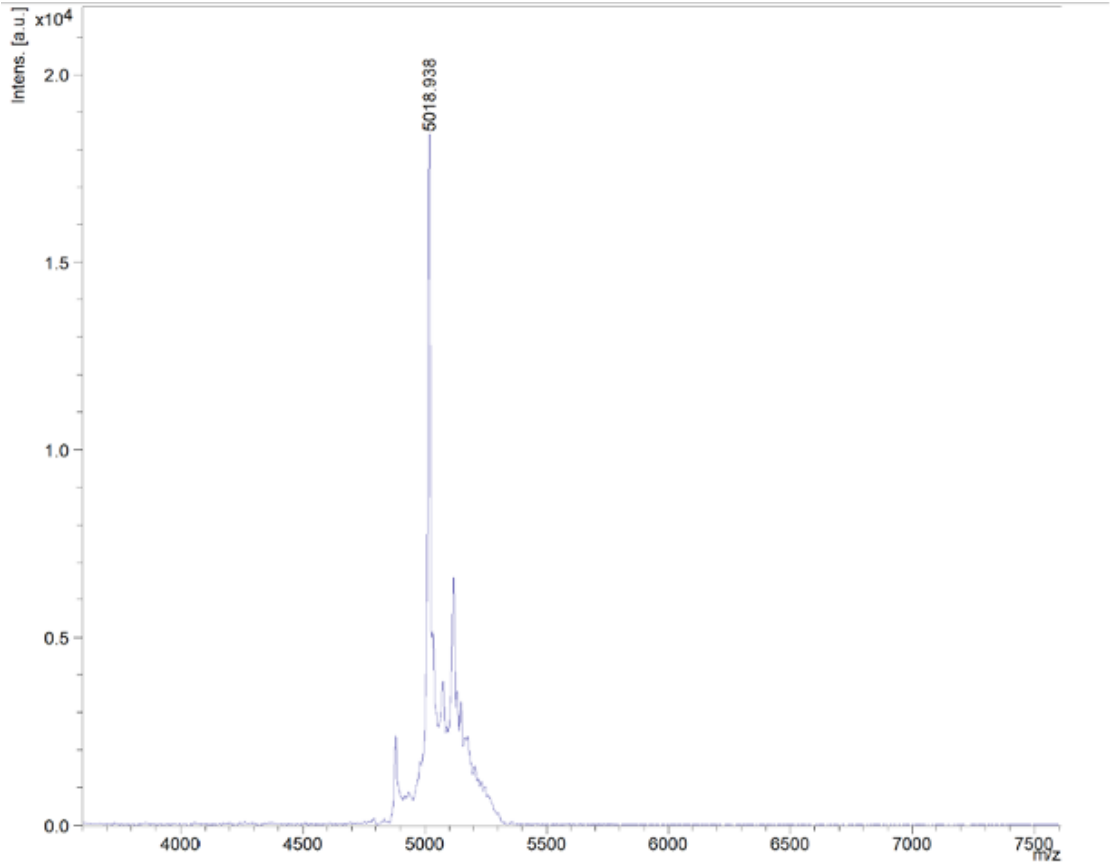
Intens. [a.u.]
x10^4
2.0
1.5
1.0
0.5
0.0
5018.938
4000
4500
5000
5500
6000
6500
7000
7500
m/z

FIG. 5

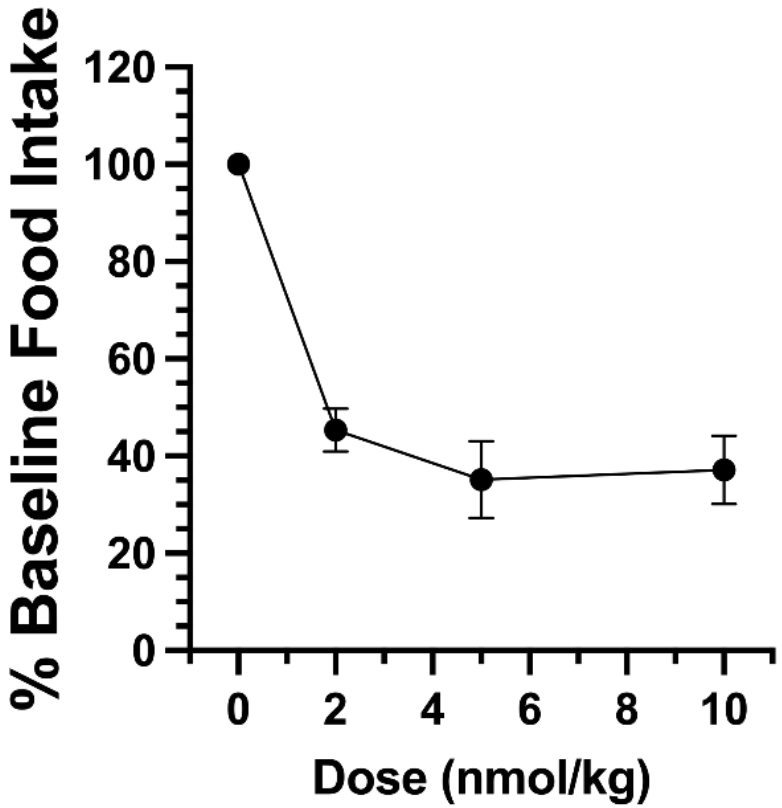
% Baseline Food Intake
120
100
80
60
40
20
0
0
2
4
6
8
10
Dose (nmol/kg)

FIG. 6

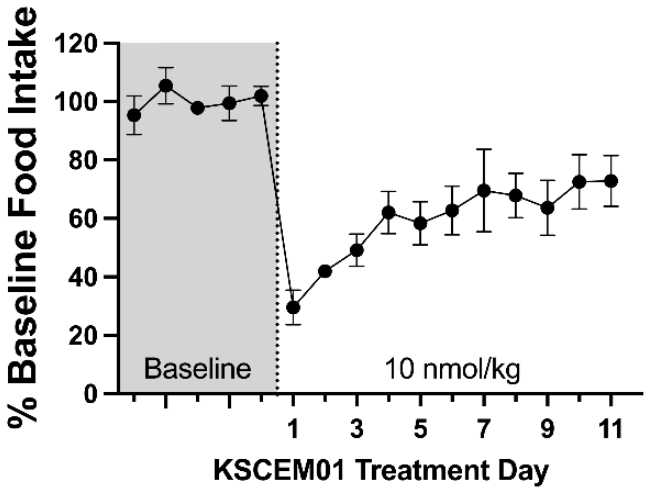
% Baseline Food Intake
120
100
80
60
40
20
0
Baseline
10 nmol/kg
1
3
5
7
9
11
KSCEM01 Treatment Day

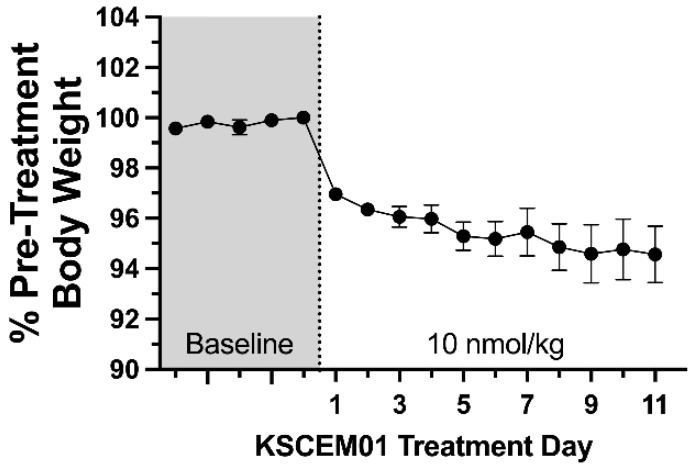
% Pre-Treatment Body Weight
104
102
100
98
96
94
92
90
Baseline
10 nmol/kg
1
3
5
7
9
11
KSCEM01 Treatment Day

FIGs. 7A-7C

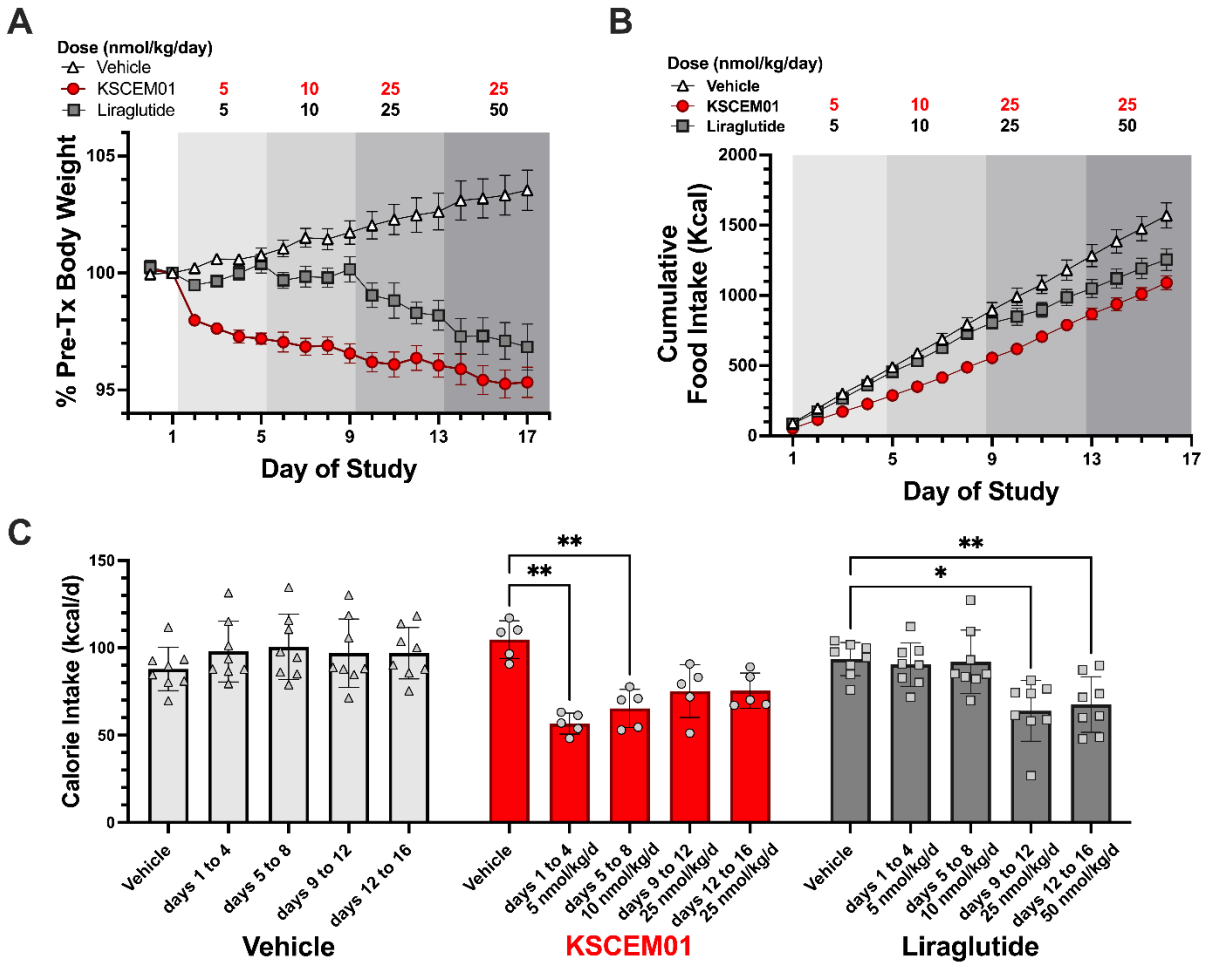
A
Dose (nmol/kg/day)
Vehicle
KSCEM01 5 10 25 25
Liraglutide 5 10 25 50
% Pre-Tx Body Weight
105
100
95
1
5
9
13
17
Day of Study
B
Dose (nmol/kg/day)
Vehicle
KSCEM01 5 10 25 25
Liraglutide 5 10 25 50
Cumulative Food Intake (Kcal)
2000
1500
1000
500
0
1
5
9
13
17
Day of Study
C
Calorie Intake (kcal/d)
150
100
50
0
**
**
**
*
Vehicle
days 1 to 4
days 5 to 8
days 9 to 12
days 12 to 16
Vehicle
days 1 to 4 5 nmol/kg/d
days 5 to 8 10 nmol/kg/d
days 9 to 12 25 nmol/kg/d
days 12 to 16 25 nmol/kg/d
Vehicle
days 1 to 4 5 nmol/kg/d
days 5 to 8 10 nmol/kg/d
days 9 to 12 25 nmol/kg/d
days 12 to 16 50 nmol/kg/d
Vehicle
KSCEM01
Liraglutide

Compositions and Methods for Controlling Food Intake, Energy Expenditure, and Body Weight for the Treatment of Obesity and Metabolic Diseases

By

Matthew R. Hayes

Robert P. Doyle

Caroline Geisler

Kylie S. Chichura

Incorporation-by-Reference of Material Submitted in Electronic Form

Incorporated herein by reference in its entirety is the sequence listing submitted via EFS-Web as a text file named SEQLIST.txt, created November 15, 2021, and having a size of 9,020 bytes.

Field of the Invention

The present invention relates to the fields of weight loss, weight maintenance, and obesity and metabolic disease treatments. More specifically, the invention provides peptide sequences and variants thereof capable of inhibiting G-Protein Receptor 75 (GPR75).

Background of the Invention

Several publications and patent documents are cited throughout the specification in order to describe the state of the art to which this invention pertains. Each of these citations is incorporated by reference herein as though set forth in full.

Obesity and its cardio-metabolic complications, particularly type 2 diabetes and coronary artery disease, account for significant morbidity and mortality globally. There is a substantial unmet medical need for safe and effective weight loss approaches and maintenance of the weight reduced state.

Lifestyle interventions on diet and physical activity are the first option for the management of obesity, but efficacy can be limited, and weight regain is common. Bariatric surgery can be highly effective for weight loss in severely obese or high-risk patients, but its use is limited by its invasive nature, cost, and risk of perioperative adverse events including perioperative death. While a few drugs have demonstrated efficacy in weight-reduction,

pharmacotherapy for the treatment of obesity is limited by the modest weight loss induced by most drugs, development of dependency, side effect profiles, contraindications, low compliance, and barriers to treatment including underprescription.

G-Protein Receptor 75 (GPR75) is a member of the G protein-coupled receptor family. GPRs are cell surface receptors that activate guanine-nucleotide binding proteins upon the binding of a ligand. GPR75 is likely coupled to heterotrimeric Gq proteins and stimulates inositol trisphosphate production and calcium mobilization upon activation. Various experiments have shown a strong association of GPR75 with obesity and metabolic diseases; however, no known molecules exist that antagonize GPR75. Clearly, GPR75 inhibitors for the treatment of obesity and metabolic diseases are urgently needed.

Summary of the Invention

In accordance with present invention, isolated or purified peptides having the amino acid sequence of SEQ ID NO: 1 or SEQ ID NO: 2 or a functional sequence having at least 95% identity thereto are provided. The peptides have anti-obesity activity and can be used for the treatment of weight management.

In a preferred embodiment, the peptides are delivered in a pharmaceutically acceptable carrier. In another aspect, isolated nucleic acids encoding amino acid sequences of SEQ ID NOS: 1 and SEQ ID NO: 2 are also disclosed. In other aspects the isolated nucleic is present in a vector for robust expression and production in an organism of interest. Administration can be via any suitable route, e.g., systemic, intramuscular, topical, oral, parenteral, transdermal patch, aerosolized, pulmonary, ophthalmic, buccal, and lingually.

In yet another embodiment, a method of treating obesity in a subject in need thereof comprising administering an effective amount of the peptides described above is disclosed. Also provided is a method of treating a metabolic disease or disorder in a subject in need thereof, the method comprising administering an effective amount of the peptide of SEQ ID NO: 1 or SEQ ID NO: 2. Metabolic diseases or disorders to be treated include, without limitation, obesity, diabetes mellitus, dyslipidemia, insulin resistance, hepatic steatosis, hypercholesterolemia, and non-alcoholic fatty liver. In certain aspects, the diabetes mellitus is selected from type 1 or type 2 diabetes. In other aspects, the method can further comprise administering a second therapeutic

agent that treats or inhibits obesity. In preferred embodiments, the weight of the patient decreases following administration of the peptide.

In another aspect, the method can further comprise assessing the patient for a reduction in obesity symptoms.

Brief Description of the Drawings

Fig. 1A -1B: Confirmation of synthesis and purity of peptides. (Fig. 1A) SU75-36 (4894.1 g/mol; 17.084 min T_R; 100% purity, (Fig. 1B) SU75-37 (4462.9 g/mol; 15.381 min T_R; 98.3% purity).

Fig. 2: Blind SU75-36/GPR75 receptor in silico docking using HPEPDOCK. SU75-36 (aqua marine; see arrow) surface binding of GPR75 consistent with SPR binding (Figure 3). Docking score 0.884.

Fig. 3: Surface Plasmon Resonance (SPR) assays tracking SU75-36 binding at GPR75. SU75-36 binds to GPR75 with a K_D of 7.76 µM.

Fig. 4: Surface Plasmon Resonance (SPR) assays tracking SU75-37 binding at GPR75. SU75-37 binds to GPR75 with a K_D of 23.8 µM.

Fig. 5: Surface Plasmon Resonance (SPR) assays comparing SU75-36 binding at hGLP-1R with positive Ex-4 control, negative ODN control, and SU75-37. SU75-37 does not bind at the hGLP-1R.

Fig. 6: Surface Plasmon Resonance (SPR) assays tracking SU75-36 binding at hGLP-1R. SU75-36 binds to hGLP-1R with a K_D of 182 µM.

Fig. 7A-7B: 4th Ventricle GPR75 Ligands Suppress Food Intake and Body Weight in HFD Rats. Effect of 4th ventricle SU75-36 (20, 100, or 200 µg/2 µL in aCSF) and SU75-37 (20 µg/2 µL in aCSF) treatment on 24h food intake (Fig. 7A) and body weight change (Fig. 7B) in HFD fed rats. All data presented as mean ± SEM.

Fig. 8A-8F: Lateral Ventricle GPR75 Ligands injection suppresses food intake and body weight in Chow and HFD Rats. Effect of lateral ventricle SU75-36 (20 or 100 µg/2µL in aCSF) or SU75-37 (20 µg/2µL in aCSF) treatment on 24h food intake in chow (Fig. 8A) and HFD fed rats (Fig. 8B), kaolin intake in chow (Fig. 8C) and HFD fed rats (Fig. 8D) and body weight change in chow (Fig. 8E) and HFD fed rats (Fig. 8F). All data presented as mean ± SEM.

Fig. 9: Secondary structure analysis of SU75-36 and SU75-37 by CD Spectroscopy at 40 µM in 0.5% saline. Percent helicity was determined to be 20.9% and 21.3% for SU75-36 and SU75-37, respectively.

Detailed Description of the Invention

As demonstrated herein, we provide novel, non-naturally occurring peptide ligands that antagonize the highly sought-after orphan receptor GPR75. These GPR75 inhibitors represent a major drug discovery in the pharmaceutical industry given the association of GPR 75 with obesity and metabolic diseases.

Definitions

Unless otherwise defined herein, scientific and technical terms used in connection with the present application shall have the meanings that are commonly understood by those of ordinary skill in the art. In addition to definitions included in this sub-section, further definitions of terms are interspersed throughout the text.

In this invention, “a”, “or” and “an” can mean “at least one” or “one or more,“ etc., unless clearly indicated otherwise by context. The term “or” means “and/or” unless stated otherwise. In the case of a multiple-dependent claim, however, use of the term “or” refers back to more than one preceding claim in the alternative only.

Furthermore, a compound “selected from the group consisting of” refers to one or more of the compounds in the list that follows, including mixtures (i.e. combinations) of two or more of the compounds. According to the present invention, an isolated, or biologically pure molecule is a compound that has been removed from its natural milieu. As such, "isolated" and "biologically pure" do not necessarily reflect the extent to which the compound has been purified. An isolated compound of the present invention can be obtained from its natural source,

can be produced using laboratory synthetic techniques or can be produced by any such chemical synthetic route.

The terms “agent”, and “test compound” denote a chemical compound, a mixture of chemical compounds, a biological macromolecule, or an extract made from biological materials such as bacteria, plants, fungi, or animal (particularly mammalian) cells or tissues. Biological macromolecules include peptides, peptide/DNA complexes, siRNA, shRNA, antisense oligonucleotides, and any nucleic acid-based molecule which encoded the proteins described herein.

It is also contemplated that the term “compound” or “compounds” refers to the compounds discussed herein and includes precursors and derivatives of the compounds, and pharmaceutically acceptable salts of the compounds, precursors, and derivatives.

The phrase "consisting essentially of" when referring to a particular nucleotide or amino acid means a sequence having the properties of a given SEQ ID NO. For example, when used in reference to an amino acid sequence, the phrase includes the sequence per se and molecular modifications that would not affect the functional and novel characteristics of the sequence.

A “derivative” of a polypeptide, polynucleotide or fragments thereof means a sequence modified by varying the sequence of the construct, e.g., by manipulation of the nucleic acid encoding the protein or by altering the protein itself. “Derivatives” of a gene or nucleotide sequence refers to any isolated nucleic acid molecule that contains significant sequence similarity to the gene or nucleotide sequence or a part thereof. In addition, "derivatives" include such isolated nucleic acids containing modified nucleotides or mimetics of naturally-occurring nucleotides.

The term “functional” as used herein implies that the nucleic or amino acid sequence is functional for the recited assay or purpose.

For purposes of the invention, “nucleic acid”, “nucleotide sequence” or a “nucleic acid molecule” as used herein refers to any DNA or RNA molecule, either single or double stranded and, if single stranded, the molecule of its complementary sequence in either linear or circular form. In discussing nucleic acid molecules, a sequence or structure of a particular nucleic acid molecule may be described herein according to the normal convention of providing the sequence in the 5' to 3' direction. With reference to nucleic acids of the invention, the term “isolated nucleic acid” is sometimes used. This term, when applied to DNA, refers to a DNA molecule

that is separated from sequences with which it is immediately contiguous in the naturally occurring genome of the organism in which it originated. For example, an "isolated nucleic acid" may comprise a DNA molecule inserted into a vector, such as a plasmid or virus vector, or integrated into the genomic DNA of a prokaryotic or eukaryotic cell or host organism. Alternatively, this term may refer to a DNA that has been sufficiently separated from (e.g., substantially free of) other cellular components with which it would naturally be associated. "Isolated" is not meant to exclude artificial or synthetic mixtures with other compounds or materials, or the presence of impurities that do not interfere with the fundamental activity, and that may be present, for example, due to incomplete purification. When applied to RNA, the term "isolated nucleic acid" refers primarily to an RNA molecule encoded by an isolated DNA molecule as defined above. Alternatively, the term may refer to an RNA molecule that has been sufficiently separated from other nucleic acids with which it would be associated in its natural state (i.e., in cells or tissues). An isolated nucleic acid (either DNA or RNA) may further represent a molecule produced directly by biological or synthetic means and separated from other components present during its production.

A "specific binding pair" comprises a specific binding member (sbm) and a binding partner (bp) which have a particular specificity for each other and which in normal conditions bind to each other in preference to other molecules. Examples of specific binding pairs are antigens and antibodies, biotin and streptavidin, ligands and receptors and complementary nucleotide sequences. The skilled person is aware of many other examples. Further, the term "specific binding pair" is also applicable where either or both of the specific binding member and the binding partner comprise a part of a large molecule. In embodiments in which the specific binding pair comprises nucleic acid sequences, they will be of a length to hybridize to each other under conditions of the assay, preferably greater than 10 nucleotides long, more preferably greater than 15 or 20 nucleotides long.

According to the present invention, an isolated or biologically pure molecule or cell is a compound that has been removed from its natural milieu. As such, "isolated" and "biologically pure" do not necessarily reflect the extent to which the compound has been purified. An isolated compound of the present invention can be obtained from its natural source, can be produced using laboratory synthetic techniques or can be produced by any such chemical synthetic route.

The term “delivery” as used herein refers to the introduction of foreign molecule (i.e., miRNA encoding the polypeptide of interest) into cells. The term “administration” as used herein means the introduction of a foreign molecule into a cell. The term is intended to be synonymous with the term “delivery”.

Peptides

The peptides of the invention inhibit or modulate GPR75 activity. The terms “inhibition” or “inhibit” refer to a decrease or cessation of any event (such as protein ligand binding) or to a decrease or cessation of any phenotypic characteristic or to the decrease or cessation in the incidence, degree, or likelihood of that characteristic. To “reduce” or “inhibit” is to decrease, reduce or arrest an activity, function, and/or amount as compared to a reference. It is not necessary that the inhibition or reduction be complete. For example, in certain embodiments, “reduce” or “inhibit” refers to the ability to cause an overall decrease of 20% or greater. In another embodiment, “reduce” or “inhibit” refers to the ability to cause an overall decrease of 50% or greater. In yet another embodiment, “reduce” or “inhibit” refers to the ability to cause an overall decrease of 75%, 85%, 90%, 95%, or greater.

The term “modulate” as used herein refers to the ability of a compound to change an activity in some measurable way as compared to an appropriate control. As a result of the presence of compounds in the assays, activities can increase or decrease as compared to controls in the absence of these compounds. Preferably, an increase in activity is at least 25%, more preferably at least 50%, most preferably at least 100% compared to the level of activity in the absence of the compound. Similarly, a decrease in activity is preferably at least 25%, more preferably at least 50%, most preferably at least 100% compared to the level of activity in the absence of the compound. A compound that increases a known activity is an “agonist”. One that decreases, or prevents, a known activity is an “antagonist.”

The term “inhibitor” refers to an agent that slows down or prevents a particular chemical reaction, signaling pathway or other process, or that reduces the activity of a particular reactant, catalyst, or enzyme.

The phrase “G-Protein Receptor 75” or “GPR75” refers to a member of the G protein-coupled receptor family. GPRs are cell surface receptors that activate guanine-nucleotide binding proteins upon the binding of a ligand. GPR75 is a protein coding gene. Among its related

pathways are Class A/1 (Rhodopsin-like receptors) and 15q13.3 copy number variation syndrome. Gene Ontology (GO) annotations related to this gene include G protein-coupled receptor activity and C-C chemokine receptor activity.

The phrase "G-Protein Receptor 75 inhibitor" or "GPR75 inhibitor" refers to a class of agents that inhibit the action of GPR75. The peptides of interest herein are GPR75 inhibitors which each adopt an α-helical secondary structure (Fig. 9). Exemplary GPR75 binding peptides are provided in Table 1.

Table 1: GPR75 Binding Peptides

Peptide	**Sequence**	**SEQ ID NO**
SU75-36	HsQGTFTSDLSKYLEEEVREFIWLKNGGPSDVNTDRPGLLDLK-NH_2	1
SU75-37	TFTSDLSKYLEEEVREFIWLKNGGPSDVNTDRPGLLDLK-NH_2	2

In certain embodiments, the present invention includes peptides that have at least 80% identity to anyone of the peptides described herein. In certain embodiments, the peptides of the invention have a sequence identity of at least 80% identity, at least 81% identity, at least 82% identity, at least 83% identity, at least 84% identity, at least 85% identity, at least 86% identity, at least 87% identity, at least 88% identity, at least 89% identity, at least 90% identity, at least 91% identity, at least 92% identity, at least 93% identity, at least 94% identity, at least 95% identity, at least 96% identity, at least 97% identity, at least 98% identity, at least 99% identity, or 100% identity.

Preferably, the peptides of the above-described sequences and functional equivalents thereof which act to modulate obesity upon administration. As used herein, the term "functional equivalent" is intended to include amino acid sequence variants having amino acid substitutions in some or all of the proteins, or amino acid additions or deletions in some of the proteins. The amino acid substitutions are preferably conservative substitutions. Examples of the conservative substitutions of naturally occurring amino acids are as follow: aliphatic amino acids (Gly, Ala, and Pro), hydrophobic amino acids (Ile, Leu, and Val), aromatic amino acids (Phe, Tyr, and Trp), acidic amino acids (Asp, and Glu), basic amino acids (His, Lys, Arg, Gln, and Asn), and sulfur-containing amino acids (Cys, and Met). The deletions of amino acids are preferably located in a region which is not directly involved in the activity of the peptide.

In the present context, the term “variant” refers to a nucleic acid sequence or polypeptide comprising a sequence, which differs (by deletion, insertion, and/or substitution of a nucleic acid or amino acid, an L or D stereoisomer an amino acid, or a non-naturally occurring amino acid) in one or more nucleic acid or amino acid positions differ from that of a wild type nucleic acid or polypeptide sequence.

In the present context, the term “linker” refers to a connection between two protein coding sequences or their protein products. Linkers comprise a stretch of contiguous nucleic acids or amino acids, which holds at least one cleavage site that enables separation of the genes or their products through cleavage of the linker. Preferably, the linker comprises a cleavage site at its 5′ end and a cleavage site at its 3′ end, or a cleavage site at its N-terminal end and a cleavage site at its C-terminal end.

The peptide may be fused to biotin, Poly-lysine, lysozyme, Green fluorescent protein (and derivatives), SUMO or other desired proteinaceous tags. Production of the desired peptide sequence can be carried out in *E.coli, , SF9, Pichia, etc.,* using existing technologies, e.g. with protein fusion tags that can either be removed or left as desired. In certain embodiments, the peptide of interest may be fused via a linker.

The peptide can be expressed as a fusion to larger proteins, facilitating expression at large scales, ease of purification, and ensuring quality of product. Expression systems can also be leveraged to generate large sequence libraries, allowing for directed evolution for targeted properties. Peptides can be produced sustainably using environmentally friendly, existing fermentation technologies.

As noted above, the invention also includes polynucleotides encoding the peptides or fusion proteins comprising the peptide described herein. Those of skill in the art understand the degeneracy of the genetic code and that a variety of polynucleotides can encode the same polypeptide. In some embodiments, the polynucleotides (i.e., polynucleotides encoding the fusion polypeptides) may be codon-optimized for expression in a particular cell including, without limitation, a plant cell, bacterial cell, or algal cell. Any polynucleotide sequences may be used which encode a desired form of the polypeptides described herein. The polynucleotide sequences which encode the polypeptides of the invention represent non-naturally occurring sequences. Computer programs for generating degenerate coding sequences are available and can

be used for this purpose. Pencil, paper, the genetic code, and a human hand can also be used to generate degenerate coding sequences.

In the present context, the term "codon optimization" refers to changing the codons of a nucleotide sequence without altering the amino acid sequence that it encodes in order to favor expression in a specific species. Codon optimization may be used to increase the abundance of the peptide or protein that the nucleotide sequence encodes since "rare" codons are removed and replaced with abundant codons.

Regarding the fusion polypeptides disclosed herein, the phrases "% sequence identity," "percent identity," or "% identity" refer to the percentage of residue matches between at least two amino acid sequences aligned using a standardized algorithm. Methods of amino acid sequence alignment are well-known. Some alignment methods take into account conservative amino acid substitutions. Such conservative substitutions generally preserve the charge and hydrophobicity at the site of substitution, thus preserving the structure (and therefore function) of the polypeptide. Percent identity for amino acid sequences may be determined as understood in the art. The structural similarity is typically at least 80% identity, at least 81% identity, at least 82% identity, at least 83% identity, at least 84% identity, at least 85% identity, at least 86% identity, at least 87% identity, at least 88% identity, at least 89% identity, at least 90% identity, at least 91% identity, at least 92% identity, at least 93% identity, at least 94% identity, at least 95% identity, at least 96% identity, at least 97% identity, at least 98% identity, or at least 99% identity.

Polypeptide sequence identity may be measured over the length of an entire defined polypeptide sequence, for example, as defined by a particular SEQ ID number, or may be measured over a shorter length, for example, over the length of a fragment taken from a larger, defined polypeptide sequence, for instance, a fragment of at least 15, at least 20, at least 30, at least 40, at least 50, at least 70 or at least 150 contiguous residues. Such lengths are exemplary only, and it is understood that any fragment length supported by the sequences shown herein, may be used to describe a length over which percentage identity may be measured.

In vitro synthesis of peptides

Peptides can be synthesized chemically either in solution or on a solid phase. The process involves directed and selective formation of an amide bond between an N-protected amino acid

and an amino acid bearing a free amino group and protected carboxylic acid. In solid phase synthesis, the carboxyl protecting group is linked to a polymer support. Following bond formation, the amino-protecting group of the dipeptide is removed, and the next N-protected amino-acid is coupled.

Solid-phase peptide synthesis (SSPS) is the most frequently used method of peptide synthesis due to its efficiency, simplicity, speed, and ease of parallelization. SPPS involves sequential addition of amino and side-chain protected amino acid residues to an amino acid or peptide attached to an insoluble polymeric support. Either an acid-labile Boc group (Boc SPPS) or base-labile Fmoc-group (Fmoc SPPS) is used for N-α-protection. After removal of this protecting group, the next protected amino acid is added using either a coupling reagent or pre-activated protected amino acid derivative. The C-terminal amino acid is anchored to the resin *via* a linker, the nature of which determines the conditions required to release the peptide from the support after chain extension. Side-chain protecting groups are often chosen so as to be cleaved simultaneously with detachment of the peptide from the resin.

Peptides of 50 amino acids can be routinely prepared although the synthesis of proteins of over 100 amino acids are commonly reported. Longer proteins can be made by native chemical ligation of fully deprotected peptides in solution. With this method, it is possible to synthesize natural peptides that are difficult to express in bacteria, to incorporate unnatural or D-amino acids, and to generate cyclic, branched, labelled, and post-translationally modified peptides.

Liquid-phase peptide synthesis, usually utilizing Boc or Z-amino protection, has been superseded by SPPS except for existing processes of large-scale synthesis of peptides for industrial purposes. Desired sequences can be developed by any one of the several commercial entities who provide this service for a fee, including Sigma Aldrich, and Avivasysbio for example.

Vectors and Production

Transgenic cells expression said polynucleotides also form an aspect of the invention. A transgenic cell may be obtained by introducing a recombinant nucleic acid molecule that encodes a protein of this disclosure. As used herein, the term “recombinant nucleic acid” refers to a polynucleotide that is manipulated by human intervention. A recombinant nucleic acid molecule can contain two or more nucleotide sequences that are linked in a manner such that the product is

not found in a cell in nature. In particular, the two or more nucleotide sequences can be operatively linked and, for example, can encode a fusion polypeptide. A recombinant nucleic acid molecule also can be based on, but manipulated so as to be different, from a naturally occurring polynucleotide, for example, a polynucleotide having one or more nucleotide changes such that a first codon, which normally is found in the polynucleotide, is biased for chloroplast codon usage, or such that a sequence of interest is introduced into the polynucleotide, for example, a restriction endonuclease recognition site or a splice site, a promoter, a DNA origin of replication, or the like.

Any appropriate technique for introducing recombinant nucleic acid molecules into cells may be used. Techniques for nuclear and chloroplast transformation are known and include, without limitation, electroporation, biolistic transformation (also referred to as micro-projectile/particle bombardment), agitation in the presence of glass beads, and Agrobacterium-based transformation.

As used herein, the term "construct" refers to recombinant polynucleotides including, without limitation, DNA and RNA, which may be single-stranded or double-stranded and may represent the sense or the antisense strand. Recombinant polynucleotides are polynucleotides formed by laboratory methods that include polynucleotide sequences derived from at least two different natural sources or they may be synthetic. Constructs thus may include new modifications to endogenous genes introduced by, for example, genome editing technologies. Constructs may also include recombinant polynucleotides created using, for example, recombinant DNA methodologies.

A "vector" is capable of transferring gene sequences to target cells. Typically, "vector construct," "expression vector," and "gene transfer vector," mean any nucleic acid construct capable of directing the expression of a gene of interest and which can transfer gene sequences to target cells. Thus, the term includes cloning and expression vehicles, as well as integrating vectors.

The constructs and vectors provided herein may be prepared by methods available to those of skill in the art. Notably each of the constructs or expression cassettes claimed are recombinant molecules and as such do not occur in nature. Generally, the nomenclature used herein and the laboratory procedures utilized in the present invention include molecular, biochemical, and recombinant DNA techniques that are well known and commonly employed in

the art. Standard techniques available to those skilled in the art may be used for cloning, DNA and RNA isolation, amplification and purification. Such techniques are thoroughly explained in the literature.

The constructs and expression cassettes provided herein may include a promoter operably linked to any one of the polynucleotides described herein but need not have a promoter and may be used for homologous recombination into the cell. Alternatively, the constructs may include a promoter and the promoter may be a heterologous promoter or an endogenous promoter associated with the polypeptide.

As used herein, the terms “heterologous promoter,” “promoter,” “promoter region,” or “promoter sequence” refer generally to transcriptional regulatory regions of a gene, which may be found at the 5′ or 3′ side of the polynucleotides described herein, or within the coding region of the polynucleotides, or within introns in the polynucleotides. Typically, a promoter is a DNA regulatory region capable of binding RNA polymerase in a cell and initiating transcription of a downstream (3′ direction) coding sequence. The typical 5′ promoter sequence is bounded at its 3′ terminus by the transcription initiation site and extends upstream (5′ direction) to include the minimum number of bases or elements necessary to initiate transcription at levels detectable above background. Within the promoter sequence is a transcription initiation site (conveniently defined by mapping with nuclease S1), as well as protein binding domains (consensus sequences) responsible for the binding of RNA polymerase.

In some embodiments, the disclosed polynucleotides are operably connected to the promoter. As used herein, a polynucleotide is “operably connected” or “operably linked” when it is placed into a functional relationship with a second polynucleotide sequence. For instance, a promoter is operably linked to a polynucleotide if the promoter is connected to the polynucleotide such that it may affect transcription of the polynucleotides. In various embodiments, the polynucleotides may be operably linked to at least 1, at least 2, at least 3, at least 4, at least 5, or at least 10 promoters.

Heterologous promoters useful in the practice of the present invention include, but are not limited to, constitutive, inducible, temporally-regulated, developmentally regulated, chemically regulated, tissue-preferred and tissue-specific promoters. The heterologous promoter may be a plant, animal, bacterial, fungal, or synthetic promoter.

Methods of Treatment and Administration

The term "reducing" or "inhibiting" as used herein refers to administering a compound prior to, or during the onset of clinical symptoms of a disease or conditions so as to reduce a physical manifestation of aberrations associated with the disease or condition.

The term "in need of treatment" as used herein refers to a judgment made by a caregiver (e.g. physician, nurse, nurse practitioner, or individual in the case of humans; veterinarian in the case of animals, including non-human mammals) that a subject requires or will benefit from treatment. This judgment is made based on a variety of factors that are in the realm of a care giver's expertise, but that includes the knowledge that the subject is ill, or will be ill, as the result of a condition that is treatable by the disclosed compounds.

In the methods described herein, the acts can be carried out in any order, except when a temporal or operational sequence is explicitly recited. Furthermore, specified acts can be carried out concurrently unless explicit claim language recites that they be carried out separately. For example, a claimed act of doing X and a claimed act of doing Y can be conducted simultaneously within a single operation, and the resulting process will fall within the literal scope of the claimed process.

As used herein, "subject" includes, but is not limited to, animals, plants, bacteria, viruses, parasites and any other organism or entity. The subject can be a vertebrate, more specifically a mammal (e.g., a human, horse, pig, rabbit, dog, sheep, goat, non-human primate, cow, cat, guinea pig or rodent), a fish, a bird, a reptile or an amphibian. The subject can be an invertebrate, more specifically an arthropod (e.g., insects and crustaceans). The term does not denote a particular age or sex. Thus, adult and newborn subjects, as well as fetuses, whether male or female, are intended to be covered. A patient refers to a subject afflicted with a disease or disorder. The term "patient" includes human and veterinary subjects.

The terms "treat," "treating," and "treatment" as used herein, refer to eliciting the desired biological response, such as a therapeutic and prophylactic effect, respectively. In some embodiments, a therapeutic effect comprises one or more of a decrease/reduction in obesity, a decrease/reduction in the severity of obesity (such as, for example, a reduction or inhibition of development or obesity), a decrease/reduction in symptoms and obesity-related effects, delaying the onset of symptoms and obesity-related effects, reducing the severity of symptoms of obesity-related effects, reducing the severity of an acute episode, reducing the number of symptoms and

obesity-related effects, reducing the latency of symptoms and obesity-related effects, an amelioration of symptoms and obesity-related effects, reducing secondary symptoms, reducing secondary infections, preventing relapse to obesity, decreasing the number or frequency of relapse episodes, increasing latency between symptomatic episodes, increasing time to sustained progression, expediting remission, inducing remission, augmenting remission, speeding recovery, or increasing efficacy of or decreasing resistance to alternative therapeutics, and/or an increased survival time of the affected host animal, following administration of the agent or composition comprising the agent. A prophylactic effect may comprise a complete or partial avoidance/inhibition or a delay of obesity development/progression (such as, for example, a complete or partial avoidance/inhibition or a delay), or an increased survival time of the affected host animal, following administration of a therapeutic protocol. Treatment of obesity encompasses the treatment of subjects already diagnosed as having any form of obesity at any clinical stage or manifestation, the delay of the onset or evolution or aggravation or deterioration of the symptoms or signs of obesity, and/or preventing and/or reducing the severity of obesity.

In another aspect, provided herein are methods for treating a patient comprising administration of the peptides of interest. In any of the embodiments described herein, the subject can be obese, or have excessive weight, elevated BMI, elevated body fat mass, percentage, or volume, and/or excessive food intake. In any of the embodiments described herein, the subject can be obese. In any of the embodiments described herein, the subject can have excessive weight. In any of the embodiments described herein, the subject can have elevated BMI. In any of the embodiments described herein, the subject can have elevated body fat mass, percentage, or volume. In any of the embodiments described herein, the subject can have excessive food intake.

Symptoms of obesity include, but are not limited to, excess body fat accumulation (particularly around the waist), breathlessness, increased sweating, snoring, inability to cope with sudden physical activity, feeling extra tired every day, back and joint pains, skin problems (from moisture accumulating in the folds of skin).

Methods of treating a subject having obesity, the methods comprising administering a GPR75 inhibitor to the subject are provided. Also disclosed are methods of treating a subject having excessive weight, the methods comprising administering a GPR75 inhibitor to the subject. The present disclosure also provides methods of treating a subject having elevated BMI,

the methods comprising administering a GPR75 inhibitor to the subject. Methods of treating a subject having elevated body fat mass, percentage, or volume, the methods comprising administering a GPR75 inhibitor to the subject are also described. Finally, treatment of a subject having excessive food intake, comprising administering a GPR75 inhibitor to the subject are also disclosed.

The present disclosure also provides methods of treating a subject to prevent weight gain or to maintain weight loss, the method comprising administering a GPR75 inhibitor to the subject.

In certain embodiments, methods of treating a metabolic disease or disorder in a subject, comprising administering an effective amount of GPR75 inhibitor to the subject are provided.

As used herein, the term “metabolic disease” or “metabolic disorder” is also called a metabolic syndrome and refers to a set of abnormal states such as an increase in body fat, an increase in blood pressure, an increase in blood sugar, and abnormal lipids in blood, which increase the risk of cerebral cardiovascular diseases and diabetes mellitus. The metabolic disease is not a single disease, but a comprehensive disease caused by genetic predisposition and environmental factors, and in the present invention, may be selected from the group consisting of obesity, diabetes mellitus, dyslipidemia, insulin resistance, hepatic steatosis, hypercholesterolemia, and non-alcoholic fatty liver disease, and may be more preferably obesity or diabetes mellitus, but is not limited thereto.

As used herein, the term “diabetes mellitus”, as a type of metabolic disease such as an insufficient amount of insulin secreted or an absence of normal function, is characterized by high blood sugar with high blood glucose concentration and causes various symptoms and signs due to hyperglycemia and glucose release from urine. Diabetes mellitus includes type 1 diabetes mellitus which occurs when insulin is not secreted largely due to the destruction of pancreatic beta cells, and type 2 diabetes mellitus which is caused by insufficient insulin secretion in the body or insulin resistance in which cells do not respond to insulin. In the present invention, diabetes mellitus includes both type 1 diabetes mellitus and type 2 diabetes mellitus. In certain embodiments, the method further comprises administering a second therapeutic agent that treats or inhibits obesity. Nonlimiting examples of therapeutic agents that treat or inhibit obesity and/or increased BMI include, but are not limited to, GLP-1R agonists, melanocortin 4 receptor (MC4R) agonists, sibutramine, orlistat, phentermine, lorcaserin, naltrexone, liraglutide,

diethylpropion, bupropion, metformin, pramlintide, topiramate, and zonisamide, or any combination thereof.

Administration of the therapeutic agents that treat or inhibit obesity and/or GPR75 inhibitors can be repeated, for example, after one day, two days, three days, five days, one week, two weeks, three weeks, one month, five weeks, six weeks, seven weeks, eight weeks, two months, or three months. The repeated administration can be at the same dose or at a different dose. The administration can be repeated once, twice, three times, four times, five times, six times, seven times, eight times, nine times, ten times, or more. For example, according to certain dosage regimens a subject can receive therapy for a prolonged period such as, for example, 6 months, 1 year, or more.

Administration of the therapeutic agents that treat or inhibit obesity and/or GPR75 inhibitors can occur by any suitable route including, but not limited to, parenteral, intravenous, oral, lingual, buccal, subcutaneous, intra-arterial, intracranial, intrathecal, intraperitoneal, topical, intranasal, or intramuscular. Pharmaceutical compositions for administration are desirably sterile and substantially isotonic and manufactured under GMP conditions. Pharmaceutical compositions can be provided in unit dosage form (i.e., the dosage for a single administration). Pharmaceutical compositions can be formulated using one or more physiologically and pharmaceutically acceptable carriers, diluents, excipients or auxiliaries. The formulation depends on the route of administration chosen. The term “pharmaceutically acceptable” means that the carrier, diluent, excipient, or auxiliary is compatible with the other ingredients of the formulation and not substantially deleterious to the recipient thereof.

The compounds can be combined with one or more pharmaceutically acceptable carriers and/or excipients that are considered safe and effective and may be administered to an individual without causing undesirable biological side effects or unwanted interactions. The carrier is all components present in the pharmaceutical formulation other than the active ingredient or ingredients. See, e.g., Remington's Pharmaceutical Sciences, latest edition, by E.W. Martin Mack Pub. Co., Easton, PA, which discloses typical carriers and conventional methods of preparing pharmaceutical compositions that can be used in conjunction with the preparation of formulations of the compounds described herein and which is incorporated by reference herein. These most typically would be standard carriers for administration of compositions to humans. In one aspect, humans and non-humans, including solutions such as sterile water, saline, and

buffered solutions at physiological pH. Other compounds will be administered according to standard procedures used by those skilled in the art.

These compositions can take the form of solutions, suspensions, emulsion, tablets, pills, capsules, powders, sustained-release formulations, and the like.

In some embodiments, the therapeutic agents that treat or inhibit obesity and/or GPR75 inhibitors (such as any of the peptide ligands disclosed herein) are administered intrathecally (i.e., introduction into the subarachnoid space of the spinal cord or into the spinal canal so that the therapeutic agent can reach the cerebrospinal fluid of a subject, or introduction into the anatomic space or potential space inside a sheath, including, by way of non-limiting examples, the arachnoid membrane of the brain or spinal cord). In some embodiments, intrathecal administration results in the therapeutic agent acting on, without limitation, the cortex, the cerebellum, the striatum, the cervical spine, the lumbar spine, or the thoracic spine. Therapeutic agents administered intrathecally may ultimately act on targets throughout the entire central nervous system. In some embodiments, the intrathecal administration is into the cisterna magna or by the lumbar area or region. In some embodiments, the intrathecal administration into the lumbar area or region results in delivery of the therapeutic agent to the distal spinal canal. Exemplary methods for intrathecal administration are described in, for example, Lazorthes et al., Advances in Drug Delivery Systems and Applications in Neurosurgery, 143-192. In some embodiments, the intrathecal administration is by injection, by bolus injection, by a catheter, or by a pump. In some embodiments, the intrathecal administration is by lumber puncture. In some embodiments, the pump is an osmotic pump. In some embodiments, the pump is implanted into subarachnoid space of the spinal canal, below the skin of the abdomen, or behind the chest wall. In some embodiments, the intrathecal administration is by an intrathecal delivery system for a therapeutic substance including a reservoir containing a volume of the therapeutic agent and a pump configured to deliver at least a portion of the therapeutic substance contained in the reservoir. In some embodiments, intrathecal administration is through intermittent or continuous access to an implanted intrathecal drug delivery device (IDDD). In some embodiments, the therapeutic substance is an inhibitory nucleic acid molecule. In some embodiments, the amount of the nucleic acid molecule or peptide molecule administered intrathecally ranges from about 10 μg to about 2 mg, from about 50 μg to about 1500 μg, or from about 100 μg to about 1000 μg. In some embodiments, the therapeutic agent is disposed within a pharmaceutical composition. In

some embodiments, the pharmaceutical composition does not comprise a preservative.

Throughout this document, values expressed in a range format should be interpreted in a flexible manner to include not only the numerical values explicitly recited as the limits of the range, but also to include all the individual numerical values or sub-ranges encompassed within that range as if each numerical value and sub-range is explicitly recited. For example, a range of "about 0.1% to about 5%" or "about 0.1% to 5%" should be interpreted to include not just about 0.1% to about 5%, but also the individual values (*e.g.*, 1%, 2%, 3%, and 4%) and the sub-ranges (*e.g.*, 0.1% to 0.5%, 1.1% to 2.2%, 3.3% to 4.4%) within the indicated range.

Parenteral Formulations

The peptides described herein can be formulated for parenteral administration. For example, parenteral administration may include administration to a patient intravenously, intradermally, intraarterially, intraperitoneally, intralesionally, intracranially, intraarticularly, intraprostatically, intrapleurally, intratracheally, intravitreally, intratumorally, intramuscularly, subcutaneously, intralingually, subconjunctivally, intravesicularly, intrapericardially, intraumbilically, by injection, and by infusion.

Parenteral formulations can be prepared as aqueous compositions using techniques known in the art. Typically, such compositions can be prepared as injectable formulations, for example, solutions or suspensions; solid forms suitable for using to prepare solutions or suspensions upon the addition of a reconstitution medium prior to injection; emulsions, such as water-in-oil (w/o) emulsions, oil-in-water (o/w) emulsions, and microemulsions thereof, liposomes, or emulsosomes.

If for intravenous administration, the compositions are packaged in solutions of sterile isotonic aqueous buffer. Where necessary, the composition may also include a solubilizing agent. The components of the composition are supplied either separately or mixed in unit dosage form, for example, as a dry lyophilized powder or concentrated solution in a hermetically sealed container such as an ampoule or sachet indicating the amount of active agent. If the composition is to be administered by infusion, it can be dispensed with an infusion bottle containing sterile pharmaceutical grade water or saline. Where the composition is administered by injection, an

ampoule of sterile water or saline can be provided so that the ingredients may be mixed prior to injection.

The carrier can be a solvent or dispersion medium containing, for example, water, ethanol, one or more polyols (e.g., glycerol, propylene glycol, and liquid polyethylene glycol), oils, such as vegetable oils (e.g., peanut oil, corn oil, sesame oil, etc.), and combinations thereof. The proper fluidity can be maintained, for example, using a coating, such as lecithin, by the maintenance of the required particle size in the case of dispersion and/or by the use of surfactants. In many cases, it will be preferable to include isotonic agents, for example, sugars or sodium chloride.

Solutions and dispersions of the active compounds as the free acid or base or pharmacologically acceptable salts thereof can be prepared in water or another solvent or dispersing medium suitably mixed with one or more pharmaceutically acceptable excipients including, but not limited to, surfactants, dispersants, emulsifiers, pH modifying agents, viscosity modifying agents, and combination thereof.

Suitable surfactants may be anionic, cationic, amphoteric, or nonionic surface-active agents. Suitable anionic surfactants include, but are not limited to, those containing carboxylate, sulfonate and sulfate ions. Examples of anionic surfactants include sodium, potassium, ammonium of long chain alkyl sulfonates, and alkyl aryl sulfonates such as sodium dodecylbenzene sulfonate; dialkyl sodium sulfosuccinates, such as sodium dodecylbenzene sulfonate; dialkyl sodium sulfosuccinates, such as sodium bis-(2-ethylthioxyl)-sulfosuccinate; and alkyl sulfates, such as sodium lauryl sulfate. Cationic surfactants include, but are not limited to, quaternary ammonium compounds, such as benzalkonium chloride, benzethonium chloride, cetrimonium bromide, stearyl dimethylbenzyl ammonium chloride, polyoxyethylene, and coconut amine. Examples of nonionic surfactants include ethylene glycol monostearate, propylene glycol myristate, glyceryl monostearate, glyceryl stearate, polyglyceryl-4-oleate, sorbitan acylate, sucrose acylate, PEG-150 laurate, PEG-400 monolaurate, polyoxyethylene monolaurate, polysorbates, polyoxyethylene octylphenylether, PEG-1000 cetyl ether, polyoxyethylene tridecyl ether, polypropylene glycol butyl ether, Poloxamer® 401, stearoyl monoisopropanolamide, and polyoxyethylene hydrogenated tallow amide. Examples of amphoteric surfactants include sodium N-dodecyl-β-alanine, sodium N-lauryl-β-iminodipropionate, myristoamphoacetate, lauryl betaine, and lauryl sulfobetaine.

The formulation can contain a preservative to prevent the growth of microorganisms. Suitable preservatives include, but are not limited to, parabens, chlorobutanol, phenol, sorbic acid, and thimerosal. The formulation may also contain an antioxidant to prevent degradation of the active agent(s).

The formulation is typically buffered to a pH of 3-8 for parenteral administration upon reconstitution. Suitable buffers include, but are not limited to, phosphate buffers, acetate buffers, and citrate buffers.

Water-soluble polymers are often used in formulations for parenteral administration. Suitable water-soluble polymers include, but are not limited to, polyvinylpyrrolidone, dextran, carboxymethylcellulose, and polyethylene glycol.

Sterile injectable solutions can be prepared by incorporating the active compounds in the required amount in the appropriate solvent or dispersion medium with one or more of the excipients listed above, as required, followed by filtered sterilization. Generally, dispersions are prepared by incorporating the various sterilized active ingredients into a sterile vehicle which contains the basic dispersion medium and the required other ingredients from those listed above. In the case of sterile powders for the preparation of sterile injectable solutions, the preferred methods of preparation are vacuum-drying and freeze-drying techniques which yield a powder of the active ingredient plus any additional desired ingredient from a previously sterile-filtered solution thereof. The powders can be prepared in such a manner that the particles are porous in nature, which can increase dissolution of the particles. Methods for making porous particles are well known in the art.

The parenteral formulations described herein can be formulated for controlled release including immediate release, delayed release, extended release, pulsatile release, and combinations thereof.

Nano- and microparticles

For parenteral administration, the one or more compounds, and optional one or more additional active agents, can be incorporated into microparticles, nanoparticles, or combinations thereof that provide controlled release of the compounds and/or one or more additional active agents. In forms wherein the formulations contain two or more peptides, the peptides can be formulated for the same type of controlled release (e.g., delayed, extended, immediate, or pulsatile) or the peptides can be independently formulated for different types of release (e.g.,

immediate and delayed, immediate and extended, delayed and extended, delayed and pulsatile, etc.).

For example, the compounds and/or one or more additional active agents can be incorporated into polymeric microparticles, which provide controlled release of the peptide(s). Release of the peptide(s) is controlled by diffusion of the protein(s) out of the microparticles and/or degradation of the polymeric particles by hydrolysis and/or enzymatic degradation. Suitable polymers include ethylcellulose and other natural or synthetic cellulose derivatives.

Polymers, which are slowly soluble and form a gel in an aqueous environment, such as hydroxypropyl methylcellulose or polyethylene oxide, can also be suitable as materials for protein containing microparticles. Other polymers include, but are not limited to, polyanhydrides, poly(ester anhydrides), polyhydroxy acids, such as polylactide (PLA), polyglycolide (PGA), poly(lactide-co-glycolide) (PLGA), poly-3-hydroxybutyrate (PHB), and copolymers thereof, poly-4-hydroxybutyrate (P4HB) and copolymers thereof, polycaprolactone and copolymers thereof, and combinations thereof.

Alternatively, the protein(s) can be incorporated into microparticles prepared from materials which are insoluble in aqueous solution or slowly soluble in aqueous solution but are capable of degrading within the GI tract by means including enzymatic degradation, surfactant action of bile acids, and/or mechanical erosion. As used herein, the term “slowly soluble in water” refers to materials that are not dissolved in water within a period of 30 minutes. Preferred examples include fats, fatty substances, waxes, wax-like substances, and mixtures thereof. Suitable fats and fatty substances include fatty alcohols (such as lauryl, myristyl stearyl, cetyl or cetostearyl alcohol), fatty acids and derivatives, including but not limited to fatty acid esters, fatty acid glycerides (mono-, di- and triglycerides), and hydrogenated fats. Specific examples include, but are not limited to hydrogenated vegetable oil, hydrogenated cottonseed oil, hydrogenated castor oil, hydrogenated oils available under the trade name Sterotex®, stearic acid, cocoa butter, and stearyl alcohol. Suitable waxes and wax-like materials include natural or synthetic waxes, hydrocarbons, and normal waxes. Specific examples of waxes include beeswax, glycowax, castor wax, carnauba wax, paraffins, and candelilla wax. As used herein, a wax-like material is defined as any material, which is normally solid at room temperature and has a melting point of from about 30 to 300ºC.

In some cases, it may be desirable to alter the rate of water penetration into the microparticles. To this end, rate-controlling (wicking) agents can be formulated along with the fats or waxes listed above. Examples of rate-controlling materials include certain starch derivatives (e.g., waxy maltodextrin and drum dried corn starch), cellulose derivatives (e.g., hydroxypropylmethyl-cellulose, hydroxypropylcellulose, methylcellulose, and carboxymethyl-cellulose), alginic acid, lactose and talc. Additionally, a pharmaceutically acceptable surfactant (e.g., lecithin) may be added to facilitate the degradation of such microparticles.

Proteins, which are water insoluble, such as zein, can also be used as materials for the formation of protein containing microparticles. Additionally, proteins, polysaccharides and combinations thereof, which are water-soluble, can be formulated with peptide into microparticles and subsequently cross-linked to form an insoluble network. For example, cyclodextrins can be complexed with individual drug molecules and subsequently cross-linked.

Method of making Nano- and Microparticles

Encapsulation or incorporation of drug into carrier materials to produce drug-containing microparticles can be achieved through known pharmaceutical formulation techniques. In the case of formulation in fats, waxes, or wax-like materials, the carrier material is typically heated above its melting temperature and the drug is added to form a mixture comprising drug particles suspended in the carrier material, drug dissolved in the carrier material, or a mixture thereof. Microparticles can be subsequently formulated through several methods including, but not limited to, the processes of congealing, extrusion, spray chilling, or aqueous dispersion. In a preferred process, wax is heated above its melting temperature, drug is added, and the molten wax-drug mixture is congealed under constant stirring as the mixture cools. Alternatively, the molten wax-drug mixture can be extruded and spheronized to form pellets or beads. These processes are known in the art.

For some carrier materials it may be desirable to use a solvent evaporation technique to produce drug-containing microparticles. In this case drug and carrier material are co-dissolved in a mutual solvent and microparticles can subsequently be produced by several techniques including, but not limited to, forming an emulsion in water or other appropriate media, spray drying or by evaporating off the solvent from the bulk solution and milling the resulting material.

In some forms, drug in a particulate form is homogeneously dispersed in a water-insoluble or slowly water-soluble material. To minimize the size of the drug particles within the composition, the drug powder itself may be milled to generate fine particles prior to formulation. The process of jet milling, known in the pharmaceutical art, can be used for this purpose. In some forms, drug in a particulate form is homogeneously dispersed in a wax or wax-like substance by heating the wax or wax-like substance above its melting point and adding the drug particles while stirring the mixture. In this case a pharmaceutically acceptable surfactant may be added to the mixture to facilitate the dispersion of the drug particles.

The particles can also be coated with one or more modified release coatings. Solid esters of fatty acids, which are hydrolyzed by lipases, can be spray coated onto microparticles or drug particles. Zein is an example of a naturally water-insoluble protein. It can be coated onto drug containing microparticles or drug particles by spray coating or by wet granulation techniques. In addition to naturally water-insoluble materials, some substrates of digestive enzymes can be treated with cross-linking procedures, resulting in the formation of non-soluble networks. Many methods of cross-linking proteins, initiated by both chemical and physical means, have been reported. One of the most common methods to obtain cross-linking is the use of chemical cross-linking agents. Examples of chemical cross-linking agents include aldehydes (gluteraldehyde and formaldehyde), epoxy compounds, carbodiimides, and genipin. In addition to these cross-linking agents, oxidized and native sugars have been used to cross-link gelatin. Cross-linking can also be accomplished using enzymatic means; for example, transglutaminase has been approved as a GRAS substance for cross-linking seafood products. Finally, cross-linking can be initiated by physical means such as thermal treatment, UV irradiation, and gamma irradiation.

To produce a coating layer of cross-linked protein surrounding drug containing microparticles or drug particles, a water-soluble protein can be spray coated onto the microparticles and subsequently cross-linked by the one of the methods described above. Alternatively, drug-containing microparticles can be microencapsulated within protein by coacervation-phase separation (for example, by the addition of salts) and subsequently cross-linked. Some suitable proteins for this purpose include gelatin, albumin, casein, and gluten.

Polysaccharides can also be cross-linked to form a water-insoluble network. For many polysaccharides, this can be accomplished by reaction with calcium salts or multivalent cations, which cross-link the main polymer chains. Pectin, alginate, dextran, amylose, and guar gum are

subject to cross-linking in the presence of multivalent cations. Complexes between oppositely charged polysaccharides can also be formed; pectin and chitosan, for example, can be complexed via electrostatic interactions.

Injectable/Implantable formulations

The compounds described herein can be incorporated into injectable/implantable solid or semi-solid implants, such as polymeric implants. In some forms, the compounds are incorporated into a polymer that is a liquid or paste at room temperature, but upon contact with aqueous medium, such as physiological fluids, exhibits an increase in viscosity to form a semi-solid or solid material. Exemplary polymers include, but are not limited to, hydroxyalkanoic acid polyesters derived from the copolymerization of at least one unsaturated hydroxy fatty acid copolymerized with hydroxyalkanoic acids. The polymer can be melted, mixed with the active substance and cast or injection molded into a device. Such melt fabrication requires polymers having a melting point that is below the temperature at which the substance to be delivered and polymer degrade or become reactive. The device can also be prepared by solvent casting where the polymer is dissolved in a solvent and the drug dissolved or dispersed in the polymer solution and the solvent is then evaporated. Solvent processes require that the polymer be soluble in organic solvents. Another method is compression molding of a mixed powder of the polymer and the drug or polymer particles loaded with the active agent.

Alternatively, the compounds can be incorporated into a polymer matrix and molded, compressed, or extruded into a device that is a solid at room temperature. For example, the compounds can be incorporated into a biodegradable polymer, such as polyanhydrides, polyhydroalkanoic acids (PHAs), PLA, PGA, PLGA, polycaprolactone, polyesters, polyamides, polyorthoesters, polyphosphazenes, proteins and polysaccharides such as collagen, hyaluronic acid, albumin and gelatin, and combinations thereof and compressed into solid device, such as disks, or extruded into a device, such as rods.

The release of the one or more compounds from the implant can be varied by selection of the polymer, the molecular weight of the polymer, and/or modification of the polymer to increase degradation, such as the formation of pores and/or incorporation of hydrolyzable linkages. Methods for modifying the properties of biodegradable polymers to vary the release profile of the compounds from the implant are well known in the art.

Enteral / Oral / Lingual Formulations

Oral / lingual formulations can include standard carriers such as pharmaceutical grades of mannitol, lactose, sodium saccharine, starch, magnesium stearate, cellulose, magnesium carbonate, etc. Such compositions will contain a therapeutically effective amount of the compound and/or antibiotic together with a suitable amount of carrier to provide the proper form to the patient based on the mode of administration to be used.

Suitable oral dosage forms include tablets, capsules, solutions, suspensions, syrups, and lozenges. Tablets can be made using compression or molding techniques well known in the art. Gelatin or non-gelatin capsules can prepared as hard or soft capsule shells, which can encapsulate liquid, solid, and semi-solid fill materials, using techniques well known in the art.

Formulations may be prepared using a pharmaceutically acceptable carrier. As generally used herein “carrier” includes, but is not limited to, diluents, preservatives, binders, lubricants, disintegrators, swelling agents, fillers, stabilizers, and combinations thereof.

Carrier also includes all components of the coating composition, which may include plasticizers, pigments, colorants, stabilizing agents, and glidants.

Examples of suitable coating materials include, but are not limited to, cellulose polymers such as cellulose acetate phthalate, hydroxypropyl cellulose, hydroxypropyl methylcellulose, hydroxypropyl methylcellulose phthalate and hydroxypropyl methylcellulose acetate succinate; polyvinyl acetate phthalate, acrylic acid polymers and copolymers, and methacrylic resins that are commercially available under the trade name EUDRAGIT® (Roth Pharma, Westerstadt, Germany), zein, shellac, and polysaccharides.

Additionally, the coating material may contain conventional carriers such as plasticizers, pigments, colorants, glidants, stabilization agents, pore formers and surfactants.

“Diluents”, also referred to as "fillers," are typically necessary to increase the bulk of a solid dosage form so that a practical size is provided for compression of tablets or formation of beads and granules. Suitable diluents include, but are not limited to, dicalcium phosphate dihydrate, calcium sulfate, lactose, sucrose, mannitol, sorbitol, cellulose, microcrystalline cellulose, kaolin, sodium chloride, dry starch, hydrolyzed starches, pregelatinized starch, silicone dioxide, titanium oxide, magnesium aluminum silicate and powdered sugar.

"Binders" are used to impart cohesive qualities to a solid dosage formulation, and thus ensure that a tablet or bead or granule remains intact after the formation of the dosage forms. Suitable binder materials include, but are not limited to, starch, pregelatinized starch, gelatin, sugars (including sucrose, glucose, dextrose, lactose and sorbitol), polyethylene glycol, waxes, natural and synthetic gums such as acacia, tragacanth, sodium alginate, cellulose, including hydroxypropylmethylcellulose, hydroxypropylcellulose, ethylcellulose, and veegum, and synthetic polymers such as acrylic acid and methacrylic acid copolymers, methacrylic acid copolymers, methyl methacrylate copolymers, aminoalkyl methacrylate copolymers, polyacrylic acid/polymethacrylic acid and polyvinylpyrrolidone.

"Lubricants" are used to facilitate tablet manufacture. Examples of suitable lubricants include, but are not limited to, magnesium stearate, calcium stearate, stearic acid, glycerol behenate, polyethylene glycol, talc, and mineral oil.

"Disintegrants" are used to facilitate dosage form disintegration or "breakup" after administration, and generally include, but are not limited to, starch, sodium starch glycolate, sodium carboxymethyl starch, sodium carboxymethylcellulose, hydroxypropyl cellulose, pregelatinized starch, clays, cellulose, alginine, gums or cross-linked polymers, such as cross-linked PVP (Polyplasdone® XL from GAF Chemical Corp).

"Stabilizers" are used to inhibit or retard drug decomposition reactions, which include, by way of example, oxidative reactions. Suitable stabilizers include, but are not limited to, antioxidants, butylated hydroxytoluene (BHT); ascorbic acid, its salts and esters; Vitamin E, tocopherol and its salts; sulfites such as sodium metabisulphite; cysteine and its derivatives; citric acid; propyl gallate, and butylated hydroxyanisole (BHA).

Oral dosage forms, such as capsules, tablets, solutions, and suspensions, can for formulated for controlled release. For example, the one or more compounds and optional one or more additional active agents can be formulated into nanoparticles, microparticles, and combinations thereof, and encapsulated in a soft or hard gelatin or non-gelatin capsule or dispersed in a dispersing medium to form an oral suspension or syrup. The particles can be formed of the drug and a controlled release polymer or matrix. Alternatively, the drug particles can be coated with one or more controlled release coatings prior to incorporation into the finished dosage form.

In another form, the one or more compounds and optional one or more additional active agents are dispersed in a matrix material, which gels or emulsifies upon contact with an aqueous medium, such as physiological fluids. In the case of gels, the matrix swells entrapping the active agents, which are released slowly over time by diffusion and/or degradation of the matrix material. Such matrices can be formulated as tablets or as fill materials for hard and soft capsules.

In still another form, the one or more compounds, and optional one or more additional active agents are formulated into a sold oral dosage form, such as a tablet or capsule, and the solid dosage form is coated with one or more controlled release coatings, such as a delayed release coatings or extended-release coatings. The coating or coatings may also contain the compounds and/or additional active agents.

The materials and methods below are provided to facilitate the practice of the present invention.

Peptide synthesis and purification

Solid-Phase Peptide Synthesis was performed on ProTide Rink amide resin (CEM Corporation cat # R002) using a microwave-assisted CEM Liberty Blue peptide synthesizer (Matthews, NC). Fmoc-protected amino acids were coupled to the resin using 0.25 M Oxyma Pure (CEM Corporation cat # S001) and 0.125 M N, N'-diisopropylcarbodiimide (Sigma-Aldrich cat # D125407) as the activator and activator base, respectively. Fmoc was removed between couplings with 20% Piperidine (Sigma-Aldrich cat # 8.22299.0500). Global deprotection and cleavage of the peptides from the solid-support resin achieved using a CEM Razor instrument over a 40-minute incubation period at 40°C in a mixture of 95% TFA (Sigma-Aldrich cat # 8.08260.2501), 2.5% TIPS (Sigma-Aldrich cat # 233781), and 2.5% water. Peptides were purified on an Agilent 1200 series High-Performance Liquid Chromatography (HPLC) instrument (10-75% HPLC-grade acetonitrile (VWR cat # BDH83639.400) for 20 minutes at 2 mL/min flow rate using an Agilent Zorbax C18 column (5µm, 9.4 x 250 mm) tracked at 280 nm.

Binding analysis of peptides at GPR75

SU75-36 binding at the human GPR75 (372-540 aa region; www.antibodies-online.com cat # ABIN5709609) was measured via a Nicoya Open SPR instrument using His-tagged GPR75 bound to an NTA-coated gold sensor (Nicoya cat # SEN-AU-100-10-NTA, range = 4.08-204 µM)

using HBSS (in-house) at 20 µL/min flow rate. Data was fit via a global, one-to-one model using Nicoya OpenSPR software.

Binding analysis of peptides at hGLP-1R

SU75-36, SU75-37, Ex-4, and ODN binding at the human GLP-1R (21-139aa region; www.rndsystems.com cat # 10956-GL) was measured via a Nicoya Open SPR instrument using His-tagged hGLP-1R bound to an NTA-coated gold sensor (Nicoya cat # SEN-AU-100-10-NTA) using HBSS (in-house) at 20 µL/min flow rate. Data was fit via a global, one-to-one model using Nicoya OpenSPR software. In-house Ex-4 and ODN were used as the positive and negative controls, respectively.

Circular dichroism (CD) spectroscopy

Peptides were prepared in 0.5% saline (pH 7.4) at 40 µM for folded-state analysis on a Chirascan VX (Applied Photophysics, Leatherhead, Surrey, England) spectropolarimeter. Samples were run as duplicate data sets, each as quartet replicates, using a 1 cm quartz cell, 200-260 nm measurement range, 100 nm/min scanning speed, 1 nm bandwidth, 4 second response time, and 1 nm data pitch. The averaged data output was converted from $\Delta\varepsilon$ (M^{-1} cm^{-1}) to molar ellipticity to then obtain their corresponding percent helicity values.

Animals

Adult male Sprague-Dawley rats (Charles River) were individually housed under a 12h-light:12h-dark cycle in a temperature and humidity-controlled satellite vivarium and had *ad libitum* access to water and chow (5001, LabDiet) or a 60% high fat diet (HFD; D12492, Research Diets) and when applicable had *ad libitum* access to kaolin pellets (K50001, Research Diets). Rats were exposed to kaolin for at least 5 days prior to measuring kaolin consumption in pica testing. Except for studies conducted in the bioDAQ, for all feeding studies rats were housed in hanging wire cages to allow for accurate measurement of food spillage. Experiments were conducted under the National Institutes for Health Guide for the Care and Use of Laboratory Animals and all procedures were approved by the Institutional Animal Care and Use Committee at the University of Pennsylvania.

Surgeries

For cannula implantation, rats were anesthetized by intraperitoneal injection of a mixture containing ketamine (90 mg/kg, Butler Animal Health Supply), xylazine (2.7 mg/kg, Anased), and acepromazine (0.64 mg/kg, Butler Animal Health Supply) (KAX) and then placed into a stereotaxic apparatus. Each rat was stereotaxically implanted with a guide cannula (26-ga, Plastics One) aimed at the fourth ventricle (guide cannula coordinates: on midline, 2.5 mm anterior to occipital suture, 5.2 mm ventral to skull; internal cannula aimed 7.2 mm ventral to skull) or the lateral ventricle (guide cannula coordinates: 1.5 mm lateral to midline, 0.9 mm posterior to bregma, 1.8 mm ventral to skull; internal cannula aimed 3.8 mm ventral to skull). For all cannulas, dummies (no projection beyond guide) were inserted in the guide cannula and left until infusions were performed. For all surgeries, rats received post-operative temperature support and analgesia was provided immediately following surgery and for two post-operative days (2 mg/kg meloxicam).

Food and Kaolin Intake Studies

For all studies measuring food intake following drug treatment, central injections were given at a volume of 2 µL using a Hamilton syringe terminating in an injector tip extending 2.0 mm beyond the guide cannula. For acute treatment days, rats were food deprived for 2 hours before the dark cycle and injections were done immediately prior to the dark cycle onset. Food and kaolin intake was measured 1, 3, 6, and 24 hours after injections were completed and food crumbs were weighed and accounted for between each timepoint. Body weight was measured during injections and 24 hours after. Injection treatments were organized in a counterbalanced, within-subjects design and separated by ≥72h.

Drugs

All drugs (SUODN36 (SU75-36) and SUODN37 (SU75-37)) used in these studies were synthesized by the Doyle lab at Syracuse University. In all cases, drugs were dissolved in artificial cerebrospinal fluid (aCSF, Harvard Apparatus). The sequence for SU75-36 and SU75-37 are provided in Table 1.

The following examples are provided to illustrate certain embodiments of the invention. They are not intended to limit the invention in any way.

Example I: Peptide Ligands that bind GPR75

Herein, we describe a novel non-naturally occurring peptide ligand for the highly sought-after orphan GPR75. GPR75 is a major drug discovery goal of the pharmaceutical industry given the association of GPR75 with obesity and metabolic diseases.

Non-naturally occurring peptides were produced using the methods described above. Table 2 provides the sequences of two novel, non-naturally occurring peptide sequences for antagonizing GPR75.

Table 2: Peptide Sequences. Peptides have been synthesized, confirmed, and purified prior to testing. Lowercase letter indicates D-amino acid. Peptides are C-terminally amidated.

Peptide	**Sequence**	**SEQ ID NO**
SU75-36	HsQGTFTSDLSKYLEEEVREFIWLKNGGPSDVNTDRPGLLDLK-NH_2	1
SU75-37	TFTSDLSKYLEEEVREFIWLKNGGPSDVNTDRPGLLDLK-NH_2	2

Peptide synthesis and purity were confirmed using High-Performance Liquid Chromatography (HPLC). Figure 1A shows SU75-36 synthesis at 100% purity while Figure 1B shows SU75-37 synthesis at 98.3% purity.

The binding of SU75-36 to GPR75 was then modeled using HPEPDOCK. Specifically, blind SU75-36/GPR75 receptor in silico docking using HPEPDOCK shows a Docking score of 0.884. Successful administration of SU75-37, as shown herein, indicates that SU75-37 binds the GPR75 receptor similarly.

The binding of SU75-36 was further analyzed using a Surface Plasmon Resonce (SPR) assay which tracks binding of SU75-36 to GPR75 over time. The assay indicated that SU75-36 binds to GPR75 with a K_D of 7.76 μM. (Figure 3) This assay was further analyzed using Nicoya OpenSPR software which showed the best fit parameters using a one-to-one model. The data obtained from this software is present in Tables 3 and 4. K_D was observed to be 7.73×10^{-6} M (7.76 μM).

TABLE 3

Evaluation type: OneToOne

Curve name	Bmax ([Signal (RU)])	ka (1/(M*s))	kd (1/s)	KD (M)	BI ([Signal (RU)])
Drug 36_49.6 µM_7962s fitted	69.54	9.56e2	7.42e-3	7.76e-6	0.00
Drug 36_24.8 µM_8902.74s fitted	69.54	9.56e2	7.42e-3	7.76e-6	0.00
Drug 36_102 µM_9594.85s fitted	69.54	9.56e2	7.42e-3	7.76e-6	0.00
Drug 36_10.2 µM_10677.88s fitted	69.54	9.56e2	7.42e-3	7.76e-6	0.00
Drug 36_68 µM_12735.07s fitted	69.54	9.56e2	7.42e-3	7.76e-6	0.00
Drug 36_102 µM_13348.46s fitted	69.54	9.56e2	7.42e-3	7.76e-6	0.00

TABLE 4

Curve name	Chi2 ([Signal (RU)]^2)	U-value: ka (%)
Drug 36_49.6 µM_7962s fitted	207.75	13.90
Drug 36_24.8 µM_8902.74s fitted	207.75	13.90
Drug 36_102 µM_9594.85s fitted	207.75	13.90
Drug 36_10.2 µM_10677.88s fitted	207.75	13.90
Drug 36_68 µM_12735.07s fitted	207.75	13.90
Drug 36_102 µM_13348.46s fitted	207.75	13.90

The SPR assay was duplicated to determine the binding of SU75-37 to GPR75 over time. The assay indicated that SU75-37 binds to GPR75 with a K_D of 23.8 µM. (Figure 4) As with SU75-36, this assay was further analyzed using Nicoya OpenSPR software. The data obtained from this software is present in Table 5. K_D was observed to be 2.38 x 10^{-5} M (23.8 µM).

TABLE 5

Curve name	Bmax ([Signal (RU)])	ka (1/(M*s))	kd (1/s)	KD (M)	BI ([Signal (RU)])
Drug37 4.93 µM_3517.28s fitted	3.57	5.92e2	1.41e-2	2.38e-5	0.10
Drug37 123.23 µM_3855.01s fitted	110.32	5.92e2	1.41e-2	2.38e-5	0.10
Drug37 12.3 µM_4332.31s fitted	9.39	5.92e2	1.41e-2	2.38e-5	0.10
Drug37 49.3 µM_4673.38s fitted	51.69	5.92e2	1.41e-2	2.38e-5	0.10
Drug37 24.65 µM_5075.24s fitted	8.98	5.92e2	1.41e-2	2.38e-5	0.10
Drug37 92.4 µM_5619.56s fitted	67.67	5.92e2	1.41e-2	2.38e-5	0.10
Drug37 12.3 µM_6783.24s fitted	11.98	5.92e2	1.41e-2	2.38e-5	0.10
Drug37 49.3 µM_6563.82s fitted	47.66	5.92e2	1.41e-2	2.38e-5	0.10
Drug37 4.9 µM_7461.88s fitted	3.80	5.92e2	1.41e-2	2.38e-5	0.10

To confirm the specificity of the peptide ligand binding, the SPR assay was duplicated for both SU75-36 and SU75-37 to determine binding at hGLP-1R with Ex-4 and ODN used as a positive and negative control respectively. SU75-37 did not bind to the hGLP-1R receptor at all.

(Figure 5). Although SU75-36 showed the ability to bind the hGLP-1R receptor, it had a K_D of 182 μM which is indicative of poor binding at this receptor. (Figure 7)

Circular dichroism (CD) spectroscopy was used to analyze the folded-states of both SU75-36 and SU75-37. The peptides each showed spectra indicative of a typical α-helix with percent helicity values greater than 20%. (Figure 9)

Example II: Peptide Ligands Administration to Rats

Herein, we describe administration of novel non-naturally occurring peptide ligand as GPR75 inhibitor for the treatment of obesity.

Diet induced obese (DIO) rats (n = 26) were administered 20μg SU75-36, 100μg SU75-36, 200μg SU75-36, or 20μg SU75-37 by intracerebroventricular injection to the 4th ventricle and observed over 24 hours. One group of rats was administered a vehicle without a GPR75 inhibitor as a negative control. All rats were given *ad libitum* access to access to water 60% high fat diet (HFD). The food intake of each rat was observed 1, 3, 6, and 24 hours after administration of the GPR75 inhibitor. (Figure 7A) Rats in each group that was administered an GPR75 inhibitor showed a significant decrease in food intake when compared to the control. Rats that were administered 200μg SU75-36 showed a further decrease when compared to the any of the other groups.

Rats were weighed at the beginning of the experiment and 24 hours after administration of the GPR75 inhibitor. The weight change of each rat after 24 hours was then calculated. Rats in the control group showed a slight increase in weight after 24 hours. Rats administered any amount of SU75-36 showed a significant decrease in weight after 24 hours. (Figure 7B).

In a separate experiment, chow maintained (n = 10) and diet-induced obese (DIO) rats (n = 12) were administered 20μg SU75-36, 200μg SU75-36, or 20μg SU75-37 by intracerebroventricular injection to the lateral ventricle and observed over 24 hours. One group of rats was administered a vehicle without a GPR75 inhibitor as a negative control. All rats were given *ad libitum* access to access to water and kaolin pellets to assess pica behavior and food, either a standard chow diet or a 60% high fat diet (HFD). The food intake of chow (Fig. 8A) or HFD (Fig. 8B), and kaolin take of chow-maintained rats (Fig. 8C) and HFD-maintained rats (Fig. 8D) of each rat was observed 1, 3, 6, and 24 hours after administration of the GPR75 inhibitor.

Rats in each group that was administered an GPR75 inhibitor showed a significant decrease in food intake when compared to the control. Rats that were administered 200μg SU75-36 showed a further decrease when compared to the any of the other groups. Additionally, the data showed an absence of kaolin intake, an established model of malaise and nausea. This indicates that antagonizing GPR75 with these novel antagonists suppresses energy balance without producing nausea/malaise.

Rats were weighed at the beginning of the experiment and 24 hours after administration of the GPR75 inhibitor. The weight change of each rat after 24 hours was then calculated. Rats in the control group fed HFD chow showed a slight increase in weight after 24 hours. Rats administered any dosage of SU75-36 or SU75-37 showed a significant decrease in weight after 24 hours when fed chow or HFD chow. (Figures 8E, 8F).

Example III: Administration of Peptide Ligands to Human Patients

The information herein above can be applied clinically to patients for therapeutic intervention. A preferred embodiment of the invention comprises clinical application of the information described herein to a patient. This can occur after a patient arrives in the clinic and presents with obesity symptoms or symptoms of a metabolic disorder. A non-limiting example of an effective dose range for a therapeutic compound described herein is from about 0.1 and 5,000 mg/kg of body weight/per day. One of ordinary skill in the art would be able to study the relevant factors and make the determination regarding the effective amount of the therapeutic compound without undue experimentation.

The therapeutic peptides described herein have been shown to be well tolerated and the symptoms were assessed using clinical scores criteria. The treatment protocol can also optionally include administration of effective amounts of one or more of therapeutic agents that treat or inhibit obesity. Such agents, include without limitation Bupropion-naltrexone, Liraglutide (Saxenda), Orlistat (Xenical, Alli), and Phentermine-topiramate. The treatment protocol can also optionally include lifestyle changes or surgeries that help with the management of weight gain.

While certain features of the invention have been described herein, many modifications, substitutions, changes, and equivalents will now occur to those of ordinary skill in the art. It is,

therefore, to be understood that the appended claims are intended to cover all such modifications and changes as fall within the scope of the invention.

What is claimed is:

1. An isolated or purified peptide having the amino acid sequence of SEQ ID NO: 1 or SEQ ID NO: 2 or a functional sequence having at least 95% identity thereto.
2. The peptide according to claim 1, wherein said peptide has an anti-obesity activity.
3. A composition comprising the peptide of claim 1 or claim 2 and a pharmaceutically acceptable carrier.
4. A nucleic acid sequence that encodes the peptide of claim 1 or claim 2.
5. A vector comprising the nucleic acid of claim 4.
6. A method of treating obesity in a subject in need thereof, the method comprising administering an effective amount of the peptide of any one of claims 1-5.
7. A method of treating a metabolic disease or disorder in a subject in need thereof, the method comprising administering an effective amount of the peptide of any one of claims 1-5.
8. The method of claim 7, wherein the metabolic disease or disorder is selected from obesity, diabetes mellitus, dyslipidemia, insulin resistance, hepatic steatosis, hypercholesterolemia, and non-alcoholic fatty liver.
9. The method of claim 8, wherein the diabetes mellitus is selected from type 1 or type 2 diabetes.
10. The method of any one of claims 6-9, further comprising administering a second therapeutic agent that treats or inhibits obesity.
11. The method of any one of claims 6-10, further comprising enforcing lifestyle interventions on diet and/or physical activity on said subject.
12. The method of any one of claims 6-11, wherein the patient has a reduced food intake for 1, 3, 6, and/or 24 hours after administration of said peptide when compared to an untreated control.
13. The method of any one of claims 6-12, wherein the weight of the patient decreases following administration of the peptide.
14. The method of any one of claims 6-13, further comprising assessing the patient for a reduction in obesity symptoms.

15. The method of any once of claims 6-14, wherein said administration is via route selected from systemic, intramuscular, topical, oral, parenteral, transdermal patch, aerosolized, pulmonary, ophthalmic, buccal, and lingually.

Abstract

Compositions and methods for the treatment of obesity and metabolic disorders using an GPR75 inhibitor are provided herein.

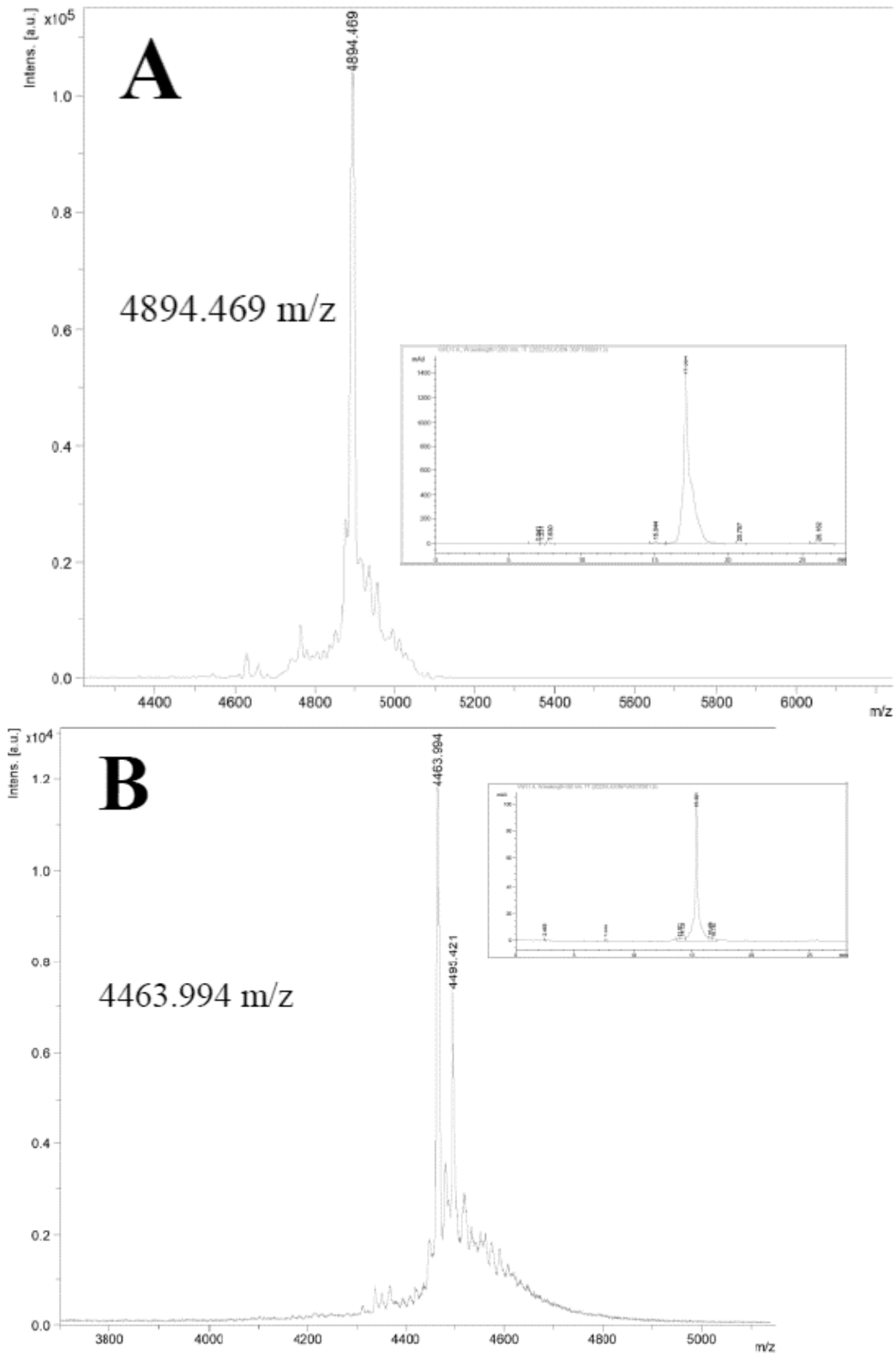
A
Intens. [a.u.]
x10^5
1.0
0.8
0.6
0.4
0.2
0.0
4894.469
4894.469 m/z
4400
4600
4800
5000
5200
5400
5600
5800
6000
m/z
B
Intens. [a.u.]
x10^4
1.2
1.0
0.8
0.6
0.4
0.2
0.0
4463.994
4495.421
4463.994 m/z
3800
4000
4200
4400
4600
4800
5000
m/z

FIGURE 1A-1B

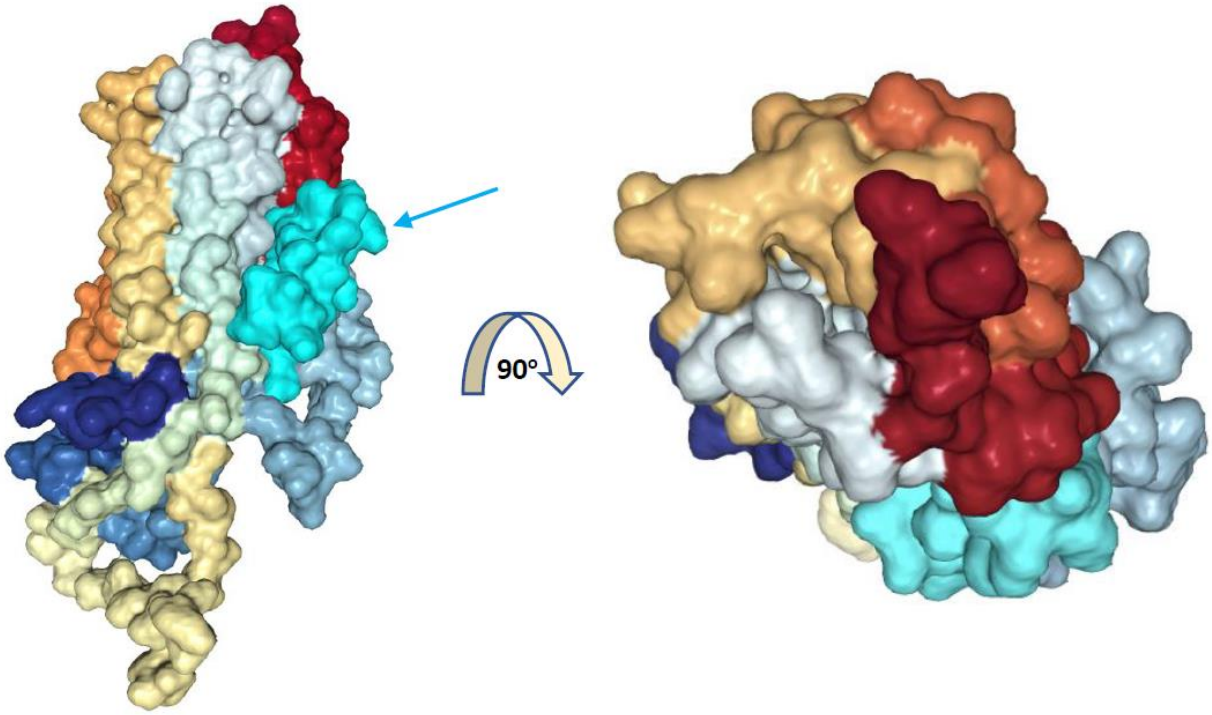

FIGURE 2

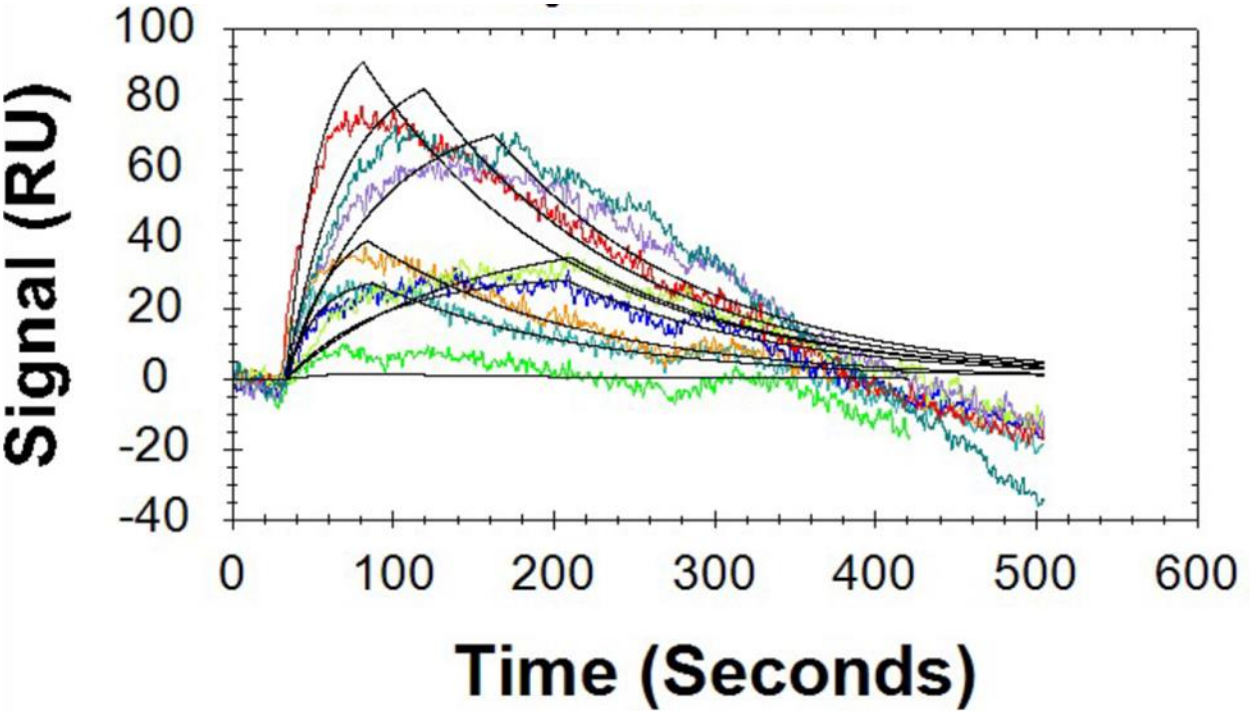

FIGURE 3

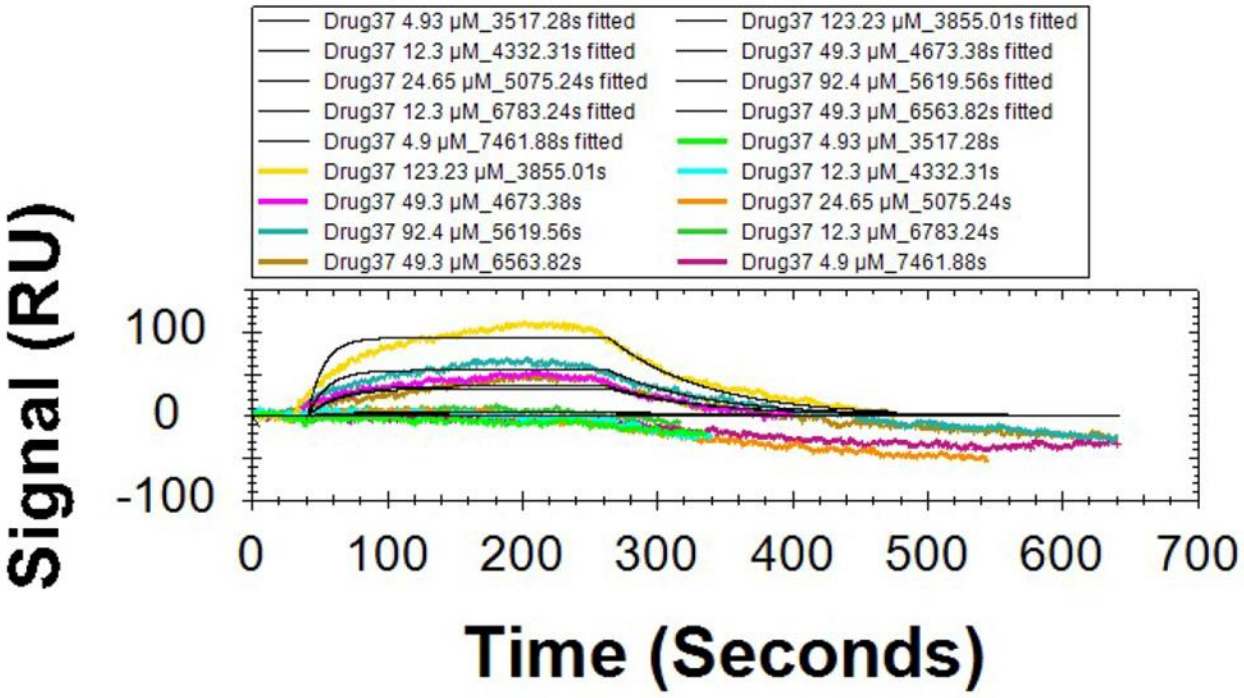

FIGURE 4

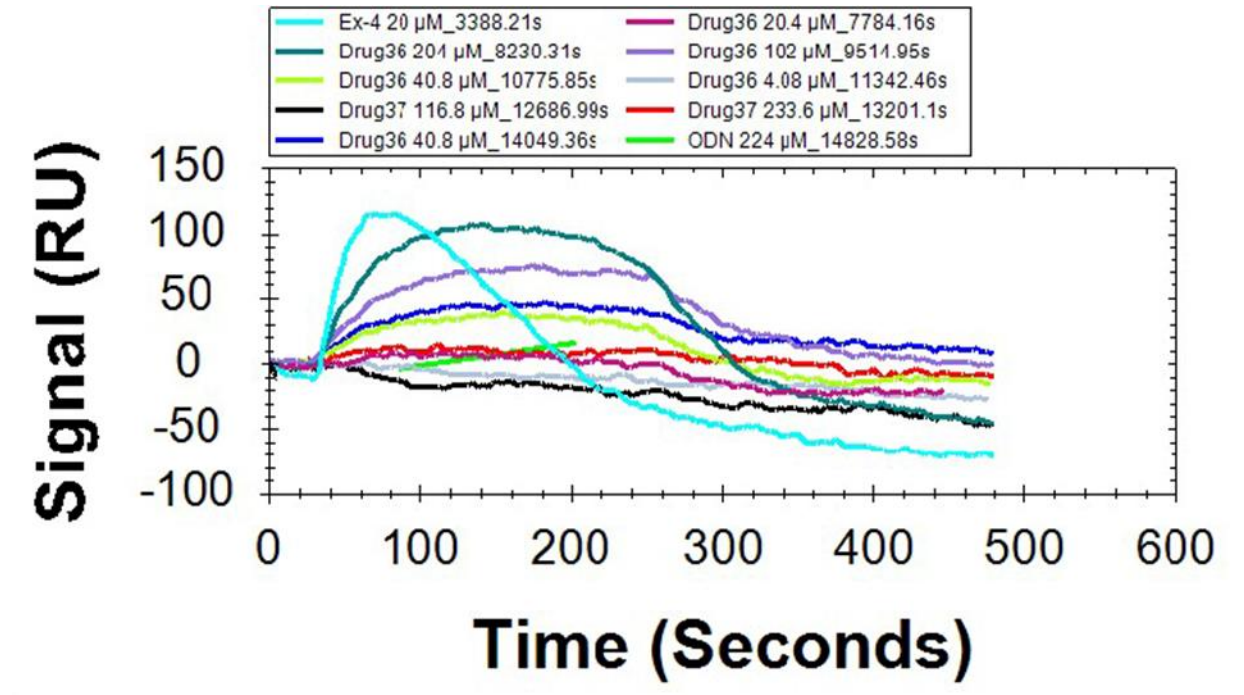

FIGURE 5

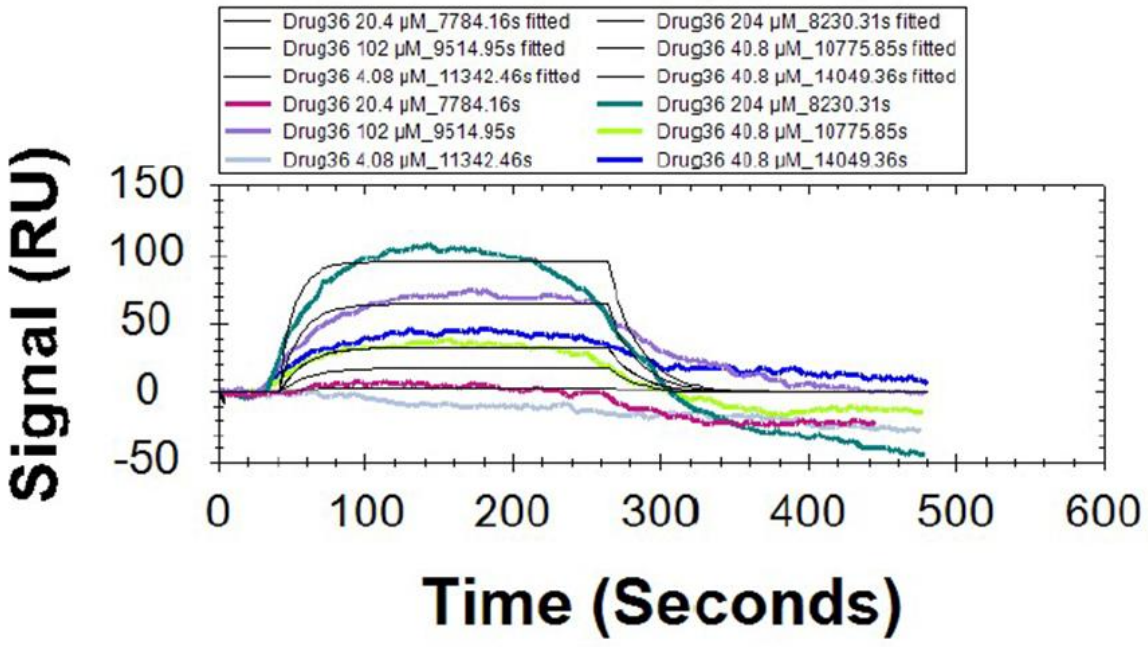
Drug36 20.4 µM_7784.16s fitted
Drug36 102 µM_9514.95s fitted
Drug36 4.08 µM_11342.46s fitted
Drug36 20.4 µM_7784.16s
Drug36 102 µM_9514.95s
Drug36 4.08 µM_11342.46s
Drug36 204 µM_8230.31s fitted
Drug36 40.8 µM_10775.85s fitted
Drug36 40.8 µM_14049.36s fitted
Drug36 204 µM_8230.31s
Drug36 40.8 µM_10775.85s
Drug36 40.8 µM_14049.36s
Signal (RU)
150
100
50
0
-50
0
100
200
300
400
500
600
Time (Seconds)

FIGURE 6

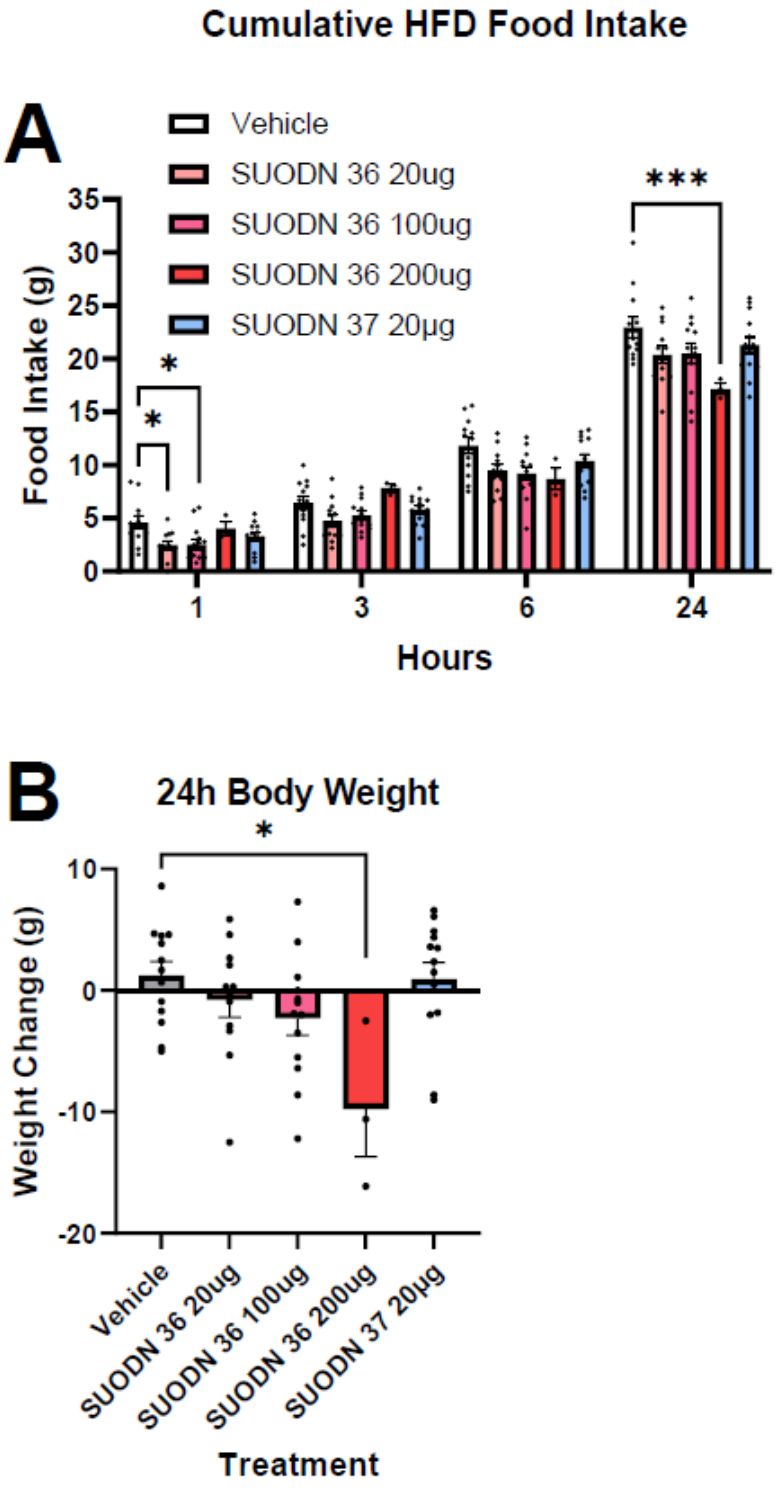
Cumulative HFD Food Intake
A
Vehicle
SUODN 36 20ug
SUODN 36 100ug
SUODN 36 200ug
SUODN 37 20µg
Food Intake (g)
35
30
25
20
15
10
5
0
*
*
***
1
3
6
24
Hours
B
24h Body Weight
*
Weight Change (g)
10
0
-10
-20
Vehicle
SUODN 36 20ug
SUODN 36 100ug
SUODN 36 200ug
SUODN 37 20µg
Treatment

FIGURE 7A-7B

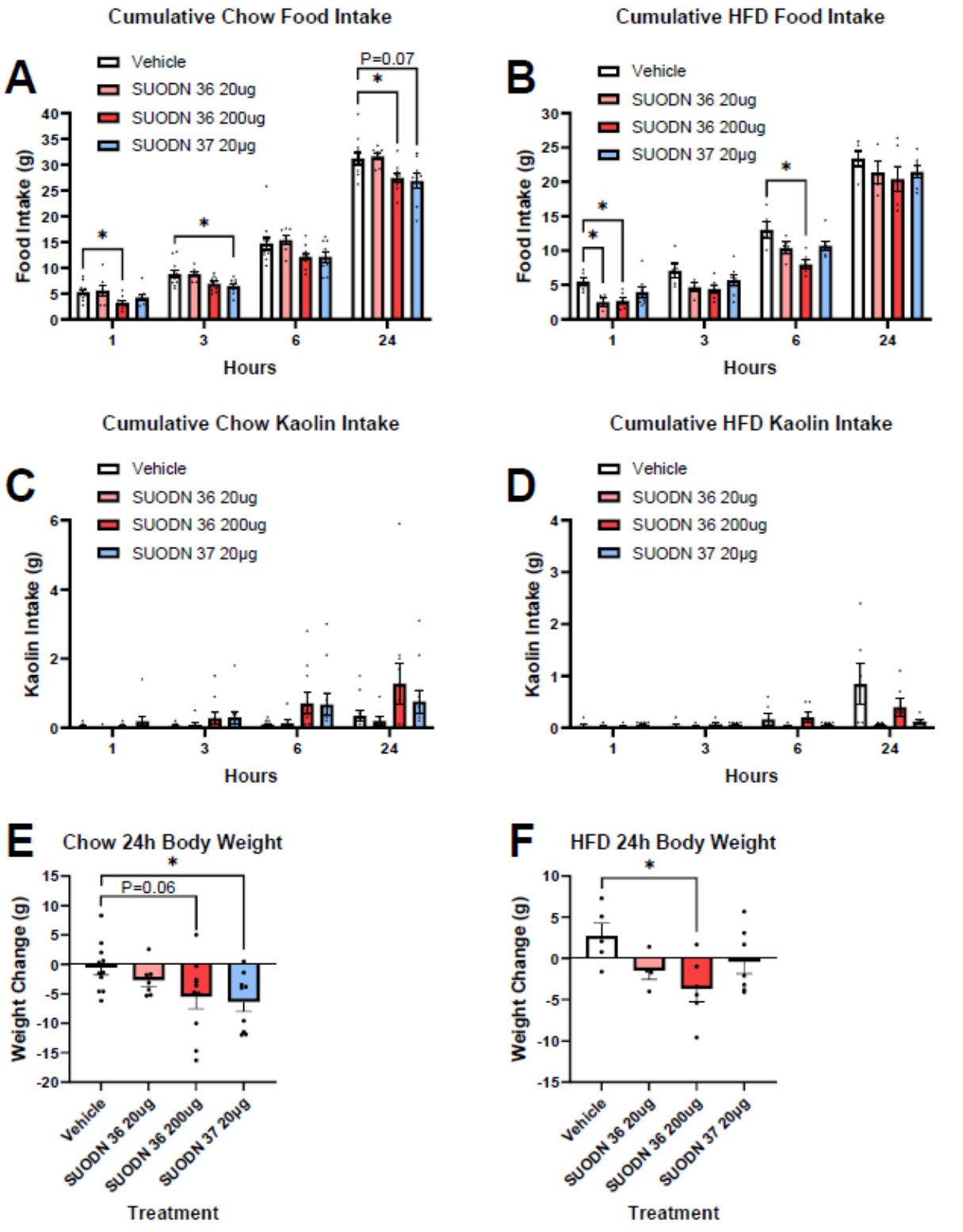
Cumulative Chow Food Intake
A
Vehicle
SUODN 36 20ug
SUODN 36 200ug
SUODN 37 20µg
P=0.07
Food Intake (g)
Hours
Cumulative HFD Food Intake
B
Cumulative Chow Kaolin Intake
C
Kaolin Intake (g)
Cumulative HFD Kaolin Intake
D
E
Chow 24h Body Weight
P=0.06
Weight Change (g)
Treatment
F
HFD 24h Body Weight

FIGURE 8A-8F

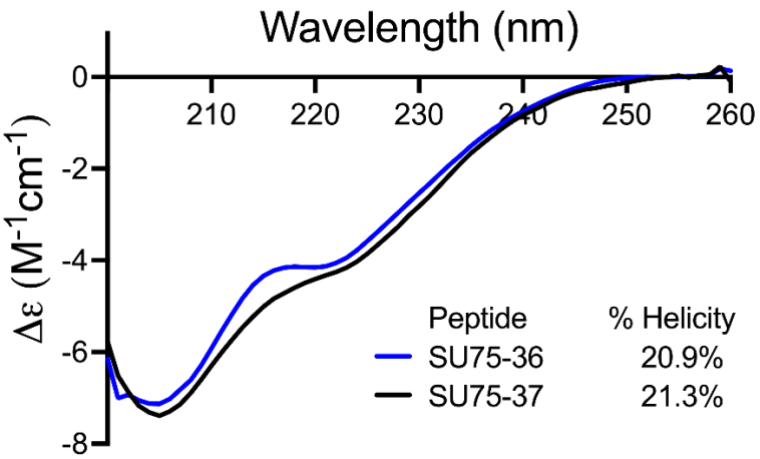
Wavelength (nm)
0
-2
-4
-6
-8
210
220
230
240
250
260
Δε (M-1cm-1)
Peptide
% Helicity
SU75-36
20.9%
SU75-37
21.3%

FIGURE 9

Compositions Comprising Octadecaneuropeptides (ODN) and Synthetic Derivatives Thereof and Methods of Use for Modulation of Food Intake, Obesity, Body Weight and Inhibition of Nausea and Emesis

By

Matthew Hayes

Richard C. Crist, III

Caroline Geisler

Benjamin Reiner

Robert Doyle

Kylie Chichura

Incorporation-by-Reference of Material Submitted in Electronic Form

The Contents of the electronic sequence listing (UPNK-114P.xml; Size: X,XXX bytes; and Date of Creation: November 2022) is herein incorporated by reference in its entirety.

Field of the Invention

The present invention relates to the fields of neuroactive compounds and methods of use thereof for the management and treatment of food intake, obesity, nausea and emesis. More specifically, certain endozepines, e.g., octadecaneuropeptide (ODN) and its precursor diazepam-binding inhibitor (DBI) peptide, and derivatives thereof are provided which act in the central nervous system and protect neurons and astrocytes from programmed cell death by reducing inflammation, apoptosis and oxidative stress.

Background of the Invention

Several publications and patent documents are cited throughout the specification in order to describe the state of the art to which this invention pertains. Each of these citations is incorporated by reference herein as though set forth in full.

Obesity affects more than 40% of the U.S. population. The excess fat in obesity was originally thought to be harmless (benign). However, data show that excess fat causes chemical changes in your blood that increase your heart disease risk. When your fat cells become enlarged, they give off hormones that produce chronic inflammation. Inflammation can lead to the body no longer using insulin efficiently, thereby producing insulin resistance. Insulin resistance is associated with trouble regulating blood sugar levels, which can result in metabolic syndrome. This condition is associated with several risk factors that increase your chance of developing heart disease, such as: High blood lipids (high LDL cholesterol, high total cholesterol and high triglycerides), high blood pressure (hypertension), high blood sugar (hyperglycemia), and low HDL cholesterol. Obesity increases other heart disease risk factors, including sleep disorders and type 2 diabetes.

Overweight and obesity are defined by the World Health Organization as abnormal or excessive fat that accumulates and presents a risk to health. Obesity is measured in body mass index (BMI), which is a person's weight (in kilograms) divided by the square of his or her height (in meters). A person with a BMI of 30 or more is generally considered obese. A person with a BMI equal to or more than 25 is considered overweight. Losing 5% to 10% of body weight can lower the risk factors for heart disease while small lifestyle changes can help improve metabolic syndrome, which lessens your heart disease risk.

Lifestyle interventions on diet and physical activity are the first option for the management of obesity and overweight, but efficacy can be limited, and weight regain is common. Bariatric surgery can be highly effective for weight loss in severely obese or high-risk patients, but its use is limited by its invasive nature, cost, risk of perioperative adverse events including perioperative death. While a few drugs have demonstrated efficacy in weight-reduction, pharmacotherapy for the treatment of obesity is limited by the modest weight loss induced by most drugs, development of dependency, side effect profile of some agents, contraindications, low compliance, and barriers to treatment including under-prescription.

Clearly, a need exists for improved, non-toxic pharmaceuticals for the treatment of obesity that lead to sustained and manageable control of food intake and a reduction in the adverse health consequences

Summary of the Invention

In accordance with the invention,

Brief Description of the Drawings

Figs. 1: Central ODN dose dependently suppresses food intake in chow and HFD rats. Effect of 4th ventricle ODN (0.2, 2, or 20 µg/2 µL in aCSF) treatment on 24h food intake (grams; A, C) and body weight change (B, D) in chow and HFD fed rats. All data presented as mean ± SEM.

Fig. 2. Meal pattern data following central ODN administration in chow fed rats. Effect of 4th ventricle ODN (0.2, 2, or 20 µg/2 µL in aCSF) treatment on food intake (grams; A-D), number of meals (E-H), time spent eating meals (seconds; I-L), meal length (seconds/meal; M-P), and meal size (grams/meal; Q-T) at time intervals 1, 6, 6-12, and 12-24 hours after administration. All data presented as mean ± SEM.

Fig. 3. Heat map representation of bout and meal parameters during the first 3 hours following central ODN administration in chow fed rats. Effect of 4th ventricle ODN (0.2, 2, or 20 µg/2 µL in aCSF) on food intake (grams; A), number of bouts (B), time spent eating bouts (seconds; C), number of meals (D), and time spent eating meals (E). * indicates difference from Veh (P=0.05). All data presented as mean ± SEM.

Fig. 4. Meal pattern data following central ODN administration in HFD fed rats. Effect of 4th ventricle ODN (0.2, 2, or 20 µg/2 µL in aCSF) treatment on food intake (grams; A-D), number of meals (E-H), time spent eating meals (seconds; I-L), meal length (seconds/meal; M-P), and meal size (grams/meal; Q-T) at time intervals 1, 6, 6-12, and 12-24 hours after administration. All data presented as mean ± SEM.

Fig. 5. Heat map representation of bout and meal parameters during the 24 hours following central ODN administration in HFD fed rats. Effect of 4th ventricle ODN (0.2, 2, or 20 µg/2 µL in aCSF) on food intake (grams; A), number of bouts (B), time spent eating bouts (seconds; C), number of meals (D), and time spent eating meals (E). * indicates difference from Veh (P=0.05). All data presented as mean ± SEM.

Fig. 6. First feeding event data following central ODN administration in chow and HFD fed rats. Effect of 4th ventricle ODN (0.2, 2, or 20 µg/2 µL in aCSF) on latency to the first meal (seconds;

A, E), size of the first meal (grams; B, F), latency to first bout (seconds; C, G), size of first bout (grams, D, H) in chow and HFD fed rats. All data presented as mean ± SEM.

Fig. 7. Effect of hindbrain 4th ventricle recombinant DBI protein on meal pattern food intake in chow and HFD rats. Central recombinant DBI protein suppresses food intake in chow fed rats. Effect of 4th ventricle recombinant DBI protein (20 µg/2 µL) on 24h food intake in chow (A) and HFD (B) fed rats and body weight change in chow and HFD rats (C). All data presented as mean ± SEM.

Fig. 8. Heat map representation of bout and meal parameters during the 24 hours following central recombinant DBI protein administration in chow fed rats. Effect of 4th ventricle recDBI (20 µg/2 µL in aCSF) on food intake (grams; A), number of bouts (B), time spent eating bouts (seconds; C), number of meals (D), and time spent eating meals (E). * indicates difference from Veh (P=0.05). All data presented as mean ± SEM.

Fig. 9. Pretreatment with an antibody against DBI attenuates central exendin-4 induced hypophagia in chow fed rats. Rats were pretreated 4th ventricle with a DBI antibody (AB 3 µg/3 µL) or vehicle followed by 4th ventricle treatment with ODN (20 µg/2 µL), Ex-4 (0.3 µg/2 µL), or vehicle. 24 hour food intake in chow (A) and HFD (B) fed rats, kaolin intake in chow (C) and HFD (D) fed rats, and body weight change in chow (E) and HFD (F) fed rats following treatments. # indicates difference from Veh/Veh (P=0.05). All data presented as mean ± SEM.

Fig. 10. Fig. 10. Pretreatment with an ODN antagonist attenuates central exendin-4 induced hypophagia. Rats were pretreated 4th ventricle with an ODN antagonist (AntOP 200 µg/2 µL) or vehicle followed by 4th ventricle treatment with ODN (20 µg/2 µL), Ex-4 (0.3 µg/2 µL), or vehicle. 24 hour food intake in chow (A) and HFD (B) fed rats, kaolin intake in chow (C) and HFD (D) fed rats, and body weight change in chow (E) and HFD (F) fed rats following treatments. # indicates difference from Veh/Veh (P=0.05). All data presented as mean ± SEM.

Fig. 11. Pretreatment with an ODN antagonist attenuates peripheral Liraglutide induced hypophagia. Rats were pretreated lateral ventricle with an ODN antagonist (AntOP 100 µg/2 µL) or vehicle followed by intraperitoneal treatment with Liraglutide (50 µg/kg), or vehicle. 48 hour food intake in chow (A) and HFD (B) fed rats, kaolin intake in chow (C) and HFD (D) fed rats,

and body weight change in chow (E) and HFD (F) fed rats following treatments. All data presented as mean ± SEM.

Fig. 12. 5-day combined treatment with ODN enhances peripheral Liraglutide induced hypophagia. Rats were treated 4th ventricle with ODN (100 µg/2 µL) or vehicle followed by intraperitoneal treatment with Liraglutide (25 µg/kg) or vehicle for 5 days. Daily (A) and cumulative (B) food intake, daily (C) and cumulative (D) kaolin intake, and daily body weight (E) in HFD fed rats following treatments. Isolated day 1 food intake (F). All data presented as mean ± SEM.

Fig. 13. Central tridecaneuropeptide (TDN; cleavage product of ODN) suppresses 24h food intake in HFD fed rats. Effect of 4th ventricle TDN (20 µg/2 µL) on 24 hour food intake in chow (A) and HFD (B) fed rats, kaolin intake in chow (C) and HFD (D) fed rats, and body weight change in chow (E) and HFD (F) fed rats following treatments. All data presented as mean ± SEM.

Fig. 14. Central TDN suppresses 24h food intake in rats. Effect of lateral ventricle TDN (20 µg/2 µL or 200 µg/2 µL) on 24 hour food intake in chow (A) and HFD (B) fed rats, kaolin intake in chow (C) and HFD (D) fed rats, and body weight change in chow (E) and HFD (F) fed rats following treatments. All data presented as mean ± SEM.

Fig. 15. Peripheral ODN suppresses 24h food intake in shrews without including emesis. Effect of intraperitoneal ODN (500 µg/kg or 5000 µg/kg) on 24 hour food intake (A) body weight change (B) and emetic episodes (C) following treatments. All data presented as mean ± SEM.

Fig. 16. Central ODN-based drugs suppress 24h food intake in HFD fed rats. Effect of 4th ventricle ODN, TDN, SUODN04, and SUODN05 (20 µg/kg) on 24 hour food intake (A) body weight change (B) following treatments. All data presented as mean ± SEM.

Fig. 17. Nutritional State and GLP-1R Agonism Regulates NTS/AP DBI Protein Expression. Rats had ad libitum access to food or were 24h fasted and received a 4th ventricle injection of vehicle of Exendin-4 (0.3 µg/2 µL) 90 minutes before sacrifice. Brains were collected and stained with a DBI antibody to detect DBI protein expression, fluorescence of which was quantified at low, moderate, and strong levels using HALO-AI software. DBI protein expression was determined in the NTS at the pre-AP level in chow (A) and HFD (B) fed rats, in the NTS at

the AP level in chow (C) and HFD (D) fed rats, in the NTS at the 4th ventricle level in chow (E) and HFD (F) fed rats, and in the AP in chow (G) and HFD (H) fed rats.

Fig. 18. Magnitude of DBI and Vimentin Co-Expression in Tanycyte Populated DVC Areas. In the AP, 87.9% of vimentin positive cells co-express DBI and 16.9% of DBI positive cells co-express vimentin. In the subpostrema border between the AP and NTS, 74.8% of vimentin positive cells co-express DBI and 47.4% of DBI positive cells co-express vimentin. In the 4th ventricle border, 58.9% of vimentin positive cells co-express DBI and 81.5% of DBI positive cells co-express vimentin.

Fig. 19. GLP-1R Agonism Upregulates DBI mRNA. 4th ventricle treatment of vehicle or Exendin-4 (0.3 µg/2 µL) in chow fed rats 90 minutes before sacrifice and mRNA quantification. All data presented as mean ± SEM.

Fig. 20. Central ODN Signaling Mediates Hindbrain Glucose Sensing. 24 hour food intake (A), 1 hour blood glucose (B), and body weight change (C) in chow fed rats pretreated 4th ventricle with an ODN agonist (OP 20 µg/2 µL) or vehicle followed by 4th ventricle treatment with 5-TG (210 µg/2 µL) or vehicle. 24 hour food intake (D), 1 hour blood glucose (E), and body weight change (F) in chow fed rats pretreated 4th ventricle with an ODN antagonist (AntOP 100 µg/2 µL) or vehicle followed by 4th ventricle treatment with glucose (5.5 mM in 3µL) or vehicle. All data presented as mean ± SEM.

Fig. 21. Rat AP/NTS DBI 10X DBI Expression Profile. Rat DBI expression was primarily seen in AP and NTS clusters 1-9, including microglia, endothelial cells, oligodendrocytes and precursors, astrocytes and tanycytes.

Fig. 22. Human AP DBI 10X DBI Expression Profile. Human DBI expression was highest in oligodendrocyte precursor cells, astrocytes, and tanycytes.

Fig. 23. Confirmation of synthesis and purity of select peptides. (A) ODN (1911.13 g/mol; 11.521 min TR; 100% pure), (B) TDN (1454.63 g/mol; 11.587 min TR; 100% pure), (C) OP (909.95 g/mol; 5.017 min TR; 96.4% pure), (D) AntOP (909.95 g/mol; 14.941 min TR; 96% pure), and (E) SUODN-03 (553.68 g/mol; 11.372 min TR; 95% pure) by MALDI-ToF MS and (inset) RP-HPLC. TR = retention time on Zorbax analytical C18 column.

Detailed Description

Endozepines are a family of astroglia-secreted proteins including the diazepam binding inhibitor (DBI) and its processing products, which have been originally isolated and characterized as endogenous ligands of benzodiazepine receptors. It is now clearly established that the octadecaneuropeptide ODN, acting through the central-type benzodiazepine receptor or an orphan metabotropic receptor, exerts important functions such as pro-conflict behavior, induction of anxiety, inhibition of pentobarbital-provoked sleep, decrease of water consumption and reduction of food intake. To mediate its effects, ODN regulates both glial cell and neuronal activities by acting on neurosteroid biosynthesis and/or neuropeptide expression. In addition, ODN stimulates astrocyte proliferation and protects both neurons and astrocytes from oxidative stress-induced cell death. The antiapoptotic effect of ODN on neural cells is mediated through activation of the ODN metabotropic receptor positively coupled to PKA, PKC and MAPK/ERK transduction pathways, which ultimately reduces the pro-apoptotic gene Bax and stimulates Bcl-2 expression, thereby inhibiting intracellular reactive oxygen species accumulation. The imbalance in favor of Bcl2 promotes mitochondria functions and blocks in turn caspases activation while at the same time, ODN also activates the endogenous antioxidant system i.e. glutathione biosynthesis, and expression and activities of antioxidant enzymes. In cultured astrocytes, DBI expression is up-regulated during moderate oxidative stress, and authentic ODN production is increased, suggesting that ODN may act as a paracrine factor protecting neighboring neurons.

Obesity alters multiple aspects of hindbrain ODN signaling, including a longer time course of ODN hypophagia, including possible difference in diazepam binding inhibitor (DBI) cleavage to ODN (recombinant DBI protein is hypophagic in chow but not high-fat diet (HFD) rats), the ODN antagonist AntOP is hypophagic in HFD but not chow rats providing a possible new site of action and/or modified target interactions.

ODN signaling may be downstream of, and partially mediate, the effects of glucagon-like peptide-1 receptor (GLP-1R) signaling, and thus partially mediates all existing GLP-1-based pharmacotherapies currently used to treat diabetes and obesity. Nonetheless, ODN and novel

peptide derivatives thereof (*e.g.* TDN) signaling appears to not be maxed out by GLP-1R agonism as ODN and GLP-1R agonist co-treatment have additive hypophagia effects.

Antagonizing ODN signaling with either an antibody targeted against DBI or a peptide antagonist of the ODN receptor (AntOP), attenuates the hypophagic and body weight effects of central and peripheral GLP-1R agonists. Because nutritional state regulates hindbrain DBI protein expression, GLP-1R signaling may contribute to this effect. ODN may facilitate transport of GLP-1R agonists across the blood brain barrier, specifically at the tanycyte borders, both across the 4th ventricle and the sub-postrema border, to regulate brain penetrance of GLP-1R agonists. Multiple cleavage products of ODN are physiologically active and suppress food intake, allowing for the creation of new forms of non-naturally occurring optimized peptides.

In the present studies the ODN receptor has been deorphanized. We have discovered that ODN, and novel peptide derivatives of ODN (e.g. TDN) are endogenous antagonists of the relaxin-3 receptor (RXFP3). Relaxin-3 is an orexigenic neuropeptide that promotes weight gain and becomes upregulated in obesity to defend against weight loss. Thus, antagonizing this signal to preserve a higher body weight may powerfully help overcome the typically observed weight loss plateau seen with current anti-obesity pharmacotherapies.

Deorphanization occurred in two critical steps. First a novel method for binding ODN-biotin onto a Nicoya streptavidin sensor chip was employed for GPCR / protein extraction of bound substances following rat tissue lysate of the dorsal vagal complex for MS/MS sequencing. Among a multitude of ODN bound proteins, MS sequencing confirmed ODN bound strongly to an extracellular protease (Rhomboid related protein 2). Detailed methods are included in Example 2 and the results provided in Tables 2 and 3 below. The bound proteins are identified in Table 4. See note below regarding out to present genes/proteins newly identified as ODN binders.

Definitions

Unless otherwise defined herein, scientific and technical terms used in connection with the present application shall have the meanings that are commonly understood by those of ordinary skill in the art. In addition to definitions included in this sub-section, further definitions of terms are interspersed throughout the text.

In this invention, “a“ or “an“ means “at least one“ or “one or more,“ etc., unless clearly indicated otherwise by context. The term “or“ means “and/or“ unless stated otherwise. In the case of a multiple-dependent claim, however, use of the term “or“ refers back to more than one preceding claim in the alternative only.

Furthermore, a compound "selected from the group consisting of" refers to one or more of the compounds in the list that follows, including mixtures (i.e. combinations) of two or more of the compounds. According to the present invention, an isolated, or biologically pure molecule is a compound that has been removed from its natural milieu. As such, "isolated" and "biologically pure" do not necessarily reflect the extent to which the compound has been purified. An isolated compound of the present invention can be obtained from its natural source, can be produced using laboratory synthetic techniques or can be produced by any such chemical synthetic route.

The terms “agent“ and “test compound“ denote a chemical compound, a mixture of chemical compounds, a biological macromolecule, or an extract made from biological materials such as bacteria, plants, fungi, or animal (particularly mammalian) cells or tissues. Biological macromolecules include peptides, peptide/DNA complexes, siRNA, shRNA, antisense oligonucleotides, , and any nucleic acid based molecule which encoded the proteins described herein.

It is also contemplated that the term “compound” or “compounds” refers to the compounds discussed herein and includes precursors and derivatives of the compounds, and pharmaceutically acceptable salts of the compounds, precursors, and derivatives.

The phrase "consisting essentially of" when referring to a particular nucleotide or amino acid means a sequence having the properties of a given SEQ ID NO. For example, when used in reference to an amino acid sequence, the phrase includes the sequence per se and molecular modifications that would not affect the functional and novel characteristics of the sequence.

A "derivative" of a polypeptide, polynucleotide or fragments thereof means a sequence modified by varying the sequence of the construct, e.g. by manipulation of the nucleic acid encoding the protein or by altering the protein itself. "Derivatives" of a polypeptide sequence refers to any isolated amino acid molecule that contains significant sequence similarity to the peptide sequence or a part thereof. In addition, "derivatives" include such isolated nucleic acids

containing modified nucleotides or mimetics of naturally-occurring nucleotides encoding the derivative peptides.

The term "functional" as used herein implies that the nucleic or amino acid sequence is functional for the recited assay or purpose.

For purposes of the invention, "nucleic acid", "nucleotide sequence" or a "nucleic acid molecule" as used herein refers to any DNA or RNA molecule, either single or double stranded and, if single stranded, the molecule of its complementary sequence in either linear or circular form. In discussing nucleic acid molecules, a sequence or structure of a particular nucleic acid molecule may be described herein according to the normal convention of providing the sequence in the 5' to 3' direction. With reference to nucleic acids of the invention, the term "isolated nucleic acid" is sometimes used. This term, when applied to DNA, refers to a DNA molecule that is separated from sequences with which it is immediately contiguous in the naturally occurring genome of the organism in which it originated. For example, an "isolated nucleic acid" may comprise a DNA molecule inserted into a vector, such as a plasmid or virus vector, or integrated into the genomic DNA of a prokaryotic or eukaryotic cell or host organism. Alternatively, this term may refer to a DNA that has been sufficiently separated from (e.g., substantially free of) other cellular components with which it would naturally be associated. "Isolated" is not meant to exclude artificial or synthetic mixtures with other compounds or materials, or the presence of impurities that do not interfere with the fundamental activity, and that may be present, for example, due to incomplete purification. When applied to RNA, the term "isolated nucleic acid" refers primarily to an RNA molecule encoded by an isolated DNA molecule as defined above. Alternatively, the term may refer to an RNA molecule that has been sufficiently separated from other nucleic acids with which it would be associated in its natural state (i.e., in cells or tissues). An isolated nucleic acid (either DNA or RNA) may further represent a molecule produced directly by biological or synthetic means and separated from other components present during its production.

A "specific binding pair" comprises a specific binding member (sbm) and a binding partner (bp) which have a particular specificity for each other and which in normal conditions bind to each other in preference to other molecules. Examples of specific binding pairs are antigens and antibodies, biotin and streptavidin, ligands and receptors and complementary nucleotide sequences. The skilled person is aware of many other examples. Further, the term

"specific binding pair" is also applicable where either or both of the specific binding member and the binding partner comprise a part of a large molecule. In embodiments in which the specific binding pair comprises nucleic acid sequences, they will be of a length to hybridize to each other under conditions of the assay, preferably greater than 10 nucleotides long, more preferably greater than 15 or 20 nucleotides long.

According to the present invention, an isolated or biologically pure molecule or cell is a compound that has been removed from its natural milieu. As such, "isolated" and "biologically pure" do not necessarily reflect the extent to which the compound has been purified. An isolated compound of the present invention can be obtained from its natural source, can be produced using laboratory synthetic techniques or can be produced by any such chemical synthetic route.

The term "delivery" as used herein refers to the introduction of foreign molecule (i.e., miRNA encoding the polypeptide of interest) into cells. The term "administration" as used herein means the introduction of a foreign molecule into the body or a cell. The term is intended to be synonymous with the term "delivery".

Peptides

The peptides of the invention inhibit or modulate ODN activity. The terms “inhibition” or “inhibit” refer to a decrease or cessation of any event (such as protein ligand binding) or to a decrease or cessation of any phenotypic characteristic or to the decrease or cessation in the incidence, degree, or likelihood of that characteristic. To “reduce” or “inhibit” is to decrease, reduce or arrest an activity, function, and/or amount as compared to a reference. It is not necessary that the inhibition or reduction be complete. For example, in certain embodiments, “reduce” or “inhibit” refers to the ability to cause an overall decrease of 20% or greater. In another embodiment, “reduce” or “inhibit” refers to the ability to cause an overall decrease of 50% or greater. In yet another embodiment, “reduce” or “inhibit” refers to the ability to cause an overall decrease of 75%, 85%, 90%, 95%, or greater.

The term “modulate” as used herein refers to the ability of a compound to change an activity in some measurable way as compared to an appropriate control. As a result of the presence of compounds in the assays, activities can increase or decrease as compared to controls in the absence of these compounds. Preferably, an increase in activity is at least 25%, more preferably at least 50%, most preferably at least 100% compared to the level of activity in the

absence of the compound. Similarly, a decrease in activity is preferably at least 25%, more preferably at least 50%, most preferably at least 100% compared to the level of activity in the absence of the compound. A compound that increases a known activity is an “agonist”. One that decreases, or prevents, a known activity is an “antagonist”.

The term “inhibitor” refers to an agent that slows down or prevents a particular chemical reaction, signaling pathway or other process, or that reduces the activity of a particular reactant, compound, or enzyme.

The term “octadecaneuropeptide” or “ODN” refers and its precursor diazepam-binding inhibitor (DBI) are peptides belonging to the family of endozepines. Endozepines are exclusively produced by astroglial cells in the central nervous system of mammals, and their release is regulated by stress signals and neuroactive compounds. There is now compelling evidence that the gliopeptide ODN protects cultured neurons and astrocytes from apoptotic cell death induced by various neurotoxic agents. a

The phrase “ODN antagonist” refers to a class of agents that inhibit the action of ODN. The phrase “ODN agonist” refers to a class of agents that potentiate or enhance ODN activity. The peptides of interest herein include naturally occurring and derivatives of ODN and are provided in Table 1.

Table 1.

ODN and ODN based peptide sequences. Peptides ODN, AntOP, TDN, OP and SUODN-03, -04, and -05 have been synthesized and assayed. Gln(alkyn), Ala(Alkyn), Gly(Alkyn) and Lys(N3) are modified amino acids for bioconjugation including lipidation and/or fluorescent tagging*.

ODN: Gln-Ala-Thr-Val-Gly-Asp-Val-Asn-Thr-Asp-Arg-Pro-Gly-Leu-Leu-Asp-Leu-Lys

AntOP: Arg-Pro-Gly-Leu-(D-Leu)-Asp-Leu-Lys

TDN (SUODN-01): Asp-Val-Asn-Thr-Asp-Arg-Pro-Gly-Leu-Leu-Asp-Leu-Lys

OP (SUODN-02): Arg-Pro-Gly-Leu-Leu-Asp-Leu-Lys

SUODN-03 Arg-Pro-Gly-Leu-Leu

SUODN-04: Asp-Val-Asn-Thr-Asp-Arg-Pro-Gly

SUODN-05: Asp-Val-Asn-Thr-Asp-Arg-Pro-Gly-Leu-Leu

SUODN-06: Gln-Ala-Thr-Val-Gly-Asp-Val-Asn-Thr-Asp-Arg-Pro-Gly

SUODN-07: Gln-Ala-Thr-Val-Gly-Asp-Val-Asn-Thr-Asp-Arg-Pro-Gly-Leu-Leu

SUODN-08: Gln(alkyn)-Ala-Thr-Val-Gly-Asp-Val-Asn-Thr-Asp-Arg-Pro-Gly-Leu-Leu-Asp-Leu-Lys(N3)
SUODN-09: Gln(alkyn)-Ala-Thr-Val-Gly-Asp-Val-Asn-Thr-Asp-Arg-Pro-Gly-Lys(N3)-Leu-Asp-Leu-Lys
SUODN-10: Gln(alkyn)-Ala-Thr-Val-Gly-Asp-Val-Asn-Thr-Asp-Arg-Pro-Gly-Leu-Lys(N3)-Asp-Leu-Lys
SUODN-11: Gln(alkyn)-Ala-Thr-Val-Gly-Asp-Val-Asn-Thr-Asp-Arg-Pro-Gly-Leu-Leu-Asp-Lys(N3)-Lys
SUODN-12: Gln-Ala(alkyn)-Thr-Val-Gly-Asp-Val-Asn-Thr-Asp-Arg-Pro-Gly-Leu-Leu-Asp-Leu-Lys(N3)
SUODN-13: Gln-Ala(alkyn)-Thr-Val-Gly-Asp-Val-Asn-Thr-Asp-Arg-Pro-Gly-Lys(N3)-Leu-Asp-Leu-Lys
SUODN-14: Gln-Ala(alkyn)-Thr-Val-Gly-Asp-Val-Asn-Thr-Asp-Arg-Pro-Gly-Leu-Lys(N3)-Asp-Leu-Lys
SUODN-15: Gln-Ala(alkyn)-Thr-Val-Gly-Asp-Val-Asn-Thr-Asp-Arg-Pro-Gly-Leu-Leu-Asp-Lys(N3)-Lys
SUODN-16: Gln-Ala-Thr-Val-Gly(alkyn)-Asp-Val-Asn-Thr-Asp-Arg-Pro-Gly-Leu-Leu-Asp-Leu-Lys(N3)
SUODN-17: Gln-Ala-Thr-Val-Gly(alkyn)-Asp-Val-Asn-Thr-Asp-Arg-Pro-Gly- Lys(N3)-Leu-Asp-Leu-Lys
SUODN-18: Gln-Ala-Thr-Val-Gly(alkyn)-Asp-Val-Asn-Thr-Asp-Arg-Pro-Gly-Leu-Lys(N3)-Asp-Leu-Lys
SUODN-19: Gln-Ala-Thr-Val-Gly(alkyn)-Asp-Val-Asn-Thr-Asp-Arg-Pro-Gly-Leu-Leu-Asp-Lys(N3)-Lys
*SEQ ID NOS; 1-21 are shown in descending order

In certain embodiments, the present invention includes peptides that have at least 80% identity to anyone of the peptides described herein. In certain embodiments, the peptides of the invention have a sequence identity of at least 90% identity, at least 91% identity, at least 92% identity, at least 93% identity, at least 94% identity, at least 95% identity, at least 96% identity, at least 97% identity, at least 98% identity, at least 99% identity, or 100% identity.

Preferably, the peptides of the above-described sequences and functional equivalents thereof which act to modulate obesity upon administration. As used herein, the term “functional equivalent” is intended to include amino acid sequence variants having amino acid substitutions in some or all of the proteins, or amino acid additions or deletions in some of the proteins. The amino acid substitutions are preferably conservative substitutions. Examples of the conservative substitutions of naturally occurring amino acids are as follow: aliphatic amino acids (Gly, Ala, and Pro), hydrophobic amino acids (Ile, Leu, and Val), aromatic amino acids (Phe, Tyr, and Trp), acidic amino acids (Asp, and Glu), basic amino acids (His, Lys, Arg, Gln, and Asn), and sulfur-containing amino acids (Cys, and Met). The deletions of amino acids are preferably located in a region which is not directly involved in the activity of the peptide.

In the present context, the term “variant” refers to a nucleic acid sequence or polypeptide comprising a sequence, which differs (by deletion, insertion, and/or substitution of a nucleic acid or amino acid including non-naturally occurring amino acid) in one or more nucleic acid or amino acid positions from that of a wild type nucleic acid or polypeptide sequence.

In the present context, the term “linker” refers to a connection between two protein coding sequences or their protein products. Linkers comprise a stretch of contiguous nucleic acids or amino acids, which holds at least one cleavage site that enables separation of the genes or their products through cleavage of the linker. Preferably, the linker comprises a cleavage site at its 5′ end and a cleavage site at its 3′ end, or a cleavage site at its N-terminal end and a cleavage site at its C-terminal end.

The peptide may be fused to biotin, Poly-lysine, lysozyme, Green fluorescent protein (and derivatives), SUMO or other desired proteinaceous tags for attachment to electrodes, nanotubes or desired surfaces (e.g. electro-transducing, mineral), as well as any protein interaction partner desired to be investigated Production of the desired peptide sequence can be carried out in *E.coli* using existing technologies, e.g. with protein fusion tags that can either be removed or left as desired. In certain embodiments, the peptide of interest may be fused via a linker.

The peptide can be expressed as a fusion to larger proteins, facilitating expression at large scales, ease of purification, and ensuring quality of product. Expression systems can also be leveraged to generate large sequence libraries, allowing for directed evolution for targeted properties. Fusion also allows the peptide to be incorporated into other proteins useful for the treatment of obesity or other metabolic disorders.

As noted above, the invention also includes polynucleotides encoding the peptides or fusion proteins comprising the peptide described herein. Those of skill in the art understand the degeneracy of the genetic code and that a variety of polynucleotides can encode the same polypeptide. In some embodiments, the polynucleotides (i.e., polynucleotides encoding the fusion polypeptides) may be codon-optimized for expression in a particular cell including, without limitation, a plant cell, bacterial cell, or algal cell. Any polynucleotide sequences may be used which encode a desired form of the polypeptides described herein. The polynucleotide sequences which encode the polypeptides of the invention represent non-naturally occurring sequences. Computer programs for generating degenerate coding sequences are available and can be used for this purpose. Pencil, paper, the genetic code, and a human hand can also be used to generate degenerate coding sequences.

In the present context, the term “codon optimization” refers to changing the codons of a nucleotide sequence without altering the amino acid sequence that it encodes in order to favor

expression in a specific species. Codon optimization may be used to increase the abundance of the peptide or protein that the nucleotide sequence encodes since “rare” codons are removed and replaced with abundant codons.

Regarding the fusion polypeptides disclosed herein, the phrases “% sequence identity,” “percent identity,” or “% identity” refer to the percentage of residue matches between at least two amino acid sequences aligned using a standardized algorithm. Methods of amino acid sequence alignment are well-known. Some alignment methods take into account conservative amino acid substitutions. Such conservative substitutions generally preserve the charge and hydrophobicity at the site of substitution, thus preserving the structure (and therefore function) of the polypeptide. Percent identity for amino acid sequences may be determined as understood in the art. The structural similarity is typically at least 90% identity, at least 91% identity, at least 92% identity, at least 93% identity, at least 94% identity, at least 95% identity, at least 96% identity, at least 97% identity, at least 98% identity, or at least 99% identity.

Polypeptide sequence identity may be measured over the length of an entire defined polypeptide sequence, for example, as defined by a particular SEQ ID number, or may be measured over a shorter length, for example, over the length of a fragment taken from a larger, defined polypeptide sequence, for instance, a fragment of at least 15, at least 20, at least 30, at least 40, at least 50, at least 70 or at least 150 contiguous residues. Such lengths are exemplary only, and it is understood that any fragment length supported by the sequences shown herein, may be used to describe a length over which percentage identity may be measured.

In vitro synthesis of peptides

Peptides can be synthesized chemically either in solution or on a solid phase. The process involves directed and selective formation of an amide bond between an N-protected amino acid and an amino acid bearing a free amino group and protected carboxylic acid. In solid phase synthesis, the carboxyl protecting group is linked to a polymer support. Following bond formation, the amino-protecting group of the dipeptide is removed, and the next N-protected amino-acid is coupled.

Solid-phase peptide synthesis (SSPS) is the most frequently used method of peptide synthesis due to its efficiency, simplicity, speed, and ease of parallelization. SPPS involves sequential addition of amino and side-chain protected amino acid residues to an amino acid or peptide attached to an insoluble polymeric support. Either an acid-labile Boc group (Boc SPPS)

or base-labile Fmoc-group (Fmoc SPPS) is used for N-α-protection. After removal of this protecting group, the next protected amino acid is added using either a coupling reagent or pre-activated protected amino acid derivative. The C-terminal amino acid is anchored to the resin *via* a linker, the nature of which determines the conditions required to release the peptide from the support after chain extension. Side-chain protecting groups are often chosen so as to be cleaved simultaneously with detachment of the peptide from the resin.

Peptides of 50 amino acids can be routinely prepared although the synthesis of proteins of over 100 amino acid are commonly reported. Longer proteins can be made by native chemical ligation of fully deprotected peptides in solution. With this method, it is possible to synthesize natural peptides that are difficult to express in bacteria, to incorporate unnatural or D-amino acids, and to generate cyclic, branched, labelled, and post -translations modified petides.

Liquid-phase peptide synthesis, usually utilizing Boc or Z-amino protection, has been superseded by solid-phase peptide synthesis except for existing processes of large-scale synthesis of peptides for industrial purposes. Desired sequences can be developed by any one of the several commercial entities who provide this service for a fee, including Sigma Aldrich, Avivasysbio for example.

Vectors and Production

Transgenic cells expression said polynucleotides also form an aspect of the invention. A transgenic cell may be obtained by introducing a recombinant nucleic acid molecule that encodes a protein of this disclosure. As used herein, the term “recombinant nucleic acid” refers to a polynucleotide that is manipulated by human intervention. A recombinant nucleic acid molecule can contain two or more nucleotide sequences that are linked in a manner such that the product is not found in a cell in nature. In particular, the two or more nucleotide sequences can be operatively linked and, for example, can encode a fusion polypeptide. A recombinant nucleic acid molecule also can be based on, but manipulated so as to be different, from a naturally occurring polynucleotide, for example, a polynucleotide having one or more nucleotide changes such that a first codon, which normally is found in the polynucleotide, is biased for chloroplast codon usage, or such that a sequence of interest is introduced into the polynucleotide, for

example, a restriction endonuclease recognition site or a splice site, a promoter, a DNA origin of replication, or the like.

Any appropriate technique for introducing recombinant nucleic acid molecules into cells may be used. Techniques for nuclear and chloroplast transformation are known and include, without limitation, electroporation, biolistic transformation (also referred to as micro-projectile/particle bombardment), agitation in the presence of glass beads, and Agrobacterium-based transformation.

As used herein, the term "construct" refers to recombinant polynucleotides including, without limitation, DNA and RNA, which may be single-stranded or double-stranded and may represent the sense or the antisense strand. Recombinant polynucleotides are polynucleotides formed by laboratory methods that include polynucleotide sequences derived from at least two different natural sources or they may be synthetic. Constructs thus may include new modifications to endogenous genes introduced by, for example, genome editing technologies. Constructs may also include recombinant polynucleotides created using, for example, recombinant DNA methodologies.

A "vector" is capable of transferring gene sequences to target cells. Typically, "vector construct," "expression vector," and "gene transfer vector," mean any nucleic acid construct capable of directing the expression of a gene of interest and which can transfer gene sequences to target cells. Thus, the term includes cloning and expression vehicles, as well as integrating vectors.

The constructs and vectors provided herein may be prepared by methods available to those of skill in the art. Notably each of the constructs or expression cassettes claimed are recombinant molecules and as such do not occur in nature. Generally, the nomenclature used herein and the laboratory procedures utilized in the present invention include molecular, biochemical, and recombinant DNA techniques that are well known and commonly employed in the art. Standard techniques available to those skilled in the art may be used for cloning, DNA and RNA isolation, amplification and purification. Such techniques are thoroughly explained in the literature.

The constructs and expression cassettes provided herein may include a promoter operably linked to any one of the polynucleotides described herein but need not have a promoter and may be used for homologous recombination into the cell. Alternatively, the constructs may include a

promoter and the promoter may be a heterologous promoter or an endogenous promoter associated with the polypeptide.

As used herein, the terms “heterologous promoter,” “promoter,” “promoter region,” or “promoter sequence” refer generally to transcriptional regulatory regions of a gene, which may be found at the 5′ or 3′ side of the polynucleotides described herein, or within the coding region of the polynucleotides, or within introns in the polynucleotides. Typically, a promoter is a DNA regulatory region capable of binding RNA polymerase in a cell and initiating transcription of a downstream (3′ direction) coding sequence. The typical 5′ promoter sequence is bounded at its 3′ terminus by the transcription initiation site and extends upstream (5′ direction) to include the minimum number of bases or elements necessary to initiate transcription at levels detectable above background. Within the promoter sequence is a transcription initiation site (conveniently defined by mapping with nuclease S1), as well as protein binding domains (consensus sequences) responsible for the binding of RNA polymerase.

In some embodiments, the disclosed polynucleotides are operably connected to the promoter. As used herein, a polynucleotide is “operably connected” or “operably linked” when it is placed into a functional relationship with a second polynucleotide sequence. For instance, a promoter is operably linked to a polynucleotide if the promoter is connected to the polynucleotide such that it may affect transcription of the polynucleotides. In various embodiments, the polynucleotides may be operably linked to at least 1, at least 2, at least 3, at least 4, at least 5, or at least 10 promoters.

Heterologous promoters useful in the practice of the present invention include, but are not limited to, constitutive, inducible, temporally-regulated, developmentally regulated, chemically regulated, tissue-preferred and tissue-specific promoters. The heterologous promoter may be a plant, animal, bacterial, fungal, or synthetic promoter.

Methods of Treatment and Administration

The term “reducing” or “inhibiting” as used herein refers to administering a compound prior to, or during the onset of clinical symptoms of a disease or conditions so as to reduce a physical manifestation of aberrations associated with the disease or condition.

The term “in need of treatment” as used herein refers to a judgment made by a caregiver (e.g. physician, nurse, nurse practitioner, or individual in the case of humans; veterinarian in the

case of animals, including non-human mammals) that a subject requires or will benefit from treatment. This judgment is made based on a variety of factors that are in the realm of a care giver's expertise, but that includes the knowledge that the subject is ill, or will be ill, as the result of a condition that is treatable by the disclosed compounds.

As used herein, "subject" includes, but is not limited to, animals, plants, bacteria, viruses, parasites and any other organism or entity. The subject can be a vertebrate, more specifically a mammal (e.g., a human, horse, pig, rabbit, dog, sheep, goat, non-human primate, cow, cat, guinea pig or rodent), a fish, a bird or a reptile or an amphibian. The subject can be an invertebrate, more specifically an arthropod (e.g., insects and crustaceans). The term does not denote a particular age or sex. Thus, adult and newborn subjects, as well as fetuses, whether male or female, are intended to be covered. A patient refers to a subject afflicted with a disease or disorder. The term "patient" includes human and veterinary subjects.

The terms "treat", "treating", and "treatment" as used herein, refer to eliciting the desired biological response, such as a therapeutic and prophylactic effect, respectively. In some embodiments, a therapeutic effect comprises one or more of a decrease/reduction in obesity, a decrease/reduction in the severity of obesity (such as, for example, a reduction or inhibition of development or obesity), a decrease/reduction in symptoms and obesity-related effects, delaying the onset of symptoms and obesity-related effects, reducing the severity of symptoms of obesity-related effects, reducing the severity of an acute episode, reducing the number of symptoms and obesity-related effects, reducing the latency of symptoms and obesity-related effects, an amelioration of symptoms and obesity-related effects, reducing secondary symptoms, reducing secondary infections, preventing relapse to obesity, decreasing the number or frequency of relapse episodes, increasing latency between symptomatic episodes, increasing time to sustained progression, expediting remission, inducing remission, augmenting remission, speeding recovery, or increasing efficacy of or decreasing resistance to alternative therapeutics, and/or an increased survival time of the affected host animal, following administration of the agent or composition comprising the agent. A prophylactic effect may comprise a complete or partial avoidance/inhibition or a delay of obesity development/progression (such as, for example, a complete or partial avoidance/inhibition or a delay), or an increased survival time of the affected host animal, following administration of a therapeutic protocol. Treatment of obesity encompasses the treatment of subjects already diagnosed as having any form of obesity at any

clinical stage or manifestation, the delay of the onset or evolution or aggravation or deterioration of the symptoms or signs of obesity, and/or preventing and/or reducing the severity of obesity.

In another aspect, provided herein are methods for treating a patient comprising administration of the peptides of interest. In any of the embodiments described herein, the subject can be obese, or have excessive weight, elevated BMI, elevated body fat mass, percentage, or volume, and/or excessive food intake. In any of the embodiments described herein, the subject can be obese. In any of the embodiments described herein, the subject can have excessive weight. In any of the embodiments described herein, the subject can have elevated BMI. In any of the embodiments described herein, the subject can have elevated body fat mass, percentage, or volume. In any of the embodiments described herein, the subject can have excessive food intake.

Symptoms of obesity include, but are not limited to, excess body fat accumulation (particularly around the waist), breathlessness, increased sweating, snoring, inability to cope with sudden physical activity, feeling very tired every day, back and joint pains, skin problems (from moisture accumulating in the folds of skin).

Methods of treating a subject having obesity, the methods comprising administering a ODN peptide or functional derivative thereof to the subject are provided. Also disclosed are methods of treating a subject having excessive weight, the methods comprising administering a ODN peptide to the subject. The present disclosure also provides methods of treating a subject having elevated BMI, the methods comprising administering an effective amount of ODN peptide to the subject. Methods of treating a subject having elevated body fat mass, percentage, or volume, the methods comprising administering an ODN peptide to the subject are also described. Finally, treatment of a subject having excessive food intake, comprising administering an ODN peptide to the subject are also disclosed.

The present disclosure also provides methods of treating a subject to prevent weight gain or to maintain weight loss, the method comprising administering an effective amount of ODN peptide to the subject.

In certain embodiments, methods of treating a metabolic disease or disorder in a subject, comprising administering an effective amount of ODN peptide to the subject are provided.

As used herein, the term “metabolic disease” or “metabolic disorder” is also called a metabolic syndrome, and refers to a set of abnormal states such as an increase in body fat, an

increase in blood pressure, an increase in blood sugar, and abnormal lipids in blood, which increase the risk of cerebral cardiovascular diseases and diabetes mellitus. The metabolic disease is not a single disease but a comprehensive disease caused by genetic predisposition and environmental factors, and in the present invention, may be selected from the group consisting of obesity, diabetes mellitus, dyslipidemia, insulin resistance, hepatic steatosis, hypercholesterolemia, and non-alcoholic fatty liver, and may be more preferably obesity or diabetes mellitus, but is not limited thereto.

As used herein, the term “diabetes mellitus”, as a type of metabolic disease such as an insufficient amount of insulin secreted or absence of normal function, is characterized by high blood sugar with high blood glucose concentration, and causes various symptoms and signs due to hyperglycemia and releases glucose from urine. Diabetes mellitus includes type 1 diabetes mellitus which occurs when insulin is not secreted largely due to the destruction of pancreatic beta cells, and type 2 diabetes mellitus caused by insufficient insulin secretion in the body or insulin resistance in which cells do not respond to insulin. In the present invention, diabetes mellitus includes both type 1 diabetes mellitus and type 2 diabetes mellitus. In certain embodiments, the method further comprises administering a second therapeutic agent that treats or inhibits obesity. Nonlimiting examples of therapeutic agents that treat or inhibit obesity and/or increased BMI include, but are not limited to, GLP1R agonists, melanocortin 4 receptor (MC4R) agonists, sibutramine, orlistat, phentermine, lorcaserin, naltrexone, liraglutide, diethylpropion, bupropion, metformin, pramlintide, topiramate, and zonisamide, or any combination thereof.

Administration of the therapeutic agents that treat or inhibit obesity and/or ODN peptide modulators can be repeated, for example, after one day, two days, three days, five days, one week, two weeks, three weeks, one month, five weeks, six weeks, seven weeks, eight weeks, two months, or three months. The repeated administration can be at the same dose or at a different dose. The administration can be repeated once, twice, three times, four times, five times, six times, seven times, eight times, nine times, ten times, or more. For example, according to certain dosage regimens a subject can receive therapy for a prolonged period of time such as, for example, 6 months, 1 year, or more.

Administration of the therapeutic agents that treat or inhibit obesity and/or ODN peptides can occur by any suitable route including, but not limited to, parenteral, intravenous, oral, buccal, subcutaneous, intra-arterial, intracranial, intrathecal, intraperitoneal, topical, intranasal, or

intramuscular. Pharmaceutical compositions for administration are desirably sterile and substantially isotonic and manufactured under GMP conditions. Pharmaceutical compositions can be provided in unit dosage form (i.e., the dosage for a single administration). Pharmaceutical compositions can be formulated using one or more physiologically and pharmaceutically acceptable carriers, diluents, excipients or auxiliaries. The formulation depends on the route of administration chosen. The term "pharmaceutically acceptable" means that the carrier, diluent, excipient, or auxiliary is compatible with the other ingredients of the formulation and not substantially deleterious to the recipient thereof.

The compounds can be combined with one or more pharmaceutically acceptable carriers and/or excipients that are considered safe and effective and may be administered to an individual without causing undesirable biological side effects or unwanted interactions. The carrier is all components present in the pharmaceutical formulation other than the active ingredient or ingredients. See, e.g., Remington's Pharmaceutical Sciences, latest edition, by E.W. Martin Mack Pub. Co., Easton, PA, which discloses typical carriers and conventional methods of preparing pharmaceutical compositions that can be used in conjunction with the preparation of formulations of the compounds described herein and which is incorporated by reference herein. These most typically would be standard carriers for administration of compositions to humans. In one aspect, humans and non-humans, including solutions such as sterile water, saline, and buffered solutions at physiological pH. Other compounds will be administered according to standard procedures used by those skilled in the art.

These compositions can take the form of solutions, suspensions, emulsion, tablets, pills, capsules, powders, sustained-release formulations and the like.

In some embodiments, the therapeutic agents that treat or inhibit obesity and/or ODN peptide modulatgors (such as any of the peptide ligands disclosed herein) are administered intrathecally (i.e., introduction into the subarachnoid space of the spinal cord or into the spinal canal so that the therapeutic agent can reach the cerebrospinal fluid of a subject, or introduction into the anatomic space or potential space inside a sheath, including, by way of non-limiting examples, the arachnoid membrane of the brain or spinal cord). In some embodiments, intrathecal administration results in the therapeutic agent acting on, without limitation, the cortex, the cerebellum, the striatum, the cervical spine, the lumbar spine, or the thoracic spine. Therapeutic agents administered intrathecally may ultimately act on targets throughout the entire

central nervous system. In some embodiments, the intrathecal administration is into the cisterna magna or by the lumbar area or region. In some embodiments, the intrathecal administration into the lumbar area or region results in delivery of the therapeutic agent to the distal spinal canal.

Exemplary methods for intrathecal administration are described in, for example, Lazorthes et al., Advances in Drug Delivery Systems and Applications in Neurosurgery, 143-192. In some embodiments, the intrathecal administration is by injection, by bolus injection, by a catheter, or by a pump. In some embodiments, the intrathecal administration is by lumber puncture. In some embodiments, the pump is an osmotic pump. In some embodiments, the pump is implanted into subarachnoid space of the spinal canal, below the skin of the abdomen, or behind the chest wall. In some embodiments, the intrathecal administration is by an intrathecal delivery system for a therapeutic substance including a reservoir containing a volume of the therapeutic agent and a pump configured to deliver at least a portion of the therapeutic substance contained in the reservoir. In some embodiments, intrathecal administration is through intermittent or continuous access to an implanted intrathecal drug delivery device (IDDD). In some embodiments, the therapeutic substance is an inhibitory nucleic acid molecule. In some embodiments, the amount of the nucleic acid molecule administered intrathecally ranges from about 10 μg to about 2 mg, from about 50 μg to about 1500 μg, or from about 100 μg to about 1000 μg. In some embodiments, the therapeutic agent is disposed within a pharmaceutical composition. In some embodiments, the pharmaceutical composition does not comprise a preservative.

Parenteral Formulations

The peptides described herein can be formulated for parenteral administration. For example, parenteral administration may include administration to a patient intravenously, intradermally, intraarterially, intraperitoneally, intralesionally, intracranially, intraarticularly, intraprostatically, intrapleurally, intratracheally, intravitreally, intratumorally, intramuscularly, subcutaneously, subconjunctivally, intravesicularly, intrapericardially, intraumbilically, by injection, and by infusion.

Parenteral formulations can be prepared as aqueous compositions using techniques known in the art. Typically, such compositions can be prepared as injectable formulations, for example, solutions or suspensions; solid forms suitable for using to prepare solutions or

suspensions upon the addition of a reconstitution medium prior to injection; emulsions, such as water-in-oil (w/o) emulsions, oil-in-water (o/w) emulsions, and microemulsions thereof, liposomes, or emulsomes.

If for intravenous administration, the compositions are packaged in solutions of sterile isotonic aqueous buffer. Where necessary, the composition may also include a solubilizing agent. The components of the composition are supplied either separately or mixed together in unit dosage form, for example, as a dry lyophilized powder or concentrated solution in a hermetically sealed container such as an ampoule or sachet indicating the amount of active agent. If the composition is to be administered by infusion, it can be dispensed with an infusion bottle containing sterile pharmaceutical grade water or saline. Where the composition is administered by injection, an ampoule of sterile water or saline can be provided so that the ingredients may be mixed prior to injection.

The carrier can be a solvent or dispersion medium containing, for example, water, ethanol, one or more polyols (e.g., glycerol, propylene glycol, and liquid polyethylene glycol), oils, such as vegetable oils (e.g., peanut oil, corn oil, sesame oil, etc.), and combinations thereof. The proper fluidity can be maintained, for example, by the use of a coating, such as lecithin, by the maintenance of the required particle size in the case of dispersion and/or by the use of surfactants. In many cases, it will be preferable to include isotonic agents, for example, sugars or sodium chloride.

Solutions and dispersions of the active compounds as the free acid or base or pharmacologically acceptable salts thereof can be prepared in water or another solvent or dispersing medium suitably mixed with one or more pharmaceutically acceptable excipients including, but not limited to, surfactants, dispersants, emulsifiers, pH modifying agents, viscosity modifying agents, and combination thereof.

Suitable surfactants may be anionic, cationic, amphoteric or nonionic surface-active agents. Suitable anionic surfactants include, but are not limited to, those containing carboxylate, sulfonate and sulfate ions. Examples of anionic surfactants include sodium, potassium, ammonium of long chain alkyl sulfonates and alkyl aryl sulfonates such as sodium dodecylbenzene sulfonate; dialkyl sodium sulfosuccinates, such as sodium dodecylbenzene sulfonate; dialkyl sodium sulfosuccinates, such as sodium bis-(2-ethylthioxyl)-sulfosuccinate; and alkyl sulfates such as sodium lauryl sulfate. Cationic surfactants include, but are not limited

to, quaternary ammonium compounds such as benzalkonium chloride, benzethonium chloride, cetrimonium bromide, stearyl dimethylbenzyl ammonium chloride, polyoxyethylene, and coconut amine. Examples of nonionic surfactants include ethylene glycol monostearate, propylene glycol myristate, glyceryl monostearate, glyceryl stearate, polyglyceryl-4-oleate, sorbitan acylate, sucrose acylate, PEG-150 laurate, PEG-400 monolaurate, polyoxyethylene monolaurate, polysorbates, polyoxyethylene octylphenylether, PEG-1000 cetyl ether, polyoxyethylene tridecyl ether, polypropylene glycol butyl ether, Poloxamer® 401, stearoyl monoisopropanolamide, and polyoxyethylene hydrogenated tallow amide. Examples of amphoteric surfactants include sodium N-dodecyl-.beta.-alanine, sodium N-lauryl-β-iminodipropionate, myristoamphoacetate, lauryl betaine, and lauryl sulfobetaine.

The formulation can contain a preservative to prevent the growth of microorganisms. Suitable preservatives include, but are not limited to, parabens, chlorobutanol, phenol, sorbic acid, and thimerosal. The formulation may also contain an antioxidant to prevent degradation of the active agent(s).

The formulation is typically buffered to a pH of 3-8 for parenteral administration upon reconstitution. Suitable buffers include, but are not limited to, phosphate buffers, acetate buffers, and citrate buffers.

Water-soluble polymers are often used in formulations for parenteral administration. Suitable water-soluble polymers include, but are not limited to, polyvinylpyrrolidone, dextran, carboxymethylcellulose, and polyethylene glycol.

Sterile injectable solutions can be prepared by incorporating the active compounds in the required amount in the appropriate solvent or dispersion medium with one or more of the excipients listed above, as required, followed by filtered sterilization. Generally, dispersions are prepared by incorporating the various sterilized active ingredients into a sterile vehicle which contains the basic dispersion medium and the required other ingredients from those listed above. In the case of sterile powders for the preparation of sterile injectable solutions, the preferred methods of preparation are vacuum-drying and freeze-drying techniques which yield a powder of the active ingredient plus any additional desired ingredient from a previously sterile-filtered solution thereof. The powders can be prepared in such a manner that the particles are porous in nature, which can increase dissolution of the particles. Methods for making porous particles are well known in the art.

The parenteral formulations described herein can be formulated for controlled release including immediate release, delayed release, extended release, pulsatile release, and combinations thereof.

Nano- and microparticles

For parenteral administration, the one or more compounds, and optional one or more additional active agents, can be incorporated into microparticles, nanoparticles, or combinations thereof that provide controlled release of the compounds and/or one or more additional active agents. In forms wherein the formulations contains two or more peptides, the peptides can be formulated for the same type of controlled release (e.g., delayed, extended, immediate, or pulsatile) or the peptides can be independently formulated for different types of release (e.g., immediate and delayed, immediate and extended, delayed and extended, delayed and pulsatile, etc.).

For example, the compounds and/or one or more additional active agents can be incorporated into polymeric microparticles, which provide controlled release of the peptide(s). Release of the peptide(s) is controlled by diffusion of the protein(s) out of the microparticles and/or degradation of the polymeric particles by hydrolysis and/or enzymatic degradation. Suitable polymers include ethylcellulose and other natural or synthetic cellulose derivatives.

Polymers, which are slowly soluble and form a gel in an aqueous environment, such as hydroxypropyl methylcellulose or polyethylene oxide, can also be suitable as materials for protein containing microparticles. Other polymers include, but are not limited to, polyanhydrides, poly(ester anhydrides), polyhydroxy acids, such as polylactide (PLA), polyglycolide (PGA), poly(lactide-co-glycolide) (PLGA), poly-3-hydroxybutyrate (PHB) and copolymers thereof, poly-4-hydroxybutyrate (P4HB) and copolymers thereof, polycaprolactone and copolymers thereof, and combinations thereof.

Alternatively, the protein(s) can be incorporated into microparticles prepared from materials which are insoluble in aqueous solution or slowly soluble in aqueous solution, but are capable of degrading within the GI tract by means including enzymatic degradation, surfactant action of bile acids, and/or mechanical erosion. As used herein, the term “slowly soluble in water” refers to materials that are not dissolved in water within a period of 30 minutes. Preferred examples include fats, fatty substances, waxes, wax-like substances and mixtures thereof.

Suitable fats and fatty substances include fatty alcohols (such as lauryl, myristyl stearyl, cetyl or cetostearyl alcohol), fatty acids and derivatives, including but not limited to fatty acid esters, fatty acid glycerides (mono-, di- and tri-glycerides), and hydrogenated fats. Specific examples include, but are not limited to hydrogenated vegetable oil, hydrogenated cottonseed oil, hydrogenated castor oil, hydrogenated oils available under the trade name Sterotex®, stearic acid, cocoa butter, and stearyl alcohol. Suitable waxes and wax-like materials include natural or synthetic waxes, hydrocarbons, and normal waxes. Specific examples of waxes include beeswax, glycowax, castor wax, carnauba wax, paraffins and candelilla wax. As used herein, a wax-like material is defined as any material, which is normally solid at room temperature and has a melting point of from about 30 to 300ºC.

In some cases, it may be desirable to alter the rate of water penetration into the microparticles. To this end, rate-controlling (wicking) agents can be formulated along with the fats or waxes listed above. Examples of rate-controlling materials include certain starch derivatives (e.g., waxy maltodextrin and drum dried corn starch), cellulose derivatives (e.g., hydroxypropylmethyl-cellulose, hydroxypropylcellulose, methylcellulose, and carboxymethyl-cellulose), alginic acid, lactose and talc. Additionally, a pharmaceutically acceptable surfactant (for example, lecithin) may be added to facilitate the degradation of such microparticles.

Proteins, which are water insoluble, such as zein, can also be used as materials for the formation of protein containing microparticles. Additionally, proteins, polysaccharides and combinations thereof, which are water-soluble, can be formulated with peptide into microparticles and subsequently cross-linked to form an insoluble network. For example, cyclodextrins can be complexed with individual drug molecules and subsequently cross-linked.

Method of making Nano- and Microparticles

Encapsulation or incorporation of drug into carrier materials to produce drug-containing microparticles can be achieved through known pharmaceutical formulation techniques. In the case of formulation in fats, waxes or wax-like materials, the carrier material is typically heated above its melting temperature and the drug is added to form a mixture comprising drug particles suspended in the carrier material, drug dissolved in the carrier material, or a mixture thereof. Microparticles can be subsequently formulated through several methods including, but not

limited to, the processes of congealing, extrusion, spray chilling or aqueous dispersion. In a preferred process, wax is heated above its melting temperature, drug is added, and the molten wax-drug mixture is congealed under constant stirring as the mixture cools. Alternatively, the molten wax-drug mixture can be extruded and spheronized to form pellets or beads. These processes are known in the art.

For some carrier materials it may be desirable to use a solvent evaporation technique to produce drug-containing microparticles. In this case drug and carrier material are co-dissolved in a mutual solvent and microparticles can subsequently be produced by several techniques including, but not limited to, forming an emulsion in water or other appropriate media, spray drying or by evaporating off the solvent from the bulk solution and milling the resulting material.

In some forms, drug in a particulate form is homogeneously dispersed in a water-insoluble or slowly water soluble material. To minimize the size of the drug particles within the composition, the drug powder itself may be milled to generate fine particles prior to formulation. The process of jet milling, known in the pharmaceutical art, can be used for this purpose. In some forms, drug in a particulate form is homogeneously dispersed in a wax or wax like substance by heating the wax or wax like substance above its melting point and adding the drug particles while stirring the mixture. In this case a pharmaceutically acceptable surfactant may be added to the mixture to facilitate the dispersion of the drug particles.

The particles can also be coated with one or more modified release coatings. Solid esters of fatty acids, which are hydrolyzed by lipases, can be spray coated onto microparticles or drug particles. Zein is an example of a naturally water-insoluble protein. It can be coated onto drug containing microparticles or drug particles by spray coating or by wet granulation techniques. In addition to naturally water-insoluble materials, some substrates of digestive enzymes can be treated with cross-linking procedures, resulting in the formation of non-soluble networks. Many methods of cross-linking proteins, initiated by both chemical and physical means, have been reported. One of the most common methods to obtain cross-linking is the use of chemical cross-linking agents. Examples of chemical cross-linking agents include aldehydes (gluteraldehyde and formaldehyde), epoxy compounds, carbodiimides, and genipin. In addition to these cross-linking agents, oxidized and native sugars have been used to cross-link gelatin. Cross-linking can also be accomplished using enzymatic means; for example, transglutaminase has been approved as a

GRAS substance for cross-linking seafood products. Finally, cross-linking can be initiated by physical means such as thermal treatment, UV irradiation and gamma irradiation.

To produce a coating layer of cross-linked protein surrounding drug containing microparticles or drug particles, a water-soluble protein can be spray coated onto the microparticles and subsequently cross-linked by the one of the methods described above. Alternatively, drug-containing microparticles can be microencapsulated within protein by coacervation-phase separation (for example, by the addition of salts) and subsequently cross-linked. Some suitable proteins for this purpose include gelatin, albumin, casein, and gluten.

Polysaccharides can also be cross-linked to form a water-insoluble network. For many polysaccharides, this can be accomplished by reaction with calcium salts or multivalent cations, which cross-link the main polymer chains. Pectin, alginate, dextran, amylose and guar gum are subject to cross-linking in the presence of multivalent cations. Complexes between oppositely charged polysaccharides can also be formed; pectin and chitosan, for example, can be complexed via electrostatic interactions.

Injectable/Implantable formulations

The compounds described herein can be incorporated into injectable/implantable solid or semi-solid implants, such as polymeric implants. In some forms, the compounds are incorporated into a polymer that is a liquid or paste at room temperature, but upon contact with aqueous medium, such as physiological fluids, exhibits an increase in viscosity to form a semi-solid or solid material. Exemplary polymers include, but are not limited to, hydroxyalkanoic acid polyesters derived from the copolymerization of at least one unsaturated hydroxy fatty acid copolymerized with hydroxyalkanoic acids. The polymer can be melted, mixed with the active substance and cast or injection molded into a device. Such melt fabrication requires polymers having a melting point that is below the temperature at which the substance to be delivered and polymer degrade or become reactive. The device can also be prepared by solvent casting where the polymer is dissolved in a solvent and the drug dissolved or dispersed in the polymer solution and the solvent is then evaporated. Solvent processes require that the polymer be soluble in organic solvents. Another method is compression molding of a mixed powder of the polymer and the drug or polymer particles loaded with the active agent.

Alternatively, the compounds can be incorporated into a polymer matrix and molded, compressed, or extruded into a device that is a solid at room temperature. For example, the compounds can be incorporated into a biodegradable polymer, such as polyanhydrides, polyhydroalkanoic acids (PHAs), PLA, PGA, PLGA, polycaprolactone, polyesters, polyamides, polyorthoesters, polyphosphazenes, proteins and polysaccharides such as collagen, hyaluronic acid, albumin and gelatin, and combinations thereof and compressed into solid device, such as disks, or extruded into a device, such as rods.

The release of the one or more compounds from the implant can be varied by selection of the polymer, the molecular weight of the polymer, and/or modification of the polymer to increase degradation, such as the formation of pores and/or incorporation of hydrolyzable linkages. Methods for modifying the properties of biodegradable polymers to vary the release profile of the compounds from the implant are well known in the art.

Enteral / Oral / Lingual Formulations

Oral formulations can include standard carriers such as pharmaceutical grades of mannitol, lactose, sodium saccharine, starch, magnesium stearate, cellulose, magnesium carbonate, etc. Such compositions will contain a therapeutically effective amount of the compound and/or antibiotic together with a suitable amount of carrier so as to provide the proper form to the patient based on the mode of administration to be used.

Suitable oral dosage forms include tablets, capsules, solutions, suspensions, syrups, and lozenges. Tablets can be made using compression or molding techniques well known in the art. Gelatin or non-gelatin capsules can prepared as hard or soft capsule shells, which can encapsulate liquid, solid, and semi-solid fill materials, using techniques well known in the art.

Formulations may be prepared using a pharmaceutically acceptable carrier. As generally used herein “carrier” includes, but is not limited to, diluents, preservatives, binders, lubricants, disintegrators, swelling agents, fillers, stabilizers, and combinations thereof.

Carrier also includes all components of the coating composition, which may include plasticizers, pigments, colorants, stabilizing agents, and glidants.

Examples of suitable coating materials include, but are not limited to, cellulose polymers such as cellulose acetate phthalate, hydroxypropyl cellulose, hydroxypropyl methylcellulose, hydroxypropyl methylcellulose phthalate and hydroxypropyl methylcellulose acetate succinate;

polyvinyl acetate phthalate, acrylic acid polymers and copolymers, and methacrylic resins that are commercially available under the trade name EUDRAGIT® (Roth Pharma, Westerstadt, Germany), zein, shellac, and polysaccharides.

Additionally, the coating material may contain conventional carriers such as plasticizers, pigments, colorants, glidants, stabilization agents, pore formers and surfactants.

“Diluents”, also referred to as "fillers," are typically necessary to increase the bulk of a solid dosage form so that a practical size is provided for compression of tablets or formation of beads and granules. Suitable diluents include, but are not limited to, dicalcium phosphate dihydrate, calcium sulfate, lactose, sucrose, mannitol, sorbitol, cellulose, microcrystalline cellulose, kaolin, sodium chloride, dry starch, hydrolyzed starches, pregelatinized starch, silicone dioxide, titanium oxide, magnesium aluminum silicate and powdered sugar.

“Binders” are used to impart cohesive qualities to a solid dosage formulation, and thus ensure that a tablet or bead or granule remains intact after the formation of the dosage forms. Suitable binder materials include, but are not limited to, starch, pregelatinized starch, gelatin, sugars (including sucrose, glucose, dextrose, lactose and sorbitol), polyethylene glycol, waxes, natural and synthetic gums such as acacia, tragacanth, sodium alginate, cellulose, including hydroxypropylmethylcellulose, hydroxypropylcellulose, ethylcellulose, and veegum, and synthetic polymers such as acrylic acid and methacrylic acid copolymers, methacrylic acid copolymers, methyl methacrylate copolymers, aminoalkyl methacrylate copolymers, polyacrylic acid/polymethacrylic acid and polyvinylpyrrolidone.

“Lubricants” are used to facilitate tablet manufacture. Examples of suitable lubricants include, but are not limited to, magnesium stearate, calcium stearate, stearic acid, glycerol behenate, polyethylene glycol, talc, and mineral oil.

“Disintegrants” are used to facilitate dosage form disintegration or "breakup" after administration, and generally include, but are not limited to, starch, sodium starch glycolate, sodium carboxymethyl starch, sodium carboxymethylcellulose, hydroxypropyl cellulose, pregelatinized starch, clays, cellulose, alginine, gums or cross linked polymers, such as cross-linked PVP (Polyplasdone® XL from GAF Chemical Corp).

“Stabilizers” are used to inhibit or retard drug decomposition reactions, which include, by way of example, oxidative reactions. Suitable stabilizers include, but are not limited to, antioxidants, butylated hydroxytoluene (BHT); ascorbic acid, its salts and esters; Vitamin E,

tocopherol and its salts; sulfites such as sodium metabisulphite; cysteine and its derivatives; citric acid; propyl gallate, and butylated hydroxyanisole (BHA).

Oral dosage forms, such as capsules, tablets, solutions, and suspensions, can for formulated for controlled release. For example, the one or more compounds and optional one or more additional active agents can be formulated into nanoparticles, microparticles, and combinations thereof, and encapsulated in a soft or hard gelatin or non-gelatin capsule or dispersed in a dispersing medium to form an oral suspension or syrup. The particles can be formed of the drug and a controlled release polymer or matrix. Alternatively, the drug particles can be coated with one or more controlled release coatings prior to incorporation into the finished dosage form.

In another form, the one or more compounds and optional one or more additional active agents are dispzr form, the one or more compounds, and optional one or more additional active agents are formulated into a sold oral dosage form, such as a tablet or capsule, and the solid dosage form is coated with one or more controlled release coatings, such as a delayed release coatings or extended release coatings. The coating or coatings may also contain the compounds and/or additional active agents.

The materials and methods below are provided to facilitate the practice of the present invention.

Animals

Adult male Sprague-Dawley rats (Charles River) were individually housed under a 12h-light:12h-dark cycle in a temperature and humidity-controlled satellite vivarium and had *ad libitum* access to water and chow (5001, LabDiet) or a 60% high fat diet (HFD; D12492, Research Diets) and when applicable had *ad libitum* access to kaolin pellets (K50001, Research Diets). Rat's were exposed to kaolin for at least 5 days prior to measuring kaolin consumption in pica testing. Except for studies conducted in the BioDaq, for all feeding studies rats were housed in hanging wire cages to allow for accurate measurement of food spillage.

Adult male shrews (Suncus murinus) weighing ~50-80 g, were bred and maintained in the De Jonghe Lab (University of Pennsylvania). These animals were offspring from a colony previously maintained at the University of Pittsburgh Cancer Institute (Dr. Charles Horn); a Taiwanese strain derived from stock originally supplied by the Chinese University of Hong

Kong). Shrews were single housed in plastic cages (37.3 x 23.4 x 14 cm, Innovive) under a 12h-light:12h-dark cycle in a temperature-and humidity-controlled environment. Animal were fed *ad libitum* with a mixture of feline (75%, Laboratory Feline Diet 5003, Lab Diet) and mink food (25%, High Density Ferret Diet 5LI4, Lab Diet) and had *ad libitum* access to tap water.

Experiments were conducted under the National Institutes for Health Guide for the Care and Use of Laboratory Animals and all procedures were approved by the Institutional Animal Care and Use Committee at the University of Pennsylvania.

Surgeries

For cannula implantation, rats were anesthetized by intraperitoneal injection of a mixture containing ketamine (90 mg/kg, Butler Animal Health Supply), xylazine (2.7 mg/kg, Anased), and acepromazine (0.64 mg/kg, Butler Animal Health Supply) (KAX) and then placed into a stereotaxic apparatus. Each rat was stereotaxically implanted with a guide cannula (26-ga, Plastics One) aimed at the fourth ventricle (guide cannula coordinates: on midline, 2.5 mm anterior to occipital suture, 5.2 mm ventral to skull; internal cannula aimed 7.2 mm ventral to skull) or the lateral ventricle (guide cannula coordinates: 1.5 mm lateral to midline, 0.9 mm posterior to bregma, 1.8 mm ventral to skull; internal cannula aimed 3.8 mm ventral to skull). For all cannulas, dummies (no projection beyond guide) were inserted in the guide cannula and left until infusions were performed. For all surgeries, rats received post-operative temperature support and analgesia was provided immediately following surgery and for two post-operative days (2 mg/kg meloxicam).

Food and Kaolin Intake Studies

For all studies measuring food intake following drug treatment, central injections were given at volume of 2 µL were administered using a Hamilton syringe terminating in an injector tip extending 2.0 mm beyond the guide cannula, and intraperitoneal injections were given based on body weight (0.1mL/100g body weight). For acute treatment days, rats were food deprived 2 hours before the dark cycle and injections were done immediately prior to the dark cycle onset. Food and kaolin intake was measured 1, 3, 6, and 24 hours after injections were completed and food crumbs were weighed and accounted for between each timepoint. Body weight was measured during injections and 24 hours after. Injection treatments were organized in a

counterbalanced, within-subjects design and separated by ≥72h. For chronic intake studies, once daily drug injections and recording of body weight, food, and kaolin intake were performed every 24h immediately prior to the dark cycle onset. For meal pattern analysis, rats living in a Biodaq system (Research Diets, Inc) were injected similarly. The BioDaq system records on a second-by-second basis for undisturbed measurements of episodic food intake. Individual bouts are initiated by the animal at onset and termination of feeding; bouts are separated by 5 second inter-bout interval (IBI). A meal is defined as at least one bout with a minimum meal size of 0.02g and separated by a 5-minute undisturbed inter-meal interval (IMI). Cumulative food intake, the number of meals, time spent consuming meals, average meal size (g/meal), and average meal length (sec/meal) was calculated for hours 0-1, 0-6, 6-12, and 12-24 relative to drug injection. Additionally, cumulative food intake (g), number of bouts, time in bouts, number of meals, and time in meals were calculated for 20 min intervals for the first 3 hours post injection in chow fed rats and for 1 hour intervals for 24 hours post injections in HFD fed rats.

Drugs

Most drugs (ODN, TDN, OP, AntOP, SUODN04, SUODN05) used in these studies were synthesized by the Doyle lab at Syracuse University. Drugs that were purchased commercially include: Rat recombinant diazepam binding inhibitor (DBI) protein (LS-G136996, Lifespan Biosciences) and exendin-4 (11096, Caymen Chemical) which were dissolved in artificial cerebrospinal fluid (aCSF, Harvard Apparatus), liraglutide (24727, Caymen Chemical) which was dissolved in 40 mM Tris HCl buffer (pH8) 0.02% Tween-80, and rabbit anti-DBI primary antibody (ab231910, Abcam) used to neutralize endogenous DBI which was not diluted and the appropriate vehicle used was a 1:1 solution of glycerol and aCSF.

Hindbrain DBI Immunohistochemistry and Quantification

Rats maintained on chow or HFD were either *ad libitum* fed or fasted for 24h. All rats received a 4th ventricle injection of aCSF or exendin-4 (0.3 µg/2 µL) 90 minutes prior to sacrifice. Rats were deeply anesthetized with KAX and transcardially perfused with 0.1 M phosphate-buffered saline (PBS; pH 7.4) followed by 4% paraformaldehyde in 0.1 M PBS on ice. Brains were removed from the crania and post-fixed in 4% paraformaldehyde for 24h, then stored in 20% sucrose in 0.1 M PBS at 4 °C until sunk. Coronal dorsal vagal complex (DVC) sections (30 µm) were sliced and collected directly onto slides (12-550-15; Superfrost Plus,

Fisher Scientific) using a cryostat and stored at −80 °C until the start of immunohistochemistry (IHC). Briefly, tissue was washed with 0.1 M PBS 3 times for 8 minutes and then incubated in blocking solution [5% normal donkey serum (Jackson Immunoresearch) in PBST; PBS with 0.3% triton X] followed by overnight incubation in rabbit anti-DBI primary antibody (1:500; ab231910, Abcam) and chicken anti-vimentin primary antibody (1:2000; ab24525, Abcam) at 4 °C. The next morning slides were washed 3 times for 8 minutes in PBST and then incubated in donkey anti-rabbit fluorescent secondary antibody (1:500; AlexaFluor 647, Jackson Immunoresearch) and donkey anti-chicken fluorescent secondary antibody (1:500; AlexaFluor 488, Jackson Immunoresearch) for 3h at room temperature. Finally, slides were washed 3 times for 5 minutes in PBST and one time in PBS before coverslipped with antifade mounting media with DAPI (H-1200, Vector Laboratories, Inc.). Slides were visualized using fluorescence microscopy (BZ-X810, Keyence). Images analysis to quantify the fluorescent intensity of DBI protein staining in the nucleus solitary tractus (NTS) and area postrema (AP) as well as the % colocalization of DBI and vimentin staining in the AP, subpostrema, and 4th ventricle boarder was done using the HALO® FISH-IF and Area Quantification FL modules.

Quantitative Real-Time (qPCR) Studies

Chow-maintained rats received a 4th ventricle injection of aCSF or exendin-4 (0.3 µg/2 µL) 90 minutes prior to sacrifice. Brains were rapidly removed, flash-frozen in −70 °C isopentane, and stored at −80 °C until processing. Micropunched tissue from the DVC was collected from each brain. Total RNA was extracted from tissue from each site using TRIzol (Invitrogen) and the RNeasy kit (Qiagen). The Advantage RT-for-PCR Kit (Clontech) was used to synthesize cDNA from 200 ng of total RNA. Relative mRNA levels of DBI were quantified using quantitative real-time PCR. Rat GapDH (VIC-MGB) was used as an internal control. PCR reactions were completed using TaqMan gene expression kits (DBI: Rn00821402_g1 and GapDH: Rn01775763_g1) and PCR reagents from Applied Biosystems. Samples were analyzed with the QuantStudio 6 Pro system (Applied Biosciences). Relative mRNA expression calculations were completed using the comparative threshold cycle method.

Hindbrain Glucose Sensing Studies

Chow-maintained rats were food deprived 2 hours before the dark cycle and 4th ventricle injections were done immediately prior to the dark cycle onset. Baseline glucose values were

taken from tail vein blood by glucometer (Concur) prior to injections and 30 and 60 minutes after injections. In one study rats received a pretreatment injection of vehicle (aCSF) or OP (20 µg/2 µL) followed by treatment with vehicle or 5-thio-d-glucose (5-TG; 210 µg/2 µL). In the other study rats received a pretreatment injection of vehicle or AntOP (20 µg/2 µL) followed by treatment with vehicle or D-glucose (5.5M in 3 µL). Food was returned 1h after injections following measurement of the last blood glucose concentrations and food intake was recorded 2, 4, 6, and 24 hours post injections. Body weight was measured during injections and 24 hours after.

Peptide synthesis and purification

Solid-Phase Peptide Synthesis was performed on ProTide Rink amide resin (CEM Corporation cat # R002) using a microwave-assisted CEM Liberty Blue peptide synthesizer (Matthews, NC). Fmoc-protected amino acids were coupled to the resin using 0.25 M Oxyma Pure (CEM Corporation cat # S001) and 0.125 M N, N'-diisopropylcarbodiimide (Sigma-Aldrich cat # D125407) as the activator and activator base, respectively. Fmoc was removed between couplings with 20% Piperidine (Sigma-Aldrich cat # 8.22299.0500). Global deprotection and cleavage of the peptides from the solid-support resin achieved using a CEM Razor instrument over a 40-minute incubation period at 40°C in a mixture of 95% TFA (Sigma-Aldrich cat # 8.08260.2501), 2.5% TIPS (Sigma-Aldrich cat # 233781), and 2.5% water. Peptides were purified on an Agilent 1200 series High-Performance Liquid Chromatography (HPLC) instrument (10-75% HPLC-grade acetonitrile (VWR cat # BDH83639.400) for 20 minutes at 2 mL/min flow rate using an Agilent Zorbax C18 column (5µm, 9.4 x 250 mm) tracked at 220 nm.

DVC Tissue Extraction from Male Sprague Dawley rats

Male Sprague Dawley rats were anesthetized by isoflurane and rapidly de-capitated, the brains removed and flash frozen in -70°C isopentane and stored at -80oC. Using a cryostat, the DVC (comprised of the area postrema, nucleus tractus solitarius, and dorsal motor nucleus of the vagus) of the rat brainstem was micropunched 1mm3 per subnuclei at the level of the AP and pooled together in a cryovial and restored at -80oC for Protein / GPCR tissue extraction procedures below.

ODN-bound Protein / GPCR extraction procedures from rat DVC tissue

Membrane proteins were extracted from rat brain tissue based on the protocol for tissues on the GPCR Extraction and Stabilization Reagent (GESR) (ThermoFisher Scientific, Rockford, Il). Briefly, the tissue samples were suspended in 1 mL of cold (4°C) PBS and washed repeatedly. The PBS was decanted, and 1 mL of cold (4°C) GESR was added to the tissue samples. The tissue samples were homogenized until an even suspension was obtained by pipetting up and down 15-20 times. The homogenate was transferred to a new tube and was incubated at 4°C for 30 minutes with end-over-end mixing. The sample was centrifuged at 16,000 x g for 20 minutes at 4°C. The supernatant containing stabilized protein receptors was saved and stored at 4°C until being analyzed.

Binding assay

Binding analysis was done on a Nicoya Open Surface plasmon resonance instrument using a Nicoya streptavidin sensor chip. The coupling procedure was according to the streptavidin sensor chip protocol, including the steps of surface conditioning and surface activation. For ligand immobilization, ODN-biotin (20 µg/mL in the PBST pH 7 running buffer) was injected over channel 2 for a 5-minute interaction time. This process was repeated several times to ensure optimal immobilization. The supernatant from the GPCR extraction procedure was injected over channels 1 and 2 of the chip, and a background-corrected binding curve was obtained. The chip was then soaked for 16 hours in 5 mL of MeOH at 4°C. An electron absorption spectrum of the MeOH used to soak the chip was obtained using a Nanodrop One. The remaining MeOH was mixed with water, freeze-dried, and sent out for MS/MS sequencing.

The following examples are provided to illustrate certain embodiments of the invention. They are not intended to limit the invention in any way.

Example 1

Synthesis and Testing of ODN peptides and derivatives

Central administration of ODN at 0.2, 2, and 20 µg/ 2 µL in the 4th ventricle dose dependently decreases food intake in the first hour after injections in chow-maintained rats (Fig.

1A) without affecting 24h body weight change (Fig. 1B), and also dose dependently decreases food intake in diet-induced obese (DIO) 60% high-fat diet (HFD)-maintained rats at hours 12 and 24 post injections (Fig. 1C) while non-significantly decreasing 24h body weight change (Fig. 1D). These data support that intracerebroventricular administration of ODN dose-dependently suppresses intake of both chow and HFD, although with differences in time course of the anorectic response. ODN acts acutely in lean chow-maintained rats but is longer-lasting and more effective at suppressing HFD intake in obese rats.

Meal pattern data examined the amount of food intake (grams), the number of meals, time spent eating meals (seconds), meal length (seconds/meal), and meal size (grams/meal) in chow-maintained rats at time intervals 0-1 hours, 0-6 hours, 6-12 hours, and 12-24 hours post ODN injection. ODN dose dependently decreased the amount of food eaten in the first hour (Fig. 2A) but not any other time frame (Figs. 2B-2D). ODN did not impact the number of meals eaten at any time frame (Figs. 2E-2H), or the time spent in meals (Figs. 2I-2L). The meal length was decreased by 0.2 µg ODN in hour 1 but not in any other time frame (Figs. 2M-2P). ODN dose dependently decreased meal size in the first hour (Fig. 2Q) but not any other time frame (Figs. 2R-2T). These data support that in chow-maintained rats, ODN suppresses food intake in the first hour post injections by decreasing meal size.

Heat map representation of food intake (Fig. 3A, grams), bout number (Fig. 3B), time spent in bours (Fig. 3C, seconds), meal number (Fig. 3D), and time spent in meals (Fig. 3E, seconds) during the first 3 hours post injections in chow-maintained rats. Compared to vehicle, 2 and 20 µg ODN decreased food intake 60 minutes after injections and 20 µg ODN also decreased food intake at 80 and 100 minutes (Fig. 3A). The number of bouts, time in bouts, and number of meals was not affected by ODN (Figs. 3B-3D), and 0.2 µg ODN decreased the time spent in meals at 80 minutes post injection relative to vehicle (Fig. 3E).

Meal pattern data examined the amount of food intake (grams), the number of meals, time spent eating meals (seconds), meal length (seconds/meal), and meal size (grams/meal) in HFD-maintained rats at time intervals 0-1 hours, 0-6 hours, 6-12 hours, and 12-24 hours post ODN injection. 20 µg ODN decreased the amount of food eaten during 6-12 hour post injections but no other time frame (Fig. 4A-4D). ODN did not affect meal pattern data at any time frame (Fig. 4E-4T).

Heat map representation of food intake (Fig. 5A, grams), bout number (Fig. 5B), time spent in bours (Fig. 5C, seconds), meal number (Fig. 5D), and time spent in meals (Fig. 5E, seconds) during the 24 hours post injections in HFD-maintained rats. 0.2, 2, and 20 µg ODN decreased food intake at 12 and 15 hours post injection, 0.2 and 20 µg also at 18 hours, and 20 µg ODN also at 24 hours (Fig. 5A). ODN did not significantly alter the number of bouts, time in bouts, number of meals, and time in meals (Figs. 5B-5E).

Meal pattern data on the first bout and meal consumed post ODN injection in chow and HFD-maintained rats. Consistent with acute effect of ODN in chow-maintained rats, ODN did not alter the latency to the first meal (Fig. 6A) but 20 µg ODN decreased the size of the first meal (Fig. 6B). 2 µg ODN increased the latency to the first bout consumed (Fig. 6C) but did not alter the size of the first bout (Fig. 6D). Consistent with the delayed impact of ODN in obese rats, ODN did not alter the latency to consume of the size of the first meal or bout (Figs 6E-6H).

ODN is a cleavage product of DBI and to understand how the parent peptide DBI regulates food intake in chow and HFD-maintained rats we injected recombinant DBI protein into the 4^{th} ventricle. In chow-maintained rats, DBI significantly reduced food intake at 4, 5, and 7-24 hours post injection (Fig. 7A). Surprisingly, DBI did not decrease food intake in HFD-maintained rats (Fig. 7B). 24h body weight change was not significantly decreased in either diet group (Fig. 7C). These results show that while ODN is more effect in obese rats, exogenous DBI does not suppress food intake, suggesting there may be some dysfunction in cleaving DBI to ODN in obesity that can be targeted to improve endogenous ODN signaling.

Heat map representation of food intake (Fig. 8A, grams), bout number (Fig. 8B), time spent in bours (Fig. 8C, seconds), meal number (Fig. 8D), and time spent in meals (Fig. 8E, seconds) during the 24 hours post recombinant DBI injections in chow-maintained rats. DBI decreased food intake at 4, 5, and 7-24 hours post injection (Fig. 8A), decreased the number of bouts at 8 and 21 hours post injection (Fig. 8B), did not alter the time spent in bouts (Fig. 8C), decreased the number of meals at 8-10 and 12-21 hours post injection (Fig. 8D), and decreased the time spent in meals 8-24 hours post injection (Fig. 8E). These data support that DBI protein strongly suppresses food intake by limiting the time spent eating meals and the number of meals consumed in chow-maintained rats.

ODN expression and release has been shown to be regulated by nutritional state, being decreased by fasting and increased by refeeding and glucose. We hypothesized that glucagon-like peptide-1 (GLP-1), which is induced post-prandially, may also regulate ODN signaling. To test the contribution of ODN signaling to the anorectic actions of GLP-1, we pretreated chow and HFD-maintained rats in the 4th ventricle with an antibody targeting DBI (AB) to neutralize endogenous DBI protein or vehicle before treatment with ODN, the GLP-1 receptor agonist, exendin-4 (Ex-4), or vehicle in the 4th ventricle. AB pretreatment reduced the anorectic effect of Ex-4 at 24 hours post injections (Fig. 9A) but did not affect HFD intake (Fig. 9B). Kaolin intake was measured to assess pica behavior. As expected, Ex-4 increased kaolin consumption in chow-maintained rats relative to controls and this was numerically but not significantly reduced by AB pretreatment (Fig. 9C). There was no difference in kaolin intake between any treatment groups in HFD-maintained rats (Fig. 9D). Ex-4 decreased 24h body weight change relative to controls in both chow and HFD-maintained rats independent of pretreatment (Figs. 9E-9F).

We repeated this study using a 4th ventricle administered ODN antagonist (AntOP) instead of the DBI targeted antibody and again demonstrated that AntOP pretreatment reduced the anorectic effect of Ex-4 in chow and HFD-maintained rats at 24h post injections (Figs. 10A-10B). Additionally, we observed that AntOP pretreatment alone decreased 24h HFD intake (Fig. 10B). Ex-4 increased kaolin intake in chow and HFD-maintained rats relative to controls, and in chow rats AntOP pretreatment to Ex-4 did not significantly elevate kaolin intake relative to controls (Figs. 10C-10D). In chow rats, AntOP pretreatment mitigated the Ex-4-induced robust decrease in body weight (Fig. 10E) and tended to do so in HFD-maintained rats (Fig. 10F). AntOP pretreatment alone also decreased 24h body weight change in HFD rats (Fig. 10F).

We next wanted to assess whether antagonizing ODN signaling could reduce the anorectic response to peripheral GLP-1 receptor agonists, so we administered AntOP or vehicle through the lateral ventricle and gave intraperitoneal injections of liraglutide or vehicle. Liraglutide decreased food intake in chow-maintained rats independent of pretreatment (Fig. 11A), and liraglutide decreased HFD intake which was attenuated by AntOP pretreatment at 1 and 3 hours post injections (Fig. 11B). Kaolin intake was increased, and body weight was decreased by liraglutide and not altered by AntOP pretreatment in chow and HFD-maintained

rats (Figs. 11C-11F). The results in figures 9-11 demonstrate that the anorectic response to central and peripheral GLP-1 receptor agonists is partially mediated by central ODN signaling.

We next investigated whether ODN and GLP-1 receptor agonism can be cooperative to decrease food intake by injecting 4th ventricle ODN or vehicle and intraperitoneal liraglutide or vehicle daily for 5 days. Liraglutide decreased daily food intake on day 1 and 2 relative vehicle and cumulative food intake on days 1-5, and ODN enhanced food intake suppression with liraglutide on day 1 (Figs. 12A-12B). Daily and cumulative kaolin intake and daily body weight was not different between any treatments (Figs. 12C-12E). Day one food intake was isolated and shows that while ODN alone did not alter food intake, it greatly enhanced the anorectic effect of liraglutide (Fig. 12F). These data suggest that as we propose ODN may be downstream of GLP-1 signaling, GLP-1 receptor agonists do not maximally stimulate ODN signaling and ODN agonists can be combined with GLP-1 agonists to provide more effective appetite control.

Tridecaneuropeptide (TDN) is a predicted cleavage product of ODN that when administered into the 4th ventricle (20 µg) did not suppress chow intake but did suppress HFD intake at 24h post injections (Figs. 13A-13B). TDN did not alter kaolin intake in chow rats but did mildly increase kaolin intake in HFD-maintained rats (Figs. 13C-13D). 24h body weight change tended to be reduced by TDN in HFD-maintained rats (Fig. 13E).

We next administered 20 and 200 µg TDN in the lateral ventricle of chow and HFD-maintained rats and observed that 200 µg TDN decreased 24h chow intake and 1 and 24h HFD intake (Figs. 14A-14B). TDN did not affect kaolin intake or significantly change 24h body weight in either diet group (Figs. 14C-14F). Figures 13 and 14 demonstrate that central TDN also shows anorectic effects.

To investigate whether ODN has anorectic effects when administered intraperitoneally and to assess the emetic response to peripheral ODN in a vomiting model, we injected intraperitoneal ODN at 500 and 5000 µg in the shrew. Both doses of ODN suppressed 24h food intake without significantly altering 24h body weight, and only one of 9 shrews had an emetic episode to the low ODN dose and no emetic episodes were observed with the high ODN dose (Figs. 15A-15C).

We tested the anorectic response to multiple novel ODN derivative peptides (ODN 20 µg, TDN 20 µg, SUODN04 20 µg, and SUODN05 20 µg) administered in the 4th ventricle. All ODN based peptides suppressed 24h HFD intake relative to vehicle and did not significantly alter 24h body weight change (Figs. 16A-16B).

DBI is synthesized by populations of glial cells in the dorsal vagal complex (DVC) of the hindbrain which comprises the area postrema (AP) and nucleus tractus solitarius (NTS). To investigate where DVC DBI protein expression is regulated by nutritional state and GLP-1 receptor signaling, we quantified the amount of fluorescently labeled DBI protein in the AP and NTS in both chow and HFD-maintained rats that we *ad libitum* fed, 24h fasted, or 24h fasted plus received a 4th ventricle injection of the GLP-1 receptor agonist exendin-4 (Ex-4). At the pre-AP level, NTS DBI expression did not change with treatment in either chow or HFD-maintained rats (Figs. 17A-17B). NTS DBI expression at the level of the AP was reduced by Ex-4 treatment compared to both fed and fasted groups in chow-maintained rats but was not different between treatments in HFD-maintained rats (Figs. 17C-17D). NTS DBI expression at the 4th ventricle level was reduced by Ex-4 treatment compared to the fasted group in chow-maintained rats but was not different between treatments in HFD-maintained rats (Figs. 17E-17F). In the AP, DBI expression was increased with fasting and decreased with Ex-4 treatment in chow-maintained rats but not different between treatments in HFD-maintained rats (Figs. 17G-17H). These data suggest that DBI protein expression in the NTS and AP is regulated by fasting and counter-regulated by Ex-4 treatment in the fasted state in chow but not HFD-maintained rats.

Tanycytes are specialized glial cells that form the border around ventricle and also form the subpostrema border between the AP, which is a circumventricular organ, and the NTS. We confirm that DBI protein expression overlaps with expression of the tanycyte marker, vimentin, in the AP, the subpostrema, and on the 4th ventricle border (Fig. 18).

4th ventricle Ex-4 treatment increases DBI mRNA expression in the DVC of chow-maintained rats (Fig. 19), supporting that ODN signaling is downstream of GLP-1 receptor agonism.

ODN has been shown to mediate glucose sensing in tanycytes of the hypothalamus, with the idea that because glucose stimulates ODN release, ODN acts as the signal to recruit a glucose-sensing neuronal circuit response. To demonstrate that ODN plays a role in glucose

sensing of the hindbrain, we tested whether the ODN analogue OP could reverse the hyperphagia and hyperglycemia of a stimulus that mimics hypoglycemia or glucoprivation (5-thio-d-glucose; 5-TG), and whether the ODN antagonist AntOP could reduce the hypophagia and hypoglycemia induced by glucose. All injections were given 4th ventricle in chow-maintained rats. 5-TG increased food intake at 2 and 24 hours post injections relative to controls, while 5-TG following OP pretreatment did not increase food intake relative to OP pretreatment alone (Fig. 20A). At 4 and 6 hours post injections, OP pretreatment to 5-TG decreased food intake relative to 5-TG treatment alone (Fig. 20A). 5-TG strongly induced a hyperglycemic response at 30 and 60 minutes post injections which was attenuated by OP pretreatment (Fig. 20B). There was no effect of any treatment on 24h body weight (Fig. 20C). Central glucose administration decreased food intake 4h post injections relative to controls and this was not seen with glucose treatment between AntOP pretreated groups (Fig. 20D). Glucose decreased blood glucose concentrations 30 minutes post injections relative to controls and within AntOP pretreated rats, glucose did not alter blood glucose levels (Fig. 20E). 24h body weight change was not different between groups (Fig. 20F). These data support that ODN signaling, which is normally enhanced post-prandially, can attenuate the physiological response to hindbrain glucoprivation sensing and that blocking ODN signaling can attenuate the physiological response to central glucose.

In total, these results demonstrate that central ODN and novel ODN based peptides decrease food intake in chow and HFD-maintained rats, that hindbrain DBI protein expression is regulated by nutritional state and GLP-1 agonism in chow rats and that this is blunted in HFD-fed rats, that central GLP-1 agonism upregulates DBI mRNA expression in chow-fed rats, that blocking ODN signaling with either an antibody targeting DBI or an ODN antagonist attenuates the anorectic effect of central and peripheral GLP-1 analogues, that ODN and GLP-1 signaling are cooperative to suppress food intake, and that ODN is involved in the hindbrain glucose sensing response.

Example 2

CHIP-Bound ODN Assays reveal new protein targets bound by ODN

Peptide sequences used in ODN-biotin-bound Rat DVC Tissue MS analyses. Both peptides were synthesized, confirmed, and purified prior to testing:

ODN QATVGDVNTDRPGLLDLK-NH_2

ODN-biotin QATVGDVNTDRPGLLDL(K-biotin)-NH_2

Binding analysis was done on a Nicoya Open Surface plasmon resonance instrument using a Nicoya streptavidin sensor chip. The coupling procedure was according to the streptavidin sensor chip protocol, including the steps of surface conditioning and surface activation. For ligand immobilization, ODN-biotin (20 µg/mL in the PBST pH 7 running buffer) was injected over channel 2 for a 5-minute interaction time. This process was repeated several times to ensure optimal immobilization. The supernatant from the GPCR extraction procedure was injected over channels 1 and 2 of the chip, and a background-corrected binding curve was obtained. The chip was then soaked for 16 hours in 5 mL of MeOH at 4°C. An electron absorption spectrum of the MeOH used to soak the chip was obtained using a Nanodrop One. The remaining MeOH was mixed with water, freeze-dried, and sent out for MS/MS sequencing.

Example 3: Screening for new druggable targets using gpcrMAX and orphanMAX assays

The gpcrMAX and orphanMAX panels are intended to provide a cost-effective means at identifying possible interactions with a selection of known GPCR or orphan GPCR targets. Compounds are typically tested at a single concentration and as a result provides a semi-quantitative determination of efficacy. Any potential interactions can be confirmed in a follow-up dose response.

gpcrMAX – Agonist Mode

Activation of GPCR by a compound acting as an agonist will result in an increase in beta-arrestin recruitment to the target GPCR. The result tables (Tables 2 and 3) provides mean, standard deviation (SD) and %CV for control values for both baseline (Control 1) and maximal control ligand response (Control 2 – Max). Compound RLU (Raw values) are provided for the test compound plus the mean RLU, standard deviation and %CV. Compound % Activity is calculated as the % activity relative to the baseline (0% activity) and Max (100% activity) values.

gpcrMAX – Antagonist Mode

Inhibition of GPCR activation by a compound acting as an antagonist of ligand binding will result in a decrease in beta-arrestin recruitment to the target GPCR. The result table provides mean, standard deviation (SD) and %CV for control values for both EC80 (Control 1) and basal ligand response (Control 2 – Basal). Compound RLU (Raw values) are provided for the test compound plus the mean RLU, standard deviation and %CV. Compound % Inhibition is calculated as the % inhibition relative to the EC80 (0% inhibition) and basal (100% inhibition) values. These assays provide a means to determine if compound activity observed in the panels is potentially significant and worthy of follow-up. Different approaches are recommended for each panel type and assay mode.

orphanMAX – Agonist Mode

Activation of Orphan GPCR by a compound acting as an agonist will result in an increase in beta-arrestin recruitment to the target orphan GPCR. The result table provides mean, standard deviation (SD) and %CV for control value for baseline activity observed. Since different GPCRs exhibit varying levels of expression and constitutive arrestin recruitment, the Baseline Mean RLU value will differ from target to target. Compound RLU (Raw values) are provided for the test compound plus the mean RLU, standard deviation and %CV. Since a known ligand is typically not available for orphan GPCR assays, % activity is calculated differently for the orphanMAX GPCR panel compared to the gpcrMAX panel. Activity is calculated relative to the baseline response only. Therefore a 2 fold increase in compound Mean RLU over baseline will generate a % Activity value of 100%. Likewise 3 fold increase is equal to 200%.

Each of the aforementioned assays can be perform on GPCR having known or unknown ligands.

Table 2

Control Dose response curves for selected GPCR Biosensor Assays

Compound Name	Project ID	Assay Name	Assay Format	Assay Target	Result Type	RC50	Unit	Hill	Curve Bottom	Curve Top	Max Response
PACAP-27	August 2022 GPCR Panel	Arrestin	Agonist	ADCYAP1R1	EC50	0.00391138	uM	1.6617	4.247	98.885	100.67
2-CHB-MECA	August 2022 GPCR Panel	Arrestin	Agonist	ADORA3	EC50	0.01525879	uM	1.1017	-4.5788	100.04	107.6
Phenylephrine	August 2022 GPCR Panel	Arrestin	Agonist	ADRA1B	EC50	0.1628722	uM	1.1119	-0.1258	99.546	102.6
UK 14,304	August 2022 GPCR Panel	Arrestin	Agonist	ADRA2A	EC50	0.006584155	uM	0.67942	0	104	103.78
UK 14,304	August 2022 GPCR Panel	Arrestin	Agonist	ADRA2B	EC50	0.1715043	uM	1.5427	-3.5776	99.007	101.76
UK 14,304	August 2022 GPCR Panel	Arrestin	Agonist	ADRA2C	EC50	0.0528202	uM	1.3001	-14.689	103.6	115.02
Isoproterenol	August 2022 GPCR Panel	Arrestin	Agonist	ADRB1	EC50	0.03615513	uM	0.9032	-1.565	98.992	103.08
Isoproterenol	August 2022 GPCR Panel	Arrestin	Agonist	ADRB2	EC50	0.01980067	uM	1.3003	0.016719	95.144	95.309
Angiotensin II	August 2022 GPCR Panel	Arrestin	Agonist	AGTR1	EC50	0.0004409406	uM	1.2265	-1.5534	98.855	106.42
Apelin-13	August 2022 GPCR Panel	Arrestin	Agonist	AGTRL1	EC50	0.00125317	uM	1.1108	-5.3927	96.774	101.08
Vasopressin	August 2022 GPCR Panel	Arrestin	Agonist	AVPR1A	EC50	0.004293781	uM	0.85042	0	99.755	103.94
Vasopressin	August 2022 GPCR Panel	Arrestin	Agonist	AVPR1B	EC50	0.001541452	uM	0.89493	-4.8549	97.66	99.458
Vasopressin	August 2022 GPCR Panel	Arrestin	Agonist	AVPR2	EC50	0.0006564323	uM	1.6806	-3.3253	101.69	104.04
LDA-Bradykinin	August 2022 GPCR Panel	Arrestin	Agonist	BDKRB1	EC50	0.003652918	uM	0.98709	-2.8311	99.753	103.16
Bradykinin	August 2022 GPCR Panel	Arrestin	Agonist	BDKRB2	EC50	0.005572115	uM	1.3847	0.091551	105.59	103.91
TAPN-Bombesin	August 2022 GPCR Panel	Arrestin	Agonist	BRS3	EC50	0.001243827	uM	0.79106	-8	91.941	100.84
C3A Receptor Agonist	August 2022 GPCR Panel	Arrestin	Agonist	C3AR1	EC50	0.1870269	uM	1.2488	0.69156	102.72	100.98
Complement C5a	August 2022 GPCR Panel	Arrestin	Agonist	C5aR1	EC50	0.001378066	uM	1.5463	0.41487	100.88	102.6
Complement C5a	August 2022 GPCR Panel	Arrestin	Agonist	C5L2	EC50	0.001570643	uM	1.1743	-9.3389	101.65	101.89
Calcitonin	August 2022 GPCR Panel	Arrestin	Agonist	CALCR	EC50	0.03093926	uM	0.98215	2.5604	105	102.54
beta CGRP	August 2022 GPCR Panel	Arrestin	Agonist	CALCRL-RAMP1	EC50	0.002395687	uM	1.7485	3.2986	98.905	99.214
Adrenomedullin	August 2022 GPCR Panel	Arrestin	Agonist	CALCRL-RAMP2	EC50	0.000999747	uM	1.7618	2.1065	101.76	101.61
Adrenomedullin	August 2022 GPCR Panel	Arrestin	Agonist	CALCRL-RAMP3	EC50	0.002876935	uM	1.3758	5.154	100.06	103.15
Calcitonin	August 2022 GPCR Panel	Arrestin	Agonist	CALCR-RAMP2	EC50	0.01643236	uM	0.89545	-4.3244	107.25	108.07
Calcitonin	August 2022 GPCR Panel	Arrestin	Agonist	CALCR-RAMP3	EC50	0.1433346	uM	0.72186	-0.87325	106	103.06
CCK-8	August 2022 GPCR Panel	Arrestin	Agonist	CCKAR	EC50	0.003881683	uM	1.1405	-2.2947	100	101.65
CCK-8	August 2022 GPCR Panel	Arrestin	Agonist	CCKBR	EC50	0.0003673388	uM	1.5527	-1.718	102.31	101.37
CCL3	August 2022 GPCR Panel	Arrestin	Agonist	CCR1	EC50	0.001041598	uM	1.1108	-10	93.69	104.89
CCL27	August 2022 GPCR Panel	Arrestin	Agonist	CCR10	EC50	0.02626274	uM	1.4073	1.8602	100	100.93
CCL2	August 2022 GPCR Panel	Arrestin	Agonist	CCR2	EC50	0.002631843	uM	1.0598	-1.4625	100	100.4
CCL13	August 2022 GPCR Panel	Arrestin	Agonist	CCR3	EC50	0.04062094	uM	0.83007	1.5878	105	100
CCL22	August 2022 GPCR Panel	Arrestin	Agonist	CCR4	EC50	0.003437795	uM	0.71432	0	102.68	101.2
CCL3	August 2022 GPCR Panel	Arrestin	Agonist	CCR5	EC50	0.007583182	uM	1.0897	1.515	100	100.91
CCL20	August 2022 GPCR Panel	Arrestin	Agonist	CCR6	EC50	0.002950529	uM	1.1253	-4.4514	100	100.8
CCL19	August 2022 GPCR Panel	Arrestin	Agonist	CCR7	EC50	0.005645118	uM	2.036	-1.7698	100.44	102.04
CCL1	August 2022 GPCR Panel	Arrestin	Agonist	CCR8	EC50	0.0458469	uM	1.3048	2.0288	100	104.05
CCL25	August 2022 GPCR Panel	Arrestin	Agonist	CCR9	EC50	0.172951	uM	1.5366	0.38159	100	100
Acetylcholine	August 2022 GPCR Panel	Arrestin	Agonist	CHRM1	EC50	1.402265	uM	0.64719	0	106.04	100.58
Acetylcholine	August 2022 GPCR Panel	Arrestin	Agonist	CHRM2	EC50	2.755396	uM	1.3779	2.6925	100	100.81
Acetylcholine	August 2022 GPCR Panel	Arrestin	Agonist	CHRM3	EC50	0.1457965	uM	0.56689	-12.236	108.49	100
Acetylcholine	August 2022 GPCR Panel	Arrestin	Agonist	CHRM4	EC50	1.900527	uM	1.1007	-6.8542	100.27	104.44
Acetylcholine	August 2022 GPCR Panel	Arrestin	Agonist	CHRM5	EC50	0.05513787	uM	1.2059	-0.59006	100.43	101.2
Chemerin	August 2022 GPCR Panel	Arrestin	Agonist	CMKLR1	EC50	0.001004986	uM	1.7846	-1.3765	100	104.08
CP55940	August 2022 GPCR Panel	Arrestin	Agonist	CNR1	EC50	0.004738708	uM	0.91424	-8.794	101.26	104.27
CP55940	August 2022 GPCR Panel	Arrestin	Agonist	CNR2	EC50	0.002215185	uM	2.9877	0.44915	98.673	99.599
Sauvagine	August 2022 GPCR Panel	Arrestin	Agonist	CRHR1	EC50	0.003279745	uM	1.8277	-1.8621	100	98.203
Sauvagine	August 2022 GPCR Panel	Arrestin	Agonist	CRHR2	EC50	0.005993492	uM	1.4129	0.49814	100	100.67
PGD2	August 2022 GPCR Panel	Arrestin	Agonist	CRTH2	EC50	0.003340105	uM	0.72799	-8.8088	100.58	100
Fractalkine	August 2022 GPCR Panel	Arrestin	Agonist	CX3CR1	EC50	0.0004444573	uM	1.1237	-8.4026	100	105.09
CXCL8	August 2022 GPCR Panel	Arrestin	Agonist	CXCR1	EC50	0.002795374	uM	0.97352	-4.9222	100	100.67
CXCL8	August 2022 GPCR Panel	Arrestin	Agonist	CXCR2	EC50	0.0003037527	uM	0.98092	0	98.662	106.94
CXCL11	August 2022 GPCR Panel	Arrestin	Agonist	CXCR3	EC50	0.0120304	uM	1.0922	3.2275	100	106.47
CXCL12	August 2022 GPCR Panel	Arrestin	Agonist	CXCR4	EC50	0.00354797	uM	0.93797	11.901	100	104.76
CXCL13	August 2022 GPCR Panel	Arrestin	Agonist	CXCR5	EC50	0.02095897	uM	1.4103	3.2801	100	100.33
CXCL16	August 2022 GPCR Panel	Arrestin	Agonist	CXCR6	EC50	0.006805656	uM	1.5222	1.7888	105	104.92
CXCL12	August 2022 GPCR Panel	Arrestin	Agonist	CXCR7	EC50	0.008011062	uM	1.6149	-1.7859	100	104.6
Dopamine	August 2022 GPCR Panel	Arrestin	Agonist	DRD1	EC50	0.3960719	uM	1.3107	1.162	100	105.47
Dopamine	August 2022 GPCR Panel	Arrestin	Agonist	DRD2L	EC50	0.1377704	uM	1.1993	-1.5603	104.48	101.1
Dopamine	August 2022 GPCR Panel	Arrestin	Agonist	DRD2S	EC50	0.0496947	uM	1.0934	-2.5746	96.826	101.97
Dopamine	August 2022 GPCR Panel	Arrestin	Agonist	DRD3	EC50	0.002081086	uM	1.5067	-6.7782	101.49	100.91
Dopamine	August 2022 GPCR Panel	Arrestin	Agonist	DRD4	EC50	0.03668766	uM	1.2385	-4.5543	101.36	103.84
Dopamine	August 2022 GPCR Panel	Arrestin	Agonist	DRD5	EC50	0.03291091	uM	1.0774	-0.024319	101.92	102.54
7a,25-Dihydroxycholesterol	August 2022 GPCR Panel	Arrestin	Agonist	EBI2	EC50	0.003632537	uM	1.1457	0.71485	103.06	101.26
S-1-P	August 2022 GPCR Panel	Arrestin	Agonist	EDG1	EC50	0.01898279	uM	1.1089	-2.857	100.31	102.86
S-1-P	August 2022 GPCR Panel	Arrestin	Agonist	EDG3	EC50	0.01059547	uM	1.1291	-3.5563	97.815	100.81
Oleoyl LPA	August 2022 GPCR Panel	Arrestin	Agonist	EDG4	EC50	1.802619	uM	1.3783	1.2853	93.075	105.68
S-1-P	August 2022 GPCR Panel	Arrestin	Agonist	EDG5	EC50	0.03718605	uM	1.7	1.1708	96.946	98.798
S-1-P	August 2022 GPCR Panel	Arrestin	Agonist	EDG6	EC50	0.03051476	uM	0.94885	-5	98.769	101.46
Oleoyl LPA	August 2022 GPCR Panel	Arrestin	Agonist	EDG7	EC50	0.1738741	uM	1.1261	1.7177	98.075	100.16
Endothelin I	August 2022 GPCR Panel	Arrestin	Agonist	EDNRA	EC50	0.002385338	uM	1.1297	-1.8519	96.562	104.63
Endothelin 3	August 2022 GPCR Panel	Arrestin	Agonist	EDNRB	EC50	0.006583851	uM	0.97303	-5.299	96.586	102.05
TFLLR-NH2	August 2022 GPCR Panel	Arrestin	Agonist	F2R	EC50	14.49439	uM	1.2839	0.6282	100	103.36
SLIGRL-NH2	August 2022 GPCR Panel	Arrestin	Agonist	F2RL1	EC50	0.5519605	uM	1.1076	-2.2601	101.71	101.05
AYPGKF-NH2	August 2022 GPCR Panel	Arrestin	Agonist	F2RL3	EC50	2.282086	uM	1.9026	-2.8768	101.99	101.77
GW9508	August 2022 GPCR Panel	Arrestin	Agonist	FFAR1	EC50	0.9588609	uM	1.0269	1.9496	101.83	103.4
WKYMVm-NH2	August 2022 GPCR Panel	Arrestin	Agonist	FPR1	EC50	0.004949029	uM	1.96	-1.2578	101.3	98.917
WKYMVm-NH2	August 2022 GPCR Panel	Arrestin	Agonist	FPRL1	EC50	0.002164662	uM	2.1405	2.3178	101.26	103.5
FSH	August 2022 GPCR Panel	Arrestin	Agonist	FSHR	EC50	0.007459333	uM	1.0758	0.71439	110	114.13
Galanin	August 2022 GPCR Panel	Arrestin	Agonist	GALR1	EC50	0.004739363	uM	2.0213	-0.48036	102.15	104.23
Galanin	August 2022 GPCR Panel	Arrestin	Agonist	GALR2	EC50	0.006805342	uM	1.5902	7.6827	102.82	100.83
Glucagon	August 2022 GPCR Panel	Arrestin	Agonist	GCGR	EC50	0.002334533	uM	1.9316	3.6064	102.29	103.15
Ghrelin	August 2022 GPCR Panel	Arrestin	Agonist	GHSR	EC50	0.008482619	uM	2.4678	0.62296	94.252	98.147
GIP	August 2022 GPCR Panel	Arrestin	Agonist	GIPR	EC50	0.004871469	uM	1.215	2.1835	106.8	110.21
Exendin-4	August 2022 GPCR Panel	Arrestin	Agonist	GLP1R	EC50	0.005824921	uM	1.2562	-0.9728	98.597	101.42
GLP II (1-33)	August 2022 GPCR Panel	Arrestin	Agonist	GLP2R	EC50	0.002297417	uM	0.78513	7.6211	102.59	100.69
Chemerin	August 2022 GPCR Panel	Arrestin	Agonist	GPR1	EC50	0.002258396	uM	1.3937	-0.015963	98.668	99.696
QRFP-26	August 2022 GPCR Panel	Arrestin	Agonist	GPR103	EC50	0.009995395	uM	0.98753	-7.5636	103.59	100.28
Nicotinic Acid	August 2022 GPCR Panel	Arrestin	Agonist	GPR109A	EC50	3.644005	uM	1.1508	1.8885	108	107.49

3-Hydroxyoctanoic Acid	August 2022 GPCR Panel	Arrestin	Agonist	GPR1066	EC50	372.9495	uM	1.3226	1.0852	105	100
Oleoyl Ethanolamide	August 2022 GPCR Panel	Arrestin	Agonist	GPR119	EC50	1.838176	uM	0.96535	-12.768	105.21	103.94
GW9508	August 2022 GPCR Panel	Arrestin	Agonist	GPR120	EC50	6.96835	uM	1.0467	-7.1742	113.42	106.32
Zaprinast	August 2022 GPCR Panel	Arrestin	Agonist	GPR35	EC50	1.740095	uM	0.65872	-4.2289	105.27	101.96
Oleoyl LPA	August 2022 GPCR Panel	Arrestin	Agonist	GPR92	EC50	0.7273777	uM	0.82717	1.1979	100.49	101.14
GRP	August 2022 GPCR Panel	Arrestin	Agonist	GRPR	EC50	0.001622146	uM	1.687	0.94683	93.998	99.427
Orexin A	August 2022 GPCR Panel	Arrestin	Agonist	HCRTR1	EC50	0.004212985	uM	1.8912	-0.62218	96.031	98.192
Orexin A	August 2022 GPCR Panel	Arrestin	Agonist	HCRTR2	EC50	0.01624904	uM	1.7906	0.17334	102.47	100.46
Histamine	August 2022 GPCR Panel	Arrestin	Agonist	HRH1	EC50	0.04169174	uM	1.0719	0	91.374	101.92
Histamine	August 2022 GPCR Panel	Arrestin	Agonist	HRH2	EC50	4.489645	uM	0.8807	4.9249	100	101.25
R-a methylhistamine	August 2022 GPCR Panel	Arrestin	Agonist	HRH3	EC50	0.1068533	uM	1.1514	-5.4023	100.87	100.75
Histamine	August 2022 GPCR Panel	Arrestin	Agonist	HRH4	EC50	0.04382884	uM	0.98004	-2.1869	102.92	104.69
Serotonin / 5-HT	August 2022 GPCR Panel	Arrestin	Agonist	HTR1A	EC50	0.04870012	uM	1.5705	-4.0678	101.04	101.92
Serotonin / 5-HT	August 2022 GPCR Panel	Arrestin	Agonist	HTR1B	EC50	0.03952119	uM	1.1066	-2.5647	101.29	102.29
Serotonin / 5-HT	August 2022 GPCR Panel	Arrestin	Agonist	HTR1E	EC50	0.003518195	uM	1.5289	-7.3023	105.51	101.99
Serotonin / 5-HT	August 2022 GPCR Panel	Arrestin	Agonist	HTR1F	EC50	0.03048808	uM	0.93606	-10.321	108.78	107.92
Serotonin / 5-HT	August 2022 GPCR Panel	Arrestin	Agonist	HTR2A	EC50	0.02168602	uM	0.96597	0.085792	99.25	99.349
Serotonin / 5-HT	August 2022 GPCR Panel	Arrestin	Agonist	HTR2C	EC50	0.001968696	uM	1.1706	-5.4272	98.587	92.1
Serotonin / 5-HT	August 2022 GPCR Panel	Arrestin	Agonist	HTR5A	EC50	0.00576647	uM	1.4028	4.5741	104.79	100.52
Kisspeptin-10	August 2022 GPCR Panel	Arrestin	Agonist	KISS1R	EC50	0.0176153	uM	1.2388	-0.57157	104.88	107.69
hCG	August 2022 GPCR Panel	Arrestin	Agonist	LHCGR	EC50	0.002273421	uM	0.65664	-6.0082	112.86	107.66
Leukotriene B4	August 2022 GPCR Panel	Arrestin	Agonist	LTB4R	EC50	0.1410552	uM	0.68356	4.511	110	122.03
Melanotan II	August 2022 GPCR Panel	Arrestin	Agonist	MC1R	EC50	0.0004369583	uM	1.2155	4.2998	100	100.11
Melanotan II	August 2022 GPCR Panel	Arrestin	Agonist	MC3R	EC50	0.0008359228	uM	1.2752	4.9004	100	100.58
Melanotan II	August 2022 GPCR Panel	Arrestin	Agonist	MC4R	EC50	0.001266889	uM	0.90099	-5.252	99.724	100.46
Melanotan II	August 2022 GPCR Panel	Arrestin	Agonist	MC5R	EC50	0.007774995	uM	0.7756	-6.5723	104.01	107.84
MCH	August 2022 GPCR Panel	Arrestin	Agonist	MCHR1	EC50	0.1674376	uM	1.4457	1.9607	100	100
MCH	August 2022 GPCR Panel	Arrestin	Agonist	MCHR2	EC50	0.005514293	uM	1.5346	3.1744	99.371	103.44
Motilin	August 2022 GPCR Panel	Arrestin	Agonist	MLNR	EC50	0.001590376	uM	0.80863	-9.2463	100	102.1
BAM(8-22)	August 2022 GPCR Panel	Arrestin	Agonist	MRGPRX1	EC50	3.504257	uM	1.2114	3.3193	100	105.15
Cortistatin 14	August 2022 GPCR Panel	Arrestin	Agonist	MRGPRX2	EC50	0.1553549	uM	0.83242	-0.33236	100	112.59
2-Iodomelatonin	August 2022 GPCR Panel	Arrestin	Agonist	MTNR1A	EC50	0.000730298	uM	1.5901	-0.91382	100.7	102.67
Neuromedin B	August 2022 GPCR Panel	Arrestin	Agonist	NMBR	EC50	0.0005755856	uM	1.2642	0	97.735	101.96
Neuromedin U-25	August 2022 GPCR Panel	Arrestin	Agonist	NMU1R	EC50	0.001429816	uM	1.6529	-0.055343	101.34	101.18
Neuropeptide W23	August 2022 GPCR Panel	Arrestin	Agonist	NPBWR1	EC50	0.002169053	uM	1.7253	6.5309	98.703	100.19
Neuropeptide W23	August 2022 GPCR Panel	Arrestin	Agonist	NPBWR2	EC50	0.003615681	uM	2.3725	-0.83886	99.167	101.21
RFRP-3	August 2022 GPCR Panel	Arrestin	Agonist	NPFFR1	EC50	0.02515244	uM	0.84424	-4.7513	100.95	100.6
Neuropeptide S	August 2022 GPCR Panel	Arrestin	Agonist	NPSR1B	EC50	0.02360206	uM	0.96946	-5.6163	97.744	106.99
Peptide YY	August 2022 GPCR Panel	Arrestin	Agonist	NPY1R	EC50	0.003925817	uM	0.86992	-9.7066	100	100.86
Peptide YY	August 2022 GPCR Panel	Arrestin	Agonist	NPY2R	EC50	0.002585294	uM	2.1905	-0.53426	100	103.69
[Lys 8,9] Neurotensin	August 2022 GPCR Panel	Arrestin	Agonist	NTSR1	EC50	0.0002377443	uM	1.8392	4.3056	105.37	101.31
DADLE	August 2022 GPCR Panel	Arrestin	Agonist	OPRD1	EC50	0.004407782	uM	0.73776	-5.8906	102.31	106.58
Dynorphin A	August 2022 GPCR Panel	Arrestin	Agonist	OPRK1	EC50	0.06292394	uM	0.91322	-2.5726	103.11	101.11
Orphanin FQ	August 2022 GPCR Panel	Arrestin	Agonist	OPRL1	EC50	0.006485448	uM	1.0555	-2.9695	101.29	103.92
[Met] Enkephalin	August 2022 GPCR Panel	Arrestin	Agonist	OPRM1	EC50	0.5881969	uM	1.1453	-2.0822	98.969	100.17
5-OxoETE	August 2022 GPCR Panel	Arrestin	Agonist	OXER1	EC50	1.143734	uM	0.75922	-0.2145	100	100
Oxytocin	August 2022 GPCR Panel	Arrestin	Agonist	OXTR	EC50	0.003228495	uM	0.75819	-1.7706	102.14	95.386
2-methylthio-ADP	August 2022 GPCR Panel	Arrestin	Agonist	P2RY1	EC50	0.02037793	uM	0.92597	-0.53627	99.336	100.4
ATP	August 2022 GPCR Panel	Arrestin	Agonist	P2RY11	EC50	371.0396	uM	4.523	1.8016	104.83	103.71
2-methylthio-ADP	August 2022 GPCR Panel	Arrestin	Agonist	P2RY12	EC50	0.002716565	uM	1.0334	-5.0447	101	102.97
UTP	August 2022 GPCR Panel	Arrestin	Agonist	P2RY2	EC50	0.4311327	uM	1.9756	2.6252	96.948	105.35
UTP	August 2022 GPCR Panel	Arrestin	Agonist	P2RY4	EC50	0.1264911	uM	0.93915	-5	98.026	101.62
UDP	August 2022 GPCR Panel	Arrestin	Agonist	P2RY6	EC50	0.01326906	uM	0.83577	-10.471	102.75	100.95
Pancreatic Polypeptide	August 2022 GPCR Panel	Arrestin	Agonist	PPYR1	EC50	0.001504423	uM	1.2096	-1.8292	97.898	96.839
PrRP-31	August 2022 GPCR Panel	Arrestin	Agonist	PRLHR	EC50	0.002440338	uM	1.5554	-0.29601	99.754	101.19
EG VEGF	August 2022 GPCR Panel	Arrestin	Agonist	PROKR1	EC50	0.01765347	uM	1.0565	-0.62347	106.22	102.59
EG VEGF	August 2022 GPCR Panel	Arrestin	Agonist	PROKR2	EC50	0.01061989	uM	1.2011	-1.0624	102.93	104.29
PAF	August 2022 GPCR Panel	Arrestin	Agonist	PTAFR	EC50	0.003823139	uM	1.8262	0.53715	100	100.46
Prostaglandin E2	August 2022 GPCR Panel	Arrestin	Agonist	PTGER2	EC50	0.6873754	uM	0.84772	-1.8177	99.103	99.417
Prostaglandin E2	August 2022 GPCR Panel	Arrestin	Agonist	PTGER3	EC50	0.003761144	uM	1.0648	-4.5647	98.536	101.62
Prostaglandin E2	August 2022 GPCR Panel	Arrestin	Agonist	PTGER4	EC50	0.0005823444	uM	1.8119	-2.9138	102.66	103.34
Cloprostenol	August 2022 GPCR Panel	Arrestin	Agonist	PTGFR	EC50	0.007043037	uM	0.96661	-0.18863	96.972	100.52
Beraprost	August 2022 GPCR Panel	Arrestin	Agonist	PTGIR	EC50	0.2187656	uM	1.3158	8.5689	100	102.4
PTH(1-34)	August 2022 GPCR Panel	Arrestin	Agonist	PTHR1	EC50	0.0008733333	uM	3.3619	3.9763	98.042	96.306
TIP-39	August 2022 GPCR Panel	Arrestin	Agonist	PTHR2	EC50	0.00148146	uM	1.9233	2.2565	100.48	101.68
Relaxin-3	August 2022 GPCR Panel	Arrestin	Agonist	RXFP3	EC50	0.01188393	uM	0.83341	-2.1488	100	103.3
Secretin	August 2022 GPCR Panel	Arrestin	Agonist	SCTR	EC50	0.001738682	uM	2.4137	-0.52064	99.971	103.23
Somatostatin 28	August 2022 GPCR Panel	Arrestin	Agonist	SSTR1	EC50	0.005690877	uM	0.9221	-0.029622	102.68	102.65
Somatostatin 28	August 2022 GPCR Panel	Arrestin	Agonist	SSTR2	EC50	0.004881576	uM	1.1232	-1.9751	99.89	107.78
Tyr-SST 14	August 2022 GPCR Panel	Arrestin	Agonist	SSTR3	EC50	0.0321048	uM	1.0935	1.3337	100	100
Somatostatin 28	August 2022 GPCR Panel	Arrestin	Agonist	SSTR5	EC50	0.007112627	uM	1.4968	3.8156	100.7	102.87
Substance P	August 2022 GPCR Panel	Arrestin	Agonist	TACR1	EC50	0.002450811	uM	1.6523	1.016	100.41	101.11
Substance P	August 2022 GPCR Panel	Arrestin	Agonist	TACR2	EC50	0.08746414	uM	0.67952	0	100	108.43
Substance P	August 2022 GPCR Panel	Arrestin	Agonist	TACR3	EC50	0.01315104	uM	0.99897	0	99.743	102.24
I-BOP	August 2022 GPCR Panel	Arrestin	Agonist	TBXA2R	EC50	0.02125299	uM	1.1152	-2.3978	100	103.12
TRH	August 2022 GPCR Panel	Arrestin	Agonist	TRHR	EC50	0.002020041	uM	1.4836	-1.4107	100	102.21
TSH	August 2022 GPCR Panel	Arrestin	Agonist	TSHR(L)	EC50	0.04951309	uM	0.82938	-0.47128	111.68	105.96
Urotensin II	August 2022 GPCR Panel	Arrestin	Agonist	UTR2	EC50	0.001186397	uM	1.0063	0	98.712	108.04
VIP	August 2022 GPCR Panel	Arrestin	Agonist	VIPR1	EC50	0.001727508	uM	1.8414	5.9378	101.12	102.57
VIP	August 2022 GPCR Panel	Arrestin	Agonist	VIPR2	EC50	0.006734727	uM	3.1618	1.3517	101.54	101.68

Table 3 Compound activity determined us GPCR Biosensor Assays

Compound Name	Project ID	Assay Name	Assay Format	Assay Target	Conc (uM)	Value 1	Value 2	Average Value	Std Deviation	% Efficacy
SUOON	US073-0024133-0	Arrestin	Antagonist	ADCYAP1R1	2.5	319600	307680	313640	8428.7	0.9
SUOON	US073-0024133-0	Arrestin	Antagonist	ADORA3	2.5	40040	42880	41460	2008.2	0.5
SUOON	US073-0024133-0	Arrestin	Antagonist	ADRA1B	2.5	74080	76960	75520	2036.5	0.1
SUOON	US073-0024133-0	Arrestin	Antagonist	ADRA2A	2.5	114520	124560	119540	7099.4	-27.2
SUOON	US073-0024133-0	Arrestin	Antagonist	ADRA2B	2.5	59920	58240	59080	1187.9	-36.8
SUOON	US073-0024133-0	Arrestin	Antagonist	ADRA2C	2.5	65360	66760	66060	990	-26.4
SUOON	US073-0024133-0	Arrestin	Antagonist	ADRB1	2.5	72600	89400	81000	11879.4	12.6
SUOON	US073-0024133-0	Arrestin	Antagonist	ADRB2	2.5	63640	59960	61800	2602.2	-11.7
SUOON	US073-0024133-0	Arrestin	Antagonist	AGTR1	2.5	73920	82880	78400	6335.7	-8.5
SUOON	US073-0024133-0	Arrestin	Antagonist	AGTRL1	2.5	183000	190920	186960	5600.3	-23.4
SUOON	US073-0024133-0	Arrestin	Antagonist	AVPR1A	2.5	66680	68400	67540	1074.8	-2.4
SUOON	US073-0024133-0	Arrestin	Antagonist	AVPR1B	2.5	16160	15960	16060	141.4	-25.7
SUOON	US073-0024133-0	Arrestin	Antagonist	AVPR2	2.5	271080	258240	264660	9079.2	-11.2
SUOON	US073-0024133-0	Arrestin	Antagonist	BDKRB1	2.5	15000	14960	14980	28.3	-8.7
SUOON	US073-0024133-0	Arrestin	Antagonist	BDKRB2	2.5	289280	280360	284820	6307.4	-1.7
SUOON	US073-0024133-0	Arrestin	Antagonist	BRS3	2.5	229520	204560	217040	17649.4	-8.8
SUOON	US073-0024133-0	Arrestin	Antagonist	C3AR1	2.5	97320	100080	98700	1951.6	4
SUOON	US073-0024133-0	Arrestin	Antagonist	C5aR1	2.5	228600	227760	228180	594	-14.2
SUOON	US073-0024133-0	Arrestin	Antagonist	C5L2	2.5	112800	128400	120600	11030.9	3.5
SUOON	US073-0024133-0	Arrestin	Antagonist	CALCR	2.5	24800	21720	23260	2177.9	-22.3
SUOON	US073-0024133-0	Arrestin	Antagonist	CALCRL-RAMP1	2.5	47120	52200	49660	3592.1	-19
SUOON	US073-0024133-0	Arrestin	Antagonist	CALCRL-RAMP2	2.5	258960	257480	258220	1046.5	-11.6
SUOON	US073-0024133-0	Arrestin	Antagonist	CALCRL-RAMP3	2.5	134000	143120	138560	6448.8	-3.5
SUOON	US073-0024133-0	Arrestin	Antagonist	CALCR-RAMP2	2.5	53400	54240	53820	594	-17.8
SUOON	US073-0024133-0	Arrestin	Antagonist	CALCR-RAMP3	2.5	10400	10720	10560	226.3	-0.1
SUOON	US073-0024133-0	Arrestin	Antagonist	CCKAR	2.5	95280	105120	100200	6957.9	-17.2
SUOON	US073-0024133-0	Arrestin	Antagonist	CCKBR	2.5	385280	359760	372520	18046.4	-7.8
SUOON	US073-0024133-0	Arrestin	Antagonist	CCR1	2.5	364000	336280	350140	19601	-6.4
SUOON	US073-0024133-0	Arrestin	Antagonist	CCR10	2.5	38360	39520	38940	820.2	-16.6
SUOON	US073-0024133-0	Arrestin	Antagonist	CCR2	2.5	142120	162680	152400	14538.1	-15.4
SUOON	US073-0024133-0	Arrestin	Antagonist	CCR3	2.5	81520	83600	82560	1470.8	-6.8
SUOON	US073-0024133-0	Arrestin	Antagonist	CCR4	2.5	304760	313960	309360	6505.4	1.3
SUOON	US073-0024133-0	Arrestin	Antagonist	CCR5	2.5	163480	173360	168420	6986.2	-16.1
SUOON	US073-0024133-0	Arrestin	Antagonist	CCR6	2.5	246240	230080	238160	11426.8	-14.8
SUOON	US073-0024133-0	Arrestin	Antagonist	CCR7	2.5	860640	822960	841800	26643.8	-19.2
SUOON	US073-0024133-0	Arrestin	Antagonist	CCR8	2.5	1337080	1294280	1315680	30264.2	-17
SUOON	US073-0024133-0	Arrestin	Antagonist	CCR9	2.5	2642000	2928040	2785020	202260.8	-10.1
SUOON	US073-0024133-0	Arrestin	Antagonist	CHRM1	2.5	52600	47360	49980	3705.2	9.3
SUOON	US073-0024133-0	Arrestin	Antagonist	CHRM2	2.5	68400	68520	68460	84.8	3.3
SUOON	US073-0024133-0	Arrestin	Antagonist	CHRM3	2.5	33440	31760	32600	1187.9	12.6
SUOON	US073-0024133-0	Arrestin	Antagonist	CHRM4	2.5	140200	154880	147540	10380.3	5.8
SUOON	US073-0024133-0	Arrestin	Antagonist	CHRM5	2.5	391840	395640	393740	2687	-1.5
SUOON	US073-0024133-0	Arrestin	Antagonist	CMKLR1	2.5	3476520	3565600	3521060	62969.1	-18.3
SUOON	US073-0024133-0	Arrestin	Antagonist	CNR1	2.5	64440	62800	63620	1159.7	-37.5
SUOON	US073-0024133-0	Arrestin	Antagonist	CNR2	2.5	86560	78000	82780	6759.9	3.6
SUOON	US073-0024133-0	Arrestin	Antagonist	CRHR1	2.5	416760	489360	453060	51336	5.4
SUOON	US073-0024133-0	Arrestin	Antagonist	CRHR2	2.5	253720	298600	276160	31735	-8.6
SUOON	US073-0024133-0	Arrestin	Antagonist	CRTH2	2.5	56200	53400	54800	1979.9	0.6
SUOON	US073-0024133-0	Arrestin	Antagonist	CX3CR1	2.5	5791720	6074960	5933340	200280.9	-0.8
SUOON	US073-0024133-0	Arrestin	Antagonist	CXCR1	2.5	1239560	1690880	1463220	321969.9	10.2
SUOON	US073-0024133-0	Arrestin	Antagonist	CXCR2	2.5	671720	727920	699820	39739.4	-9.8
SUOON	US073-0024133-0	Arrestin	Antagonist	CXCR3	2.5	1269680	1238920	1254300	21750.6	-7.5
SUOON	US073-0024133-0	Arrestin	Antagonist	CXCR4	2.5	15800	13680	14740	1499.1	-28.5
SUOON	US073-0024133-0	Arrestin	Antagonist	CXCR5	2.5	672240	666520	669380	4044.6	-18.9
SUOON	US073-0024133-0	Arrestin	Antagonist	CXCR6	2.5	6040	6240	6140	141.4	-1.3
SUOON	US073-0024133-0	Arrestin	Antagonist	CXCR7	2.5	2383280	2751880	2582580	281862.8	-9.6
SUOON	US073-0024133-0	Arrestin	Antagonist	DRD1	2.5	31160	28680	29920	1753.6	5.7
SUOON	US073-0024133-0	Arrestin	Antagonist	DRD2L	2.5	24440	23560	24000	622.2	-16.8
SUOON	US073-0024133-0	Arrestin	Antagonist	DRD2S	2.5	167880	163960	165920	2771.9	-13.4
SUOON	US073-0024133-0	Arrestin	Antagonist	DRD3	2.5	91680	86680	89180	3535.5	-1
SUOON	US073-0024133-0	Arrestin	Antagonist	DRD4	2.5	6120	6400	6260	198	2.5
SUOON	US073-0024133-0	Arrestin	Antagonist	DRD5	2.5	34240	34920	34580	480.8	4.2
SUOON	US073-0024133-0	Arrestin	Antagonist	EBI2	2.5	459960	392240	426100	47885.3	-27.3
SUOON	US073-0024133-0	Arrestin	Antagonist	EDG1	2.5	175200	199560	187380	17225.1	-25.9
SUOON	US073-0024133-0	Arrestin	Antagonist	EDG3	2.5	365840	496760	431300	92574.4	15.4
SUOON	US073-0024133-0	Arrestin	Antagonist	EDG4	2.5	83080	79840	81460	2291	4.6
SUOON	US073-0024133-0	Arrestin	Antagonist	EDG5	2.5	186160	194720	190440	6052.8	-11.2
SUOON	US073-0024133-0	Arrestin	Antagonist	EDG6	2.5	359400	376760	368080	12275.4	4.5
SUOON	US073-0024133-0	Arrestin	Antagonist	EDG7	2.5	95800	97720	96760	1357.6	5
SUOON	US073-0024133-0	Arrestin	Antagonist	EDNRA	2.5	46000	49080	47540	2177.9	2.5
SUOON	US073-0024133-0	Arrestin	Antagonist	EDNRB	2.5	58040	53520	55780	3196.1	-9.9
SUOON	US073-0024133-0	Arrestin	Antagonist	F2R	2.5	36440	44800	40620	5911.4	-17
SUOON	US073-0024133-0	Arrestin	Antagonist	F2RL1	2.5	282720	263680	273200	13463.3	-9.2
SUOON	US073-0024133-0	Arrestin	Antagonist	F2RL3	2.5	444280	402360	423320	29641.9	-25.9
SUOON	US073-0024133-0	Arrestin	Antagonist	FFAR1	2.5	111920	105840	108880	4299.2	-3.9
SUOON	US073-0024133-0	Arrestin	Antagonist	FPR1	2.5	384840	369200	377020	11069.2	-11.1
SUOON	US073-0024133-0	Arrestin	Antagonist	FPRL1	2.5	193080	196400	194740	2347.6	-17.7
SUOON	US073-0024133-0	Arrestin	Antagonist	FSHR	2.5	23840	21880	22860	1385.9	-16.9
SUOON	US073-0024133-0	Arrestin	Antagonist	GALR1	2.5	381800	474280	428040	65393.2	-22.5
SUOON	US073-0024133-0	Arrestin	Antagonist	GALR2	2.5	474160	412960	443560	43274.9	-29.7
SUOON	US073-0024133-0	Arrestin	Antagonist	GCGR	2.5	138720	143080	140900	3083	-17.2
SUOON	US073-0024133-0	Arrestin	Antagonist	GHSR	2.5	162640	137200	149920	17988.8	-7.4
SUOON	US073-0024133-0	Arrestin	Antagonist	GIPR	2.5	13680	14160	13920	339.4	-18.9
SUOON	US073-0024133-0	Arrestin	Antagonist	GLP1R	2.5	173160	164680	168920	5996.3	-11
SUOON	US073-0024133-0	Arrestin	Antagonist	GLP2R	2.5	58800	57040	57920	1244.5	-15.4
SUOON	US073-0024133-0	Arrestin	Antagonist	GPR1	2.5	118880	110160	114520	6166	-1.3
SUOON	US073-0024133-0	Arrestin	Antagonist	GPR103	2.5	24560	23920	24240	452.6	14.6
SUOON	US073-0024133-0	Arrestin	Antagonist	GPR109A	2.5	107680	105360	106520	1640.5	-16

SUOON	US073-0024133-O	Arrestin	Antagonist	GPR109B	2.5	433560	449200	441380	11059.2	-17
SUOON	US073-0024133-O	Arrestin	Antagonist	GPR119	2.5	57680	55320	56500	1668.8	-1
SUOON	US073-0024133-O	Arrestin	Antagonist	GPR120	2.5	12160	14000	13080	1301.1	22.7
SUOON	US073-0024133-O	Arrestin	Antagonist	GPR35	2.5	183680	167160	175520	11822.8	-12.2
SUOON	US073-0024133-O	Arrestin	Antagonist	GPR92	2.5	111400	109720	110560	1187.9	10.6
SUOON	US073-0024133-O	Arrestin	Antagonist	GRPR	2.5	118560	109520	114040	6392.2	-12.2
SUOON	US073-0024133-O	Arrestin	Antagonist	HCRTR1	2.5	326440	320840	323640	3959.8	-1.7
SUOON	US073-0024133-O	Arrestin	Antagonist	HCRTR2	2.5	285920	279520	282720	4525.5	-2.7
SUOON	US073-0024133-O	Arrestin	Antagonist	HRH1	2.5	135360	118960	127160	11596.6	-38.5
SUOON	US073-0024133-O	Arrestin	Antagonist	HRH2	2.5	36840	31440	34140	3818.4	-13.3
SUOON	US073-0024133-O	Arrestin	Antagonist	HRH3	2.5	12280	12240	12260	28.3	-8.6
SUOON	US073-0024133-O	Arrestin	Antagonist	HRH4	2.5	3240	3040	3140	141.4	5.2
SUOON	US073-0024133-O	Arrestin	Antagonist	HTR1A	2.5	320640	334600	327720	9729.8	-6.2
SUOON	US073-0024133-O	Arrestin	Antagonist	HTR1B	2.5	194200	164960	179580	20675.8	-11.9
SUOON	US073-0024133-O	Arrestin	Antagonist	HTR1E	2.5	3640	3640	3640	0	-3.8
SUOON	US073-0024133-O	Arrestin	Antagonist	HTR1F	2.5	65080	62160	63620	2064.8	-23.3
SUOON	US073-0024133-O	Arrestin	Antagonist	HTR2A	2.5	238960	219800	229380	13548.2	-9.7
SUOON	US073-0024133-O	Arrestin	Antagonist	HTR2C	2.5	166680	155720	161200	7749.9	2.2
SUOON	US073-0024133-O	Arrestin	Antagonist	HTR5A	2.5	515760	512760	514260	2121.3	-0.3
SUOON	US073-0024133-O	Arrestin	Antagonist	KISS1R	2.5	26000	22480	24240	2489	13.2
SUOON	US073-0024133-O	Arrestin	Antagonist	LHCGR	2.5	13280	14520	13900	876.8	7.2
SUOON	US073-0024133-O	Arrestin	Antagonist	LTB4R	2.5	107160	106480	106820	480.8	10.3
SUOON	US073-0024133-O	Arrestin	Antagonist	MC1R	2.5	17760	17960	17860	141.4	0.4
SUOON	US073-0024133-O	Arrestin	Antagonist	MC3R	2.5	5400	5200	5300	141.4	-2.1
SUOON	US073-0024133-O	Arrestin	Antagonist	MC4R	2.5	14720	14160	14440	396	-4.6
SUOON	US073-0024133-O	Arrestin	Antagonist	MC5R	2.5	22560	18880	20720	2602.2	5.9
SUOON	US073-0024133-O	Arrestin	Antagonist	MCHR1	2.5	6840	6600	6720	169.7	5.1
SUOON	US073-0024133-O	Arrestin	Antagonist	MCHR2	2.5	36520	32280	34400	2998.1	-10.5
SUOON	US073-0024133-O	Arrestin	Antagonist	MLNR	2.5	94320	93560	93940	537.4	-5.5
SUOON	US073-0024133-O	Arrestin	Antagonist	MRGPRX1	2.5	222520	199640	211080	16178.6	3.8
SUOON	US073-0024133-O	Arrestin	Antagonist	MRGPRX2	2.5	210400	221720	216060	8004.4	-23.5
SUOON	US073-0024133-O	Arrestin	Antagonist	MTNR1A	2.5	15480	15200	15340	198	2.2
SUOON	US073-0024133-O	Arrestin	Antagonist	NMBR	2.5	121880	111440	116660	7382.2	-7.7
SUOON	US073-0024133-O	Arrestin	Antagonist	NMU1R	2.5	121560	105000	113280	11709.7	-34.2
SUOON	US073-0024133-O	Arrestin	Antagonist	NPBWR1	2.5	84640	84680	84660	28.3	-15
SUOON	US073-0024133-O	Arrestin	Antagonist	NPBWR2	2.5	139040	136760	137900	1612.2	-1.1
SUOON	US073-0024133-O	Arrestin	Antagonist	NPFFR1	2.5	33920	37760	35840	2715.3	-4.2
SUOON	US073-0024133-O	Arrestin	Antagonist	NPSR1B	2.5	6520	6920	6720	282.8	15.5
SUOON	US073-0024133-O	Arrestin	Antagonist	NPY1R	2.5	39200	42080	40640	2036.5	-2.7
SUOON	US073-0024133-O	Arrestin	Antagonist	NPY2R	2.5	346520	314120	330320	22910.3	-10.3
SUOON	US073-0024133-O	Arrestin	Antagonist	NTSR1	2.5	267280	230400	248840	26078.1	-21.4
SUOON	US073-0024133-O	Arrestin	Antagonist	OPRD1	2.5	36720	39520	38120	1979.9	10
SUOON	US073-0024133-O	Arrestin	Antagonist	OPRK1	2.5	6720	6320	6520	282.8	-4.5
SUOON	US073-0024133-O	Arrestin	Antagonist	OPRL1	2.5	142080	137080	139580	3535.5	-6.6
SUOON	US073-0024133-O	Arrestin	Antagonist	OPRM1	2.5	188640	187280	187960	961.7	-21.1
SUOON	US073-0024133-O	Arrestin	Antagonist	OXER1	2.5	37440	40400	38920	2093	-39.7
SUOON	US073-0024133-O	Arrestin	Antagonist	OXTR	2.5	64080	67120	65600	2149.6	1.3
SUOON	US073-0024133-O	Arrestin	Antagonist	P2RY1	2.5	82720	80560	81640	1527.4	-6.4
SUOON	US073-0024133-O	Arrestin	Antagonist	P2RY11	2.5	40480	41000	40740	367.7	-5.6
SUOON	US073-0024133-O	Arrestin	Antagonist	P2RY12	2.5	104360	98520	101440	4129.5	-11
SUOON	US073-0024133-O	Arrestin	Antagonist	P2RY2	2.5	107080	107520	107300	311.1	-5.2
SUOON	US073-0024133-O	Arrestin	Antagonist	P2RY4	2.5	160480	142400	151440	12784.5	12.9
SUOON	US073-0024133-O	Arrestin	Antagonist	P2RY6	2.5	237200	228560	232880	6109.4	-15.1
SUOON	US073-0024133-O	Arrestin	Antagonist	PPYR1	2.5	85600	86280	85940	480.8	-11.4
SUOON	US073-0024133-O	Arrestin	Antagonist	PRLHR	2.5	16560	15560	16060	707.1	-22.2
SUOON	US073-0024133-O	Arrestin	Antagonist	PROKR1	2.5	44200	46760	45480	1810.2	-12.4
SUOON	US073-0024133-O	Arrestin	Antagonist	PROKR2	2.5	11640	12640	12140	707.1	-17.5
SUOON	US073-0024133-O	Arrestin	Antagonist	PTAFR	2.5	445960	588840	517400	101031.4	-7.3
SUOON	US073-0024133-O	Arrestin	Antagonist	PTGER2	2.5	20480	18200	19340	1612.2	2.1
SUOON	US073-0024133-O	Arrestin	Antagonist	PTGER3	2.5	131160	151200	141180	14170.4	-10
SUOON	US073-0024133-O	Arrestin	Antagonist	PTGER4	2.5	125840	117320	121580	6024.6	-15.1
SUOON	US073-0024133-O	Arrestin	Antagonist	PTGFR	2.5	16760	18000	17380	876.8	-8.4
SUOON	US073-0024133-O	Arrestin	Antagonist	PTGIR	2.5	86520	81280	83900	3705.2	-20
SUOON	US073-0024133-O	Arrestin	Antagonist	PTHR1	2.5	659000	631160	645080	19685.8	-8.7
SUOON	US073-0024133-O	Arrestin	Antagonist	PTHR2	2.5	423800	430920	427360	5034.6	4.5
SUOON	US073-0024133-O	Arrestin	Antagonist	RXFP3	2.5	19800	19680	19740	84.8	31.4
SUOON	US073-0024133-O	Arrestin	Antagonist	SCTR	2.5	354160	317120	335640	26191.2	7.7
SUOON	US073-0024133-O	Arrestin	Antagonist	SSTR1	2.5	3920	3480	3700	311.1	-1.6
SUOON	US073-0024133-O	Arrestin	Antagonist	SSTR2	2.5	61400	63960	62680	1810.2	-20.5
SUOON	US073-0024133-O	Arrestin	Antagonist	SSTR3	2.5	137800	143880	140840	4299.2	4.2
SUOON	US073-0024133-O	Arrestin	Antagonist	SSTR5	2.5	86040	79880	82960	4355.8	-17.3
SUOON	US073-0024133-O	Arrestin	Antagonist	TACR1	2.5	838600	790120	814360	34280.5	-17.6
SUOON	US073-0024133-O	Arrestin	Antagonist	TACR2	2.5	141560	124560	133060	12020.8	8.3
SUOON	US073-0024133-O	Arrestin	Antagonist	TACR3	2.5	144760	157080	150920	8711.6	-6.8
SUOON	US073-0024133-O	Arrestin	Antagonist	TBXA2R	2.5	89600	90400	90000	565.7	16.2
SUOON	US073-0024133-O	Arrestin	Antagonist	TRHR	2.5	11320	13840	12580	1781.9	-6.6
SUOON	US073-0024133-O	Arrestin	Antagonist	TSHR(L)	2.5	4560	4800	4680	169.7	-19.1
SUOON	US073-0024133-O	Arrestin	Antagonist	UTR2	2.5	17800	17960	17880	113.1	-27.2
SUOON	US073-0024133-O	Arrestin	Antagonist	VIPR1	2.5	407880	387440	397660	14453.3	-11.6
SUOON	US073-0024133-O	Arrestin	Antagonist	VIPR2	2.5	442360	396720	419540	32272.4	-6.7

Abstract

Compositions and methods for the management and treatment of obesity, metabolic disorders, nausea and emesis using an ODN peptides and derivatives thereof are disclosed.

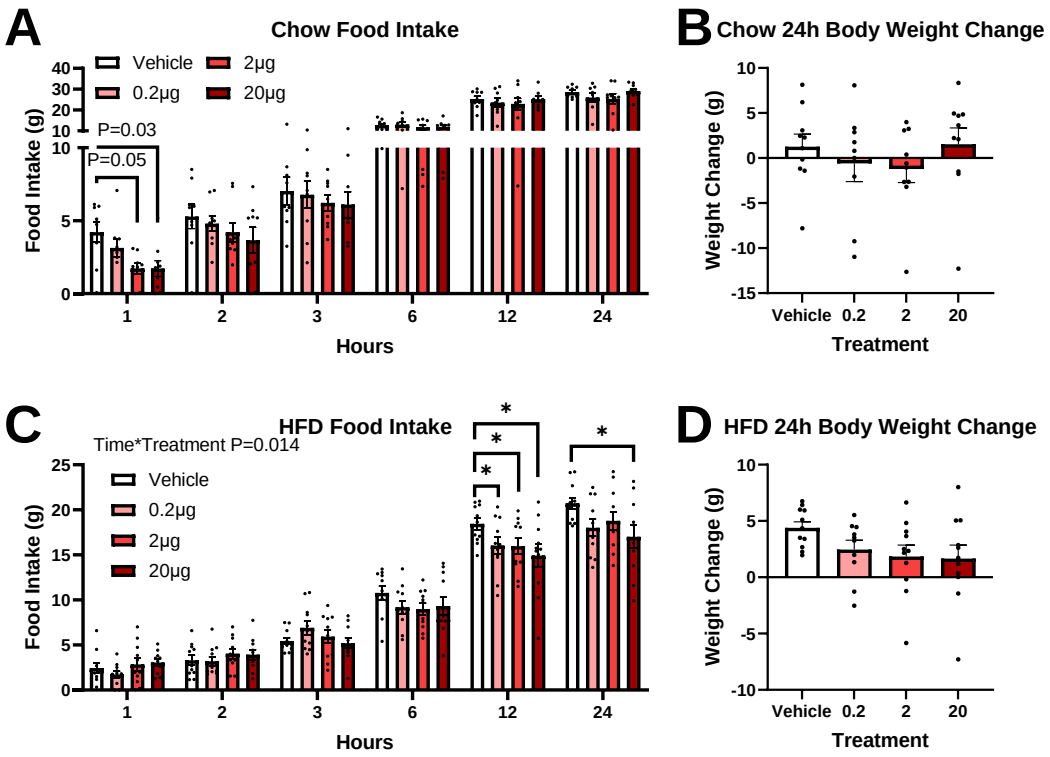
A
Chow Food Intake
Vehicle
0.2µg
2µg
20µg
P=0.03
P=0.05
Food Intake (g)
Hours
B
Chow 24h Body Weight Change
Weight Change (g)
Vehicle
0.2
2
20
Treatment
C
HFD Food Intake
Time*Treatment P=0.014
Vehicle
0.2µg
2µg
20µg
Food Intake (g)
Hours
D
HFD 24h Body Weight Change
Weight Change (g)
Vehicle
0.2
2
20
Treatment

Fig. 1.

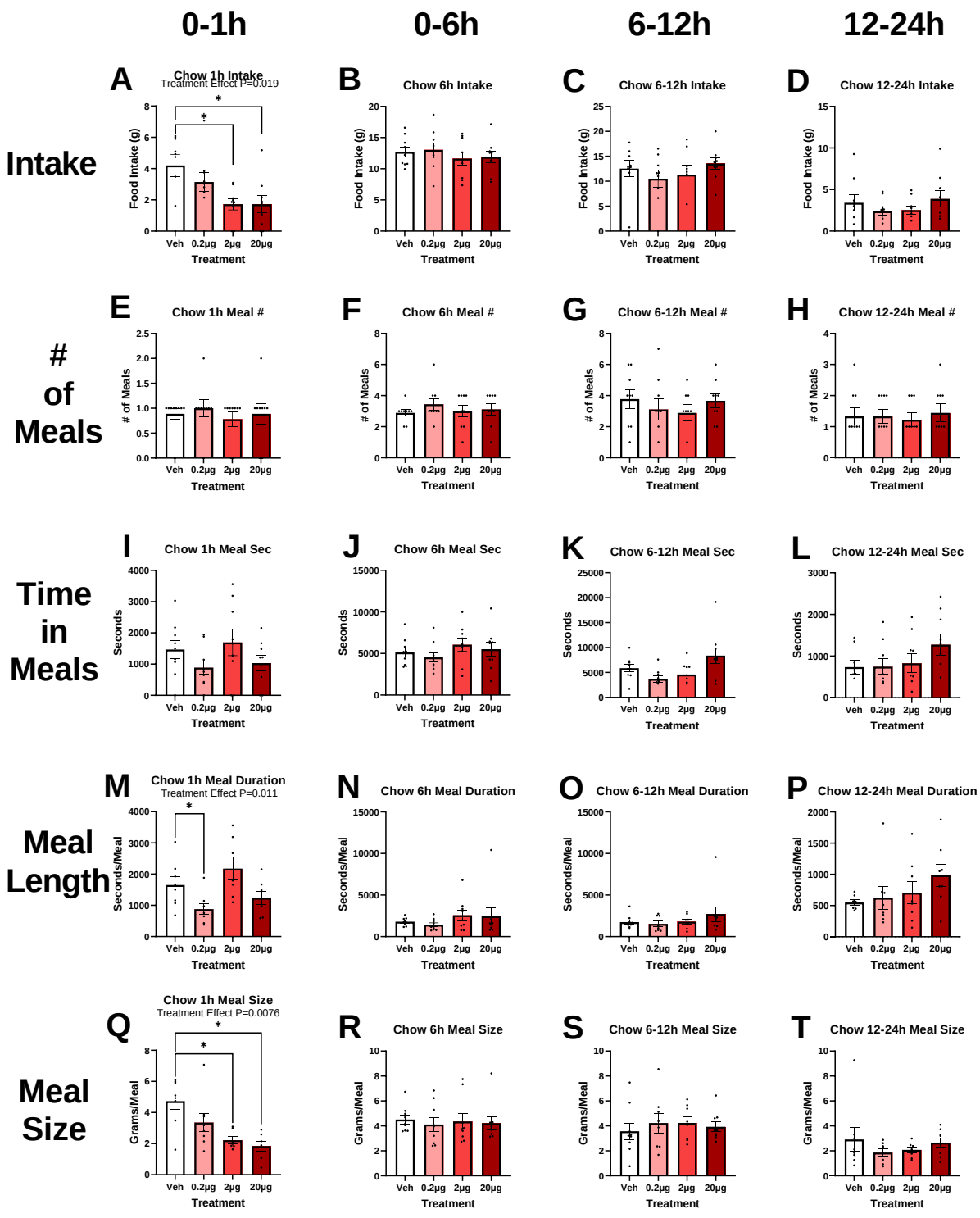
0-1h
0-6h
6-12h
12-24h
Intake
# of Meals
Time in Meals
Meal Length
Meal Size
A
Chow 1h Intake
Treatment Effect P=0.019
B
Chow 6h Intake
C
Chow 6-12h Intake
D
Chow 12-24h Intake
E
Chow 1h Meal #
F
Chow 6h Meal #
G
Chow 6-12h Meal #
H
Chow 12-24h Meal #
I
Chow 1h Meal Sec
J
Chow 6h Meal Sec
K
Chow 6-12h Meal Sec
L
Chow 12-24h Meal Sec
M
Chow 1h Meal Duration
Treatment Effect P=0.011
N
Chow 6h Meal Duration
O
Chow 6-12h Meal Duration
P
Chow 12-24h Meal Duration
Q
Chow 1h Meal Size
Treatment Effect P=0.0076
R
Chow 6h Meal Size
S
Chow 6-12h Meal Size
T
Chow 12-24h Meal Size
Food Intake (g)
# of Meals
Seconds
Seconds/Meal
Grams/Meal
Veh
0.2µg
2µg
20µg
Treatment

Fig. 2.

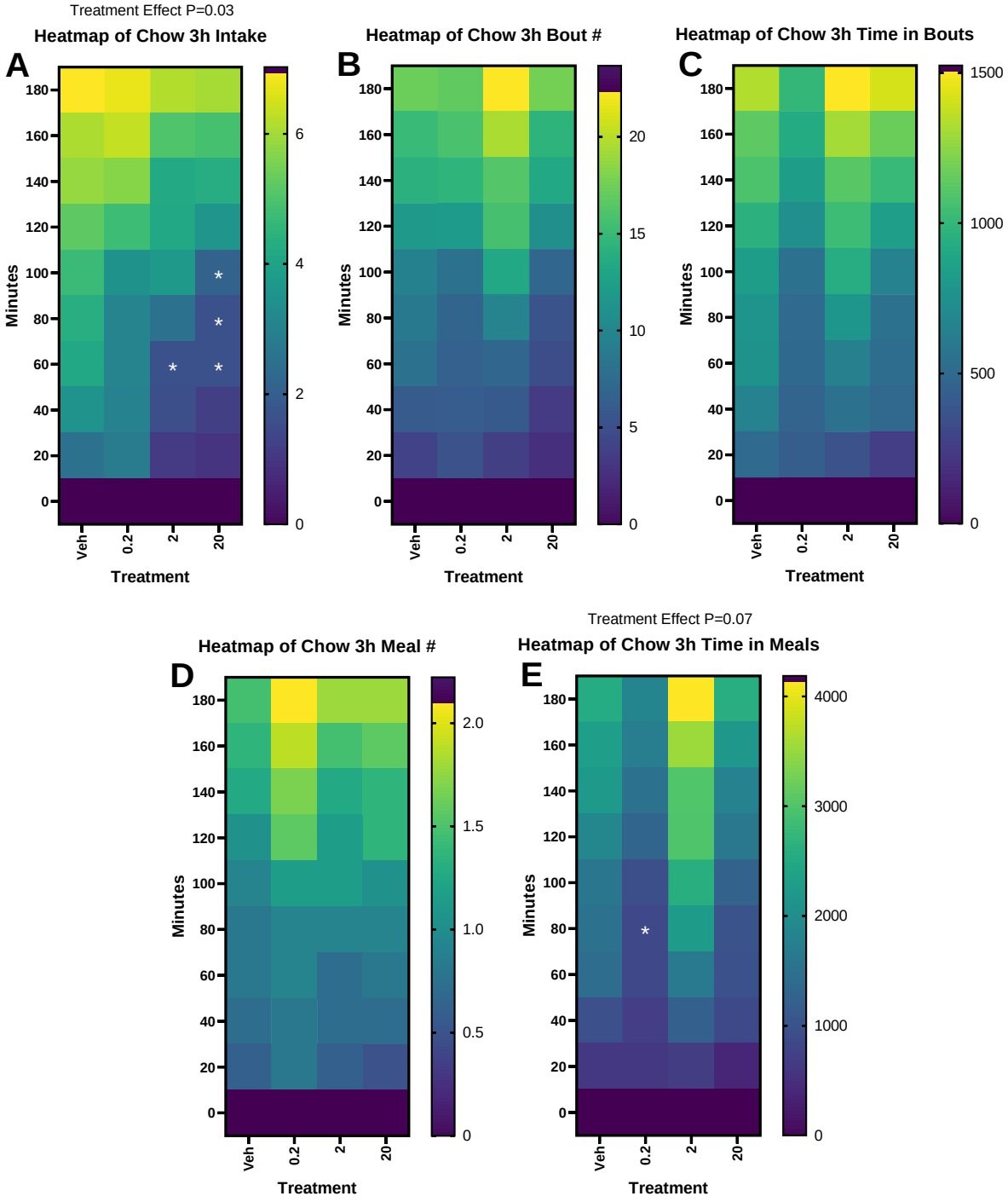
Treatment Effect P=0.03
Heatmap of Chow 3h Intake
A
Minutes
Treatment
Veh
0.2
2
20
Heatmap of Chow 3h Bout #
B
Heatmap of Chow 3h Time in Bouts
C
Treatment Effect P=0.07
Heatmap of Chow 3h Meal #
D
Heatmap of Chow 3h Time in Meals
E

Fig. 3.

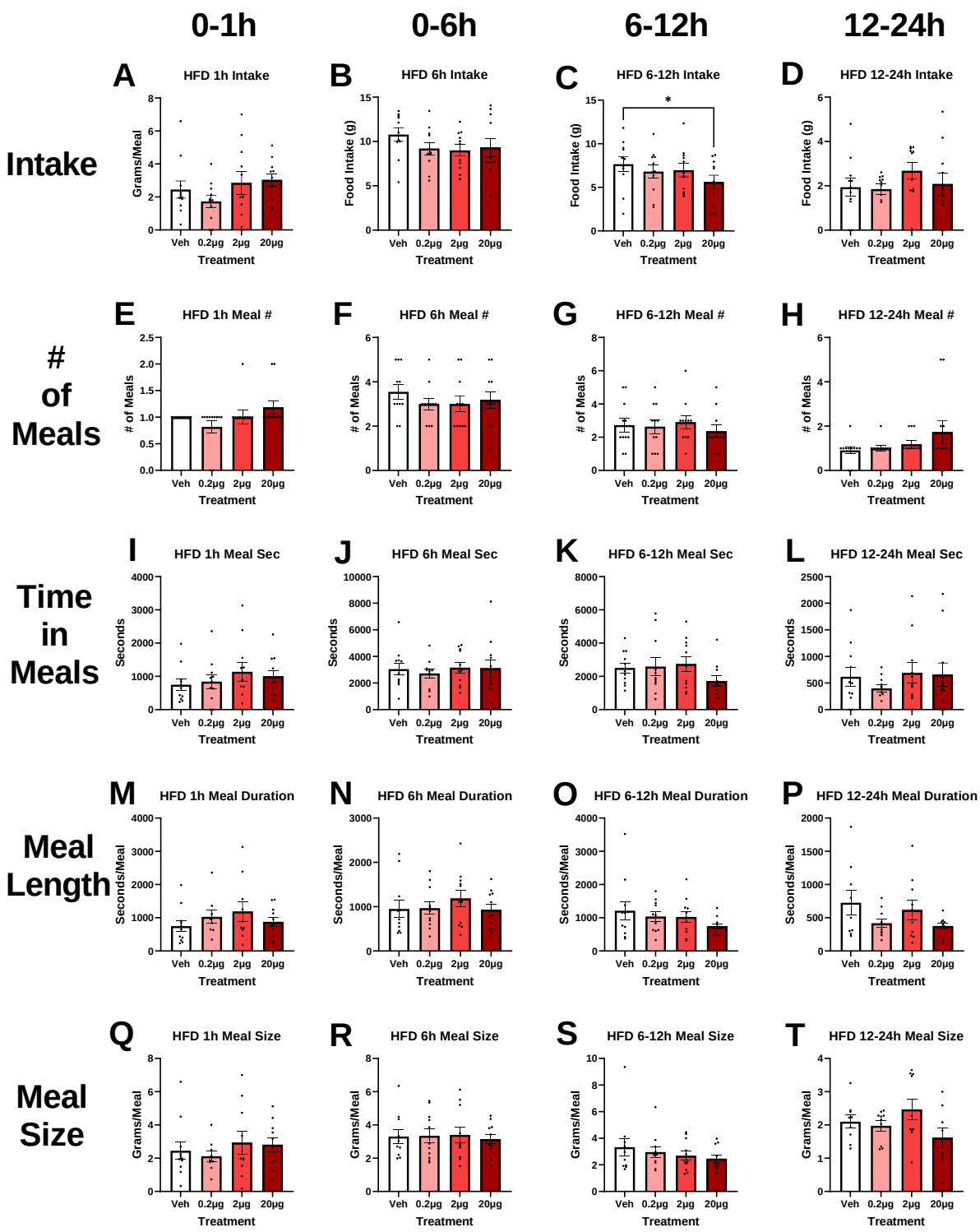
0-1h
0-6h
6-12h
12-24h
Intake
# of Meals
Time in Meals
Meal Length
Meal Size
A HFD 1h Intake
B HFD 6h Intake
C HFD 6-12h Intake
D HFD 12-24h Intake
E HFD 1h Meal #
F HFD 6h Meal #
G HFD 6-12h Meal #
H HFD 12-24h Meal #
I HFD 1h Meal Sec
J HFD 6h Meal Sec
K HFD 6-12h Meal Sec
L HFD 12-24h Meal Sec
M HFD 1h Meal Duration
N HFD 6h Meal Duration
O HFD 6-12h Meal Duration
P HFD 12-24h Meal Duration
Q HFD 1h Meal Size
R HFD 6h Meal Size
S HFD 6-12h Meal Size
T HFD 12-24h Meal Size
Grams/Meal
Food Intake (g)
# of Meals
Seconds
Seconds/Meal
Veh
0.2µg
2µg
20µg
Treatment
*

Fig. 4.

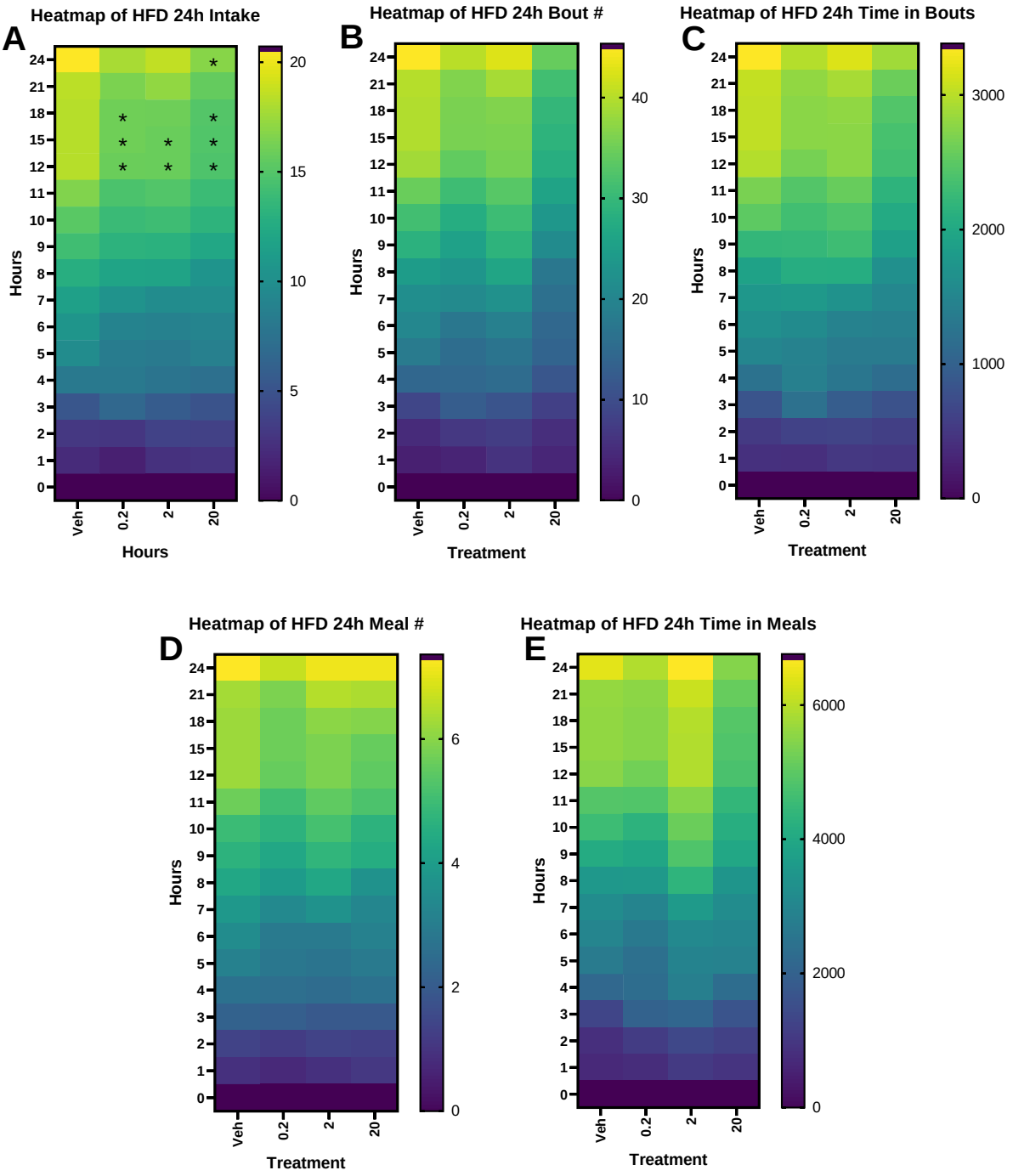
A
Heatmap of HFD 24h Intake
Hours
Hours
Veh
0.2
2
20
B
Heatmap of HFD 24h Bout #
Hours
Treatment
C
Heatmap of HFD 24h Time in Bouts
Hours
Treatment
D
Heatmap of HFD 24h Meal #
Hours
Treatment
E
Heatmap of HFD 24h Time in Meals
Hours
Treatment

Fig. 5.

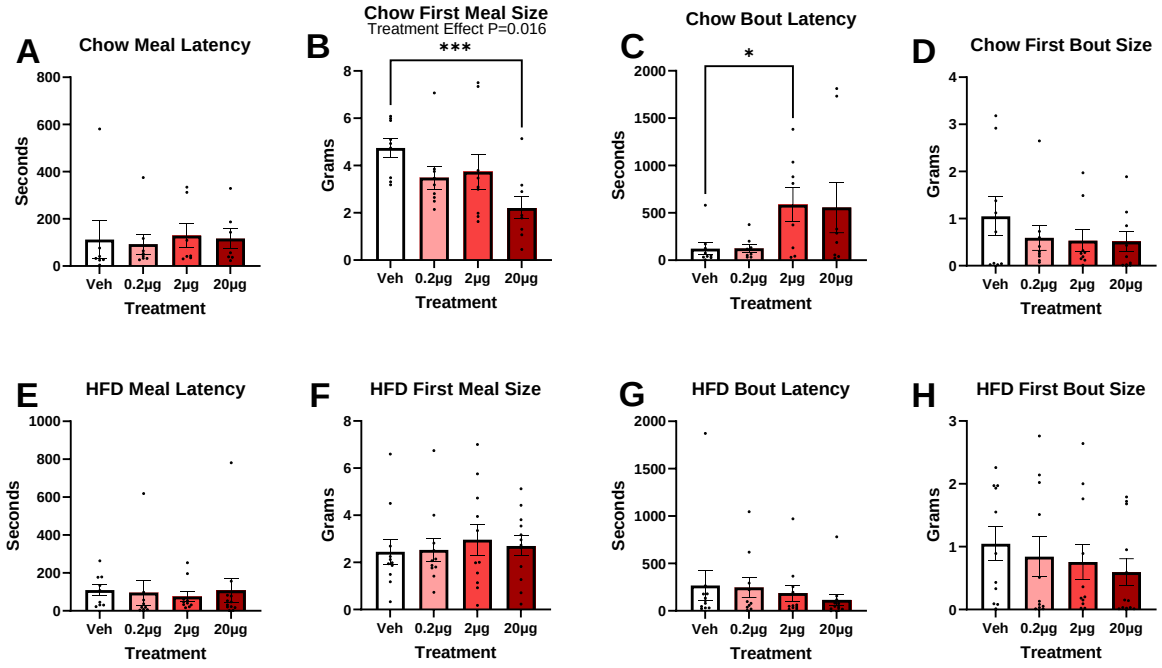
A
Chow Meal Latency
Seconds
Treatment
B
Chow First Meal Size
Treatment Effect P=0.016
***
Grams
C
Chow Bout Latency
*
Seconds
D
Chow First Bout Size
Grams
E
HFD Meal Latency
Seconds
F
HFD First Meal Size
Grams
G
HFD Bout Latency
Seconds
H
HFD First Bout Size
Grams
Veh
0.2µg
2µg
20µg

Fig. 6.

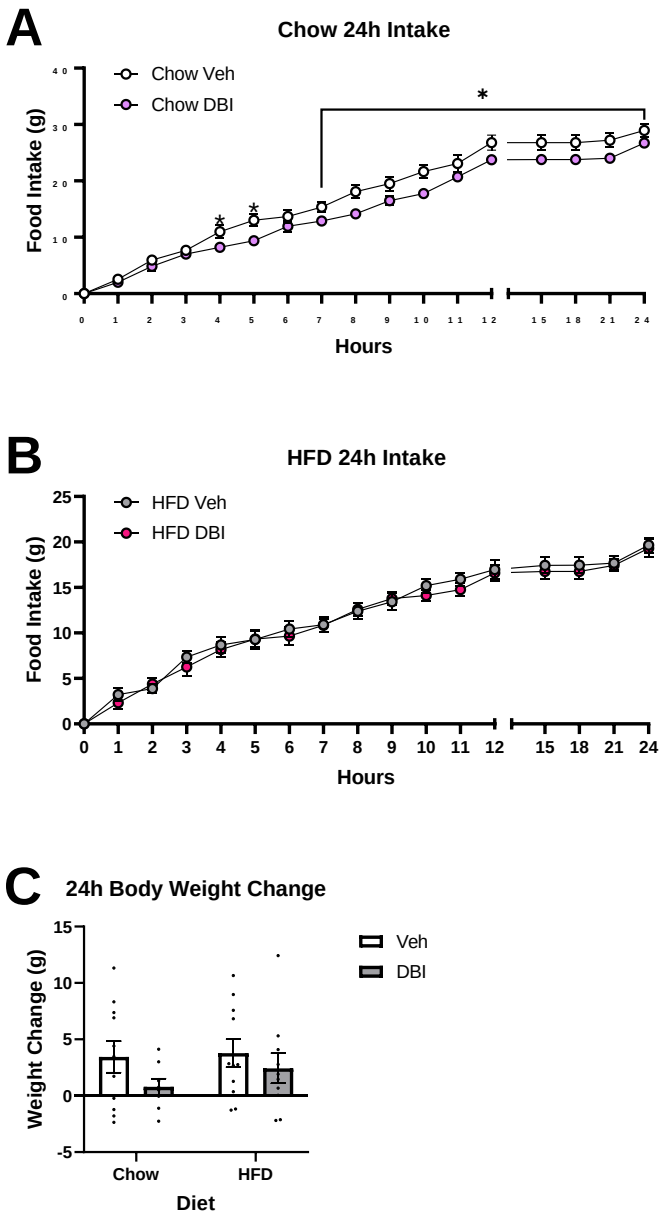
A
Chow 24h Intake
Chow Veh
Chow DBI
Food Intake (g)
Hours
B
HFD 24h Intake
HFD Veh
HFD DBI
Food Intake (g)
Hours
C
24h Body Weight Change
Veh
DBI
Weight Change (g)
Chow
HFD
Diet

Fig. 7.

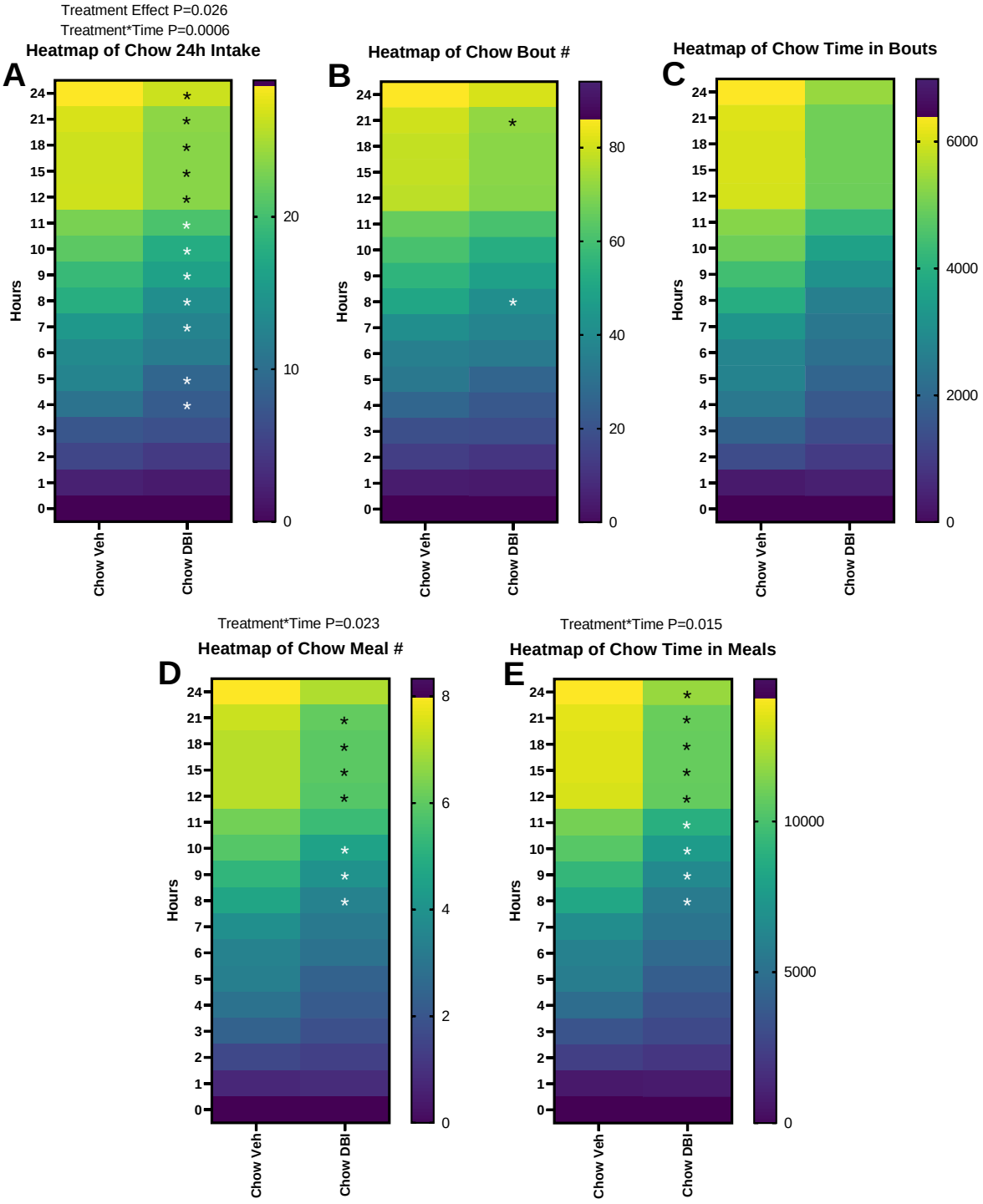
Treatment Effect P=0.026
Treatment*Time P=0.0006
Heatmap of Chow 24h Intake
A
Hours
Chow Veh
Chow DBI
Heatmap of Chow Bout #
B
Heatmap of Chow Time in Bouts
C
Treatment*Time P=0.023
Heatmap of Chow Meal #
D
Treatment*Time P=0.015
Heatmap of Chow Time in Meals
E

Fig. 8.

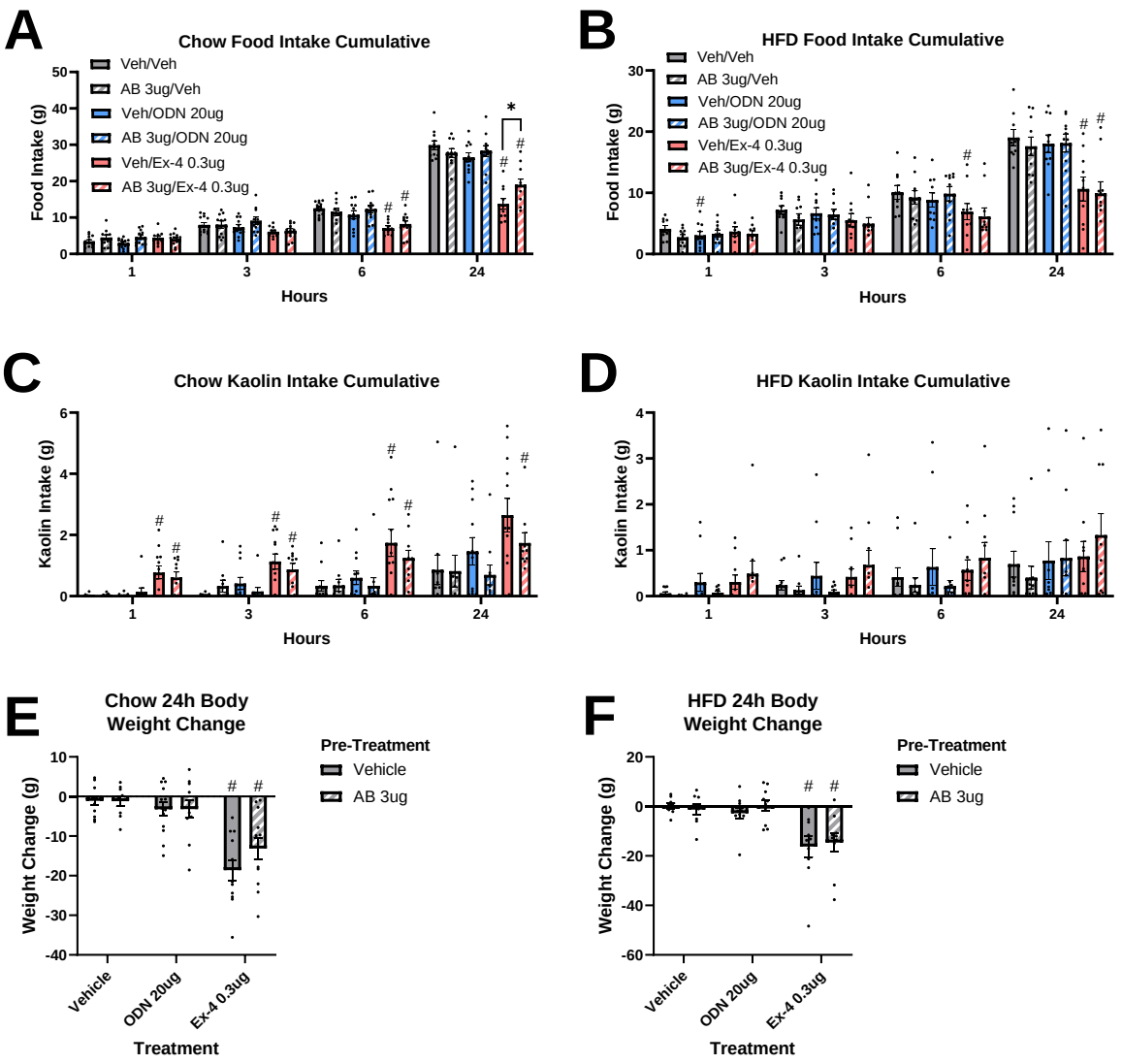
A
Chow Food Intake Cumulative
Veh/Veh
AB 3ug/Veh
Veh/ODN 20ug
AB 3ug/ODN 20ug
Veh/Ex-4 0.3ug
AB 3ug/Ex-4 0.3ug
Food Intake (g)
Hours
B
HFD Food Intake Cumulative
C
Chow Kaolin Intake Cumulative
Kaolin Intake (g)
D
HFD Kaolin Intake Cumulative
E
Chow 24h Body Weight Change
Pre-Treatment
Vehicle
AB 3ug
Weight Change (g)
Vehicle
ODN 20ug
Ex-4 0.3ug
Treatment
F
HFD 24h Body Weight Change

Fig. 9.

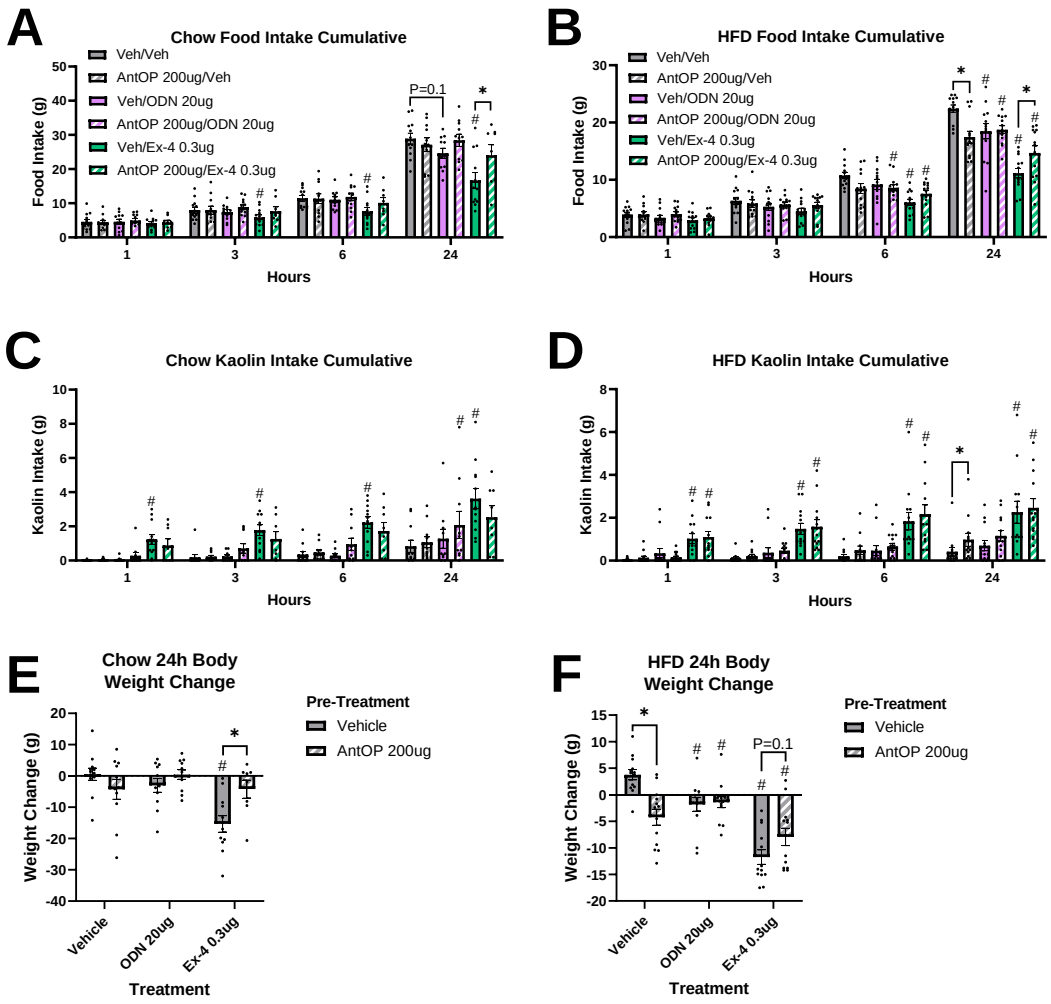
A
Chow Food Intake Cumulative
Veh/Veh
AntOP 200ug/Veh
Veh/ODN 20ug
AntOP 200ug/ODN 20ug
Veh/Ex-4 0.3ug
AntOP 200ug/Ex-4 0.3ug
Food Intake (g)
Hours
P=0.1
B
HFD Food Intake Cumulative
C
Chow Kaolin Intake Cumulative
Kaolin Intake (g)
D
HFD Kaolin Intake Cumulative
E
Chow 24h Body Weight Change
Weight Change (g)
Pre-Treatment
Vehicle
AntOP 200ug
Vehicle
ODN 20ug
Ex-4 0.3ug
Treatment
F
HFD 24h Body Weight Change

Fig. 10.

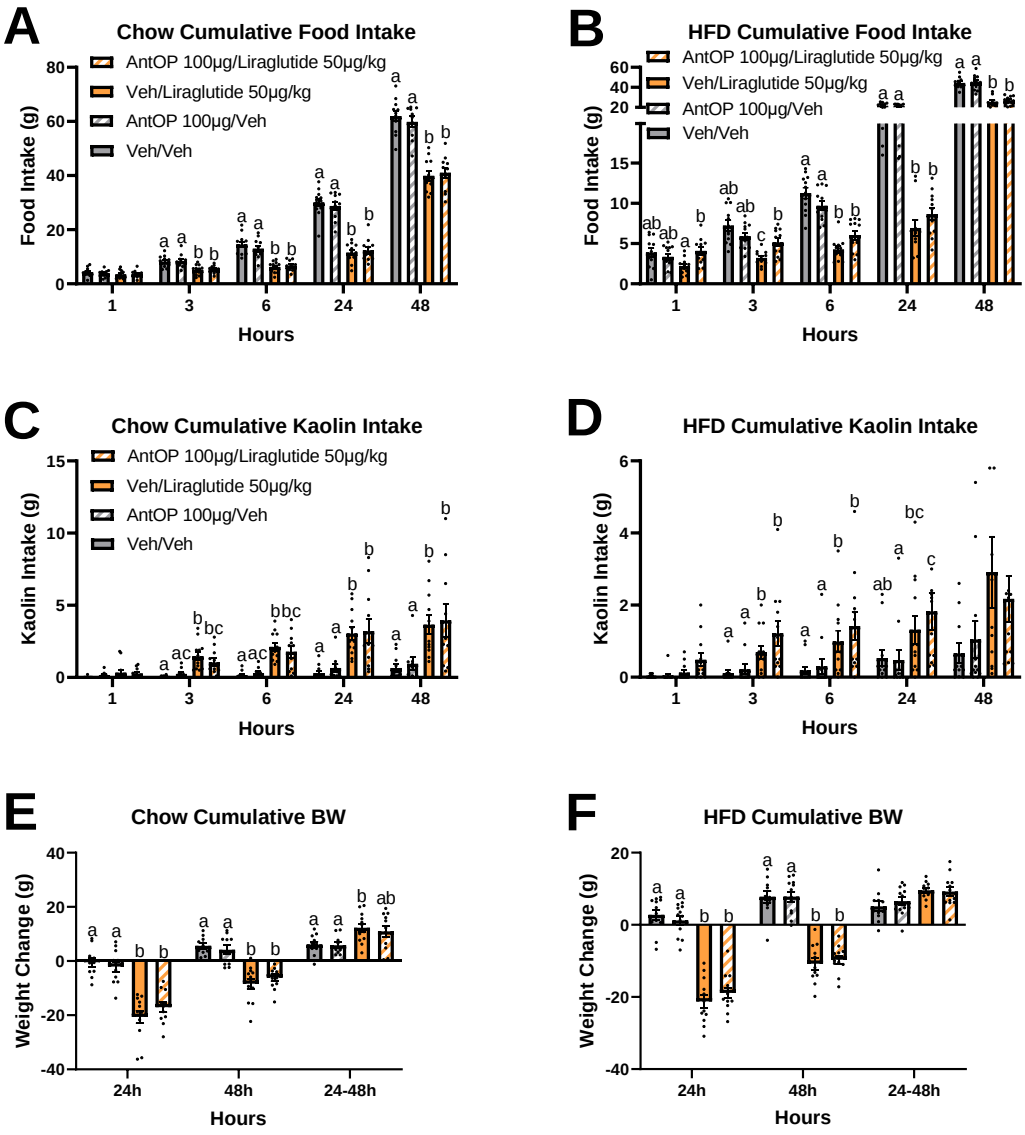
A
Chow Cumulative Food Intake
AntOP 100µg/Liraglutide 50µg/kg
Veh/Liraglutide 50µg/kg
AntOP 100µg/Veh
Veh/Veh
Food Intake (g)
Hours
B
HFD Cumulative Food Intake
C
Chow Cumulative Kaolin Intake
Kaolin Intake (g)
D
HFD Cumulative Kaolin Intake
E
Chow Cumulative BW
Weight Change (g)
24h
48h
24-48h
F
HFD Cumulative BW

Fig. 11.

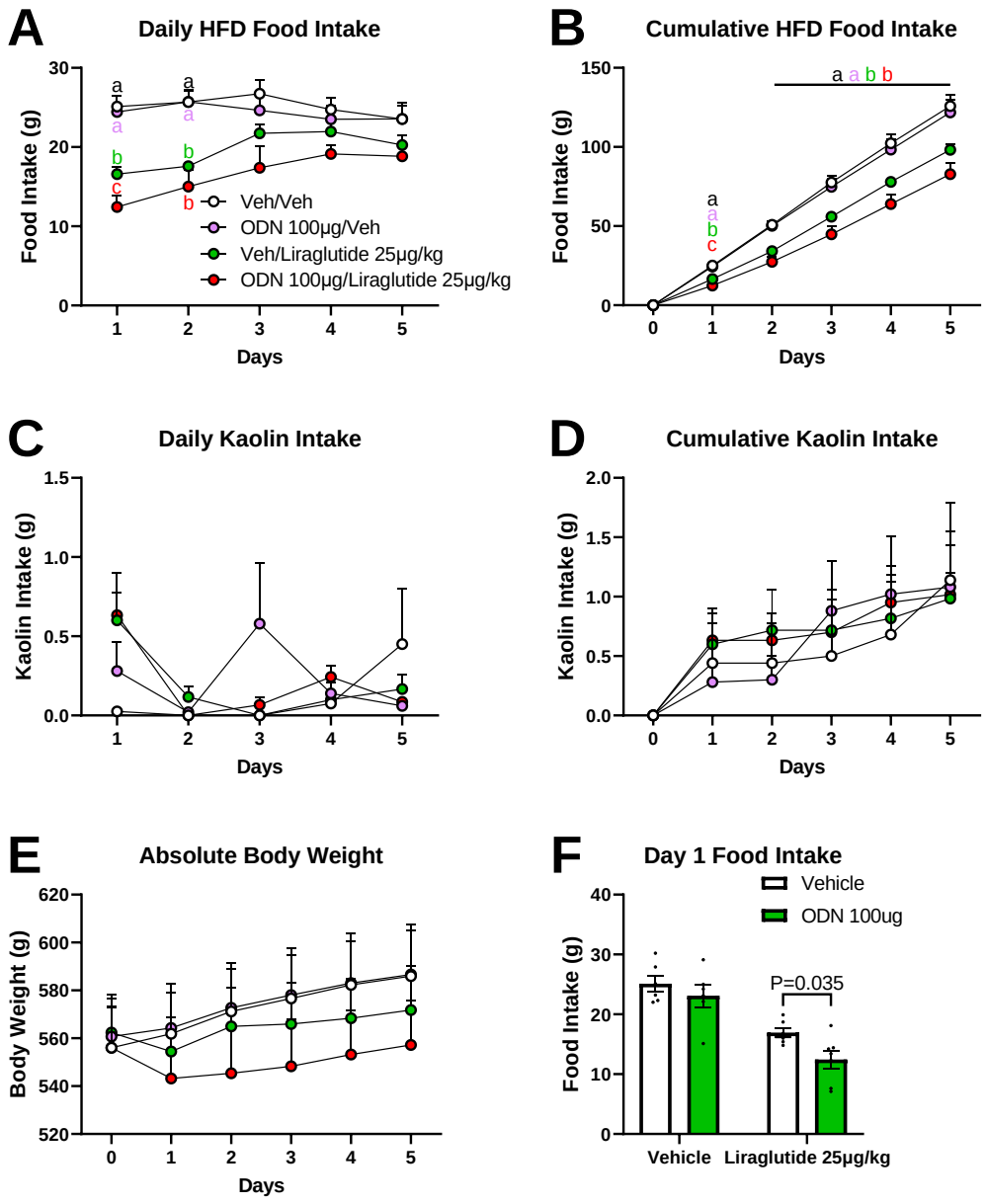
A
Daily HFD Food Intake
Food Intake (g)
Days
Veh/Veh
ODN 100µg/Veh
Veh/Liraglutide 25µg/kg
ODN 100µg/Veh/Liraglutide 25µg/kg
B
Cumulative HFD Food Intake
Food Intake (g)
Days
a a b b
C
Daily Kaolin Intake
Kaolin Intake (g)
Days
D
Cumulative Kaolin Intake
Kaolin Intake (g)
Days
E
Absolute Body Weight
Body Weight (g)
Days
F
Day 1 Food Intake
Vehicle
ODN 100ug
Food Intake (g)
P=0.035
Vehicle
Liraglutide 25µg/kg

Fig. 12.

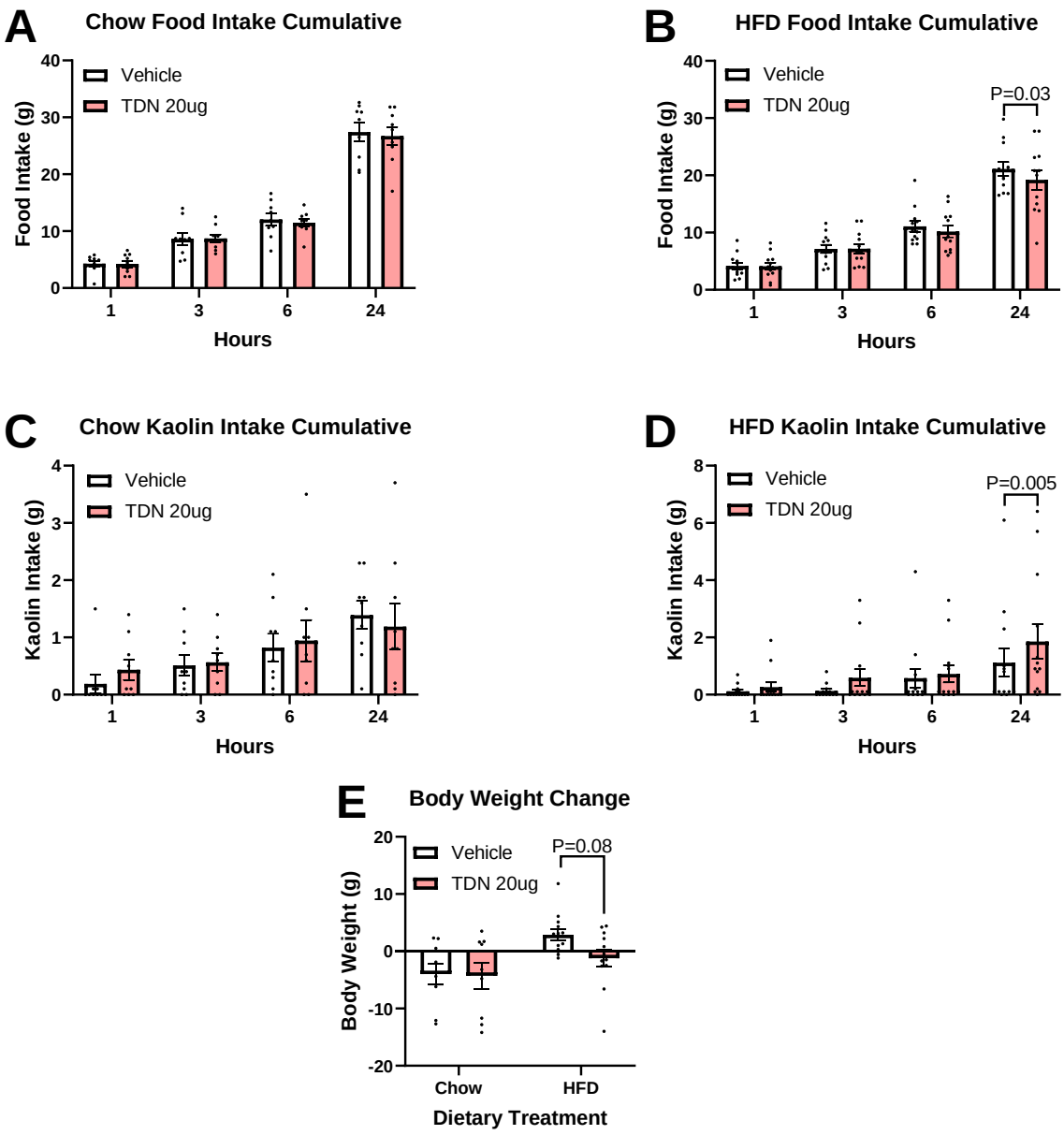
A
Chow Food Intake Cumulative
Vehicle
TDN 20ug
Food Intake (g)
Hours
B
HFD Food Intake Cumulative
P=0.03
C
Chow Kaolin Intake Cumulative
Kaolin Intake (g)
D
HFD Kaolin Intake Cumulative
P=0.005
E
Body Weight Change
P=0.08
Body Weight (g)
Chow
HFD
Dietary Treatment

Fig. 13.

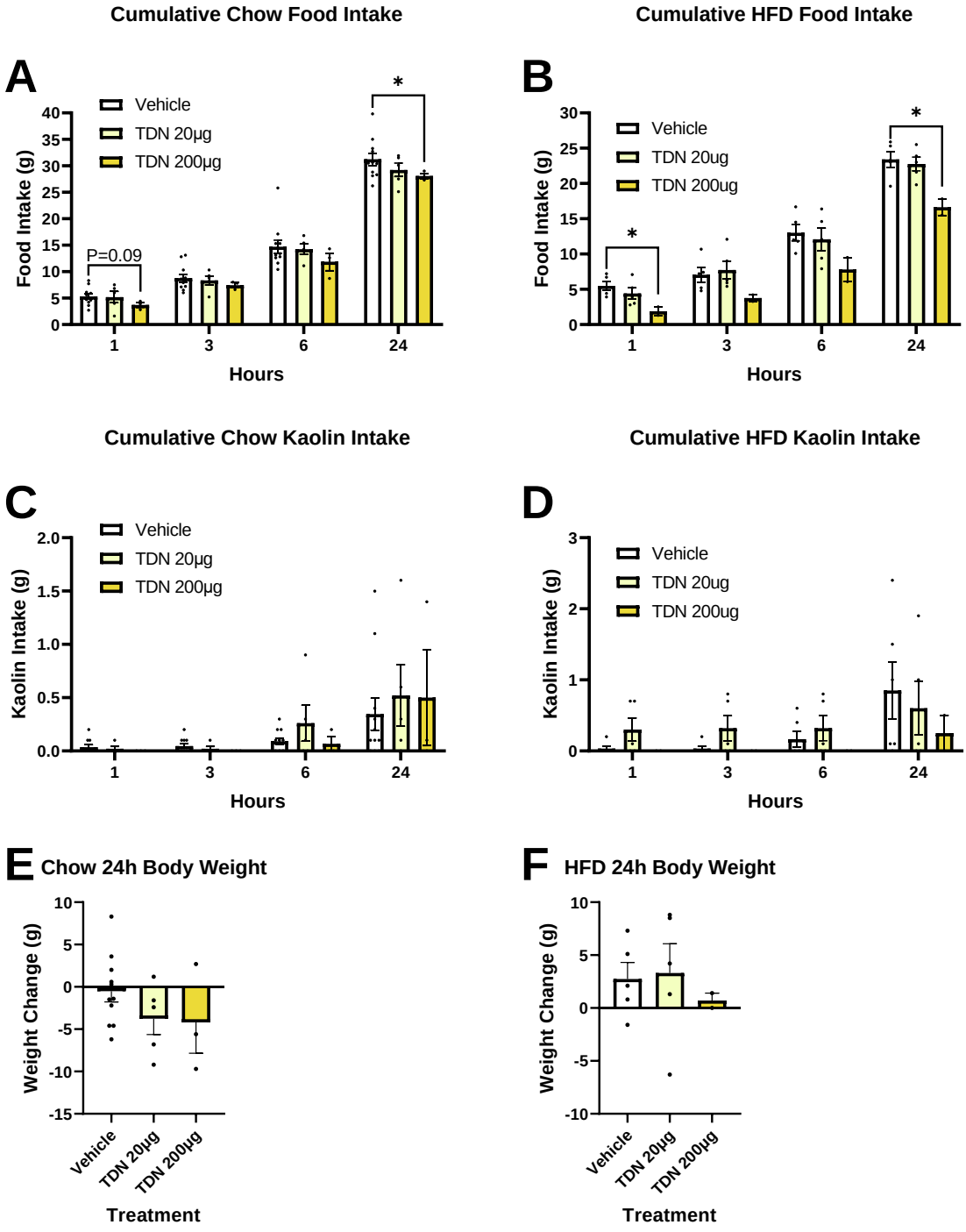
Cumulative Chow Food Intake
A
Vehicle
TDN 20µg
TDN 200µg
Food Intake (g)
P=0.09
*
Hours
Cumulative HFD Food Intake
B
Vehicle
TDN 20ug
TDN 200ug
Food Intake (g)
*
*
Hours
Cumulative Chow Kaolin Intake
C
Vehicle
TDN 20µg
TDN 200µg
Kaolin Intake (g)
Hours
Cumulative HFD Kaolin Intake
D
Vehicle
TDN 20ug
TDN 200ug
Kaolin Intake (g)
Hours
E
Chow 24h Body Weight
Weight Change (g)
Vehicle
TDN 20µg
TDN 200µg
Treatment
F
HFD 24h Body Weight
Weight Change (g)
Vehicle
TDN 20µg
TDN 200µg
Treatment

Fig. 14.

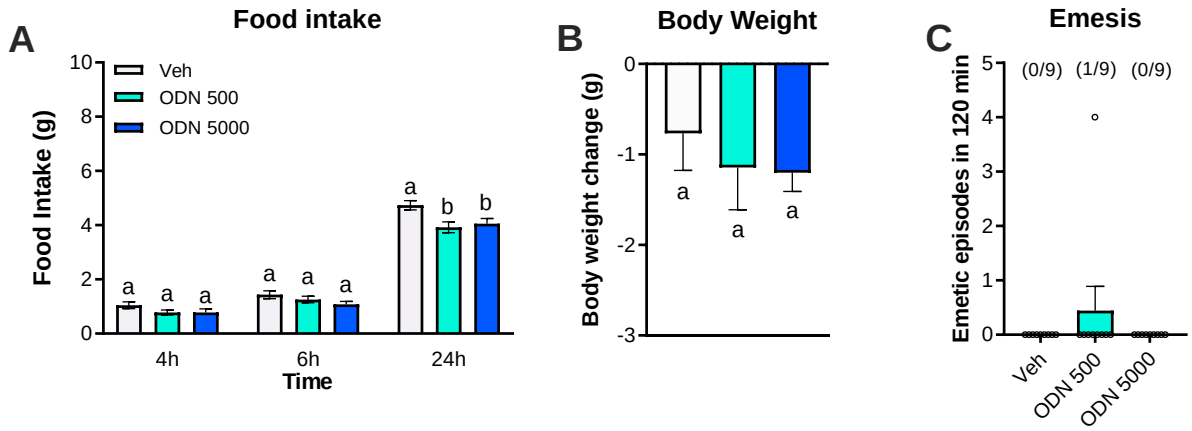
A
Food intake
Food Intake (g)
Veh
ODN 500
ODN 5000
a
a
a
a
a
a
a
b
b
4h
6h
24h
Time
B
Body Weight
Body weight change (g)
a
a
a
C
Emesis
Emetic episodes in 120 min
(0/9)
(1/9)
(0/9)
Veh
ODN 500
ODN 5000

Fig. 15.

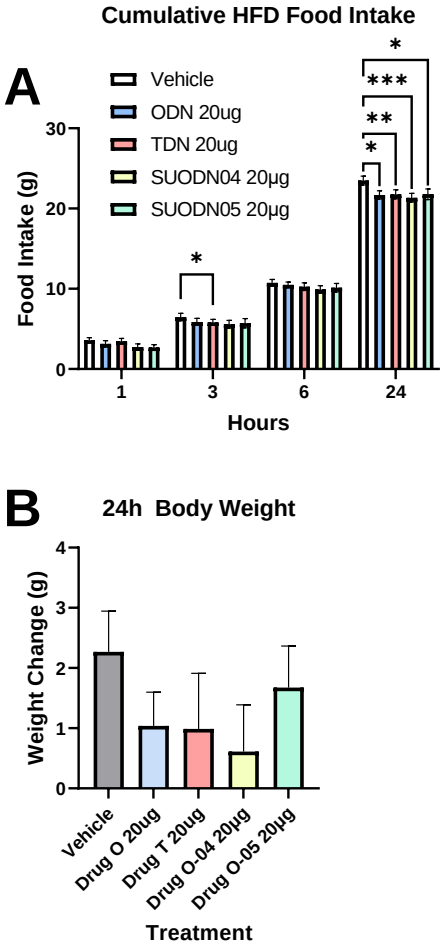
A
Cumulative HFD Food Intake
Vehicle
ODN 20ug
TDN 20ug
SUODN04 20μg
SUODN05 20μg
Food Intake (g)
Hours
B
24h Body Weight
Weight Change (g)
Vehicle
Drug O 20ug
Drug T 20ug
Drug O-04 20μg
Drug O-05 20μg
Treatment

Fig. 16.

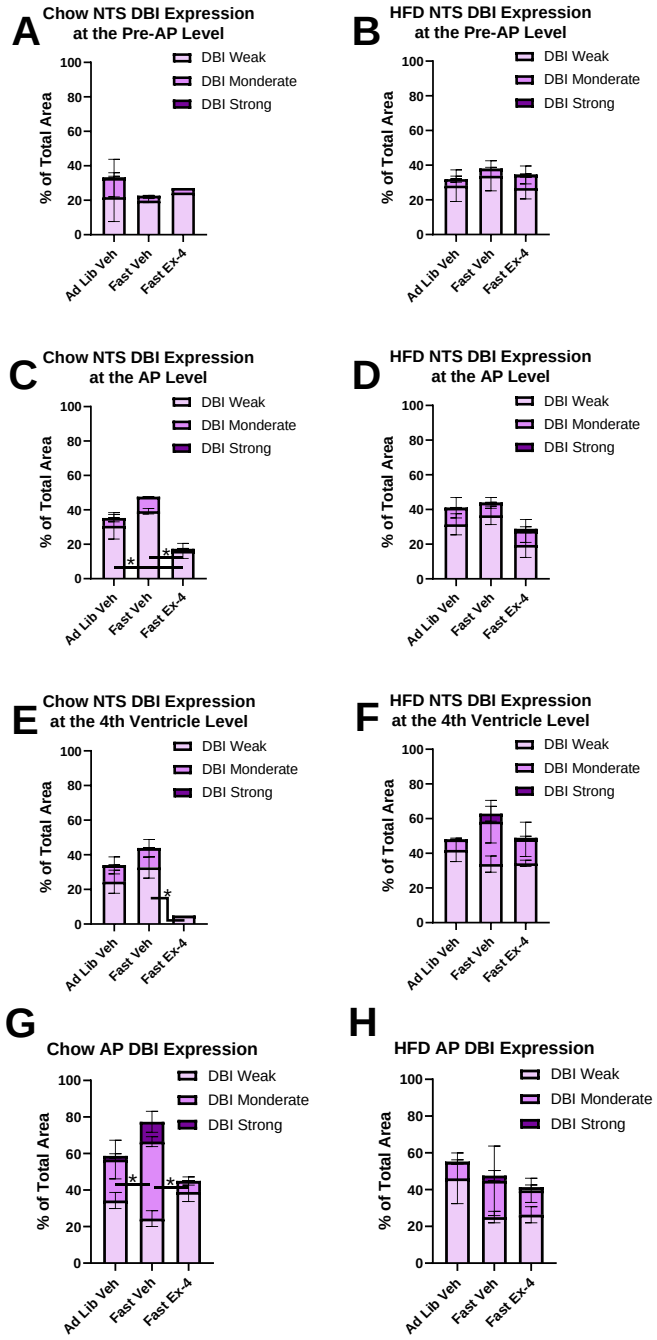
A
Chow NTS DBI Expression at the Pre-AP Level
B
HFD NTS DBI Expression at the Pre-AP Level
C
Chow NTS DBI Expression at the AP Level
D
HFD NTS DBI Expression at the AP Level
E
Chow NTS DBI Expression at the 4th Ventricle Level
F
HFD NTS DBI Expression at the 4th Ventricle Level
G
Chow AP DBI Expression
H
HFD AP DBI Expression
DBI Weak
DBI Monderate
DBI Strong
% of Total Area
0
20
40
60
80
100
Ad Lib Veh
Fast Veh
Fast Ex-4
*

Fig. 17.

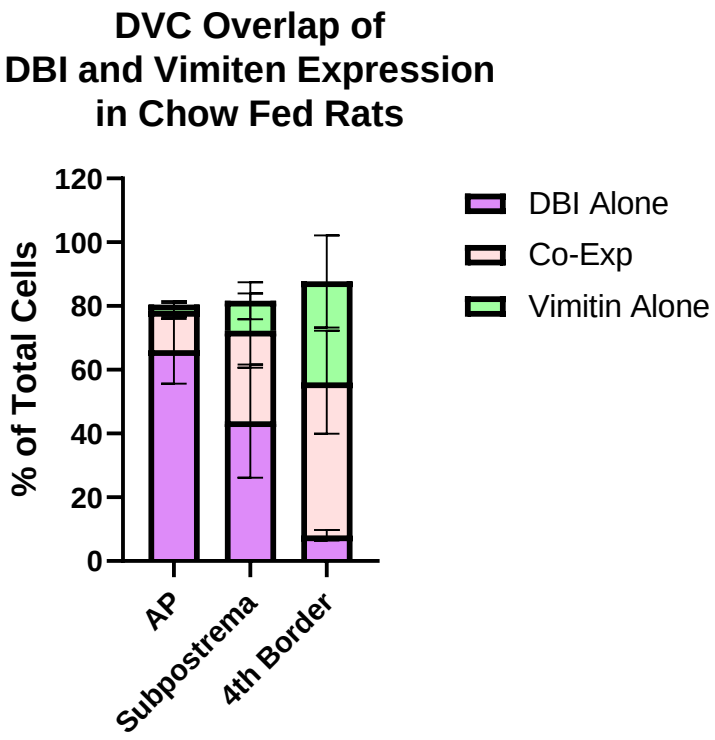
DVC Overlap of
DBI and Vimiten Expression
in Chow Fed Rats
% of Total Cells
120
100
80
60
40
20
0
AP
Subpostrema
4th Border
DBI Alone
Co-Exp
Vimitin Alone

Fig. 18.

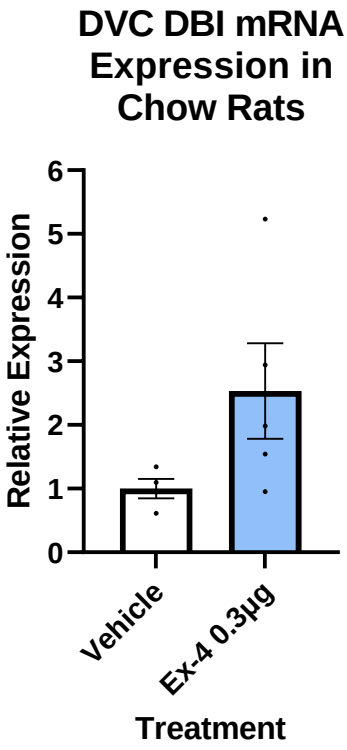
DVC DBI mRNA Expression in Chow Rats
Relative Expression
0
1
2
3
4
5
6
Vehicle
Ex-4 0.3µg
Treatment

Fig. 19.

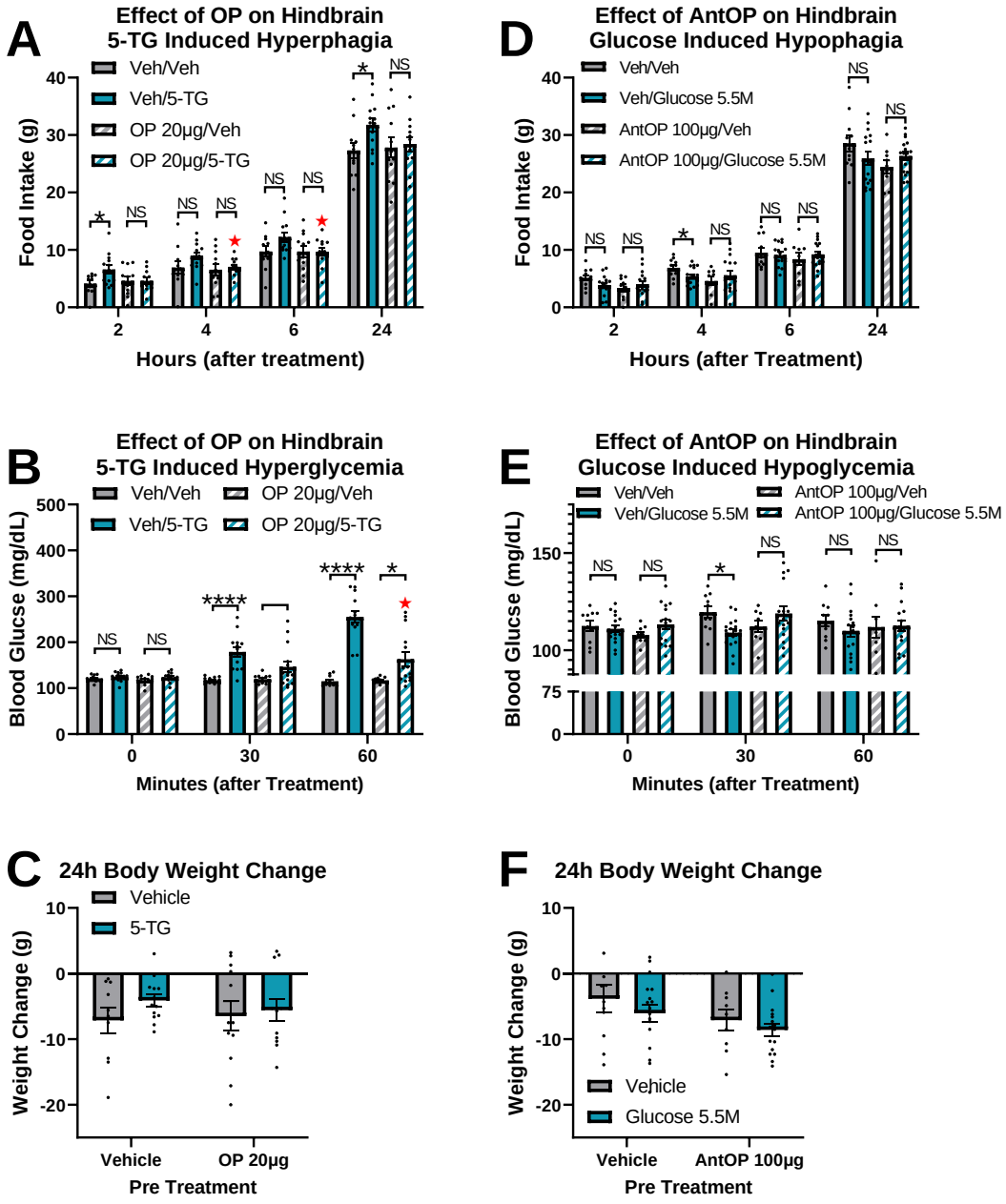
A
Effect of OP on Hindbrain
5-TG Induced Hyperphagia
Veh/Veh
Veh/5-TG
OP 20µg/Veh
OP 20µg/5-TG
Food Intake (g)
Hours (after treatment)
D
Effect of AntOP on Hindbrain
Glucose Induced Hypophagia
Veh/Veh
Veh/Glucose 5.5M
AntOP 100µg/Veh
AntOP 100µg/Glucose 5.5M
Food Intake (g)
Hours (after Treatment)
B
Effect of OP on Hindbrain
5-TG Induced Hyperglycemia
Veh/Veh
Veh/5-TG
OP 20µg/Veh
OP 20µg/5-TG
Blood Glucse (mg/dL)
Minutes (after Treatment)
E
Effect of AntOP on Hindbrain
Glucose Induced Hypoglycemia
Veh/Veh
Veh/Glucose 5.5M
AntOP 100µg/Veh
AntOP 100µg/Glucose 5.5M
Blood Glucse (mg/dL)
Minutes (after Treatment)
C
24h Body Weight Change
Vehicle
5-TG
Weight Change (g)
Vehicle
OP 20µg
Pre Treatment
F
24h Body Weight Change
Weight Change (g)
Vehicle
Glucose 5.5M
Vehicle
AntOP 100µg
Pre Treatment

Fig. 20.

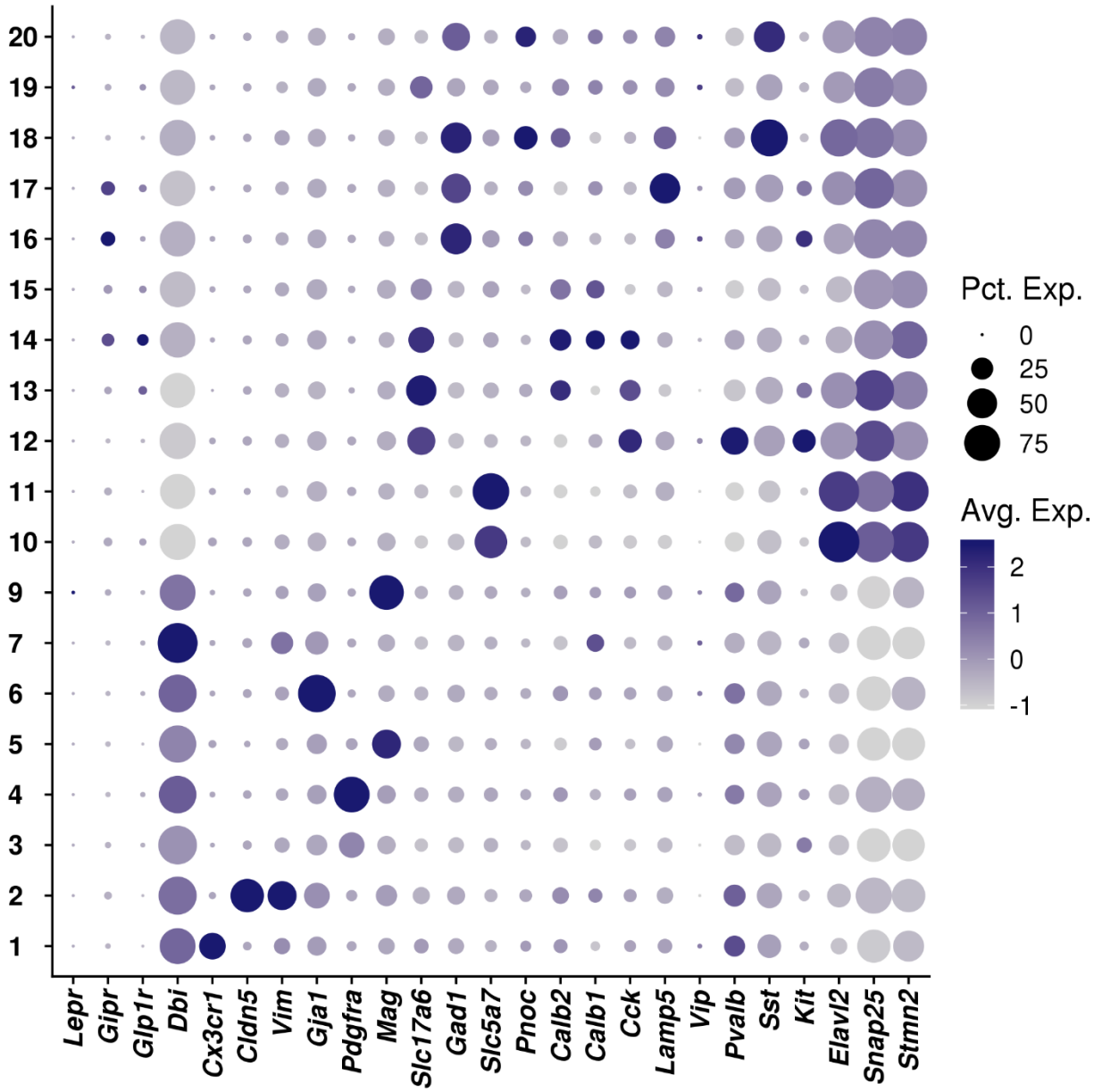
20
19
18
17
16
15
14
13
12
11
10
9
7
6
5
4
3
2
1
Lepr
Gipr
Glp1r
Dbi
Cx3cr1
Cldn5
Vim
Gja1
Pdgfra
Mag
Slc17a6
Gad1
Slc5a7
Pnoc
Calb2
Calb1
Cck
Lamp5
Vip
Pvalb
Sst
Kit
Elavl2
Snap25
Stmn2
Pct. Exp.
0
25
50
75
Avg. Exp.
2
1
0
-1

Fig. 21.

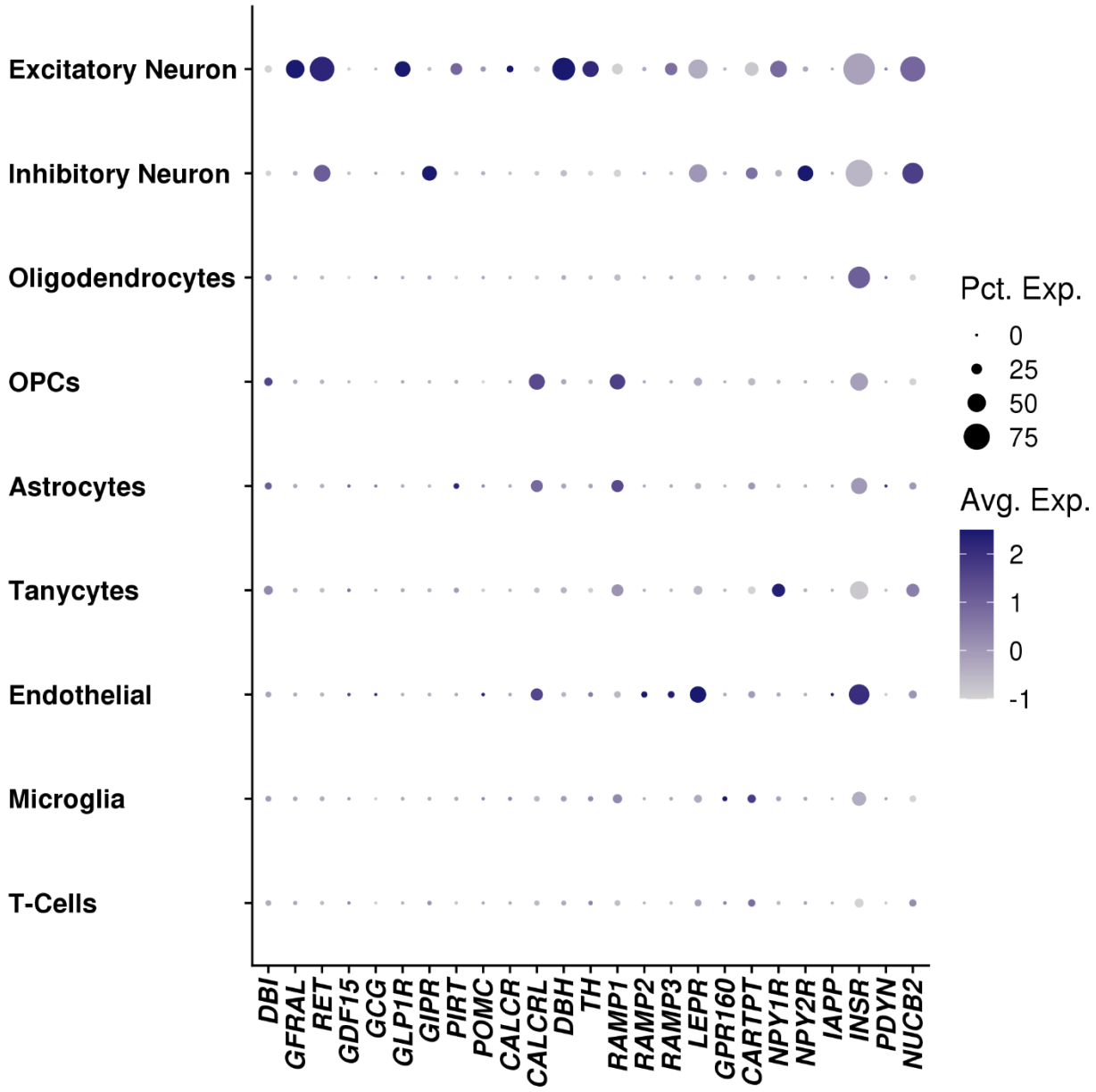
Excitatory Neuron
Inhibitory Neuron
Oligodendrocytes
OPCs
Astrocytes
Tanycytes
Endothelial
Microglia
T-Cells
DBI
GFRAL
RET
GDF15
GCG
GLP1R
GIPR
PIRT
POMC
CALCR
CALCRL
DBH
TH
RAMP1
RAMP2
RAMP3
LEPR
GPR160
CARTPT
NPY1R
NPY2R
IAPP
INSR
PDYN
NUCB2
Pct. Exp.
0
25
50
75
Avg. Exp.
2
1
0
-1

Fig. 22.

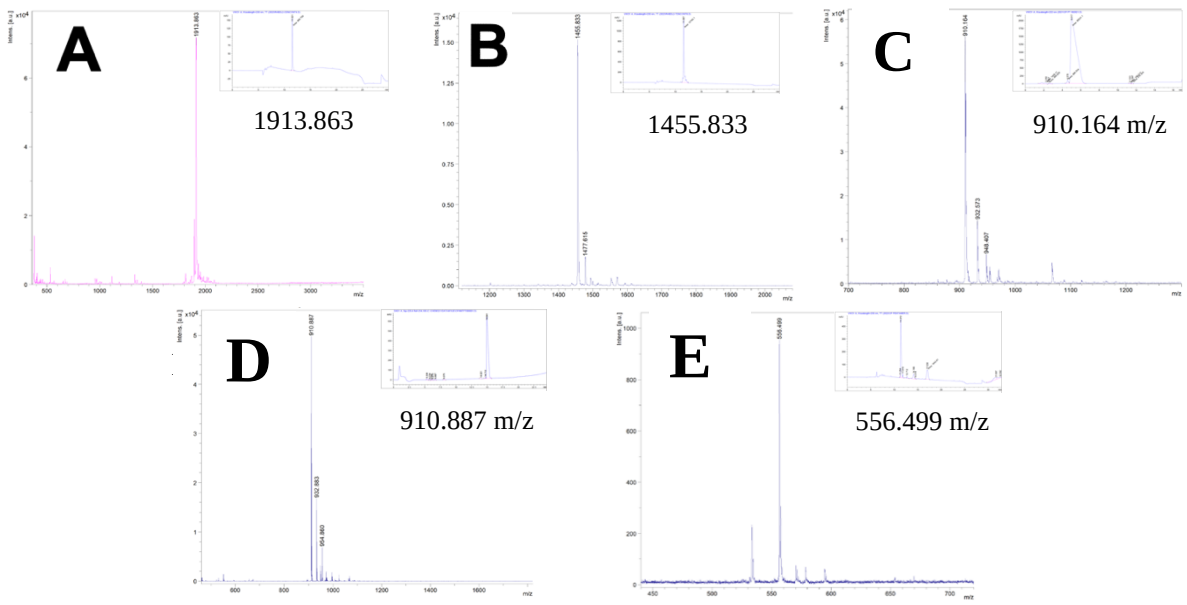

Fig. 23.

A Peptide Triple Agonist of GLP-1, Neuropeptide Y1, and Neuropeptide Y2 Receptors Promotes Glycemic Control and Weight Loss

Kylie S. Chichura,[1,8] Clinton T. Elfers,[2,8] Therese Salameh,[2] Varun Kamat,[3] Oleg G. Chepurny,[4] Aelish McGivney,[1] Brandon T. Milliken,[1] George G. Holz,[4,5] Sarah V. Applebey,[6] Matthew R. Hayes,[6] Ian R. Sweet,[3] Christian L. Roth,[2,7,9,*] and Robert P. Doyle[1,4,5,9,10,*]

[1]Syracuse University, Department of Chemistry, 111 College Place, Syracuse, NY 13244, USA
[2]Seattle Children's Research Institute, 1900 Ninth Ave, Seattle WA 98101, USA
[3]University of Washington, Diabetes Research Institute and Division of Metabolism, Endocrinology, and Nutrition, Seattle, WA 98195, USA
[4]State University of New York, Upstate Medical University, Department of Medicine, Syracuse, NY 13210, USA
[5]State University of New York, Upstate Medical University, Department of Pharmacology, Syracuse, NY 13210, USA
[6]Department of Psychiatry, Perelman School of Medicine, University of Pennsylvania, Philadelphia, PA 19104, USA
[7]Seattle Children's Hospital, University of Washington, Department of Pediatrics, Seattle, WA 98105, USA
[8]These authors contributed equally
[9]These authors contributed equally
[10]Lead Contact
[*]Correspondence: Christian.roth@seattlechildrens.org; Rpdoyle@syr.edu

SUMMARY

Mechanisms underlying long-term sustained weight loss and glycemic normalization after obesity surgery include changes in gut hormone levels, including glucagon-like peptide 1 (GLP-1) and peptide YY (PYY). We demonstrate that two peptide biased agonists (GEP44 and GEP12) of the GLP-1, neuropeptide Y1, and neuropeptide Y2 receptors (GLP-1R, Y1-R, and Y2-R, respectively) elicit Y1-R antagonist controlled, GLP-1R-dependent stimulation of insulin secretion in both rat and human pancreatic islets, thus revealing the counteracting effects of Y1-R and GLP-1R agonism. These agonists also promote insulin-independent Y1-R-mediated glucose uptake in muscle tissue ex vivo and more profound reductions in food intake and body weight than liraglutide when administered to diet-induced obese rats. Our findings support a role for Y1-R signaling in glucoregulation and highlight the therapeutic potential of simultaneous receptor targeting to achieve long-term benefits for millions of patients.

KEYWORDS
GLP-1R, Y1-R, Y2-R, biased agonism, T2DM, obesity, insulin secretion, metabolism

INTRODUCTION

The pathophysiology of obesity is driven by the dysregulation of numerous interrelated pathways. Thus, interventions that are effective at treating obesity will most likely be those that target multiple receptors in complementary neurocircuits and regulate energy balance. Patients who have undergone obesity surgery typically experience changes in the levels of gut hormones, primarily glucagon-like peptide-1 (GLP-1) and peptide YY (PYY) (Chandarana, Gelegen et al. 2013, Guida, Stephen et al. 2019, Dischinger, Hasinger et al. 2020, De Bandt, Rives-Lange et al. 2022). Current pharmacotherapies, including GLP-1 receptor agonists (GLP-1RAs), primarily target a single receptor and signaling pathway. These receptor agonists have been used successfully to treat type 2 diabetes mellitus (T2DM), which is a frequent co-morbidity of obesity. However, the use of these drugs has been associated with several notable side effects, including malaise, nausea, and emesis, as well as other gastrointestinal issues. These drugs also have similar shortcomings when used to treat obesity alone (Borner, Tinsley et al. 2022). In response to these concerns, several novel dual or triple agonists have been created based on the structures of gut hormone agonists that are complementary to GLP-1, including glucagon, glucose-dependent insulinotropic polypeptide (GIP), and peptide YY_{3-36} (PYY_{3-36}) (Talsania, Anini et al. 2005, Chepurny, Bonaccorso et al. 2018, Frias, Nauck et al. 2018, Kjaergaard, Salinas et al. 2019, Milliken, Elfers et al. 2021, Ostergaard, Paulsson et al. 2021, Battelino, Bergenstal et al. 2022, Boland, Laker et al. 2022, Heise, Mari et al. 2022, Jastreboff, Aronne et al. 2022, Metzner, Herzog et al. 2022, Zhao, Yan et al. 2022).

$PYY_{1–36}$ is a gut hormone that binds to the Y1-R in pancreatic islets and central nervous system (CNS) nuclei that control appetite regulation in the brain including the brainstem area postrema (AP) and nucleus tractus solitarius (NTS), where it has an anorectic effect (Walther, Morl et al. 2011). The results of recent work reveal that GLP-1R is expressed in neuropeptide Y (NPY)-positive neurons in the AP and that GLP-1 can directly or indirectly inhibit neuronal signaling in the anorexigenic NPY system via

agonism of GLP-1R (Ruska, Szilvasy-Szabo et al. 2022). Likewise, results from a considerable body of research revealed that PYY_{1-36} agonism of Y1-R plays a key role in promoting β-cell survival; this pathway has been recognized as critical to the reversal of diabetes and the recovery of impaired islet function after bariatric treatment (Guida, Stephen et al. 2017, Guida and Ramracheya 2020, Lafferty, Flatt et al. 2021). Acute administration of a Y1-R agonist may also reduce the rate of insulin secretion by pancreatic β-cells (Guida, Stephen et al. 2017, Guida, Stephen et al. 2019). Recent results demonstrating agonism at the arcuate nucleus (ARC) revealed that signaling via Y1-Rs protected female mice from obesity (Paterlini, Panelli et al. 2021, Oberto, Bertocchi et al. 2022). Other studies performed in mice demonstrate that pancreatic Y1-R activation facilitates the trans-differentiation of α-cells into β-cells, thereby improving insulin sensitivity (Lafferty, Flatt et al. 2021). The authors of this study noted that the pancreatic islets clearly benefited from Y1-R activation regardless of the diabetes status of the host (Lafferty, Flatt et al. 2021). Tanday et al., (2022) have since described a role for Y1-R agonism in inducing periods of β-cell rest that, when combined with GLP-1R agonism, proved beneficial in obesity-driven models of diabetes.

$PYY_{3–36}$, a truncated peptide agonist derived from dipeptidyl peptidase IV (DPPIV)-mediated proteolysis of full-length $PYY_{1–36}$, is of particular interest as it binds preferentially to the anorectic neuropeptide Y2-R (Talsania, Anini et al. 2005, Kjaergaard, Salinas et al. 2019, Merkel, Moreno et al. 2021, Ostergaard, Paulsson et al. 2021, Metzner, Herzog et al. 2022). PYY_{3-36} crosses the blood-brain-barrier (Nonaka, Shioda et al. 2003) and inhibits food intake via its interactions with Y2-R in brain areas that regulate energy homeostasis, including the ARC of the hypothalamus and the AP and NTS of the hindbrain (Shaw, Gackenheimer et al. 2003, Fetissov, Byrne et al. 2004, Neary, Small et al. 2005, Blevins, Chelikani et al. 2008). While circulating levels of PYY_{3-36} are frequently reduced in individuals with obesity (Batterham, Cohen et al. 2003, Roth, Enriori et al. 2005, Batterham, Heffron et al. 2006, Rahardjo, Huang et al. 2007, Roth, Bongiovanni et al. 2010), these levels typically return to those

detected in average-weight individuals following a reduction in body weight and/or gastric bypass surgery (Roth, Enriori et al. 2005, Batterham, Heffron et al. 2006) (Roth, Bongiovanni et al. 2010). Peripheral administration of PYY_{3-36} reduces caloric intake, increases postprandial insulin levels, and enhances insulin sensitivity, thermogenesis, lipolysis, and fat oxidation in both lean and obese humans as well as in nonhuman primates (Koegler, Enriori et al. 2005, Moran, Smedh et al. 2005) (Vrang, Madsen et al. 2006, Sloth, Davidsen et al. 2007, Abdel-Hamid, Abdalla et al. 2019). Administration of PYY_{3-36} also results in improved glucose control, improved lipid metabolism, and diminished insulin resistance in rodent models (Vrang, Madsen et al. 2006, van den Hoek, Heijboer et al. 2007, Chandarana, Gelegen et al. 2013). However, several significant limitations have hampered the development of PYY_{3-36} as an anti-obesity drug, including its short half-life (~12 min) (Addison, Minnion et al. 2011) and its inability to sustain weight reduction beyond a 1–2-week period (Reidelberger, Haver et al. 2011). The inability to sustain weight loss may be due to PYY_{3-36}-induced Y2-R down-regulation and tolerance (i.e., tachyphylaxis) and/or activation of compensatory mechanisms in response to reduced food intake. Recent work suggested that the reduction in both food intake and body weight observed in response to combined treatment with GLP-1RAs and PYY_{3-36} results in synergistically-enhanced activation of discrete hypothalamic and brainstem circuits that regulate appetite, including the arcuate nucleus (ARC), the paraventricular nuclei of the hypothalamus (PVNs), the central nucleus of the amygdala (CeA), and the hindbrain (AP/NTS) (Dischinger, Corteville et al. 2019, Kjaergaard, Salinas et al. 2019, Lafferty, Flatt et al. 2021, Metzner, Herzog et al. 2022). Combination therapy has also resulted in improved glucoregulation via an increase in insulin sensitivity, an observation that has been linked to the recovery of pancreatic β-cell function (Lafferty, Flatt et al. 2021).

Based on previous research and promising clinical data (Guida, Stephen et al. 2017, Guida and Ramracheya 2020), we have designed a single chimeric peptide intended to target GLP-1R, Y1-R, and Y2-R-mediated pathways simultaneously. While other multi-agonists that target a variety of receptors have been explored, this specific approach has not been utilized in any previous studies. This approach

offers a unique combination of potent weight-loss, glucoregulation with b-cell mass protection/proliferation, devoid of nausea/malaise.

To this end, we recently published the first description of GEP44, a chimeric peptide monomer that includes partial amino acid sequences of the GLP-1RA, Exendin-4 (Ex-4), and PYY. Results from our previous study revealed that GEP44 binds to GLP-1R, Y1-R, and Y2-R (Milliken, Elfers et al. 2021). Administration of GEP44 resulted in potent anorectic effects in two-to-five-day treatment studies in both lean and diet-induced obese (DIO) rats. Notably, administration of GEP44 resulted in an 80% reduction in food intake and a more profound loss of body weight than what could be achieved in response to treatment with several of the US Food and Drug Administration (FDA)-approved GLP-1RAs, including Ex-4 and liraglutide (LIRA). Furthermore, administration of GEP44 resulted in no visceral malaise, as determined in experiments with both rats and shrews (Milliken, Elfers et al. 2021).
In this manuscript, we develop the biochemical and preclinical aspects of GEP44. We found that GEP44 exhibits biased agonism at the Y2-R, as documented by its inability to induce Y2-R-mediated internalization. As a further development of the biased agonist approach, we introduce the GEP44 analog, GEP12. GEP12 was designed to incorporate findings published by Jones, Buenaventura et al. (2018), who reported that conversion of the N-terminal histidine (His) of Ex-4 to phenylalanine (Phe) resulted in reduced GLP-1R-mediated internalization and prolonged signal response. Interestingly, while administration of GEP12 did not result in a reduction in GLP-1R internalization, when evaluated in the presence of a Y1-R antagonist, it elicited increased insulin secretion in rat islets compared to results obtained with either GEP44 or Ex-4. These findings are consistent with the reduced rates of insulin secretion observed in islets in response to agonism at Y1-R (Yang, Ann-Onda et al. 2022).

Our findings highlight the potential of simultaneously targeting GLP-1R, Y1-R, and Y2-R and provide evidence suggesting a significant role for Y1-R agonism in the control of food intake and glucoregulation.

This approach offers the possibility of achieving the long-term benefits of obesity surgery with a noninvasive approach. This will help millions of patients who are currently suffering from obesity and its comorbidities, especially those for whom surgery is not an option.

RESULTS

GEP44 binds to and activates GLP-1R, Y1-R, and Y2-R via biased agonism

The addition of GEP44 to H188-GLP-1R transduced HEK293 cells resulted in elevated levels of cAMP with an EC_{50} value of 417 pM (Fig. 1A). The overall magnitude of response to GEP44 (and GEP12, vide infra) was nearly equivalent to the response to Ex-4 (Fig. 1A), but with differences noted in EC_{50} values for GEP44 (492.6 pM), GEP12 (17.3 nM) and Ex-4 (28.7 pM) at the GLP-1R (Fig. 1A). GEP44 agonism at Y1-R and Y2-R was validated in assays that monitored their ability to counteract adenosine-stimulated cAMP production in HEK293 C24 cells that were transiently transfected with Y1-R or Y2-R (Milliken, Doyle et al. 2020, Milliken, Elfers et al. 2021). As we reported previously (Milliken, Elfers et al. 2021), pre-treatment of these cells with GEP44 for 20 min resulted in a concentration-dependent inhibitory effect (Fig.1B and 1C) with IC_{50} values of 34 nM and 27 nM for Y2-R and Y1-R, respectively. As shown in Fig. 1D–F, half-maximal GEP44 binding at GLP-1R was observed at 113 nM (versus 5.85 nM for Ex-4), 65.8 nM at Y2-R (versus 1.51 nM for PYY_{3-36}), and 86.6 nM at Y1-R (versus 7.9 nM for PYY_{1-36}).

Fig. 1

Biased agonism is a term used to describe ligand-mediated activation of a specific subset of the intracellular signaling pathways linked to a single receptor (Andresen 2011). With this in mind, we explored the GEP44-mediated internalization of Y2-R and internalization and recruitment of b-arrestin-2 at GLP-1R (Fig. 1G–I). Our results revealed that GEP44 did not promote internalization of Y2-R (Fig. 1I). This is notable given that Y2-R internalization is a critical step in receptor desensitization; this most likely results from strong allosteric effects associated with Y2-R/Ga interactions that place the cell in a refractory state and prevent further signaling (Ziffert, Kaiser et al. 2020).

By contrast, GEP44 elicited responses that were similar to those of the peptide agonist Ex-4 in assays designed to examine both internalization (Fig. 1G) and b-arrestin recruitment (Fig. 1H) at GLP-1R. Our findings revealed EC_{50} values of 3.97 nM and 2.43 nM for GLP-1R internalization mediated by GEP44 and Ex-4, respectively, and EC_{50}s of 1.59 nM and 7.13 nM for GEP44 and Ex-4, respectively, for b-arrestin-2 recruitment.

A recent publication by Jones, Buenaventura et al. (Jones, Buenaventura et al. 2018), reported the impact of GLP-1R trafficking on insulin release and noted specifically that Ex-4 analogs with reduced capacity to elicit internalization and b-arrestin recruitment were more efficacious at inducing insulin release than the parent Ex-4 peptide. These results suggest that ligand-induced insulin secretion tracks inversely with b-arrestin recruitment. The authors reported that conversion of the N-terminal His to Phe resulted in an Ex-4 analog with improved efficacy at inducing insulin release while eliciting reduced levels of receptor internalization and b-arrestin-2 recruitment (Jones, Buenaventura et al. 2018). We used this information to create GEP12 (Fig. 1) which is a GEP44 analog with an analogous N-terminal His to Phe modification. We found that GEP12 functioned as a GLP-1R agonist with an EC_{50} of 17.3 nM (Fig. 1A) and bound to this receptor with an IC_{50} of 19.2 nM (Fig. 1D). As predicted, we observed no measurable GEP12-mediated internalization of GLP-1R in response to concentrations as high as 400 nM (Fig. 1G). Thus, we explored the responses to both GEP12 and GEP44 in ex vivo studies of insulin secretion in rat and human islets (Fig. 2A and B) as discussed in detail in the section to follow.

Effects of GEP44 and GEP12 on islets and muscle are mediated by both GLP-1R and Y1-R

Insulin secretion from rat and human islets was measured in the presence of 20 mM glucose and the presence or absence of various test compounds using both static and perifusion analyses. As shown in Fig. 2A and B, a static analysis revealed that both Ex-4 and GEP44 potentiated the insulin secretion rate (ISR) by 62% and 37%, respectively, over 20 mM glucose alone. However, a stimulatory response of GEP44 was observed only in the presence of Y1-R-specific antagonists (PD160170 or BIBO3304 - Fig. 2A and B), as expected if Y1-R agonism by GEP44 serves to counteract GLP-1R agonism by the same

peptide. Our findings from perifusion experiments were consistent with those obtained from the static analysis. The results shown in Fig. 2C confirmed that GEP44 had a stimulatory effect on ISR in both rat and human islets and that this response occurred only in the presence of a Y1-R antagonist. The perifusion experiments also documented similar kinetic ISR responses to Ex-4 and GEP44 when islets were treated with a Y1-R antagonist (Fig. 2C). Nonetheless, the impact of GEP44 with a Y1-R antagonist in the doses used in this experiment is significant and greater than the responses observed to 5 nM Ex-4, which is the typical pharmacologic level of this agent (Fig. 2B). Interestingly, GEP12 elicited stronger increases in the ISR (Fig. 2A and B). Likewise, responses to both GEP44 and GEP12 were accompanied by significant increases in cAMP levels in both rat and human islets when measured the presence of glucose and Y1-R antagonists (Fig. 2D and E).

Taken together, the ISR and cAMP findings support the hypothesis that GLP-1R-mediated increases in cAMP potentiate insulin secretion, but that simultaneous occupation of Y1-R prevents binding to GLP-1R and/or the capacity to elicit relevant downstream responses. However, to explore the possibility that these peptides might modulate glucose homeostasis via their effects on circulating levels of glucagon, glucagon secretion from islets treated with GEP44 or GEP12 was measured, both in the presence and the absence of Y1-R antagonists (Fig. 2F). Our findings revealed that all agents and relevant combinations (i.e., GEP44 and GEP12 with Y1-R antagonists or Ex-4 alone) resulted in decreased glucagon release. Interestingly, this was the opposite of their individual impacts on the ISR (Fig. 2F). These data are consistent with one of two scenarios, either (1) direct peptide-stimulated inhibition of GLP-1R and Y1-R on α-cells, or (2) indirect peptide-mediated insulin release leading to inhibition of glucagon release, as observed in previous studies (Vergari, Knudsen et al. 2019); (Bansal and Wang 2008).

FIG. 2

GEP44 activates insulin-independent glucose uptake in muscle tissue via its interactions with Y1-R

Despite the positive ISR data and hypothesis that GEP12 would prove superior to GEP44, we noted in

in vivo studies (vide infra) that it was considerably inferior to GEP44 in terms of food intake and body weight reduction. GEP12 is also poorly soluble and unstable (i.e., forms aggregates in solution). Based on these observations with GEP12, and on our unexpected findings that GEP44-mediated increases in ISR and decreases in glucagon release can be detected only in the presence of Y1-R antagonists, we proceeded to characterize the contributions of Y1-R to glucose uptake in muscle tissue. Uptake of the radiolabeled glucose analog, ^{3}H-2-deoxyglucose (2-DG; Fig. 2G), was used to measure the impact of acute stimulation of glucose transport in freshly harvested rat quadriceps muscle. Our findings revealed that Y1-R signaling directly stimulated glucose uptake in muscle tissue via a pathway that is independent of insulin-stimulation. Addition of wortmannin, a biochemical inhibitor of AKT signaling that is central to insulin-mediated stimulation of glucose transport (Thiel, Guethlein et al. 2021) effectively blocked insulin-stimulated glucose uptake in muscle tissue. However, wortmannin had no impact on glucose uptake stimulated by the Y-1R agonist, PYY_{1-36} (Fig. 2G). Thus, based on the clear and direct role of Y1-R in promoting glucose uptake in muscle, the lack of any response to GLP-1R agonism, and the glucose-reducing effects of GEP44 observed in our previous studies (Milliken, Elfers et al. 2021), we predicted that GEP44 would also promote glucose uptake via interactions with the Y1-R. Accordingly, we performed parallel studies designed to measure the impact of PYY_{1-36}, GEP44, and GEP44 together with the Y1-R-specific antagonist, PD160170, on glucose uptake into muscle (Fig. 2G). In contrast to the results of our previous experiments performed using pancreatic islets (i.e., those in which GEP44-mediated effects were more prominent in the presence of the Y1-R antagonist), we found that GEP44 directly increased glucose uptake in muscle tissue to a degree similar to that elicited by PYY_{1-36} and that GEP44-mediated glucose uptake was inhibited by Y1-R antagonism. To reinforce these findings, we also measured the release of lactate from muscle using a flow system (Fig. 2H). Based on our findings that revealed the ability of PYY_{1-36} to stimulate insulin-independent glucose transport, we further investigated the impact of this peptide and GEP44 on glycolysis. We reasoned that stimulation of glucose transport would have an impact on the rate of glycolysis as reflected by lactate release and if so, would provide a demonstration this novel effect of Y1R agonism on muscle based on the results of two different assay

systems. Accordingly, we used the flow system that was featured previously in our experiments focused on islet analysis and observed a doubling of lactate production in response to GEP44 (Fig. 2H).

Detection of GEP44 in Y1-R, Y2-R, and GLP-1R-expressing cells in caudal brainstem nuclei associated with appetite control (AP/NTS)

To visualize GEP44 localization in the brain, we injected rats with fluorescently labeled (f)-Cy5-GEP44 either intraperitoneally (IP; 15.5 μg/kg) or directly into the fourth ventricle (intracerebroventricular injection [ICVI]; 1 μg/μl) to target caudal brainstem regions (e.g., the AP and the NTS) involved in food intake and control of nausea/malaise. To evaluate f-Cy5-GEP44 localization in Y1-R, Y2-R, and/or GLP-1Rexpressing cells in the rat hindbrain, we performed RNAscope fluorescent in situ hybridization (FISH) as previously described (Fortin, Lipsky et al. 2020) combined with immunohistochemistry (IHC) of coronal sections prepared from the rat brainstem. f-Cy5-GEP44 administered IP (Fig. 3A) or by ICVI (Fig. 3B) was detected in the brainstem at 60 min post-injection, specifically in Y1-R and/or GLP-1R-expressing cells within the AP and the NTS. We also detected f-Cy5-GEP44 in Y1-R, Y2-R, and GLP-1R-expressing cells in these regions (Fig. 3C). Localization of f-Cy5-GEP44 in cells expressing Y1-R or Y2-R was observed primarily within the medial NTS, while GEP44 localization in cells expressing GLP-1R was detected primarily within the AP.

Fig 3

In vivo dose-response on food intake/body weight in diet-induced obese (DIO) rats

In our first preclinical experiment, we performed a dose escalation study in DIO rats to compare responses to treatment with GEP44 and Ex-4. Our results revealed similar reductions in food intake in response to daily injections of GEP44 or Ex-4 at concentrations ranging from 0.5–10 nmol/kg. However, rats treated with GEP44 at 20 nmol/kg/day exhibited greater reductions in food intake compared to those treated with the same concentration of Ex-4 (predicted mean difference, -18.5%; 95% confidence interval [CI], -36.3% to -0.7%, p=0.0382). Notably, rats receiving Ex-4 at doses of 5 nmol/kg and higher exhibited a lack of activity during the first 30 min of the dark cycle relative to rats injected with vehicle

alone. With doses of 10 nmol/kg and higher, rats exhibited not only a lack of activity, but also notable changes in facial expressions associated with pain and nausea including orbital tightening and nose/cheek flattening compared to rats treated with vehicle alone. Thus, we limited the doses of Ex-4 used in these experiments to ≤20 nmol/kg/day. By contrast, we were able to continue the dose escalation in rats treated with GEP44. Our findings revealed that rats receiving 50 or 100 nmol/kg/day responded with ~77% and ~90% reductions in food intake relative to baseline, respectively (Fig. 4A). The minimal effective dose (MED) determined for both drugs was 0.5 nmol/kg/day. Our results indicated a 'no observed adverse effect level' (NOAEL) of 2 nmol/kg/day for Ex-4 and a maximal tolerated dose (MTD) of 20 nmol/kg/day.

By contrast, the DIO rats tolerated much higher doses (up to 100 nmol/kg/day) of GEP44 with no indication of malaise. We did detect mild staining around the mouth and nose of one rat treated with 50 nmol/kg/day GEP44 and one additional rat when treated with a single 100 nmol/kg dose of GEP44. Staining did not appear to be the result of inattention to grooming and was not consistent with porphyrin secretion. All animals remained alert and responsive with no other notable changes in appearance, activity, or behavior compared to rats treated with vehicle alone. Thus, we established a NOAEL for GEP44 at 20 nmol/kg/day. No MTD was determined.

In additional experiments, treatment of DIO rats with GEP12 at 10 nmol/kg/day resulted in significant reductions in food intake and body weight (food intake: mean difference -41.3 kcal/day, 95% CI -62.8 to -19.9 kcal/day, p=0.0019; body weight: mean difference -32.6 g, 95% CI -53.5 to -11.7 g, p=0.0062). By contrast, no significant differences were observed in response to GEP12 at 5 nmol/kg/day (food intake: mean difference -20.0 kcal/day, 95% CI -41.4 to 1.5 kcal/day, p=0.067; body weight: mean difference -8.7 g, 95% CI -29.6 to 12.24 g, p=0.479). The impact of GEP12 on food intake relative to baseline was notably less than that observed in response to GEP44 (at 5 nmol/kg/day: mean difference 36.5%, 95% CI 14.9% to 58.0%, p=0.0009; at 10 nmol/kg/d: mean difference 34.6%, 95% CI -13.0% to 56.1%, p=0.0015). An analysis of 24-h food intake patterns revealed the GEP12-mediated suppression of food intake was of substantially shorter duration than that observed in response to GEP44 (Fig. 4B and C).

No appreciable kaolin consumption was recorded.

Fig.4

Our first longer-term experiment was a vehicle-controlled study designed to examine the responses of DIO rats to equimolar doses of GEP44 and liraglutide (LIRA) beginning with 10 nmol/kg/day and increasing to 25 nmol/kg/day after day 10. The rats treated with GEP44 exhibited notably larger reductions in both body weight (day 10: predicted mean difference -4.9%, 95% CI -6.6 to -3.3%, p<0.0001; day 16: predicted mean difference -7.9%, 95% CI -9.7 to -6.1%, p <0.0001) and food intake (10 nmol/kg/day: predicted mean difference -29.8 kcal/day, 95% CI -45.4 to -14.3 kcal/day, p=0.0001; 25 nmol/kg/day, predicted mean difference -34.1 kcal/day, 95% CI -49.7 to -18.6 kcal/day, p <0.0001) compared to rats treated with LIRA. Treatment with LIRA had no impact on body weight or food intake when administered at 10 nmol/kg/day and induced only mild transient changes at 25 nmol/kg/day (Fig. 5A and B). At the 25 nmol/kg/day dose, food intake was reduced by 62% in rats treated with GEP44 compared to 25% in rats treated with LIRA. At the end of the 16-day treatment protocol, we found that rats that received 25 nmol/kg/day exhibited an average body weight reduction of -12.1% compared to -3.2% in rats treated with LIRA. Blood glucose levels (Table 1) were lower on average in DIO rats treated with GEP44 compared to those treated with vehicle alone (estimated treatment effect, -8.1 mg/dL, 95% CI -15.3 to -1.0 mg/dL, p=0.026), while no difference was noted in LIRA vs. vehicle treated animals (estimated treatment effect, -3.4 mg/dL, 95% CI -10.2 to 3.3 mg/dL, p=0.309).

Fig 5

The second long-term study focused on efforts to sustain these effects via a gradual dose escalation from 5 to 50 nmol/kg/day. The results of this study recapitulated the larger reductions in body weight (mean difference -5.8%, 95% CI -7.9 to -3.7%, p<0.0001) and food intake (mean difference -309 kcal, 95% CI -549 to -70 kcal, p=0.004) observed in response to GEP44 compared to equivalent doses of LIRA during the first 12 days of treatment (Fig. 5C and D). During the remaining 15 days, GEP44 treatment continued to yield greater reductions in food intake relative to baseline (mean difference -14.3%, 95% CI -25.4 to -3.3%, p=0.01), even though the rats were treated with stronger doses of LIRA

on days 13 through 20. At the end of the 27-day treatment protocol, the observed reductions in body weight compared to the vehicle were -15% and -9% for rats treated with GEP44 and LIRA, respectively. Similarly, the cumulative reduction in food intake reduction was -39% for rats treated with GEP44 versus -20% for rats treated with LIRA. At the end of the 27-d treatment, body weight reduction compared to vehicle was -15% (GEP44) vs. -9% (LIRA), and cumulative food intake reduction was -39% (GEP44) vs. -20% (LIRA) (Table 1).

Table 1

Finally, while reductions of mean body weight were consistently less for vehicle-treated rats that were pair-fed with those treated GEP44 or LIRA compared to their peptide-treated counterparts, the differences did not achieve statistical significance. Rats receiving either GEP44 or LIRA exhibited lower post-treatment fasting insulin levels compared to those treated with vehicle alone. Interestingly, vehicle-treated rats that were pair-fed to those receiving GEP44 exhibited comparatively lower fasting serum cholesterol and HDL levels than did their peptide-treated counterparts. No differences in fasting blood glucose, triglycerides, or hepatic transaminase levels were observed (Table 2).

Table 2

DISCUSSION

In this manuscript, we present the properties of the unimolecular triple agonist peptide, GEP44. GEP44 interacts with GLP-1, Y1, and Y2 receptors to regulate insulin secretion in both rat and human pancreatic islets, and it promotes insulin-independent Y1-R-mediated glucose uptake in rat muscle tissue ex vivo. Furthermore, the administration of GEP44 results in profound reductions in food intake and body weight in DIO rats. We modified GEP44 at its N-terminus to generate GEP12. As hypothesized, this modification resulted in reduced internalization at the GLP-1R. However, while there is a stronger stimulation of insulin secretion in response to GEP12 vs. GEP44, GEP12 it is less potent than GEP44 when administered in vivo to reduce food intake and body weight.

There are many seemingly conflicting reports on the effects of Y1-R agonism versus antagonism found

in the recent literature. While receptor levels, animal diet, dosing, and the presence of a GLP-1RA have a profound impact on insulin secretion and associated endocrine outcomes, the effects of dual or triple agonism of Y1-R and Y2-R, in the presence of a GLP-1RA remain unclear. Several groups have designed monomeric dual and triple agonists based on the interactions of GLP-1 with glucagon (Day, Gelfanov et al. 2012, Sanchez-Garrido, Brandt et al. 2017, Ambery, Parker et al. 2018) and/or GIP (Finan, Yang et al. 2015, Nowak, Nowak et al. 2022, Tan, Akindehin et al. 2022). This is a novel and promising approach to the development of drugs for the treatment of human obesity. However, many of these drugs are poorly tolerated and are associated with significant adverse events. For example, once weekly dosing of tirzepatide (a dual GIPR and GLP-1R co-agonist) has superior efficacy for weight reduction compared to the GLP-1R agonist, semaglutide; at least 50% of patients receiving 10 or 15 mg of tirzepatide per week achieved a weight loss of 20% and more (Willard, Douros et al. 2020, Min and Bain 2021, Rosenstock, Wysham et al. 2021, Jastreboff, Aronne et al. 2022, Nowak et al. 2022).Tirzepatide was also superior to semaglutide at reducing levels of glycated hemoglobin (Frias, Davies et al. 2021). However, tirzepatide treatment resulted in mild to moderate gastrointestinal symptoms, including nausea (12–24%), diarrhea (15–17%) and vomiting (6–10%). These symptoms led to the discontinuation of treatment in 3-7% of those patients (Jastreboff, Aronne et al. 2022). Thus, our goal was to design a peptide agonist that overcomes these shortcomings and compare glucoregulation/appetite control driven by the incorporation of Y1-R/Y2-R agonism, a property not shared by tirzepatide incorporation. GEP44 was developed based on extensive structure-activity relationship studies and earlier preliminary in vivo studies that demonstrated its greater efficacy at reducing both food intake and body weight compared to the agonist peptide, Ex-4, without triggering gastrointestinal distress (as assessed by kaolin intake and behavioral scoring as a proxy for nausea in rats and direct evidence of emesis in shrews) (Milliken, Elfers et al. 2021).

Despite reports of positive outcomes from simultaneous agonism of both GLP-1R and Y2-R, this approach alone has not generated the same clinical benefits as obesity surgery (Ye, Hao et al. 2014,

Boland, Mumphrey et al. 2019, Dischinger, Heckel et al. 2021). In one study, exogenous administration of combined GLP-1R/Y2-R agonists partially mimicked the positive effects of bariatric surgery but did not lead to the anticipated overall metabolic improvements (Metzner, Herzog et al. 2022) suggesting other pathways are also involved. Results of a study published by Dischinger, Hasinger et al. (2020) support this concept. Specifically, while obesity surgery and LIRA/PYY_{3-36} co-administration resulted in comparable changes in body weight in obese rats, only surgery resulted in profound changes to the hypothalamic transcriptome; these findings may explain in part the limited nature of the metabolic improvements observed in response to pharmacologic intervention (Dischinger, Hasinger et al. 2020, Metzner, Herzog et al. 2022). Others have demonstrated that the positive outcomes of obesity surgery (i.e., changes in body weight and improved glucose homeostasis) are sustained in mice in the absence of GLP-1R or Y2-R, or both GLP-1R and Y2-R (Ye, Hao et al. 2014, Boland, Mumphrey et al. 2019). These findings support the hypothesis that numerous intersecting and redundant pathways are involved in these physiologic responses. Bearing in mind the observed agonism and binding across GLP-1R, Y1-R and Y2-R (Fig. 1), we also determined that GEP44 delivered either peripherally or directly via ICVI localizes in hindbrain regions involved in the control of food intake. GEP44 was detected in AP/NTS cells that express GLP-1R, Y1-R, or Y2-R (Fig. 3). This result highlights a potential mechanism used by GEP44 to suppress food intake and promote reduction in body weight.

Binding, agonism, internalization, and b-arrestin recruitment

Studies published by (Jones, Buenaventura et al. 2018) and (Ziffert, Kaiser et al. 2020) have documented the physiologic relevance of internalization and b-arrestin recruitment in response to specific interactions with both the GLP-1R and Y2-R. (Jones, Buenaventura et al. 2018) demonstrated that the extent of internalization and receptor trafficking mediated by Ex-4 (the scaffold upon which GEP44 is built) has a direct impact on the ISR and that efforts to retain GLP-1R on the cell surface result in enhanced and sustained insulin release. Similarly, (Ziffert, Kaiser et al. 2020) reported that Y2-R internalization results in receptor desensitization accompanied by a G_i-refractory state. Thus, we evaluated GEP44-mediated

GLP-1R and Y2-R internalization and compared the results to those obtained using Ex-4 or PYY_{3-36}, respectively. Interestingly, GEP44 and Ex-4 were similarly effective at promoting GLP-1R internalization, with EC_{50} values of 3.97 nM and 2.43 nM, respectively. By contrast, while PYY_{3-36} exhibited the anticipated efficacy at Y2-R in this assay (IC_{50}, 8.83 nM), GEP44 was not internalized. This unanticipated outcome may provide critical clues to the mechanism underlying GEP44-mediated weight loss observed in experiments performed in vivo. Thus, we modified GEP44 with the intent of also reducing its capacity to induce internalization at the GLP-1R. We hypothesized that this modified peptide would elicit improved ISRs in both rat and human islets. Based on information published (Jones, Buenaventura et al. 2018), we synthesized GEP12, a peptide with a single N-terminal amino acid change (His to Phe) from GEP44 (Fig. 1). GEP12 (IC_{50} = 19.2 nM) exhibited >4-fold greater binding affinity at human GLP-1R compared to GEP44 (IC_{50} = 90.4 nM) and elicited an increased ISR compared to either GEP44 (in the presence of a Y1-R antagonist) or Ex-4 alone. The N-terminal Phe residue in GEP12 likely contributes to its increased affinity for the extracellular binding domain of GLP-1R. As predicted, GEP12 elicits little to no GLP-1R internalization, a finding that is consistent with and confirms the observations of (Jones, Buenaventura et al. 2018), and is consistent with the concept of biased agonism. Biased agonism may be a critical factor underlying the observed effects of GEP44 and its GEP12 analog; similar results have been reported in studies that characterized the recent FDA-approved single molecule tirzepatide. These studies revealed that tirzepatide is an imbalanced and biased dual GIP-R/GLP-1R co-agonist, which stimulates GIP receptors in a manner analogous to its parent peptide but favors cAMP generation over β-arrestin recruitment at the GLP-1R. Thus, tirzepatide promotes enhanced insulin secretion when compared with responses to native GLP-1 (Willard, Douros et al. 2020).

Y1-R-mediated effects on pancreatic islets

Our experiments were also designed to determine whether peptides that are efficacious at lower concentrations and/or those that promote modified internalization/β-arrestin recruitment might be capable of sustaining the beneficial effects beyond those currently observed while also reducing the

frequency of adverse events. These improvements are likely to increase patient compliance and improve their overall quality of life. Our results suggest that the responses to GEP44 are most likely mediated via integrated responses from several tissues. We show in this manuscript that Y1-R signaling facilitates insulin-independent glucose uptake in muscle. This finding complements findings from an earlier study that revealed a role for Y1-R agonism in facilitating trans-differentiation of α-cells into β-cells (Lafferty, Flatt et al. 2021).

Initially, we anticipated that GEP44 would reduce serum glucose levels via binding to GLP-1R. Of note, we found that Ex-4 binding to GLP-1R leads to increased cAMP levels, an elevated ISR, and reduced glucagon secretion, all consistent with previous findings. However, our experimental studies with GEP44 revealed that interactions with Y1-R could mask the effects of GLP-1R agonism in isolated pancreatic islets. We found that GEP44 had little to no impact on glucose-stimulated insulin secretion in isolated islets in the absence of Y1-R antagonists. These findings may result from a direct interaction between Y1-R and GLP-1R and/or the impact of Y1-R signaling on GLP-1R-mediated induction of cAMP; the latter explanation is suggested by our results (see Fig. 2). The absence of GEP44-mediated changes to the ISR in the absence of a Y1-R antagonist suggests two possible mechanisms that would be consistent with the serum glucose-lowering effects observed in response to this chimeric peptide in vivo. First, we considered the possibility that responses mediated by GLP-1R might be modulated by the state of the Y1-R. In support of this hypothesis, we found that the Y1-R ligand, PYY_{1-36}, inhibited Ex-4-mediated stimulatory responses. We also observed a direct correlation between cAMP levels and the ISR. Conversely, we also note the inverse relationship between glucagon release and the ISR. It is not yet clear whether this is the direct result of insulin-mediated inhibition of glucagon secretion or inhibition resulting from the activation of an α-cell receptor.

Our data suggest a role for Y1-R on pancreatic b-cell function, a role also suggested by other recent results (Yan, Zeng et al. 2021) documenting up-regulation of Y1-R mRNA in brown adipose tissue,

inguinal white adipose tissue, and skeletal muscle of obese mice and humans. Other studies have documented up-regulation of the Y1-R agonist, PYY_{1-36}, in pancreatic islets after obesity surgery; this ligand is then converted to the Y2-R agonist PYY_{3-36} via enzymatic cleavage by DPPIV (Chan, Mun et al. 2006); (Ballantyne 2006). Thus, DPPIV inhibitors may function by prolonging the half-lives of both GLP-1 and PYY_{1-36} in vivo (Aaboe, Knop et al. 2010). A 12-week study in which patients diagnosed with T2DM were treated with the DPPIV inhibitor, sitagliptin, revealed increased serum levels of PYY_{1-36} and improvement of glucose and non-glucose dependent insulin secretion (Aaboe, Knop et al. 2010). Therefore, DPPIV inhibitors might promote glucoregulation in part because of resulting elevated levels of PYY_{1-36}, albeit with associated losses in food intake and body weight reduction. GEP44 mediates insulin-independent glucose uptake in muscle via interactions with Y1-R GEP44 may also reduce serum glucose levels via direct interactions resulting in increased glucose uptake in muscle tissue. Given the known role of Y1-R in GLP-1R-mediated regulation of insulin secretion, we were surprised to find that Y1-R also stimulated glucose uptake in muscle via a mechanism that was fully independent of insulin stimulation. GEP44-mediated increases in glucose transport also correlated with its stimulation of lactate production and thus a downstream impact on muscle metabolism; however, Y1-R agonism may also stimulate a reaction step in the glycolytic pathway. Given that previous findings suggested a role for insulin-independent glucose uptake in pathways leading to glucose homeostasis (Wiernsperger 2005, Diener, Mowbray et al. 2021), the contributions of Y1-R may be physiologically significant. As GEP44 acts directly on muscle tissue, while its effects on islets require concomitant Y1-R antagonism, activation of Y1-R expressed in muscle tissue may ultimately prove to be a critical factor in reducing serum glucose levels, alongside any potential effects on insulin secretion and glucagon release.

Our results revealed that Y1-R agonism resulted in insulin-independent glucose uptake into muscle, but only in the presence of elevated glucose levels. (Magnone, Emionite et al. 2020) Although long-term treatment with GEP44 treatment results in profound reductions of serum glucose levels in DIO rats, it

stimulates the ISR to a much smaller degree than is observed in response to Ex-4. However, GEP44 coadministered with one of two different Y1-R antagonists resulted in more profound increases in the ISR; these results suggest that Y1-R signaling may activate acute responses of GEP44 mediated by GLP-1R.

Both GLP-1R and Y1-R are coupled to the $G\alpha_i$ subunit, in association with reduced levels of cAMP and protein kinase A (PKA) signaling. Given that PKA-mediated signaling is required for glucose-stimulated insulin release, this could be perceived as a contradiction between this mechanism and reports of enhanced insulin secretion under these conditions (Shi, Loh et al. 2015). There are several potential explanations for these observations, including (1) coupling with different G subunits may lead to the activation of protein kinase C (PKC) and ultimately an increase in β-cell mass, especially under conditions of chronic administration, (2) their role in promoting protection against necrotizing or apoptotic β-cell death (Tito, Rudnicki et al. 1993, Sam, Gunner et al. 2012), and (3) activation of phosphatidylinositol 3 kinase γ-subunit (PI3Kγ), a kinase identified as a component of the neuropeptide Y signaling cascade which may aid in the correct localization of insulin granules to facilitate insulin secretion (MacDonald 2009); (Goldberg, Taimor et al. 1998).

Impact of GEP44 on food intake, body weight, and metabolic outcomes in DIO rats compared to responses to Ex-4 and LIRA

Data from the dose escalation experiment conducted in DIO rats indicated that treatment with low doses (0.5 to 10 nmol/kg) of GEP44 and Ex-4 resulted in similar anorectic effects. However, GEP44 has a superior therapeutic window, as rats could be treated with higher doses with no notable adverse effects. As reported in our earlier studies (Milliken, Elfers et al. 2021), GEP44 treatment elicited no indicators of malaise in rats at doses as high as 100 nmol/kg/day. Testing was discontinued at this dose due to extreme reductions in food intake. When comparing the results from the current dose escalation experiment in DIO Wistar rats to those from our earlier experiments performed with lean rats (Milliken, Elfers et al. 2021), and found that GEP44 treatment results in comparable anorectic effects in both

models. By contrast, the data presented in this study suggest that Ex-4 treatment results in a more robust anorectic effect in DIO rats compared to their lean counterparts.

Findings from an initial 16-day experiment performed in DIO rats revealed that GEP44 treatment resulted in more profound reductions of food intake and body compared to treatment with equimolar doses (10 and 25 nmol/kg/day) of LIRA, which is a well-established GLP-1RA currently approved for the treatment of obesity. Similar results were observed in a follow-up 27-day treatment study, in which GEP44 continued to elicit more profound reductions in food intake than equimolar doses of LIRA (5, 10, and 25 nmol/kg/day). As part of this longer 27-day treatment study, pair-fed controls were used to determine whether GEP44 or LIRA had any impact on energy expenditure (EE) and the potential to induce weight loss beyond what would be anticipated from reduced food intake alone. Interestingly, mean body weight reductions observed in the two pair-fed groups of DIO rats were consistently lower throughout the experiment compared to those treated with GEP44 and LIRA; however, no significant differences in change of body weight were identified between either of the treated and their respective pair-fed groups. These results are consistent with earlier studies in humans in which LIRA had no impact on EE (Harder, Nielsen et al. 2004); however, current findings do not rule out the possibility of long-term increases in EE associated with drug treatment (Maciel, Beserra et al. 2018).

Preliminary in vivo studies of GEP12 on food intake and body weight compared to GEP44 in DIO rats

Initial in vivo testing with GEP12 (5 and 10 mg/kg/day) resulted in robust reductions in food intake and body weight, albeit somewhat less than responses observed in rats treated with equivalent doses of GEP44. As in prior experiments with GEP44, no indicators of nausea or malaise (e.g., changes in responsiveness, behavior, coat appearance, or facial expressions such as orbital tightening and nose/cheek flattening) were observed with GEP12 dosing.

CONCLUSION

In summary, the results presented in this manuscript provide pre-clinical validation of a poly-agonistic chimeric peptide targeting GLP-1R, Y1-R and Y2-R. Our findings demonstrate their metabolic stability

and selective agonism at Y1-R, Y2-R, and GLP-1R that lead to stimulation of insulin secretion from pancreatic islets and muscle glucose uptake in vitro and profound reductions in food intake and body weight in experiments performed in vivo. Subsequent work will focus on the use of lipidated analogs of GEP44 and the possibility of one-per-week dosing. This is a promising and innovative route toward the development of unimolecular peptide drugs with superior efficacy than those currently available for the treatment of obesity and T2DM.

AUTHOR CONTRIBUTIONS

R.P.D. and B.T.M. designed GEP44. R.P.D. and K.S.C. designed GEP12. C.L.R., I.R.S., and R.P.D. developed the study rationale and the experimental designs. K.S.C., C.L.R., I.R.S., and R.P.D. drafted the manuscript, which was reviewed and edited by all authors. All fluorescent probes were designed by K.S.C., B.T.M., and R.P.D. and were synthesized, purified, and characterized by K.S.C., A.M.G., or B.T.M. In vitro receptor agonism assays were performed and analyzed by O.G.C. and G.G.H. Ex vivo islet and muscle experiments were designed by I.R.S. and conducted by V.K. FISH/RNAScope experiments were performed by S.V.A. and analyzed by S.V.A. and M.R.H. The in vivo experiments were performed by C.T.E. and T.S.S. with assistance from K.S.C. and A.M.G. and analyzed by C.T.E. and C.L.R. All authors approved the final version of the manuscript.

Funding sources, conflicts of interest, and acknowledgments

This work was supported by the United States Department of Defense through a Congressionally Directed Medical Research Program Award (W81XWH1010299) to R.P.D. and C.L.R. and funding from the National Institutes of Health (R01 DK17047, the DRC Cell Function Analysis Core) and the National Science Foundation (STTR 1853066) to I.R.S. G.G.H. received funding via subcontract under National Institutes of Health (R01 DK128443) to R.P.D., M.R.H. and Bart C. De Jonghe. Biochemical analyses were performed at the University of Washington Nutrition and Obesity Research Center (UW NORC) which is supported by grant P30 DK035816 from the National Institute of Diabetes and Digestive and Kidney Diseases. R.P.D. acknowledges the SOURCE program at Syracuse University for funding provided for A.M.G. R.P.D. is a Scientific Advisory Board member of Balchem Corporation, New Hampton, NY, and Xeragenx LLC. (St. Louis, MO); these organizations played no role in the design, execution, or analysis of the results of these studies. R.P.D. and B.T.M. are named authors of a patent pursuant to this work that is owned by Syracuse University. I.R.S. has financial ties to EnTox Sciences, Inc. (Mercer Island, WA), the manufacturer/distributor of the BaroFuse perifusion system used in this study. M.R.H. receives funding from Zealand Pharma, Novo Nordisk, Eli Lilly & Co., and Boehringer Ingelheim; these funds were not used to support these studies. M.R.H. and R.P.D. are co-founders and co-owners of Cantius Therapeutics (Lansdale, PA), which also played no role in these studies.

Figure 1. Design and in vitro evaluation of chimeric peptides GEP44 and GEP12. Shown are the amino acid sequences of Ex-4, PYY_{1-36} and PYY_{3-36} overlaid with those of GEP44 and GEP12 with lowercase single-letter amino acid code denoting a D-isomer. (A) Dose-dependent agonism (% change in FRET ratio tracking levels of cAMP) of Ex-4, GEP44, and GEP12 at the GLP-1R. (B) Dose-dependent agonism (% change in FRET ratio tracking levels of cAMP) of PYY_{3-36}, GEP44, and GEP12 at the Y2-R. (C) Dose-dependent agonism of PYY_{1-36}, GEP44, and GEP12 at the Y1-R. (D) Percent binding of Ex-4, GEP44, and GEP12 at the GLP-1R. (E) Percent binding of PYY_{3-36}, GEP44, and GEP12 at the Y2-R. (F) Percent binding of PYY_{1-36}, GEP44, and GEP12 at the Y1-R. (G) % internalization of GEP44 and GEP12

at the GLP-1R. (H) % recruitment of β-arrestin-2 by Ex-4 and GEP44 at the GLP-1R. (I) % internalizationof Ex-4 and GEP44 at the Y2-R.

Figure 2. Action of GEP44 and GEP12 are mediated by GLP-1R and Y1-R in isolated pancreatic islets and muscle tissue. Rat (A) and human (B) islets were incubated for 60 min in 20 mM glucose and additional agents as indicated. Supernatants were then assayed for insulin, cAMP, and glucagon concentrations. (C) Insulin secretion rates (ISRs) were measured by perifusion over a one-hour incubation period in rat islets in 20 mM glucose with 5 or 50 nM peptides with or without Y1-R antagonist, as indicated (C). Impact of GEP44 on (D) cAMP, (E) the ISR to cAMP ratio, and (F) glucagon secretion, relative to glucose-mediated stimulation alone in the absence of test compounds. cAMP levels corresponded directly, and glucagon secretion corresponded inversely with the ISR. (G) Uptake of ^{3}H-2-deoxyglucose (2-DG) and (H) lactate production (± 5 mM glucose) in response to GEP44 and other agents known to interact with GLP-1R, Y1-R, and Y2-R in the rat quadriceps muscle ex vivo. Horizontal dashed line in 2A, B, D, and F represents response to 20 mM glucose alone in assay as described. [a] =PD 160170; [b] = BIIE0246; [c] = BIBO; [d] = Bay K, [e] = Wortmannin.

Figure 3. FISH and IHC visualization of f-Cy5-GEP44 and its colocalization with Y1-R, Y2-R, and GLP-1R in cells in the NTS/AP regions of the rat brain. (A) f-Cy5-GEP44 (green) administered IP colocalized with Y1-R and GLP-1R (yellow) in the AP. (B) f-Cy5-GEP44 administered ICVI colocalized with Y1-R (yellow) and GLP-1R (magenta) in the AP. See Supplementary Video 1 for a three-dimensional (3D) rotational image of the area within the inset. (C) f-Cy5-GEP44 administered ICVI colocalized with Y2-R (yellow) and GLP-1R (magenta) in cells of the AP. See Supplementary Video 2 for a 3D rotational image of the area within the inset. Images are shown at 40x magnification.

Figure 4. Dose-escalation study reveals a robust reduction of food intake in response to GEP44. (A) The dose-escalation study shows a robust reduction of food intake in response to GEP44 (●, n=8 DIO rats) vs. Ex-4 (n, n=4 DIO rats). Food intake was averaged over three days of treatment at each drug dose and was normalized to the earliest three days during which all animals received injections with the vehicle control. Escalation of the Ex-4 dose was stopped at 20 nmol/kg due to multiple indicators of malaise. (B, C) Shown is the average 24-hour cumulative food intake for the three-day vehicle-treated baseline and three-day GEP12 treatment phases (q, n=8 DIO rats) at (B) 5 nmol/kg/day and (C) 10 nmol/kg/day doses. Data from equivalent dose-testing performed as part of the GEP44 (●) doseescalation study were included in these figures to facilitate a qualitative comparison. Data shown are means ± standard error of the mean (SEM); *p<0.05, ** p <0.01, *** p <0.001.

Figure 5. GEP44-mediated reductions in body weight and food intake were stronger than those elicited by LIRA during a 16-day and 27-day dose escalation protocol. (A, B) DIO Wistar rats were treated with vehicle (r) or with GEP44 (●) or LIRA at 10 nmol/kg/day for 9 days followed by 25 nmol/kg/day for 7 days (n=4–6) rats/group. In a second experiment, (C) changes in body weight and (D) food intake was evaluated during 27 days of treatment with vehicle, GEP44, vehicle-treated rats that were pair-fed to those receiving GEP44, LIRA, and vehicle-treated rats that were pair-fed to those receiving LIRA; n=8 per group. DIO male Wistar rats were matched based on baseline food intake and initial body weight gain trajectory. Changes in body weight were evaluated in response to GEP44 (●) at doses escalating from 5 to 50 nmol/kg/day. Rats underwent pair-feeding to match the amount of food consumed by their GEP44-treated counterparts (o). Other groups included rats treated with salinevehicle control, LIRA, and rats that were pair-fed to their LIRA-treated counterparts. Symbols representing the results from pair-fed animals are overlayed by those from the GEP44 and LIRA treatment groups. Data shown are means ± SEM; *p <0.05, ***p <0.001, ****p <0.0001.

Table 1. Characteristics of treatment groups at baseline and after 27 days of treatment with GEP44 or LIRA. The data shown are means ± standard deviation (SD). Data were compared by ANCOVA

followed by pairwise comparisons of marginal linear predictions using a Bonferroni correction; n=8 rats per group. Abbreviations: Tx, treatment; *p <0.05, **p <0.01, ***p <0.001 vs. vehicle control; #p <0.05, ##p <0.01, ###p <0.001 vs. LIRA. Pair-fed comparisons were made with no difference detected.
Table 2. Outcomes after 27 days of treatment with GEP44 or LIRA. Data shown are means ± SD. Cross-sectional analyses were performed using an ANOVA followed by pairwise comparisons of means using a Bonferroni correction; n=8 rats per group. Abbreviations: ALT, alanine aminotransferase; AST, aspartate aminotransferase; Trig, triglycerides; HDL, high-density lipoprotein; calc, calculated; LDL, lowdensity lipoprotein; † p <0.05, †† <0.01 vs. pair-fed counterparts.

STAR*METHODS
Detailed methods are provided in the online version of this paper and include the following:
• KEY RESOURCES TABLE
• RESOURCES AVAILABILITY
o Lead Contact
o Materials Availability
o Data and Code Availability
• METHOD DETAILS
• Peptide syntheses and purification
• Competitive binding assays at GLP-1R
• Competitive binding assay at Y2-R
• Competitive binding assay at Y1-R
• Internalization of GLP-1R
• Internalization of Y2-R
• β-Arrestin recruitment at GLP-1R
• In vitro receptor agonism at Y1-R, Y2-R, and GLP-1R
• Rat islet isolation and culture
• Static measurement of rates of insulin secretion, glucagon secretion, and cAMP release
• Perifusion measurements to determine rates of insulin secretion
• Assays performed on supernatants collected from static incubation and outflow fractions of perifusion experiments
• Insulin measured by radioimmunoassay (RIA)
• Glucagon measured by immunoassay
• Quantitative evaluation of cAMP levels by ELISA
• Glucose uptake in muscle
• Lactate production by perfused muscle tissue
• Fluorescent in situ hybridization (FISH) and immunohistochemical (IHC) visualization of fluorescent GEP44 (f-Cy5-GEP44) colocalized with GLP-1R and Y1-R or Y2-R on neurons in the AP/NTS
• Animal experiments
• Preparation and administration of drugs
• Dose escalation study in diet-induced obese male rats
• Long-term drug intervention
• QUANTIFICATION AND STATISTICAL ANALYSIS
All data were expressed as means ± standard deviation (SD) unless otherwise noted. For behavioral studies, data were analyzed by ANCOVA, a repeated-measures one-way ANOVA, or a two-way ANOVA followed by Tukey's or Bonferroni's post hoc test as appropriate. For all statistical tests, a pvalue less than 0.05 was considered significant. All data were analyzed using Prism GraphPad 9 or Stata/SE 14.2.

Key Resources Table

REAGENT or RESOURCE	SOURCE	IDENTIFIER
Antibodies		
Anti-anti-Cy5 Antibody (B-2) Alexa Fluor 647	Santa Cruz Biotechnology	sc-166896 AF647
Bacterial and virus strains		
H188 Adenovirus	Lab of Prof. Kees Jalink, Division of Cell Biology, the Netherlands Cancer Institute, Amsterdam, the Netherlands.	N/A
Biological samples		
Rat Islets	Harvested from Sprague-Dawley rats (n=23; ~250g; Envigo/Harlan)	N/A
Human Islets	Human islets were provided by the NIH-funded Integrated Islet Distribution Program	N/A
Rat brain tissue	Extracted from adult male Sprague-Dawley rats (n=23; ~400g; Charles River Laboratories)	N/A
Chemicals, peptides, and recombinant proteins		
Exendin-4	In-house (Syracuse University)	N/A
Liraglutide	Selleck Chemicals (Houston, TX)	S8256
GEP44	GenScript (Piscataway, NJ)	N/A
GEP12	In-house (Syracuse University)	N/A
PYY(3-36)	In-house (Syracuse University)	N/A
PYY(1-36)	In-house (Syracuse University)	N/A
PD160170	Tocris	2200
BIBO3304	Tocris	2412
^{3}H-2-deoxyglucose	Perkin Elmer	NET328A250UC
Wortmannin	Sigma Aldrich	W1628
Y1-R antibodies	online Inc.	ABIN4888949
Glucagon-Like Peptide 1 Receptor (GLP-1R) protein (His tag)	antibodies-online Inc.	ABIN3080888
Neuropeptide Y Receptor Y1 (NPY1R) protein (His tag)	antibodies-online Inc.	ABIN7086253
ProTide Rink amide resin	CEM Corporation	R002
Triisopropylsilane	Sigma-Aldrich	233781
Trifluoroacetic acid	Sigma-Aldrich	8.08260.2501
N,N'-Diisopropylcarbodiimide	Sigma-Aldrich	D125407
Oxyma Pure	CEM Corporation	S001
Piperidine	Sigma-Aldrich	8.22299.0500
N,N'-Dimethylformamide	VWR (Radnor, PA)	BDH83634.400
α-cyano-4-hydroxycinnamic acid	Acros Organics	163440050

Acetonitrile HiSolv VWR BDH83639.400
Diethyl ether VWR BDH67003.400
Dulbecco's Modified Eagle Medium Sigma-Aldrich D6429
Penicillin-streptomycin ThermoFisher Scientific 15140122
Bovine serum albumin Sigma-Aldrich A3059
Fetal bovine serum Sigma-Aldrich 12303C
Liberase Roche Molecular Biochemicals (Indianapolis, IN) 05339880001
Euthasol, 390 mg/ml sodium pentobarbital Virbac RXEUTHASOL
Insulin MilliporeSigma 91077C
Catheter lock solution (500 USP units/ml heparin in 50% glycerol) Instech Labs (Plymouth Meeting, PA) USP-HGS-500-10-VBP-5
DAPI-containing mounting media VECTASHIELD Antifade Mounting Medium H1200
Lactate MilliporeSigma L9795
Standard Extracellular Saline (SES) Solution In-house (Upstate Medical University) N/A
Normal donkey serum Sigma Aldrich 566460
5-thio-D-glucose Santa Cruz Biotechnology sc-221044A
Meloxicam Midwest Veterinary Supply N/A
isoflurane Butler Schein
sulfo-Cyanine5 DBCO Lumiprobe 433F0
Bay-K8644 Sigma-Aldrich B112
Critical commercial assays and kits
hY2-R Binding Assay EuroscreenFast (Gosselies, Belgium) FAST-0321B
hGLP-1R Agonist-Based Internalization Eurofins Discovery (Fremont, CA) 86-0010P-2029AG
hY2-R Agonist-Based Internalization Eurofins Discovery (Fremont, CA) 86-0010P-2037AG
hGLP-1R Agonist-Based Arrestin Recruitment Eurofins Discovery (Fremont, CA) 86-0001P-2166AG
Leptin, IL-1b, IL-6, and TNF-a Magnetic Bead Panel Assay MilliporeSigma RECYTMAG-65K
Insulin ELISA MilliporeSigma EZRMI-13K
Adiponectin ELISA MilliporeSigma EZRADP-62K
cAMP Kit ThermoFisher 4412182
Amplex Red Glucose/Glucose Oxidase Assay Kit ThermoFisher A22189
Lactate Oxidase from Aerococcus viridans MilliporeSigma L9795
Beuthanasia-D Schering-Plough Animal Health Corp., Union, NJ N/A
Experimental models: Cell lines
HEK293 cells stably transfected to express hGLP-1R

In-house N/A
HEK293 cells American Type Culture Collection
(Manassas, VA)
N/A
HEK293 C24 American Type Culture Collection
(Manassas, VA)
N/A
Experimental models: Organisms/strains
Adult male Wistar rats Charles River Laboratories
(Wilmington, MA)
003
Adult male Sprague Dawley rats Envigo Harlan (Indianapolis, IN) 002
Adult male DIO Wistar rats Charles River Laboratories
(Wilmington, MA)
003
Software and algorithms
GraphPad PRISM GraphPad Software N/A
Stata/SE 14.2 STATACorp LLC N/A
ProData Viewer Software JASCO J-715 spectropolarimeter N/A
FlexStation 3 microplate reader Molecular Devices N/A
Imaris 8.1.2 software Bitplane N/A
HPEPDOCK Server Huang Lab (Huazhong University
of Science and Technology,
Wuhan, China)
N/A
Other
High-Fat diet Research Diets, Inc. (New
Brunswick, NJ)
D12492
BioDAQ cages Research Diets, Inc. (New
Brunswick, NJ)
E2 Electronic
DietMax Food Monitoring System OmniTech Electronics, Inc.
(Columbus, OH)
Normal chow LabDiet (St. Louis, MO) PicoLab Rodent 5053
Kaolin (powdered) Sigma Aldrich K1512
OneTouch Ultra Mini Glucometer Lifescan (Malvern, PA)
OneTouch Ultra Glucose test strips Lifescan (Malvern, PA) N/A
Microvette® 100 K_3 EDTA Sarstedt 20.1278.100
Superfrost Plus slides Fisher Scientific
RNAscope® Multiplex Fluorescent Reagent Kit v2 ACDBio 323100
RNAscope probe Rn-NPY1-R-C1 ACDBio 414471
RNAscope probe Rn-GLP-1R-C2 ACDBio 315221-C2
RNAscope probe Rn-NPY2-R-C1 ACDBio 414481
BZ-X800 microscope Keyence
Liquid scintillation counter Beckman Model LS6500
26-gauge cannula Plastics One
Spectrophotometer, plate reader, Synergy 4 BioTek (Winooski, VT) Model S4MLFPTA
Wizard 2, 5-channel gamma counter Perkin Elmer Model 2470-0050
BaroFuse Multi-Channel perifusion system EnTox Sciences Model 001-08
pcDNA3.1-hY2 receptor plasmid DNA cDNA Resource Center NPYR20TN00

pcDNA3.1-hY1 receptor plasmid DNA cDNA Resource Center NPYR10TN00
OpenSPR Nicoya (Kitchener, ON, Canada) N/A
Nitrilotriacetic acid (NTA) sensor chip Nicoya Store (Kitchener, ON, Canada)
SEN-AU-100-10-NTA
Zorbax C18 column (5μm, 9.4 x 250 mm) Agilent 880995-202
Resource Availability
Lead Contact
Further information and requests for resources and reagents should be directed to and will be fulfilled by the lead contact Professor Robert P. Doyle (rpdoyle@syr.edu).
Materials Availability
This study generated new unique reagents. R.P.D is the named author of a patent pursuant to this work that is owned by Syracuse University and will supply the reagent under MTA upon reasonable request.
Data and Code Availability
The published article includes all data generated or analyzed during this study. No code was used or generated in this study.

METHOD DETAILS

Peptide Syntheses and Purification

Solid-phase peptide synthesis was performed on ProTide Rink amide resin using a microwave-assisted CEM Liberty Blue peptide synthesizer (Matthews, NC, USA). Fmoc-protected amino acids were coupled to the resin using Oxyma Pure (0.25 M) and N, N'-diisopropyl carbodiimide (0.125 M) as the activator and activator base, respectively. Fmoc was removed between couplings with 20% piperidine. Global deprotection and cleavage of the peptides from the solid-support resin were achieved using a CEM Razor instrument via a 40-minute incubation at 40°C in a mixture of 95% trifluoroacetic acid, 2.5% triisopropylsilane, and 2.5% water. Peptides were precipitated with cold (4°C) diethyl ether and purified on an Agilent 1200 series High-Performance Liquid Chromatography (HPLC) instrument (10–75% HPLC-grade acetonitrile for 20 minutes at a 2 mL/min flow rate over an Agilent Zorbax C18 column (5 μm, 9.4 x 250 mm) tracked at 220, 254, and 280 nm. Peptides were purified to >95%. Peptide binding was assayed by EuroscreenFast (Gosselies, Belgium) or in-house with a Nicoya Open Surface Plasmon Resonance (SPR) instrument. Internalization and b-arrestin recruitment assays were performed by Eurofins Discovery (Fremont, CA, USA).

Competitive Binding Assays at GLP-1R

GEP44 and Ex-4 binding to the human GLP-1R was measured using a TagLite fluorescent competitive binding assay in CHO-K1 cells. $GLP\text{-}1_{red}$ was used as the agonist tracer and Ex-4 as the reference competitor. IC_{50} values were measured in duplicate in independent runs at eight concentrations per run. GEP12 binding to the human GLP-1R was measured in-house by SPR using His-tagged GLP-1R bound to a nitrilotriacetic acid (NTA) sensor. The GEP12 dose-response (0.1 nM – 100 nM) binding assay was performed in a duplicate.

Competitive Binding Assays at Y2-R

Peptide binding to the human Y2-R was measured in a dose-responsive manner (1 pM –1 μM) using a radioligand competitive binding assay in CHO-K1 cells. Peptide binding was assayed in duplicate independent runs with eight concentrations per run. The peptide $PYY_{3\text{-}36}$ was used as a positive control.

Competitive Binding Assays at Y1-R

Peptide binding to human Y1-R was performed in-house by SPR. The dose response to GEP44 (4 pM - 19 μM) was evaluated using $PYY_{1\text{-}36}$ as positive and $PYY_{3\text{-}36}$ as negative controls.

Internalization of GLP-1R

Human GLP-1R (G_s-coupled) cell-based agonist-activated internalization assays were performed by Eurofins Discovery. Dose-response assays (30 pM - 1 μM) were performed in duplicate with Ex-4 as a positive control.

Internalization of Y2-R

A human Y2-R (G_s-coupled) dose-response (5.51 pM - 551 nM) cell-based agonist-activated internalization assay was performed in duplicate with $PYY_{3\text{-}36}$ as a positive control.

β-Arrestin Recruitment at GLP-1R

Human GLP-1R cell-based arrestin assays were performed by Eurofins Discovery (Fremont, CA, USA; assay #86-0001P-2166AG) as described by the company. Dose-response assays (5.51 pM – 551 nM) were performed in duplicate with Ex-4 as a positive control.

In vitro Receptor Agonism at Y1-R, Y2-R, and GLP-1R

H188 virally transduced HEK293 cells stably expressing human GLP-1R were obtained from Novo Nordisk A/S for use in FRET assays. HEK293 C24 cells stably expressing the H188 FRET reporter were obtained by G418 selection and grown in monolayers to ~70% confluency in 100 cm^2 tissue culture dishes and were then transfected with plasmids (11 μg/dish) encoding human GLP-1R, human Y2-R, or human Y1-R. Transfected cells were then incubated for 48 h in fresh culture media. For real-time FRET kinetic assays, cells were harvested, resuspended in 21 mL of SES buffer, and plated at 196 μL per well. Plated cells were pretreated with 4 μL of agonist, or antagonist (Ex_{9-39} (GLP-1R antagonist) or BIIE0246 (Y2-R antagonist)), at a given target concentration and incubated for 20 min before performing the assay. Y1-R and Y2-R agonism to stimulate G_i proteins and to inhibit adenylyl cyclase was monitored by detecting the ability of PYY peptides, GEP44, or GEP12 to counteract the ability of Adenosine (acting through endogenous A2B receptor and Gs proteins) to increase levels of cAMP. For these assays, increased levels of cAMP were measured as an increase of the 485/535 nm FRET ratio serving as a readout for binding of cAMP to the H188 biosensor that is based on the exchange protein activated by cAMP (Chepurny, Bonaccorso et al. 2018).

Rat islet isolation and culture. Islets were harvested from Sprague-Dawley rats (~250 g) that were anesthetized by an intraperitoneal injection of pentobarbital sodium (150 mg/kg). All procedures were approved by the University of Washington Institutional Animal Care and Use Committee (IACUC Protocol 4091-01). Islets were prepared and purified as described (Rountree, Neal et al. 2014). Briefly, islets were prepared by injecting collagenase (10 mL of Liberase at 0.23 mg/mL) into the pancreatic duct

followed by surgical removal of the pancreas. The isolated pancreata were placed into 15 mL conical tubes containing 10 mL of 0.23 mg/mL Liberase and incubated at 37C for 30 min. The digests were then filtered and rinsed with Hank's buffered salt solution (HBSS). Islets were purified using an Optiprep gradient (Nycomed, Oslo, Norway) as previously described (Brandhorst, Brandhorst et al. 1999) and cultured for 18 h in a 37˚C in a 5% CO_2 incubator in Roswell Park Memorial Institute (RPMI) medium supplemented with 10% heat-inactivated fetal bovine serum before use in experiments.

Static measurements to determine rates of insulin secretion, glucagon secretion, and cAMP release. Rates of insulin, glucagon, and cAMP release were determined statically under multiple conditions as previously described (Jung, Reed et al. 2009). Briefly, islets were handpicked, transferred to a petri dish containing 11 mL of Krebs-Ringer bicarbonate (KRB) buffer supplemented with 0.1% bovine serum albumin (BSA) and 3 mM glucose, and incubated at 37˚C and 5% CO_2 for 60 min. Islets were then selected and transferred into wells of 96-well plates containing 0.2 mL of KRB with 20 mM glucose and various test compounds as indicated and incubated for an additional 60 min. Subsequently, the supernatants were assayed for insulin, glucagon, and cAMP. These values were used to calculate the secretion rate as the concentration in the assay (ng/ml for insulin and glucagon, and pmol/mL for cAMP) times the volume of KRB in each well during the assay (0.2 mL) divided by the assay time (60 minutes). Data was then normalized by dividing by the secretion rate in the presence of test compounds over that obtained at 20 mM glucose alone.

Preparation of test compounds for in vitro experiment. Adding test compounds to solutions for either static or perifusion protocols involved making up a stock solution and then adding a small volume to the wells (for static) or inflow buffer (for perifusion). Stock solutions of test compounds that are water soluble were made up at 20 times the final assay concentration in buffer (including glucose, GEP44, GEP12, exendin-4, PYY_{1-36} and insulin). For test compounds that were insoluble in water (Y1-R

antagonists) stocks were made up at 1000 times the assay concentration in DMSO, so that final concentration of DMSO in the assay was 0.1%.

Perifusion measurements to determine rates of insulin secretion. Insulin production was evaluated using a commercially available perifusion system (BaroFuse; EnTox Sciences, Mercer Island, WA). Ten isolated rat islets were placed into each of eight channels that were operating at a flow rate of 50 μL/min of KRB (continuously equilibrated with 21% O_2 and 5% CO_2 and balance of N_2) containing 0.1% BSA and 3 mM glucose for 90 minutes. Subsequently, varying amounts of glucose and test compounds were injected into the inflow of the flow system as indicated and outflow fractions were collected every 10 minutes and assayed for insulin as described in the section to follow. The insulin secretion rate was calculated as insulin times the flow rate of KRB divided by the number of islet x 100 yielding the ng/min/100 islets. Data was graphed after normalizing each insulin time course by dividing by the secretion rate at each time point by the rate obtained in the presence of 20 mM glucose prior to the addition of test compounds. Assays performed on supernatants collected from static incubation and outflow fractions of perifusion experiments. Assays using commercially available kits were performed according to the manufacturers' instructions.

Insulin measured by radioimmunoassay (RIA). Briefly, specific anti-insulin antiserum was incubated with the sample together with defined amounts of ^{125}I-labeled insulin. Antibody-bound tracer was separated from the unbound tracer by precipitation in solution provided in the kit containing 3% PEG and 0.05% Triton X-100 in 0.05M Phosphosaline with 0.025M EDTA and 0.08% sodium azide. The ^{125}I remaining in the tube was assessed quantitatively on a five-channel gamma counter. The amount of ^{125}I detected in the supernatant is inversely proportional to the amount of insulin in the original sample.
Glucagon measured by immunoassay. Briefly, samples were incubated with two manufacturersupplied anti-glucagon monoclonal antibodies that were covalently linked to either SmBiT or LgBiT. After the detection substrate was added, the resulting luminescence was measured using a

spectrophotometer. The luminescent signal detected is directly proportional to the amount of glucagon present in the sample.

Quantitative evaluation of cAMP levels by ELISA. Samples and diluted cAMP-alkaline phosphatase (AP) reagent were added to wells of a pre-coated assay plate (Thermofisher; Waltham, MA) and mixed by repetitive pipetting. After a one-hour incubation, the solutions were removed from wells which were then washed six times with wash buffer. A substrate/enhancer solution was then added, and the plates were incubated for 30 min. The luminescent signal was measured using a spectrophotometer at room temperature protected from light.

Glucose uptake in muscle. ^{3}H-2-deoxyglucose (DG) uptake into muscle tissue was evaluated as previously described (Sweet, Cook et al. 2004), with the exception that the bound radiolabeled compound was separated from free radiolabel by washing the tissue multiple times in radiolabel-free medium. Sprague-Dawley rats (~250 g) were anesthetized by intraperitoneal injection of Beuthanasia-D (38 mg pentobarbital sodium and 6 mg phenytoin sodium/230 g rat) (Schering-Plough Animal Health Corp., Union, NJ). While the rats remained under anesthesia, strips of quadriceps muscle were collected and transferred to a Petri dish containing HBSS with 0.1% BSA. While still under anesthesia, animals were then euthanized by cutting the diaphragm. The muscle strip was cut into smaller pieces (~2 mg each) using a scalpel. Three pieces were then transferred into polystyrene 12 x 75 test tubes containing 190 mL of KRB (with 5 mM bicarbonate) solution and compounds as described in each experiment. Each condition was evaluated in triplicate. The tubes were placed in racks that were partially submerged in a shaking water bath maintained at 37˚C. At precisely the times indicated, 10 μL of the radioactive dose (typically 0.25 μCi) was spiked into each tube to bring the final volume to 200 mL. The tubes were capped and shaken in the water bath at 120 rpm for precisely 45 minutes. Free radiolabel was removed by washing the muscle fragments three times with 5 mL cold (4˚C) KRB solution. After the third wash, 100 μL of KRB was added to each tube and the muscle and solution were then transferred to a

microcentrifuge tube. The muscle pieces were then fragmented further by sonication (Branson) at maximum power and 50% duty cycle for 20 seconds. The contents of the microfuge tube were then transferred to a 7 mL scintillation vial. A liquid scintillation cocktail (5 mL, Ecolume) was added, the samples were shaken, and radioactivity was evaluated using a liquid scintillation counter

Lactate production by perifused muscle tissue Muscle fragments (6 x 2 mg each) were placed into each of six channels of a commercially available perifusion system (BaroFuse) operating at a flow rate of 30 μL/min of KRB with 0.1% BSA and varying amounts of glucose. Outflow fractions were collected every 10 minutes and measured using a glucose/glucose oxidase kit in which lactate oxidase was used to replace glucose oxidase. Manufacturer supplied solutions of horseradish peroxidase, Amplex Red, and lactate oxidase were added to samples in wells of a 96-well microplate which was then incubated at room temperature for 30 minutes.

Fluorescence was measured with a spectrophotometer.

Fluorescent in situ hybridization (FISH) and immunohistochemical (IHC) visualization of fluorescent GEP44 (f-Cy5-GEP44) and its localization AP/NTS neurons that express GLP-1R and Y1-R or Y2-R. Male Sprague-Dawley rats were briefly anesthetized with isoflurane (5% induction followed by 2–3% maintenance) to facilitate implantation of an in-dwelling cannula (26 gauge) directed at the 4th cerebroventricular region (coordinates: on the midline, 2.5 mm anterior to the occipital suture and 5.2 mm ventral to the skull.) Postoperative analgesia (2 mg/kg meloxicam) was administered subcutaneously for two days, and the rats were allowed to recover for one week. Proper placement and cannula patency were verified via 5-thio-D-glucose (210 μg)-induced hyperglycemia, as previously described (Mietlicki-Baase, Liberini et al. 2018). Rats with appropriate cannula placement and patency were included in the experiments to follow. Rats (n=2) received an ICVI of f-Cy5-GEP44 (1 μg) dissolved in 1 μL 0.9% normal saline solution. Additional rats (n=2) received an intraperitoneal injection of f-Cy5-GEP44 (15.5 μg/kg). One hour later, rats were anesthetized with ketamine (90 mg/kg), xylazine (2.8 mg/kg), and acepromazine (0.72 mg/kg) and transcardially perfused with 0.1 M phosphate-buffered

saline (PBS) followed by 4% paraformaldehyde (PFA) in PBS. Brains were collected and stored in 4% PFA for 24 hours after which they were transferred to 20% sucrose for cryoprotection at 4ÅãC. Serial coronal sections (16 μm thickness) of each brain were prepared using a cryostat, mounted onto Superfrost Plus slides, and stored at −80 ÅãC. One series that included the rostral-caudal extent of the NTS was used to detect RNA levels of Y1-R (RNAscope Probe Rn-NPY1-R-C1), GLP-1R (RNAscope Probe Rn-GLP-1R-C2), and f-Cy5-GEP44; another series was used separately to detect RNA levels of Y2-R (RNAscope Probe Rn-Y2-R-C1), GLP-1R, and f-Cy5-GEP44. Fluorescent in situ hybridization (FISH) was performed as per the manufacturer's instructions for the RNAscope. Multiplex Fluorescent Reagent Kit v2. Sections were washed three times for 5 min each in 0.1 M PBS, followed by incubation in 50% ethanol for 30 min. Sections were then rinsed again (three times x 5 min each with 0.1 M PBS). Sections were then washed in freshly prepared 0.1% sodium borohydride for 20 min and washed again in 0.1 M PBS (three times, 5 min each). To restore Cy5-GEP44 fluorescence, sections were then incubated overnight with an Alexa Fluor 647-linked mouse anti-Cy5 antibody (1:100). After washing (three times x 5 min each with 0.1 M PBS, the tissues were immersed in DAPI-containing mounting media, cover-slipped, and stored at 4 C. Images were acquired 24 – 48 hrs later, on a Keyence BZ-X800 microscope using negative control sections to adjust for background fluorescence. Images were taken using filter cubes for DAPI, GFP, Cy3, and Cy5 at 20x and 40x magnification. Image z-stacks were collected with a step-size of 1 μm and rendered as three-dimensional rotational animations using Imaris 8.1.2 software (Supplementary videos 1 and 2).

Animal experiments

All procedures performed in rats were approved by the Institutional Animal Care and Use Committee at the Seattle Children's Research Institute (IACUC00064) and were in accordance with the National Institutes of Health (NIH) Guide for Care and Use of Laboratory Animals. This facility is approved by the Association of the Assessment and Accreditation of Laboratory Animal Care International (AAALAC). Wistar rats purchased from Charles River Laboratories (Wilmington, MA) were used in this study. The

rats were provided with ad libitum access to food and water and were kept on a 12 h light/12 h dark cycle. For all other experiments, male rats (51–75g; approximately 4 weeks of age) were fed a diet with 60% of the calories provided by fat (D12492; Research Diets, Inc; New Brunswick, NJ; 5.21 kcal/g) for approximately five months before the start of the study generate diet-induced obesity (DIO). Animals were individually housed in a temperature (22 ± 1C) and humidity-controlled (57 ± 4%) room. All body weight measurements were taken just before the start of the dark cycle.

Preparation and administration of drugs

GEP44 stock solutions were prepared using sterile ultra-pure H_2O and gently agitated at 4ÅãC for >24 h and then aliquoted and stored at -20ÅãC. Ex-4 was produced by the Doyle lab and dissolved in 1 mL of sterile ultra-pure H_2O. LIRA was dissolved in 1 mL of sterile ultra-pure H_2O. The stock solutions were aliquoted and stored at -20C. Stock solutions for both Ex-4 and LIRA were diluted to working solutions in 0.9% normal saline and mixed gently before use. GEP12 (aliquots up to 5 mg) was dissolved in 100 µL DMSO and mixed at 1000 rpm for three min to create a stock solution. Stock solutions were diluted to working solutions in 0.9% normal saline, resulting in a final DMSO concentration of <2%. The unused portion of the stock solution was stored at -20ÅãC for up to 7 days. Working solutions were stored at 4C for up to two days and mixed gently before use. Normal saline solution was used as the vehicle control in all studies. Working solutions of GEP44, GEP12, Ex-4, LIRA, or vehicle control were administered by subcutaneous injection once daily at the start of the dark cycle using a 1 cc 29G insulin syringe. The concentration of each drug solution was adjusted to maintain the dosing volume at 0.5 mL/kg.

Dose escalation study in diet-induced obese male rats

Male Wistar rats (Ex-4 group, n=4; GEP44 group, n=8) were provided with a high-fat (HF) diet (60% cal from fat, 5.21 kcal/g) for 20 weeks before the start of the study. Rats were singly housed in BioDAQ cages and allowed to acclimate for at least 10 days before the start of this study. The average baseline weight of the rats in this study was 685 Å} 38 g. Baseline measurements of body weight and food intake

were taken for three days to balance the groups. The study design included sequential rounds of a three-day vehicle-treated baseline phase, a three-day treatment phase, and a two-to-three-day washout phase. Dosing began at 0.5 nmol/kg/day and was increased in approximately one-third-log increments ($10_{n/3}$) until the MTD was established. The doses tested included 0.5, 1, 2, 5, 10, 20, 50, and 100 nmol/kg/day administered subcutaneously just before the start of the dark cycle. The 100 nmol/kg dose of GEP44 was tested for one day only. Body weight was assessed daily just before the start of the dark cycle. Food and water were available ad libitum and consumption was monitored continuously.

A preliminary GEP12 dosing test was performed in male DIO Wistar rats (n=8). These rats were fed the HF diet for 40 weeks before the start of the study and weighed an average of 862 Å} 82 g at baseline. The study design included two rounds of a three-day vehicle-treated baseline phase, a three-day treatment phase, and a two-to-three-day washout phase. Doses of 5 to 10 nmol/kg/day were administered via subcutaneous injection just before the start of the dark cycle. Body weight was assessed daily just before the start of the dark cycle. Food and water were available ad libitum and consumption was continuously monitored using a BioDAQ system. In this experiment, cages were modified to facilitate the use of the DietMax food monitor system for continuous recording of powdered kaolin consumption. Animals were allowed to acclimate for at least 10 days before the start of the study.

Long-term drug intervention

Male Wistar rats (n=4) were fed a 60% HF diet for 20 weeks before the start of the study. Rats were then housed singly in BioDAQ cages and allowed to acclimate to their new environment for 10 days. Baseline measures of body weight and food intake were collected for one week to balance the groups and create feeding pairs. Two independent experiments were performed. In the first experiment, three cohorts of eight animals each received daily injections of vehicle or increasing doses of either GEP44 or LIRA starting at 10 nmol/kg for 9 days and followed by 25 nmol/kg for 7 days. Rats averaged 802 Å} 86 g at baseline with equivalent variances between the groups. In the second experiment, five cohorts of eight animals each received daily injections of GEP44 alone, vehicle pair-fed with GEP44, LIRA alone, vehicle

pair-fed to LIRA, and vehicle alone. Rats averaged 661 Å} 68 g at baseline with equivalent variances between the groups. GEP44 was administered as follows: 5 nmol/kg/day for 4 days, 10 nmol/kg/day for 4 days, 25 nmol/kg/day for 12 days, and 50 nmol/kg/day for 8 days. LIRA was administered as follows: 5 nmol/kg/day for 4 days, 10 nmol/kg/day for 4 days, 25 nmol/kg/day for 4 days, and 50 nmol/kg/day for 16 days. Food intake was monitored continuously throughout the experiment. Body weights were measured daily immediately before the start of the dark cycle. Pre- and post-treatment fasting plasma samples were obtained from blood collected via tail nick using a microvette to assess insulin levels. Blood glucose concentrations were obtained at the same time using a handheld glucometer. Blood was collected by cardiac puncture at the time of euthanasia which was two hours after the final injection. Commercially available enzyme-linked immunosorbent assays (ELISAs) were used to perform quantitative assessments of both insulin and adiponectin. A commercially-available magnetic bead panel was used to perform quantitative assessments of leptin, IL-1b, IL-6, and TNF-a. Serum samples were diluted 1:500 for the adiponectin ELISA using the sample diluent provided with the kit. All ELISAs were performed following the manufacturers' recommendations. Serum levels of glucose, cholesterol (total, high-density lipoprotein [HDL], and calculated low-density lipoprotein [LDL]), triglycerides, alanine transaminase (ALT), and aspartate transaminase (AST) were determined using a Modular P chemistry analyzer (Roche Diagnostics, Germany) by the University of Washington NORC Core, Seattle, WA.

QUANTIFICATION AND STATISTICAL ANALYSIS

All data were expressed as mean ± SD unless otherwise noted. For behavioral studies, data were analyzed by ANCOVA, or repeated-measures one-way or two-way ANOVA followed by Tukey's or Bonferroni's post hoc test as appropriate. For all statistical tests, a p-value <0.05 was considered significant. All data were analyzed using Prism GraphPad 9 or Stata/SE 14.2.

REFERENCES

Aaboe, K., F. K. Knop, T. Vilsboll, C. F. Deacon, J. J. Holst, S. Madsbad and T. Krarup (2010). "Twelve weeks treatment with the DPP-4 inhibitor, sitagliptin, prevents degradation of peptide YY and improves glucose and non-glucose induced insulin secretion in patients with type 2 diabetes mellitus." Diabetes

Obes Metab 12(4): 323-333.
Abdel-Hamid, H. A., M. M. I. Abdalla, N. M. Zenhom and R. F. Ahmed (2019). "The effect of peptide tyrosine tyrosine (PYY3-36), a selective Y2 receptor agonist on streptozotocin-induced diabetes in albino rats." Endocr Regul 53(1): 26-33.
Addison, M. L., J. S. Minnion, J. C. Shillito, K. Suzuki, T. M. Tan, B. C. Field, N. Germain-Zito, C. Becker-Pauly, M. A. Ghatei, S. R. Bloom and K. G. Murphy (2011). "A role for metalloendopeptidases in the breakdown of the gut hormone, PYY 3-36." Endocrinology 152(12): 4630-4640.
Ambery, P., V. E. Parker, M. Stumvoll, M. G. Posch, T. Heise, L. Plum-Moerschel, L. F. Tsai, D. Robertson, M. Jain, M. Petrone, C. Rondinone, B. Hirshberg and L. Jermutus (2018). "MEDI0382, a GLP-1 and glucagon receptor dual agonist, in obese or overweight patients with type 2 diabetes: a randomised, controlled, double-blind, ascending dose and phase 2a study." Lancet 391(10140): 2607-2618.
Andresen, B. T. (2011). "A pharmacological primer of biased agonism." Endocr Metab Immune Disord Drug Targets 11(2): 92-98.
Ballantyne, G. H. (2006). "Peptide YY(1-36) and peptide YY(3-36): Part II. Changes after gastrointestinal
surgery and bariatric surgery." Obes Surg 16(6): 795-803.
Bansal, P. and Q. Wang (2008). "Insulin as a physiological modulator of glucagon secretion." Am J Physiol Endocrinol Metab 295(4): E751-761.
Battelino, T., R. M. Bergenstal, A. Rodriguez, L. Fernandez Lando, R. Bray, Z. Tong and K. Brown (2022).
"Efficacy of once-weekly tirzepatide versus once-daily insulin degludec on glycaemic control measured by continuous glucose monitoring in adults with type 2 diabetes (SURPASS-3 CGM): a substudy of the randomised, open-label, parallel-group, phase 3 SURPASS-3 trial." Lancet Diabetes Endocrinol 10(6): 407-417.
Batterham, R. L., M. A. Cohen, S. M. Ellis, C. W. Le Roux, D. J. Withers, G. S. Frost, M. A. Ghatei and S. R. Bloom (2003). "Inhibition of food intake in obese subjects by peptide YY3-36." N Engl J Med 349(10): 941-948.
Batterham, R. L., H. Heffron, S. Kapoor, J. E. Chivers, K. Chandarana, H. Herzog, C. W. Le Roux, E. L. Thomas, J. D. Bell and D. J. Withers (2006). "Critical role for peptide YY in protein-mediated satiation and body-weight regulation." Cell Metab 4(3): 223-233.
Blevins, J. E., P. K. Chelikani, A. C. Haver and R. D. Reidelberger (2008). "PYY(3-36) induces Fos in the arcuate nucleus and in both catecholaminergic and non-catecholaminergic neurons in the nucleus tractus solitarius of rats." Peptides 29(1): 112-119.
Boland, B., M. B. Mumphrey, Z. Hao, B. Gill, R. L. Townsend, S. Yu, H. Munzberg, C. D. Morrison, J. L. Trevaskis and H. R. Berthoud (2019). "The PYY/Y2R-Deficient Mouse Responds Normally to High-Fat Diet and Gastric Bypass Surgery." Nutrients 11(3): 585.
Boland, B. B., R. C. Laker, S. O'Brien, S. Sitaula, I. Sermadiras, J. C. Nielsen, P. Barkholt, U. Roostalu, J. Hecksher-Sorensen, S. R. Sejthen, D. D. Thorbek, A. Suckow, N. Burmeister, S. Oldham, S. Will, V. G. Howard, B. M. Gill, P. Newton, J. Naylor, D. C. Hornigold, J. Austin, L. Lantier, O. P. McGuinness, J. L. Trevaskis, J. S. Grimsby and C. J. Rhodes (2022). "Peptide-YY3-36/glucagon-like peptide-1 combination treatment of obese diabetic mice improves insulin sensitivity associated with recovered pancreatic beta-cell function and synergistic activation of discrete hypothalamic and brainstem neuronal circuitries." Mol Metab 55: 101392.
Boland, B. B., M. B. Mumphrey, Z. Hao, R. L. Townsend, B. Gill, S. Oldham, S. Will, C. D. Morrison, S. Yu, H. Munzberg, C. J. Rhodes, J. L. Trevaskis and H. R. Berthoud (2019). "Combined loss of GLP-1R and Y2R does not alter progression of high-fat diet-induced obesity or response to RYGB surgery in mice." Mol Metab 25: 64-72.
Borner, T., I. C. Tinsley, R. P. Doyle, M. R. Hayes and B. C. De Jonghe (2022). "Glucagon-like peptide-1 in diabetes care: Can glycaemic control be achieved without nausea and vomiting?" Br J Pharmacol 179(4): 542-556.

Brandhorst, H., D. Brandhorst, B. J. Hering and R. G. Bretzel (1999). "Significant progress in porcine islet mass isolation utilizing liberase HI for enzymatic low-temperature pancreas digestion." Transplantation 68(3): 355-361.
Chan, J. L., E. C. Mun, V. Stoyneva, C. S. Mantzoros and A. B. Goldfine (2006). "Peptide YY levels are elevated after gastric bypass surgery." Obesity (Silver Spring) 14(2): 194-198.
Chandarana, K., C. Gelegen, E. E. Irvine, A. I. Choudhury, C. Amouyal, F. Andreelli, D. J. Withers and R. L. Batterham (2013). "Peripheral activation of the Y2-receptor promotes secretion of GLP-1 and improves glucose tolerance." Mol Metab 2(3): 142-152.
Chepurny, O. G., R. L. Bonaccorso, C. A. Leech, T. Wollert, G. M. Langford, F. Schwede, C. L. Roth, R. P. Doyle and G. G. Holz (2018). "Chimeric peptide EP45 as a dual agonist at GLP-1 and NPY2R receptors." Sci Rep 8(1): 3749.
Day, J. W., V. Gelfanov, D. Smiley, P. E. Carrington, G. Eiermann, G. Chicchi, M. D. Erion, J. Gidda, N. A. Thornberry, M. H. Tschop, D. J. Marsh, R. SinhaRoy, R. DiMarchi and A. Pocai (2012). "Optimization of co-agonism at GLP-1 and glucagon receptors to safely maximize weight reduction in DIO-rodents." Biopolymers 98(5): 443-450.
De Bandt, D., C. Rives-Lange, Y. Frigout, D. Bergerot, A. Blanchard, M. Le Gall, J. M. Lacorte, J. M. Chevallier, S. Czernichow, T. Poghosyan, C. Carette and J. Le Beyec (2022). "Similar Gut Hormone Secretions Two Years After One Anastomosis Gastric Bypass and Roux-en-Y Gastric Bypass: a Pilot Study." Obes Surg 32(3): 757-762.
Diener, J. L., S. Mowbray, W. J. Huang, D. Yowe, J. Xu, S. Caplan, A. Misra, A. Kapur, J. Shapiro, X. Ke, X. Wu, A. Bose, D. Panza, M. Chen, V. Beaulieu and J. Gao (2021). "FGF21 Normalizes Plasma Glucose in Mouse Models of Type 1 Diabetes and Insulin Receptor Dysfunction." Endocrinology 162(9): bqab092.
Dischinger, U., C. Corteville, C. Otto, M. Fassnacht, F. Seyfried and M. K. Hankir (2019). "GLP-1 and PYY3-36 reduce high-fat food preference additively after Roux-en-Y gastric bypass in diet-induced obese rats." Surg Obes Relat Dis 15(9): 1483-1492.
Dischinger, U., J. Hasinger, M. Konigsrainer, C. Corteville, C. Otto, M. Fassnacht, M. Hankir and F. J. D. Seyfried (2020). "Toward a Medical Gastric Bypass: Chronic Feeding Studies With Liraglutide + PYY3-36 Combination Therapy in Diet-Induced Obese Rats." Front Endocrinol (Lausanne) 11: 598843.
Dischinger, U., T. Heckel, T. Bischler, J. Hasinger, M. Konigsrainer, A. Schmitt-Bohrer, C. Otto, M. Fassnacht, F. Seyfried and M. K. Hankir (2021). "Roux-en-Y Gastric Bypass and Caloric Restriction but Not Gut Hormone-Based Treatments Profoundly Impact the Hypothalamic Transcriptome in Obese Rats." Nutrients 14(1): 116.
Fetissov, S. O., L. C. Byrne, H. Hassani, P. Ernfors and T. Hokfelt (2004). "Characterization of neuropeptide Y Y2 and Y5 receptor expression in the mouse hypothalamus." J Comp Neurol 470(3): 256-265.
Finan, B., B. Yang, N. Ottaway, D. L. Smiley, T. Ma, C. Clemmensen, J. Chabenne, L. Zhang, K. M. Habegger, K. Fischer, J. E. Campbell, D. Sandoval, R. J. Seeley, K. Bleicher, S. Uhles, W. Riboulet, J. Funk, C. Hertel, S. Belli, E. Sebokova, K. Conde-Knape, A. Konkar, D. J. Drucker, V. Gelfanov, P. T. Pfluger, T. D. Muller, D. Perez-Tilve, R. D. DiMarchi and M. H. Tschop (2015). "A rationally designed monomeric peptide triagonist corrects obesity and diabetes in rodents." Nat Med 21(1): 27-36.
Fortin, S. M., R. K. Lipsky, R. Lhamo, J. Chen, E. Kim, T. Borner, H. D. Schmidt and M. R. Hayes (2020).
"GABA neurons in the nucleus tractus solitarius express GLP-1 receptors and mediate anorectic effects of liraglutide in rats." Sci Transl Med 12(533): eaay8071.
Frias, J. P., M. J. Davies, J. Rosenstock, F. C. Perez Manghi, L. Fernandez Lando, B. K. Bergman, B. Liu, X. Cui, K. Brown and S.-. Investigators (2021). "Tirzepatide versus Semaglutide Once Weekly in Patients with Type 2 Diabetes." N Engl J Med 385(6): 503-515.
Frias, J. P., M. A. Nauck, J. Van, M. E. Kutner, X. Cui, C. Benson, S. Urva, R. E. Gimeno, Z. Milicevic, D. Robins and A. Haupt (2018). "Efficacy and safety of LY3298176, a novel dual GIP and GLP-1 receptor

agonist, in patients with type 2 diabetes: a randomised, placebo-controlled and active comparatorcontrolled
phase 2 trial." Lancet 392(10160): 2180-2193.
Goldberg, Y., G. Taimor, H. M. Piper and K. D. Schluter (1998). "Intracellular signaling leads to the hypertrophic effect of neuropeptide Y." Am J Physiol 275(5): C1207-1215.
Guida, C. and R. Ramracheya (2020). "PYY, a Therapeutic Option for Type 2 Diabetes?" Clin Med Insights Endocrinol Diabetes 13: 1179551419892985.
Guida, C., S. Stephen, R. Guitton and R. D. Ramracheya (2017). "The Role of PYY in Pancreatic Islet Physiology and Surgical Control of Diabetes." Trends Endocrinol Metab 28(8): 626-636.
Guida, C., S. D. Stephen, M. Watson, N. Dempster, P. Larraufie, T. Marjot, T. Cargill, L. Rickers, M. Pavlides, J. Tomlinson, J. F. L. Cobbold, C. M. Zhao, D. Chen, F. Gribble, F. Reimann, R. Gillies, B. Sgromo, P. Rorsman, J. D. Ryan and R. D. Ramracheya (2019). "PYY plays a key role in the resolution of diabetes following bariatric surgery in humans." EBioMedicine 40: 67-76.
Harder, H., L. Nielsen, D. T. Tu and A. Astrup (2004). "The effect of liraglutide, a long-acting glucagon-like peptide 1 derivative, on glycemic control, body composition, and 24-h energy expenditure in patients with type 2 diabetes." Diabetes Care 27(8): 1915-1921.
Heise, T., A. Mari, J. H. DeVries, S. Urva, J. Li, E. J. Pratt, T. Coskun, M. K. Thomas, K. J. Mather, A. Haupt and Z. Milicevic (2022). "Effects of subcutaneous tirzepatide versus placebo or semaglutide on pancreatic islet function and insulin sensitivity in adults with type 2 diabetes: a multicentre, randomised, double-blind, parallel-arm, phase 1 clinical trial." Lancet Diabetes Endocrinol 10(6): 418-429.
Jastreboff, A. M., L. J. Aronne, N. N. Ahmad, S. Wharton, L. Connery, B. Alves, A. Kiyosue, S. Zhang, B. Liu, M. C. Bunck, A. Stefanski and S.-. Investigators (2022). "Tirzepatide Once Weekly for the Treatment of Obesity." N Engl J Med 387(3): 205-216.
Jones, B., T. Buenaventura, N. Kanda, P. Chabosseau, B. M. Owen, R. Scott, R. Goldin, N. Angkathunyakul, I. R. Correa, Jr., D. Bosco, P. R. Johnson, L. Piemonti, P. Marchetti, A. M. J. Shapiro, B. J. Cochran, A. C. Hanyaloglu, A. Inoue, T. Tan, G. A. Rutter, A. Tomas and S. R. Bloom (2018). "Targeting GLP-1 receptor trafficking to improve agonist efficacy." Nat Commun 9(1): 1602.
Jung, S. R., B. J. Reed and I. R. Sweet (2009). "A highly energetic process couples calcium influx through L-type calcium channels to insulin secretion in pancreatic beta-cells." Am J Physiol Endocrinol Metab. 297(3): E717-727.
Kjaergaard, M., C. B. G. Salinas, J. F. Rehfeld, A. Secher, K. Raun and B. S. Wulff (2019). "PYY(3-36) and exendin-4 reduce food intake and activate neuronal circuits in a synergistic manner in mice." Neuropeptides 73: 89-95.
Koegler, F. H., P. J. Enriori, S. K. Billes, D. L. Takahashi, M. S. Martin, R. L. Clark, A. E. Evans, K. L. Grove, J. L. Cameron and M. A. Cowley (2005). "Peptide YY(3-36) inhibits morning, but not evening, food intake and decreases body weight in rhesus macaques." Diabetes 54(11): 3198-3204.
Lafferty, R. A., P. R. Flatt and N. Irwin (2021). "Established and emerging roles peptide YY (PYY) and exploitation in obesity-diabetes." Curr Opin Endocrinol Diabetes Obes 28(2): 253-261.
MacDonald, P. (2009). "Control of secretory granule access to the plasma membrane by PI3 kinasegamma." Islets 1(3): 266-268.
Maciel, M. G., B. T. S. Beserra, F. C. B. Oliveira, C. M. Ribeiro, M. S. Coelho, F. A. R. Neves and A. A. Amato (2018). "The effect of glucagon-like peptide 1 and glucagon-like peptide 1 receptor agonists on energy expenditure: A systematic review and meta-analysis." Diabetes Res Clin Pract 142: 222-235.
Magnone, M., L. Emionite, L. Guida, T. Vigliarolo, L. Sturla, S. Spinelli, A. Buschiazzo, C. Marini, G. Sambuceti, A. De Flora, A. M. Orengo, V. Cossu, S. Ferrando, O. Barbieri and E. Zocchi (2020). "Insulin-independent stimulation of skeletal muscle glucose uptake by low-dose abscisic acid via AMPK activation." Sci Rep 10(1): 1454.
Merkel, R., A. Moreno, Y. Zhang, R. Herman, J. Ben Nathan, S. Zeb, S. Rahematpura, K. Stecyk, B. T. Milliken, M. R. Hayes, R. P. Doyle and H. D. Schmidt (2021). "A novel approach to treating opioid use disorders: Dual agonists of glucagon-like peptide-1 receptors and neuropeptide Y2 receptors." Neurosci Biobehav Rev 131: 1169-1179.

Metzner, V., G. Herzog, T. Heckel, T. Bischler, J. Hasinger, C. Otto, M. Fassnacht, A. Geier, F. Seyfried and U. Dischinger (2022). "Liraglutide + PYY3-36 Combination Therapy Mimics Effects of Roux-en-Y Bypass on Early NAFLD Whilst Lacking-Behind in Metabolic Improvements." J Clin Med 11(3): 753.
Mietlicki-Baase, E. G., C. G. Liberini, J. L. Workinger, R. L. Bonaccorso, T. Borner, D. J. Reiner, K. Koch-Laskowski, L. E. McGrath, R. Lhamo, L. M. Stein, B. C. De Jonghe, G. G. Holz, C. L. Roth, R. P. Doyle and M. R. Hayes (2018). "A vitamin B12 conjugate of exendin-4 improves glucose tolerance without associated nausea or hypophagia in rodents." Diabetes Obes Metab 20(5): 1223-1234.
Milliken, B. T., R. P. Doyle, G. G. Holz and O. G. Chepurny (2020). "FRET Reporter Assays for cAMP and Calcium in a 96-well Format Using Genetically Encoded Biosensors Expressed in Living Cells." Bio Protoc 10(11): e3641.
Milliken, B. T., C. Elfers, O. G. Chepurny, K. S. Chichura, I. R. Sweet, T. Borner, M. R. Hayes, B. C. De Jonghe, G. G. Holz, C. L. Roth and R. P. Doyle (2021). "Design and Evaluation of Peptide Dual-Agonists of GLP-1 and NPY2 Receptors for Glucoregulation and Weight Loss with Mitigated Nausea and Emesis." J Med Chem 64(2): 1127-1138.
Min, T. and S. C. Bain (2021). "The Role of Tirzepatide, Dual GIP and GLP-1 Receptor Agonist, in the Management of Type 2 Diabetes: The SURPASS Clinical Trials." Diabetes Ther 12(1): 143-157.
Moran, T. H., U. Smedh, K. P. Kinzig, K. A. Scott, S. Knipp and E. E. Ladenheim (2005). "Peptide YY(3-36) inhibits gastric emptying and produces acute reductions in food intake in rhesus monkeys." Am J Physiol Regul Integr Comp Physiol 288(2): R384-388.
Neary, N. M., C. J. Small, M. R. Druce, A. J. Park, S. M. Ellis, N. M. Semjonous, C. L. Dakin, K. Filipsson, F. Wang, A. S. Kent, G. S. Frost, M. A. Ghatei and S. R. Bloom (2005). "Peptide YY3-36 and glucagon-like
peptide-17-36 inhibit food intake additively." Endocrinology 146(12): 5120-5127.
Nonaka, N., S. Shioda, M. L. Niehoff and W. A. Banks (2003). "Characterization of blood-brain barrier permeability to PYY3-36 in the mouse." J Pharmacol Exp Ther 306(3): 948-953.
Nowak, M., W. Nowak and W. Grzeszczak (2022). "Tirzepatide - a dual GIP/GLP-1 receptor agonist - a new antidiabetic drug with potential metabolic activity in the treatment of type 2 diabetes." Endokrynol Pol 73(4): 745-755.
Oberto, A., I. Bertocchi, A. Longo, S. Bonzano, S. Paterlini, C. Meda, S. Della Torre, P. Palanza, A. Maggi and C. Eva (2022). "Hypothalamic NPY-Y1R Interacts with Gonadal Hormones in Protecting Female Mice against Obesity and Neuroinflammation." Int J Mol Sci 23(11): 6351.
Ostergaard, S., J. F. Paulsson, M. Kjaergaard Gerstenberg and B. S. Wulff (2021). "The Design of a GLP-1/PYY Dual Acting Agonist." Angew Chem Int Ed Engl 60(15): 8268-8275.
Paterlini, S., R. Panelli, L. Gioiosa, S. Parmigiani, P. Franceschini, I. Bertocchi, A. Oberto, A. Bartolomucci, C. Eva and P. Palanza (2021). "Conditional Inactivation of Limbic Neuropeptide Y-1 Receptors Increases Vulnerability to Diet-Induced Obesity in Male Mice." Int J Mol Sci 22(16): 8745.
Rahardjo, G. L., X. F. Huang, Y. Y. Tan and C. Deng (2007). "Decreased plasma peptide YY accompanied by elevated peptide YY and Y2 receptor binding densities in the medulla oblongata of diet-induced obese mice." Endocrinology 148(10): 4704-4710.
Reidelberger, R. D., A. C. Haver, B. A. Apenteng, K. L. Anders and S. M. Steenson (2011). "Effects of exendin-4 alone and with peptide YY(3-36) on food intake and body weight in diet-induced obese rats." Obesity (Silver Spring) 19(1): 121-127.
Rosenstock, J., C. Wysham, J. P. Frias, S. Kaneko, C. J. Lee, L. Fernandez Lando, H. Mao, X. Cui, C. A. Karanikas and V. T. Thieu (2021). "Efficacy and safety of a novel dual GIP and GLP-1 receptor agonist tirzepatide in patients with type 2 diabetes (SURPASS-1): a double-blind, randomised, phase 3 trial." Lancet 398(10295): 143-155.
Roth, C. L., K. D. Bongiovanni, B. Gohlke and J. Woelfle (2010). "Changes in dynamic insulin and gastrointestinal hormone secretion in obese children." J Pediatr Endocrinol Metab 23(12): 1299-1309.
Roth, C. L., P. J. Enriori, K. Harz, J. Woelfle, M. A. Cowley and T. Reinehr (2005). "Peptide YY is a regulator of energy homeostasis in obese children before and after weight loss." J Clin Endocrinol Metab 90(12): 6386-6391.

Rountree, A. M., A. S. Neal, M. Lisowski, N. Rizzo, J. Radtke, S. White, D. S. Luciani, F. Kim, C. S. Hampe and I. R. Sweet (2014). "Control of insulin secretion by cytochrome C and calcium signaling in islets with impaired metabolism." J Biol Chem 289(27): 19110-19119.
Ruska, Y., A. Szilvasy-Szabo, D. Kovari, A. Kadar, L. Macsai, R. Sinko, E. Hrabovszky, B. Gereben and C. Fekete (2022). "Expression of glucagon-like peptide 1 receptor in neuropeptide Y neurons of the arcuate nucleus in mice." Brain Struct Funct 227(1): 77-87.
Sam, A. H., D. J. Gunner, A. King, S. J. Persaud, L. Brooks, K. Hostomska, H. E. Ford, B. Liu, M. A. Ghatei, S. R. Bloom and G. A. Bewick (2012). "Selective ablation of peptide YY cells in adult mice reveals their role in beta cell survival." Gastroenterology 143(2): 459-468.
Sanchez-Garrido, M. A., S. J. Brandt, C. Clemmensen, T. D. Muller, R. D. DiMarchi and M. H. Tschop (2017). "GLP-1/glucagon receptor co-agonism for treatment of obesity." Diabetologia 60(10): 1851-1861.
Shaw, J. L., S. L. Gackenheimer and D. R. Gehlert (2003). "Functional autoradiography of neuropeptide Y Y1 and Y2 receptor subtypes in rat brain using agonist stimulated [35S]GTPgammaS binding." J Chem Neuroanat 26(3): 179-193.
Shi, Y. C., K. Loh, M. Bensellam, K. Lee, L. Zhai, J. Lau, J. Cantley, J. Luzuriaga, D. R. Laybutt and H. Herzog (2015). "Pancreatic PYY Is Critical in the Control of Insulin Secretion and Glucose Homeostasis in Female Mice." Endocrinology 156(9): 3122-3136.
Sloth, B., L. Davidsen, J. J. Holst, A. Flint and A. Astrup (2007). "Effect of subcutaneous injections of PYY1-36 and PYY3-36 on appetite, ad libitum energy intake, and plasma free fatty acid concentration in obese males." Am J Physiol Endocrinol Metab 293(2): E604-609.
Sweet, I. R., D. L. Cook, A. Lernmark, C. J. Greenbaum, A. R. Wallen, E. S. Marcum, S. A. Stekhova and K. A. Krohn (2004). "Systematic screening of potential beta-cell imaging agents." Biochem Biophys Res Commun 314(4): 976-983.
Talsania, T., Y. Anini, S. Siu, D. J. Drucker and P. L. Brubaker (2005). "Peripheral exendin-4 and peptide YY(3-36) synergistically reduce food intake through different mechanisms in mice." Endocrinology 146(9): 3748-3756.
Tan, Q., S. E. Akindehin, C. E. Orsso, R. C. Waldner, R. D. DiMarchi, T. D. Muller and A. M. Haqq (2022). "Recent Advances in Incretin-Based Pharmacotherapies for the Treatment of Obesity and Diabetes." Front Endocrinol (Lausanne) 13: 838410.
Thiel, G., L. A. Guethlein and O. G. Rossler (2021). "Insulin-Responsive Transcription Factors." Biomolecules 11(12): 1886.
Tito, J. M., M. Rudnicki, D. H. Jones, H. D. Alpern and M. S. Gold (1993). "Peptide YY ameliorates cerulein-induced pancreatic injury in the rat." Am J Surg 165(6): 690-696.
van den Hoek, A. M., A. C. Heijboer, P. J. Voshol, L. M. Havekes, J. A. Romijn, E. P. Corssmit and H. Pijl (2007). "Chronic PYY3-36 treatment promotes fat oxidation and ameliorates insulin resistance in C57BL6 mice." Am J Physiol Endocrinol Metab 292(1): E238-245.
Vergari, E., J. G. Knudsen, R. Ramracheya, A. Salehi, Q. Zhang, J. Adam, I. W. Asterholm, A. Benrick, L. J. B. Briant, M. V. Chibalina, F. M. Gribble, A. Hamilton, B. Hastoy, F. Reimann, N. J. G. Rorsman, Spiliotis, II, A. Tarasov, Y. Wu, F. M. Ashcroft and P. Rorsman (2019). "Insulin inhibits glucagon release by SGLT2-induced stimulation of somatostatin secretion." Nat Commun 10(1): 139.
Vrang, N., A. N. Madsen, M. Tang-Christensen, G. Hansen and P. J. Larsen (2006). "PYY(3-36) reduces food intake and body weight and improves insulin sensitivity in rodent models of diet-induced obesity." Am J Physiol Regul Integr Comp Physiol 291(2): R367-375.
Walther, C., K. Morl and A. G. Beck-Sickinger (2011). "Neuropeptide Y receptors: ligand binding and trafficking suggest novel approaches in drug development." J Pept Sci 17(4): 233-246.
Wiernsperger, N. F. (2005). "Is non-insulin dependent glucose uptake a therapeutic alternative? Part 2: Do such mechanisms fulfil the required combination of power and tolerability?" Diabetes Metab 31(6): 521-525.
Willard, F. S., J. D. Douros, M. B. Gabe, A. D. Showalter, D. B. Wainscott, T. M. Suter, M. E. Capozzi, W. J. van der Velden, C. Stutsman, G. R. Cardona, S. Urva, P. J. Emmerson, J. J. Holst, D. A. D'Alessio, M. P. Coghlan, M. M. Rosenkilde, J. E. Campbell and K. W. Sloop (2020). "Tirzepatide is an imbalanced

and biased dual GIP and GLP-1 receptor agonist." JCI Insight 5(17): e140532.
Yan, C., T. Zeng, K. Lee, M. Nobis, K. Loh, L. Gou, Z. Xia, Z. Gao, M. Bensellam, W. Hughes, J. Lau, L. Zhang, C. K. Ip, R. Enriquez, H. Gao, Q. P. Wang, Q. Wu, J. J. Haigh, D. R. Laybutt, P. Timpson, H. Herzog and Y. C. Shi (2021). "Peripheral-specific Y1 receptor antagonism increases thermogenesis and protects against diet-induced obesity." Nat Commun 12(1): 2622.
Yang, C. H., D. Ann-Onda, X. Lin, S. Fynch, S. Nadarajah, E. G. Pappas, X. Liu, J. W. Scott, J. S. Oakhill, S. Galic, Y. Shi, A. Moreno-Asso, C. Smith, T. Loudovaris, I. Levinger, D. L. Eizirik, D. R. Laybutt, H. Herzog, H. E. Thomas and K. Loh (2022). "Neuropeptide Y1 receptor antagonism protects beta-cells and improves glycemic control in type 2 diabetes." Mol Metab 55: 101413.
Ye, J., Z. Hao, M. B. Mumphrey, R. L. Townsend, L. M. Patterson, N. Stylopoulos, H. Munzberg, C. D. Morrison, D. J. Drucker and H. R. Berthoud (2014). "GLP-1 receptor signaling is not required for reduced body weight after RYGB in rodents." Am J Physiol Regul Integr Comp Physiol 306(5): R352-362.
Zhao, S., Z. Yan, Y. Du, Z. Li, C. Tang, L. Jing, L. Sun, Q. Yang, X. Tang, Y. Yuan, J. Han and N. Jiang (2022). "A GLP-1/glucagon (GCG)/CCK2 receptors tri-agonist provides new therapy for obesity and diabetes." Br J Pharmacol 179(17): 4360-4377.
Ziffert, I., A. Kaiser, S. Babilon, K. Morl and A. G. Beck-Sickinger (2020). "Unusually persistent Galphaisignaling of the neuropeptide Y2 receptor depletes cellular Gi/o pools and leads to a Gi-refractory state." Cell Commun Signal 18(1): 49.

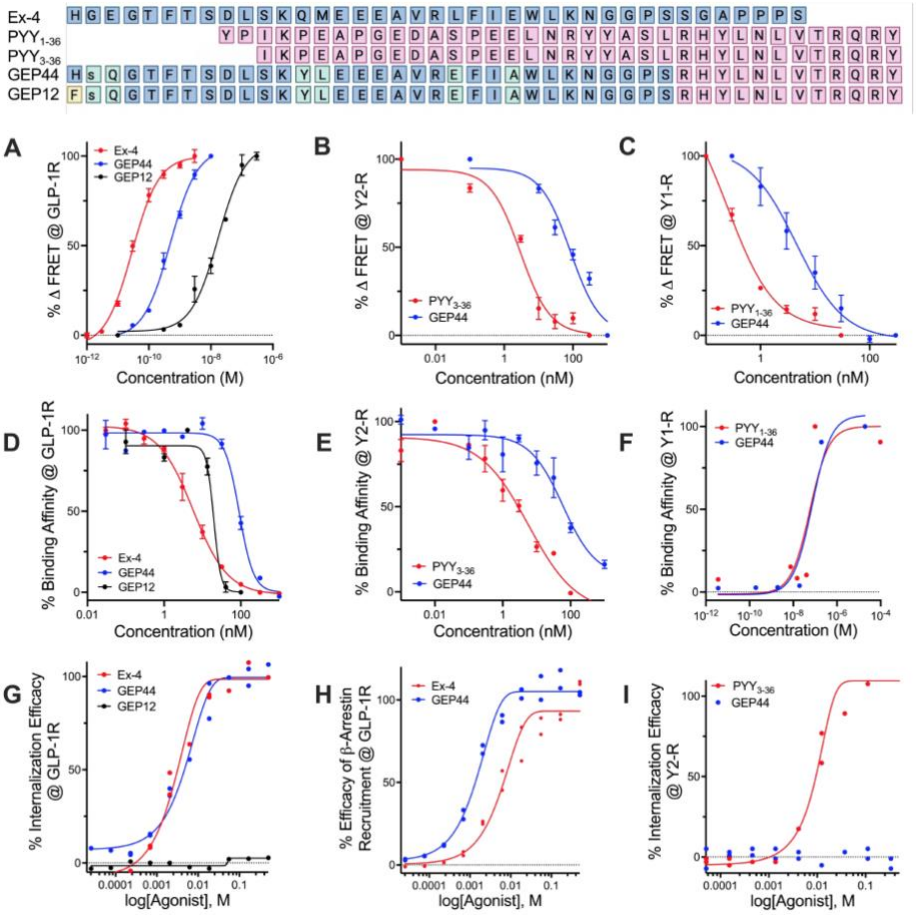
Ex-4 H G E G T F T S D L S K Q M E E E A V R L F I E W L K N G G P S S G A P P P S
PYY1-36 Y P I K P E A P G E D A S P E E L N R Y Y A S L R H Y L N L V T R Q R Y
PYY3-36 I K P E A P G E D A S P E E L N R Y Y A S L R H Y L N L V T R Q R Y
GEP44 H s Q G T F T S D L S K Y L E E E A V R E F I A W L K N G G P S R H Y L N L V T R Q R Y
GEP12 F s Q G T F T S D L S K Y L E E E A V R E F I A W L K N G G P S R H Y L N L V T R Q R Y
A
% Δ FRET @ GLP-1R
Ex-4
GEP44
GEP12
Concentration (M)
B
% Δ FRET @ Y2-R
PYY3-36
GEP44
Concentration (nM)
C
% Δ FRET @ Y1-R
PYY1-36
GEP44
Concentration (nM)
D
% Binding Affinity @ GLP-1R
Ex-4
GEP44
GEP12
Concentration (nM)
E
% Binding Affinity @ Y2-R
PYY3-36
GEP44
Concentration (nM)
F
% Binding Affinity @ Y1-R
PYY1-36
GEP44
Concentration (M)
G
% Internalization Efficacy @ GLP-1R
Ex-4
GEP44
GEP12
log[Agonist], M
H
% Efficacy of β-Arrestin Recruitment @ GLP-1R
Ex-4
GEP44
log[Agonist], M
I
% Internalization Efficacy @ Y2-R
PYY3-36
GEP44
log[Agonist], M

Figure 1

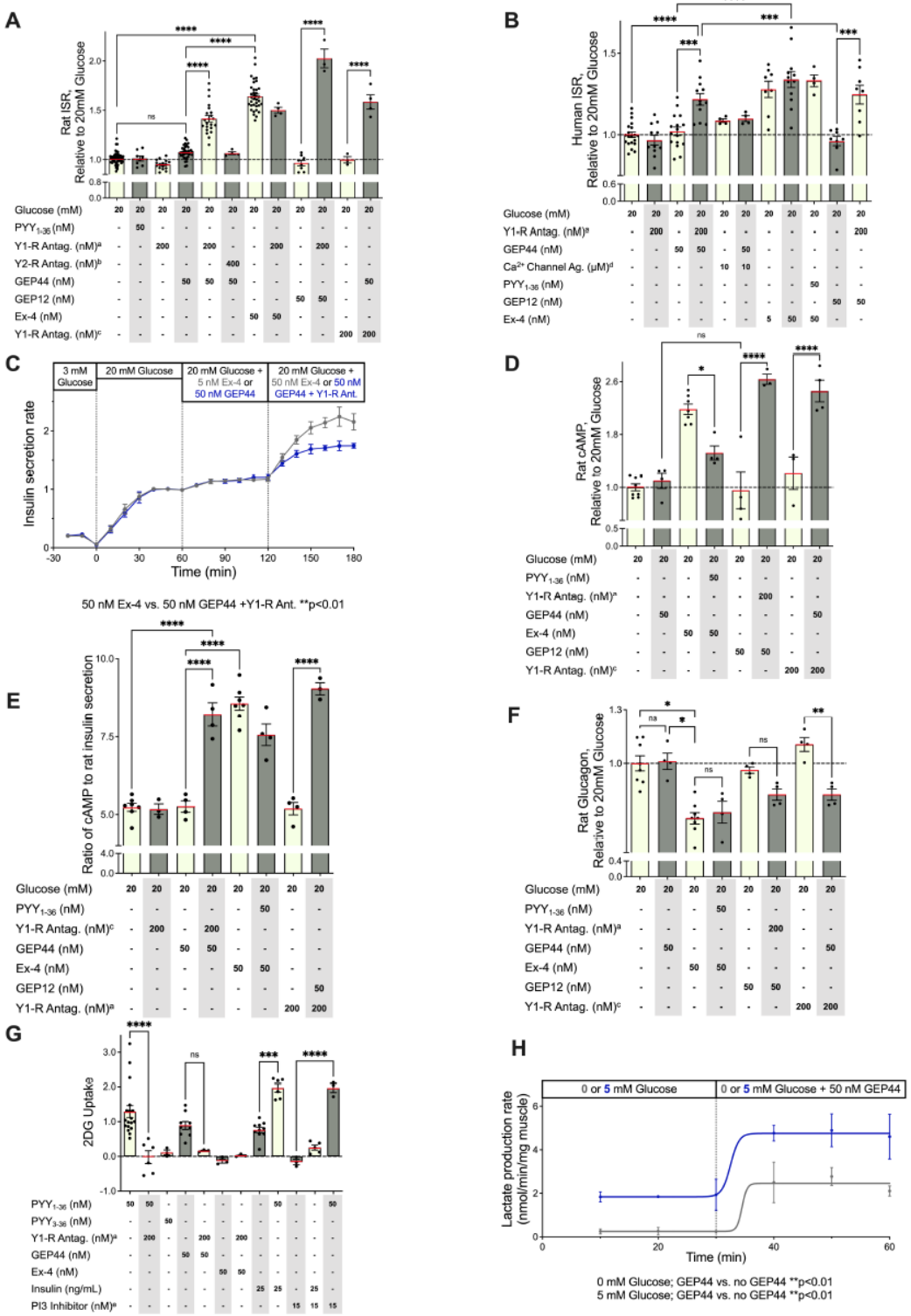
A
Rat ISR, Relative to 20mM Glucose
B
Human ISR, Relative to 20mM Glucose
C
3 mM Glucose
20 mM Glucose
20 mM Glucose + 5 nM Ex-4 or 50 nM GEP44
20 mM Glucose + 50 nM Ex-4 or 50 nM GEP44 + Y1-R Ant.
Insulin secretion rate
Time (min)
50 nM Ex-4 vs. 50 nM GEP44 +Y1-R Ant. **p<0.01
D
Rat cAMP, Relative to 20mM Glucose
E
Ratio of cAMP to rat insulin secretion
F
Rat Glucagon, Relaive to 20mM Glucose
G
2DG Uptake
H
0 or 5 mM Glucose
0 or 5 mM Glucose + 50 nM GEP44
Lactate production rate (nmol/min/mg muscle)
Time (min)
0 mM Glucose; GEP44 vs. no GEP44 **p<0.01
5 mM Glucose; GEP44 vs. no GEP44 **p<0.01

Figure 2

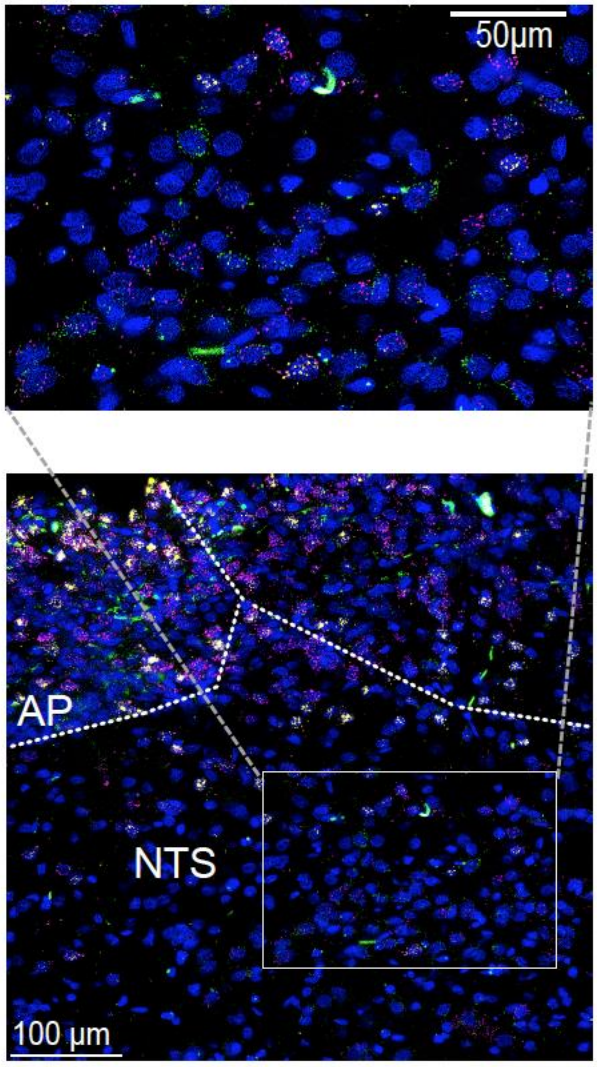

Figure 3A

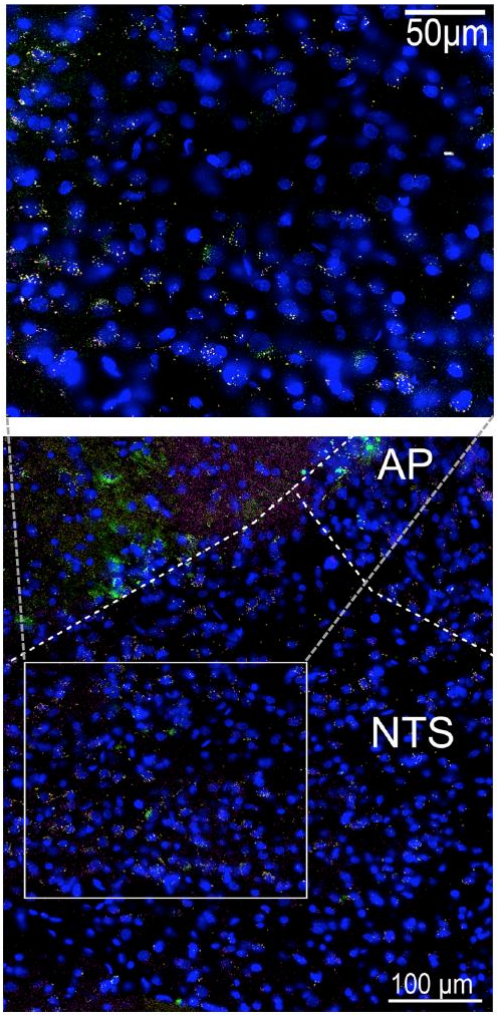

Figure 3B

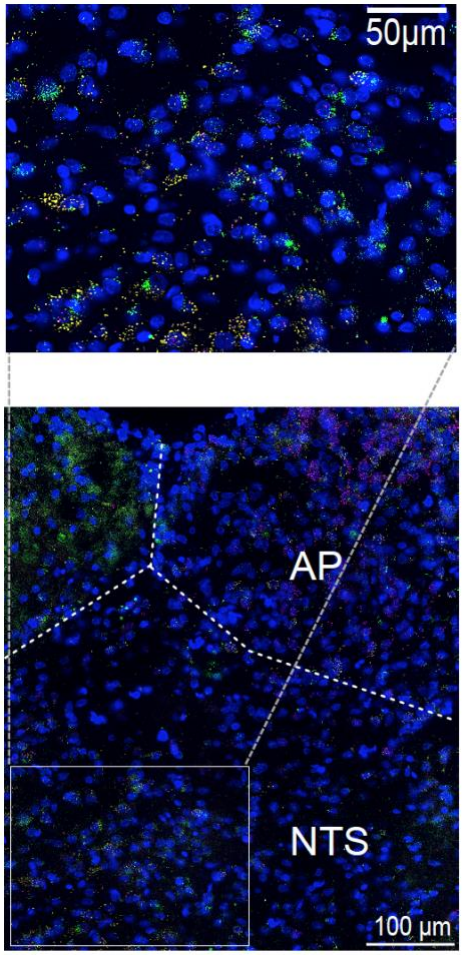

Figure 3C

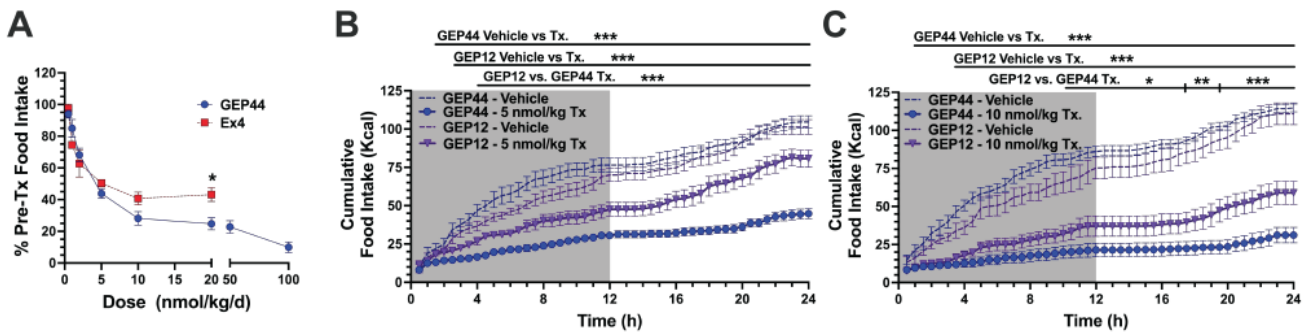

Figure 4

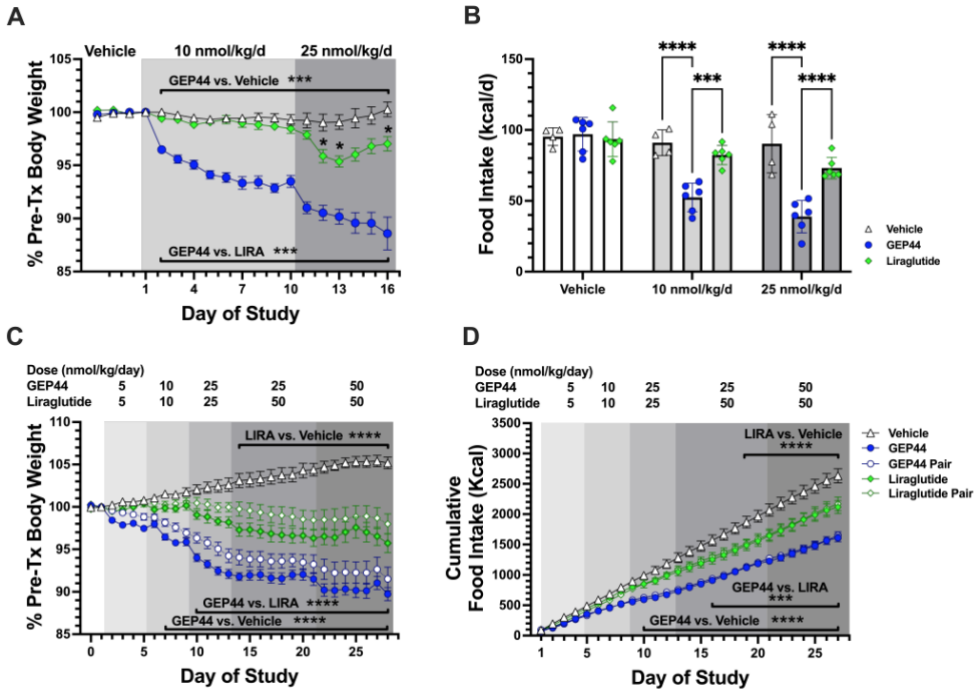

Figure 5

	Vehicle	GEP44	GEP44 pair-fed	Liraglutide	Liraglutide pair-fed
Body Weight (g)					
Baseline	660 ± 94	660 ± 55	667 ± 63	660 ± 65	658 ± 75
Post-Tx	695 ± 104	592 ± 55 *** ##	611 ± 70 ***	631 ± 79 ***	647 ± 86 ***
Food Intake					
5d Baseline (kcal/d)	88.6 ± 12.6	95.6 ± 8.9	94.2 ± 14.4	93.1 ± 8.7	91.3 ± 4.3
Last 5d of Tx (kcal/d)	91.8 ± 10.4	65.5 ± 10.0 *** ##	65.6 ± 10.2 ***	78.3 ± 11.1 ***	78.5 ± 10.6 *
Cumulative (kcal)	2633 ± 329	1610 ± 184 *** ##	1637 ± 186 ***	2116 ± 300 **	2166 ± 327 *
Glucose (mg/dL)					
Baseline	120 ± 10	110 ± 8	119 ± 13	119 ± 10	119 ± 5
Post-Tx	93 ± 8	83 ± 6 *	90 ± 6	89 ± 3	93 ± 9
Insulin (ng/mL)					
Baseline	14 ± 10	13 ± 5	16 ± 6	14 ± 5	14 ± 4
Post-Tx	14 ± 8	7 ± 2 **	6 ± 3	8 ± 3 *	8 ± 3

Table 1

	Vehicle	GEP44	GEP44 pair-fed	Liraglutide	Liraglutide pair-fed
ALT (U/L)	195 ± 37	205 ± 30	192 ± 30	191 ± 32	184 ± 14
AST (U/L)	64 ± 88	34 ± 16	25 ± 11	32 ± 10	31 ± 23
Cholesterol (mg/dL)	256 ± 190	214 ± 170 ††	183 ± 92	175 ± 126	163 ± 106
Trig (mg/dL)	74 ± 15	83 ± 16	55 ± 11	71 ± 13	60 ± 14
HDL (mg/dL)	76 ± 23	64 ± 14 ††	55 ± 15	61 ± 16	56 ± 15
calc LDL (mg/dL)	23 ± 3	26 ± 3 †	18 ± 3	22 ± 3	19 ± 4

Table 2

Figure 1. Design and in vitro evaluation of chimeric peptides GEP44 and GEP12. Shown are the amino acid sequences of Ex-4, PYY_{1-36} and PYY_{3-36} overlaid with those of GEP44 and GEP12 with lowercase single-letter amino acid code denoting a D-isomer. (A) Dose-dependent agonism (% change in FRET ratio tracking levels of cAMP) of Ex-4, GEP44, and GEP12 at the GLP-1R. (B) Dose-dependent agonism (% change in FRET ratio tracking levels of cAMP) of PYY_{3-36}, GEP44, and GEP12 at the Y2-R. (C) Dose-dependent agonism of PYY_{1-36}, GEP44, and GEP12 at the Y1-R. (D) Percent binding of Ex-4, GEP44, and GEP12 at the GLP-1R. (E) Percent binding of PYY_{3-36}, GEP44, and GEP12 at the Y2-R. (F) Percent binding of PYY_{1-36}, GEP44, and GEP12 at the Y1-R. (G) % internalization of GEP44 and GEP12 at the GLP-1R. (H) % recruitment of β-arrestin-2 by Ex-4 and GEP44 at the GLP-1R. (I) % internalization of Ex-4 and GEP44 at the Y2-R.

Figure 2. Action of GEP44 and GEP12 are mediated by GLP-1R and Y1-R in isolated pancreatic islets and muscle tissue. Rat (A) and human (B) islets were incubated for 60 min in 20 mM glucose and additional agents as indicated. Supernatants were then assayed for insulin, cAMP, and glucagon concentrations. (C) Insulin secretion rates (ISRs) were measured by perifusion over a one-hour incubation period in rat islets in 20 mM glucose with 5 or 50 nM peptides with or without Y1-R antagonist, as indicated (C). Impact of GEP44 on (D) cAMP, (E) the ISR to cAMP ratio, and (F) glucagon secretion, relative to glucose-mediated stimulation alone in the absence of test compounds. cAMP levels corresponded directly, and glucagon secretion corresponded inversely with the ISR. (G) Uptake of ^{3}H-2-deoxyglucose (2-DG) and (H) lactate production (Å} 5 mM glucose) in response to GEP44 and other agents known to interact with GLP-1R, Y1-R, and Y2-R in the rat quadriceps muscle ex vivo. Horizontal dashed line in 2A, B, D, and F represents response to 20 mM glucose alone in assay as described. $_{a}$ =PD 160170; $_{b}$ = BIIE0246; $_{c}$ = BIBO; $_{d}$ = Bay K, $_{e}$ = Wortmannin.

Figure 3. FISH and IHC visualization of f-Cy5-GEP44 and its colocalization with Y1-R, Y2-R, and GLP-1R in cells in the NTS/AP regions of the rat brain. (A) f-Cy5-GEP44 (green) administered IP colocalized with Y1-R and GLP-1R (yellow) in the AP. (B) f-Cy5-GEP44 administered ICVI colocalized with Y1-R (yellow) and GLP-1R (magenta) in the AP. See Supplementary Video 1 for a three-dimensional (3D) rotational image of the area within the inset. (C) f-Cy5-GEP44 administered ICVI colocalized with Y2-R (yellow) and GLP-1R (magenta) in cells of the AP. See Supplementary Video 2 for a 3D rotational image of the area within the inset. Images are shown at 40x magnification.

Figure 4. Dose-escalation study reveals a robust reduction of food intake in response to GEP44. (A) The dose-escalation study shows a robust reduction of food intake in response to GEP44 (●, n=8 DIO rats) vs. Ex-4 (n, n=4 DIO rats). Food intake was averaged over three days of treatment at each drug dose and was normalized to the earliest three days during which all animals received injections with the vehicle control. Escalation of the Ex-4 dose was stopped at 20 nmol/kg due to multiple indicators of malaise. (B, C) Shown is the average 24-hour cumulative food intake for the three-day vehicle-treated baseline and three-day GEP12 treatment phases (q, n=8 DIO rats) at (B) 5 nmol/kg/day and (C) 10 nmol/kg/day doses. Data from equivalent dose-testing performed as part of the GEP44 (●) dose-escalation study were included in these figures to facilitate a qualitative comparison. Data shown are means ± standard error of the mean (SEM); *p<0.05, ** p <0.01, *** p <0.001.

Figure 5. GEP44-mediated reductions in body weight and food intake were stronger than those elicited by LIRA during a 16-day and 27-day dose escalation protocol. (A, B) DIO Wistar rats were treated with vehicle (r) or with GEP44 (●) or LIRA (¿) at 10 nmol/kg/day for 9 days followed by 25 nmol/kg/day for 7 days (n=4–6) rats/group. In a second experiment, (C) changes in body weight and (D) food intake was evaluated during 27 days of treatment with vehicle, GEP44, vehicle-treated rats that were pair-fed to those receiving GEP44, LIRA, and vehicle-treated rats that were pair-fed to those receiving LIRA; n=8 per group. DIO male Wistar rats were matched based on baseline food intake and initial body weight gain trajectory. Changes in body weight were evaluated in response to GEP44 (●) at

doses escalating from 5 to 50 nmol/kg/day. Rats underwent pair-feeding to match the amount of food consumed by their GEP44-treated counterparts (o). Other groups included rats treated with saline-vehicle control, LIRA, and rats that were pair-fed to their LIRA-treated counterparts. Symbols representing the results from pair-fed animals are overlayed by those from the GEP44 and LIRA treatment groups. Data shown are means Å} SEM; *p <0.05, ***p <0.001, ****p <0.0001.

Table 1. Characteristics of treatment groups at baseline and after 27 days of treatment with GEP44 or LIRA. The data shown are means Å} standard deviation (SD). Data were compared by ANCOVA followed by pairwise comparisons of marginal linear predictions using a Bonferroni correction; n=8 rats per group. Abbreviations: Tx, treatment; *p <0.05, **p <0.01, ***p <0.001 vs. vehicle control; #p <0.05, ##p <0.01, ###p <0.001 vs. LIRA.

Table 2. Outcomes after 27 days of treatment with GEP44 or LIRA. Data shown are means Å} SD. Cross-sectional analyses were performed using an ANOVA followed by pairwise comparisons of means using a Bonferroni correction; n=8 rats per group. Abbreviations: ALT, alanine aminotransferase; AST, aspartate aminotransferase; Trig, triglycerides; HDL, high-density lipoprotein; calc, calculated; LDL, lowdensity
lipoprotein; *p <0.05, **p <0.01 vs. pair-fed counterparts.

7.2 Curriculum vitae

I am a medicinal chemist with an interest in designing and optimizing potential pharmaceuticals for future clinical translation. I have experience in peptide-based drug design, synthesis, characterization, and modification by lipidation, unnatural amino acid incorporation, and CLICK chemistry. As a Ph.D. candidate, I have focused on the rational design, synthesis, and characterization of monomeric, peptide-based, multi-agonists of the GLP-1R, Y1-R, and Y2-R in addition to their subsequent *in vivo* validation (in collaboration with Dr. Christian Roth, Seattle Children's Research Institute) for the treatment of type II diabetes and obesity devoid of gastrointestinal side effects. Simultaneously, I am working in collaboration with Prof. Matthew Hayes at the University of Pennsylvania to deorphanize a GPCR which, when antagonized, has pharmaceutical potential as a new avenue for treatment of obesity and metabolic disorders.

Publications

Chichura, K. S., Elfers, C., Salameh, T., Kamat, V., Chepurny, O. G., McGivney, A., Milliken, B. T., Holz, G. G., Applebey, S. V., Hayes, M. R., Sweet, I. R., Roth, C. L., Doyle, R. P. A Peptide Tri-agonist of the GLP-1-, Neuropeptide Y1-, and Neuropeptide Y2-Receptors for Glycemic Control and Weight Loss. **2023**, Accepted to *Scientific Reports*.

Chepurny, O. G.†, Liles, A.†, **Chichura, K. S.**, Milliken, B. T., Leech, C. A., Liapakis, G., Matsoukas, M., Doyle, R. P., Holz, G. G. Novel GPCR agonist properties of peptide chimeras based on GLP-1, Exendin-4, α-Latrotoxin and Peptide YY. **2022**, *Awaiting submission.*

Milliken, B., Elfers, C., Chepurny, O. G., **Chichura, K. S.**, Sweet, I. R., Borner, T., Hayes, M. R., De Jonghe, B. C., Holz, G. G., Roth, C. L., Doyle, R. P. Design and Evaluation of Peptide Dual-Agonists of GLP-1 and NPY2 Receptors for Glucoregulation and Weight Loss with Mitigated Nausea and Emesis. *J. Med. Chem*. **2021**, 64, 2.

Milly, T. A., Engler, E. R., **Chichura, K. S.**, *et al*. Harnessing multiple, non-proteogenic substitutions to optimize CSP:comD hydrophobic interactions in group 1 Streptococcus pneumoniae. *ChemBioChem*. **2021**, 22, 1940-1947.

Patents

Chichura, K. S., Elfers, C., Roth, C. L., Doyle, R. P. (2022) *Melanocortin and GLP-1 Receptor Agonists and Methods of Use*. *Under review*.

Chichura, K. S., Geisler, C. E., Doyle, R. P., Hayes, M. R. (2022) *Novel GPR75 ligands for controlling food intake, energy expenditure, body weight and treatment of obesity and metabolic diseases*. Web_50322. *Under review.*

Chichura, K. S., Geisler, C. E., Reiner, B. C., Crist, R. C., Doyle, R. P., Hayes, M. R. (2022) *Octadecaneuropeptide (ODN) and novel derived neuropeptides activity in the brain for food intake, obesity, body weight and prevention of nausea/emesis*. *Under review*.

Honors and Awards

Henning Andersen Award, 60th Annual Meeting of the European Society for Paediatric Endocrinology (ESPE)
Rome, Italy, September 2022
Outstanding Abstract Award, The Endocrine Society's Endo 2022 Meeting
Atlanta, GA, June 2022

Education

Syracuse University, 900 South Crouse Ave. Syracuse, NY 13244
Doctor of Philosophy in Chemistry, Expected: April 2023
Title: Design, synthesis, and characterization of a library of peptide multi-agonists of the GLP-1 and Neuropeptide Y1- and Y2-receptors for the mitigation of gastrointestinal side effects such as nausea and emesis involved with the treatment of type II diabetes and obesity. PI: Dr. Robert P. Doyle

Syracuse University, 900 South Crouse Ave. Syracuse, NY 13244
Master of Philosophy in Chemistry
GPA: 3.80

Moravian College, 1200 Main Street, Bethlehem, PA 18018
ACS-certified Bachelor of Science in Chemistry with Honors, Minor in Math, May 2019

Presentations

American Chemical Society National Meeting and Exposition, General Orals Session, Indianapolis, IN, March 2023

Chichura, K. S., Elfers, C., Salameh, T., Kamat, V., Chepurny, O. G., McGivney, A., Milliken, B. T., Holz, G. G., Applebey, S. V., Hayes, M. R., Sweet, I. R., Roth, C. L., Doyle, R. P.

Development of anorexigenic and glucoregulatory chimeric peptides with multi-agonism of the GLP-1R, Y2-R, and Y1-R to simultaneously treat obesity and type 2 diabetes.

60th Annual Meeting of the European Society for Pediatric Endocrinology,
Rome, Italy, September 2022

Christian Roth, **Kylie S. Chichura**, Ian Sweet, Clinton Elfers, Therese Salameh, Varun Kamat, Brandon Milliken, Robert Doyle

Development of Anorexigenic and Glucoregulatory Chimeric Peptides.

29th Annual Society for the Study of Ingestive Behavior Meeting,
Porto, Portugal, July 2022

Sarah V. Applebey, **Kylie Chichura**, Antonia Caffrey, Heath D. Schmidt, Robert P. Doyle, Matthew R. Hayes

Evaluating the role of hindbrain GLP-1R and NPY2-R signaling in sensory-specific satiety.

The Endocrine Society's Endo 2022,
Atlanta, GA, June 2022

Kylie Chichura, Clinton Elfers, Dr. Christian L. Roth, Dr. Robert P. Doyle
A Monomeric Tri-Agonist of GLP-1, NPY1 and NPY2 Receptors.
256th American Chemical Society National Meeting and Exposition,
Boston, MA, August 2018

Kylie Chichura, Bimal Koirala, Dr. Michael A. Bertucci, Dr. Yftah Tal-Gan
Effects of multiple amino acid mutations of a key quorum sensing peptide, CSP-1.

Skills

Laboratory

Proficiency in RP-HPLC, MALDI-TOF mass spectrometry, Bioconjugate and CEM microwave-assisted solid-phase peptide synthesis, ESI-MS, Copper-free CLICK chemistry, CD spectroscopy, UV-Vis spectroscopy, NMR, Surface plasmon resonance, cell assays

Technological

GraphPad Prism, PyMOL, HPEPDOCK